Mobile Information Systems

Edge Intelligence in Internet of Things using Machine Learning

Lead Guest Editor: Mian Ahmad Jan
Guest Editors: Muhammad Usman, Muhammad Babar, Xingwang Li, and Muhammad Bilal

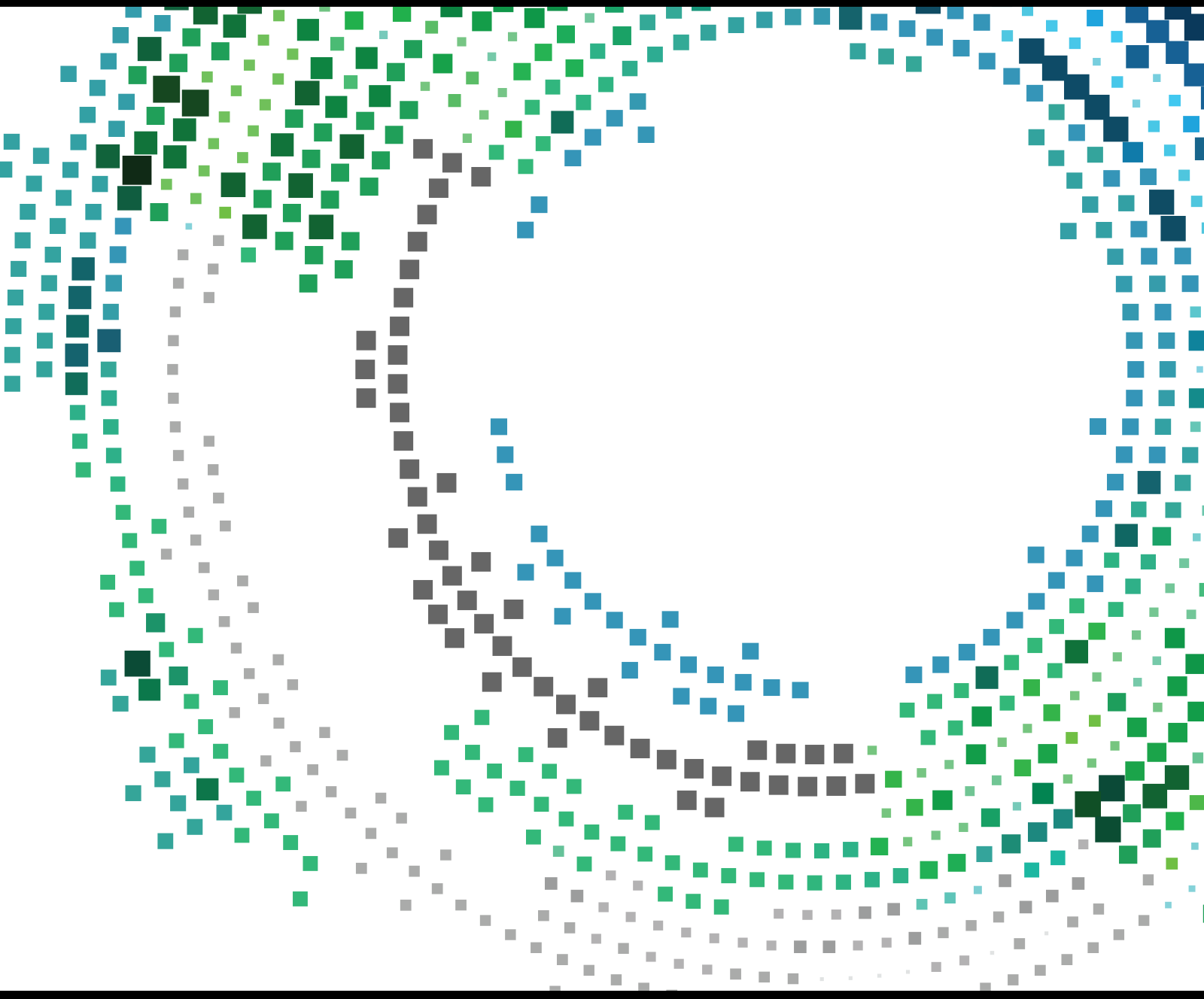

Edge Intelligence in Internet of Things using Machine Learning

Mobile Information Systems

Edge Intelligence in Internet of Things using Machine Learning

Lead Guest Editor: Mian Ahmad Jan
Guest Editors: Muhammad Usman, Muhammad Babar, Xingwang Li, and Muhammad Bilal

Copyright © 2023 Hindawi Limited. All rights reserved.

This is a special issue published in “Mobile Information Systems.” All articles are open access articles distributed under the Creative Commons Attribution License, which permits unrestricted use, distribution, and reproduction in any medium, provided the original work is properly cited.

Chief Editor

Alessandro Bazzi, Italy

Academic Editors

Mahdi Abbasi, Iran
Abdullah Alamoodi, Malaysia
Markos Anastassopoulos, United Kingdom
Marco Anisetti, Italy
Claudio Agostino Ardagna, Italy
Ashish Bagwari, India
Dr. Robin Singh Bhadoria, India
Nicola Bicocchi, Italy
Peter Brida, Slovakia
Puttamadappa C., India
Carlos Calafate, Spain
Pengyun Chen, China
Yuh-Shyan Chen, Taiwan
Wenchi Cheng, China
Gabriele Civitarese, Italy
Massimo Condoluci, Sweden
Rajesh Kumar Dhanaraj, India
Rajesh Kumar Dhanaraj, India
Almudena Díaz Zayas, Spain
Filippo Gandino, Italy
Jorge Garcia Duque, Spain
Francesco Gringoli, Italy
Wei Jia, China
Adrian Kliks, Poland
Adarsh Kumar, India
Dongming Li, China
Juraj Machaj, Slovakia
Mirco Marchetti, Italy
Elio Masciari, Italy
Zahid Mehmood, Pakistan
Eduardo Mena, Spain
Massimo Merro, Italy
Aniello Minutolo, Italy
Jose F. Monserrat, Spain
Raul Montoliu, Spain
Mario Muñoz-Organero, Spain
Francesco Palmieri, Italy
Marco Picone, Italy
Alessandro Sebastian Podda, Italy
Maheswar Rajagopal, India
Amon Rapp, Italy
Filippo Sciarrone, Italy
Floriano Scioscia, Italy
Mohammed Shuaib, Malaysia
Michael Vassilakopoulos, Greece
Ding Xu, China
Laurence T. Yang, Canada
Kuo-Hui Yeh, Taiwan

Contents

Retracted: Real-Time Data Scheduling of Flexible Job in Papermaking Workshop Based on Deep Learning and Improved Fuzzy Algorithm
Mobile Information Systems
Retraction (1 page), Article ID 9819581, Volume 2023 (2023)

Retracted: Prediction of College Students' Psychological Crisis Based on Data Mining
Mobile Information Systems
Retraction (1 page), Article ID 9803212, Volume 2023 (2023)

Retracted: Multimedia Teaching of College Musical Education Based on Deep Learning
Mobile Information Systems
Retraction (1 page), Article ID 9763973, Volume 2023 (2023)

Retracted: Intelligent Sports Training System Based on Artificial Intelligence and Big Data
Mobile Information Systems
Retraction (1 page), Article ID 9875791, Volume 2023 (2023)

Subspace Learning and Joint Distribution Adaptation for Unsupervised Cross-Database Microexpression Recognition
Yanliang Zhang, Ying Liu, Geng Li, and Hongxing Peng
Research Article (8 pages), Article ID 5572096, Volume 2021 (2021)

A Cross-Border E-Commerce Approach Based on Blockchain Technology
Zhao Hongmei
Research Article (10 pages), Article ID 2006082, Volume 2021 (2021)

Smart Application Division and Time Allocation Policy for Computational Offloading in Wireless Powered Mobile Edge Computing
Abdullah Numani, Zaiwar Ali, Ziaul Haq Abbas, Ghulam Abbas, Thar Baker, and Dhiya Al-Jumeily
Research Article (13 pages), Article ID 9993946, Volume 2021 (2021)

Open Innovation Mode of Green Innovation System for Manufacturing Industry
Shao Bo and Bi Kexin
Research Article (11 pages), Article ID 9948683, Volume 2021 (2021)

KoRASA: Pipeline Optimization for Open-Source Korean Natural Language Understanding Framework Based on Deep Learning
Myeong-Ha Hwang, Jikang Shin, Hojin Seo, Jeong-Seon Im, and Hee Cho
Research Article (9 pages), Article ID 9987462, Volume 2021 (2021)

Deep Learning-Driven Gaussian Modeling and Improved Motion Detection Algorithm of the Three-Frame Difference Method
Dingchao Zheng, Yangzhi Zhang, and Zhijian Xiao
Research Article (7 pages), Article ID 9976623, Volume 2021 (2021)

Construction of Video Courses of Physical Education and Health Education in Colleges and Universities under the MOOC Platform
Shuai Yang
Research Article (8 pages), Article ID 9925838, Volume 2021 (2021)

An Internet of Things Evaluation Algorithm for Quality Assessment of Computer-Based Teaching
Jing Huang
Research Article (10 pages), Article ID 9919399, Volume 2021 (2021)

[Retracted] Intelligent Sports Training System Based on Artificial Intelligence and Big Data
Chunguang Li and Jianbiao Cui
Research Article (11 pages), Article ID 9929650, Volume 2021 (2021)

Intelligent Decision-Making System for Martial Arts Competition Using Deep Learning
Shisen Li, Shenglu Huo, and Wei Ke
Research Article (8 pages), Article ID 9920751, Volume 2021 (2021)

E-Commerce Enterprise Supply Chain Financing Risk Assessment Based on Linked Data Mining and Edge Computing
Qiao Qu, Cheng Liu, and Xinzhong Bao
Research Article (9 pages), Article ID 9938325, Volume 2021 (2021)

An Action Recognition Algorithm for Sprinters Using Machine Learning
Fengqing Jiang and Xiao Chen
Research Article (10 pages), Article ID 9919992, Volume 2021 (2021)

A Classification Method of Tourism English Talents Based on Feature Mining and Information Fusion Technology
Xin Wei
Research Article (9 pages), Article ID 5520079, Volume 2021 (2021)

Identification of Pneumonia Disease Applying an Intelligent Computational Framework Based on Deep Learning and Machine Learning Techniques
Yar Muhammad, Mohammad Dahman Alshehri, Wael Mohammed Alenazy, Truong Vinh Hoang, and Ryan Alturki
Research Article (20 pages), Article ID 9989237, Volume 2021 (2021)

[Retracted] Prediction of College Students' Psychological Crisis Based on Data Mining
Jingjing Liu, Guangyuan Shi, Jing Zhou, and Qiumei Yao
Research Article (7 pages), Article ID 9979770, Volume 2021 (2021)

Cross-Cultural Communication of Regional Images Based on Multimodal Discourse Analysis and Network Security
Qing Xu and Guangming Wang
Research Article (10 pages), Article ID 9956593, Volume 2021 (2021)

Contents

Application of Data Envelopment and Internet of Things Technology for Asset Value Evaluation
Lunsheng Wang, Mingwu Gao, and Zhenlu Liang
Research Article (8 pages), Article ID 9934090, Volume 2021 (2021)

Systematic Study on Expression of Vocal Music and Science of Human Body Noise Based on Wireless Sensor Node
Yifei Xu
Research Article (9 pages), Article ID 9993019, Volume 2021 (2021)

Moving Object Detection Technology of Line Dancing Based on Machine Vision
Liyun Liu
Research Article (9 pages), Article ID 9995980, Volume 2021 (2021)

Fatigue Load Spectrum of Highway Bridge Vehicles in Plateau Mountainous Area Based on Wireless Sensing
Li Rui, Xie Xiaoyu, and Duan Xueyan
Research Article (8 pages), Article ID 9955988, Volume 2021 (2021)

Interactive Teaching System of Basketball Action in College Sports Based on Online to Offline Mixed Teaching Mode
Wenbo Guo and Yunjie Niu
Research Article (10 pages), Article ID 9994050, Volume 2021 (2021)

Local Cultural IP Development and Cultural Creative Design Based on Big Data and Internet of Things
Wei Bi and Guangming Wang
Research Article (9 pages), Article ID 5521144, Volume 2021 (2021)

Analysis of Influencing Factors of Social Mental Health Based on Big Data
Yixuan Zhao and Qinghua Tang
Research Article (8 pages), Article ID 9969399, Volume 2021 (2021)

Evaluation of Potential Correlation of Piano Teaching Using Edge-Enabled Data and Machine Learning
Sibing Sun
Research Article (11 pages), Article ID 6616284, Volume 2021 (2021)

[Retracted] Real-Time Data Scheduling of Flexible Job in Papermaking Workshop Based on Deep Learning and Improved Fuzzy Algorithm
Shihong Dang and Wei Tang
Research Article (12 pages), Article ID 9930740, Volume 2021 (2021)

Multimedia Interaction-Based Computer-Aided Translation Technology in Applied English Teaching
Hongxia Wu
Research Article (10 pages), Article ID 5578476, Volume 2021 (2021)

Multilabel CNN-Based Hybrid Learning Metric for Pedestrian Reidentification
Yinjun Zhang, Ryan Alturki, Hasan J. Alyamani, Mohammed Abdulaziz Ikram, Ateeq ur Rehman, and Muhammad Haleem
Research Article (7 pages), Article ID 5512382, Volume 2021 (2021)

[Retracted] Multimedia Teaching of College Musical Education Based on Deep Learning
Wei Li
Research Article (10 pages), Article ID 5545470, Volume 2021 (2021)

An Early Risk Warning of Cross-Border E-Commerce Using BP Neural Network
Zhichao Deng, Meiji Yan, and Xu Xiao
Research Article (8 pages), Article ID 5518424, Volume 2021 (2021)

Sonar Image Target Detection and Recognition Based on Convolution Neural Network
Wu Yanchen
Research Article (8 pages), Article ID 5589154, Volume 2021 (2021)

Intelligent Integrated Community Model for Ethnic Minority Areas Using Data Analysis and Machine Learning
Xiaoxue Liu
Research Article (8 pages), Article ID 5579709, Volume 2021 (2021)

Prediction of Volleyball Competition Using Machine Learning and Edge Intelligence
Qiang Liu and Qiannan Liu
Research Article (8 pages), Article ID 5595833, Volume 2021 (2021)

A 3D Machine Vision-Enabled Intelligent Robot Architecture
Yanjun Zhang, Jianxin zhao, and Heyong Han
Research Article (11 pages), Article ID 6617286, Volume 2021 (2021)

RSSI-Controlled Long-Range Communication in Secured IoT-Enabled Unmanned Aerial Vehicles
Inam Ullah Khan, Ryan Alturki, Hasan J. Alyamani, Mohammed Abdulaziz Ikram, Muhammad Adnan Aziz, Vinh Truong Hoang, and Tanweer Ahmad Cheema
Research Article (11 pages), Article ID 5523553, Volume 2021 (2021)

Analyzing and Evaluating Smart Cities for IoT Based on Use Cases Using the Analytic Network Process
Chao Huang and Shah Nazir
Research Article (13 pages), Article ID 6674479, Volume 2021 (2021)

A Dual-Mode Medium Access Control Mechanism for UAV-Enabled Intelligent Transportation System
Muhammad Asghar Khan, Tanweer Ahmad Cheema, Insaf Ullah, Fazal Noor, Sajjad Ur Rehman, Ateeq Ur Rehman, and Muhammad Adnan Aziz
Research Article (13 pages), Article ID 5578490, Volume 2021 (2021)

Contents

Innovative Marketing Framework for Enterprises Using Edge-Enabled Data Analysis
Guangming Wang and Yifeng Wang
Research Article (8 pages), Article ID 6699420, Volume 2021 (2021)

Big Data Insights and Comprehensions in Industrial Healthcare: An Overview
Weiwei He, Shah Nazir, and Zahid Hussain
Review Article (11 pages), Article ID 6628739, Volume 2021 (2021)

Hindawi
Mobile Information Systems
Volume 2023, Article ID 9819581, 1 page
https://doi.org/10.1155/2023/9819581

Retraction

Retracted: Real-Time Data Scheduling of Flexible Job in Papermaking Workshop Based on Deep Learning and Improved Fuzzy Algorithm

Mobile Information Systems

Received 8 August 2023; Accepted 8 August 2023; Published 9 August 2023

Copyright © 2023 Mobile Information Systems. This is an open access article distributed under the Creative Commons Attribution License, which permits unrestricted use, distribution, and reproduction in any medium, provided the original work is properly cited.

This article has been retracted by Hindawi following an investigation undertaken by the publisher [1]. This investigation has uncovered evidence of one or more of the following indicators of systematic manipulation of the publication process:

(1) Discrepancies in scope

(2) Discrepancies in the description of the research reported

(3) Discrepancies between the availability of data and the research described

(4) Inappropriate citations

(5) Incoherent, meaningless and/or irrelevant content included in the article

(6) Peer-review manipulation

The presence of these indicators undermines our confidence in the integrity of the article's content and we cannot, therefore, vouch for its reliability. Please note that this notice is intended solely to alert readers that the content of this article is unreliable. We have not investigated whether authors were aware of or involved in the systematic manipulation of the publication process.

Wiley and Hindawi regrets that the usual quality checks did not identify these issues before publication and have since put additional measures in place to safeguard research integrity.

We wish to credit our own Research Integrity and Research Publishing teams and anonymous and named external researchers and research integrity experts for contributing to this investigation.

The corresponding author, as the representative of all authors, has been given the opportunity to register their agreement or disagreement to this retraction. We have kept a record of any response received.

References

[1] S. Dang and W. Tang, "Real-Time Data Scheduling of Flexible Job in Papermaking Workshop Based on Deep Learning and Improved Fuzzy Algorithm," *Mobile Information Systems*, vol. 2021, Article ID 9930740, 12 pages, 2021.

Hindawi
Mobile Information Systems
Volume 2023, Article ID 9803212, 1 page
https://doi.org/10.1155/2023/9803212

Retraction

Retracted: Prediction of College Students' Psychological Crisis Based on Data Mining

Mobile Information Systems

Received 8 August 2023; Accepted 8 August 2023; Published 9 August 2023

Copyright © 2023 Mobile Information Systems. This is an open access article distributed under the Creative Commons Attribution License, which permits unrestricted use, distribution, and reproduction in any medium, provided the original work is properly cited.

This article has been retracted by Hindawi following an investigation undertaken by the publisher [1]. This investigation has uncovered evidence of one or more of the following indicators of systematic manipulation of the publication process:

(1) Discrepancies in scope
(2) Discrepancies in the description of the research reported
(3) Discrepancies between the availability of data and the research described
(4) Inappropriate citations
(5) Incoherent, meaningless and/or irrelevant content included in the article
(6) Peer-review manipulation

The presence of these indicators undermines our confidence in the integrity of the article's content and we cannot, therefore, vouch for its reliability. Please note that this notice is intended solely to alert readers that the content of this article is unreliable. We have not investigated whether authors were aware of or involved in the systematic manipulation of the publication process.

Wiley and Hindawi regrets that the usual quality checks did not identify these issues before publication and have since put additional measures in place to safeguard research integrity.

We wish to credit our own Research Integrity and Research Publishing teams and anonymous and named external researchers and research integrity experts for contributing to this investigation.

The corresponding author, as the representative of all authors, has been given the opportunity to register their agreement or disagreement to this retraction. We have kept a record of any response received.

References

[1] J. Liu, G. Shi, J. Zhou, and Q. Yao, "Prediction of College Students' Psychological Crisis Based on Data Mining," *Mobile Information Systems*, vol. 2021, Article ID 9979770, 7 pages, 2021.

Hindawi
Mobile Information Systems
Volume 2023, Article ID 9763973, 1 page
https://doi.org/10.1155/2023/9763973

Retraction

Retracted: Multimedia Teaching of College Musical Education Based on Deep Learning

Mobile Information Systems

Received 8 August 2023; Accepted 8 August 2023; Published 9 August 2023

Copyright © 2023 Mobile Information Systems. This is an open access article distributed under the Creative Commons Attribution License, which permits unrestricted use, distribution, and reproduction in any medium, provided the original work is properly cited.

This article has been retracted by Hindawi following an investigation undertaken by the publisher [1]. This investigation has uncovered evidence of one or more of the following indicators of systematic manipulation of the publication process:

(1) Discrepancies in scope

(2) Discrepancies in the description of the research reported

(3) Discrepancies between the availability of data and the research described

(4) Inappropriate citations

(5) Incoherent, meaningless and/or irrelevant content included in the article

(6) Peer-review manipulation

The presence of these indicators undermines our confidence in the integrity of the article's content and we cannot, therefore, vouch for its reliability. Please note that this notice is intended solely to alert readers that the content of this article is unreliable. We have not investigated whether authors were aware of or involved in the systematic manipulation of the publication process.

Wiley and Hindawi regrets that the usual quality checks did not identify these issues before publication and have since put additional measures in place to safeguard research integrity.

We wish to credit our own Research Integrity and Research Publishing teams and anonymous and named external researchers and research integrity experts for contributing to this investigation.

The corresponding author, as the representative of all authors, has been given the opportunity to register their agreement or disagreement to this retraction. We have kept a record of any response received.

References

[1] W. Li, "Multimedia Teaching of College Musical Education Based on Deep Learning," *Mobile Information Systems*, vol. 2021, Article ID 5545470, 10 pages, 2021.

Hindawi
Mobile Information Systems
Volume 2023, Article ID 9875791, 1 page
https://doi.org/10.1155/2023/9875791

Retraction

Retracted: Intelligent Sports Training System Based on Artificial Intelligence and Big Data

Mobile Information Systems

Received 8 August 2023; Accepted 8 August 2023; Published 9 August 2023

Copyright © 2023 Mobile Information Systems. This is an open access article distributed under the Creative Commons Attribution License, which permits unrestricted use, distribution, and reproduction in any medium, provided the original work is properly cited.

This article has been retracted by Hindawi following an investigation undertaken by the publisher [1]. This investigation has uncovered evidence of one or more of the following indicators of systematic manipulation of the publication process:

(1) Discrepancies in scope
(2) Discrepancies in the description of the research reported
(3) Discrepancies between the availability of data and the research described
(4) Inappropriate citations
(5) Incoherent, meaningless and/or irrelevant content included in the article
(6) Peer-review manipulation

The presence of these indicators undermines our confidence in the integrity of the article's content and we cannot, therefore, vouch for its reliability. Please note that this notice is intended solely to alert readers that the content of this article is unreliable. We have not investigated whether authors were aware of or involved in the systematic manipulation of the publication process.

Wiley and Hindawi regrets that the usual quality checks did not identify these issues before publication and have since put additional measures in place to safeguard research integrity.

We wish to credit our own Research Integrity and Research Publishing teams and anonymous and named external researchers and research integrity experts for contributing to this investigation.

The corresponding author, as the representative of all authors, has been given the opportunity to register their agreement or disagreement to this retraction. We have kept a record of any response received.

References

[1] C. Li and J. Cui, "Intelligent Sports Training System Based on Artificial Intelligence and Big Data," *Mobile Information Systems*, vol. 2021, Article ID 9929650, 11 pages, 2021.

Hindawi
Mobile Information Systems
Volume 2021, Article ID 5572096, 8 pages
https://doi.org/10.1155/2021/5572096

Research Article

Subspace Learning and Joint Distribution Adaptation for Unsupervised Cross-Database Microexpression Recognition

Yanliang Zhang, Ying Liu, Geng Li, and Hongxing Peng

School of Physics and Electronic Information Engineering, Henan Polytechnic University, Jiaozuo 454150, China

Correspondence should be addressed to Hongxing Peng; phx@hpu.edu.cn

Received 24 February 2021; Revised 6 May 2021; Accepted 25 June 2021; Published 20 July 2021

Academic Editor: Floriano Scioscia

Copyright © 2021 Yanliang Zhang et al. This is an open access article distributed under the Creative Commons Attribution License, which permits unrestricted use, distribution, and reproduction in any medium, provided the original work is properly cited.

Microexpression recognition has been widely favored by researchers due to its many potential applications, such as business negotiation and lie detection. Cross-database microexpression recognition is more challenging and attractive than normal microexpression recognition because the training and testing samples come from different databases. The ensuing challenge is that the feature distributions between training and testing samples differ too much. As a result, the performance of current well-performing microexpression recognition methods often fails to achieve the desired effect. In this paper, we overcome this problem by introducing Subspace Learning and Joint Distribution Adaptation (SLJDA) by projecting the source and target domains into the subspace and later reducing the distance between them and then minimizing the distance between the marginal and conditional probability distributions of the data between the source domain and the target domain. To evaluate its performance, a large number of cross-database experiments are performed in the SMIC database and CASMEII database. The experimental results show the superiority of the method compared with existing microexpression recognition methods.

1. Introduction

Microexpression is a special, weak facial expression that usually lasts only 1/25 to 1/5 seconds [1]. Different from ordinary facial expressions, microexpressions are spontaneous expressions that occur when people try to hide their inner emotions [2]. In other words, microexpressions can show the true thoughts of a person's heart. Therefore, automatic microexpression recognition technology can be applied in many practical scenarios such as marital relationship prediction [3], clinical diagnosis, and teaching assessment [4, 5], and even in the future, it may be extended to communication security [6–9], intelligent devices, etc.

In recent years, with the development of intelligent technology, researchers have gradually focused their attention on it, and microexpression recognition has made some progress. However, both training and testing samples for microexpression recognition come from the same microexpression database. This is not the case in practical applications, where the training and testing samples for microexpression recognition come from different databases. Different database recording environments, camera devices, genders, ages, and so on will vary. They lead to the destruction of the consistency of feature distribution that exists in traditional microexpression recognition methods. Therefore, the microexpression recognition methods with good performance often fail to achieve the ideal effect in many practical applications. In order to solve this problem, it is necessary to study cross-database microexpression recognition; that is, the training set (train domain) and the testing set (target domain) are not the same database.

Yan et al. [10] classified cross-database facial expression recognition into two cases, semisupervised and unsupervised. Similarly, according to the presence or absence of label information in the target domain, cross-database microexpression recognition can also be divided into two categories, unsupervised cross-database microexpression recognition (CDMER) and semisupervised cross-database microexpression recognition. Unsupervised cross-database microexpression recognition can only be trained using the

sample label information of the source domain, while the latter can also incorporate a small amount of label information of the target domain. Therefore, this paper will focus on unsupervised cross-database microexpression recognition.

Domain adaptation is one of transfer learning methods [11], aiming at how to reduce the distribution differences between source and target domains data under the assumption that the source and target domain feature space and category space are the same and the feature distribution is different. In recent two years, Zong et al. [12] proposed cross-database microexpression recognition based on domain adaptive method for the first time and achieved good results. Current transfer learning methods can be roughly divided into three categories: data distribution [13–17], feature selection [18, 19], and subspace learning [20–23]. At present, the classical work based on these methods includes Transfer Component Analysis (TCA) [13], which finds a feature mapping while retaining the original information of the source domain and the target domain, so that the conditional distribution between the two domains after the mapping is relatively close. But such feature mapping may not exist. The feature selection-based approach, Structural Correspondence Learning (SCL) [19], assumes the existence of common data features in the source and target domains and uses shared features for modeling. However, when the characteristics of the two are very different, it can lead to failure. Based on the subspace learning method Subspace Alignment (SA) [20], the SA method is to directly seek a linear transformation by projecting the source and target domains into a subspace, through which the transformation alignment of different data is realized. However, such methods tend to ignore the distribution shift between the projected data in the two subspaces. In the face of this challenge, we integrate the subspace learning method with the data distribution adaptation method, namely, Subspace Learning and Joint Distribution Adaptation (SLJDA). First, the source and target domains are mapped to the corresponding subspaces, followed by maximizing the interclass distance and minimizing the intraclass distance in turn to preserve the discriminative features of the source domain data. Maximize the target domain variance samples, minimize the differences in the distribution of the corresponding subspaces of the projected source and target domains, and minimize the distances between subspaces to reduce the difference between source and target domains and improve the recognition of unsupervised cross-database microexpression.

In general, this paper contains the following main contributions:

(1) After considering the practical situation, the subspace-based learning method and the data distribution-based adaptive method are cleverly combined to reduce the difference between the source and target domains. The original information is preserved, and there is no need to search for feature mappings that may not exist to a large extent. In addition, the data distribution shift in the projected subspace is reduced, and the distance between them is geometrically reduced.

(2) We conducted more extensive CDMER experiments to assess the performance of the SLJDA approach.

The rest of this paper is arranged as follows. Section 2 reviews the recent research on unsupervised cross-database microexpression. In Section 3, we describe the SLJDA for CDMER in detail. For better evaluating this method, extensive experiments and analyses on SMIC and CASMEII are shown in Section 4. Finally, the conclusion and the future planning of this paper are drawn in Section 5.

2. Related Work

As mentioned above, most of the existing cross-database emotion recognition problems (including cross-database voice emotion recognition, facial expression recognition, and microexpression recognition) usually solve the mismatch of feature distribution between source domain and target domain by domain adaptive DA method. In the recent two years, a domain adaptive approach was first proposed by Zong et al. [12]. In addition, Target Sample Re-Generator (TSRG) was proposed to learn a sample regenerator that can regenerate the samples of source domain and target domain, and the samples of both have the same characteristic distribution, where the regenerated source domain microexpression samples will remain unchanged in the feature space. Li et al. [24] proposed to use the Target-Adapted Least-Squares Regression (TALSR) method to learn the regression coefficient matrix according to the source domain data information and make the regression coefficient matrix fit the target database.

Before this, most researchers focused on cross-database facial expression and cross-database speech recognition related to cross-database microexpression and put forward many effective methods. For example, Zhu et al. [25] first proposed to use domain adaptation to solve the facial expression recognition problem and achieve good results. In the work of [26], Transductive Transfer Regularized Least-Squares Regression (TTRLSR) was proposed to solve the cross-database facial expression recognition problem. The core idea is to learn a discriminant subspace and use the source domain with complete data information and the dataset selected from the target domain sample to predict the facial expression category in the target domain. Chu et al. [27, 28] discovered a new method, selective transfer machine (STM), which can use target samples to learn a set of weights of the source samples, so that the weighted source samples and the target samples have the same or similar characteristic distribution. Then the learned classifier is used to predict the information of the target domain samples. In addition, Yan et al. [10] innovatively came up with Unsupervised Domain-Adaptive Dictionary Learning (UDADL), with the aim of learning a dictionary from the samples of source domain and target domain and solving the problem of cross-database facial expression recognition by using the basic idea of common subspace. In the Domain-Adaptive Subspace Learning (DoSL) model [29], the source

and target domain samples are mapped into the common subspace by learning a mapping matrix, and the regenerated source and target domain samples follow the same or similar feature distributions.

In the early research of cross-database speech emotion recognition, a series of good methods appeared. For example, Hassan et al. [30] proposed to use the Importance weighted support vector machine (IW-SVM) method to deal with the challenge of cross-database speech emotion recognition. The method was developed by combining three domain adaptive methods; namely, kernel mean matching (KMM) [31], Kullback–Leibler importance estimation procedure (KLIEP) [32], and unconstrained least-squares importance fitting (uLSIF) [33] were combined. It is used to alleviate the problem that the sample feature distribution of source domain and target domain does not match. Zong et al. [34] introduced the domain-adaptive least-squares regression (DALSR) method to learn a regression coefficient matrix using the source domain sample information and the auxiliary set selected from the target database. At the same time, the mean and variance of the speech sample in the source and target domain after regression are also constrained to make the sample in the two domains have similar feature distributions.

3. Subspace Learning and Joint Distribution Adaptation

3.1. Problem Definition. Assume that n and m denote the number of samples in the source and target domains, respectively, d represents the dimensionality of the microexpression feature vector, and $X_s \in \mathbb{R}^{d\times n}$ and $X_t \in \mathbb{R}^{d\times m}$ are the microexpression samples in the source and target domains. Given a labeled source domain $\Omega_s = \{(x_j, y_j)\}_{j=1}^{n}$ and an unlabeled target domain $\Omega_t = \{x_i\}_{i=1}^{m}$, assume that the feature space and the category space are the same; that is, $\mathcal{X}_s = \mathcal{X}_t$ and $\mathcal{Y}_s = \mathcal{Y}_t$. The margin distribution is different $P_s(x_s) \neq P_t(x_t)$. Moreover, the mapping relationship is not the same in the source and target domains.

For better cross-database MER, we fuse data distribution and subspace learning methods to reduce domain differences. By mapping the source and target domains to the corresponding subspaces, we then maximize the target domain sample variance and preserve the source domain discriminative features while minimizing the two subspace differences and the subspace data distribution differences. The details are described next.

3.2. Subspace Learning and Joint Distribution Adaptation. Since the source domain contains not only sample information but also label information, we should make the best use of the discriminatory features of the source domain to achieve the best possible differentiation between different classes. By using the minimization of intraclass scatter and the maximization of interclass scatter, similar samples in the source domain can be close to each other, while different samples can be far away from each other as far as possible, thus facilitating a learning algorithm with good performance.

$$\min_{Y} \operatorname{Tr}\left(Y^T S_w Y\right), \tag{1}$$

$$S_w = \sum_{c=1}^{C} X_s^{(c)} H_s^{(c)} \left(X_s^{(c)}\right)^T, \tag{2}$$

where S_w is the within-class scatter matrix, $H_s^{(c)} = I_s^{(c)} - 1/n_c 1_s^{(c)} (1_s^{(c)})^T$ is the center matrix of class c in the source domain, $X_s^{(c)} \in \mathbb{R}^{d\times n_c}$, n_c is the number of class c, $1_s \in \mathbb{R}^{n_c}$ is the row vector of unit 1, and $1_s^{(c)} \in \mathbb{R}^{n_c\times n_c}$ is the identity matrix.

$$\max_{Y} \operatorname{Tr}\left(Y^T S_b Y\right), \tag{3}$$

$$S_b = \sum_{c=1}^{C} n_c \left(\mu_j - \mu\right)\left(\mu_j - \mu\right)^T, \tag{4}$$

where S_b is the interclass scatter matrix, μ_j is the sample mean of class c in the source domain, and μ is the sample mean of the source domain.

In order to preserve the data attributes to the classification of the target domain as much as possible, it is necessary to project the feature dimensions onto the relevant dimensions and therefore maximizing the target domain variance in the relevant subspace [35].

Maximize the target variance as follows:

$$\operatorname{Tr}\left(Z^T X_t H_t X_t^T Z\right), \tag{5}$$

where $H_t = I_t - 1/m 1_t 1_t^T$ is the centering matrix and $1_t \in \mathbb{R}^m$ is a row vector of unit 1.

Similar to the principle of data-centric domain adaptive methods, we compare the data differences between two domains by MMD distance to minimize the maximum mean difference between the source and target domains in k-dimensional embedding and further improve the marginal distribution differences.

$$\left\| \frac{1}{n} \sum_{x_j \in X_s} Y^T x_j - \frac{1}{m} \sum_{x_i \in X_t} Z^T x_i \right\|_F^2. \tag{6}$$

Because the label of the target domain is unknown, the conditional distribution of the target domain cannot be obtained directly, so the method proposed by [16] is usually used. Pseudo labels are obtained by using the classifier in the source domain to predict directly on the target domain. Since some pseudo labels may be incorrect and thus lead to poor recognition, an iterative approach is used to continuously improve the classification accuracy and thus reduce the difference between the two conditional distributions. The conditional distribution difference is

$$\sum_{c=1}^{C} \left\| \frac{1}{n_c} \sum_{x_j \in X_s^{(c)}} Y^T x_j - \frac{1}{m_c} \sum_{x_i \in X_t^{(c)}} Z^T x_i \right\|_F^2. \tag{7}$$

Therefore, by integrating equations (6) and (7), the distribution difference between source domain and target domain can be obtained:

$$\min_{Y,Z} \mathrm{Tr}\left(\begin{bmatrix} Y^T & Z^T \end{bmatrix} \begin{bmatrix} X_s\left(M_0 + \sum_{c=1}^{C} M_c\right)X_s^T & X_s\left(M_0 + \sum_{c=1}^{C} M_c\right)X_t^T \\ X_t\left(M_0 + \sum_{c=1}^{C} M_c\right)X_s^T & X_t\left(M_0 + \sum_{c=1}^{C} M_c\right)X_t^T \end{bmatrix} \begin{bmatrix} Y \\ Z \end{bmatrix} \right). \tag{8}$$

To simplify equation (8), we write it as follows:

$$\min_{Y,Z} \mathrm{Tr}\left[\begin{bmatrix} Y^T & Z^T \end{bmatrix} \begin{bmatrix} W_{s,s} & W_{s,t} \\ W_{t,s} & W_{t,t} \end{bmatrix} \begin{bmatrix} Y \\ Z \end{bmatrix} \right], \tag{9}$$

where

$$W_{s,s} = X_s\left(M_0 + \sum_{c=1}^{C} M_c\right)X_s^T,$$

$$(M_c)_{ji} = \begin{cases} \dfrac{1}{n_c^2}, & x_i, x_j \in X_s^{(c)}, \\ \dfrac{1}{m_c^2}, & x_i, x_j \in X_t^{(c)}, \\ -\dfrac{1}{m_c n_c}, & \begin{cases} x_j \in X_s^{(c)}, x_i \in X_t^{(c)} \\ x_j \in X_t^{(c)}, x_i \in X_s^{(c)} \end{cases}, \\ 0, & \text{otherwise}, \end{cases} \tag{10}$$

$$(M_0)_{ji} = \begin{cases} \dfrac{1}{n^2} 1_s 1_s^T, & x_i, x_j \in X_s, \\ \dfrac{1}{m^2} 1_t 1_t^T, & x_i, x_j \in X_t, \\ -\dfrac{1}{mn} 1_s 1_t^T, & x_j \in X_s, x_i \in X_t, \\ -\dfrac{1}{mn} 1_t 1_s^T, & x_i \in X_t, x_j \in X_s. \end{cases}$$

Unlike the subspace learning method SA, which requires finding an alignment matrix and aligning the source and target domain subspaces to reduce the distance between the source and target domains, this method is mapped to their respective subspaces, and we optimize both Y and Z while making the two subspaces closer together.

$$\min_{Y,Z} \|Y - Z\|_F^2. \tag{11}$$

3.3. Optimization Problem. By integrating the five equations (1), (3), (5), (9), and (11), we can get the final SLJDA method:

$$\max \frac{\gamma(5) + \beta(3)}{\lambda(11) + (9) + \beta(1)}, \tag{12}$$

where λ, β, and γ are the hyperparameters by $\mathrm{Tr}(Z^T Z)$ to constrain Z. Furthermore, the two coupled projections Y and Z are obtained using the following optimization function calculated:

$$\max_{Y,Z} \frac{\mathrm{Tr}\left(\begin{bmatrix} Y^T & Z^T \end{bmatrix} \begin{bmatrix} \beta S_b & 0 \\ 0 & \gamma S_t \end{bmatrix} \begin{bmatrix} Y \\ Z \end{bmatrix} \right)}{\mathrm{Tr}\left(\begin{bmatrix} Y^T & Z^T \end{bmatrix} \begin{bmatrix} W_{s,s} + \lambda I + \beta S_w & W_{s,t} - \lambda I \\ W_{t,s} - \lambda I & W_{t,t} + (\lambda + \gamma) I \end{bmatrix} \begin{bmatrix} Y \\ Z \end{bmatrix} \right)}. \tag{13}$$

Since $\begin{bmatrix} Y \\ Z \end{bmatrix}$ can be stretched without changing the final result, we can simply keep the bottom constant and only calculate the top. So the final optimization problem becomes

$$\begin{aligned} &\max_{Y,Z} \mathrm{Tr}\left(\begin{bmatrix} Y^T & Z^T \end{bmatrix} \begin{bmatrix} \beta S_b & 0 \\ 0 & \gamma S_t \end{bmatrix} \begin{bmatrix} Y \\ Z \end{bmatrix} \right) \\ &s.t. \quad \mathrm{Tr}\left(\begin{bmatrix} Y^T & Z^T \end{bmatrix} \begin{bmatrix} W_{s,s} + \lambda I + \beta S_w & W_{s,t} - \lambda I \\ W_{t,s} - \lambda I & W_{t,t} + (\lambda + \gamma) I \end{bmatrix} \begin{bmatrix} Y \\ Z \end{bmatrix} \right) = 1. \end{aligned} \tag{14}$$

Denote $\Phi = \mathrm{diag}(\lambda_1, \ldots, \lambda_d)$ as the Lagrange multiplier, and then Lagrange function for equation (14) is

$$\begin{aligned} L = &\mathrm{Tr}\left(\begin{bmatrix} Y^T & Z^T \end{bmatrix} \begin{bmatrix} \beta S_b & 0 \\ 0 & \gamma S_t \end{bmatrix} \begin{bmatrix} Y \\ Z \end{bmatrix} \right) \\ &+ \mathrm{Tr}\left(\left(\begin{bmatrix} Y^T & Z^T \end{bmatrix} \begin{bmatrix} W_{s,s} + \lambda I + \beta S_w & W_{s,t} - \lambda I \\ W_{t,s} - \lambda I & W_{t,t} + (\lambda + \gamma) I \end{bmatrix} \begin{bmatrix} Y \\ Z \end{bmatrix} - I \right) \Phi \right). \end{aligned} \tag{15}$$

Setting the derivative $\partial L / \partial A = 0$, we can obtain

$$\begin{bmatrix} \beta S_b & 0 \\ 0 & \gamma S_t \end{bmatrix} A = \begin{bmatrix} W_{s,s} + \lambda I + \beta S_w & W_{s,t} - \lambda I \\ W_{t,s} - \lambda I & W_{t,t} + (\lambda + \gamma) I \end{bmatrix} A \Phi, \tag{16}$$

where $\begin{bmatrix} Y \\ Z \end{bmatrix} = A$, and the matrix composed of eigenvectors corresponding to d minimum eigenvalues obtained by the

generalized value decomposition of equation (16) is A. Then the subspaces Y and Z are obtained.

4. Experiments

4.1. Microexpression Database. In this chapter, we conduct wide-ranging experiments in two popularly known databases, CASMEII and SMIC, to evaluate the performance of this method in a comprehensive manner. One of them, CASMEII [36], established by the Institute of Psychology of the Chinese Academy of Sciences, requires subjects not only to watch videos with large mood swings but more importantly to simultaneously attempt to mask their emotions. At the same time, the subjects' expressions were recorded at a frame rate of 200 fps without watching the video. With this elicitation mechanism, 247 video sequences from 26 individuals were acquired. Seven microexpression categories (*Happy, Surprised, Disgusted, Depressed, Sad, Scared, Other)* were included within this dataset. The SMIC dataset [37, 38] was established by the University of Oulu, Finland, using a similar induction mechanism to ensure the reliability of the data. The database contains 164 video sequences of 16 individuals (10 males and 6 females) containing 3 categories of microexpressions categories *(Positive, Surprised, Negative)*. SMIC contains three datasets SMIC (HS, VIS, and NIR). The SMIC (VIS) and SMIC (NIR) were recorded in the Visual Identity System (VIS) and Near Infrared (NIR) environments, respectively, using a camera with a frame rate of 25 FPS. The results were also recorded by HS using a 100 FPS high-speed camera, and the three will be used as separate datasets in this experiment. As shown above, the SMIC and CASMEII databases contain inconsistent microexpression categories. To face this problem, we selected and reannotated the categories in CASMEII. Specifically, firstly, the *Happy* sample is changed to *Positive*, the *Surprised* sample is kept unchanged, then the *Other* category is deleted, and finally the *Disgusted* and *Depressed* samples correspond to *Negative*. The details are shown in Table 1.

4.2. Experimental Setup. Regarding SMIC (VIS, HS, and NIR) and CASMEII, we designed 24 sets of cross-database microexpression experiments. Among them, no. 1–no. 6 and no. 13–no. 18 are treated as the first type of experiment, which is labeled as type-1, and no. 7–no. 12 and no. 19–no. 24 are treated as the second type of experiment, which is labeled as type-2. We use LBP-TOP [39] and HIGO-TOP [40] spatiotemporal descriptors for feature extraction. For the former, the neighborhood radius R and neighborhood point P are set to 1 and 8, respectively. HIGO-TOP has only one important parameter P, which is set to 8. Whether it is LBP-TOP or HIGO-TOP, the feature vector subsets of each plane are sequentially concatenated to form a supervector, that is, to form a microexpression facial feature vector.

As we can see from Table 1, the CASMEII and SMIC databases have extremely unbalanced samples for each category. Therefore, in addition to the weighted average recall (WAR), we also used unweighted average recall (UAR) [41] as the measurement criterion to compare the performance of various methods in the CDMER experiment. WAR is the rate of correctness. UAR is the average of the recognition rates calculated for each category of samples, regardless of the number of samples in each category. In summary, the combined WAR and UAR provide a fairer measure of the true performance of a method when the categories are unbalanced.

Table 1: Sample composition of the reconstituted CASMEII and SMIC databases.

	Database			
Category	CASMEII	SMIC (HS)	SMIC (NIR)	SMIC (VIS)
Positive	32	51	23	23
Surprise	25	43	20	20
Negative	91	70	28	28
Total	148	164	71	71

In order to show the performance of SLJDA, we choose other domain adaptation methods which have better performance in cross-database recognition to carry out comparative experiments. These methods include Support Vector Machine (SVM) [42], Domain Regeneration in the original Feature Space with unchanged Target domain (DRFS-T), Domain Regeneration in the original Label Space (DRLS), Target Sample Re-Generator (TSRG), SA, Joint Distribution Analysis (JDA), and Transfer Joint Matching (TJM). Parameter settings of all the above methods in the CDMER experiment are shown as follows:

(1) For SVM, set $C = 1$ (linear), and use it as a traditional method. The results of experiments conducted directly with SVM will be used as a baseline method for comparison.

(2) DRFS-T, DRLS, and TSRG involve two important parameters, that is, λ and μ. Following this work, we search for the best values of these two parameters in $\lambda \in [0.001, 0.01, 0.1, 1, 10, 100, 1000]$ and $\mu \in [0.001: 0.001: 0.009, 0.01: 0.01: 0.09, 0.1: 0.1: 1, 2: 10]$.

(3) We set $\lambda \in [0.1, 1, 10]$ according to the author's suggestion in [18], and JDA follows the original design of $\lambda \in [0.01, 0.1, 1, 10, 100]$. In addition, optimal dimensionality reduction dimension $d \in [10: 10: \max]$. For SA, we will traverse all possible dimensions d, that is, search $[1: 1: \max]$.

(4) Finally, with respect to SLJDA in this paper, we choose β from $[0.00005: 0.00001: 0.00009, 0.0001: 0.0001: 0.0009, 0.001: 0.001: 0.009, 0.01: 0.01: 0.09, 0.1: 0.1: 1, 2: 10]$, for $d \in [20: 10: \max]$.

4.3. Analysis of Experimental Results. Tables 2–5 show the results compared to the current better performing cross-database methods, and the bolded ones are the best performing methods in each group of experiments. Observing the table, we can find that the SLJDA method performs best in 8 out of 12 groups of experiments. In addition, we reperformed feature extraction with HIGO and compared it

Table 2: Type-1 experimental results of unsupervised CDMER based on LBP-TOP feature extraction (WAR).

No.	Task	SVM	DRLS	DRFS-T	TSRG	SLJDA
1	CASMEII-SMIC (HS)	44.51	54.27	43.90	45.73	**57.93**
2	CASMEII-SMIC (NIR)	62.16	**79.73**	70.95	68.92	54.73
3	CASMEII-SMIC (VIS)	35.21	54.93	32.39	40.85	**56.34**
4	SMIC (HS)-CASMEII	33.78	**63.51**	54.73	62.16	58.11
5	SMIC (NIR)-CASMEII	38.03	56.34	35.21	45.07	**73.24**
6	SMIC (VIS)-CASMEII	35.14	**70.95**	52.03	61.49	57.43

Table 3: Type-1 experimental results of unsupervised CDMER based on LBP-TOP feature extraction (UAR).

No.	Task	SVM	DRLS	DRFS-T	TSRG	SLJDA
1	CASMEII-SMIC (HS)	35.96	53.71	34.88	37.81	**55.46**
2	CASMEII-SMIC (NIR)	34.67	**73.46**	51.12	47.71	46.77
3	CASMEII-SMIC (VIS)	36.67	55.15	33.33	43.33	**56.30**
4	SMIC (HS)-CASMEII	40.32	**66.22**	55.86	35.05	54.11
5	SMIC (NIR)-CASMEII	40.00	36.67	58.94	48.33	**72.27**
6	SMIC (VIS)-CASMEII	49.94	54.70	49.16	33.33	67.85

Table 4: Type-2 experimental results of unsupervised CDMER based on LBP-TOP feature extraction (WAR).

No.	Task	SVM	DRLS	DRFS-T	TSRG	SLJDA
7	SMIC (HS)-SMIC (NIR)	61.97	73.24	**78.87**	73.24	64.79
8	SMIC (NIR)-SMIC (HS)	46.34	**60.98**	57.32	58.54	**60.98**
9	SMIC (HS)-SMIC (VIS)	76.06	88.73	78.87	81.69	**95.77**
10	SMIC (VIS)-SMIC (HS)	54.88	64.63	59.15	56.71	**65.85**
11	SMIC (NIR)-SMIC (VIS)	78.87	81.69	80.28	77.46	**85.92**
12	SMIC (VIS)-SMIC (NIR)	66.20	77.46	78.87	77.46	**81.69**

Table 5: Type-2 experimental results of unsupervised CDMER based on LBP-TOP feature extraction (UAR).

No.	Task	SVM	DRLS	DRFS-T	TSRG	SLJDA
7	SMIC (HS)-SMIC (NIR)	60.52	72.32	**78.34**	72.57	65.13
8	SMIC (NIR)-SMIC (HS)	58.02	62.85	58.02	59.87	**62.97**
9	SMIC (HS)-SMIC (VIS)	77.17	88.31	79.50	83.01	**95.21**
10	SMIC (VIS)-SMIC (HS)	59.15	**67.74**	60.47	60.41	66.73
11	SMIC (NIR)-SMIC (VIS)	77.86	82.23	79.53	77.15	**86.36**
12	SMIC (VIS)-SMIC (NIR)	65.24	76.06	78.29	75.63	**82.02**

with the currently popular domain adaptive methods. As shown in Tables 6 and 7, more than half of the experimental results show that this method has a clear advantage over other methods.

Observing the table, we can find that the experimental results of no. 7–no. 12 (type-2) and no. 19–no. 24 (type-2) are better than those of no. 1–no. 6 (type-1) and no. 13–no. 18 (type-1). The analysis may be due to the fact that the differences between CASMEII and SMIC samples are greater than differences between three datasets of SMIC. This is because the SMIC (HS), SMIC (VIS), and SMIC (NIR) only differ in the camera pixels taken between them. However, between CASMEII and SMIC, the filming equipment, recording environment, ethnicity of the subjects, and so on were different. It is worth noting that SMIC (VIS) experimental results are better than SMIC (NIR) experimental results under the same conditions, both as source and target domain datasets, for example, no. 3 and no. 5. Combining 4.1, we analyze that this may be due to the image quality difference problem.

Table 6: Type-1 experimental results of unsupervised CDMER based on HIGO-TOP feature extraction (WAR).

No.	Task	SA	JDA	TJM	SLJDA
13	CASMEII-SMIC (HS)	**61.95**	53.05	56.1	53.05
14	CASMEII-SMIC (NIR)	**66.89**	43.92	45.95	56.76
15	CASMEII-SMIC (VIS)	50.7	**57.75**	52.11	53.52
16	SMIC (HS)-CASMEII	48.65	45.95	45.27	**54.73**
17	SMIC (NIR)-CASMEII	57.75	59.15	61.97	**66.20**
18	SMIC (VIS)-CASMEII	49.32	46.62	47.3	**58.78**

Table 7: Type-2 experimental results of unsupervised CDMER based on HIGO-TOP feature extraction (WAR).

No.	Task	SA	JDA	TJM	SLJDA
19	SMIC (HS)-SMIC (NIR)	**73.24**	71.83	**73.24**	70.42
20	SMIC (NIR)-SMIC (HS)	59.15	60.98	49.39	**61.59**
21	SMIC (HS)-SMIC (VIS)	77.46	92.96	**94.37**	**94.37**
22	SMIC (VIS)-SMIC (HS)	58.54	60.37	59.76	**65.24**
23	SMIC (NIR)-SMIC (VIS)	84.51	74.65	76.06	**87.32**
24	SMIC (VIS)-SMIC (NIR)	74.65	**78.87**	77.46	77.46

In addition, an interesting phenomenon prevails in all the methods covered in this paper; when CASMEII and HS are used as target domains, the difference between WAR and UAR of the former is greater than that of the latter. For example, in Tables 2–5, the difference between WAR and UAR of no. 5 and no. 6 is significantly larger than the difference between no. 8 and no. 10. Looking at Table 1, it can be observed that the CASMEII dataset and the SMIC (HS) dataset are unbalanced in terms of microexpression categories, with the former having a majority of negative emotions (91/148). At the same time, the proportion of negative emotions in SMIC (HS) (70/164) is smaller than that of CASMEII. Analysis of this reason may be due to the imbalance of categories in the dataset. Further observation of both SMIC (NIR) and SMIC (VIS) databases showed consistent proportions of microexpression categories. When SMIC (NIR) or SMIC (VIS) is the target domains (no. 7 or no. 11), the difference between WAR and UAR is smaller than that between SMIC (HS) and CASMEII, which are also the target domains. This further proves that the category imbalance of microexpression database has a certain influence on MER.

5. Conclusion and Discussion

In this paper, we integrate data distribution methods with subspace learning methods from practical situations as a way to reduce the differences between source and target domains. That is, the SLJDA method is used to perform unsupervised cross-database microexpression recognition. Extensive experiments are conducted on CASMEII and SMIC databases, and the experimental results show that this method significantly outperforms other state-of-the-art domain adaptive methods for unsupervised CDMER tasks. However, there are still some issues to be investigated. As shown above, category imbalance in microexpression database is an important factor affecting the results of CDMER. Therefore, to improve the recognition results, we need to work on reducing the impact caused by the database category imbalance.

Data Availability

The data used to support this study are available from the corresponding author upon request.

Conflicts of Interest

The authors declare that they have no conflicts of interest.

Authors' Contributions

Y. Zhang and Y. Liu jointly designed the study. Y. Liu collected and analyzed the data. G. Li and H. Peng reviewed and edited the manuscript.

Acknowledgments

This work was supported by the Key Research Project of Henan Higher Education Institution (Project no. 17B440001), Henan University of Science and Technology Enterprise Commissioning Project (JG017), and Henan Provincial Science and Technology Tackling Program Grant Project 212102210504.

References

[1] P. Ekman, *Telling Lies: Clues to Deceit in the Marketplace, Politics, and Marriage*, WW Norton & Company, New York, NY, USA, 2009.

[2] P. Ekman, "Darwin, deception, and facial expression," *Annals of the New York Academy of Sciences*, vol. 1000, no. 1, pp. 205–221, 2003.

[3] J. M. Gottman and R. W. Levenson, "A two-factor model for predicting when a couple will divorce: exploratory analyses using 14-year longitudinal data," *Family Process*, vol. 41, no. 1, pp. 83–96, 2002.

[4] J. Whitehill, Z. Serpell, Y.-C. Lin, A. Foster, and J. R. Movellan, "The faces of engagement: automatic recognition of student engagementfrom facial expressions," *IEEE Transactions on Affective Computing*, vol. 5, no. 1, pp. 86–98, 2014.

[5] L. Dacre Pool and P. Qualter, "Improving emotional intelligence and emotional self-efficacy through a teaching intervention for university students," *Learning and Individual Differences*, vol. 22, no. 3, pp. 306–312, 2012.

[6] X. Li, J. Li, Y. Liu, Z. Ding, and A. Nallanathan, "Residual transceiver hardware impairments on cooperative NOMA networks," *IEEE Transactions on Wireless Communications*, vol. 19, no. 1, pp. 680–695, 2020.

[7] X. Li, M. Zhao, M. Zeng et al., "Hardware impaired ambient backscatter NOMA system: reliability and security," *IEEE Transactions on Communications*, vol. 69, no. 4, pp. 2723–2736, 2021.

[8] X. Li, M. Zhao, Y. Liu, L. Li, Z. Ding, and A. Nallanathan, "Secrecy analysis of ambient backscatter NOMA systems under I/Q imbalance," *IEEE Transactions on Vehicular Technology*, vol. 69, no. 10, pp. 12286–12290, 2020.

[9] X. Li, Q. Wang, M. Liu et al., "Cooperative wireless-powered NOMA relaying for B5G IoT networks with hardware impairments and channel estimation errors," *IEEE Internet of Things Journal*, vol. 8, no. 7, pp. 5453–5467, 2020.

[10] K. Yan, W. Zheng, Z. Cui, and Y. Zong, "Cross-database facial expression recognition via unsupervised domain adaptive dictionary learning," *International Conference on Neural Information Processing*, Springer, vol. 9948, pp. 427–434, Berlin, Germany, 2016.

[11] S. J. Pan and Q. Yang, "A survey on transfer learning," *IEEE Transactions on Knowledge and Data Engineering*, vol. 22, no. 10, pp. 1345–1359, 2010.

[12] Y. Zong, W. Zheng, X. Huang, J. Shi, Z. Cui, and G. Zhao, "Domain regeneration for cross-database micro-expression recognition," *IEEE Transactions on Image Processing*, vol. 27, no. 5, pp. 2484–2498, 2018.

[13] S. J. Pan, I. W. Tsang, J. T. Kwok, and Q. Yang, "Domain adaptation via transfer component analysis," *IEEE Transactions on Neural Networks*, vol. 22, no. 2, pp. 199–210, 2011.

[14] J. Wang, Y. Chen, L. Hu, X. Peng, and P. S. Yu, "Stratified transfer learning for cross-domain activity recognition," in *Proceedings of the IEEE International Conference on Pervasive Computing and Communications*, pp. 1–10, Athens, Greece, March 2018.

[15] K. Saito, Y. Ushiku, and T. Harada, "Asymmetric tri-training for unsupervised domain adaptation," in *Proceedings of the 34th International Conference on Machine Learning*, pp. 2988–2997, Sydney, Australia, February 2017.

[16] M. Long, J. Wang, G. Ding, J. Sun, and P. S. Yu, "Transfer feature learning with joint distribution adaptation," in *Proceedings of the IEEE International Conference on Computer Vision*, pp. 2200–2207, Sydney, Australia, December 2013.

[17] J. Wang, Y. Chen, S. Hao, W. Feng, and Z. Shen, "Balanced distribution adaptation for transfer learning," in *Proceedings of the IEEE International Conference on Data Mining*, pp. 1129–1134, New Orleans, LA, USA, November 2017.

[18] M. Long, J. Wang, G. Ding, J. Sun, and P. S. Yu, "Transfer joint matching for unsupervised domain adaptation," in *Proceedings of the IEEE Conference on Computer Vision and Pattern Recognition*, pp. 1410–1417, Columbus, OH, USA, June 2014.

[19] J. Blitzer, R. McDonald, and F. Pereira, "Domain adaptation with structural correspondence learning," in *Proceedings of the 2006 Conference on Empirical Methods in Natural Language Processing*, pp. 120–128, Sydney, Australia, July 2006.

[20] B. Fernando, A. Habrard, M. Sebban, and T. Tuytelaars, "Unsupervised visual domain adaptation using subspace alignment," in *Proceedings of the IEEE International Conference on Computer Vision*, pp. 2960–2967, Sydney, NSW, Australia, December 2013.

[21] B. Sun and K. Saenko, "Deep coral: correlation alignment for deep domain adaptation," *European Conference on Computer Vision*, Springer, Berlin, Germany, pp. 443–450, 2016.

[22] B. Sun and K. Saenko, "Subspace distribution alignment for unsupervised domain adaptation," in *Proceedings of the British Machine Vision Conference 2015*, vol. 4, pp. 24–31, Lowell, MA, USA, September 2015.

[23] B. Gong, Y. Shi, F. Sha, and K. Grauman, "Geodesic flow kernel for unsupervised domain adaptation," in *Proceedings of the IEEE Conference on Computer Vision and Pattern Recognition*, pp. 2066–2073, Providence, RI, USA, June 2012.

[24] L. Li, X. Zhou, Y. Zong et al., "Unsupervised cross-database micro-expression recognition using target-adapted least-squares regression," *IEICE Transactions on Information and Systems*, vol. E102.D, no. 7, pp. 1417–1421, 2019.

[25] R. Zhu, T. Zhang, Q. Zhao, and Z. Wu, "A transfer learning approach to cross-database facial expression recognition," in *Proceedings of the International Conference on Biometrics*, pp. 293–298, Phuket, Thailand, May 2015.

[26] W. Zheng and X. Zhou, "Cross-domain color facial expression recognition using transductive transfer subspace learning," *IEEE Transactions on Affective Computing*, vol. 9, no. 1, pp. 21–37, 2016.

[27] W. S. Chu, F. De La Torre, and J. F. Cohn, "Selective transfer machine for personalized facial action unit detection," in *Proceedings of the IEEE Conference on Computer Vision and Recognition*, pp. 3515–3522, Portland, OR, USA, June 2013.

[28] W.-S. Chu, F. De La Torre, and J. F. Cohn, "Selective transfer machine for personalized facial expression analysis," *IEEE Transactions on Pattern Analysis and Machine Intelligence*, vol. 39, no. 3, pp. 529–545, 2017.

[29] N. Liu, Y. Zong, B. Zhang et al., "Unsupervised cross-corpus speech emotion recognition using domain-adaptive subspace learning," in *Proceedings of the IEEE International Conference on Acoustics, Speech and Signal Processing*, pp. 5144–5148, Calgary, Canada, April 2018.

[30] A. Hassan, R. Damper, and M. Niranjan, "On acoustic emotion recognition: compensating for covariate shift," *IEEE Transactions on Audio, Speech, and Language Processing*, vol. 21, no. 7, pp. 1458–1468, 2013.

[31] J. Huang, A. J. Smola, A. Gretton, K. M. Borgwardt, and B. Scholkopf, "Correcting sample selection bias by unlabeled data," in *Advances in Neural Information Processing Systems*, pp. 601–608, MIT Press, Cambridge, MA, USA, 2007.

[32] M. Sugiyama, T. Suzuki, S. Nakajima et al., "Direct importance estimation with model selection and its application to covariate shift adaptation," *Advances in Neural Information Processing Systems*, vol. 20, pp. 1433–1440, 2007.

[33] T. Kanamori, S. Hido, and M. Sugiyama, "A least-squares approach to direct importance estimation," *Journal of Machine Learning Research*, vol. 10, no. 48, pp. 1391–1445, 2009.

[34] Y. Zong, W. Zheng, T. Zhang, and X. Huang, "Cross-corpus speech emotion recognition based on domain-adaptive least-squares regression," *IEEE Signal Processing Letters*, vol. 23, no. 5, pp. 585–589, 2016.

[35] J. Zhang, W. Li, and P. Ogunbona, "Joint geometrical and statistical alignment for visual domain adaptation," in *Proceedings of the IEEE Conference on Computer Vision and Pattern Recognition*, pp. 5150–5158, Honolulu, HI, USA, May 2017.

[36] W. J. Yan, Q. Wu, Y. J. Liu, S.-J. Wang, and X. Fu, "CASME database: a dataset of spontaneous micro-expressions collected from neutralized faces," in *Proceedings of the IEEE International Conference and Workshops on Automatic Face and Gesture Recognition*, pp. 1–7, Shanghai, China, April 2013.

[37] X. Li, T. Pfister, X. Huang, G. Zhao, and M. Pietikäinen, "A spontaneous micro-expression database: inducement, collection and baseline," in *Proceedings of the IEEE International Conference and Workshops on Automatic Face and Gesture Recognition*, pp. 1–6, Shanghai, China, April 2013.

[38] T. Pfister, X. Li, G. Zhao, and M. Pietikäinen, "Recognising spontaneous facial micro-expressions," in *Proceedings of the International Conference on Computer Vision*, pp. 1449–1456, Barcelona, Spain, November 2011.

[39] G. Zhao and M. Pietikainen, "Dynamic texture recognition using local binary patterns with an application to facial expressions," *IEEE Transactions on Pattern Analysis and Machine Intelligence*, vol. 29, no. 6, pp. 915–928, 2007.

[40] N. Dalal and B. Triggs, "Histograms of oriented gradients for human detection," in *Proceedings of the IEEE Computer Society Conference on Computer Vision and Pattern Recognition*, vol. 1, pp. 886–893, San Diego, CA, USA, June 2005.

[41] B. Schuller, B. Vlasenko, F. Eyben et al., "Cross-corpus acoustic emotion recognition: variances and strategies," *IEEE Transactions on Affective Computing*, vol. 1, no. 2, pp. 119–131, 2011.

[42] J. A. K. Suykens and J. Vandewalle, "Least squares support vector machine classifiers," *Neural Processing Letters*, vol. 9, no. 3, pp. 293–300, 1999.

Hindawi
Mobile Information Systems
Volume 2021, Article ID 2006082, 10 pages
https://doi.org/10.1155/2021/2006082

Research Article

A Cross-Border E-Commerce Approach Based on Blockchain Technology

Zhao Hongmei

Hunan Sany Polytechnic College, Hunan, Changsha 412006, China

Correspondence should be addressed to Zhao Hongmei; t20071490@csuft.edu.cn

Received 23 June 2021; Accepted 6 July 2021; Published 16 July 2021

Academic Editor: Muhammad Usman

Copyright © 2021 Zhao Hongmei. This is an open access article distributed under the Creative Commons Attribution License, which permits unrestricted use, distribution, and reproduction in any medium, provided the original work is properly cited.

In the current cross-border electronic commerce (e-commerce) system, various document recording and authorization processes are cumbersome, record sharing efficiency is low, and identity verification is difficult. A method of asymmetric encryption technology combining Blockchain technology and cryptography is proposed. The advantages of asymmetric encrypted communications include high security and ease of multiparties communication collaboration, being applied to a peer-to-peer network formed by Blockchain technology, and making cross-border e-commerce record cross-domain sharing traceable, data immutable, and identity verification simplified. First of all, based on the immutable modification of Blockchain technology and asymmetric encryption technology, file synchronization contracts and authorization contracts are designed. Its distributed storage advantages ensure the privacy of users' cross-border e-commerce information. Second, the design of the cross-domain acquisition contract can effectively verify the identity and transmission efficiency of both parties to the data sharing, so that illegal users can be safely filtered without a third-party notary institution. The simulation experiment results show that the solution proposed in this paper has obvious advantages in data antitheft, multiparty authentication, and saving system overhead compared with traditional cloud computing methods to solve the problem of sharing medical records. It provides a reference for solving the security problems in the process of data sharing by using the advantages of Blockchain's decentralization and auditability and provides reference ideas for solving the problems of data sharing and cross-domain authentication.

1. Introduction

In recent years, with the rapid development of China's local e-commerce and the continuous improvement of its business model, it has not only stepped into the forefront of the world but also brought unprecedented opportunities for the development of China's cross-border e-commerce. Therefore, it is imperative to build a balanced and sustainable cross-border e-commerce system. But at present, the traditional e-commerce model, especially the centralized e-commerce model, cannot meet the sustainable development of cross-border e-commerce. Especially in the aspects of traceability, collaboration, payment, and contract, they are facing great challenges. At the same time, the emergence of digital currency represented by bitcoin, especially the underlying technology bitcoin relies on Blockchain technology, has aroused widespread concern in academic circles. In 2016, Blockchain technology has developed rapidly in the world, so it is also known as the first year of Blockchain application. Blockchain technology is considered to be another subversive technological innovation after Internet technology, and it is also permeating into cross-border e-commerce, network financial services, the Internet of things, and other fields. Its rapid development momentum is expected to lead the transformation of the Internet economy mode from application-driven innovation mode to technology-driven innovation mode. One belt, one road, and the other cross-border electric business, which are advocated by China, will also provide new directions for the development of cross-border electricity providers.

Cross-border e-commerce is a kind of business activity, which takes the transactions belonging to different customs as the main body and makes the two sides reach a certain agreement through the e-commerce platform, to carry out

payment and settlement and transport goods across the border, to complete the transaction. In recent years, as the growth rate of the global economy and trade gradually tends to be flat, the circulation of goods is slow. To solve this problem, we should constantly accelerate the circulation of goods, open up overseas markets, and improve the growth rate of the economy and trade. More and more enterprises to shorten the distance with foreign consumers accelerate commodity sales. In this economic environment, cross-border e-commerce should be shipped out; now cross-border e-commerce is still developing rapidly, gradually affecting the world's economic trend. The emergence of cross-border e-commerce greatly reduces the transaction cost between e-commerce enterprises and foreign customers, simplifies the transaction process, directly and effectively speeds up the capital turnover, and provides an efficient cross-border trade channel for the world.

In the process of cross-border transactions, the credit rating of cross-border e-commerce enterprises is different due to the differences in economy, culture, and system between different countries. At present, there is no open enterprise credit sharing platform between countries, which makes it difficult for enterprises of different countries to evaluate each other's credit effectively in the process of cross-border transactions, which makes it difficult for enterprises of both sides of the transaction to trust each other, so that enterprises have adverse selection consequences, and then affect the overall development of cross-border e-commerce.

It has realized the traceability function of logistics, but it is not satisfactory in cross-border e-commerce logistics. The driving force of cross-border trade is to export products with comparative advantages to other countries. For example, oil in the Middle East, machinery products in Europe, food in Central America, and manufacturing in Asia all have their comparative advantages. However, the asymmetric information of the importing and exporting countries often leads to adverse selection in the transaction of such products. Even more, some domestic illegal businesses turn domestic fake and shoddy goods into imported goods by counterfeiting logistics information. These not only damage the fundamental interests of consumers but also harm the development of cross-border e-commerce and even lead to international disputes.

Due to the geographical location of cross-border e-commerce and the differences in foreign exchange control policies of different countries, the current cross-border payment means generally cannot achieve real-time arrival, and the rapid change of exchange rate increases the risk of exchange rate fluctuation caused by the enterprise's foreign exchange exposure in the payment process to a certain extent. Besides, today's cross-border e-commerce transactions are generally conducted through the cross-border e-commerce platform and all transaction data is also stored on the virtual platform. Therefore, the security risks in the payment process cannot be completely avoided. Under the current cross-border e-commerce system, the cross-border payment platform cannot effectively restrict the cross-border e-commerce platform. At the same time, the inconsistency of financial policies and regulations in the world also makes it difficult to effectively supervise cross-border payment. This lack of supervision needs the mode of enterprise self-discipline, which objectively increases the credit risk and transaction cost of enterprises in the transaction process.

Because cross-border e-commerce is the trade between countries behind individual and enterprise transactions, the complexity of cross-border e-commerce is much higher than that of domestic e-commerce. Due to the need for the participation of customs, inspection and quarantine, logistics, and other subjects, it also needs to spend a lot of manpower and material costs in the aspects of the review, reconciliation, customs clearance, and so forth. Therefore, enterprises engaged in cross-border e-commerce not only need to deal with cross-border logistics, exchange rate, and other uncertain factors but also need to get through many links, thus pushing up the economic cost and time cost.

The rest of this paper is organized as follows. In Section 2, related work is presented followed by the system model and proposed work in Section 3. In Section 4, performance analysis is presented followed by experimental evaluation in Section 5. Finally, the paper is concluded in Section 6.

2. Related Work

Satoshi Nakamoto introduced a fully decentralized digital currency exchange system based on distributed systems and cryptography in 2008 [1]. This is the first time Blockchain technology has been used. Blockchain demonstrated the ability to execute peer-to-peer digital currency payments in an untrustworthy setting. In [2], the author launched the Ethereum plan, which enables people to create transactions to fulfill any system transfer function and automate processes by constructing a Blockchain framework in Turing's full language. In [3, 4], Melanie Swan first released the block exchange innovation trading platform, which was a significant landmark in the modern financial market's decentralization development. The British government published a report on Blockchain in [5]. "Distributed Ledger Technology: Beyond Block Chain" is a research study that advocates the use of Blockchain for financial and government affairs. The People's Bank of China held a digital currency workshop to look into the possibility of using Blockchain technology to offer digital currency in order to increase the quality, convenience, and transparency of the financial transactions. In [6], the authors explain the Blockchain in terms of data design, encryption properties, and network structure. The blockchain is cryptographically promised, and it is not changeable and emissions reductions decentralized ledger, a data structure composed of a relational database, and a data structure composed of a relational database. In [7], the authors developed Blockchain research from 2014 to 2018, claiming that Blockchain work is still in its infancy in terms of theoretical context, methodological heterogeneity, and empirically based study. According to the authors in [8], Blockchain innovations have the ability to address economic inequality by overcoming the 4 times more likely of geographical exposure, high costs, inadequate banking goods, and economic ignorance. The authors in [9] presented multiple research studies and discussed the effect of

Blockchain on supply chain management. Reference [10] showed early signs of Blockchain being used in supply chain operations to improve liability and clearness. This investigation shows how Blockchain can help supply chain managers achieve their goals through a range of techniques. The Blockchain is used to solve the quality control issue in the agriculture supply chain in [11]. In [12], the authors addressed the market continuity equation of the supply chain quality control issue. The authors in [13] looked into the actions of individual consumers when it came to the use of Blockchain in the supply chain. Life span of results, social impact, enabling conditions, openness, and confidence have all been shown to have varying levels of control on users' actions intentions against Blockchain. The authors in [14] gathered empirical evidence and concluded that intense competition, sophistication, expense, and comparative have major effects on Blockchain adoption. The rest of the work is organized as follows: in Section 3, the proposed model for cross-border e-commerce approach based on Blockchain technology is explained; in Section 4, performance evaluation is discussed; in Section 5, the experimental work is explained; and in Section 6, the conclusion is explained.

3. System Model

The block diagram of our proposed cross-border e-commerce approach based on Blockchain technology is presented in Figure 1, wherein the users first register themselves in a hospital of a particular country. After users' (patient and doctor) registration, they verify themselves by requesting to EHRs manager; else, a penalty is generated on this specific ID. Following effective authentication, the approved user can now upload/download healthcare data, which can then be stored on the Blockchain after concerned patient and practitioner approval. This approved data become a transaction and store in the Interplanetary File System (IPFS) by calculating the desired hash; this IPFS is a distributed storage mostly used in Blockchain technology. After storage, the block is stored in the transaction pool which consists of two types of transaction, that is, the transactions received from the Blockchain and the transaction that need to be store on the Blockchain. After successful mining, the block is added to the Blockchain network by the approval of the Policy List, that is, checking the rules/regulations for different countries in order to interact with the Blockchain [15–20].

The block structure of the proposed system is presented in Figure 2; it includes Hash of previous block, Nonce, Time Stamp, Version, and Markel Root (consists of hash of the transactions); the block calculates its own hash, which can be given to other blocks as its previous block hash.

3.1. Application Scenarios. Traditional cross-border e-commerce record solutions are limited by the efficiency of each platform in terms of storage and real-time viewing of transaction records. For cross-border e-commerce merchants, this will be a great time overhead. In addition, once a platform loses this transaction record, it cannot provide a complete record in the subsequent e-commerce transaction process, so that it may not be able to provide a credible record in cross-border aspects. Due to the increasing development of the current network, the evaluation of e-commerce transactions requires multiple inspections, and sometimes even more than 10 items are inspected. Effective and complete preservation of these transaction records is essential. For cross-border e-commerce transaction records, the transaction records often store the private information of the transaction personnel. Our work is how to ensure that the transaction information stored in the database is not obtained by criminals. To solve the above problems, this solution addresses the four core issues currently in the field of transaction records: (1) how to store e-commerce transaction records safely and effectively, (2) how to upload transaction records in real time, (3) how to set access control to filter illegal persons, and (4) how to conveniently download transaction records across domains. Design three Ethereum smart contracts based on Ethereum: file synchronization contract, authorization contract, and cross-domain acquisition contract.

3.2. Smart Contract Algorithm. This algorithm can be explained in the following sections.

3.2.1. File Synchronization Contract. To ensure the files uploaded to RSME are safe, we use an asymmetric encryption algorithm to encrypt the user in the encryption layer. In the platform of this scheme, we use three encryption algorithms to save the digital password: hash algorithm, ECC algorithm, and transaction record algorithm. The hash algorithm SHA-256 encrypts the user ID, ECC encrypts the public-private key pair, and the transaction record algorithm is responsible for recording the intermediate events in the folder FOLDAADDRESS [21–24]. We use the IPNs protocol to hash and encrypt the folder. The early worker information is represented by the following:

$$\begin{aligned}&\text{merchants}\{\text{ID}(\text{Identity}), \text{PK}(\text{Public}-\text{key}),\\ &\quad \text{SK}(\text{Private}-\text{key}), \text{Folder}-\text{Address}, \text{Permission}\}.\end{aligned} \tag{1}$$

The user's unique ID is used to uniquely identify the e-commerce identity after SHA-256 hash algorithm was used to encrypt the data. The ECC algorithm encrypts the SK (private key) pair, PK (public key) is used to encrypt the transaction of the e-commerce, and a single file ID, that is, HashID, is gained after encryption. It can be expressed by the following formula [25–29]:

$$\begin{aligned}&\text{SHA}-256(\text{PK}(\text{Public Key}), \text{EMR})\\ &\quad = \text{HashID}(\text{Hash value of ID}).\end{aligned} \tag{2}$$

The encryption and synchronization procedures can be seen in Figure 3.

The e-commerce company itself holds a public key and private key pairs, i.e., PK and SK. Afterwards, the platform transaction is finalized and the PK is assigned to platform A. The platform uses formula (2) to encrypt the e-commerce transaction record file to gain the desired encrypted file, i.e.,

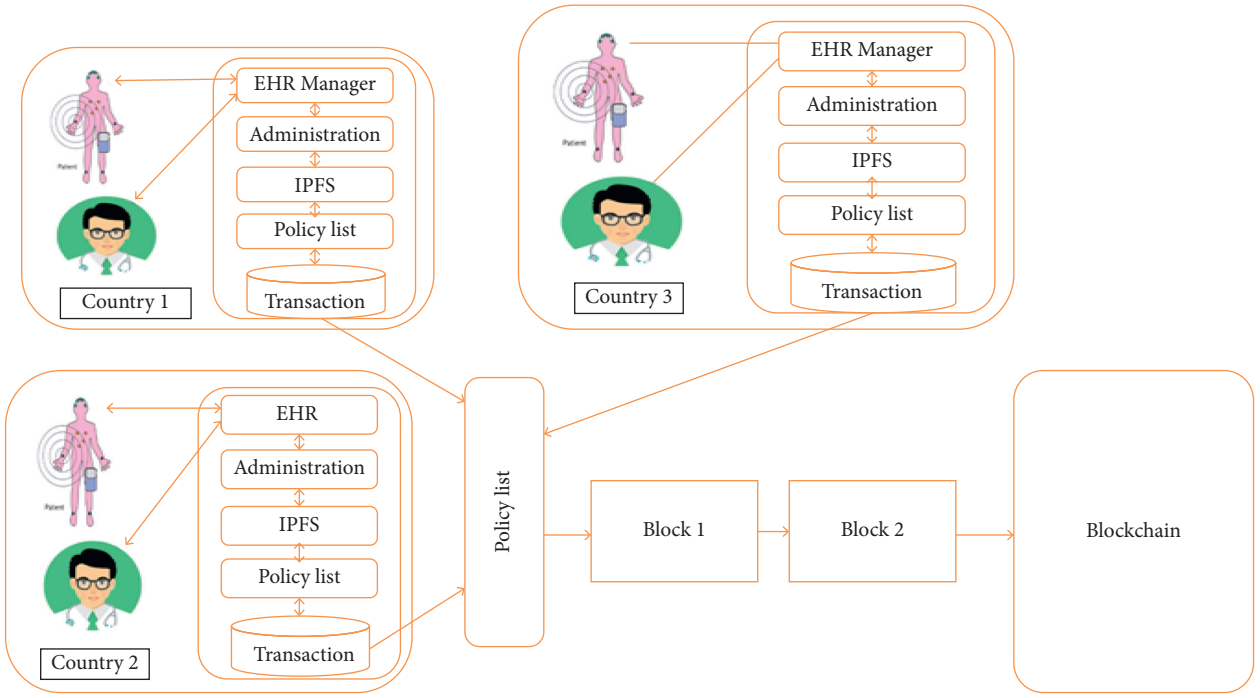

Figure 1: Network model of the proposed cross-border e-commerce approach based on Blockchain technology.

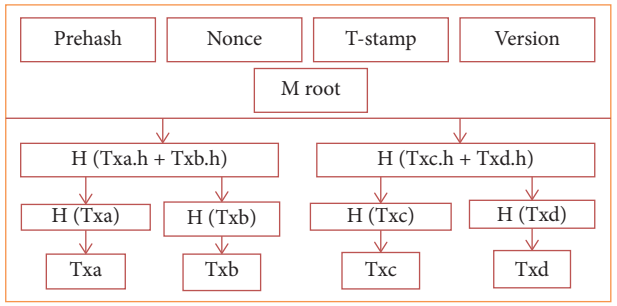

Figure 2: Block structure of the proposed cross-border e-commerce approach based on Blockchain technology.

SecFile, and its record file is kept in the file address of the transaction record folder for uploading to the IPFS service [30–36].

The user's authentication protocol is explained in Algorithm 1. First, the smart device (SD) encodes the requested user ID using the EHR Manager's public key and assigns it to an encrypted message, which is then transmit to the EHR Manager to decrypt it using the EHR Manager's private key. The ID is then sent to the Admin Unit, where it can be reviewed under Policy in the Policy List; if it appears there, authentication is successful; else, a penalty is applied to this ID, which will serve as a message of warning to the recipient in our scheme.

The proposed system's algorithm (Algorithm 2) describes how to add a fresh block to the Blockchain. To begin, a list of possible miners is given by the miner, who is bound by the Policy List's clear limit. The block header is then computed. The targeted hash along with nonce is determined if the target becomes accurate. If the chosen miner is validated and all of the situations are met, the block is implemented; else, the block is rejected.

The entire encryption process is given in Algorithm 3.

3.2.2. License Agreement. In this section, we mainly describe the file transfer process, which is mainly described by the automatically executed intelligent contract file and transmits the Blockchain in the Ethernet. This process is as follows.

First, the layer encrypted by the hash algorithm is to output the unique file ID and encryption security file securityfile. Secondly, when the intelligent contract receives the encrypted ciphertext file securityfile, these files will be automatically transferred to the private protocol network, and before the file is uploaded, the private protocol will automatically check if these files are copied, so the purpose is to save bandwidth. When all difficulties are successful, we have a unique file ID through formula (3), but these records usually include the following types [37, 38]:

$$\text{SHA 256}\{\text{PK}, \text{RecordFile}\ (\text{Pic1}\&\text{Picn}, \text{Video1}\&\text{Videon}, \text{Text1}\&\text{Textn})\} = \text{HashID1}. \tag{3}$$

A folder value of hash obtained by encryption comprises many files, which are represented by the following symbols in this article:

(i) $\text{Pic}_{11},\ldots,\text{Pic}_{1n}$

(ii) $\text{Video}_{11},\ldots,\text{Video}_{1n}$

(iii) $\text{Text}_{11},\ldots,\text{Text}_{1n}$

In the process of transaction, if a company has transaction records on multiple platforms, then, in these private

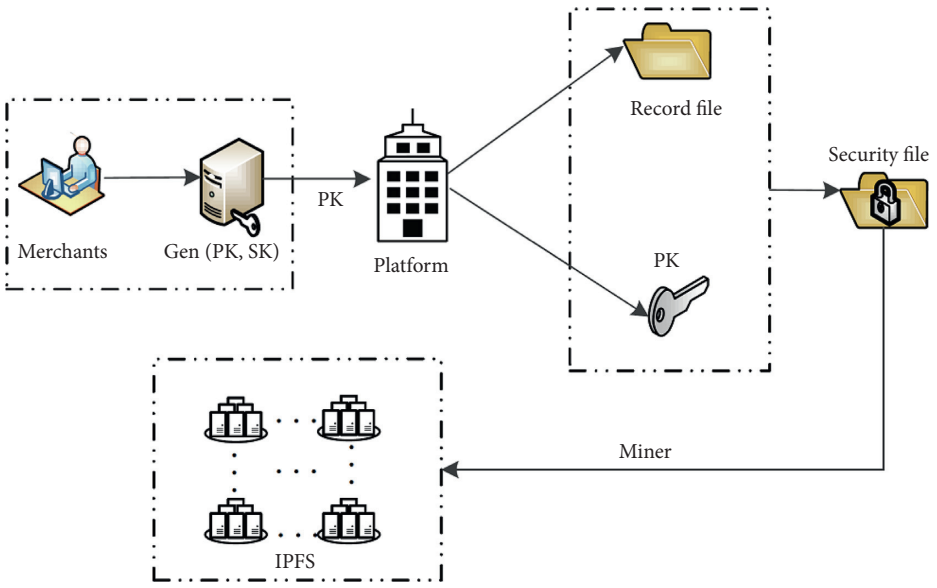

Figure 3: File synchronization process.

Input: identity of *j*-th users.
Output: result
(1) Start authentication for *j*-th users
(2) EncrypMi ⟵ Encrypt (PKEHRi, u*j*)
(3) EHR Manager receives encrypted message which is EncryptMi
(4) decrypEHRi ⟵ dec (SKEHRi, EncryptMi)
(The message is decrypted by EHR manager with its SK)
EHR Manager sends user u*j* to Administration Unit
(5) if policy list (u*j*) == correct then
(6) Result ⟵ ("authentication successful")
(7) Acknowledged user
(8) Else
(9) Result ⟵ penalty (u*j*, action)
(10) End if
Return "Result"

Algorithm 1: User authentication.

Input: Hash of the previous block (PBH), randomly generated list of miners (i.e., Mi).
Output: {Reception of the block}
(1) Arrive M [*i*] from miners that are available
Selected_Miner [*j*] ⟵ M [*i*]
(2) If Selected_Miner [*j*] == true then
(3) Build-up MarkelTree(MT)
(4) BlockHeader ⟵ (T_stamp||MR||V||PBH) (Designed Header of Block)
(5) Compute nonce for the block
(6) BlockHash ⟵ (T_stamp||MR||V||PBH||nonce)
(7) If Miner [*j*] == verified and sig == true and Hash of Block == target-Hash, nonce = correct and Time stamp(TS) == correct then
(8) Result ⟵ Block Accepted
(9) Else
(10) Result Block not Accepted
(11) End if
(12) Return: Result
(13) End if

Algorithm 2: Acceptance of block to add in the Blockchain network.

```
(1) Input: public key (PK) and file of record (RecordFile)
(2) Output: SecFile
(3) begin
(4) while(The user uses the RSMR system for the 1st time)
(5) if(e-commerce meets the circumstances of use)
(6) {Generate structured data for e-commerce:
(7) Patient{ID, PK, SK, address of folder (FolderAddress)}}
(8) if(GenerateFoldAddress = = Success and Get transaction log file)
(9) {Use the formula SHA256(PK,EHR) = HashID to encrypt SecFile}
(10) return SecFile;
(11) if(hash of SecurityFile value repeatability check approved)
(12) {Upload SecFile to the IPFS and the copy will be synchronized in different network locations on the private network at the same
     time}
(13) else
(14) {The file has been uploaded, no need to upload repeatedly, saving bandwidth}
(15) end
```

Algorithm 3: File synchronization contract (execution process).

network protocols, we can use the same pair of keys to correspond to different folders. In this paper, we use $EC_A(HashID_1,\ldots,HashID_A)$ to represent the transaction files of different platforms corresponding to the same company.

In the private protocol, we divide the verified and uploaded files into sequences ($sequence_1,\ldots,sequence_n$); in this way, even if the host is shut down or unexpected errors occur, transactions on other platforms will not be affected because we have stored a copy of the file, as shown in Figure 4.

4. Performance Evaluations

The performance evaluation of the proposed scheme can be explained as follows.

4.1. Solution Deployment. In the experiment process of this program, five third-generation B-type Raspberry Pis (ARMCortex-A53 1.2 GHz, 1G RAM, Ubuntu OS) are used as hardware carriers to simulate the functions of nodes A, B, C, D, and E, and the software program uses the protocol described earlier in this article which is distributed on every hardware carrier. In order to solve the Byzantine problem in the topology, the node management tool IPFS-Cluster is selected for the simulation experiment part of this article, which is divided into the server side and the management side. On the transaction server, the control terminal is typically installed. The aim of this paper is to install the control terminal on point A so that it can handle files and perform the same activities on multiple nodes, such as uploading, upgrading, and file transfer. To execute file transfers, mount the server on B, C, D, and E equipment.

Node object: all participating objects of the trading organization, including platform computers, computers at home for transactions, or a personal PC where transaction records are e-commerce. Model nodes: five nodes, nodes A, B, C, D, and E.

Node A: the computer where the platform wants to synchronize transaction record information

Node B: the computer where the e-commerce company wants to keep personal transaction records

Node C: personal computers of relatives and neighbors related to e-commerce

Nodes D and E: virtual machine image on the platform server

For the smart contract part, this solution uses Remix-IDE as the Ethernet smart contract development tool, written in Solidity language and deployed on the Ropsten Test Network and the Ethernet test network.

4.2. Experimental Process. In this paper, we design the following experiments.

4.2.1. Design Key and Synchronize Key. We share all nodes to a public key. If we generate a public key on node a, the smart contract will automatically synchronize to other nodes after execution, which will not affect the node's decryption of the encrypted file, because only the first key generated by point A (node) can decrypt the EMR file.

4.2.2. Start Up the Node. In this paper, we use the cluster management method to take node A as the starting node. Of course, you can also use other nodes as boot nodes. Its main task is to be responsible for and perform tasks, including public key encryption and uploading files in private protocol and synchronization, so as to form a Blockchain system. The rest of the nodes are copied from the boot node. After the startup, we assign a unique hash ID (qmbxy g9bp), which we use as the single ID of the address of the computer and connect to the 04 host addresses of the other nodes.

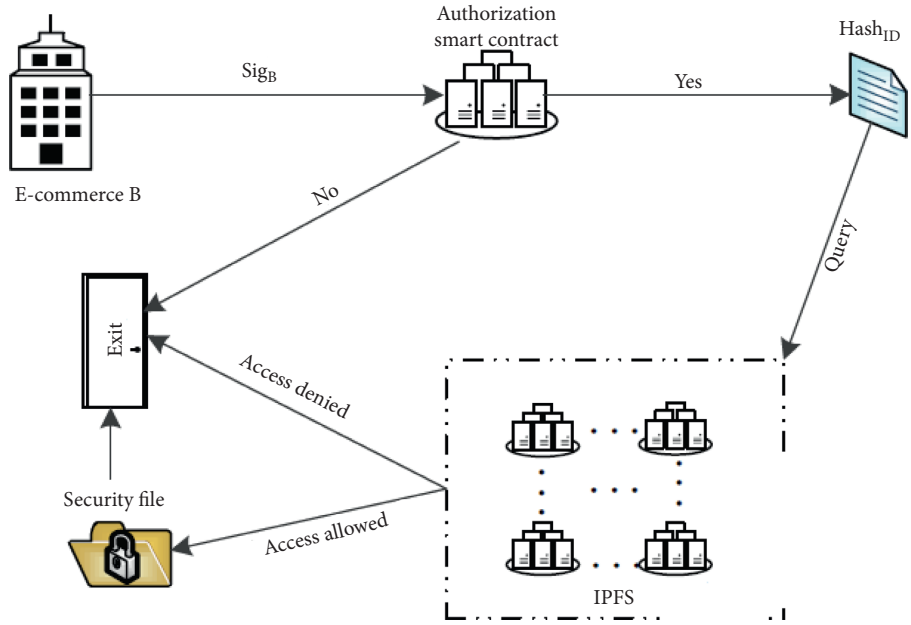

Figure 4: Authorization process.

Table 1: Contrast of the features of our scheme with existing schemes.

S. no.	Feature	[15]	[16]	[17]	[18]	[19]	Proposed system
1.	Scalability of the system	Yes	No	Yes	Yes	No	Yes
2.	Authentication of users	No	No	Yes	No	No	Yes
3.	Integrity of the system	No	Yes	Yes	No	Yes	Yes
4.	Confidentiality of records	No	Yes	Yes	No	Yes	Yes
5.	Access control mechanism	Yes	Yes	Yes	Yes	Yes	Yes
6.	File synchronization	No	No	No	No	No	Yes
7.	Document traceability	No	No	No	No	No	Yes

4.2.3. Upload Files. In Figure 3, we upload the file obtained by using the encryption algorithm. This file only has a unique hash address and upload time. This address is the only address for this article. All identifications are based on this address. Digitize the sequence mentioned above and get an encrypted file.

4.2.4. Transaction Confirmation. When node A uploads to the private protocol network, it can obtain the hash value and time stamp, so that, among all nodes, we only know the upload time and other information, but we cannot see other information in this network. According to the working mechanism of Ethernet, we can also synchronize to the remaining private nodes.

4.2.5. Document Traceability. In the model scenario of this paper, if cross-border business occurs, if e-commerce wants to obtain the files of e-commerce A on the domestic platform, it must obtain the license of the domestic e-commerce platform before downloading and provide the key file. The update of the downloaded transaction information is through the file directory under the management terminal. According to the characteristics of the Blockchain, the file downloads need to synchronize the information of other nodes, so as to realize the file traceability. As shown in Figure 3, when the user enters a hash value, the e-commerce can download the EMR file locally, trigger the algorithm in the smart contract, and then use the private key to decrypt the source file.

The contrast of different features of our proposed scheme with the present schemes is shown in Table 1. From Table 1, it is clear that our proposed system has all the features which the existing schemes have and also has additional features like file synchronization, document traceability, and authentication.

5. Experiment Analyses

The intelligent contract part: this program uses Remix-IDE as an Ether Fang Intelligent Contract Development Tool, written in Solidity language, and deploys running on the Etheriquat test network Ropsten Test Network. Experimental hardware and software are shown in Table 2.

Generally speaking, the size of a file is in the range of 1~5 M. In this solution, the upload and download of a file is less than 100 ms. However, in actual application scenarios, an e-commerce platform may usually access hundreds or

Table 2: Hardware and software parameters.

Software/hardware	Versions
Rospberry Pi	3B
CPU	Broadcom CortexA53@1.4GHz
RAM	1GB LPDDR2
Operation system	Ubuntu 16.04 LTS
IDE	Remix
Programming language	Solidity 0.4.7
Compiler environment	JavaScript VM
Ethernet	MetaMask
Test network	Ropsten Test Network

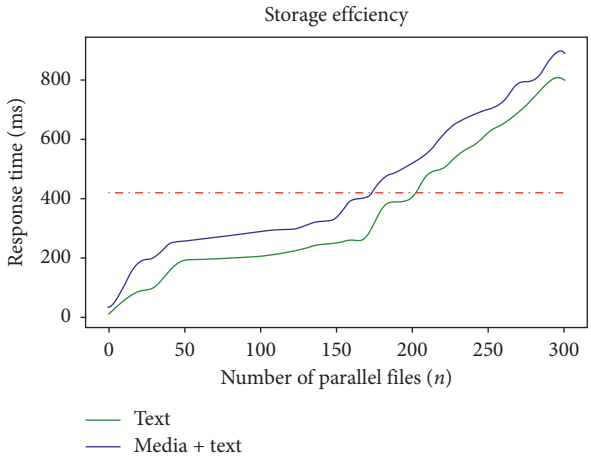

Figure 5: Comparison of storage efficiency.

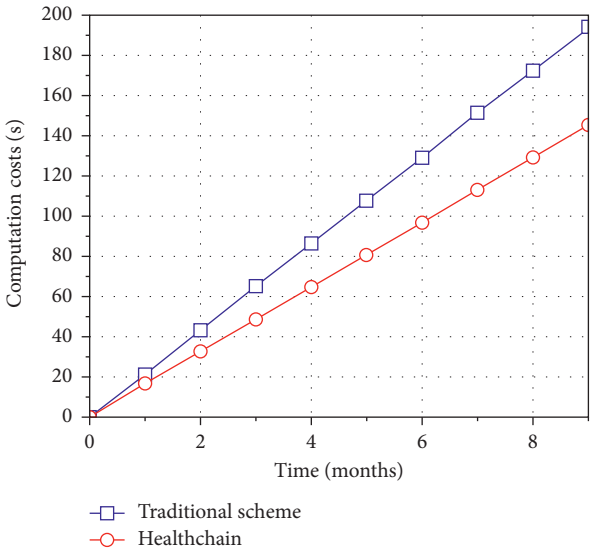

Figure 6: Computation overhead of our proposed system compared to the traditional one.

thousands of transaction files at the same time. Under such high concurrent file access conditions, this experiment simulates parallel transactions from 1 to 300 transaction files. At the same time, considering the actual situation, some transaction files are multimedia files, and some are pure

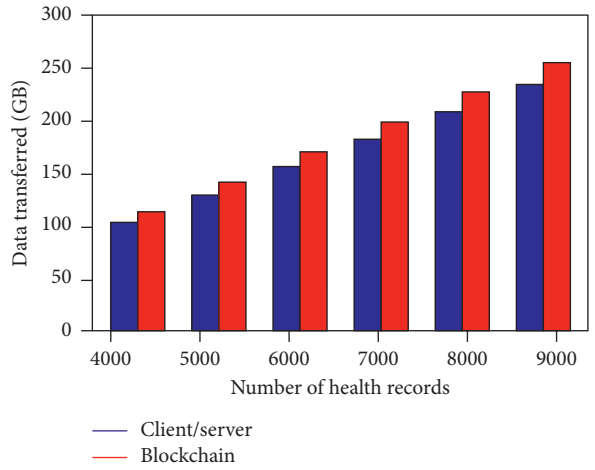

Figure 7: Throughput of our proposed system.

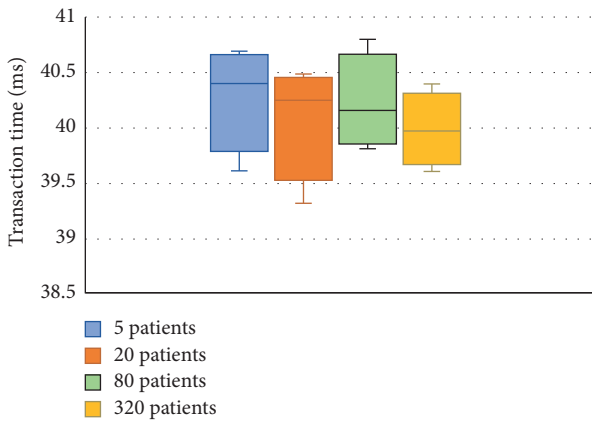

Figure 8: The average transaction processing time.

electronic document files. The experimental performance of two different types of files is shown in Figure 5.

It can be seen from Figure 5 that the growth trend of plain text files and multimedia fusion files is basically the same. With the increase of files, the pressure of node confirmation increases and the response time slows down. It can be seen that the response speed of uploading transaction files at the same time is less than 180 files, and the response time is about 400 ms or less. However, when the number of files is more than 180, the response time has increased rapidly. The possible reason is that, in the experiment based on the POW consensus mechanism, there are too few packaging contract nodes (mining nodes), which leads to slow transactions. In theory, the experiment arranged to the efficiency in the public network will be further optimized. However, in the case of 180 files, the requirements in the model can be fully met, and users will not feel significant delay. Generally speaking, the system performed well without obvious clogging, which was in line with the initial expectations of the study.

The computation overhead of transaction generation of our proposed system and the traditional system is shown in

Figure 6, the throughput of the proposed system with increasing number of records is shown in Figure 7, and the average transaction of the proposed system per processing time is shown in Figure 8.

6. Conclusions

In this research, the application scenario of Blockchain technology in a cross-border e-commerce environment is proposed: cross-domain record sharing and traceability. And the advantages and disadvantages of the proposed modification scheme are analyzed in terms of data protection, access performance, security, implementation difficulty, simplicity of use, and so on. We explained Blockchain and its working according to our work and designed different algorithms which increase the efficiency of our proposed scheme. The experimental results indicate that in spite of success metrics, in the above aspects, the scheme proposed by this research has an effective storage server, low transaction latency, tracking, and reduced power. Though, as multiparty participation and multiparty supervision technology, Blockchain can ensure that transaction records can be traced at any time, but it may also suffer from security issues such as artificial leakage of keys during propagation. In the future, this research will use cryptography such as attribute encryption, homomorphic encryption, and proxy encryption technology, combined with the characteristics of multiparty participation and nontampering in Blockchain technology, to protect user privacy information.

Data Availability

The data used to support the findings of this study are included within the article.

Conflicts of Interest

The author declares that there are no conflicts of interest regarding the publication of this study.

References

[1] S. Nakamoto, "Bitcoin: a peer-to-peer electronic cash system," 2008, https://bitcoin.org/en/bitcoin-paper.

[2] V. Buterin, "A next-generation smart contract and decentralized application platform," 2014, https://github.com/ethereum/wiki/wiki/White-Paper.

[3] X. Yu, Y. Chu, F. Jiang, Y. Guo, and D. Gong, "SVMs classification based two-side cross domain collaborative filtering by inferring intrinsic user and item features," *Knowledge-Based Systems*, vol. 141, pp. 80–91, 2018.

[4] UK Government Chief Scientific Adviser, "Distributed Ledger technology: beyond Blockchain," 2016, https://assets.publishing.service.gov.uk/government/uploads/system/uploads/attachment_data/file/492972/gs-16-1-distributed-ledger-technology.pdf.

[5] X. Yu, Q. Hu, H. Li, J. Du, J. Gao, and L. Sun, "Cross-domain recommendation based on latent factor alignment," *Neural Computing and Applications*, vol. 14, 2021.

[6] Y. Yuan and F. Wang, "Blockchain: the state of the art and future trends," *Acta Automatica Sinica*, vol. 42, no. 4, pp. 481–494, 2016.

[7] J. Frizzo-Barker, P. A. Chow-White, P. R. Adams, J. Mentanko, D. Ha, and S. Green, "Blockchain as a disruptive technology for business: a systematic review," *International Journal of Information Management*, vol. 51, 2020.

[8] M. Usman, M. A. Jan, and A. Jolfaei, "SPEED: a deep learning assisted privacy-preserved framework for intelligent transportation systems," *IEEE Transactions on Intelligent Transportation Systems*, vol. 3, pp. 1–9, 2020.

[9] R. Cole, M. Stevenson, and J. Aitken, "Blockchain technology: implications for operations and supply chain management," *Supply Chain Management: An International Journal*, vol. 24, no. 4, pp. 469–483, 2019.

[10] N. Kshetri, "1 Blockchain's roles in meeting key supply chain management objectives," *International Journal of Information Management*, vol. 39, pp. 80–89, 2018.

[11] M. A. Jan, J. Cai, X. C. Gao et al., "Security and Blockchain convergence with Internet of Multimedia Things: current trends, research challenges and future directions," *Journal of Network and Computer Applications*, vol. 175, pp. 102918–102935, 2021.

[12] Y. Chang, E. Iakovou, and W. Shi, "Blockchain in global supply chains and cross border trade: a critical synthesis of the state-of-the-art, challenges and opportunities," *International Journal of Production Research*, vol. 58, no. 7, pp. 2082–2099, 2019.

[13] S. Fosso Wamba, A. Gunasekaran, R. Dubey, and E. W. T. Ngai, "Big data analytics in operations and supply chain management," *Annals of Operations Research*, vol. 270, no. 1-2, pp. 1–4, 2018.

[14] L.-W. Wong, L.-Y. Leong, J.-J. Hew, G. W.-H. Tan, and K.-B. Ooi, "Time to seize the digital evolution: adoption of Blockchain in operations and supply chain management among Malaysian SMEs," *International Journal of Information Management*, vol. 52, 2020.

[15] P. Zhang, M. A. Walker, J. White, D. C. Schmidt, and G. Lenz, "Metrics for assessing Blockchain-based healthcare decentralized apps," in *Proceedings of the 2017 IEEE 19th International Conference One-Health Networking, Applications and Services (Healthcom)*, pp. 1–4, Dalian, China, October 2017.

[16] A. Azaria, A. Ekblaw, T. Vieira, and A. Lippman, "Medrec: using Blockchain for medical data access and permission-management," in *Proceedings of the 2016 2nd International Conference on Openand Big Data (OBD)*, pp. 25–30, Vienna, Austria, August 2016.

[17] Q. Xia, E. B. Sifah, K. O. Asamoah, J. Gao, X. Du, and M. Guizani, "Medshare: trust-less medical data sharing among cloud service providers via Blockchain," *IEEE Access*, vol. 5, pp. 14757–14767, 2017.

[18] Q. Xia, E. Sifah, A. Smahi, S. Amofa, and X. Zhang, "Bbds: Blockchain-based data sharing for electronic medical records in cloud environments," *Information*, vol. 8, no. 2, p. 44, 2017.

[19] M. A. Jan, F. Khan, R. Khan et al., "A lightweight mutual authentication and privacy-preservation scheme for intelligent wearable devices in industrial-CPS," *IEEE Transactions on Industrial Informatics*, vol. 17, no. 8, pp. 5829–5839, 2021.

[20] D. Wang and Z. Xie, "Application path and legal regulatory framework of Blockchain technology in the collaborative development of cross-border e-commerce," *Journal of Xinjiang University of Finance and Economics*, vol. 1, no. 3, pp. 64–71, 2020.

[21] J. Wang, W. Zhao, R. Gao, and J. Cao, "Research on the application of Blockchain technology in cross border e-commerce," *Jilin Financial Research*, vol. 3, no. 8, pp. 11–13 + 30, 2020.
[22] L. Liu, D. Cheng, and X. Su, "Analysis of consumer trust mechanism based on Blockchain technology," *Commercial Economy Research*, vol. 11, no. 15, pp. 32–36, 2020.
[23] Z. Jin, "Application of Blockchain technology in e-commerce logistics industry," *Electronic Technology and Software Engineering*, vol. 6, no. 15, pp. 175-176, 2020.
[24] C. Qian, "Analysis on the financial management of e-commerce enterprises based on "Blockchain + Internet"," *Journal of Times Finance*, vol. 4, no. 21, pp. 79-80, 2020.
[25] M. Wu and Y. Liu, "Research on the construction of cross-border payment system driven by Blockchain technology—from the perspective of cost control," *Journal of Guangdong Polytechnic of Light Industry*, vol. 19, no. 2, pp. 14–18, 2020.
[26] H. Jia, "Application of "Blockchain + e-commerce" in the field of e-commerce of agricultural products in Weinan City," *Computer Technology and Development*, vol. 30, no. 6, pp. 191–196, 2020.
[27] J. Pang and H. Huize, "Analysis and supervision of cross-border payment model based on Blockchain technology," *Journal of Economist*, vol. 6, no. 6, pp. 56-57, 2020.
[28] X. Chen, "Optimization of financial activities of cross border e-commerce enterprises based on Blockchain technology," *Commercial Economy*, vol. 7, no. 5, pp. 146–148, 2020.
[29] X. Jiang, *Research on the Application of Blockchain in Cross Border E-Commerce*, Tianjin University of Commerce, Tianjin, China, 2020.
[30] S. Yang, Z. Huang, and D. Li, "Application scenarios and value analysis of the Blockchain in cross border e-commerce," *Cyberspace Security*, vol. 11, no. 4, pp. 44–48, 2020.
[31] Y. Liu and L. Qiu, "Solving mechanism of "trust" gap of cross-border e-commerce under Blockchain technology," *Commercial Economy Research*, vol. 10, no. 7, pp. 150–153, 2020.
[32] Y. Yi, "Prospects for the development of cross border logistics finance in China based on Blockchain technology—taking accompanying payment as an example," *Foreign Trade Practice*, vol. 11, no. 4, pp. 77–80, 2020.
[33] D. Yan and F. Zhu, "Research on breaking the credit crisis of China's cross-border e-commerce under the background of Blockchain," *Time-Honored Brand Marketing*, vol. 6, no. 4, pp. 18–20, 2020.
[34] M. Yin and X. Xu, "Challenges faced by cross-border e-commerce export trade and Countermeasures: from the perspective of Blockchain technology application," *Commercial Economy Research*, vol. 2, no. 6, pp. 149–152, 2020.
[35] Q. Yi, H. Yang, and K. Wang, "Review on the application of Blockchain technology in logistics," *Logistics Technology*, vol. 39, no. 3, pp. 129–133, 2020.
[36] X. Yu, J. Yang, and Z. Xie, "Training SVMs on a bound vectors set based on Fisher projection," *Frontiers of Computer Science*, vol. 8, no. 5, pp. 793–806, 2014.
[37] X. Yu, F. Jiang, J. Du, and D. Gong, "A cross-domain collaborative filtering algorithm with expanding user and item features via the latent factor space of auxiliary domains," *Pattern Recognition*, vol. 94, pp. 96–109, 2019.
[38] J. Ge, S. Jiao, and C. Weng, "Development opportunities and challenges of "Blockchain + cross border e-commerce"," *Modern Economic Information*, vol. 8, no. 24, pp. 310-311, 2019.

Hindawi
Mobile Information Systems
Volume 2021, Article ID 9993946, 13 pages
https://doi.org/10.1155/2021/9993946

Research Article

Smart Application Division and Time Allocation Policy for Computational Offloading in Wireless Powered Mobile Edge Computing

Abdullah Numani,[1] **Zaiwar Ali**,[1] **Ziaul Haq Abbas**,[2] **Ghulam Abbas**,[3] **Thar Baker**,[4] **and Dhiya Al-Jumeily**[5]

[1]*Telecommunications and Networking (TeleCoN) Research Lab, GIK Institute of Engineering Sciences and Technology, Topi, Swabi 23640, Pakistan*
[2]*Faculty of Electrical Engineering, GIK Institute of Engineering Sciences and Technology, Topi, Swabi 23640, Pakistan*
[3]*Faculty of Computer Sciences and Engineering, GIK Institute of Engineering Sciences and Technology, Topi, Swabi 23640, Pakistan*
[4]*Department of Computer Science, University of Sharjah, Sharjah, UAE*
[5]*Department of Computer Science, Liverpool John Moores University, Liverpool, UK*

Correspondence should be addressed to Thar Baker; tshamsa@sharjah.ac.ae

Received 3 April 2021; Revised 29 May 2021; Accepted 24 June 2021; Published 2 July 2021

Academic Editor: Yugen Yi

Copyright © 2021 Abdullah Numani et al. This is an open access article distributed under the Creative Commons Attribution License, which permits unrestricted use, distribution, and reproduction in any medium, provided the original work is properly cited.

Limited battery life and poor computational resources of mobile terminals are challenging problems for the present and future computation-intensive mobile applications. Wireless powered mobile edge computing is one of the solutions, in which wireless energy transfer technology and cloud server's capabilities are brought to the edge of cellular networks. In wireless powered mobile edge computing systems, the mobile terminals charge their batteries through radio frequency signals and offload their applications to the nearby hybrid access point in the same time slot to minimize their energy consumption and ensure uninterrupted connectivity with hybrid access point. However, the smart division of application into k subtasks as well as intelligent partitioning of time slot for harvesting energy and offloading data is a complex problem. In this paper, we propose a novel deep-learning-based offloading and time allocation policy (DOTP) for training a deep neural network that divides the computation application into optimal number of subtasks, decides for the subtasks to be offloaded or executed locally (offloading policy), and divides the time slot for data offloading and energy harvesting (time allocation policy). DOTP takes into account the current battery level, energy consumption, and time delay of mobile terminal. A comprehensive cost function is formulated, which uses all the aforementioned metrics to calculate the cost for all k number of subtasks. We propose an algorithm that selects the optimal number of subtasks, partial offloading policy, and time allocation policy to generate a huge dataset for training a deep neural network and hence avoid huge computational overhead in partial offloading. Simulation results are compared with the benchmark schemes of total offloading, local execution, and partial offloading. It is evident from the results that the proposed algorithm outperforms the other schemes in terms of battery life, time delay, and energy consumption, with 75% accuracy of the trained deep neural network. The achieved decrease in total energy consumption of mobile terminal through DOTP is 45.74%, 36.69%, and 30.59% as compared to total offloading, partial offloading, and local offloading schemes, respectively.

1. Introduction

Due to the advancements in cellular technologies and applications of Internet of things (IoT), our daily life activities, such as smart healthcare, smart homes, and smart driving, are becoming dependent on mobile terminals (MTs) [1, 2]. The aforementioned applications are computation-intensive and energy-hungry and require large storage and faster execution [3]. To meet these requirements, an attempt is the cloud computing system that contains centralized servers

having higher processing powers and storage capabilities [4, 5]. However, the delay-sensitive applications such as online simulators, live streaming, and online games cannot be executed through cloud servers due to the inherited problem of high latency caused by long distances of cloud servers from the MTs [6, 7]. The problems of high latency and centralized architecture can be overcome to a certain limit through fog nodes closer to the request generators in fog computing. However, there are challenges of tasks offloading, resource distribution, and degraded performance of network links [8].

An alternative for the delay-sensitive applications is mobile edge computing (MEC) that offers services similar to that of cloud computing in a distributed manner and can be called the cloud computing at the edge of cellular networks. In the MEC environment, an MT can offload its computational applications to the nearby mobile edge server (MES) available with the lowest delays as compared to the cloud servers. The challenging problems of MTs, that is, limited computational power, storage, and higher time delays in execution, are entirely dependent on the battery life of MT. Unfortunately, the MTs have limited battery life that leads to the compromised performance [9]. To ensure the connectivity of MT with a nearby base station (BS), the battery of MT needs regular charging that requires more hardware and physical cost. The technology of wireless energy transfer (WET) is explained in [10], in which the battery of MTs can be charged wirelessly through radio frequency (RF) signals. However, energy harvesting from RF signals transmitted for information exchange leads to security issues at physical layer. Hence, either the deployment of multiple antennas at MT and exploiting diversity techniques or energy transmitter (ET) at the BS is preferred [11]. Recently, incorporation of WET technology in MEC system is a hot area of research. A model that utilizes the advantages of both WET technology and MEC is called wireless powered MEC (WP-MEC) [12]. The use of such model can facilitate the MT with the harvesting of energy to improve the battery life and with the computational offloading to enhance the computational capability of MT simultaneously.

There are two main types of computational offloading. In coarse-grained computational offloading, the whole application is either executed locally at the MT or offloaded to the remote MES [13]. Meanwhile, in fine-grained computational offloading [14], the whole application of size M is first divided into a k number of subtasks and can be offloaded with 2^k possible policies. For example, if an application of 10 GB is divided into 4 subtasks, then these 4 subtasks can be offloaded according to $2^4 = 16$ offloading policies as shown in Table 1.

Number of subtasks per application and selection of offloading policy mainly contribute to energy consumption and time delay of MT. Therefore, it is important to divide the application in an optimal number of subtasks and select an offloading policy that has minimum cost.

In WP-MEC system, an MT offloads its computational application to the hybrid access point (HAP) and harvests energy from RF signals of energy transmitter (ET). The MT harvests energy in some part of time slot and offloads data in the remaining time of the same time slot. Therefore, the intelligent division of time slot into fractions for energy harvesting and data offloading is a crucial point of consideration, known as time allocation policy. The possible number of time allocation policies is dependent on resolution of time, τ_r, and is equal to $(1/\tau_r) + 1$. Decrease in τ_r increases the number of time allocation policies. We can find the cost of all possible policies and then select the optimal one that has minimum cost. For example, the possible time allocation policies for $\tau_r = 0.2$ are given in Table 2. Both the battery life and computation power can be improved through the optimal selection of number of subtasks per application and time allocation policy for energy harvesting and data offloading. The time allocation policy is investigated through the Lyapunov function optimization technique in [15] for WP-MEC system. However, such numerical solutions suffer from huge computational overhead, which increases the complexity of algorithm and time delay of execution. To avoid the problem of huge computational overhead in such offloading, the emerging artificial intelligence (AI) concepts can be used.

Table 1: Offloading policies for an application divided into 4 subtasks.

Offload to HAP = 1, execute on MT = 0				
Policy	Subtask 1	Subtask 2	Subtask 3	Subtask 4
1	0	0	0	0
2	0	0	0	1
3	0	0	1	0
4	0	0	1	1
5	0	1	0	0
6	0	1	0	1
7	0	1	1	0
8	0	1	1	1
⋮	⋮	⋮	⋮	⋮
16	1	1	1	1

In this paper, we propose a deep learning approach to find the best time allocation policy and partial offloading policy with optimal number of subtasks per application. Our proposed cost function depends on time delay, energy consumption, and current battery level of the MT. Initially, if the battery level is 100%, our cost function focuses on time delay of application execution. The cost function gives more importance to the energy consumption when the battery is low. The considered WP-MEC system consists of an HAP (containing an ET, MES, and an AP) and MTs. Due to the size limitation, MT is considered to have one antenna that can be used for both energy harvesting and computational offloading. In contrast, the larger size of HAP allows separate antennas for transmitting energy and data communication, as shown in Figure 1. The target of the proposed approach is to utilize the WET and partial offloading technique with optimal number of subtasks per application to improve the battery life of MT and make the execution of applications faster. Novelty and contributions of the proposed work are outlined as follows:

Table 2: Time allocation policies for time resolution of $\tau_r = 0.2$.

Possible options	Time fraction for harvesting energy (t_0)	Time fraction for data offloading (t_1)
Policy 1	0	1
Policy 2	0.2	0.8
Policy 3	0.4	0.6
Policy 4	0.6	0.4
Policy 5	0.8	0.2
Policy 6	1	0

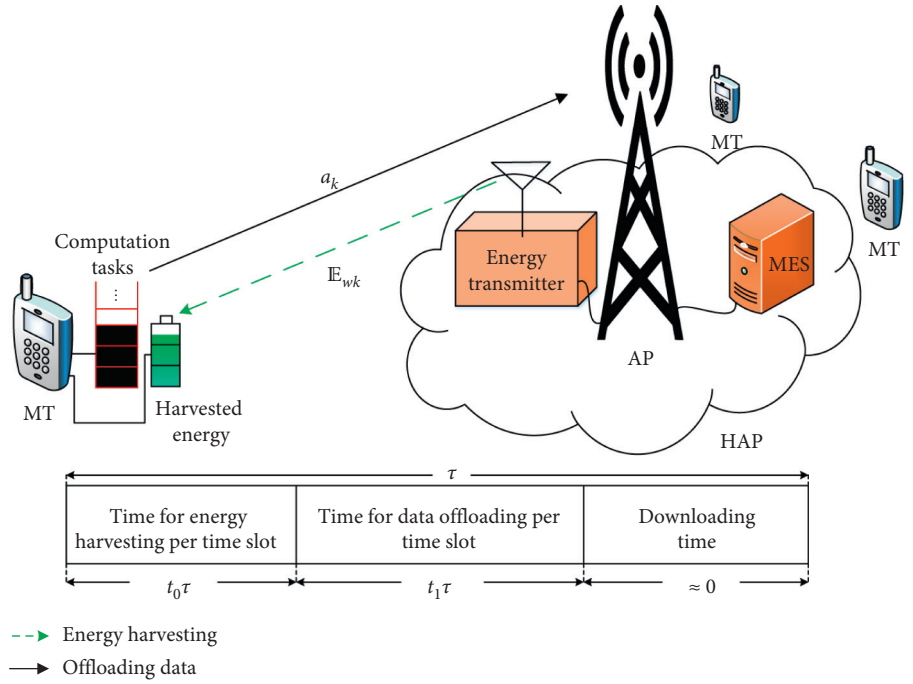

Figure 1: Wireless powered mobile edge computing system.

(i) We find the time allocation policy for energy harvesting and data offloading, partial offloading policy, and optimal number of subtasks per application, simultaneously, through deep learning approach in WP-MEC system to improve the battery life of MT and execution delay.

(ii) We formulate a cost function which depends on energy consumption, time delay, and current battery life of MT. There are two main parts of the cost function: energy consumption part and time delay part. The minimum cost value means that the energy consumption and time delay will be minimum; however, our cost function updates itself through weighting coefficients dependent on battery level, which decide the contribution of time delay part or energy consumption part in the cost function.

(iii) Simulation results show that our proposed algorithm prolongs the battery life and ensures faster execution and minimum energy consumption.

The remainder of the paper is organized as follows: Section 2 provides the related work of the proposed technique. Section 3 presents the mathematical model and the proposed algorithm. In Section 4, the numerical simulations and results are discussed. Section 5 concludes the paper and suggests some future directions.

2. Related Work

For the improvement of MT's battery life and ensured connectivity with HAP during partial offloading technique, the time slot for data offloading is further divided into two parts: (a) the time fraction in which the MT will charge its battery through RF signal and (b) the time fraction in which the MT will offload data to the HAP. This division of time slot, referred to as time allocation policy, is discussed in [15, 16]. The problem of time allocation policy (for power transfer and data offloading) and offloading mode selection (for offloading or local execution of an application) is studied in [12], and a total computational offloading technique for all energy harvesting MTs is proposed. Based on computation rate, a maximization problem is studied in [17] for the decrease in propagation loss that severely affects harvested energy and computation performance of MT. For the joint optimization of time allocation among MTs, CPU frequencies, transmitted energy at the AP, and number of

offloaded bits, a multiuser WP-MEC is considered in [18]. The authors in [15] propose an algorithm for the improvement of computation rate by joint consideration of computational offloading and time allocation policies in a WP-MEC system with one MT. The enhancement in computational performance of active MTs by the user cooperation technique is investigated in [19], where the inactive MTs use their harvested energy for the help of active ones. For the computational offloading policy, the authors in [19] consider frequency division multiple access (FDMA) to improve computation rate. The maximum-minimum energy efficiency optimization problem (MMEP) with joint optimization of energy consumption, time slots for computational offloading and energy transfer, and transmitted power at HAP in WP-MEC system are focused on in [20], and, by the application of block coordinate descent (BCD) and fractional programming theory, the authors present algorithms with lower complexity. In [21], the computational energy efficiency of entire system is improved by the joint consideration of optimal allocation for MT's transmitted power, CPU frequency, and time for transmission in WP-MEC system. In [22], the maximization problem of system energy efficiency by the joint consideration of optimal time allocation, local computing capacity, energy consumption, and application offloading is discussed. In [23], the authors consider a stochastic method for battery management and resource allocation decisions in a time slot and propose an algorithm derived from Lyapunov optimization technique. In [24], the authors utilize the Lyapunov optimization for the evaluation of tradeoff between delay and energy efficiency of a multiuser WP-MEC system. In all the abovementioned work, the improvement in computation rate is mainly focused. However, the battery life of MT is ignored and the number of subtasks in which an application should be divided for partial offloading is assumed to be a fixed value.

In most studies on WP-MEC, the investigation of time allocation and resource allocation policies is based on the numerical optimization techniques such as Lyapunov and Lagrange multipliers. However, for the complex optimization problems of allocating resources in WP-MEC, the said techniques do not guarantee global minima/maxima, and thus the performance of algorithms based on these methods becomes poor. Additionally, these approaches make use of long calculations and thus involve larger computational overheads that affect the time delays for computations and energy consumption of MTs. The greater amount of energy consumption badly affects the battery life of MTs and consequently the connectivity of MTs with HAP becomes limited. An alternate solution for fast computation of application division in subtasks and provision of optimal decisions for time allocation and resource allocation policies with minimum energy consumption and improved battery life is required. This requirement leads to the deep learning approach that decreases computational complexity by learning from predefined dataset training.

Little work is done for optimal time allocation and offloading policies in WP-MEC systems using deep learning approach. In [25], the authors investigate deep reinforcement learning for online offloading to reduce the computational complexity of large-size networks for offloading decisions and resource allocations, while ignoring the cost function. The main focus of the authors in [25] is on the minimization of execution latency, while battery life of MT, energy consumption, and optimal division of application are not taken into account. In [26, 27], the authors consider metrics such as subtask energy consumption, MT's remaining energy, computational load, and network conditions and propose a deep-learning-based offloading policy. However, their work ignores the energy harvesting capability of HAP and considers only MES at the edge of cellular network. A comparison table of the work related to deep-learning-based offloading and time allocation policy (DOTP) is given in Table 3.

From the study of related work on binary offloading policies in WP-MEC systems, we find two options for an application execution. (1) If an application is locally executed at the MT, it can reduce energy consumption; however, due to limited computational resources, the time delay will be higher. (2) If all the subtasks of an application are remotely executed on MES, the computational time delay will be smaller as the MES is assumed to have sufficient computational resources; however, in offloading data, the energy consumption of the MT will be higher. The third option is the partial offloading policy, that is, to divide the application into a number of subtasks. Then, some of the subtasks will be locally executed, while some subtasks are offloaded to the MES for remote execution. In this case, the option for subtask to be executed either locally on MT or remotely on the MES is dependent on the cost calculated through the cost function. This paper focuses on a deep-learning-based approach to find the optimal number of subtasks (optimal in terms of cost) in which we should divide the application and then apply the partial offloading policy. In the offloading option of a subtask, the time allocation policy is applied to find the time fraction for MT's energy harvesting and data offloading per time slot. The proposed cost function jointly considers the remaining battery level, time delay, and energy consumption of MT in the cost calculation for an application. Simulation results show that the proposed DOTP technique performs better than the benchmark schemes in terms of battery life, time delay, and energy consumption.

3. System Model

In our WP-MEC system model, we consider an HAP communicating with single MT. From implementation point of view, the HAP is assumed to have two antennas used in a time division duplex (TDD) manner for energy transmission and data communication separately, in the same frequency band. Meanwhile, the MT is considered to have single antenna; therefore, it utilizes the protocol of first-harvest-then-offload through the same antenna on downlink (DL) and uplink (UL), respectively. During the remote execution, MT first harvests energy for some part of the time slot and then transmits its subtask for execution to the MES in the rest of time slot. Moreover, the HAP is assumed to have sufficient resources of energy and processing, while the

Table 3: Comparison of related works with the proposed DOTP technique in WP-MEC system.

Technique	Considers battery life?	Considers optimal number of subtasks per application?	Considers energy consumption?	Considers time delay?	Considers energy harvesting (WET technology)?	Considers deep learning approach?
Lyapunov optimization [23] (2016)	Yes	No	Yes	No	Yes	No
Wang et al. [18]	No	No	Yes	Yes	Yes	No
Mao et al. [20]	No	No	Yes	No	Yes	No
ADMM [12] (2018)	No	No	Yes	Yes	Yes	No
Zhou et al. [17]	No	No	Yes	No	Yes	No
Lagrange multipliers [19] (2018)	No	No	Yes	No	Yes	No
OSRM [15] (2019)	No	No	Yes	No	Yes	No
Mao et al. [24]	No	No	Yes	Yes	Yes	No
DROO [25] (2019)	No	No	No	Yes	Yes	Yes
EEDOS [26] (2019)	No	Yes	Yes	Yes	No	Yes
SEEM [22] (2020)	Yes	No	Yes	No	Yes	No
MADS [21] (2020)	No	No	Yes	No	Yes	No
JTAOP [16] (2021)	No	No	Yes	No	Yes	No
CEDOT [27] (2021)	No	Yes	Yes	Yes	No	Yes
DOTP (our proposed technique)	Yes	Yes	Yes	Yes	Yes	Yes

MT is considered to have limited computational resources and battery. Thus, the MT will use the energy transmitted by HAP to prolong its battery life for offloading and local execution of subtasks. In partial offloading, some of the components are offloaded to MES for execution. We divided a time slot for offloading in two parts, called time allocation policy. In the first part, the MT harvests energy and in the second part it offloads its data to the MES. The downloading time is small as compared to the transmitting time; therefore, the downloading time is assumed to be negligible. The time allocation policy is denoted by $t = \{t_0, t_1\}$, where t_0 is the percent time of a single time slot for which the MT will harvest energy from HAP and t_1 is the percent time of the same time slot in which the MT will offload its subtask to the MES. We introduce a binary variable B_k for subtask k which defines the decision of local execution or remote execution. $B_k = 0$ indicates the local execution of a subtask k on MT and $B_k = 1$ indicates the remote execution of a subtask k at the MES. A detailed list of notations used in this paper is given in Table 4. Two models are considered, namely, local execution model and remote execution model.

3.1. Local Execution. For local execution of subtask k, that is, $B_k = 0$, the time delay of local execution, D_{lk}, is calculated as

$$D_{lk} = \frac{a_k C}{\nu_{mk}}, \tag{1}$$

where ν_{mk} is the CPU frequency of MT for subtask k, C is the number of CPU cycles used for the execution of one byte of data, and a_k is the input data of subtask k, executed locally at the MT. The energy consumption of MT for a single subtask k in local execution is formulated as

$$\mathbb{E}_{lk} = \eta \nu_{mk}^3 D_{lk}, \tag{2}$$

where η, a dimensionless quantity, represents the effective switching capacitance factor that is dependent on the architecture of chip [28]. The product $\eta\nu_{mk}$ shows the computation power of MT. The total cost for subtask k executed locally at the MT is defined as the summation of normalized energy consumption and normalized time delay for subtask k and is given by

$$\lambda_{lk} = \varepsilon \mathbb{E}_{lk} + \psi D_{lk}, \tag{3}$$

where ε and ψ are the unit balancing coefficients defined, respectively, as

$$\begin{aligned} \varepsilon &= \frac{\sigma_1}{\mathbb{E}_{\max}}, \\ \psi &= \frac{\sigma_2}{D_{\max}}. \end{aligned} \tag{4}$$

For the whole application, $\mathbb{E}_{\max}$ and $D_{\max}$ are the maximum energy consumption and maximum time delay, respectively, having fixed values. σ_1 and σ_2 are the weighting coefficients that are dependent on the current level of MT's battery. These coefficients are used for providing priority to either data offloading or energy harvesting of MT. The cost function checks the current level of battery and decides the time fraction for energy harvesting. Initially, when the battery level is high, the time fraction for energy harvesting is low and the time fraction for offloading is high. However,

Table 4: Notations.

Notations	Meaning
a_k	Input data of subtask k
a_{k+1}	Output data of subtask k
α_u, α_d	Uplink and downlink small scale fading channel power gains, respectively
B_k	Boolean variable for offloading option of subtask k
b^*	Optimal offloading policy
$\mathscr{B}_i$	Current available energy of MT's battery
$\mathscr{B}_{i+1}$	Energy of MT's battery for coming time slot
$\mathscr{B}_{\%}$	Percent current level of MT's battery
β	Available bandwidth
C	CPU cycles to execute 1 byte of data
D_{dk}, D_{uk}	MT's downlink reception and uplink transmission time delays, respectively
D_{ek}, D_k	Processing and total time delays for subtask k, respectively
$D_{\max}$	Maximum time delay for single application
D_{lk}, D_{ok}	Time delays for local and remote execution of subtask k, respectively
$\mathbb{E}_{lk}$, $\mathbb{E}_{ok}$	Local and remote execution energy consumption for subtask k, respectively
$\mathbb{E}_{\max}$	Maximum energy consumption for single application
$\mathbb{E}_{wk}$	Harvested energy of MT during subtask k
η	Effective switching capacitance factor
ε and ψ	Unit balancing coefficients
G_k	Channel power gain for subtask k
γ_k^{ul}, γ_k^{dl}	MT's uplink and downlink channel data rates, respectively
k	Number of subtasks
λ	Cost function
λ_{lk}, λ_{ok}	Cost functions for local execution and remote execution of subtask k, respectively
λ^*	Optimal cost
M	Size of application
N_0	Noise spectral density
n	Number of subtasks per application
n^*	Optimal number of subtasks
ν_h, ν_{mk}	CPU frequencies of MES and MT, respectively
OP	Matrix of all possible offloading policies
ϕ	Path loss exponent
$\mathbb{P}_{hk}$, $\mathbb{P}_{mk}$	Transmitted powers of HAP and MT, respectively
$\mathbb{P}_x$	Downlink power of HAP
ρ	Path loss constant
s	Distance between MT and HAP
s_0	Reference distance
σ_1 and σ_2	Weighting coefficients
t_0, t_1	MT's time fractions for harvesting energy and data offloading, respectively
t_0^*, t_1^*	Optimal time fractions for energy harvesting and data offloading, respectively
τ_r	Time resolution

when the battery level decreases and falls below a threshold value, our cost function increases the time fraction for energy harvesting to its maximum value.

3.2. Remote Execution. For remote execution, that is, $B_k = 1$, the subtask k is offloaded to the HAP to utilize the processing power of MES. The processing power of MES and transmission power of HAP are assumed to be sufficient. Consequently, the delay of downloading from HAP to the MT is taken as zero and the total time is divided into two parts only, that is, $t_0 + t_1 \approx 1$ [22]. The UL channel data rate from MT to HAP, γ_k^{ul}, can be obtained using the Shannon-Hartley theorem as follows:

$$\gamma_k^{ul} = \beta \log_2\left(1 + \frac{G_k \mathbb{P}_{mk}}{\beta N_0}\right), \tag{5}$$

where $\mathbb{P}_{mk}$ denotes the transmitted power of MT for subtask k. For the UL, noise spectral density is represented by N_0 and β is the available bandwidth. The wireless channel between MT and HAP is considered to be independent and identically distributed block fading channel. α_u represents the UL small scale fading channel power gain. The channel power gain from MT to HAP is calculated as $G_k = \rho\alpha_u (s_0/s)^{\phi}$, where ρ is the path loss constant, s_0 is the reference distance, ϕ is the path loss exponent, and s is the distance between MT and HAP [29]. In a similar way, the DL channel data rate from HAP to the MT, γ_k^{dl}, can be formulated as

$$\gamma_k^{dl} = \beta \log_2\left(1 + \frac{G_k \mathbb{P}_{hk}}{\beta N_0}\right), \tag{6}$$

where $\mathbb{P}_{hk}$ represents the transmitted power of HAP for subtask k.

For calculating the time delay for remote execution, the UL time for data transmission, the DL time for data reception, and the execution time for data at MES are considered. The UL time delay in transmission of data from MT to the HAP, D_{uk}, is given as

$$D_{uk} = \frac{a_k}{\gamma_k^{ul}}. \tag{7}$$

In a similar way, the DL time delay in reception of data from HAP to the MT, D_{dk}, is formulated as

$$D_{dk} = \frac{a_{k+1}}{\gamma_k^{dl}}, \tag{8}$$

where a_{k+1} is the output data of subtask k and the input data of subtask $k+1$. The execution time delay for data a_k at the MES, D_{ek}, is calculated as

$$D_{ek} = \frac{a_k}{\nu_h}, \tag{9}$$

where ν_h is the CPU frequency of MES. The offloading time delay for a subtask k, D_{ok}, is obtained as

$$D_{ok} = t_1 \left(D_{uk} + D_{dk} + D_{ek}\right). \tag{10}$$

The MES is considered to have high computation power due to a large number of CPUs in it. Thus, due to high CPU frequency of MES, the execution time delay, D_{ek}, may be ignored. Moreover, the output data for k subtask, a_{k+1}, is very small as compared to the input data, a_k, and hence the DL time delay, D_{dk}, can be considered as approximately zero. Consequently, the offloading time delay of subtask k, D_{ok}, can be approximated as

$$D_{ok} \approx t_1 D_{uk}. \tag{11}$$

The MT's offloading energy consumption of subtask k, $\mathbb{E}_{ok}$, in remote execution model is formulated as

$$\mathbb{E}_{ok} = D_{ok} \mathbb{P}_{mk}. \tag{12}$$

The total cost for subtask k, executed remotely at the MES, is given by

$$\lambda_{ok} = \varepsilon \mathbb{E}_{ok} + \psi D_{ok}, \tag{13}$$

where ε and ψ are the unit balancing coefficients, as in (3).

The total time delay of a subtask k, D_k, can be defined as

$$D_k = \begin{cases} D_{ok}, & B_k = 1, \\ D_{lk}, & B_k = 0. \end{cases} \tag{14}$$

The cost of subtask k either locally executed on MT or remotely executed at the MES is formulated as

$$\lambda_k = \begin{cases} \lambda_{ok}, & B_k = 1, \\ \lambda_{lk}, & B_k = 0. \end{cases} \tag{15}$$

The total time delay for an application containing n number of subtasks, D_a, can be obtained as

$$D_a = \sum_{k=1}^{n} D_{ok} B_k + \sum_{k=1}^{n} D_{lk} \left(1 - B_k\right). \tag{16}$$

In this paper, it is considered that the MT has a chargeable battery, which can provide and store energy for the consumption of MT and can harvest energy from HAP. The harvested energy of MT is calculated as

$$\mathbb{E}_{wk} = t_0 D_{ok} \mu \mathbb{P}_x \alpha_d, \tag{17}$$

where $\mu = \left[0 \;\; 1\right]$ is a constant for energy harvesting and describes how efficiently the MT receives the transmitted energy of HAP [6]. For broadcasting RF signals to the MTs, $\mathbb{P}_x$ is the transmitted power of HAP. α_d represents the DL channel power gain. For the purpose of simplicity, it is assumed that α_d is equal to the UL channel power gain G_k. For subtask k, the total energy consumption of MT, $\mathbb{E}_k$, is written as

$$\mathbb{E}_k = \begin{cases} \mathbb{E}_{ok}, & B_k = 1, \\ \mathbb{E}_{lk}, & B_k = 0. \end{cases} \tag{18}$$

The current available energy of MT's battery is denoted by $\mathscr{B}_i$ and satisfies the condition

$$\mathbb{E}_k \leq \mathscr{B}_i + \mathbb{E}_{wk}. \tag{19}$$

The available energy of MT's battery is updated as follows:

$$\mathscr{B}_{i+1} = \mathscr{B}_i - \mathbb{E}_k + \mathbb{E}_{wk}, \tag{20}$$

where $\mathscr{B}_{i+1}$ is the energy of MT's battery for coming time slot. The total energy consumption of MT for single application, containing n number of subtasks, $\mathbb{E}_a$, is defined as

$$\mathbb{E}_a = \sum_{k=1}^{n} \mathbb{E}_{ok} B_k + \sum_{k=1}^{n} \mathbb{E}_{lk} \left(1 - B_k\right). \tag{21}$$

For the comparison of different techniques, a cost function is modeled as

$$\lambda = \sum_{k=1}^{n} \lambda_{ok} B_k + \sum_{k=1}^{n} \lambda_{lk} \left(1 - B_k\right), \tag{22}$$

where λ is the cost for a single application execution.

Initially, if the battery level is 100%, the energy consumption weight should be less than the weight of time delay because, in that case, faster execution is more important. The energy consumption part in the cost function becomes more important when the battery of MT is low. Therefore, we calculate these weighting coefficients by using the current battery level of MT as

$$\begin{aligned} \sigma_1 &= \frac{\mathscr{B}_{\%}}{\mathbb{E}_{\max}}, \\ \sigma_2 &= 1 - \sigma_1, \end{aligned} \tag{23}$$

where $\mathscr{B}_{\%}$ represents the percent current level of battery.

3.3. Proposed DOTP Algorithm. The number of possible values for energy harvesting time t_0 is represented by Z and is given as $Z = (1/\tau_r) + 1$. In the proposed DOTP technique, described in Algorithm 1, we calculate the local and remote costs for all possible number of subtasks per application, $k \in \{1, 2, 3, \ldots, n\}$, number of possible values for $t_0 \in \{0{:}\ \tau_r{:}\ 1\}$, that is Z, and offloading policies (2^n). Thus, the complexity of algorithm is $O(n \times Z \times 2^n)$. **OP** is a matrix of all possible offloading policies and has the order of $(n \times 2^n)$. For subtask k, local and remote costs are calculated using (3) and (13), respectively. With optimal number of subtasks, n^*, optimal time allocation policy, $t_0^* \in \{t_{01}^*, t_{02}^*, t_{03}^*, t_{04}^*, t_{05}^*, t_{06}^*, t_{07}^*, t_{08}^*, t_{09}^*\}$, and optimal offloading policy, b^*, the minimum cost is denoted by λ^* in Algorithm 1, where t_{01}^* is the harvesting time for subtask 1, t_{02}^* is the harvesting time for subtask 2, and so on.

Due to huge computational overhead of finding λ^*, n^*, t_0^*, and b^*, the service delay and energy consumption of MTs increase. Computations of these values are also explained through the flowchart in Figure 2. With the help of cost function, we generate a training dataset and train a DNN to reduce the computational overhead, energy consumption, and service delay of MTs.

The input layer of our DNN takes the size of application (M), number of subtasks per application (n), distance of MT from HAP (s), CPU frequency (ν_m), transmitted power $(\mathbb{P}_m)$, and the available battery level of MT $(\mathscr{B}_i)$, while the output layer gives the optimal number of subtasks (n^*), partial offloading policy (b^*), and the optimal time for harvesting energy (t_0^*). For the two hidden layers and the output layer, the rectified linear unit (ReLU) and Softmax activation functions are used, respectively.

We calculate the minimum cost and store the corresponding inputs and outputs as a training dataset. After obtaining a training dataset of size 5000, these data are divided into training dataset (70% of training dataset), validation dataset (15% of the training dataset), and test dataset (15% of the training dataset). The DNN is trained on training dataset and then its performance is validated through validation dataset. When the DNN is trained, the accuracy of DNN is checked through test dataset. The results of our DOTP algorithm are compared with the exiting benchmark schemes, that is, local execution, total offloading, and partial offloading.

4. Simulation and Results

The simulations environment used was MATLAB (R2019a) and the processor was Intel Core i7 with clock speed of 3.4 GHz. An application can be divided into more than 10 subtasks; however, for simulation purpose, we have assumed that an application can be divided into a maximum of 10 subtasks. For time allocation policy, the time resolution is assumed to be 0.01. Practically, the distance for WET is up to 12 m. However, to check the mobility effect of MT in a more comprehensive way, the maximum distance of MT from HAP is assumed to be 200 m. The reference distance of MT from HAP is assumed to be 1 m. The experimentation is performed on the basis of randomly generated data to show the stochastic nature of the problem and have more realistic results. The randomly generated input data for our graphs are the CPU frequency of MT, transmitted power of MT, distance of MT from HAP, and the application size. The advanced smart phones have the heterogeneous frequency capability and use different frequencies in different scenarios [30]. Thus, the CPU frequency of MT is taken randomly from a uniform distribution in the range of $[\,0.1 \;\; 1\,]$ GHz. Similarly, the transmitted power of smartphones is variable and changes as the distance of MT from HAP varies. This stochastic nature of transmitted power of MT is incorporated by considering it as a uniform distribution in $[\,0.8 \;\; 1.5\,]$ Watts. Different applications may have different sizes and that is why we have considered the size of application to be randomly selected from a uniform distribution in $[\,0.1 \;\; 1\,]$ G bits. To incorporate the mobility effect of MT in the simulation, the distance of MT from HAP is selected randomly from a uniform distribution in the range of $[\,3 \;\; 200\,]$ m.

CPU cycles of MT to execute one byte of data, C, are taken as 737.5 cycles/byte, each application is divided into n number of subtasks, and the value of n lies between 1 and 10. The value of effective switching capacitance factor, η, is taken as 10^{-25}, MT's efficiency of energy harvesting, μ, is taken as 0.8, path loss constant, ρ, has the value of −30 dB, path loss exponent $\phi \geq 2$, and reference distance of MT from HAP, s_0, is 1 m. The available bandwidth, β, and noise spectral density, N_0, are 0.5 MHz and −174 dBm/Hz, respectively. The trained DNN has 32 neurons in the input layer (one for MT's currently available battery level, $\mathscr{B}_i$, one for application size, M, ten for MT's CPU frequencies, ν_m, ten for MT's transmitted powers, $\mathbb{P}_m$, and ten for the distances of MT from HAP, s). The simulation parameters are given in Table 5. The number of subtasks in which an application of size M will be divided is taken from 1 to 10. Therefore, in the output layer, 10 neurons are specified for the number of subtasks per application. In the partial offloading policy, as considered in this paper, a maximum of 9 subtasks out of 10 can be offloaded to the remote MES. Thus, there are 9 neurons for the optimal time allocation policy, t_0^*. In one neuron at the output layer, the optimal partial offloading policy, b^*, is stored. Thus, the total number of neurons in the output layer of DNN is 20. There are two hidden layers and 100 neurons in each hidden layer. The accuracy of trained DNN achieved is 75%. The detailed architecture of DNN is shown in Figure 3.

The benchmark techniques considered for comparison of simulation results in this paper are described as follows:

(i) Total offloading technique [18]: in total offloading, no policy for offloading decisions is considered and the whole application is offloaded to the MES.

(ii) Local execution [19]: in local execution, the whole application is executed locally on MT and there is no offloading to MES.

(iii) Partial offloading technique [14]: in partial offloading, the application is divided into a number of

Input: $a \in [a_1, a_2, \ldots, a_n], \nu_m \in [\nu_{\min}, \nu_{\max}], \mathbb{P}_m \in [\mathbb{P}_{\min}, \mathbb{P}_{\max}], s \in [s_{\min}, s_{\max}], \mathscr{B}_i$
Output: $\{n^*, b^*, t_0^*\}$

for $i = 1: n$ **do**
  for $b = 1: 2^i$ **do**
    OP $\longleftarrow$ matrix of all possible offloading policies
    $B \longleftarrow \mathbf{OP}(b, :)$
    for $k = 1: i$ **do**
      if $(B(k) = 0)$ **then**
        while (a_k execution completion) **do**
          $D_{lk} \longleftarrow (a_k C/\nu_{mk})$ (1)
          $\mathbb{E}_{lk} \longleftarrow \eta \nu_{mk}^3 D_{lk}$ (2)
          $\lambda_1(k) \longleftarrow \lambda_{lk}$ (3)
        end while
        $t_0(k) = 0$
      else
        $\overline{t_0} = 0: \tau_r: 1$
        for $j = 1:$ length$(\overline{t_o})$ **do**
          while (a_k execution completion) **do**
            $D_{ok} \longleftarrow t_1 D_{uk}$ (11)
            $\mathbb{E}_{ok} \longleftarrow D_{ok} \mathbb{P}_{mk}$ (12)
            $\mathbb{E}_{wk} = t_0 D_{ok} \mu \mathbb{P}_x \alpha_d$ (17)
            $\mathscr{B}_{i+1} = \mathscr{B}_i - \mathbb{E}_k + \mathbb{E}_{wk}$ (20)
            $\lambda_2(j) \longleftarrow \lambda_{ok}$ (13)
          end while
        end for
      end if
      [index, $\lambda_1(k)$] = min(λ_2)
      $t_0(k) \longleftarrow \overline{t_0}$(index)
    end for
    $\lambda_2(b) \longleftarrow$ sum(λ_1)
    $t_2(b, :) \longleftarrow t_0$
  end for
  [index, $\lambda_3(i)$] = min(λ_2)
  $\mathbf{OP}_1(i, :) \longleftarrow \mathbf{OP}$(index, :)
  $t_3(i, :) \longleftarrow t_2$(index, :)
end for
[index, λ^*] $\longleftarrow$ min(λ_3)
$t_0^* \longleftarrow t_3$(index, :)
$\mathbf{OP}^* \longleftarrow \mathbf{OP}_1$(index, :)
$n^* \longleftarrow$ index
Save inputs: input $\longleftarrow \{a_k, \nu_{mk}, \mathbb{P}_{mk}, s_k\}$
Save outputs: labels $\longleftarrow \{n^*, b^*, t_0^*\}$
Repeat this for different size of applications
Train the DNN: Trained_DNN $\longleftarrow$ train(input, labels)
Test trained DNN
Accuracy $\longleftarrow$ number of correct decisions/number of total decisions

Algorithm 1: DOTP algorithm.

subtasks. An offloading policy is made for the decision of subtasks to be executed either locally or remotely.

All the above techniques find the offloading policy that has minimum cost and consider time delay and energy consumption for a fixed number of subtasks per application. They also ignore the battery life of MT and optimal time allocation policy for harvesting. Our proposed DOTP considers the optimal number of subtasks per application and the optimal offloading policy. Furthermore, the DOTP also considers the current battery level of MT for improvement through harvesting energy from HAP by utilizing an optimal time allocation policy.

In Figure 4, the remaining energy of MT is plotted against various sizes of application. The battery of MT for benchmark schemes dissipates faster as compared to the proposed DOTP due to their high energy consumption. The battery level in the benchmark schemes approaches negative (practically, battery of MT does not get negative

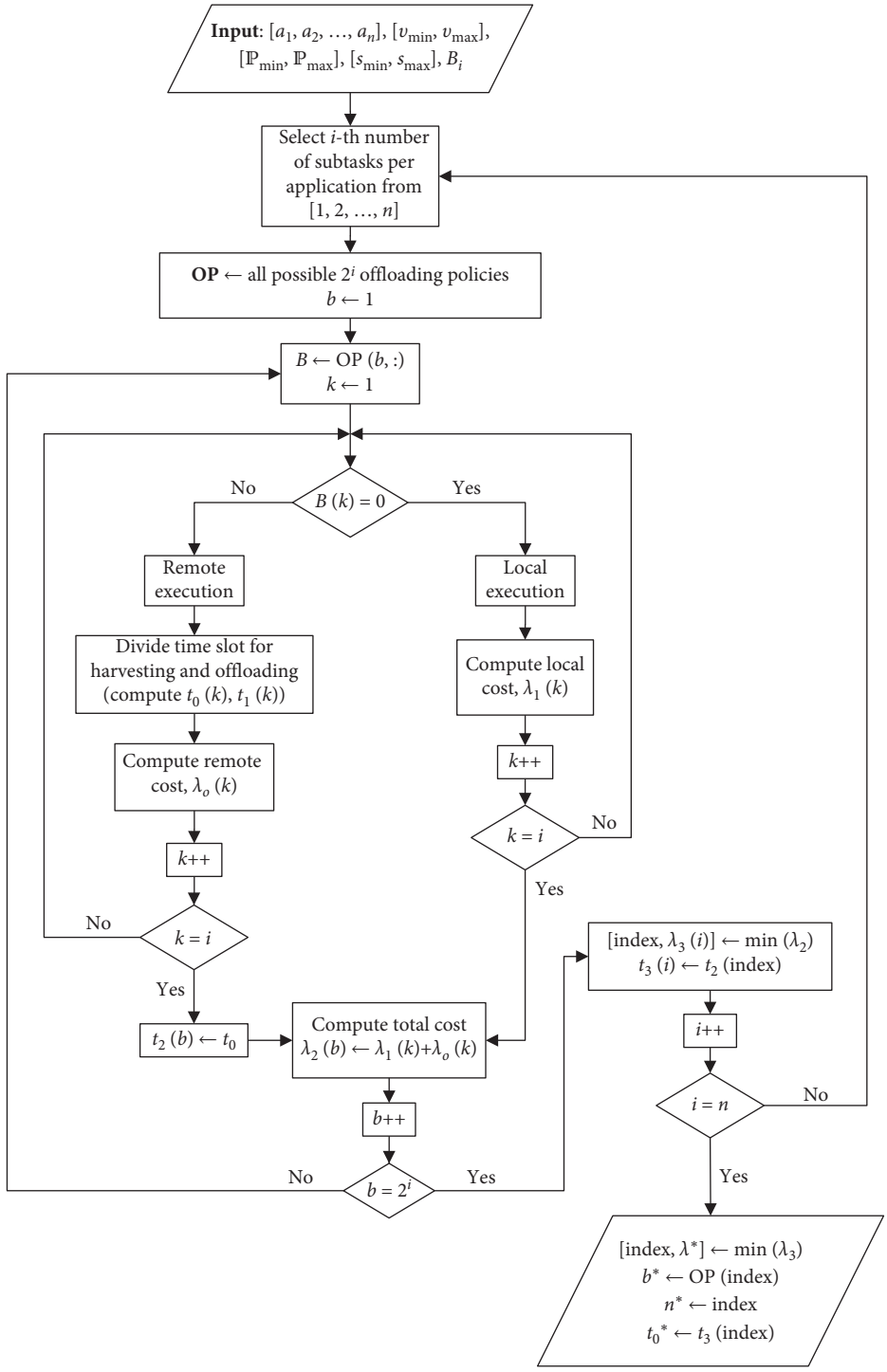

Figure 2: Flowchart of proposed DOTP algorithm.

values, and it is possible only in the simulations; in simulation results, negative values for MT's battery denote the shutdown state of MT) that results in the shutdown of MT, and consequently disconnection with HAP occurs. The total remaining energy for DOTP increases after a task size of 12 GBs because the harvesting energy time fraction of MT is dependent upon the remaining battery of MT. As the battery of MT decreases below a threshold level, the MT increases the time for harvesting energy and decreases the time for data offloading by changing the weighting coefficients' values described in the mathematical model. In contrast, there is no intelligent division of time slot for energy harvesting and data offloading in the benchmark schemes. Therefore, the remaining energy of MT for other schemes further decreases after task size of 12 GBs. Thus, in the DOTP scheme, a reserved battery level always remains available in the MT, which ensures that neither the MT will be

Table 5: Simulation parameters [15].

Parameter	Value
β	0.5 MHz
n	$\{1, 2, 3, \ldots, 10\}$
C	737.5 cycles/byte
s	$[3 \;\; 200]$ m
ν_m	$[0.1 \;\; 1]$ GHz
η	10^{-25}
$\mathbb{P}_m$	$[0.8 \;\; 1.5]$ Watt
N_o	−174 dBm/Hz
M	$[0.1 \;\; 1]$ G bits
μ	0.8
ρ	−30 dB
s_0	1 m
t_0	$[0 \;\; 1]$
τ_r	0.01
ϕ	≥2

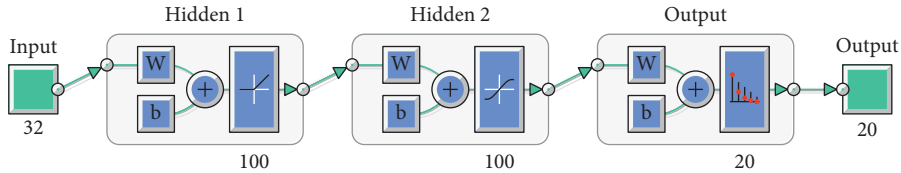

Figure 3: Detailed architecture of DNN.

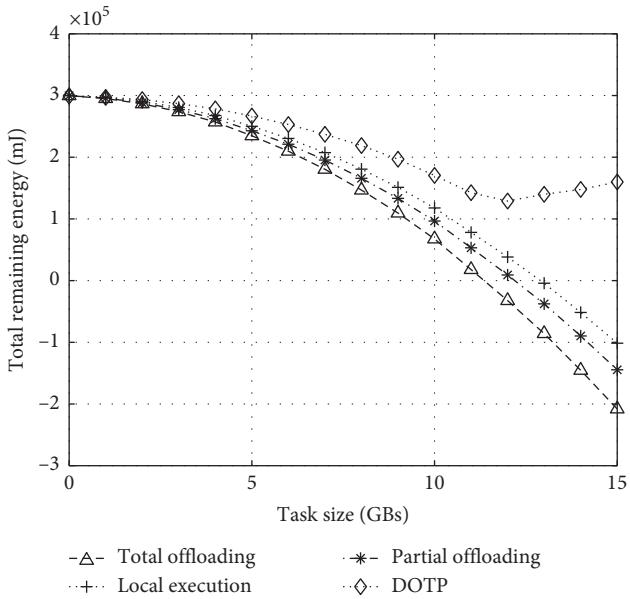

Figure 4: Battery life of MT with varying application sizes.

disconnected from HAP nor the battery level will go to negative values.

Figure 5 depicts the plot of total energy consumption with varying application sizes for all the mentioned techniques. The minimum energy consumption of DOTP can be observed from the figure. This is due to the consideration of different energy consumptions in the cost function (ignored in the benchmark schemes) and then the selection of offloading policy based on optimal number of subtasks. The different energy consumption behavior of first increasing and then decreasing when a threshold level is reached is due to the reason that the amount of energy being harvested is greater than that of the consumed energy. As MT prefers energy harvesting, the total energy consumption decreases at the task size of 12 GB. It is due to the energy consumption for comparatively smaller time fraction in the data offloading, while the energy consumption for the other schemes continuously increases due to the absence of smart time allocation policy. To the best of our knowledge, this smart time allocation policy is ignored in all the considered benchmark techniques.

Figure 6 compares the time delay versus different application sizes plot of DOTP with the benchmark schemes. The better performance of the proposed DOTP is evident from the figure through achievement of smaller time delays. This better performance of DOTP is due to the selection of optimal number of subtasks per application, which is considered constant in the mentioned benchmark schemes. The total offloading has minimum time delay, but this technique's energy consumption is the highest, as depicted in Figure 5. The greater rise in the execution time of DOTP is due to the lower battery level of MT; that is, most of the time the MT will harvest energy to level up its battery and in the same time slot little offloading of data takes place. The MT harvests energy for greater part of a time slot; therefore, an application will be offloaded in more time.

In Figure 7, the cost of the proposed DOTP is compared with those of the three benchmark schemes. From the figure, it is evident that the DOTP has the lowest cost as compared

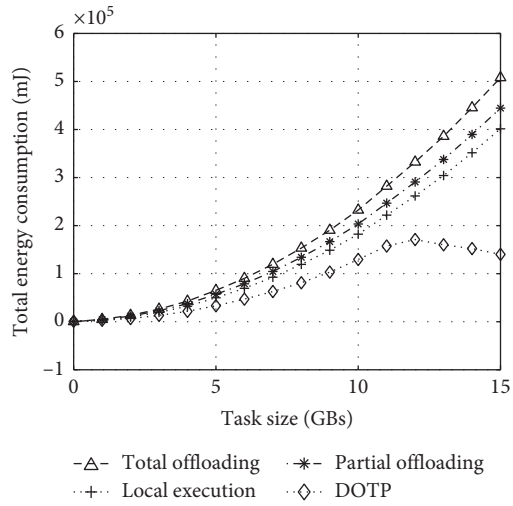

Figure 5: Total energy consumption for various application sizes.

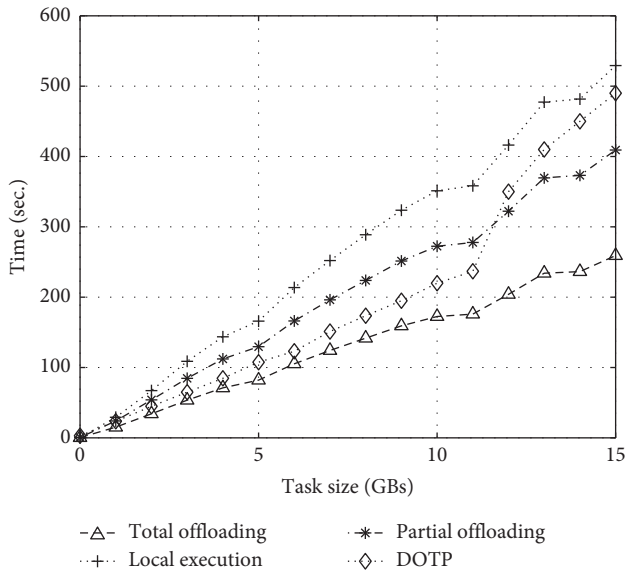

Figure 6: Time delay of MT with varying application sizes.

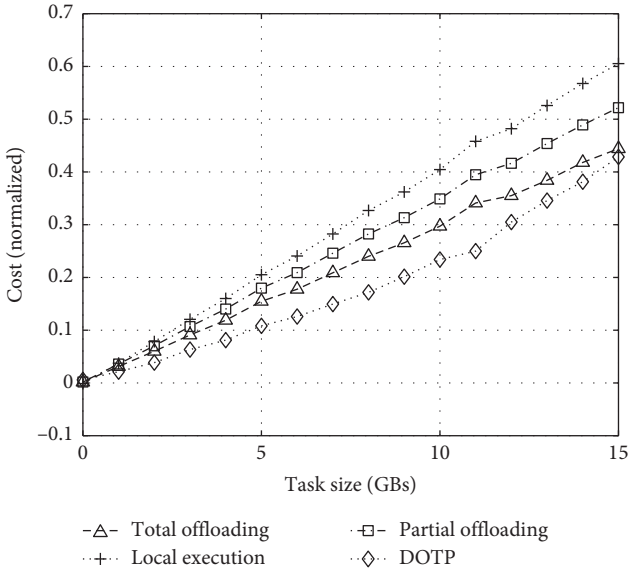

Figure 7: Cost for different application sizes.

to the other techniques. This minimum cost is the result of selecting optimal number of subtasks per application and considering the energy consumption, time delay, and energy harvesting in the cost function. In the cost function, weighting coefficients are dependent on the remaining energy of MT. These coefficients are used for providing priority to either data offloading or energy harvesting of MT. In contrast, the benchmark schemes consider fixed number of subtasks per application and focus on either energy consumption or time delay but not both simultaneously. The minimum cost of DOTP demonstrates the better performance for computational offloading in terms of energy consumption, time delay, and battery life.

5. Conclusions

In this paper, the battery life of MT, time allocation policy for energy harvesting and data offloading, and offloading policy based on optimal number of subtasks are investigated for single MT in WP-MEC system. The application for computational offloading is divided into optimal number of subtasks and then, through offloading policy, the decision to follow either remote execution or local execution is made. A detailed cost function is formulated, which jointly considers time delay and energy consumption for offloading policy. In addition, the cost function includes the current battery level of MT and thus prolongs the battery life of MT. The deep learning approach is used to find the optimal number of subtasks per application and partial offloading policy along with time allocation policy for energy harvesting simultaneously. The DOTP algorithm provides time allocation policy that results in extended battery life as compared to the benchmark schemes. A DNN is trained on a pregenerated dataset through mathematical model for the achievement of aforementioned objectives in order to reduce the energy consumption and time delay that incur for traditional optimization methods and make the decisions faster. It is evident from the numerical results that our proposed DOTP demonstrates extended battery life, lower energy consumption, and lower time delay for application execution in comparison with the benchmark techniques. In the future, the scenario can be extended to multiple MTs and HAPs, as well as to vehicular networks. In addition, reinforcement approach can be used, and routing strategies can be investigated for handover management during mobility from one HAP to another.

Data Availability

The data used in this study are random and are generated through our proposed mathematical model and Algorithm 1. Using the simulation parameters, given in Table 5, the required data can be generated as explained in Section 3.3.

Conflicts of Interest

The authors declare that they have no conflicts of interest.

References

[1] A. Ahad, M. Tahir, M. Aman Sheikh, K. I. Ahmed, A. Mughees, and A. Numani, "Technologies trend towards 5G network for smart health-care using IoT: a review," *Sensors*, vol. 20, no. 14, p. 4047, 2020.

[2] Z. Ali, Z. H. Abbas, and F. Y. Li, "A stochastic routing algorithm for distributed IoT with unreliable wireless links," in *Proceedings of the 2016 IEEE 83rd Vehicular Technology Conference (VTC Spring)*, pp. 1–5, IEEE, Nanjing, China, May 2016.

[3] A. Shakarami, M. Ghobaei-Arani, and A. Shahidinejad, "A survey on the computation offloading approaches in mobile edge computing: a machine learning-based perspective," *Computer Networks*, vol. 182, p. 107496, 2020.

[4] Z. Ali, S. Khaf, Z. H. Abbas, G. Abbas, F. Muhammad, and S. Kim, "A deep learning approach for mobility-aware and energy-efficient resource allocation in mec," *IEEE Access*, vol. 8, pp. 179530–179546, 2020.

[5] X. Jin, Z. Wang, and W. Hua, "Cooperative runtime offloading decision algorithm for mobile cloud computing," *Mobile Information Systems*, vol. 2019, Article ID 8049804, 17 pages, 2019.

[6] J. Ren, G. Yu, Y. He, and G. Y. Li, "Collaborative cloud and edge computing for latency minimization," *IEEE Transactions on Vehicular Technology*, vol. 68, no. 5, pp. 5031–5044, 2019.

[7] Z. Ali, S. Khaf, Z. H. Abba, G. Abbas et al., "A comprehensive utility function for resource allocation in mobile edge computing," *Computers, Materials & Continua*, vol. 66, no. 2, pp. 1461–1477, 2020.

[8] S. P. Singh, A. Nayyar, R. Kumar, and A. Sharma, "Fog computing: from architecture to edge computing and big data processing," *The Journal of Supercomputing*, vol. 75, no. 4, pp. 2070–2105, 2019.

[9] F. O. Ombongi, H. O. Absaloms, and P. L. Kibet, "Resource allocation in millimeter-wave device-to-device networks," *Mobile Information Systems*, vol. 2019, Article ID 5051360, 16 pages, 2019.

[10] O. L. López, H. Alves, R. D. Souza, S. Montejo-Sánchez, E. M. Fernandez, and M. Latva-Aho, "Massive wireless energy transfer: enabling sustainable IoT towards 6G era," *IEEE Internet of Things Journal*, vol. 8, no. 11, pp. 8816–8835, 2021.

[11] D. D. Tran, D. B. Ha, and A. Nayyar, "Wireless power transfer under secure communication with multiple antennas and eavesdroppers," in *Proceedings of the International Conference on Industrial Networks and Intelligent Systems*, pp. 208–220, Da Nang, Vietnam, August 2018.

[12] S. Bi and Y. J. Zhang, "Computation rate maximization for wireless powered mobile-edge computing with binary computation offloading," *IEEE Transactions on Wireless Communications*, vol. 17, no. 6, pp. 4177–4190, 2018.

[13] H. Eom, R. Figueiredo, H. Cai, Y. Zhang, and G. Huang, "Malmos: machine learning-based mobile offloading scheduler with online training," in *Proceedings of the 2015 3rd IEEE International Conference on Mobile Cloud Computing, Services, and Engineering*, pp. 51–60, San Francisco, CA, USA, March 2015.

[14] Z. Kuang, L. Li, J. Gao, L. Zhao, and A. Liu, "Partial offloading scheduling and power allocation for mobile edge computing systems," *IEEE Internet of Things Journal*, vol. 6, no. 4, pp. 6774–6785, 2019.

[15] C. Li, W. Chen, H. Tang, Y. Xin, and Y. Luo, "Stochastic computation resource allocation for mobile edge computing powered by wireless energy transfer," *Ad Hoc Networks*, vol. 93, p. 101897, 2019.

[16] A. Irshad, Z. H. Abbas, Z. Ali, G. Abbas, T. Baker, and D. Al-Jumeily, "Wireless powered mobile edge computing systems: simultaneous time allocation and offloading policies," *Electronics*, vol. 10, no. 8, p. 965, 2021.

[17] F. Zhou, Y. Wu, R. Q. Hu, and Y. Qian, "Computation rate maximization in UAV-enabled wireless-powered mobile-edge computing systems," *IEEE Journal on Selected Areas in Communications*, vol. 36, no. 9, pp. 1927–1941, 2018.

[18] F. Wang, J. Xu, X. Wang, and S. Cui, "Joint offloading and computing optimization in wireless powered mobile-edge computing systems," *IEEE Transactions on Wireless Communications*, vol. 17, no. 3, pp. 1784–1797, 2017.

[19] D. Wu, F. Wang, X. Cao, and J. Xu, "Wireless powered user cooperative computation in mobile edge computing systems," in *Proceedings of the 2018 IEEE GLOBECOM Workshops (GC Wkshps)*, pp. 1–7, Abu Dhabi, UAE, December 2018.

[20] S. Mao, S. Leng, K. Yang, X. Huang, and Q. Zhao, "Fair energy-efficient scheduling in wireless powered full-duplex mobile-edge computing systems," in *Proceedings of the GLOBECOM 2017-2017 IEEE Global Communications Conference*, pp. 1–6, Singapore, December 2017.

[21] A. Mahmood, A. Ahmed, M. Naeem, and Y. Hong, "Partial offloading in energy harvested mobile edge computing: a direct search approach," *IEEE Access*, vol. 8, pp. 36757–36763, 2020.

[22] C. Li, M. Song, L. Zhang, W. Chen, and Y. Luo, "Offloading optimization and time allocation for multiuser wireless energy transfer based mobile edge computing system," *Mobile Networks and Applications*, vol. 25, pp. 1–9, 2020.

[23] D. Zhang, Z. Chen, M. K. Awad, N. Zhang, H. Zhou, and X. S. Shen, "Utility-optimal resource management and allocation algorithm for energy harvesting cognitive radio sensor networks," *IEEE Journal on Selected Areas in Communications*, vol. 34, no. 12, pp. 3552–3565, 2016.

[24] S. Mao, S. Leng, S. Maharjan, and Y. Zhang, "Energy efficiency and delay tradeoff for wireless powered mobile-edge computing systems with multi-access schemes," *IEEE Transactions on Wireless Communications*, vol. 19, no. 3, pp. 1855–1867, 2019.

[25] L. Huang, S. Bi, and Y.-J. A. Zhang, "Deep reinforcement learning for online computation offloading in wireless powered mobile-edge computing networks," *IEEE Transactions on Mobile Computing*, vol. 19, no. 11, pp. 2581–2593, 2019.

[26] Z. Ali, L. Jiao, T. Baker, G. Abbas, Z. H. Abbas, and S. Khaf, "A deep learning approach for energy efficient computational offloading in mobile edge computing," *IEEE Access*, vol. 7, pp. 149623–149633, 2019.

[27] Z. H. Abbas, Z. Ali, G. Abbas et al., "Computational offloading in mobile edge with comprehensive and energy efficient cost function: a deep learning approach," *Sensors*, vol. 21, no. 10, p. 3523, 2021.

[28] T. D. Burd and R. W. Brodersen, "Processor design for portable systems," *Journal of VLSI Signal Processing Systems for Signal, Image and Video Technology*, vol. 13, no. 2, pp. 203–221, 1996.

[29] Y. Mao, J. Zhang, S. Song, and K. B. Letaief, "Power-delay tradeoff in multi-user mobile-edge computing systems," in *Proceedings of the 2016 IEEE Global Communications Conference (GLOBECOM)*, pp. 1–6, Washington, DC, USA, December 2016.

[30] Y. G. Kim, M. Kim, and S. W. Chung, "Enhancing energy efficiency of multimedia applications in heterogeneous mobile multi-core processors," *IEEE Transactions on Computers*, vol. 66, no. 11, pp. 1878–1889, 2017.

Hindawi
Mobile Information Systems
Volume 2021, Article ID 9948683, 11 pages
https://doi.org/10.1155/2021/9948683

Research Article

Open Innovation Mode of Green Innovation System for Manufacturing Industry

Shao Bo[1] **and Bi Kexin**[1,2]

[1]*School of Economics and Management, Harbin University of Science and Technology, Harbin 150080, China*
[2]*School of Economics and Management, Harbin Engineering University, Harbin 150080, China*

Correspondence should be addressed to Bi Kexin; xuanfeng@hrbust.edu.cn

Received 7 March 2021; Revised 28 March 2021; Accepted 18 June 2021; Published 28 June 2021

Academic Editor: Mian Ahmad Jan

Copyright © 2021 Shao Bo and Bi Kexin. This is an open access article distributed under the Creative Commons Attribution License, which permits unrestricted use, distribution, and reproduction in any medium, provided the original work is properly cited.

The open mode of the manufacturing innovation system under conventional conditions makes it difficult to realize the open operation of the green innovation system, which also lacks operational capability and has low analysis coverage. Therefore, an open model of the green innovation system in the manufacturing industry is put forward. The opening and functional elements of the model are determined. The mechanism of the environmental aspects is clarified. The adaptability of different levels of the innovation process is discussed, and its evolution theory is derived. Finally, the best open innovation model's selection rules are chosen to realize the analysis of the open innovation model's mechanism. Its established operational index and model mechanism are discovered for the manufacturing industry. The experimental data show that our proposed model of the green innovation system is more efficient than the conventional model as its operational ability is increased by 33.42%, and the coverage rate is enhanced by 54.32%.

1. Introduction

The open mode of the manufacturing industry's innovation system (under the conventional conditions) aims to provide services only to the manufacturing enterprises. Because of the restrictions imposed on the structure itself, it is challenging to realize the open, innovative operation of the green innovation system. Besides, there is a shortage of poor operational ability and low analysis coverage [1]. Therefore, green innovation of the manufacturing industry under the Internet is proposed. Based on the Internet conditions, the main elements of enterprises, governments, universities, and intermediaries are analyzed, and the internal relationships are established according to Oswald's market innovation theory [2]. The functional elements of knowledge development and knowledge diffusion are clarified, the available subjects of universities and governments are determined, and the natural environment, resources, and infrastructure are clearly defined. Green computing has a vibrant range of meanings, including power saving. It is also necessary to build a green manufacturing industry and play an essential role in constructing smart cities [3].

This study expounds on the open innovation evolution theory. It sets up the information selection rules of the open innovation mode by using the best choice of different subjects' internal or external elements to realize the open innovation model machine [4]. Based on the open innovation mechanism, we built our model, and the related indexes such as aggregation, nonlinearity, and diversity are determined [5, 6]. To ensure our open innovation model's effectiveness, the manufacturing industry's experimental environment is simulated. The operational capability and the analysis coverage simulation test are carried out using two open innovation models [7]. In [8], the authors studied the open innovation mode based on the Internet platform. They found that it is composed of the external system and internal system. The external system includes environment, policy, and technology. The internal system is strategy, value, incentive, and feedback. The internal and external systems work together to realize the open innovation mode. In [9], the authors

proposed that open innovation breaks enterprises' boundaries by interconnecting internal resources and external resources, continuously injects innovative ideas into enterprises, and improves enterprises' innovation levels. In [10], the authors used a case study to analyze the open innovation mode of Shenyang Machine Tool Co., Ltd. They found that its open innovation mode aims to achieve intelligent manufacturing, based on the Internet platform. Combined with the enterprise's internal management system, it promotes the development of enterprise's innovation level.

Till date, numerous studies have been conducted on industrial innovation applications, green innovation system, and open innovation mode. However, it can be found that the research of the open innovation mode mostly focuses on the manufacturing enterprise level. It rarely involves the industry level or the open innovation mode of the green innovation system. The research of the green innovation system mainly focuses on the construction and function of the enterprise's green innovation system, and the open innovation mode is the open innovation mode for the enterprise. Research on the impact and evaluation of innovation performance is less about the open innovation mode of industry and the innovation mode of the green innovation system. The conclusion of this paper can also enrich the academic research results in related research fields. The main contributions of this work are as follows.

(1) We suggest the selection of the open innovation mode for the industrial green innovation system. It starts from the resource theory and demand life cycle theory. It is considered that the specific requirements of the open innovation mode for the industrial green innovation system at different development stages are also different. Therefore, according to the specific analysis of the development stage of the green innovation system, it is necessary to select the open innovation mode suitable for the development stage innovative mode.

(2) The simulation model research results are more convincing. In this paper, the system dynamics model's test method is used to analyze the industrial green innovation system, and then, according to the software operation results, the future operation trend of the industrial green innovation system is evaluated. At the same time, according to the changes of the variables in the system, the simulation time period of the industrial green innovation system is divided into four development stages, and the simulation time is divided into four stages. Each stage of development has its own characteristics.

The rest of this paper is organized as follows. In Section 2, the establishment of an open innovation mode for the green innovation system in manufacturing industry is discussed. In Section 3, an analysis of the open innovation model is provided. In Section 4, the construction mechanism for an open innovation model is provided. In Section 5, experimental results are provided for our model. Finally, we conclude this paper in Section 6.

2. The Establishment of Open Innovation Mode for Green Innovation System in Manufacturing Industry

Elements are the basic components of the open innovation model of the green innovation system in the manufacturing industry [11]. This paper divides them into three main parts: main elements, functional elements, and environmental elements based on Internet conditions' advantages. The functional elements are the pioneering activities of green innovation, knowledge development (learning), knowledge diffusion, research orientation, market formation, resource flow, creation of legitimacy, and resistance to change. The environmental elements include the material environment (including the natural environment, resource environment, and infrastructure) and soft environment (including institutional environment, market environment, and cultural environment). There is a linkage between the main body, function, and environmental elements [12].

2.1. Determination of the Open Elements of the Subject. In the open mode of the innovation system, enterprises are the core body, which play a vital role. The enterprises directly face the market, first understand the market demand, and make the feedback in time. Its market reflection ability, information feedback ability, and green technology innovation ability play a key role in the operation of the whole green innovation system. According to Oswald's market innovation theory, the role of enterprises in the green innovation system can be expressed using the following equation:

$$\text{antcb} = \frac{\sum_{i=1}^{n} kH \cdot t}{C + F}. \tag{1}$$

In this equation, antcb represents the function element of the enterprise in the innovation system, k represents the market randomness, n represents the number of active enterprises in the market, C represents the reaction ability of the market, F represents the green innovation technical ability, and H represents the market feedback capability.

The relationship between the enterprises will help to form the scale of the industry, enhance the overall competitiveness of a single enterprise, and promote the development of the green innovation system of the whole manufacturing industry. School-enterprise cooperation is conducive to increasing the cooperative relationship between schools and enterprises [13]. It will increase knowledge accumulation and provide intellectual support for enterprises [14]. Moreover, cooperation between enterprises

and intermediaries is conducive to the smooth communication and connection between enterprises and internal bodies of the green innovation system, which build a key bridge between the enterprises and the various subjects [14]. Freeman pointed out that the role of the government in green innovation can be expressed using the following equation [15]:

$$F = \left[\frac{G - gV}{v_{\max}}, \frac{G - gV}{v_{\max}}\right]. \quad (2)$$

In this equation, F represents the government's influence on the green innovation subject, G represents the relevant policies formulated by the government, V represents the implementation of the policy, g represents the external elements, and v represents the feasibility [16].

The role of the government in the green innovation system of manufacturing industry has two sides [17]. On the one hand, it is a participant in the green innovation system, which plays the role of making various policies and regulating the laws and implementing them within the system. On the other hand, the government is the macroregulator of the whole green innovation system. It is necessary to rationally configure the resources within the whole system and guide the behavior of the main body [18].

Universities and research institutes provide knowledge sources for the green innovation system of the whole manufacturing industry. Institutions of higher learning and scientific research institutes are determined by their own attributes so that they can concentrate on the research and development of green technology. They often do not worry too much about market risk or market value. It is easier to develop a breakthrough technology with high market value and high technology content than the enterprises [19].

On the contrary, universities and scientific research institutes also carry out the cultivation of green creative talents. Talent is the carrier of knowledge. Many green innovation talents pour into the market, enrich the knowledge base of the green innovation system, and provide a large amount of resources for the system of knowledge reserve and talent reserve. At the same time, it is also conducive to the spread and diffusion of green technology and further promotes the operation of the green innovation system. The implementation of the green innovation system in universities can be expressed by the following equation [20]:

$$F_1 = \frac{G - SgV - W}{v_{\max} - g}. \quad (3)$$

Different from the enterprises and the government, the calculation of the ability to carry out the green innovation system is relatively simple, and the influence elements are few. In the equation, F_1 represents the ability of the green innovation system in universities, G represents the relevant policies formulated by the government, g represents the external influence elements, V represents the teacher's ability, and W represents the hardware environment of the university. The relationship between the faculty, the hardware environment, and the ability of the green innovation system in universities is shown in Figure 1.

It can be seen from the curve that there is a monotonic linear relationship between the faculty, hardware environment, and ability of the green innovation system in universities. The stronger the teachers and hardware capabilities of universities, the stronger the ability to implement the green innovation system described in.

Intermediaries play an important role in the current market economy under incomplete information. In the green innovation system, intermediary agencies do not participate in green innovation activities directly, but it is indispensable. The communication between enterprises, government, scientific research institutions, and other innovative bodies cannot be separated from intermediary agencies. The role of agencies in the green innovation system is shown as follows:

$$F_2 = \int\int g^p F^q f(x, y) d_x d_y. \quad (4)$$

On the one hand, intermediary agencies provide services for enterprises, including information dissemination, consulting services, and financial support, so as to reduce the number of invalid transactions under the condition of incomplete information. On the other hand, intermediaries are an adhesive in the green innovation system and can well coordinate the behavior between the various green innovation subjects.

2.2. Determination of Functional Elements. The so-called system function refers to something that the green innovation system of manufacturing industry is engaged in. Researchers around the globe have conducted multiple studies on the functions of innovation systems [21–24]. Based on these studies, combined with the computer conditions, the analysis of functional elements includes the following aspects.

If there is no entrepreneur and if innovation is impossible, then the green innovation system of manufacturing will not come into being. The role of entrepreneurs is to transform new knowledge development capabilities, networks, and markets to generate and utilizes industry opportunities:

$$g(i, j) = \frac{f(i, j) - f_{\min}}{f_{\max} - f_{\min}}. \quad (5)$$

In this equation, $g(i, j)$represents the learning mechanism function of knowledge development (learning), $f(i, j)$ represents the entrepreneur function in the green innovation system of manufacturing industry, $f_{\max}$ represents the maximum function coefficient, and $f_{\min}$ represents the minimum function coefficient.

The authors in [25] believe that the basic function of the innovation system is information exchange, i.e., knowledge diffusion. In the green innovation system, knowledge diffusion is also important in a strict R&D environment, while the development schedule will also be influenced by norms and value changes. From this point of view, the network interaction of the green innovation system in manufacturing industry is a prerequisite for interactive learning. If it is a

consumer producer network, then it can be seen as learning in use. Combined with equation (5), we get the knowledge diffusion function $u(i, j)$and the relation curve with $g(i, j)/f(i, j)$, as shown in Figure 2.

According to the curve, we can get better knowledge diffusion when the entrepreneur and learning mechanism are sound. On the contrary, when entrepreneurs or learning mechanisms are not perfect, it is difficult to obtain better knowledge diffusion. For example, the government issued a statement aimed at achieving a certain proportion of renewable energy in the next few years. The implementation of sustainable energy technology development has stimulated the flow of resources needed to promote this development. At the same time, there are exceptions because accidental exceptions may lead to a specific theme, resulting in a specific direction of change.

Resource flow that includes financial resources and human resources are important inputs for all activities in the green innovation system of manufacturing industry. Especially in biotechnology, the rich availability of biological resources is a potential element determining the success or failure of projects. It can be defined as follows:

$$M = L - L_0 + kA. \tag{6}$$

We must create a sense of legitimacy/change resistance, and new technology must become part of the existing system or overturn it. Interested bodies often object to this creative destruction. In this way, advocating joint will become a catalyst to promote the legalization of new technologies and hinder opposition to change.

2.3. Determination of Environmental Elements. The system has the same function and its restraint and standardization. If the current system is not coordinated with the development of the green innovation system in the manufacturing industry, the development will be restricted, and the relevant departments of the government and other relevant departments should be adjusted accordingly. Therefore, in order to ensure the continuous progress and perfection of the green innovation system in the manufacturing industry, the institutional environment must be constantly changed and self-rectified to promote the smooth development of the green innovation activities of the manufacturing industry. It can be described by the following equation:

$$H = \frac{\partial^2 M}{\partial V \cdot \partial (A_1 + A_2)}. \tag{7}$$

A good market environment will play a positive role in stimulating the green innovation system of manufacturing industry. First, the market can test whether green innovation is successful. Under the conditions of the fully developed market economy, a successful new technology, which is welcomed by the consumer, will quickly occupy the monopoly position, form the technical barrier, obtain the excess profit, and not be easily imitated action of a good competition mechanism. In the market, competition and cooperation are the same. Green technology innovation in manufacturing industry has high risk and uncertainty, constantly learning, improving and self-improving, and seeking survival in the competition. The schematic diagram of the green innovation system of manufacturing industry can be expressed in Figure 3. At the same time, the correlation between hard environment element (A_1) and soft environment coefficient (A_2) can be reflected from the following diagram.

Social culture environment is a subtle spiritual force that indirectly affects the open mode of the green innovation system in manufacturing industry. In the green innovation system of manufacturing industry, a good social and cultural environment is conducive to the development of green innovation activities among various subjects. At the same time, it is also beneficial to the communication and study among various subjects and to realize the long-term and benign operation.

3. Analysis of the Mechanism of Open Innovation Model Construction

In this section, first we analyze the theory of open innovation evaluation followed by the formulation of information selection rules of the open innovation mode.

3.1. Analysis of the Theory of Open Innovation Evolution. In 1994, John Holland formally proposed the open innovation system theory (OST). The theory is based on the open innovation evolution perspective to analyze the origin of open innovation. The adaptability of the macrolevel is the process of investigating how the subject can present with the external knowledge and technology in the macroenvironment of the external economy and the globalization of technology. The core idea of open innovation theory is to create openness with adaptability. The basic characteristic function of its open innovation mode is shown in the following equation:

$$\begin{cases} F\dfrac{\partial y}{\partial x} = MU + A\dfrac{\partial P}{\partial x} + qS, \\ \\ M\left(\dfrac{\partial}{\partial t} + U\dfrac{\partial}{\partial x}\right)^2 y + (qS + MU)\dfrac{\partial y}{\partial x} + F = 0. \end{cases} \tag{8}$$

In this equation, M represents the return rate of the green innovation system in manufacturing industry, F represents green innovation technical ability, A is the return item, U represents adaptive subjectivity, x and y represent the adaptability of the environment and individual, q represents the macroreaction coefficient, and S represents the microcosmic reaction coefficient.

3.2. Formulation of the Information Selection Rules of the Open Innovation Model. Through the integration of internal and external resources of the enterprise, the utility maximization can be obtained, and the open innovation pattern awareness maximizes the innovation performance through the integration of internal and external resources. Innovation

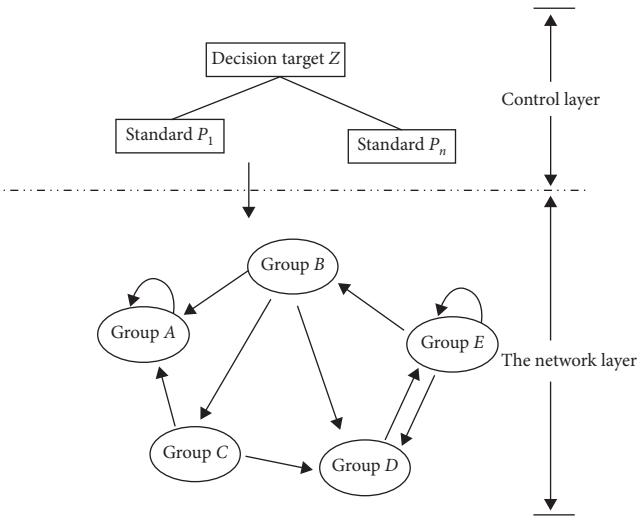

Figure 1: The relationship between the faculty, hardware environment, and ability of the green innovation system in universities.

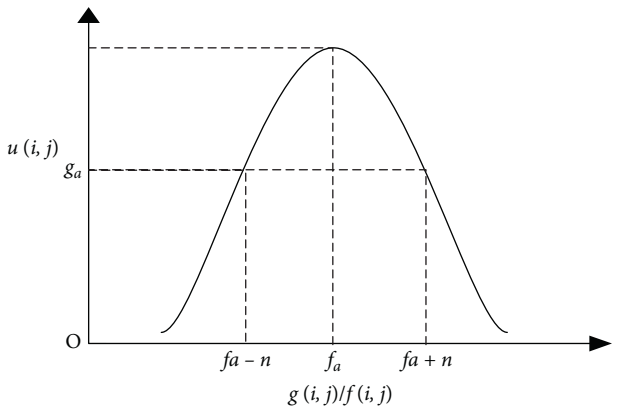

Figure 2: The relationship between knowledge diffusion and entrepreneurial learning mechanism.

adaptability is a rule to distinguish information through a kind of internal information. When exploring the current system information, it can judge the current form and take action. The open innovation model is also when a subject develops new technology or new product. The results are passed so that other enterprises can learn from them. It can use Figure 4 to represent the optimal selection curve of the two different subjects inside or outside. The best choice curve between the two subjects inside or outside is shown in Figure 4.

Open innovation is an innovative activity integrating knowledge innovation, technology innovation, and system innovation. In the innovation activities, the innovation elements will flow and change, especially the innovation elements such as funds, information, technology, knowledge and talents, and continuous transformation between enterprises and environment. The innovative and open characteristics of the open innovation require that the innovative subjects need to continuously improve their adaptability to meet the changes in the internal and external environment of innovation. Open innovation also has the characteristics of the green innovation system. The characteristic function can be expressed in the following equation:

$$\begin{cases} R(x) = r_{n-1}x^{n-1} + r_{n-2}x^{n-2} + \cdots + r_1 x + r, \\ C(x) = c_{n-1}x^{n-1} + c_{n-2}x^{n-2} + \cdots + c_1 x + c, \\ E(x) = e_{n-1}x^{n-1} + e_{n-2}x^{n-2} + \cdots + e_1 x + c. \end{cases} \tag{9}$$

In this equation, $R(x)$ represents the knowledge innovation of open innovation, $C(x)$ represents the technological innovation of open innovation, $E(x)$ represents the system innovation of open innovation, r represents knowledge innovation ability, c represents system innovation ability, and e represents system innovation ability.

4. Construction of Open Innovation Model

In this section, first we determine the operating index followed by the operation mechanism of the open innovation model.

4.1. Determination of the Operating Index. The concept of the green innovation system mainly revolves around "four characteristics and three mechanisms." Four characteristics are reflected by aggregation, nonlinearity, flow, and diversity, and the three mechanisms are through identification, internal mechanism, and building blocks. The characteristics of the subject are the process of adapting to the environment under the action of the green innovation system in order to adapt to the change of the environment. The mechanism is the lubricant and coordination agent in the process of the subject adaptation, reflecting the application process of the main whole and the external environment. Similarly, in the open innovation mode, we can find the corresponding process of how the main body and mechanism of enterprises change. The formula can be expressed as

$$G = \frac{\partial^2 a}{\partial \delta} \cdot \sum_{i=1}^{n} \lambda p \cdot \left(mv^2 + oz + G_0\right) - G\alpha. \tag{10}$$

Here, G represents a unified dimensional unit, a represents the overall coefficient, δ represents the integrity of 7 indicators, λ represents aggregation, p represents nonlinear, m represents flow (flows), v represents diversity identification, α represents internal model, O represents building blocks, and z represents diversity. The specific meaning is as follows:

(i) Aggregation: the subject is based on the similarity and commonality of R&D to gather the available bodies together through the features of "adhesion." The effect of aggregation is the mechanism of R&D activities at different levels after a low level of screening. In the innovation model of the equipment manufacturing industry, the main body of innovation consists of a large number of interacted entities, such as enterprises, universities, scientific research institutions, government, and technical intermediaries. These bodies can form more

advanced subjects through interaction, such as industrial alliance, industry research alliance, and official production. This can highlight the characteristics of aggregation at different levels. The aggregation formula is shown in equation (11); λ represents aggregation, λ_0 represents initial aggregation, e stands for R&D similarity, and f represents R&D commonality:

$$\lambda = p\lambda_0 + \log\left(a^n + ef\right). \tag{11}$$

The main body of the equipment manufacturing system in China has the mechanism of adaptation and learning. It is not a direct purchase application and a simple imitation, but through digestion and absorption of relevant content, so as to gradually improve innovation capabilities.

(ii) Diversity: it reflects the different characteristics of the subject, and the advantages of the enterprise in a certain aspect, such as some of the automobile enterprises are good at developing the engine, display screen, and design, and the versatility is the prerequisite for the continuous evolution of the system. In China's equipment manufacturing system, each subject has his own unique technology, product, service characteristics, scientific research achievements, and scientific research expertise, which determine the diversity of different subjects. The influence function on diversity is shown in the following equation:

$$z = \frac{\sum_{i=1}^{n}\left(a_i - \overline{a}\right)\left(f_i - \overline{f}\right)\cdot 1}{\sum_{i=1}^{n}\left(h_i - \overline{h}\right)}. \tag{12}$$

Here, z stands for diversity, a stands for theme embodiment, f represents relative advantages, and h represents acceptance of the masses.

(iii) Tagging: tagging refers to the ability of a subject to recognize and respond from different information through its choice of diversity. It is the process of selecting valuable information in diversity, and different subjects have different tags and response mechanisms for the information obtained. In China's equipment manufacturing system, enterprises, universities, government, research institutions, and other industrial technologies are all tags; the aggregation of the various main bodies forms the different industries, enterprise groups, industry and research community, knowledge community, and so on.

(iv) Internal model: the mechanism that the main body will collect and transform the innovation source within the enterprise and innovate it. The subject is required to enter the selected innovation source into the internal structure model of the system and select the structure of the model in the innovation system. In this internal model, the innovation body can foresee the output structure obtained by the input. For enterprises, universities, scientific research institutions, and government, they all have the foreseen mechanism and ability. If we meet the innovation pressure, we can improve the innovation ability by changing the internal structure, such as the innovation model.

(v) Building blocks: also known as the component, it is the key element in the open innovation model, such as the technical personnel of scientific research, capital, equipment, science and technology, knowledge and information, management system, and operation mechanism:

$$O = \frac{p\sum_{i=1}^{n}\left(r_i - \overline{r}\right)\left(c_i - \overline{c}\right)\cdot 1}{\left[\sum_{i=1}^{n}\left(b_i - \overline{b}\right)\right] + \log\left(r^n + ui\right)}. \tag{13}$$

Here, O represents building blocks, r represents relevant technical personnel, c represents equipment, b represents funds, n represents technology and technology knowledge, u represents the information management system, and i represents the operation mechanism.

4.2. Operation Mechanism of Open Innovation Model. The open innovation of equipment manufacturing industry includes seven elements, namely, four characteristics and three mechanisms, which are involved in the innovation system. It mainly includes the basic and core elements of the model, which can be described in an open innovation module with signs, attributes, and behavior.

(i) Logo: the characteristics of the element identification included in the innovation adaptive system are also to distinguish the signs of other enterprises because each open innovation is different from the other open innovation, and each subject has its own unique characteristics. That is to say, each open innovation has special logos in the microenvironment and macroenvironment. The initiative adaptability of open innovation is to start with identifying logos.

(ii) Property: the characteristics of diversity are included in the innovation adaptive system because open innovation is a unique symbol; in the process of stimulus response modeling, we need to consider the properties of the physical, space, and quality of the main body. The attributes in the model are the characteristics of other subjects encountered by the enterprise in the external environment. These attributes will be applied to the implementation process of the main body. It is also the basis of the decision analysis of the subject.

(iii) Behavior: that is to say, the system will finally show the process of aggregation, nonlinearity, flow, internal models, and building blocks. After determining the main body in the innovation adaptive system, the innovation results are generated by the interaction of material flow, information flow, and

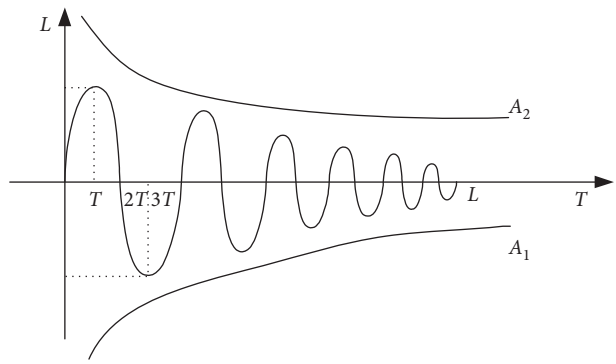

Figure 3: Dynamic schematic diagram of a green innovation system in the manufacturing industry.

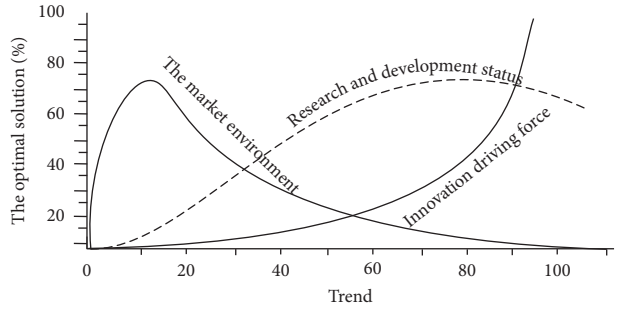

Figure 4: The best choice curve between the two subjects inside or outside.

energy flow in the mechanism of the innovation adaptive system through mutual learning. This is the process of which the main body acts, makes decisions, and adapts. That is the necessary condition for the stimulus response mode. It describes the correlation relationship, as shown in Figure 5.

The main model of the green innovation system theory is the stimulus response mechanism: this model can reflect the behavior pattern of the main body at the microlevel. The adaptive evolution of each adaptive subject requires three aspects of a detector, an effector, and an IF/THEN rule. The stimulus that the main body uses the detector to receive the external environment is also the input of relevant information, knowledge, and technology. The effector is the output of the external stimulus through a certain adaptive process. The IF/THEN rule is the process of responding to the input stimulus. In response to realistic activities, OST theory sets different rules, and different ways can be chosen for different stimuli. The open innovation mode of equipment manufacturing industry based on the stimulus response is shown in Figure 6.

On one hand, the green innovation system of manufacturing industry can optimize the market structure, improve the degree of rationalization of the industrial structure, and promote the innovation of the system. On the other hand, the green innovation system in manufacturing industry is also beneficial to the improvement of the economic level and the quality of the products. Facing the resource crisis, we made contributions to effectively implement green innovation activities for energy conservation and emission reduction.

5. Experimental Analyses

In order to ensure the effectiveness of the open innovation mode of the green innovation system in manufacturing industry under the Internet condition, the simulation analysis is carried out. During the test, different manufacturing industries were used as the test objects to carry out the simulation test of operational capability and analysis coverage. The different production types and scale of manufacturing are simulated.

5.1. Data Preparation. The parameter settings for the original data are shown in Table 1.

5.2. Analysis of Test Results. The operation capability and the analysis coverage simulation test are carried out only for the different manufacturing industries and the open innovation model of different innovation systems. The test curve of its operating capacity is shown in Figure 7.

In the above figure, Figure 7(a) is the test curve of the traditional method's running ability and Figure 7(b) is the running ability curve of the proposed method. According to the test curve, the operation ability of the traditional method is 65%, and the operation ability of the proposed method is 98.42. The open innovation mode of the green innovation system is 33.42% higher than that of the conventional model.

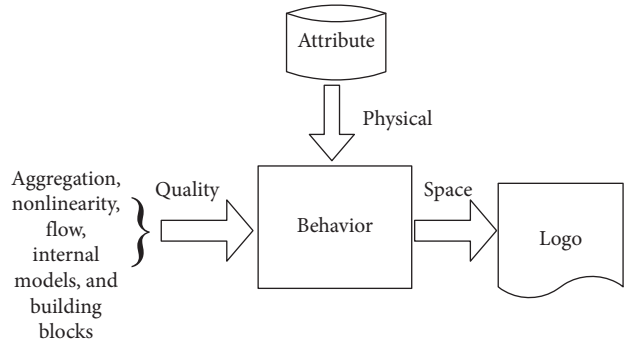

Figure 5: The correlation relationship.

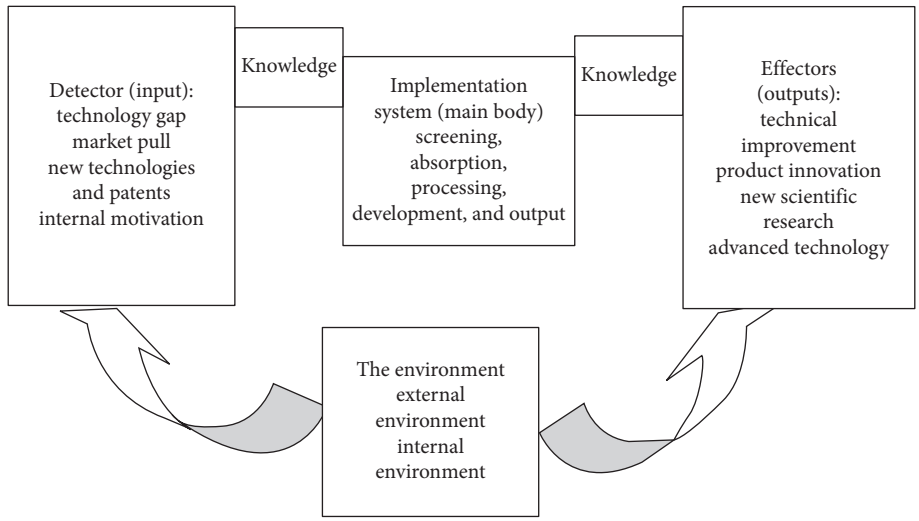

Figure 6: Open innovation model of equipment manufacturing industry based on the stimulus response.

Table 1: Test parameters' setting.

Manufacturing type	Manufacturing scale/5 million	The production type
Agricultural and sideline food processing industry	50	Engineer to order
Manufacturing of railway, ship, aerospace, and other transportation equipment	200	Engineer to project
Wine, drinks, and refined tea	450	Make to order
Nonferrous metal smelting and rolling industry	650	Assemble to order
Black metal smelting and rolling industry	750	Make to stock
Textile and clothing industry	200	Repetitive
Leather, fur, feathers and their products, and footwear	450	Batch
Wood processing and wood, bamboo, rattan, brown, and grass products	650	Continuous
Manufacturing of computers, communications, and other electronic equipment	20	Engineer to order
Metal products, machinery, and equipment repair	4	Engineer to project
Printing and recording media reproduction	3850	Make to order
Education, industry, sports, and entertainment industries	350	Assemble to order
Petroleum processing, coking, and nuclear fuel processing industries	12	Make to stock

At the same time, two different methods are used to analyze the coverage test. Analysis of coverage test curves is shown in Figure 8.

Figure 8(a) is the test curve of the traditional method's running ability under the low difficulty. Figure 8(b) is the running ability curve of this method under the low difficulty. Figure 8(c) is the test curve of the traditional method running ability under the high difficulty, and Figure 8(d) is the running ability curve of this method under the high difficulty. Through third party analysis software, the average value of the arithmetic is taken. The two methods run under different difficulty levels, and the coverage rate is not obvious. The open innovation model of the green innovation system is compared with the conventional model; the

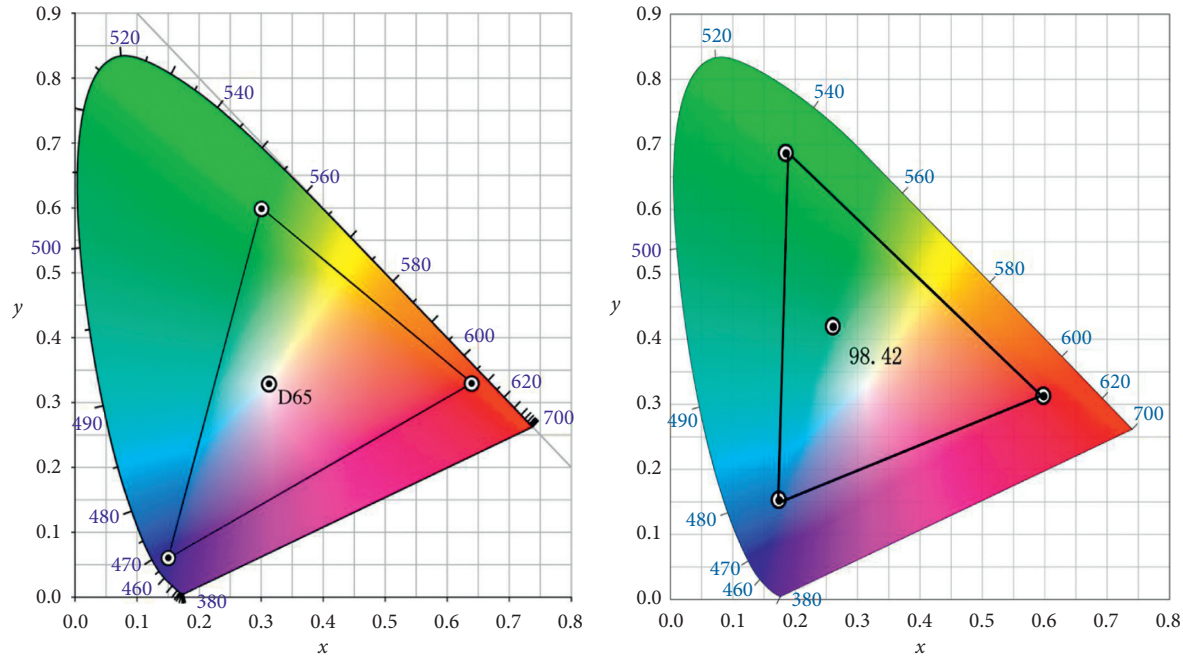

(a) (b)

Figure 7: Running capacity test curve.

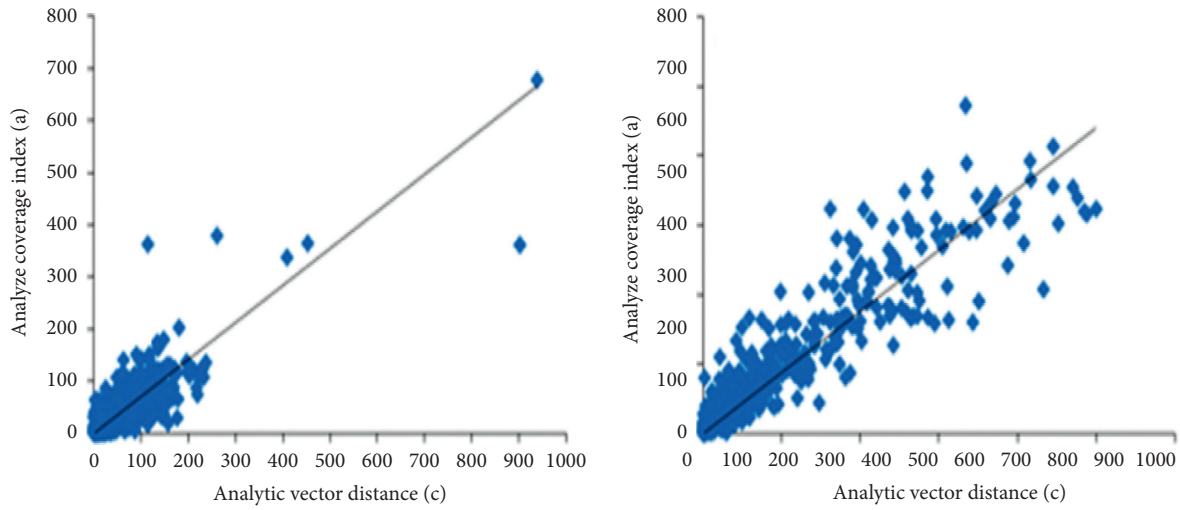

(a) (b)

Figure 8: Continued.

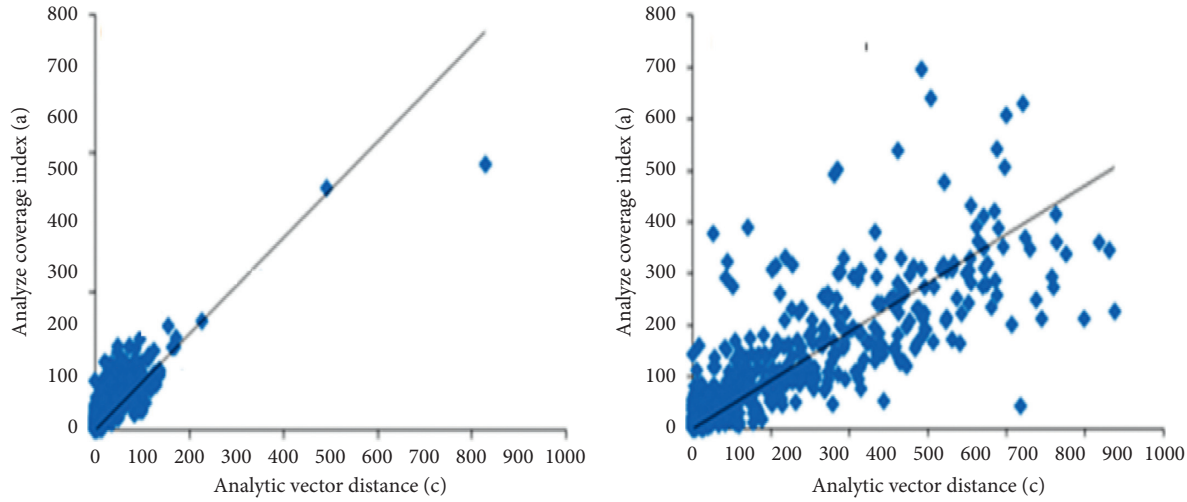

Figure 8: Analysis of coverage test curves.

coverage rate is raised by 54.32%. It can realize the open and innovative operation of the green innovation system.

6. Conclusion

In this paper, an open innovation model of a green innovation system in the manufacturing industry is put forward. Its mechanism is analyzed, and the model is built to realize the objective of this paper. The influencing factors of the open innovation model based on the industrial green innovation system are clarified. Through the relevant literature research and the understanding of related concepts, the model's influencing factors, i.e., the system's participants, the openness, and the technological environment, are examined. The influence of the system participants mainly comes from the participants' innovation strength, the innovation resources owned by the participants, the number of participants, etc. The influence of openness primarily comes from the industrial green innovation system's exposure, the openness of the innovation subjects within the system, etc. The technological environment's influence mainly comes from the integration of technology and industrial production chain and the integration of technology under the environment. The understanding of these factors provides a basic reference for the classification of the open innovation model. Moreover, this paper classifies the open innovation mode, based on the industrial green innovation system, into numerous influencing factors: innovation alliance mode, investment and merger mode, resource integration mode, and open platform mode. According to the resource-based theory and life cycle theory, the selection ideas and research methods of the open innovation mode are determined.

Data Availability

The data used to support the findings of this study are available from the corresponding author upon request.

Conflicts of Interest

The authors declare that they have no conflicts of interest.

References

[1] Y. Xing and H. Li, "A simulation study on optimization and forecast of material supply demand in automobile manufacturing industry," *Computer Simulation*, vol. 33, no. 10, pp. 421–424, 2016.

[2] P. Lu, Y. Mou, and Z. Zhang, "Study on the detection method of unreachable function call path in complex system," *Computer Simulation*, vol. 33, no. 9, pp. 426–430, 2016.

[3] Y. Xu, G. Y. Zhang, and D. Sheng, "Research on the growth model of scientific and technological innovation talents based on hierarchical clustering," *Computer Simulation*, vol. 34, no. 8, pp. 351–355, 2017.

[4] H. H. Chen, S. Chen, and Y. Lan, "Attaining a sustainable competitive advantage in the smart grid industry of China using suitable open innovation intermediaries," *Renewable & Sustainable Energy Reviews*, vol. 62, pp. 1083–1091, 2016.

[5] H. K. Jin, S. Kim, and K. Kim, "The role of learning capability in market-oriented firms in the context of open innovation-based technology acquisition: empirical evidence from the Korean manufacturing sector," *International Journal of Technology Management*, vol. 70, no. 2-3, p. 135, 2016.

[6] M. Usman, M. A. Jan, X. He, and J. Chen, "A survey on big multimedia data processing and management in smart cities," *ACM Computing Surveys (CSUR)*, vol. 52, no. 3, pp. 1–29, 2019.

[7] G. Wang, X. Tian, Y. Hu et al., "Manufacturing process innovation-oriented knowledge evaluation using MCDM and fuzzy linguistic computing in an open innovation environment," *Sustainability*, vol. 9, no. 9, pp. 1–19, 2017.

[8] S. O. Shim and K. B. Park, "Technology for production scheduling of jobs for open innovation and sustainability with fixed processing property on parallel machines," *Sustainability*, vol. 8, no. 9, p. 904, 2016.

[9] S. Ortega-Requena and S. Rebouillat, "ChemInform abstract: bigger data open innovation: potential applications of value-added products from milk and sustainable valorization of by-

products from the dairy industry," *Green Chemistry*, vol. 47, no. 7, pp. 5100–5113, 2016.

[10] A. Zobel, "Benefiting from open innovation: a multidimensional model of absorptive capacity," *Journal of Product Innovation Management*, vol. 34, no. 3, pp. 269–288, 2017.

[11] X. Zhu, M. C. Dong, J. Gu et al., "How do informal ties drive open innovation? the contingency role of market dynamism," *IEEE Transactions on Engineering Management*, vol. 64, no. 2, pp. 208–219, 2017.

[12] B. Yuan and Q. Xiang, "Environmental regulation, industrial innovation and green development of Chinese manufacturing: based on an extended CDM model," *Journal of Cleaner Production*, vol. 176, pp. 895–908, 2018.

[13] N. Nilsson and T. Minssen, "Unlocking the full potential of open innovation in the life sciences through a classification system," *Drug Discovery Today*, vol. 23, no. 4, pp. 771–775, 2018.

[14] J. Hou, H. Chen, and J. Xu, "External knowledge sourcing and green innovation growth with environmental and energy regulations: evidence from manufacturing in China," *Sustainability*, vol. 9, no. 3, p. 342, 2017.

[15] N. Miglietta, E. Battisti, and F. Campanella, "Value maximization and open innovation in food and beverage industry: evidence from US market," *British Food Journal*, vol. 119, no. 11, pp. 2477–2492, 2017.

[16] J. L. Wadin, K. Ahlgren, and L. Bengtsson, "Joint business model innovation for sustainable transformation of industries-a large multinational utility in alliance with a small solar energy company," *Journal of Cleaner Production*, vol. 160, pp. 139–150, 2017.

[17] M. A. Jan, W. Zhang, M. Usman, Z. Tan, F. Khan, and E. Luo, "SmartEdge: an end-to-end encryption framework for an edge-enabled smart city application," *Journal of Network and Computer Applications*, vol. 137, pp. 1–10, 2019.

[18] Z. Feng and W. Chen, "Environmental regulation, green innovation, and industrial green development: an empirical analysis based on the spatial durbin model," *Sustainability*, vol. 10, no. 1, p. 223, 2018.

[19] A. Akbar, M. Ibrar, M. A. Jan, A. K. Bashir, and L. Wang, "SDN-enabled adaptive and reliable communication in IoT-fog environment using machine learning and multi-objective optimization," *IEEE Internet of Things Journal*, vol. 8, no. 5, pp. 3057–3065, 2020.

[20] E. A. Severo, J. C. F. D. Guimarães, and E. C. H. Dorion, "Cleaner production and environmental management as sustainable product innovation antecedents: a survey in Brazilian industries," *Journal of Cleaner Production*, vol. 142, no. 1, pp. 87–97, 2018.

[21] F. Khan, A. ur Rehman, and M. A. Jan, "A secured and reliable communication scheme in cognitive hybrid ARQ-aided smart city," *Computers & Electrical Engineering*, vol. 81, pp. 291–302, 2020.

[22] S. Lin, J. Sun, D. Marinova et al., "Evaluation of the green technology innovation efficiency of China's manufacturing industries: DEA window analysis with ideal window width," *Technology Analysis & Strategic Management*, vol. 30, no. 1, pp. 1–16, 2018.

[23] X. Xie, J. Huo, G. Qi et al., "Green process innovation and financial performance in emerging economies: moderating effects of absorptive capacity and green subsidies," *IEEE Transactions on Engineering Management*, vol. 63, no. 1, pp. 101–112, 2016.

[24] M. Usman, M. A. Jan, A. Jolfaei, M. Xu, X. He, and J. Chen, "A distributed and anonymous data collection framework based on multilevel edge computing architecture," *IEEE Transactions on Industrial Informatics*, vol. 16, no. 9, pp. 6114–6123, 2019.

[25] Y. Guo, X. Xia, S. Zhang et al., "Environmental regulation, government R&D funding and green technology innovation: evidence from China provincial data," *Sustainability*, vol. 51, no. 4, pp. 1563–2157, 2017.

Hindawi
Mobile Information Systems
Volume 2021, Article ID 9987462, 9 pages
https://doi.org/10.1155/2021/9987462

Research Article

KoRASA: Pipeline Optimization for Open-Source Korean Natural Language Understanding Framework Based on Deep Learning

Myeong-Ha Hwang, Jikang Shin, Hojin Seo, Jeong-Seon Im, and Hee Cho

Digital Solution Laboratory, Korea Electric Power Research Institute (KEPRI), Daejeon, Republic of Korea

Correspondence should be addressed to Myeong-Ha Hwang; mh.hwang@kepco.co.kr

Received 15 March 2021; Revised 27 May 2021; Accepted 14 June 2021; Published 24 June 2021

Academic Editor: Muhammad Bilal

Copyright © 2021 Myeong-Ha Hwang et al. This is an open access article distributed under the Creative Commons Attribution License, which permits unrestricted use, distribution, and reproduction in any medium, provided the original work is properly cited.

Since the emergence of deep learning-based chatbots for knowledge services, numerous research and development projects have been conducted in various industries. A high demand for chatbots has drastically increased the global market size; however, the limited functional scalability of open-domain chatbots is a challenge to their application to industries. Moreover, as most chatbot frameworks employ English, it is necessary to create chatbots customized for other languages. To address this problem, this paper proposes KoRASA as a pipeline-optimization method, which uses a deep learning-based open-source chatbot framework to understand the Korean language. KoRASA is a closed-domain chatbot that is applicable across a wide range of industries in Korea. KoRASA's operation consists of four stages: tokenization, featurization, intent classification, and entity extraction. The accuracy and $F1$-score of KoRASA were measured based on datasets taken from common tasks carried out in most industrial fields. The algorithm for intent classification and entity extraction was optimized. The accuracy and $F1$-score were 98.2% and 98.4% for intent classification and 97.4% and 94.7% for entity extraction, respectively. Furthermore, these results are better than those achieved by existing models. Accordingly, KoRASA can be applied to various industries, including mobile services based on closed-domain chatbots using Korean, robotic process automation (RPA), edge computing, and Internet of Energy (IoE) services.

1. Introduction

Chatbots are communication tools that can be used to achieve a goal through automated dialog without human intervention [1]. Similar to a personal assistant, chatbots have been used in various applications, such as booking restaurant reservations, assisting with shopping, and conducting web searches. In recent years, many businesses around the world have strengthened their competitiveness by using chatbots and, as a result, many industries in Korea have also introduced chatbots in their services [2]. The global market size of chatbots is increasing at a rapid pace, as the benefits they provide have produced a high demand. Accordingly, large companies such as Facebook, Google, and Naver have started providing chatbot services as part of their professional services [3]. For example, in April 2016, eight years after Steve Jobs introduced the App Store, Mark Zuckerberg of Facebook announced the launch of Facebook Messenger platform, which includes chatbots. The number of users on that platform has reached over one billion, which exceeds the number of iPhone users that existed at the launch of the App Store.

However, application of open-domain chatbots is not effective in every industry because of the limited functional scalability of these chatbots. Moreover, as most chatbot frameworks employ English, it is necessary to create chatbots customized for other languages. To this end, this paper proposes KoRASA as a pipeline-optimization method using a deep learning-based open-source chatbot framework to understand the Korean language. KoRASA, which is a closed-domain chatbot, consists of four stages: (1) a tokenization step, which separates the corpus into tokens, i.e., language elements that cannot be further grammatically divided; (2) a featurization step, which extracts the features of each token; (3) an intent classification step, which classifies the intent of each question posed to the chatbot; and

(4) an entity extraction step, which extracts the relevant entity from the question sentence. In the present study, an optimization experiment was performed at each stage with respect to the Korean language understanding. Based on datasets reflecting common tasks in industry, the accuracy and $F1$-score of our proposed method were 98.2% and 98.4% for intent classification and 97.4% and 94.7% for entity extraction, respectively. Accordingly, KoRASA can be used not only for developing a closed-domain chatbot for the Korean language, but also for various industrial purposes such as mobile chatbot services, edge computing services, and robotic process automation (RPA) services.

The remainder of this paper is organized as follows. In Section 2, related work is discussed. The method of our proposed work is explained in Section 3 and we provide experimental results in Section 4. Finally, we conclude the paper with future research directions in Section 5.

2. Related Work

2.1. Chatbot Framework. As numerous companies have started introducing and utilizing chatbots in recent years, various research and development projects have been conducted to improve the functionality of chatbots. Adamopoulou et al. [4] introduced the history, technologies, and applications of chatbots, and Cahn [5] proposed the architecture and design of chatbots and the process of chatbot development, thereby presenting guidelines for chatbot researchers and developers to follow. Figure 1 shows the architecture of a typical chatbot. When a user inputs a message, the intent is classified, and an entity is extracted by the natural language understanding (NLU) component. A tracker maintains a conversation state, while the intent and entity (which have been classified and extracted by NLU) are put into slots to await further processing. A dialog management system then designates the next action based on previous actions, action results, and the contents of the slots. The message generator then provides the user with a corresponding response. If it is necessary to extract data from a database or URL, an application programming interface (API) is used for communication, transmission, and reception.

Gwendal et al. [6] suggested a Xatkit framework to develop a multimodal low-code chatbot. Xatkit comes with a runtime engine that automatically deploys the chatbot application and manages the defined conversation logic over the platforms of choice. Addi et al. [7] developed a chatbot based on knowledge graphs, which led to the emergence of chatbots capable of learning diverse data types. Furthermore, Park et al. [8] developed a framework for developing dialog systems in a smart home environment. The framework ontologically presents the knowledge required for the task-oriented dialog system's process and can build a dialog system by editing the dialog knowledge. Reshmi and Balakrishnan [9] proposed an interface framework for providing customer service chatbots. More specifically, they proposed an integration method with big data as a knowledge base for the chatbots that can enable the generation of dynamic responses to user queries and improve the analytical capability of chatbots with data from a distributed environment. By using chatbots in this manner, developers can create services that are tailored to specific fields and increase the productivity of companies. However, because the chatbots proposed by these studies are based on frameworks that were designed for specific purposes, their development and use in a broad range of industries are limited.

2.2. Natural Language Understanding (NLU). The key technology used in chatbots is NLU, which involves transforming natural language expressions into a machine-readable format. Figure 2 illustrates the architecture of NLU. The preprocessing stage of NLU is divided into two substages. The first substage is tokenization, in which a corpus is divided into tokens, which are the grammatically indivisible units of a language. The second substage is featurization, wherein the features of each token are extracted. After the preprocessing stage, intent is classified to ensure that the user's request message is sufficiently understood, and an entity is extracted to provide a suitable response. Through this process, a user-friendly chatbot system can be developed.

There are two types of NLU [10]: rule-based and deep-learning-based. Rule-based NLU depends on features extracted by humans, which means that it takes an extended period to manually extract features from sample user input. In addition, the accuracy of rule-based NLUs decreases as document volume increases. Deep-learning-based NLU automatically extracts and learns features from the data. Compared with the existing rule-based NLUs, it enables wider contextual processing and can also be used to build multimodal models by combining it with models that learn other types of data, such as images and voices. Accordingly, many recent studies have actively employed deep-learning-based NLU.

For example, Radford and Narasimhan [11] conducted research on improving natural language understanding using the generative pretraining model. Liu et al. [12] designed and developed multitask deep neural networks for natural language understanding. Jiao et al. [13] developed a method using the popular transformer-based machine learning technique BERT for natural language understanding. In the field of NLU research, studies on understanding natural language using transformer are becoming increasingly popular [14].

Among the different deep-learning-based NLU services, LUIS, Watson Conversation, API.ai, and RASA have been widely used in recent years [15–18]. Braun et al. [19] evaluated these NLU services for conversational question-answering systems (see Table 1). Such NLU services share the same basic concept: users can train intent classification and entity extraction based on example data. In the performance evaluation of the NLU services of chatbots, RASA and LUIS achieved an F-score of 0.94, whereas Watson Conversation and API.ai only achieved scores of 0.74 and 0.68, respectively. In particular, RASA, an open-source chatbot framework, is a strong framework as it enables users to easily

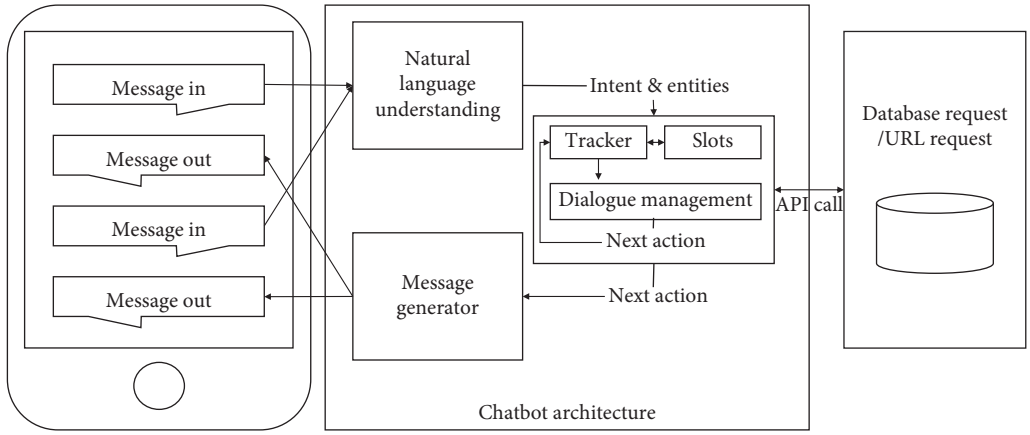

Figure 1: Chatbot architecture.

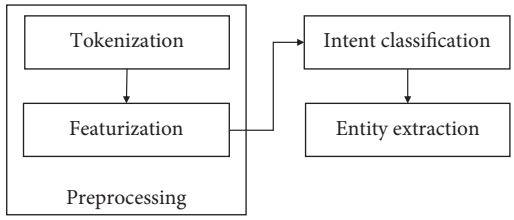

Figure 2: Architecture of natural language understanding (NLU).

develop the functions of machine-learning-based dialog management and natural language understanding. Therefore, in the present study, we adopted RASA as a deep learning-based open-source chatbot framework [18]. However, RASA is optimized for English; thus, to develop a chatbot for use in Korean industries, the framework must be optimized through performance experiments, examining the different stages in the pipeline, to enable it to understand the Korean language.

Recently, deep learning has been actively applied in various industrial as well as NLU fields. O'Shea and Hoydis [20] developed a new fundamental method of considering communications system design as an end-to-end reconstruction task. They demonstrated the application of convolutional neural networks on raw IQ samples for modulation classification. Aceto et al. [21, 22] proposed a general framework for deep learning-based mobile and encrypted traffic classification based on a rigorous definition of its milestones. They overcame the design limitations of previous works by envisioning the simultaneous use of multimodal and multitask techniques. Hwang et al. [23] proposed Gen2Vec, a search engine-based framework for operating power plants using deep learning. Gen2Vec can be the core engine of the knowledge system for power plant operators and can be used in search and chatbot services for power plant operation programs and new employee training. Wang et al. [24] proposed a deep learning-based ensemble approach for probabilistic wind power forecasting. They could effectively extract the nonlinear and stochastic nature exhibited in each wind power frequency, and the latter could cancel out the diverse errors. Wang et al. [25] proposed a method of detecting potential adverse drug reactions (ADRs) using a deep neural network model. They could not only discover the potential ADRs of drugs but also predict the possible ADRs of new drugs. Roman et al. [26] proposed a machine learning pipeline for battery state-of-health estimation, providing insights into the design of scalable data-driven models for battery SOH estimation, emphasizing the value of confidence bounds around the prediction.

Table 1: *F*-scores for the different NLU services.

Service	*F*-score
LUIS	0.94
Watson	0.74
API.ai	0.68
RASA	0.94

3. KoRASA: Pipeline Optimization for Open-Source Korean Natural Language Understanding Based on Deep Learning

3.1. Pipeline Architecture of KoRASA. KoRASA is an optimization method that uses a deep learning-based open-source chatbot framework to understand the Korean language. KoRASA is developed based on the RASA framework [18], and it follows a typical NLU process, including tokenization, featurization, intent classification, and entity extraction, as shown in Figure 2. Figure 3 illustrates the pipeline architecture of KoRASA as proposed in this study. The tokenizer uses the Korean version of Mecab, and a count vector featurizer is adopted [27, 28]. Then, the Dual Intent Entity Transformer (DIET) is used for intent classification and entity extraction of KoRASA [29]. DIET is capable of fast learning using a common baseline model. However, as KoRASA is intended to be applied to the industrial field; the focus is not on the learning speed of the model but on its ability to perform intent classification and entity extraction. Accordingly, the architecture in this study was optimized by tuning its parameters. Moreover, to maximize the performance of entity extraction, a mapping function was added using the Entity Synonym Mapper, and the Transformer Embedding Dialogue (TED) policy was applied [18, 30].

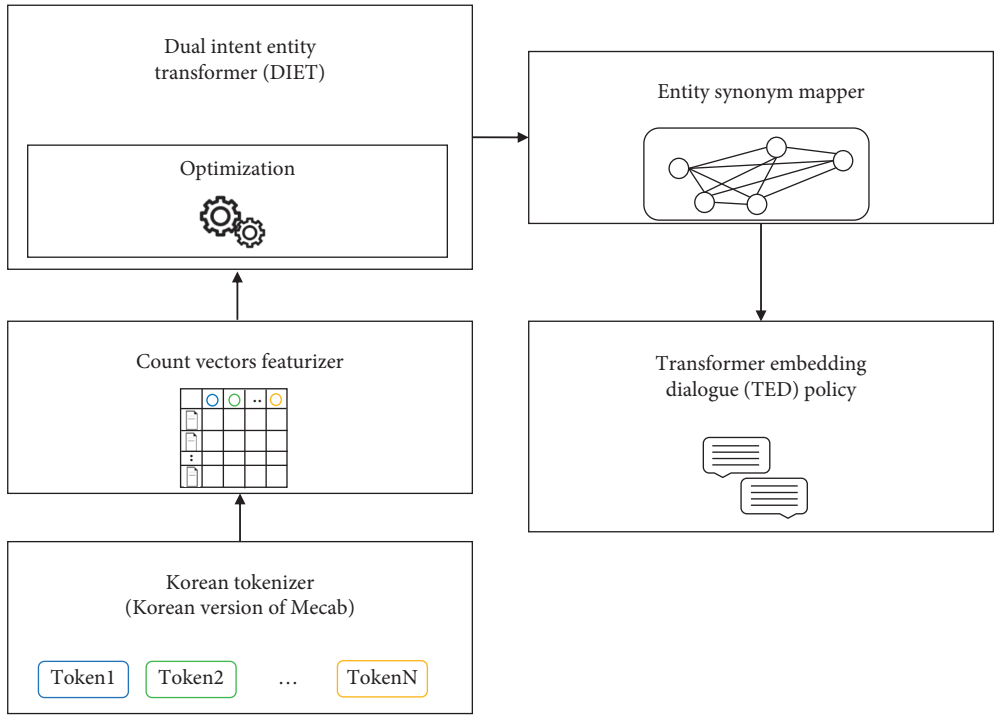

Figure 3: Pipeline architecture of KoRASA.

3.2. Optimized Structure of DIET Model (DIET-Opt). Figure 4 shows the optimization architecture of the DIET model of KoRASA (DIET-Opt). We refer to the Rasa blog for parameter optimization in KoRASA [31]. Tokens are extracted by the Korean tokenizer and are then input into the transformer layer through feed-forward layers. The sequence (a), which is the output from the transformer layer, becomes the sequence (y_{entity}) of entity labels and an input value for the conditional random field (CRF) algorithm. As shown in equation (1), the entity loss (L_{Entity}) can be calculated using the negative log-likelihood of CRF.

$$L_{\text{Entity}} = L_{\text{CRF}}\left(a,\ y_{\text{entity}}\right). \tag{1}$$

The CLS token (a_{CLS}) and intent labels (y_{intent}), which refer to the sentence encoding of an input sentence, are input into the respective embedding layers ($h_{\text{CLS}} = E(a_{\text{CLS}})$, $h_{\text{intent}} = E(y_{\text{intent}})$, where $h \in \mathbb{R}^{20}$). In addition, as expressed in equation (2), the dot-product loss used here not only maximizes the target label (y^{+}_{intent}) and the similarity measure ($S^{+}_{\text{Intent}} = h^{T}_{\text{CLS}} h^{+}_{\text{intent}}$) but also minimizes negative samples (y^{-}_{intent}) and similarities ($S^{-}_{\text{Intent}} = h^{T}_{\text{CLS}} h^{-}_{\text{intent}}$) [27].

$$L_{\text{Intent}} = -< S^{+}_{\text{Intent}} - \log\left(e^{S^{+}_{\text{Intent}}} + \sum_{\Omega^{-}_{\text{Intent}}} e^{S^{-}_{\text{Intent}}} \right) >. \tag{2}$$

Tokens include mask tokens, and values that are output from the transformer layer following the feed-forward layer are then input into the embedding layers. There are two embedding layers: an embedding layer for mask tokens and another for unmasked actual tokens. In practice, 15% of the input tokens are randomly selected in each sequence. A total of 70% of the tokens selected are then replaced by a special mask token MASK, and 10% of them are replaced by random tokens. For the remaining 20%, the original tokens are used directly as input. As shown in equation (3), the output of the transformer (a_{MASK}) for each selected token (y_{token}) is provided through a dot-product loss that is similar to the intent loss.

$$L_{\text{Mask}} = -< S^{+}_{\text{Mask}} - \log\left(e^{S^{+}_{\text{Mask}}} + \sum_{\Omega^{-}_{\text{Mask}}} e^{S^{-}_{\text{Mask}}} \right) >. \tag{3}$$

Finally, the model is trained to minimize the total loss (L_{Total}), which can be expressed by

$$L_{\text{Total}} = L_{\text{Intent}} + L_{\text{Entity}} + L_{\text{Mask}}. \tag{4}$$

Although the overall architecture of KoRASA is similar to the baseline model of DIET (DIET-Base), various experiments were performed to improve the performance of its intent classification and entity extraction processes. An experiment was conducted to determine the optimal number of epochs for best performance. Instead of the traditionally used 300 epochs, 500 epochs were adopted as the optimal number. The number of transformer layers was also increased from 2 to 4, while the weight sparsity was decreased from 0.8 to 0.7. The number of embedding dimensions was increased from 20 to 30, and the hidden layer size increased from 256 to 512, thus optimizing the parameters (see Table 2).

4. Experiments and Results

4.1. Dataset. For the experiments performed in this study, datasets were built based on common tasks applicable to most industries. For the intent classification experiment, a

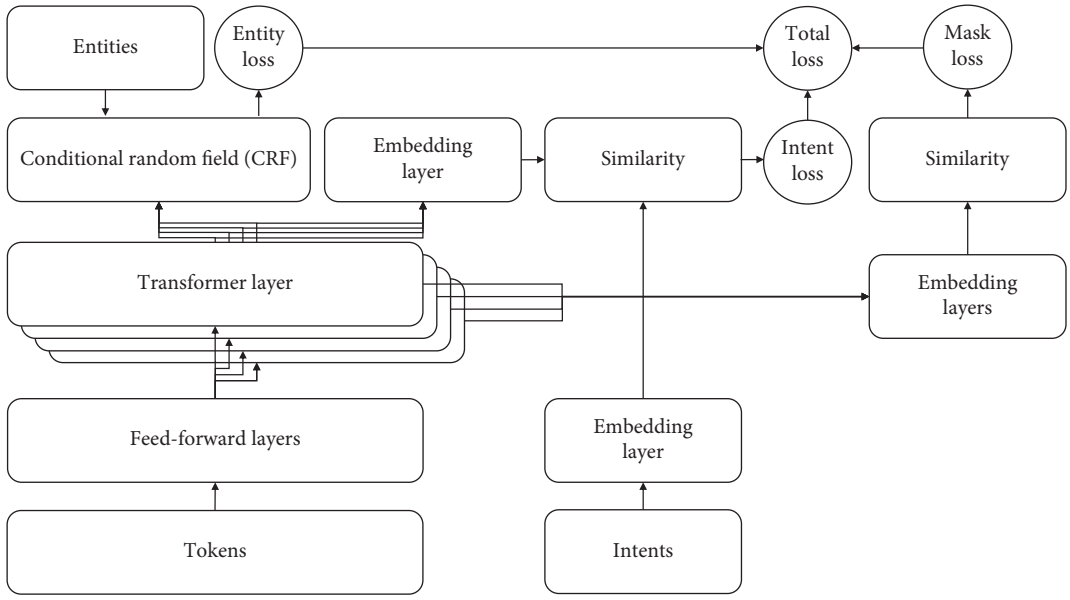

Figure 4: Architecture of DIET-Opt (KoRASA).

Table 2: Parameter comparison between DIET-Base and DIET-Opt (KoRASA).

Parameter	DIET-Base	DIET-Opt (KoRASA)
Epoch	300	500
The number of transformer layers	2	4
Transformer size	256	256
Masked language model	True	True
Drop rate	0.25	0.25
Weight sparsity	0.8	0.7
Embedding dimension	20	30
Hidden layer size	(256, 128)	(512, 128)

total of 487 datasets were generated with the following six components: greeting (Greet), closing (Goodbye), menu (Food_Menu), department contact (Dept_Contact), division of work (Pers_Work), and calculator (Calc) (see Table 3).

For the entity extraction experiment, a total of 3,354 datasets were generated with the following seven entities: date (Date), department (Dept), work (Work), name (Name), time (Time), number (Num), and absence of entity (No_Entity) (see Table 4).

4.2. Preprocessing. As shown in Figure 2, the preprocessing of the NLU can be divided into tokenization and featurization stages. In terms of tokenization, the performance of intent classification and entity extraction was measured by applying three tokenizers: the WhiteSpace Tokenizer, ConveRT Tokenizer, and Korean version of Mecab [18, 27, 32]. The count vector featurizer (CV), fallback classifier, and DIET-Base, which are the three baseline models recommended by RASA, were used as algorithms for featurization, intent classification, and entity extraction [18]. The tokenizers were compared with respect to the intent

Table 3: Intent dataset.

Number	Intent	Meaning	Count
1	Greet	Greeting	8
2	Goodbye	Closing	6
3	Food_Menu	Menu	53
4	Dept_Num	Department contact	60
5	Pers_Work	Division of works	355
6	Calc	Calculator	5

Table 4: Entity dataset.

Number	Entity	Meaning	Count
1	Date	Date	100
2	Dept	Department	246
3	Work	Work	640
4	Name	Name	54
5	Time	Time	13
6	Num	Number	20
7	No_Entity	Absence of entity	2,281

classification and entity extraction performance. The intent classification performance was similar to that of the tokenizer. With regards to entity extraction, however, the WhiteSpace Tokenizer and the ConveRT Tokenizer had an accuracy of 0.073 and $F1$-score of 0.050, whereas the Mecab tokenizer exhibited significantly better performance with an accuracy of 0.989 and an $F1$-score of 0.959 (see Table 5).

For featurization, a comparative experiment was conducted by applying the following three featurizers: Regex Featurizer, Lexical Syntactic Featurizer (LS), and Count Vector Featurizer (CV), while the Korean version of the Mecab tokenizer (Mecab (Ko)) was being applied [18]. Combinations of these featurizers were applied, and the top three performance results were charted. The entity extraction performance of the Count Vector Featurizer was 0.905 ($F1$-score), which was at least 0.3% higher than those of the

Table 5: Tokenization.

Model	Intent classification				Entity extraction			
	Train		Test		Train		Test	
	Acc	F1	Acc	F1	Acc	F1	Acc	F1
WhiteSpace	1.000	1.000	0.984	0.981	0.085	0.073	0.073	0.050
ConveRT	1.000	1.000	0.982	0.978	0.085	0.073	0.071	0.047
Mecab (Ko)	1.000	1.000	0.980	0.985	0.993	0.989	0.959	0.905

Table 6: Featurization.

Model	Intent classification				Entity extraction			
	Train		Test		Train		Test	
	Acc	F1	Acc	F1	Acc	F1	Acc	F1
Regex + LS + CV	1.000	1.000	0.980	0.980	0.988	0.089	0.949	0.882
Regex	1.000	1.000	0.980	0.978	0.993	0.989	0.959	0.902
CV	1.000	1.000	0.980	0.985	0.993	0.989	0.959	0.905

combined Regex + LS + CV Featurizer and the Regex Featurizer (see Table 6).

4.3. Intent Classification and Entity Extraction. A comparative experiment was performed to identify the optimal number of epochs for constructing the DIET-Opt model of KoRASA (see Figure 5). The accuracies and *F*1-scores for intent classification and entity extraction were analyzed when the model was trained with 100 to 900 epochs. In the experiment, when the epoch number was set to 500, the accuracy and *F*1-score of intent classification were found to be 0.982 and 0.984, respectively, and those of entity extraction were found to be 0.974 and 0.947, respectively.

The intent classifier of KoRASA proposed in this study was also compared with other intent classifiers on its intent classification and entity extraction performance. To this end, an experiment was conducted for the keyword classifier, fallback classifier, and DIET-Base classifier models (see Table 7) [18, 29]. The performance evaluation results revealed that the *F*1-score of KoRASA was 19.8%, 0.3%, and 0.4% higher in intent classification and 3.9%, 4.2%, and 3.7% higher in entity extraction than those of the keyword classifier, fallback classifier, and DIET-Base classifier, respectively.

An example of the results of intent classification conducted on the experimental data is shown in the following confusion matrix (see Table 8). After performing a total of six different types of intent classification, the greeting (Greet) and the closing (Goodbye) datasets were recognized as being composed of similar words, meaning that it was difficult to classify intent between those datasets. However, the intents of some of the other datasets, such as menu (Food_Menu), department contact (Dept_Num), and calculator (Calc), were completely classified.

In addition, the entity extractor of KoRASA was compared with other entity extractors. An experiment was conducted to compare the performance of KoRASA with CRF, a combination of DIET-Base and CRF (DIET-Base + CRF), and DIET-Base (see Table 9) [29, 33]. The

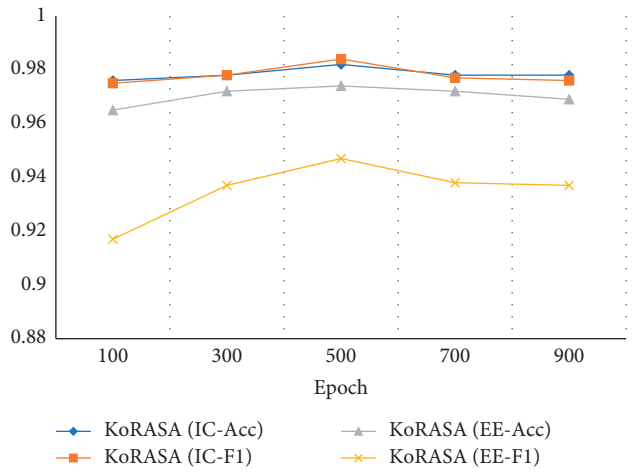

Figure 5: Performance comparison of epoch in KoRASA (IC: intent classification; EE : entity extraction).

Table 7: Performance comparison of intent classification.

Model	Intent classification				Entity extraction			
	Train		Test		Train		Test	
	Acc	F1	Acc	F1	Acc	F1	Acc	F1
Keyword	0.975	0.982	0.782	0.786	0.993	0.989	0.957	0.908
Fallback	1.000	1.000	0.980	0.981	0.993	0.989	0.959	0.905
DIET-Base	1.000	1.000	0.982	0.980	0.993	0.989	0.962	0.910
KoRASA	1.000	1.000	0.982	0.984	0.993	0.989	0.974	0.947

experimental results revealed that the *F*1-score of KoRASA was 1.5%, 1.2%, and 0.4% higher in intent classification and 4.2%, 4.3%, and 3.7% higher in entity extraction than those of CRF, DIET-Base + CRF, and DIET-Base, respectively.

Exemplary results from the experimental evaluation of entity extraction conducted are shown in the confusion matrix in Table 10. The results from seven different types of entity extraction show that our model demonstrated high accuracy for numerical datasets such as date (Date) and time

Table 8: Result example of confusion matrix for intent classification.

True/predict	Greet	Goodbye	Food_Menu	Dept_Num	Pers_Work	Calc
Greet	6	2	0	0	0	0
Goodbye	2	4	0	0	0	0
Food_Menu	0	0	53	0	0	0
Dept_Num	0	0	0	60	0	0
Pers_Work	1	0	0	1	353	0
Calc	0	0	0	0	0	5

Table 9: Performance comparison of entity extraction.

Model	Intent classification				Entity extraction			
	Train		Test		Train		Test	
	Acc	F1	Acc	F1	Acc	F1	Acc	F1
CRF	1.000	1.000	0.974	0.969	0.993	0.989	0.964	0.905
DIET-Base + CRF	1.000	1.000	0.976	0.972	0.993	0.989	0.964	0.904
DIET-Base	1.000	1.000	0.982	0.980	0.993	0.989	0.962	0.910
KoRASA	1.000	1.000	0.982	0.984	0.993	0.989	0.974	0.947

Table 10: Result example of confusion matrix for entity extraction.

True/predict	Date	Dept	Work	Name	Time	Num	No_Entity
Date	100	0	0	0	0	0	0
Dept	0	242	0	0	0	4	0
Work	4	4	567	2	0	0	63
Name	0	0	20	29	0	0	5
Time	0	0	0	0	13	0	0
Num	5	0	0	0	0	15	0
No_Entity	0	2	23	3	0	0	2253

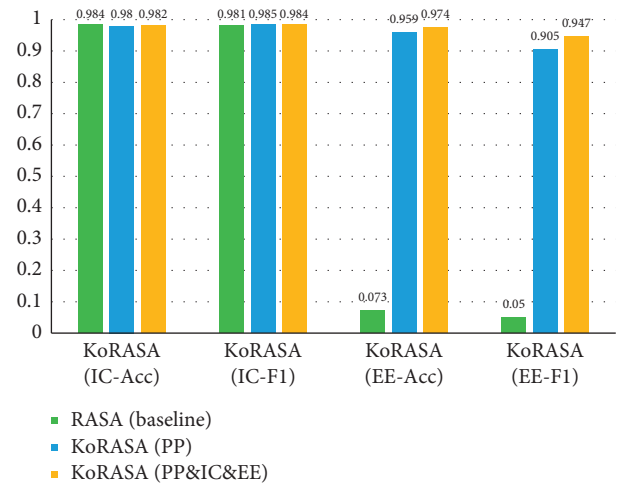

Figure 6: Performance comparison (PP: preprocessing; IC: intent classification; EE: entity extraction).

(Time), as well as for proper nouns such as department (Department) and work (Work). Alternatively, the performance with the name (Name) dataset was lower in terms of accuracy than with the other datasets.

To understand the optimization performance of each stage, we compared the experimental results between (1) the baseline model of RASA; (2) the optimized preprocessing model, which included tokenization and featurization stages (KoRASA(PP)); and (3) the model with optimized preprocessing, intent classification, and entity extraction stages, i.e., the model applying DIET-Opt (KoRASA(PP&IC&EE)) (see Figure 6). Compared with the baseline model of RASA, the results of the KoRASA (PP) model demonstrated comparable performance for intent classification. In contrast, entity extraction performance increased by 88.6% (accuracy) and 85.5% ($F1$-score). Finally, the model in which KoRASA (PP&IC&EE) was applied demonstrated similar results for intent classification. Contrarily, the entity extraction performance increased by 90.1% (accuracy) and 89.7% ($F1$-score).

5. Conclusion

This paper proposed KoRASA as a pipeline-optimization method for a deep learning-based open-source chatbot framework designed to understand the Korean language. KoRASA is a closed-domain chatbot applicable to most industries in Korea. It consists of four stages (tokenization, featurization, intent classification, and entity extraction) and is optimized to understand the Korean language. The tokenization stage uses the Korean version of the Mecab tokenizer, and the featurization stage adopts the Count Vector featurizer. For the intent classification and entity extraction stages, this study developed the DIET-Opt model by parameter tuning and optimizing the DIET-Base model. According to our experimental results, our model demonstrated an accuracy of 98.2% and an $F1$-score of 98.4% for intent classification. These scores were 19.8%, 0.3%, and 0.4% higher than those of the keyword classifier, fallback classifier, and DIET-Base classifier, respectively, which are popular existing intent classifier algorithms. Regarding entity extraction, the experimental results demonstrate that our model had an accuracy of 97.4% and an $F1$-score of 94.7%. Thus, the DIET-Opt model had 1.5%, 1.2%, and 0.4% better performance than those of the CRF, DIET-Base + CRF, and DIET-Base models, respectively, which are popular existing entity extraction algorithms. When the

results of intent classification and entity extraction are charted using the Confusion Matrix, the improved performance of our proposed method was confirmed across the different datasets, with the exception of the greeting (Greet), closing (Goodbye), and employee name (Name) datasets, which are recognized as being composed of similar words. Therefore, we confirmed the necessity of constructing an accurate dataset for effective chatbot training. The results of our experiment demonstrate that KoRASA is useful not only for developing a closed-domain chatbot for the Korean language, but also for various industrial areas such as mobile chatbot services, RPA interworking services, edge computing, Internet of Energy (IoE), and smart grids. We will apply KoRASA to RPA Chatbot and optimize its tokenization method using word embedding for Korean language. In addition, we will construct an open dataset and develop an automatic optimization function to adapt to additional datasets.

Data Availability

No data were used to support this study.

Conflicts of Interest

The authors declare that there are no conflicts of interest regarding the publication of this study.

Acknowledgments

This work was funded by the Korea Electric Power Corporation (KEPCO).

References

[1] K. Shinichiro, *CHATBOT: AI To Robot No Shinka Ga Henkakusuru Mirai*, Sotechsha Co.,, Tokyo, Japan, 2016.

[2] A. M. Rahman, A. A. Mamun, and A. Islam, "Programming challenges of chatbot: current and future prospective," in *Proceedings of the IEEE Region 10 Humanitarian Technology Conference (R10-HTC)*, pp. 75–78, Dhaka, Bangladesh, December 2017.

[3] H. J. Kang and S. I. Kim, "Evaluation on the usability of chatbot intelligent messenger mobile services -focusing on google (allo) and facebook (M messenger)," *Journal of the Korea Convergence Society*, vol. 8, no. 9, pp. 271–276, 2017.

[4] E. Adamopoulou and L. Moussiades, "Chatbots: history, technology, and applications," *Machine Learning with Applications*, vol. 2, 2020.

[5] J. Cahn, *CHATBOT: Architecture, Design, and Development*, 2017.

[6] D. Gwendal, C. Jordi, D. Laurent et al., "Xaikit: a multimodal low-code chatbot development framework," *IEEE Access*, vol. 8, pp. 15332–15346, 2020.

[7] A. M. Addi and L. Xjang, "KBot: a knowledge graph based ChatBot for natural language understanding over linked data," *IEEE Access*, vol. 8, pp. 149220–149230, 2020.

[8] Y. M. Park, S. W. Kang, and J. G. Seo, "An efficient framework for development of task-oriented dialog systems in a smart home environment," *Sensors*, vol. 181581 pages, 2018.

[9] S. Reshmi and K. Balakrishnan, "Empowering chatbots with business intelligence by big data integration," *International Journal of Advanced Research in Computer Science*, vol. 9, no. 1, 2018.

[10] L. Deng and Y. Liu, *Deep Learning in Natural Language Processing*, Springer, Berlin, Germany, 2018.

[11] A. Radford, K. Narasimhan, Tim Salimans et al., "Improving language understanding by generative pre-training," 2018, https://s3-us-west-2.amazonaws.com/openaiassets/research-covers/language-unsupervised/language_understanding_paper.pdf URL.

[12] X. Liu, P. He, W. Chen et al., "Multi-task deep neural networks for natural language understanding," 2019, http://arxiv.org/abs/1901.11504v2.

[13] X. Jiao, Y. Yin, L. Shang et al., "TinyBERT: distilling BERT for natural language understanding," 2020, http://arxiv.org/abs/1909.10351v5.

[14] A. Vaswani, N. Shazeer, N. Parmar et al., "Attention is all you need," in *Proceedings of the 31st Conference on Neural Information Processing Systems (NIPS 2017)*, pp. 1–11, Long Beach, CA, USA, 2017.

[15] Microsoft, https://luis.ai, 2021.

[16] IBM, https://www.ibm.com/watson/developercloud/conversation.html, 2021.

[17] Google, https://www.api.ai, 2021.

[18] Rasa Technologies Inc., https://rasa.com, 2021.

[19] D. Braun, A. H. Mendez, F. Matthes et al., "Evaluating natural language understanding services for conversational question answering systems," in *Proceedings of the SIGDIAL 2017 Conference*, pp. 174–185, Saarbrücken, Germany, August 2017.

[20] T. O'Shea and J. Hoydis, "An introduction to deep learning for the physical layer," *IEEE Transactions on Cognitive Communications and Networking*, vol. 3, no. 4, pp. 563–575, 2017.

[21] G. Aceto, D. Ciuonzo, A. Montieri, and A. Pescape, "Mobile encrypted traffic classification using deep learning: experimental evaluation, lessons learned, and challenges," *IEEE Transactions on Network and Service Management*, vol. 16, no. 2, pp. 445–458, 2019.

[22] G. Aceto, D. Ciuonzo, A. Montieri, and A. Pescapé, "Toward effective mobile encrypted traffic classification through deep learning," *Neurocomputing*, vol. 409, pp. 306–315, 2020.

[23] M.-H. Hwang, I.-T. Lee, C.-H. Chae, and N.-J. Jung, "Gen2Vec: deep learning based distributed representation framework of words and documents for diagnostic services of power generation facility," *The Transactions of The Korean Institute of Electrical Engineers*, vol. 69, no. 12, pp. 1808–1815, 2020.

[24] H.-Z. Wang, G.-Q. Li, G.-B. Wang, J.-C. Peng, H. Jiang, and Y.-T. Liu, "Deep learning based ensemble approach for probabilistic wind power forecasting," *Applied Energy*, vol. 188, pp. 56–70, 2017.

[25] C. Wang, P. Lin, C. Cheng et al., "Detecting potential adverse drug reactions using deep neural network model," *Journal of Medical Internet Research*, vol. 21, no. 2, pp. 1–12, 2019.

[26] D. Roman, S. Saxena, V. Robu, M. Pecht, and D. Flynn, "Machine learning pipeline for battery state-of-health estimation," *Nature Machine Intelligence*, vol. 3, no. 5, pp. 447–456, 2021.

[27] T. Kudo, *Mecab: Yet Another Part-Of-Speech and Morphological Analyzer*, https://sourceforge.net/projects/mecab/, 2012.

[28] F. Pedregosa, G. Varoquaux, A. Gramfort et al., "Scikit-learn: machine learning in Python," *Journal of Machine Learning Research*, vol. 12, pp. 2825–2830, 2011.

[29] B. Tanja, V. Daksh, V. Vladimir et al., "DIET: lightweight language understanding for dialogue systems," 2020, http://arxiv.org/abs/2004.09936v3.
[30] V. Vladimir, E. M. M. Johannes, and N. Alan, "Dialogue transformers," 2020, http://arxiv.org/abs/1910.00486v3.
[31] Rasa Blog., https://blog.rasa.com, 2021.
[32] M. Henderson, C. Inigo, M. Nikola et al., "ConveRT: efficient and accurate conversational representations from transformers," *Findings of the Association for Computational Linguistics: EMNLP*, vol. 2020, pp. 2161–2174, 2020.
[33] J. D. Lafferty, A. McCallum, and F. C. N. Pereira, "Conditional random fields: probabilistic models for segmenting and labelling sequence data," in *Proceedings of the 18th International Conference on Machine Learning(ICML)*, pp. 282–289, Williamstown, MA, USA, 2001.

Hindawi
Mobile Information Systems
Volume 2021, Article ID 9976623, 7 pages
https://doi.org/10.1155/2021/9976623

Research Article

Deep Learning-Driven Gaussian Modeling and Improved Motion Detection Algorithm of the Three-Frame Difference Method

Dingchao Zheng, Yangzhi Zhang, and Zhijian Xiao

Digital Engineering Academy, Zhejiang Dongfang Polytechnic, Wenzhou 325200, China

Correspondence should be addressed to Zhijian Xiao; xiaozhijiandigital@126.com

Received 17 March 2021; Revised 24 April 2021; Accepted 19 May 2021; Published 8 June 2021

Academic Editor: Mian Ahmad Jan

Copyright © 2021 Dingchao Zheng et al. This is an open access article distributed under the Creative Commons Attribution License, which permits unrestricted use, distribution, and reproduction in any medium, provided the original work is properly cited.

To enhance the effect of motion detection, a Gaussian modeling algorithm is proposed to fix holes and breaks caused by the conventional frame difference method. The proposed algorithm uses an improved three-frame difference method. A three-frame image sequence with one frame interval is selected for pairwise difference calculation. The logical "OR" operation is used to achieve fast motion detection and to reduce voids and fractures. The Gaussian algorithm establishes an adaptive learning model to make the size and contour of the motion detection more accurate. The motion extracted by the improved three-frame difference method and Gaussian model is logically summed to obtain the final motion foreground picture. Moreover, a moving target detection method, based on the U-Net deep learning network, is proposed to reduce the dependency of deep learning on the number of training datasets. It helps the algorithm to train models on small datasets. Next, it calculates the ratio of the number of positive and negative samples in the dataset and uses the reciprocal of the ratio as the sample weight to deal with the imbalance of positive and negative samples. Finally, a threshold is set to predict the results for obtaining the moving object detection accuracy. Experimental results show that the algorithm can suppress the generation and rupture of holes and reduce the noise. Also, it can quickly and accurately detect movement to meet the design requirements.

1. Introduction

Motion detection refers to the process of extracting and identifying objects in image sequences or videos of which spatial position changes as foreground motion [1]. Due to the dynamic changes of the scene, it is not easy to reliably and effectively detect and segment motion. In the field of computer vision, it has always been a common research subject. Operations such as tracking, processing, recognition, and behavior discrimination can be performed through effective segmentation of moving objects. These are widely applied to live production, such as video surveillance, motion recognition, and multimedia applications, among others [2].

At present, the frame difference method [3], optical flow method [4], and background subtraction method [5] are standard methods for motion detection, in addition to the feature matching method, K-nearest neighbor method, and ViBe algorithm [6]. Two adjacent frames of the image sequence are taken to perform pixel-based time difference and binarization to extract the motion area in the image for the frame difference method. The advantages of this method are as follows: its simple principle and a fast calculation speed. However, the noise resistance is poor, and holes and breaks are easy to be produced [7]. The ViBe algorithm stores a sample set for each pixel. In the sample collection, the sampling value is the pixel's previous pixel value and the pixel values of its neighbors. The first frame of the image can be taken to complete the creation of the background model's sample set. The sample set can then be compared to each new pixel value to see if it belongs to the context point. The calculation efficiency is high, but it is easy to cause breaks and other problems. In the optical flow method, the motion information of objects between adjacent frames is determined using changes in the time domain of pixels in the image series and the correlation between adjacent frames, based on the relationship between the previous frame and

the current frame. Although the entire area of motion can be detected, there is a large amount of calculation. With a complex structure, it can be easily affected by external factors.

In this study, we propose an optimized Gaussian model and improved three-frame difference method for motion detection. The main contributions are as follows.

(1) We present an optimized Gaussian model and improved three-frame difference method to solve the shortcomings of the aforementioned algorithm, which is used for this task till date

(2) We compare the optimized Gaussian model with the improved three-frame difference method. First, the traditional three-frame difference method is improved to obtain the foreground motion. Then, the Gaussian model is optimized. According to the motion obtained by the Gaussian model, logical operation and morphological processing are performed on the two motions to obtain the final foreground motion. This algorithm can effectively overcome holes and adapt to environmental changes with good robustness.

The rest of this study is organized as follows. In Section 2, we discuss the improved three-frame difference method followed by the optimized Gaussian modeling in Section 3. In Section 4, the improved U-Net model is discussed. In Section 5, the experimental results and analysis are provided. Finally, the study is concluded and future research directions are provided in Section 6.

2. Improved Three-Frame Difference Method

In the traditional three-frame difference method, the first two frames and the last two frames of the adjacent three frames of images are taken for the difference operation. The two frames of difference images are then subjected to the "AND" operation to obtain the result [8]. Due to the continuity of the video sequence, the change between adjacent frames will be minimal if there is no motion in the area. If there is a motion, there will be apparent changes between consecutive frames [9]. Although motions can be quickly detected by this method, problems such as holes and double shadows are likely to appear.

To solve the aforementioned problems, the traditional three-frame difference method is improved in this study. The difference operation is conducted on the three-frame images of the video sequence interval. The "OR" operation instead of the "AND" operation is conducted for different images. The specific steps are as follows:

(1) Three-frame images with one frame interval are collected and converted into grayscale images. Then, filtering processing to remove noise is performed to obtain the corresponding three-frame images, denoted as $f_{k-2}(x, y)$, $f_k(x, y)$, $f_{k+2}(x, y)$.

(2) The k frame of the image is taken as the current frame, and the difference operation is performed with the $k+2$ and $k-2$ frames, respectively, to obtain the absolute value of difference $D_1(x, y)$ and $D_2(x, y)$ as shown in the following equations.

$$D_1(x, y) = \left| f_{k-2}(x, y) - f_k(x, y) \right|, \tag{1}$$

$$D_2(x, y) = \left| f_{k+2}(x, y) - f_k(x, y) \right|. \tag{2}$$

(3) The obtained difference of the above equations is binarized, and an OR operation is performed as shown in the following equation.

$$D(x, y) = D_1(x, y) \oplus D_2(x, y). \tag{3}$$

(4) Finally, appropriate morphological processing is performed on the results

According to the above principles, the code is written to realize the motion detection of a video image by the traditional three-frame difference and the improved three-frame difference. The detection effect is shown in Figure 1.

In Figures 1(a) and 1(b), images at different periods in the same video are shown. The left side image in each figure is the original video image. The middle is the motion detected by the traditional three-frame difference method. The motion observed by the enhanced three-frame difference method is seen on the right. The detection results show that improving the three-frame difference approach will help solve the holes' problem to some degree. However, the motion is deformed to a certain extent, so it needs to be improved or combined with other algorithms for processing.

3. Optimized Gaussian Modeling

The value or feature of each pixel in the image is distributed within a specific range around a certain central point in a short time, and this distribution is regular. According to statistical laws, if the amount of data is large enough, it will be normally distributed, known as Gaussian distribution. According to this feature, if the pixel's value is far from the center point, the pixel belongs to the foreground; otherwise, it belongs to the background [10]. In motion detection, the Gaussian modeling is taken for each background pixel by mixing K Gaussian distributions (3–5 is generally taken for K). Clearer motions can be extracted by Gaussian modeling, and the background can be updated and adaptive. The improved three-frame difference method can be combined to achieve complementary advantages and disadvantages and enhance the detection of motions [11].

3.1. Background Model Building. The grayscale histogram of an image reflects the frequency of a specific grayscale value in the image. Suppose the motion area in the image is larger than the background area. There is a certain difference in grayscale between the background and motion area. In that case, the grayscale histogram of the image presents a double peak-valley shape. One of the peaks corresponds to the motion, and the other peak corresponds to the central grayscale of the background. For complex images, they are generally multipeak. By treating the multipeak characteristics of the histogram as the superposition of multiple

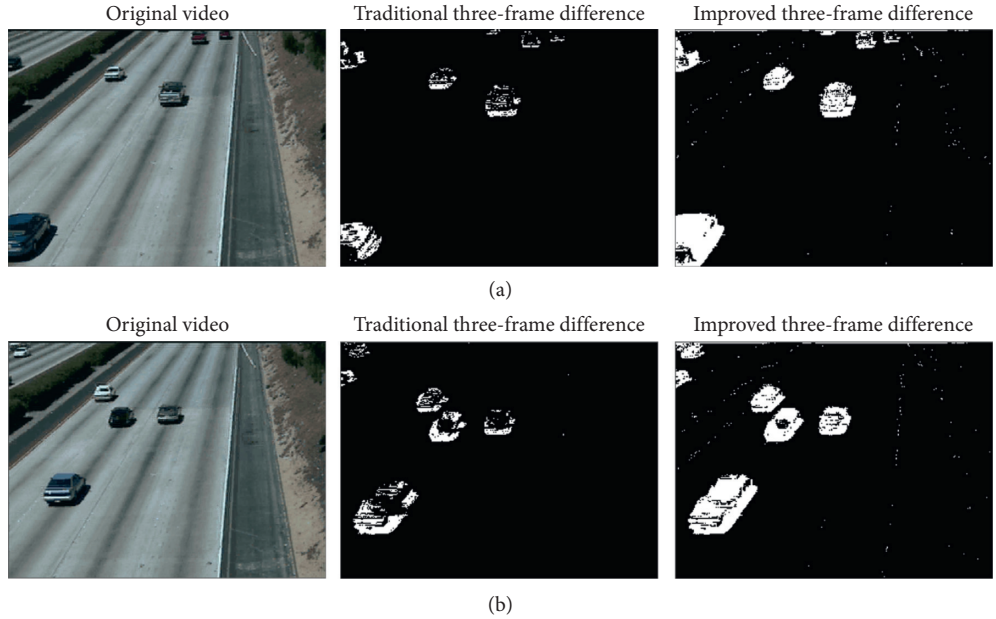

Figure 1: Motion detection by the three-frame difference method.

Gaussian distributions, the image segmentation problem can be solved [12].

Each pixel of the background image is modeled by a Gaussian mixture model composed of K Gaussian distributions as shown in the following equation.

$$P(x_t) = \sum_{i=1}^{k} \omega_{i,t} \eta\left(x_t, \mu_{i,t}, \tau_{i,t}\right), \tag{4}$$

where k is the total number of distribution patterns, and $\omega_{i,t}$ represents the estimated value of the weight coefficient of the i^{th} Gaussian distribution in the Gaussian mixture model at time t, $\eta(x_t, \mu_{i,t}, \tau_{i,t})$ is the i^{th} Gaussian distribution at time t, and η represents the probability density function of the Gaussian distribution. x_t represents the value of i^{th} pixel at time t. $\mu_{i,t}, \tau_{i,t}$ represent the mean vector and covariance matrix of the i^{th} Gaussian distribution in the Gaussian mixture model at time t.

The patterns are arranged in descending order of the value of ω/δ^2. The larger the value, the more likely the k^{th} distribution is the background model. Then, the first B Gaussian distributions were selected as the background models. As shown in the following equation, T represents the proportion of the background.

$$B = \arg\left(\min\left(\sum_{k=1}^{b} \omega_k > T \right) \right), \tag{5}$$

3.2. Foreground Motion Detection. After the background model is established, each pixel value x_t of the new input image frame is matched with B Gaussian distributions in the background model. If the pixel value matches any Gaussian distribution, the pixel is the background point; otherwise, it is the foreground, thus completing the motion detection. Each new pixel value x_t is compared with the current K models. As generally shown in equation (6), the mean deviation coefficient is generally 2.5.

$$|x_t - \mu_{i,t-1}| \leq 2.5\sigma_{i,t-1}. \tag{6}$$

3.3. Background Update. The context model must be changed during the motion detection process. The context model is learning to enable the detection to adapt to changes in the environment, and a is the learning rate. Suppose a frame of image does not match any Gaussian distribution during the detection process. In that case, the pattern with the most negligible weight is replaced. The weight of the pattern is represented by equation (7), and its mean and standard deviation remain unchanged.

$$\omega_{k,t} = (1 - \alpha) * \omega_{k,t-1}. \tag{7}$$

Suppose, it is detected that at least one Gaussian distribution in the background model matches the pixel. In that case, the parameters of the Gaussian model are updated using the following equations.

$$\omega_{k,t} = (1 - \alpha) * \omega_{k,t-1} + \alpha, \tag{8}$$

$$\rho = \alpha * \eta\left(x_t | \mu_k, \sigma_k\right), \tag{9}$$

$$\mu_t = (1 - \rho) * \mu_{t-1} + \rho * x_t, \tag{10}$$

$$\sigma^2 = (1 - \rho) * \sigma_{t-1}^2 + \rho * \left(x_t - \mu_t\right)^T \left(x_t - \mu_t\right). \tag{11}$$

The effect of motion detection by Gaussian modeling is shown in Figure 2. The left side is the original video image, and the right side is the motion detection image. From figure, it can be seen that the Gaussian model can better

Figure 2: Motion detection by Gaussian modeling.

overcome the problem of holes. Simultaneously, the appearance of the motion is not elongated, and the outline is evident [13].

3.4. Combining the Improved Three-Frame Difference Method. The frame difference approach has a simple operation and quick speed. However, due to its low noise resistance, holes are easy to appear. For the enhanced three-frame difference process, three nonadjacent frames are taken, and the OR operation is used instead of the original, which may not only eliminate gaps but also trigger issues such as elongated movements and blurred outlines. Therefore, the Gaussian model is combined to establish a learning background model for motion detection. The outline of the motion detected by the Gaussian model method is relatively straightforward, and the appearance is not elongated.

In the detection process of motions, first, the motions are extracted by the improved three-frame difference method and Gaussian modeling. Then, the logical AND operation is conducted for the motion images obtained by these two algorithms. Next, connectivity detection and morphological operations are taken to the process, and finally, the completed motion is achieved. The flow chart of the algorithm is shown in Figure 3.

4. Improved U-Net Model

The top-down image detection algorithm based on deep learning [14–18] extracts global image information and high-level semantic information by self-learning image features. In contrast, the bottom-up image detection algorithm based on low-level visual features extracts low-level image color and texture. Image features can extract rich image local and spatial information. Therefore, fuse the semantic information and global information of the top-down image detection algorithm with the bottom-up saliency detection algorithm's spatial information. The local information can help the high-level network obtain the local image information to locate the salient target and improve the image detection effect.

Therefore, this study adds the saliency map extracted by the bottom-up motion detection algorithm in the decoder stage of U-Net and realizes the accurate prediction of the saliency image by fusing high-level global information and low-level local information. Specifically, the algorithm first reduces the saliency map extracted by the bottom-up image detection algorithm, generates a priori map of the same size as the feature map of the U-Net network decoder stage, and then combines the a priori map with upsampling. Feature fusion is performed on the feature map of the stage. Furthermore, the channel attention module is added after sampling at each layer to extract more important channel information. Finally, the saliency map output of each layer is upsampled to construct a weighted loss function to continuously optimize the learning process of the neural network [16, 19–22]. The specific structure of the model is shown in Figure 4.

5. Experimental Results and Analysis

To verify the algorithm's effectiveness in the study, a highway surveillance video for testing was selected for the experiment. The hardware environment of the experimental platform is an ordinary computer, with an I3 processor, main frequency 2.1 GHz, and memory 4G. The software environment is Visual Studio 2019 and OpenCV3 computer vision open source library. The programming language is C#. Gaussian modeling, improved three-frame difference method, and combination of Gaussian modeling and improved three-frame difference method were taken to the test. The effect diagram of the test is shown in Figure 5. For the improved U-Net model, this article uses python language, and the deep learning framework uses Keras.

In Figure 5, the original video sequence is in the first column. The result of the improved three-frame difference method is in the second column. The third column is the result obtained by Gaussian modeling. The last column is the motion obtained by combining the two methods. Figure 5(a)–5(c) are the detection effect diagrams of the same video at different periods.

In Figure 6, we compare the accuracy of our work against the conventional Gaussian model and improved three-frame different model. We compare the accuracy of these schemes for different time frames. This figure shows that our proposed work has much better accuracy as compared to the existing schemes.

Figure 7 shows the comparison experiment results of the average time complexity under different time frames. Our scheme outperforms the existing models, and it has much better results for varying number of frames.

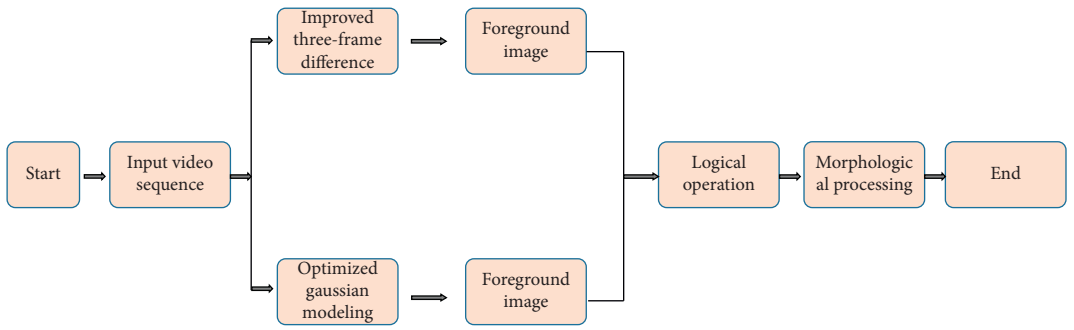

Figure 3: Flow chart of the algorithm.

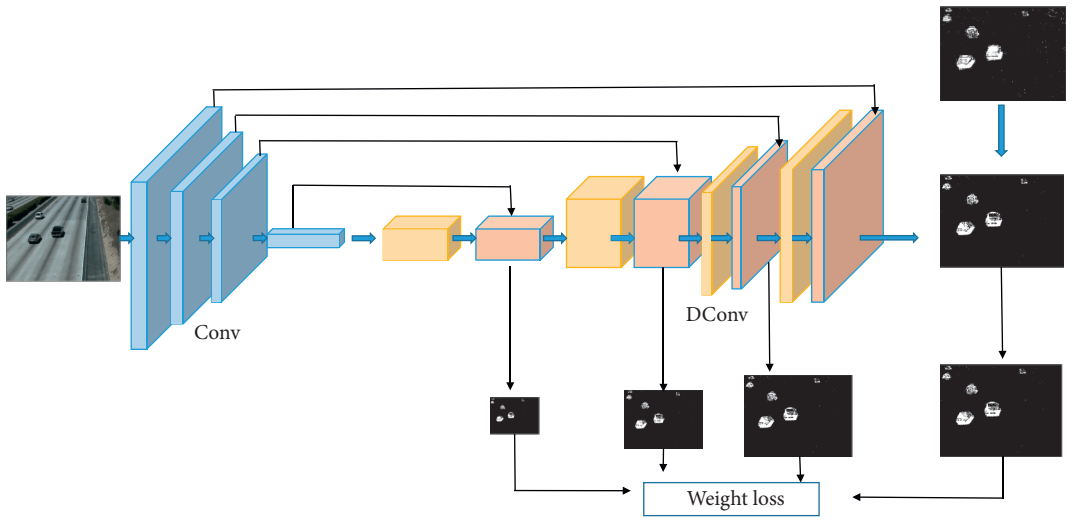

Figure 4: Improved U-Net architecture diagram.

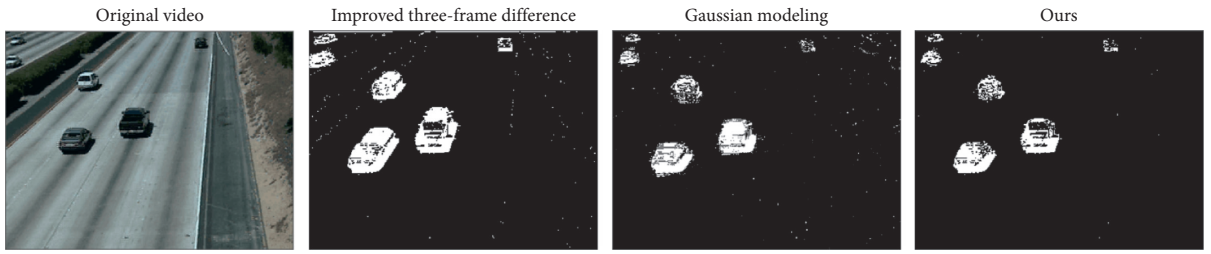

(a)

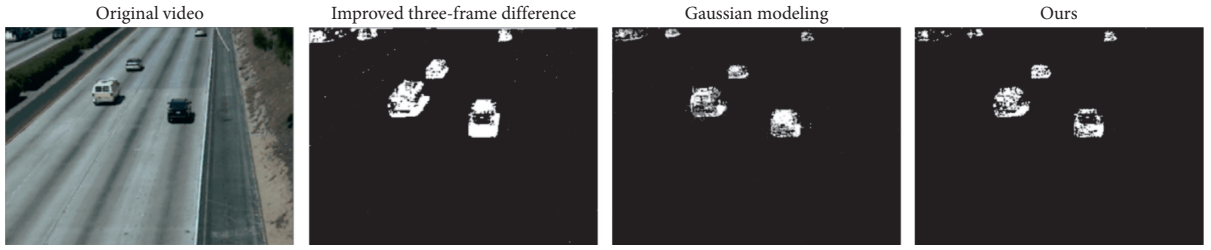

(b)

Figure 5: Continued.

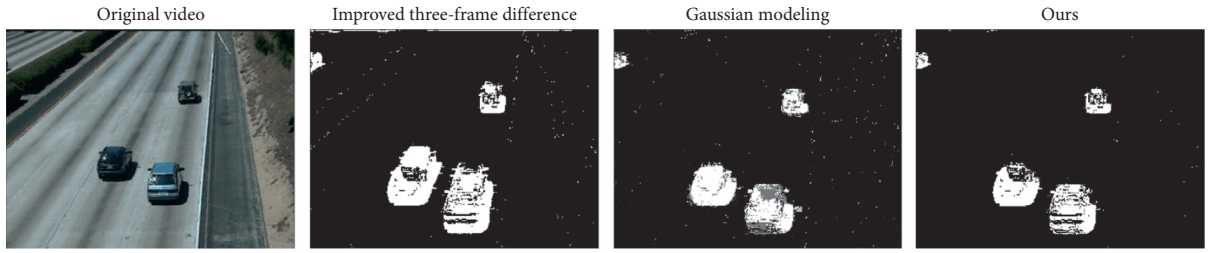

(c)

Figure 5: Effect diagram for three kinds of motion detection.

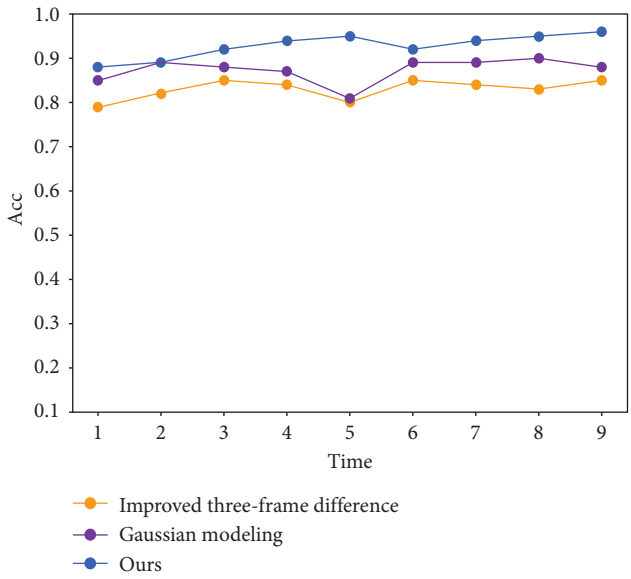

Figure 6: Accuracy comparison experiment results in different time frames.

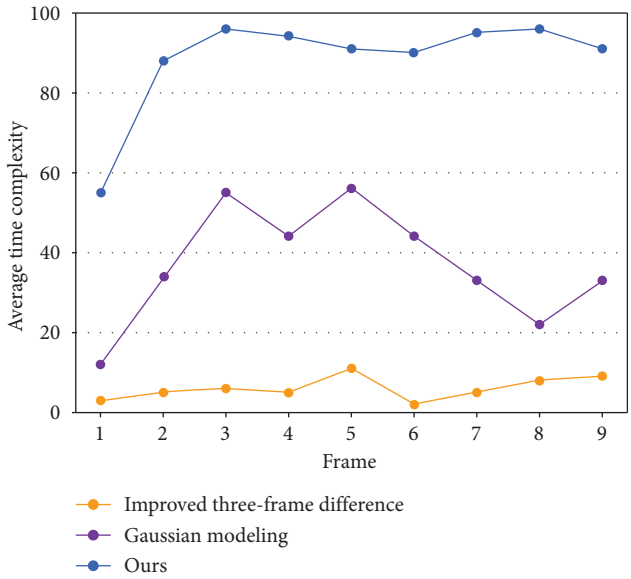

Figure 7: Comparison of experimental results of average time complexity in different time frames.

6. Conclusions

A motion detection algorithm based on Gaussian modeling and an improved three-frame difference method is proposed in the study. Adjacent frames of images are taken in the traditional three-frame difference method. Images of non-adjacent frames are taken in the improved algorithm, and "OR" operation is performed upon them. We use Gaussian modeling to adapt to environmental changes. After the two algorithms are tested, improved, and combined, the deformation, holes, noise, and other motion problems caused by the frame difference method can be effectively improved. It helps in raising the detection efficiency of motion detection. The antiinterference is enhanced, which can meet the requirements of motion detection, with certain practicability and value.

Data Availability

The data used to support the findings of this study are included within the article.

Conflicts of Interest

The authors declare that they have no conflicts of interest.

References

[1] H. Hu, *Video Motion Detection in Complex Traffic Scenes*, Anhui University, Hefei, China, 2020.

[2] Y. Zhang, *Research on Video-Based Motion Detection Algorithm*, Shanghai Normal University, Shanghai, China, 2020.

[3] L. Xiao, Y. Yang, and Y. Xu, "Motion detection by four-frame difference and improved Gaussian mixture model," *Science Technology and Engineering*, vol. 20, no. 15, pp. 6141–6150, 2020.

[4] Y. Jin, Y. Yang, and Y. Du, "Motion tracking algorithm based on optical flow feature points in power monitoring scenes," *Electric Power Science and Engineering*, vol. 36, no. 5, pp. 40–47, 2020.

[5] S. Sui, "Overview of pixel-based background subtraction technology[J]," *Science and Technology Innovation*, vol. 9, pp. 63–66, 2019.

[6] Y. Mou and L. Jin, "Improved ViBe algorithm for motion detection[J]," *Information Technology and Informatization*, vol. 6, pp. 75–77, 2020.

[7] H. Gao and X. Duan, "Motion detection at sea based on frame difference method and Gaussian mixture," *Computer and Digital Engineering*, vol. 47, no. 5, pp. 1140–1144, 2019.

[8] Q. Sun, X. Zhao, and X. Zhang, "Research on the detection method of small motion trajectory based on improved three-frame difference method," *Equipment Manufacturing Technology*, vol. 3, pp. 135–137, 2019.

[9] W. Jiang, *Research on Conspicuous Video Motion Detection Algorithm Based on Biological Vision Mechanism*, University of Electronic Science and Technology of China, Chengdu, China, 2020.

[10] R. Cao and H. Xiaoli, "Improved vibe algorithm based on Gaussian mixture model and threshold adaptation," *Journal of Taiyuan University of Technology*, vol. 51, no. 4, pp. 516–521, 2020.

[11] C. Zhang, Y. Zhang, Y. Chen, Y. Wang, and D. Zhao, "Motion detection and recognition based on five-frame difference and template matching," *Laser and Infrared*, vol. 48, no. 12, pp. 1554–1560, 2018.

[12] Y. Yang, B. Hui, Z. Chang, and Y. Ma, "Motion detection algorithm at sea based on Gaussian mixture model," *Application Research of Computers*, vol. 37, no. 1, pp. 310–313, 2020.

[13] Z. Li and X. Tan, "Motion detection algorithm based on Gaussian mixture model and five-frame difference," *Computer and Digital Engineering*, vol. 46, no. 2, pp. 284–288, 2018.

[14] L. Zhang, W. Li, X. Ning, X. Dong, and W. Liu, "A finger vein recognition method based on histogram of oriented lines and (2D)2FPCA," *Journal of Computer-Aided Design & Computer Graphics*, vol. 30, no. 2, pp. 254–261, 2018.

[15] X. Zhang, Y. Yang, Z. Li, X. Ning, Y. Qin, and W. Cai, "An improved encoder-decoder network based on strip pool method applied to segmentation of farmland vacancy field," *Entropy*, vol. 23, no. 4, p. 435, 2021.

[16] S. Li, X. Ning, L. Yu et al., "Multi-angle head pose classification when wearing the mask for face recognition under the COVID-19 coronavirus epidemic," in *Proceedings of the 2020 International Conference on High Performance Big Data and Intelligent Systems (HPBD&IS)*, pp. 1–5, Shenzhen, China, May 2020.

[17] W. Cai and Z. Wei, "Remote sensing image classification based on a cross-attention mechanism and graph convolution," *IEEE Geoscience and Remote Sensing Letters*, vol. 13, 2020.

[18] X. Ning, Y. Wang, W. Tian, L. Liu, and W. Cai, "A biomimetic covering learning method based on principle of homology continuity," *ASP Transactions on Pattern Recognition and Intelligent Systems*, vol. 1, no. 1, pp. 8–15, 2021, https://www.aspress.org/index.php/tpris/article/view/9.

[19] W. Cai, B. Liu, Z. Wei, M. Li, and J. Kan, "TARDB-Net: triple-attention guided residual dense and BiLSTM networks for hyperspectral image classification," *Multimedia Tools and Applications*, vol. 80, no. 7, pp. 11291–11312, 2021.

[20] J. Chen, C. Du, Y. Zhang, P. Han, and W. Wei, "A clustering-based coverage path planning method for autonomous heterogeneous UAVs," *IEEE Transactions on Intelligent Transportation Systems*, vol. 21, pp. 1–11, 2021.

[21] Z. L. Yang, S. Y. Zhang, Y. T. Hu, Z. W. Hu, and Y. F. Huang, "VAE-Stega: linguistic steganography based on variational auto-encoder," *IEEE Transactions on Information Forensics and Security*, vol. 16, pp. 880–895, 2020.

[22] X. Ning, X. Wang, S. Xu et al., "A review of research on co-training. concurrency and computation: practice and experience," , 2021.

Hindawi
Mobile Information Systems
Volume 2021, Article ID 9925838, 8 pages
https://doi.org/10.1155/2021/9925838

Research Article

Construction of Video Courses of Physical Education and Health Education in Colleges and Universities under the MOOC Platform

Shuai Yang

Insititute of Higher Education Research, Beihang University, Beijing 100191, China

Correspondence should be addressed to Shuai Yang; by1511114@buaa.edu.cn

Received 11 March 2021; Revised 9 April 2021; Accepted 23 May 2021; Published 4 June 2021

Academic Editor: Mian Ahmad Jan

Copyright © 2021 Shuai Yang. This is an open access article distributed under the Creative Commons Attribution License, which permits unrestricted use, distribution, and reproduction in any medium, provided the original work is properly cited.

In the traditional construction process of educational video courses for physical and health education in universities, numerous problems are encountered, such as small storage capacity, significant delay error, and decreased information throughput rate. Therefore, an educational video course for physical and health education in universities based on the Massive Open Online Course (MOOC) platform is constructed. The course is built by constructing a creative environment for video courses, establishing a video course model under the MOOC platform, and the caching code design for video courses. Upon numerous modifications and test runs, with the campus network's help, the construction of a network teaching video for physical and health theory courses is realized. Our proposed approach's experimental result shows that the designed course's frame rate is 10% higher than that of the traditional course designing. The node's storage capacity is up to 130%, the delay error is significantly reduced, and the information throughput rate is not affected by the increase of network load.

1. Introduction

Video course is a new multimedia teaching mode that excels in developing modern computer network technology and video technology. The educational video courses of sports and health, based on the MOOC platform in universities, are an effective way to promote the reform of physical and health education in universities and promote the network and science of physical and health education in universities. Video courses break through the time and space limitations of traditional teaching activities and make the boring teaching content in the classroom more vivid through video. With the application of computer network technology, the all-around exchange and interaction between the two sides of teaching are realized [1]. Wireless network technology provides technical support for the construction of videos. Moreover, it remains an essential tool for the development and use of videos. In a nutshell, essential applications, including PPT presentation, are wireless network technology contributions [2].

With the popularity of the MOOC model for higher education, the development of video courses has gradually become one of the most important topics in the field of higher education. Only by keeping pace with the modern era and the technological trends, we can ensure the quality and effectiveness of education [3]. Therefore, this paper studies the related problems in the construction process of video courses for physical and health education under the platform of MOOC in universities. Initially, a method for constructing the MOOC platform is discussed, which helps to identify the issues related to designing an effective and robust course model for video courses [4]. It is anticipated that it can provide some references for the scientific construction of video courses for universities' physical and health education.

The rest of this paper is organized as follows. Section 2 is about constructing the MOOC platform, and Section 3 proposes the video courses model. Section 4 describes the video course's cache code design, and Section 5 gives the experimental results and performance analysis. Section 6 summarizes this paper and the future research direction.

2. Construction of MOOC Platform

To construct the MOOC platform, we have the following setup in place [5]. A PowerEdge R710 server is used to build a web server, and it also bears the function of a reverse proxy server. Two PowerEdge R720 servers are used as streaming media servers, and load balancing is achieved through a reverse proxy server. PowerEdge R710 is configured as a two eight-core Xeon E5620 processors with 32 GB DDR3 and two 500G SAS hard drives to install and 6 1T hard disks to store instructional video data. The development language is Java. The system is built based on the J2EE development system, and the multilayer architecture of the J2EE is shown in Figure 1 [6]. The architecture features of the business layer and the business logic processing layer make full use of the services provided by the J2EE business server [7].

The application server, represented by BEA WebLogic, provides perfect services for various programs, such as threads, transactions, database connection pools, and security. These services are very stable [8]. The server software environment installs the Windows Server 2008 Enterprise R2 version on the R710 server and installs NETFRAMEWORK3.5 and other running frameworks. IS7.5 is used as the main station's server program, and the NGINX reverse proxy is installed on this server, and it is mapped to two other R720 servers to make the load balanced when accessing the videos [9]. Flash Media Server is installed on the two servers, and the video management program based on FMS is deployed to the server to achieve the control of video playback [10]. This system has no special requirements for client hardware. It only needs browser to be installed on the system, and FLASH plug-ins have to be installed. The bulletin information is shown in Table 1.

3. The Proposed Video Courses Model

First, the overall design of the model function, the course video script's production, the collection of text material, and the entry and editing of the text information are discussed. The physical and health curriculum models in universities can be analyzed from various angles, namely, the concept of ideology, curriculum, teaching, the system of operation, and implementation. Image material is compressed in JPG format and image processing software such as Photoshop and Fore work are used for image production [11]. A camera is used to photograph the teaching staff's technical movements. The editing of images, commentaries, and captions is carried out on the nonlinear editing system and stored in AVI or FLV format. Multimedia camera technology is used to convert the image material into WMV format and played on Internet [12]. The Microsoft SQL Server database, ASP technology, and page development software, i.e., Dreamweaver MX web, are used to integrate all kinds of obtained materials on the Windows XP server operating system. After many modifications and test runs, with the campus network's help, the construction of a network teaching video for physical and health theory courses is realized. The construction's flow chart is shown in Figure 2, which is similar to the one proposed by Mei [13].

The resource information table is used to store all kinds of teaching resources in schools, which is shown in Table 2 [14].

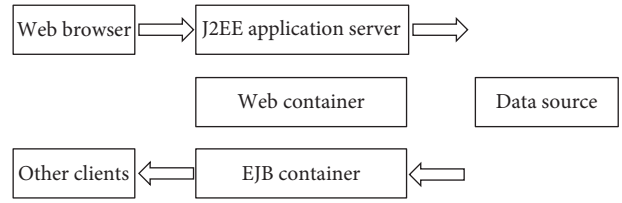

Figure 1: Multilayer architecture of MOOC platform using J2EE.

Table 1: Bulletin information.

Serial number	Attribute	Field type	Field length	Primary key
1	Bulletin number	Int	10	Yes
2	Content	Varchar	100	No
3	Release time	Date	8	No
4	Release people	Varchar	10	No
5	Type	Varchar	15	No

The permission information table is used to store the contents of each user's permission scope in the system, which is shown in Tables 3 and 4 [15].

The performance of virtual data migrating from one level to another is an important indicator of a system [16]. The following equations are used to calculate the migration performance:

$$\mathrm{MT}_T = \frac{M_{\mathrm{VM}}}{N_{\mathrm{BW}}},$$
$$P_V = \int_T^{T+\mathrm{MT}_T} U_{\mathrm{CPU}}, \tag{1}$$

where MT_T is the total time of migration, M_{VM} is the memory utilization of the virtual machine, N_{BW} is the available network broadband, P_{VM} indicates the degradation rate of the virtual machine, and U_{CPU} represents the occupancy of virtual machine [17]. Through these two equations, the degradation rate of virtual machine and the performance of application can be obtained.

The system uses the ZIP-LIKE distribution to simulate the video popularity test. The video is sorted according to the probability of clicking from high to low, and the probability of video being clicked is as follows:

$$f_i = \frac{P_V}{c \times i^{a_V}}, \tag{2}$$

where c is the memory space and a_v indicates the ZIP-LIKE distribution parameters. The user behavior generator is used to simulate the released data, and the byte hit rate is used as the criterion of the algorithm. For this purpose, the equation is as follows:

$$\mathrm{BHR} = fi\frac{B_{\mathrm{cache}}}{B_{\mathrm{req}}}, \tag{3}$$

where B_{cache} is the amount of data provided by the cache server and B_{req} is the total amount of data that is requested for the user [18].

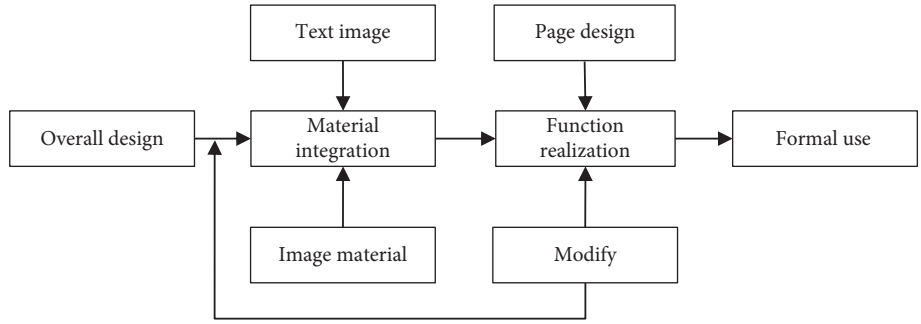

Figure 2: Course model for network teaching mode.

Table 2: Resource information table.

Serial number	Attribute	Field type	Field length	Primary key
1	Resource ID	Int	10	Yes
2	Name	Varchar	10	No
3	Format	Varchar	10	No
4	Profile	Varchar	200	No
5	Upload time	Date	16	No
6	Upload person	Varchar	15	No
7	Data amount	Int	10	No

Table 3: Permission information table.

Serial number	Attribute	Field type	Field length	Primary key
1	Permission ID	Int	10	Yes
2	User ID	Int	10	No
3	User name	Varchar	10	No
4	Access module	Int	15	No

Table 4: Transcoding server information.

Serial number	Attribute	Field type	Field length	Primary key
1	Transcode ID	Int	10	Yes
2	Equipment type	Varchar	5	No
3	IP addresses	Varchar	10	No
4	Server port	Varchar	20	No

The type of knowledge point is an important analysis dimension. In order to ensure the validity of the data, the knowledge content of the teaching video course is classified and the reliability is analyzed. The reliability formula of the content analysis is as follows:

$$R = \frac{n \times K}{1 + (n-1) \times \mathrm{BHRK}}, \tag{4}$$

where R is the reliability, n is the number of judges, and k is the average mutual agreement degree.

$$K = R\frac{2M}{N_1 + N_2}. \tag{5}$$

In this equation, M is the number of analytic categories agreed on by two adjudicators, N_1 is the number of cases analyzed by the first adjudicator, and N_2 is the number of cases analyzed by the adjudicator. If the coefficient Cronbach α is used to examine the overall and internal consistency reliability, then the reliability coefficient α is

$$\alpha = \frac{\mathrm{k}}{k-1}\left(1 - \frac{\sum_{i=1}^{k} S_i^2}{S_\chi^2}\right), \tag{6}$$

where K is the number of questions on the test, S_i is the variance of the score for the questions, and S_χ is the variance of the total score of the test. According to the different parameters, physical video courses can be divided into three modes. The following are the specific formulas used for each mode:

(i) Single-parameter mode:

$$p(\theta) = K\frac{\alpha}{1 + l^{-D(\theta-b)}}. \tag{7}$$

(ii) Dual-parameter mode:

$$p(2\theta) = K\frac{\alpha}{1 + l^{-D_a(\theta-b)}}. \tag{8}$$

(iii) Three-parameter mode:

$$p(3\theta) = c + (1-c)\frac{K}{1 + l^{-D_a(\theta-b)}}, \tag{9}$$

where $D = 1.702$, θ is the value of the students' ability, a is the division of the topic, b is the difficulty of the topic, and c is the guessing coefficient of the topic. $p(\theta)$ is the probability of answering the question to the students with the ability of θ.

The construction of video courses can be divided into six levels: hardware level, basic platform level, data level, business support level, application level, and user level. The hardware layer improves the hardware support of the application platform so as to ensure that the program can run stably and efficiently and realize remote access to the system under the guarantee of network conditions. The basic platform layer is the operation system, database management system, NGINX reverse proxy service, host storage and backup system, and information security. The data layer is designed according to the needs of the system, the video files, and related configuration files designed according to the system requirements. The business support layer provides some general operation interfaces, including database access support, form service support, and message queuing. The application layer implements the specific functional modules of the system, and the user layer is the ultimate user.

The website uses ASP.NET MVC, LINQ to SQL, SQL SERVER 2005, FMS, AJAX, and other technologies to achieve the whole system construction. All kinds of technologies complement each other and ensure the overall integrity and efficiency of the system. The relationship diagram of each part of MVC is shown in Figure 3.

The implementation of ASP.NET MVC based on ASP.NET can be compatible with existing ASP.NET applications by multiple components in ASP.NET to realize data binding. In ASP.NET MVC, a controller is usually a class that inherits the system. When a request is sent to the server, the system looks up the corresponding action in the corresponding Controller through the URL address and the system routing setup. The relationship between the Controller, Model, and View in the ASP.NET MVC is shown in Figure 4.

The ASP.NET MVC framework is highly compatible and can use any.NET-based Database, ORM framework, or other tools. LINQ to SQL is an O/RM component included in the.NET F3.5 version. This component can implement RDB modeling and then use LINQ to implement the operation of the model. Through the relational mapping, the data in the database can be checked, updated, added, and deleted. Besides the above functions, LINQ to SQL can also support stored procedures, views, and transactions, creating a bridge between business logic and the model, in a simple way. Microsoft SQL Server 2005 data engine combines analysis, reporting, integration, and notification capabilities. Figure 5 shows the functions of uploading, downloading, selecting lessons, and inquiring modules for students.

The tight integration with Microsoft Visual Studio, the Microsoft Office System, and the new development kit makes Microsoft SQL Server 2005 unique. Microsoft SQL Server 2005 is suitable for all types of research and development (R&D) personnel, such as developers, database administrators, and decision makers, providing powerful technical support and solutions. Adobe Flash Media Server is a major component of the Adobe Flash Platform with compatibility.

The online course management module includes teaching resource management, job management, examination related management, interactive management and

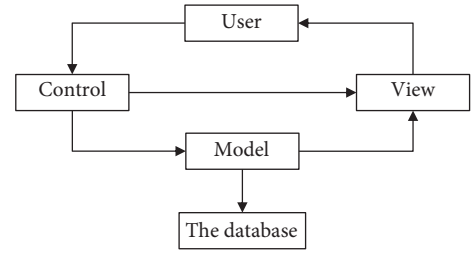

Figure 3: MVC model.

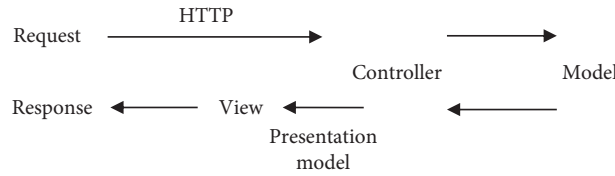

Figure 4: The relationship between the Controller, Model, and View.

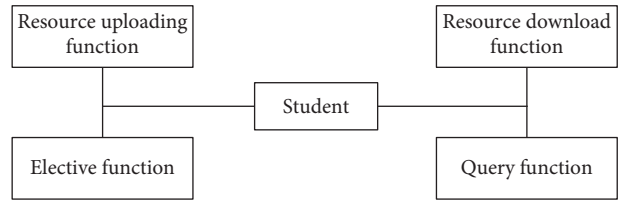

Figure 5: Uploading, downloading, selecting lessons, and inquiring modules for students.

resource uploading, and download management modules. The interactive management module is BBS, online questions and answers (Q&A), and video communication. The cloud storage system is shown in Figure 6.

The transcoding server management function module is constituted by the transcoding server manage class and the transcoding server manages User Interface (UI) class. The transcoding server manages the UI class by implementing the front interface of the function module, and the transcod server manage class implements the business logic of the function module, in which the classes relying on three control classes are the transcoding server info manage class and the server transcoding class, as three subfunctions that implement transcoding server information management, server configuration, and server transcoding. Among them, the transcoding server info manage class has add, modify, and delete methods, depending on the transcoding server info entity class. The server confugurst class has a parameter set method, which depends on the transcoding server info entity class. The server transcoding class has a transcoding method and depends on the transcoding server info entity class. The storage server management module is composed of the Storage_server manage class and the Storage_server_manage_UI class. The Storage_server_manage_UI class implements the front-end interface of the functional module, and the

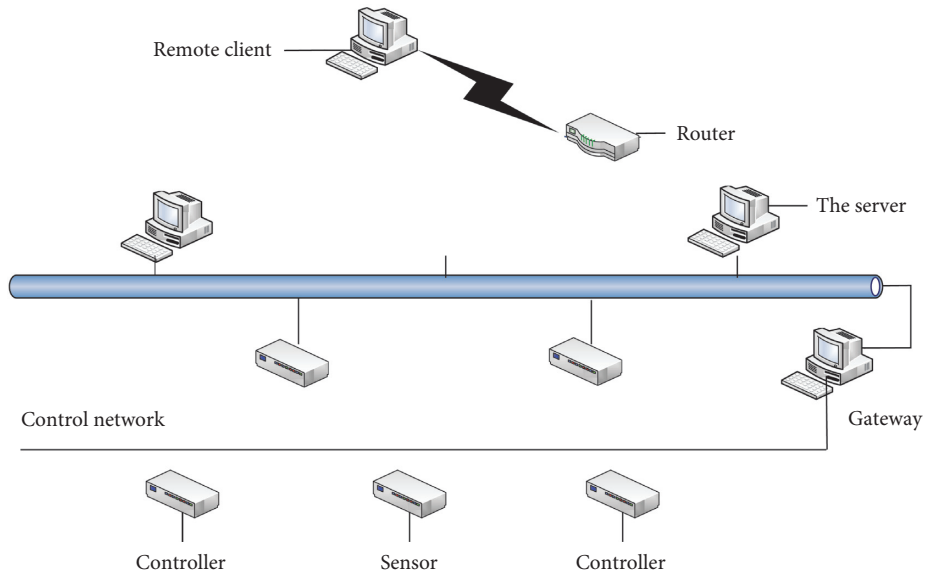

Figure 6: Service-oriented cloud storage system.

Storage_server_manage class implements the business logic of the functional module.

4. The Design of Video Course Cache Code

Since the key of the cached data is unique when the key value is known, the value can be changed within the valid time of the cached data. In the Django framework, first set the key value and value through the Django's own cache, and then introduce the Memcached module; the Memcached client is also set to the machine and then through the previously set key value to change the value and finally verified.

With the same key value test, we can get two values. But, in the same memory, the key value is unique, but there are two values. There is only one possibility. The test in the cache and the test in Memcached are not of a single value. In order to prove the conjecture, through the study of Django, we found that the Django framework encapsulates the key value. It added ":1:" before the key value to avoid the key worthy of repetitiveness.

The Django framework encapsulates the key value and ensures the uniqueness and security of the cached data by redefining the prefix. Memcached is a free, open-source, high-performance caching tool, which improves access rates in dynamic web and allows multiple users to access cached data at the same time. Figure 7 shows the working principle of Memcached.

From Figure 7, one can see that the single arrow indicates that the data is obtained from the RDBMS when the page is accessed for the first time and then stored in Memcached. The double arrow indicates that when the user accesses the page for the second time, he/she will obtain the data from Memcached. Because the Memcached server has no distributed functions, its distributed function can only be implemented by the client. Memcached servers store data independently. Multiple servers cannot share data and cannot communicate with each other.

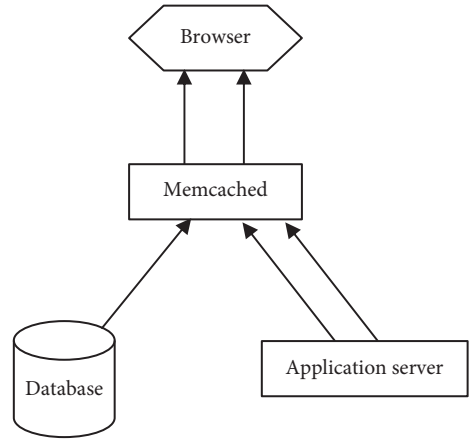

Figure 7: The working principle of Memcached.

As the number of user increases, the background will be gradually expanded. When a large number of users request the database at the same time and in case there is no caching technology, it can be imagined that the database will soon crash. In order to solve this problem along with the expandability, the two APP Server caches are merged under the Django framework.

It can be seen from the above code that the IP addresses of the two APP Servers are 101.200.0.130 and 101.200.0.162, respectively, and the service port number is 11211. When a user needs to expand the server due to business needs, he/she only needs to add the corresponding server address and port number to the code. The following code is the measured data, the relevant parameters are sent using JSON format, and it is explicitly specified that HTTP header information is not cached.

The serialization in Django is mainly used to return the retrieved data in the database to the client. In the video sharing system, the requested raw data is converted to JSON

format and then visualized and returned to the client or browser user. After formatting the video template list object through JSON, it is passed to the view module and then returned to browser.

5. Experimental Results and Analysis

In order to verify the effectiveness of the video system designed in this paper, the following comparative experiments are designed.

The traditional teaching video is the control group with two computers as the experimental object. The teaching video in this paper is the control group. Under the premise of controlling the single variable, the two groups of experiments are recorded and compared, respectively. Table 5 denotes the experimental parameter setting, and Table 6 denotes the network performance requirements.

Provided that the computers of the experimental group and the control group enter the working state at the same time and record the ring frame rate separately, in order to avoid the interference caused by unexpected events on experimental results, multiple experiments were conducted to compare the results. Figure 8 shows the comparison of frame rate for the two algorithms.

Analysis of Figure 8 shows that, with the increase of the time, the ring frame rate of the experimental group shows a trend of rising first and then decreasing. In the second experiment, the ring frame rate reaches a maximum value of 0.30. The ring frame rate of the control group also showed a trend of increasing first and then decreasing. When the second experiment was run, the ring frame rate reached a maximum value of 0.40. The initial ring frame rate of the experimental group was about 0.10, and the initial ring frame rate of the control group was about 0.70. During the third experiment, both groups of experiments reached the minimum ring frame rate. It was about 0.13 in the experimental group and it was 0.10 in the control group. Overall, compared with the control group, the experimental group presented small amplitude fluctuations, and as the number of experiments increased, the ring frame rate of the experimental group was higher than that of the control group. Figure 9 shows the comparison of node storage capacity for the two algorithms.

It can be clearly seen from Figure 9 that the node storage capacity of the curriculum system designed in this paper increases with the increase of number of relay nodes, and the increase rate is much larger than the traditional curriculum system. Figure 10 shows the comparison of time delay for the two algorithms.

It is clearly evident from Figure 11 that the delay error of the experimental group increases slowly with time, and the upward trend is slow, while the delay error of the control group rises rapidly with the time, and the uptrend is steep compared to the experimental group. Figure 11 shows the relationship between the throughput and the network load.

Table 5: Experimental parameter setting.

Project components	Server configuration	Client configuration
CPU	Intel i7	More than I3 of Intel
Memory	32 G	2 GB
Hard disk	2 TB	500 G
Operating system	More than Windows 7	Windows Server 2008
Browser	Above IE8.0	Above IE8.0
Database system	MYSQL5.5	MYSQL5.5

Table 6: Network performance requirements.

Transport protocol type	Packet loss	Network delay	Delay jitter
TCP	<1/100	<200	<50
UDP	<1/100	<500	<100

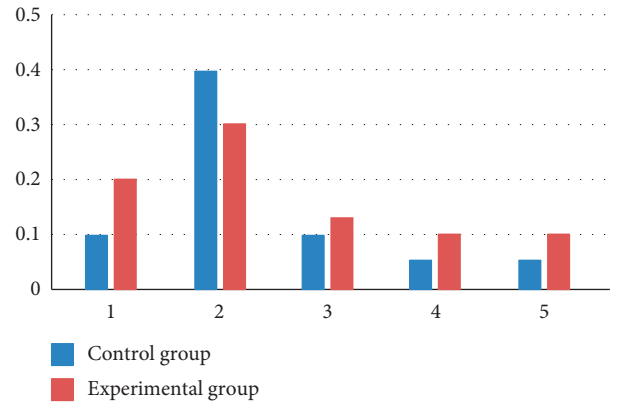

Figure 8: Comparison of frame rate for the two algorithms.

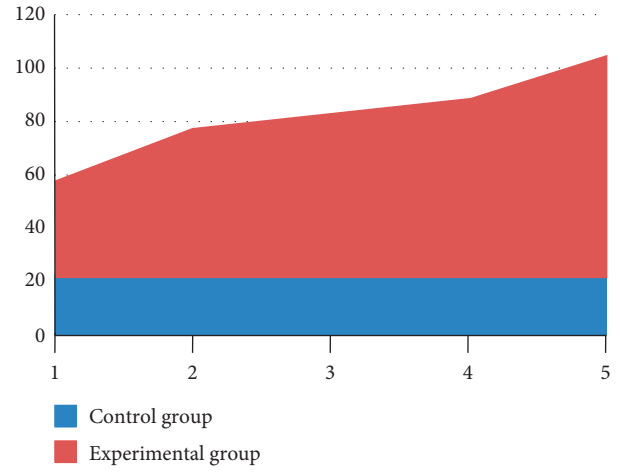

Figure 9: Comparison of node storage capacity for the two algorithms.

As shown in Figure 11, it can be seen that the throughput of the control group of the traditional method gradually decreases as the network load increases, and the throughput rate of the experimental group shows an upward trend with the increase of the network load. In summary, the video course system designed in this article is real and effective.

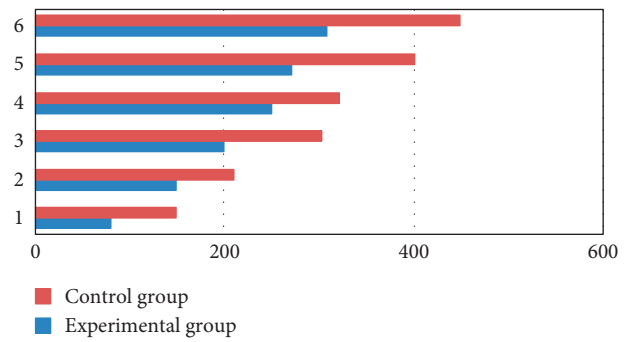

Figure 10: Comparison of time delay for the two algorithms.

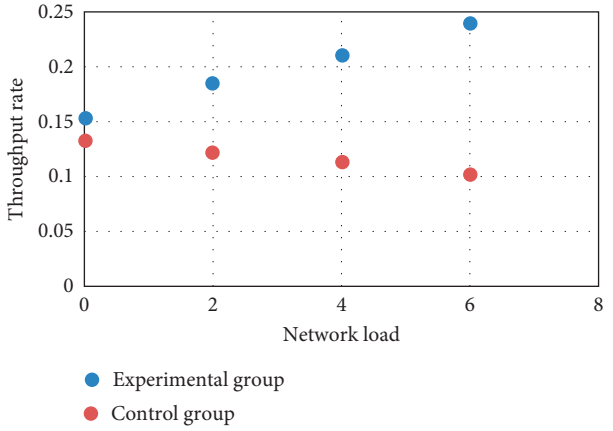

Figure 11: The relationship between the throughput and the network load.

6. Conclusion

In this paper, a video course construction method for college sports and health education under the MOOC platform is proposed. This platform verifies the advantages of the existing methods in practical real environment. Using hardware and software platforms, this paper realizes the construction of sports and health education courses and, at the same time, ensures that the system is reliable and effective. These courses are built by constructing a creative environment for video lectures, which is established using a MOOC platform. The experimental results of this approach show that the designed course's frame rate is 10% higher than that of the traditional course designing. The node's storage capacity is up to 130%, the delay error is significantly reduced, and the information throughput rate is not affected by the increase of network load.

Data Availability

The datasets used and/or analyzed during the current study are available from the corresponding author upon reasonable request.

Conflicts of Interest

The author declares that he has no conflicts of interest.

References

[1] Y. Wang, E. Zio, X. Wei, D. Zhang, and B. Wu, "A resilience perspective on water transport systems: the case of Eastern Star," *International Journal of Disaster Risk Reduction*, vol. 33, pp. 343–354, 2019.

[2] S. Froehlich, D. Grose, and R. Drechsler, "One method-all error-metrics: a three-stage approach for error-metric evaluation in approximate computing," in *Proceedings of the 2019 design, automation & test in europe conference & exhibition (DATE)*, vol. 89, pp. 754–768, Florence, Italy, March 2019.

[3] J. Frey and J. Reich, "Evaluation and application of the eclipse epsilon framework for the online execution of model-based reasoning algorithms in the context of cooperative system safety," M.Sc. thesis, Fraunhofer Institute for Experimental Software Engineering, Kaiserslautern, Germany, 2019.

[4] F. D. Ramalho, P. Y. Ekel, W. Pedrycz et al., "Multicriteria decision making under conditions of uncertainty in application to multiobjective allocation of resources," *Information Fusion*, vol. 45, no. 8, pp. 12–25, 2019.

[5] M. Y. Zhang, D. Zhang, F. Goerlandt, X. Yan, and P. Kujala, "Use of HFACS and fault tree model for collision risk factors analysis of icebreaker assistance in ice-covered waters," *Safety Science*, vol. 111, pp. 128–143, 2018.

[6] G. Wang and M. Liu, "Dynamic trust model based on service recommendation in big data," *Computers, Materials & Continua*, vol. 58, no. 3, pp. 845–857, 2019.

[7] Z. Gao, S. Zhang, H. Li, and N. Cao, "Modeling and analysis the effects of EMP on the balise system," *Computers, Materials & Continua*, vol. 58, no. 3, pp. 859–878, 2019.

[8] G. Xu, Y. Zhu, L. Deng, G. Wang, B. Li, and K.-C. Hui, "Efficient construction of B-spline curves with minimal internal energy," *Computers, Materials & Continua*, vol. 58, no. 3, pp. 879–892, 2019.

[9] C. Bingbing, "MOOCS curriculum model: contribution and dilemma," *Foreign Language Audio-Visual Teaching*, vol. 3, pp. 39-40, 2014.

[10] M. Sekula, S. Datta, and S. Datta, "optCluster: an R package for determining the optimal clustering algorithm," *Bioinformation*, vol. 13, no. 3, pp. 101–103, 2017.

[11] B. Wu, X. Yan, Y. Wang, and C. G. Soares, "An evidential reasoning-based CREAM to human reliability analysis in maritime accident process," *Risk Analysis*, vol. 37, no. 10, pp. 1936–1957, 2017.

[12] V. P. Ananthi, P. Balasubramaniam, and T. Kalaiselvi, "A new fuzzy clustering algorithm for the segmentation of brain tumor," *Soft Computing*, vol. 20, no. 12, pp. 1–21, 2015.

[13] G. Xu, Y. Zong, P. Jin, R. Pan, and Z. Wu, "KIPTC: a kernel information propagation tag clustering algorithm," *Journal of Intelligent Information Systems*, vol. 45, no. 1, pp. 95–112, 2015.

[14] H. Chen, J. Xu, G. Xiao, Q. Wu, and S. Zhang, "Fast auto-clean CNN model for online prediction of food materials," *Journal of Parallel and Distributed Computing*, vol. 117, pp. 218–227, 2018.

[15] C. Wan, X. Yan, D. Zhang, Z. Qu, and Z. Yang, "An advanced fuzzy Bayesian-based FMEA approach for assessing maritime supply chain risks," *Transportation Research Part E: Logistics and Transportation Review*, vol. 125, pp. 222–240, 2019.

[16] B. Wu, L. Zong, X. Yan, and C. Guedes Soares, "Incorporating evidential reasoning and TOPSIS into group decision-making under uncertainty for handling ship without command," *Ocean Engineering*, vol. 164, pp. 590–603, 2018.

[17] A. Alrawais, A. Alhothaily, C. Hu, and X. Cheng, "Fog computing for the Internet of Things: security and privacy issues," *IEEE Internet Computing*, vol. 21, no. 2, pp. 34–42, 2017.

[18] T. Zhou, C. Wu, J. Zhang, and D. Zhang, "Incorporating CREAM and MCS into Fault Tree analysis of LNG carrier spill accidents," *Safety Science*, vol. 96, pp. 183–191, 2017.

Hindawi
Mobile Information Systems
Volume 2021, Article ID 9919399, 10 pages
https://doi.org/10.1155/2021/9919399

Research Article

An Internet of Things Evaluation Algorithm for Quality Assessment of Computer-Based Teaching

Jing Huang

Department of Information and Electronic Engineering, Hunan City University, Yiyang 413000, Hunan, China

Correspondence should be addressed to Jing Huang; huangjing@hncu.edu.cn

Received 17 March 2021; Revised 20 April 2021; Accepted 26 April 2021; Published 26 May 2021

Academic Editor: Muhammad Usman

Copyright © 2021 Jing Huang. This is an open access article distributed under the Creative Commons Attribution License, which permits unrestricted use, distribution, and reproduction in any medium, provided the original work is properly cited.

Internet of Things has the ability to revolutionize computer-based teaching and assess the quality of teaching at the same time. The assessment of teaching efficiency is hampered by two issues: the evaluation index method (EIS) is insufficient, and the assessment framework is incapable of dealing with complicated fuzzy indexes. To address these issues, the theory of fuzzy stratification from IoT perspective is presented for the first time in this paper. This theory is based on the related theory of fuzzy assessment by measuring the teaching quality evaluation index. Initially, theoretical analysis and model measurement were merged to build a better multiangle EIS for teaching quality. To manage fuzzy indexes, a teaching quality assessment model was developed using both quantitative and qualitative studies. The suggested EIS and fuzzy assessment model can effectively evaluate the standard of teaching in schools, colleges, universities, and institutes, according to implementation results. This qualitative assessment approach is empirical and rational, and it strongly promotes the quality enhancement of educational effectiveness, based on our experimental and simulation results.

1. Introduction

Teaching evaluation is an important part of the entire teaching process. It is based on a certain teaching aspects and syllabus requirements of each subject to investigate, evaluate, and appraise teaching activities, so as to make value judgments on the quality and effect of teaching. Therefore, it is an indispensable part of the teaching process. It is an important means for in-depth education reform and improvement of teaching quality. However, the current teaching evaluation methods still remain at the level of relying on personal experience and focusing on qualitative analysis. First of all, the evaluation of teaching quality often involves multiple factors (indicators), and it must be comprehensively evaluated based on these indicators, not just from one or a few. Secondly, in comprehensive evaluation, the method of scoring each individual indicator is usually used, and then weighted average is applied. In fact, in the comprehensive evaluation problems encountered in practice, the single-factor evaluation [1–3] is often vague, and it is not appropriate to use a value absolutely. It should be represented by a fuzzy set. Therefore, in the evaluation of teaching quality, it is more appropriate to use a fuzzy comprehensive evaluation method.

Computer comprehensive evaluation is a very effective multifactor decision-making method. It is widely used in software engineering and soft science research, for example, software development cost estimation, design scheme selection, software product quality evaluation, teaching or other work quality assessments, etc. All these approaches can use the computer comprehensive assessment law [4–6].

This article will apply the relevant theories of fuzzy mathematics, combined with the multilevel indicator system of teaching quality, and propose a comprehensive computer evaluation algorithm for teaching quality. Along with that, we will discuss the role of Internet of Things in the field of education. As Internet of Things (IoT) technology has the potential to transform education at all levels, including school, college, and university, similarly, the Internet of Things (IoT) has a direct and indirect effect on learning by facilitating overall work and improving educational efficiency. In simple words, it has a broad impact on the

teaching and learning process. That is why the evaluation area of education requires serious attention, and Internet of Things (IoT) is well suited for application in this field. Finally, the experimental results and testing of the proposed scheme are relatively analyzed. It is estimated that the planned scheme will support the teachers in the accurate teaching evaluation.

The rest of this paper is organized as follows. In Section 2, a literature review is provided. In Section 3, we provide a comprehensive description of our proposed approach along with the application of IoT in education. In Section 4, we provide extensive simulation results. Finally, the paper is concluded and research directions for future work are provided in Section 5.

2. Literature Review

The use of the Internet of Things (IoT) in the educational field has provided a fantastic way to communicate and educate kids. The IoT has a major impact on the learning field. The traditional teaching practice as well as the structure of education institutions has been significantly improved with the use of IoT [7]. In the educational field, the IoT is viewed as a platform for improving an institution's infrastructure and teaching the fundamentals of computer science [8]. For an instructor or a student, be it in the classroom or on campus, IoT is equally beneficial. The effect of IoT on learning was seen in the use of sensors like Super Mechanical's Twine7 [9]. IoT allows students, instructors, and physical and virtual objects to communicate easily and efficiently [10]. The IoT is an appealing subject for learners to study the fundamentals of computer science [11]. Because of the importance of IoT, the Open University in the United Kingdom created a course called "My Digital Life" for undergraduates in the computer science department that focuses on IoT fundamentals. This program taught students how to use IoT to better understand the world and know their needs [12]. The English language will be taught using an interactive platform focused on IoT. For correcting the speech and shape of English learners' mouths, this model uses speech and visual sensors [13]. IoT is also used to teach students the fundamentals of programming. Analytical learning approaches are used to collect data and build students' learning paths. The use of the IoT as a tool to improve and simplify the educational process was comprehensively discussed in recent years. A genuine effort was made to use and apply IoT at the University of Padova [14]. Their research focused primarily on improving a web payment system for wireless communication. Their research examines the use of computing and the IoT in incorporating educational resource systems and proposes an analysis framework. Chen and Dong [15] discussed the impact of different technologies such as the IoT, cloud computing, and data mining to provide up-to-date education. Bagheri and Movahed [16] provided an overview of the educational climate as well as a distinction among intellectual and digital campuses using IoT and cloud computing. Mershad and Wakim [17] proposed an integrated model that was planned to enhance IoT in an educational world. Apart from these studies, there are many other researches in which the authors have used IoT in the educational field, as well as in other projects.

3. Application of IoT in Education and Our Proposed Model

The Internet of Things (IoT) appears to be changing education in terms of teaching and learning, school administration, research and education, school buildings, and so on [18]. Realistic IoT implementations in educational settings can be divided into numerous categories. For example, the data from IoT devices may be used to enhance management strategies and academic life. Learner analytics, greater access to knowledge, and personalizing learning by the use of connected devices could all be used to improve the efficacy of education and assessment. In this section, we discuss the various aspects that can benefit from the application of IoT.

3.1. Management Level. In administration, IoT may be used to simplify everyday operations that school administration would perform in order to free up further space and time for educational processes. While such IoT applications do not have a specific impact on learning, they can help prepare the school atmosphere for learning events and also save time that otherwise would have been wasted on everyday tasks. Mobile sensors, for instance, may be used to track equipment and relieve teachers of the responsibility of taking attendance and submitting to the management company on a daily basis [19]. Furthermore, IoT can endorse conventional systems engineering systems, assist in power management and conservation, control access control systems, and implement environmental monitoring and safety mechanisms for teachers and school staff [20]. Likewise, IoT devices can help track temperatures in the class room, which could have a positive impact on learning because physical surroundings temperature has been shown to influence students' awareness and behaviors [21]. In this way, the Internet of Things improves the cost-effectiveness of academic institutions. There is, however, a scarcity of research that examines the indirect effects of IoT systems on training. Rather, it is widely acknowledged that a much more relaxed and secure learning atmosphere will help students achieve better results. That is, the anticipated benefit of implementing IoT to address school administration problems. Furthermore, since these projects are typically costly to set up, many schools across the country will be unable to make predictions of funds to carry out such initiatives [22].

3.2. Learning/Teaching Level. The number of planned IoT frameworks at the instructional level is closely relevant to the construction problems, but this period at the person level. This includes the use of smart technology and other IoT-based participant tracking systems. For example, the authors of [23] proposed using a wrist tracker to gather information on learners' sleep habits and blood pressure. Because they argue, such information may be used to increase students' self-awareness of their sleeping and pressure habits, allowing

them to determine the best time to study and relax when planning their timetable. As can be seen in these examples, IoT devices appear to have a significant effect on what academic technologists refer to as "smart schools." Many IoT initiatives, on the other hand, are focused on a specific feature of the use of IoT for academic purposes.

3.3. Algorithm for Computer Comprehensive Evaluation. Computer comprehensive evaluation is a complex recursive calculation process. Not only can there be any limited number of evaluation objects, but each evaluation object can contain a variety of characteristics. Therefore, computer comprehensive evaluation must take into account all aspects and repeat it to get a more ideal result.

3.3.1. Algorithm Description. The basic algorithm of computer comprehensive evaluation is as follows.

Step 1. Determine the evaluation object set F, factor set U, and comment set V.

Determine the object to be evaluated according to actual needs, and construct the entire object into a set, and then use fuzzy mathematical analysis to determine the set of evaluation factors and the set of comments:

$$\text{Object set: } F = \{F_1, F_2, F_3, \ldots, F_L\}$$
$$\text{Factor set: } U = \{U_1, U_2, U_3, \ldots, U_n\}$$
$$\text{Comment set: } V = \{V_1, V_2, V_3, \ldots, V_m\}$$

Among them, L is the number of objects to be evaluated; n is the number of evaluation factors; m is the number of comments. In view of the fact that there are many factors that need to be considered in practical application problems, and the factors have hierarchical relationships, computer comprehensive evaluation usually adopts "multilevel comprehensive evaluation" algorithm (for the convenience of presentation, this article takes the second-level comprehensive evaluation as an example). At this time, a given factor set U needs to be divided into n subfactor sets $U_1, U_2, U_3, \ldots, U_n$, and the result of division should satisfy

$$U = U_1 \cup U_2 \cup \cdots \cup U_n, U_i \cap U_j = \Phi, (i \neq j), \quad (1)$$

and have

$$U_i = \{U_{i1}, U_{i2}, \ldots, U_{ik_i}\}, \quad i = 1, 2, \ldots, n. \quad (2)$$

U_i is the first level index (composite index). Since each U_i contains K_i evaluation indexes, there are $\sum_{i=1}^{n} K_i$ in the total factor set U, one evaluation index, that is, the second level index (base indicator).

Step 2. Establish a factor weight distribution matrix $A_i (i = 1, 2, \ldots, n)$ for each subfactor set $U_i (i = 1, 2, \ldots, n)$. Each factor in the evaluation factor set is in the "evaluation of the goal" process having different status and functions; that is, each evaluation factor occupies a different proportion in the comprehensive evaluation. This proportion is called the "priority weight value," or "weight value" for short. There are many ways to determine the "weight value"; for example, the "relative importance level calculation method" can be used.

The "weight value" determines whether it is reasonable and effective, which has a great impact on the computer comprehensive evaluation results.

Step 3. Make a single-level comprehensive evaluation of K_i evaluation indicators in each subfactor set U_i.

For example, $U_i = \{u_{i1}, u_{i2}, \ldots, u_{ik_i}\}$: the weight values of various factors are assigned as $a_i (a_{i1}, a_{i2}, \ldots, a_{ik_i})$, where $a_{ij} > 0$, and the comment set of U_i is $V_i = \{v_{i1}, v_{i2}, \ldots, v_{ik_i}\}$. Carrying out a single-factor evaluation on each factor of U_i, the evaluation matrix S_i can be obtained, which is,

$$S_i = \begin{bmatrix} s_{i1} \\ s_{i2} \\ \vdots \\ s_{ik_i} \end{bmatrix}. \quad (3)$$

Among them, $s_{i1}, s_{i2}, \ldots, s_{ik_i}$ represent the score of each factor evaluation object.

The so-called single-level comprehensive evaluation of the subfactor set U_i is actually to calculate the single-factor comprehensive evaluation matrix $R_i (i = 1, 2, \ldots, n)$.

$$R_i = A_i \cdot S_i. \quad (4)$$

This means after implementing S_i transformation on the input matrix (array) A_i, the output matrix (array) R_i can be obtained. Obviously, when A_i and S_i are known, compound operations can be performed:

$$R_i = A_i \cdot S_i = \{r\}. \quad (5)$$

Theoretically speaking, the above compound expressions have infinitely many kinds of calculation models. However, in the actual application process, the "weighted average" comprehensive evaluation calculation model is the most effective, because it balances all the evaluation factors according to the "weight value," which are applicable to situations where overall indicators are required.

In the "weighted average" comprehensive evaluation operation model, the weighted average operator is denoted as M (●, +). Here, "●" means ordinary real number multiplication and "ten" means ordinary real number addition.

Step 4. After comprehensively evaluating the n factors U_i of U, the total comprehensive evaluation matrix R is obtained:

$$R = \begin{Bmatrix} R_1 \\ R_2 \\ \vdots \\ R_n \end{Bmatrix}. \quad (6)$$

Step 5. Perform matrix compound operation to calculate the comprehensive evaluation result (comprehensive evaluation value) B of the object to be evaluated.

Suppose the weight value distribution matrix of U is A. Then $B = A \times R$. The operator is the same as above. It is not only the result of U's secondary computer comprehensive evaluation, but also the comprehensive evaluation result of all factors of U. That is:

$$B = A \cdot R = A \begin{bmatrix} R_1 \\ R_2 \\ \vdots \\ R_n \end{bmatrix} = A \cdot \begin{bmatrix} A_1 \circ S_1 \\ A_2 \circ S_2 \\ \vdots \\ A_n \circ S_n \end{bmatrix}. \quad (7)$$

According to the abovementioned two-level computer comprehensive evaluation principle (Steps 2–5), the evaluation of L objects to be evaluated can be successfully completed and finally the comprehensive evaluation values of L different objects to be evaluated, namely $B_1, B_2, \ldots, B_L$.

Step 6. Sort the L comprehensive evaluation values B_i ($i = 1, 2, \ldots, L$) 21 and output the sorting result.

At this point, the entire computer comprehensive evaluation work is announced. Obviously, for teaching quality evaluation, the larger the evaluation value, the higher the teaching quality level, and the smaller the evaluation value, the lower the teaching quality level.

3.3.2. Block Diagram of Algorithm Programming. In order to facilitate computer implementation, the following is a flowchart (simplified diagram) of the computer comprehensive evaluation algorithm. This flowchart of Figure 1 is based on the basic computer comprehensive evaluation algorithm.

Users can choose any program design according to their needs. Language compiles computer comprehensive evaluation program.

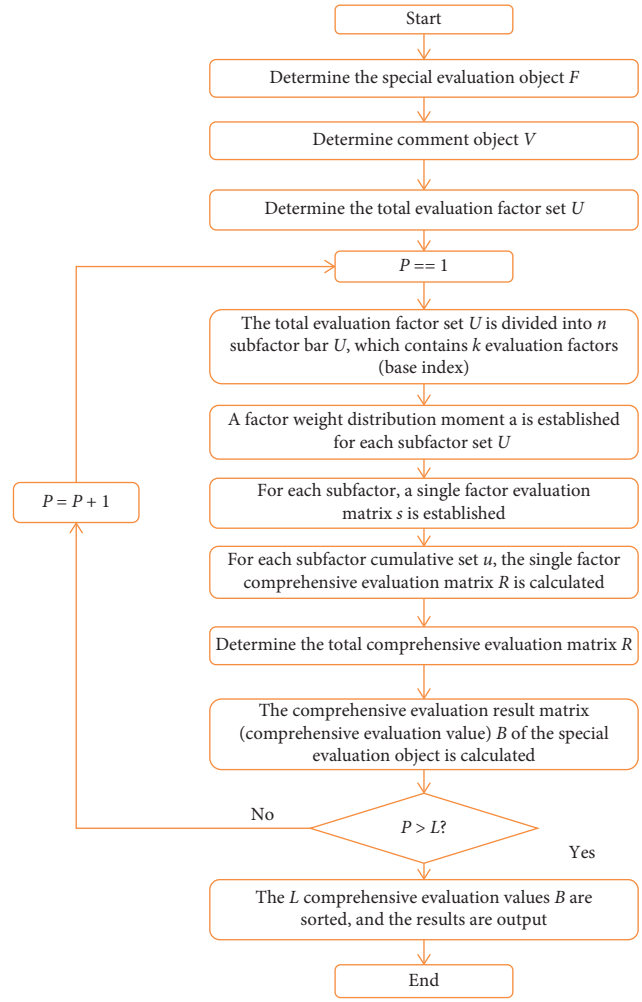

Figure 1: Flow chart of computer comprehensive evaluation (level 2).

3.3.3. Computer Comprehensive Evaluation Index System for Teaching Quality. Teaching quality is a fuzzy concept. When people form a concept in their minds, it has a certain connotation and extension. The entire set of objects that conform to this concept is the extension of this concept. For teaching quality, it is both there is no clear extension and the connotation is quite complicated. For its evaluation, generally only a few representative indicators can be selected for assessment.

Considering that the teaching process is complex composed of many factors, the quality of teaching is often reflected from different aspects. Therefore, when evaluating teaching, it is necessary to carry out many aspects of the teaching process from different perspectives and different aspects. It is necessary to evaluate the final teaching effect, but also pay attention to the role played by each link in the teaching process and treat them as a whole. When applying fuzzy mathematics to analyze practical problems, the first step is to establish a hierarchy in the substructure diagram, the highest level is the general goal, the middle level is the criteria to be followed when making decision analysis, and the lowest level is the evaluation index level. Generally speaking, the indicators reflecting the quality of teaching can be summarized into the following 5 aspects:

(1) Teacher preparation: this indicator reflects the overall level of teacher preparation, such as teaching purpose, teaching preparation, and homework design.

(2) Textbook processing: this indicator reflects the ability of teachers to control textbooks and teach students in accordance with their aptitude. Such as the scientific nature of knowledge transfer, the processing of key and difficult points, and the cultivation of student abilities.

(3) Implementation of teaching methods: it reflects whether the structure and arrangement of classroom teaching are reasonable, whether the selection and combination of teaching methods are appropriate, and whether the cooperation between teachers and students is tacitly compatible, such as the overall design of the classroom, teaching bilateral activities, the combination of teaching methods, and the use of teaching methods.

(4) Teaching quality: it reflects the degree of influence of teachers' teaching quality on teaching quality, including teaching attitude, teaching language, blackboard writing, and demonstration.

(5) Teaching effect: it reflects the final result of the teaching process, including the classroom teaching atmosphere, the situation of completing the teaching plan, the situation of students mastering knowledge, and the improvement of students' thinking ability.

The above five types of indicators constitute an indicator system that reflects the level of teaching quality, which can be expressed as a hierarchical analysis diagram. In actual application, the indicators should be independent and inclusive of each other.

3.3.4. Determination of the Weight Value of the Comprehensive Evaluation Index of Teaching Quality. The comprehensive evaluation indicator system has multiple indicators and multiple levels, and each indicator has different effects on the indicators of the previous layer. In actual comprehensive evaluation, different weight values are often used to indicate the size of its effect. But the determination of the weight value is often subjective factors. In order to make the weight value of each indicator reflect the objective reality as much as possible, the method of 0~4 score in Table 1 is used to determine the relative importance weight of these indicators.

The specific steps are as follows.

(1) Draw up an expert score sheet and ask each expert to fill it out separately.

Scoring method: compare n evaluation indicators in pairs; the very important side scores 4 points, the less important side scores 0 points, the more important side scores 3 points, the less important side scores 1 point, and the two equally important sides score 2 points. The total score of 0~4 is $\sum_{i=1}^{n} C_i = 2n(n-1)$, where n is the number of indicators.

(2) There are m experts to participate in the scoring, and the j^{th} expert's scoring value for the i^{th} index is $C_{ij}(i = 1, 2, \ldots, m)$ calculating the score Z of each index,

$$Z_i = \sum_{j=1}^{m} C_{ij}, \quad i = 1, 2 \ldots, n. \tag{8}$$

(3) Calculate the total score

$$Z = 2mm(n-1). \tag{9}$$

(4) Calculate the weight value of each indicator

$$A_i = \frac{z_i}{z}, \quad i = 1, 2 \ldots, n. \tag{10}$$

According to the above method, fill in the form through the scores of the experts, and calculate the importance weight of each level index relative to the upper level index as shown in Table 2.

Table 1: 0~4 score table.

Index	$X_1, X_2, \ldots, X_n$	Score	Proportion
X_1		C_1	$C_1/\sum C_1$
X_2		C_2	$C_1/\sum C_1$
...		...	...
X_n		C_n	$C_n/\sum C_n$
$\sum$		$\sum C_i$	1.000

3.3.5. Mathematical Model of Computer Comprehensive Evaluation of Teaching Quality. Suppose the object set to be evaluated is $F = \{F_1, F_2, F_3, \ldots, F_L\}$, the comment set is $V = [0, 1]$, and a continuous real number interval is acceptable. Hence, the following needs to be considered.

(1) Determine the Score Value of Each Base Indicator. The scoring value of each base indicator is scored by the members of the teaching quality assessment team on the 17 base indicators on a percentile system, and these scoring values are relatively independent.

(2) Evaluation of Base Indicators. The evaluation of the base index is to determine the membership function $\mu s\,(X_i)$ of each base index X to the comment set V and find its evaluation value s_j. According to the theory of fuzzy mathematics, the membership function can be defined as the following evaluation model:

$$s_i = \mu_s(X_i) = \begin{cases} 0\,(0 \le X_i < 50), \\ \\ \dfrac{1}{50} X_i - 1\,(50 \le X_i \le 100). \end{cases} \tag{11}$$

3.3.6. Evaluation of Composite Indicators. The evaluation of the composite index is the multilevel computer comprehensive evaluation. Let U be the ith ($i = 1, 2, ..., 5$) evaluation subset in the overall goal of teaching quality, and the corresponding importance weight vector is A, and the membership degree (evaluation value) vector that has been obtained from the evaluation of the base index is S. Use the fuzzy relation composition operation (the operator is M (●, +)) to obtain the evaluation value of the composite index for the overall goal of teaching quality for

$$R_i = A_i \cdot S_i = \sum_{i=1}^{k} a_{ij} s_{ij}, \tag{12}$$

where $a_{ij} \in [0, 1]$ and $\sum_{i=1}^{k} a_{ij} = 1$, $s_{ij} \in [0, 1]$, $k = 3$ or 4.

3.3.7. Comprehensive Evaluation of the General Objective. The comprehensive evaluation of the overall goal is a multilevel and two-level computer comprehensive evaluation, which is a comprehensive evaluation based on a composite index evaluation.

Table 2: The importance weight for each level index relative to the upper level index.

Index	Weight	Index	Weight
F_1: teachers prepare lessons	0.19	X_7: overall classroom design	0.27
F_2: textbook processing	0.16	X_8: bilateral teaching activities	0.22
F_3: teaching method implementation	0.20	X_9: teaching methods	0.26
F_4: teaching quality	0.19	X_{10}: application of teaching means	0.25
F_5: teaching effect	0.26	$\sum$	1.00
$\sum$	1.00	X_{11}: teaching attitude	0.38
X_1: teaching purpose	0.35	X_{12}: teaching language	0.32
X_2: teaching preparation	0.41	X_{13}: blackboard writing and demonstration	0.30
X_3: job design	0.24	$\sum$	1.00
$\sum$	1.00	X_{14}: classroom atmosphere	0.20
X_4: the science of knowledge transfer	0.37	X_{15}: completion of teaching plan	0.23
X_5: treatment of key and difficult points	0.32	X_{16}: students' knowledge	0.27
X_6: the cultivation of students' ability	0.31	X_{17}: the improvement of students' thinking ability	0.30
$\sum$	1.00	$\sum$	1.00

$$B = A \cdot R = \sum_{i=1}^{5} A_i R_i. \quad (13)$$

$B \in [0, 1]$ is the final evaluation value.

Through the above Steps 1–4, the relative evaluation results of the L objects to be evaluated $F, F_z, , F_L$ to measure the teaching quality can be obtained $Y = B_1, B_2, ..., B_L$, where $B \in [0, 1]$ and the value of B reflects the level of teaching quality. The larger the value, the higher the teaching quality. According to this, $F_1, F_2, ..., F_m$ represents the order of teaching quality.

3.3.8. Application Examples. As for the application of the abovementioned comprehensive computer evaluation algorithm for teaching quality, four teachers from different teaching and research sections of a technical secondary school are selected as the evaluation objects. According to the evaluation index system of teaching quality, from teacher preparation, textbook processing, teaching method implementation, teaching quality, and teaching effect 5 subobjectives, we comprehensively evaluate the teaching quality of 4 teachers: *A*, *B*, *C*, and *D* and sort them by the size of the evaluation value. The scoring of the base index is the basis of the entire evaluation process. In order to make the scoring value of the base index true, it reflects the actual teaching situation of teachers. For different basic indicators, different methods are used to score the following.

(1) Test Method. Use different forms such as written examination, oral examination, and practical operation to assess students' mastery, understanding, and application of knowledge.

(2) Observation Method. The members of the evaluation team are immersive and obtain first-hand information of teaching activities in a natural state and then make a score. It is mainly used to score basic indicators such as teachers' teaching attitude, teaching language, classroom teaching atmosphere, and teaching bilateral activities.

(3) Investigation Method. These methods include holding a symposium, filling out a written survey form, interviewing students and parties, understanding the situation, and making an assessment.

(4) Inspection Method. Check the teacher's lesson preparation notes, homework correction records, student work, etc., to understand the information to be mastered when grading. After completing the above preparations, you can start the evaluation.

3.3.9. Base Index Evaluation. The members of the teaching quality evaluation team scored the 4 teachers one by one according to 17 base indicators and then calculated the average score for each base indicator as the score value of the base indicator. Score one by one, and calculate the average score for each base indicator as the score value of the base indicator. Substitute the score value into the membership function to calculate the degree of membership, which is the evaluation result of the base index.

3.3.10. Evaluation of Composite Indicators. According to the importance weight of the base index and the composite index evaluation mathematical model, the evaluation results of all composite indicators can be calculated. For example, the calculation of the composite indicator Ui of teacher *A* in Table 3:

$$R_1 = (0.35, 0.41, 0.24) \cdot \begin{bmatrix} 0.76 \\ 0.68 \\ 0.82 \end{bmatrix} = 0.35 \cdot 0.76 + 0.41. \quad (14)$$

In the same way, all the composite index evaluation values of each teacher can be calculated, as shown in Table 3.

3.3.11. Comprehensive Evaluation of the Overall Goal. According to the composite index importance weight and the overall objective comprehensive evaluation mathematical model, the comprehensive evaluation results of the four teachers' teaching quality are calculated (as shown in Table 4).

Table 3: Evaluation results of composite indicators.

Composite index	Evaluation value	JIA	YI	BING	DING
U_1	R_1	0.7416	0.7074	0.6736	0.8266
U_2	R_2	0.5272	0.4208	0.5230	0.5672
U_3	R_3	0.6150	0.6006	0.6660	0.6500
U_4	R_4	0.5700	0.4656	0.6528	0.5928
U_5	R_5	0.6526	0.6246	0.5782	0.6188

Table 4: Comprehensive evaluation results.

Teacher	JIA	YI	BING	DING
Comprehensive evaluation value b	0.6263	0.5727	0.6192	0.6513

For example, we have the overall goal U for teacher A and comprehensive evaluation value calculation.

$$B = (0.19, 0.16, 0.20, 0.19, 0.26) \cdot \begin{bmatrix} 0.7416 \\ 0.5272 \\ 0.6510 \\ 0.6526 \end{bmatrix} = 0.19 \cdot 0.7416 + 0.16 \cdot 0.5272 + 0.20 \cdot 0.6510 + 0.26 \cdot 0.6526 = 0.6263. \quad (15)$$

In the same way, the comprehensive evaluation value B of other teachers can be obtained. It can be seen that the order of the four teachers' teaching quality level from high to low is D, A, C, B.

From the final evaluation results, it can better reflect the actual teaching quality level of the four teachers, achieve the expected evaluation goals, and achieve satisfactory results.

3.3.12. Fuzzy Logic Assessment. We proposed an infrastructure that enables a first evaluation of the learners' approach [24, 25] to solve the first challenges they may face, when designing their solution. Without any of the involvement of a teacher, students will ask the system what is incorrect with the answer they are creating. Our goal is to build a framework that aids learners in comprehending what they are learning. There are several methods to assess computer learning practices, where [26] has a strong survey on static or dynamic evaluation of computer software as shown in Figure 2.

As seen in the diagram above, the instructor first asks for an integration of the optimal estimated algorithm for solving a problem. Following that, a number of software parameters that influence its architecture will be determined. As a result, we have an example of the ideal estimated algorithm. Then, by each parameter, fuzzy numbers will be generated in the following way: each fuzzy set will begin as a default triangular function centered on the estimated algorithm's metric value; the teacher may easily change the fuzzy set suggesting the following:

(i) The solution's highest values that the educator finds low

(ii) The bare min of validity

(iii) The highest possible score for accuracy

(iv) The solution's min value that the educator finds high

4. Experimental Results

4.1. Experiment. The experimental results of our proposed system can be divided into the following stages.

4.1.1. Choice of Teaching Quality Analysis Cases. This paper will conduct performance testing of related models after choosing the model method and design. Developers of network teaching methods have increasingly developed many common course models for various educational needs in recent times. Traditional personal mentoring programmes, student-centered personal mentoring classes, personalized online education classes, knowledge-first personal mentoring classes, explorative personal mentoring classes, and conceptual personal mentoring classes are some of the new trajectory structures available. This article suggests an Internet of Things evaluation algorithm for Computer Teaching Quality Model which is a combination of wireless sensor networks and fuzzy comprehensive evaluation algorithms to address the aforementioned issues. On this foundation, we will choose teaching quality diagnostic situations for performance monitoring based on relevant regulations.

4.1.2. Test for Teaching Quality Diagnostic Performance. As compared to other models, the design has obtained strong experimental performance, as seen in Figure 3. The failure rate of network detection of teaching quality diagnosis reduced as the number of test samples increased, and much more accurate results have been obtained. The efficiency of the convolutional neural network is quite high as

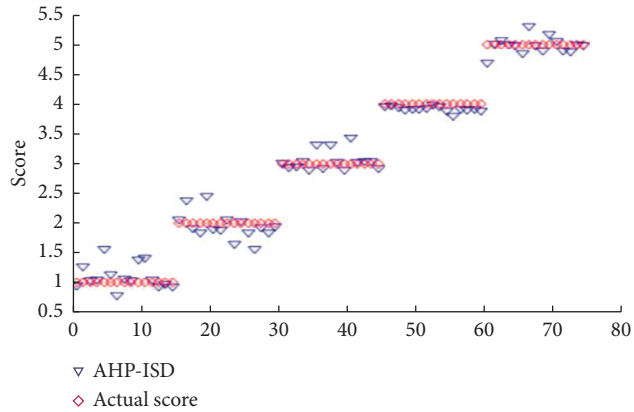

Figure 2: Fuzzy logic.

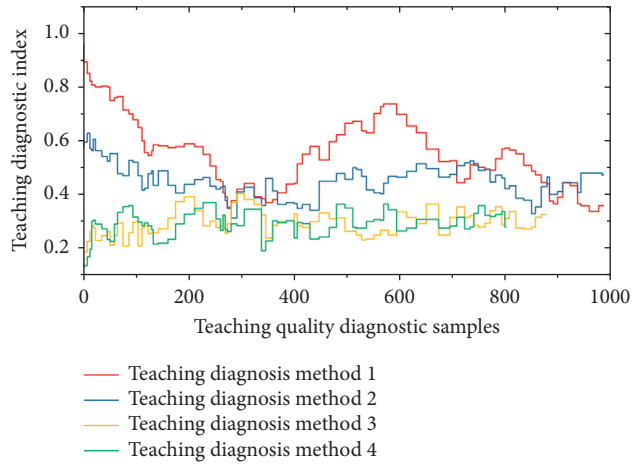

Figure 3: Judgment achievement rate of the teaching quality diagnosis system.

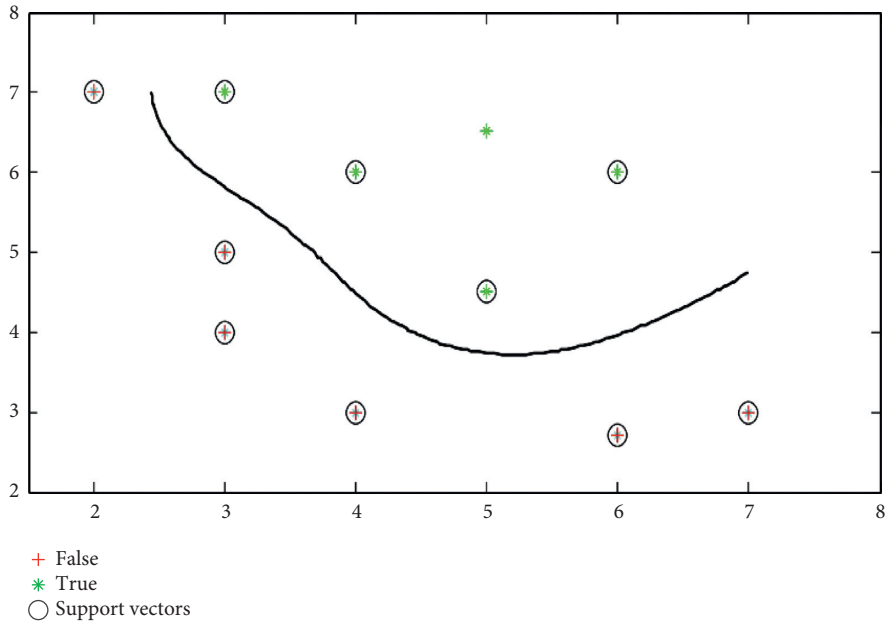

Figure 4: SVM exercise outcomes when $\lambda = 0.6$ evaluation result.

compared to many other algorithms, as per the results. As a result, the test results reveal that convolutional neural networks' extraction performance is significantly higher than other approaches' data mining capacities and that they can give better effective information mining and retrieval for the teaching quality diagnosis process.

4.2. Teaching Quality Evaluation (TQE) of Support Vector Machine (SVM) Grounded on Analytic Hierarchy Process-ASD. The following is the SVM teaching quality assessment method focused on AHP-ISD:

Stage 1. The data from each assessment is normalized in this process, and a teaching quality decision matrix is developed

Stage 2. During this stage, the weight of AHP as well as ISD is designed

Stage 3. During this stage, the comprehensive weight of AHP-ISD is designed

Stage 4. During this stage, the development directory data is separated into two sets such as test set and trained set

Stage 5. Here the SVM prediction model is set up by our trained data set

Stage 6. This is the last stage, where the SVM teaching quality evaluation design is tested

The evaluation result of SVM exercise outcomes when $\lambda = 0.6$ can be explained in Figure 4.

5. Conclusion

This paper applies the related theories of fuzzy mathematics and uses the analytic hierarchy process to put forward a new idea of comprehensive evaluation of teaching quality by computer, so as to make a preliminary exploration of the transformation of teaching quality evaluation from qualitative analysis to quantitative analysis. We have addressed different issues of teaching quality and designed a model to solve these issues. We have the theoretical analysis and model measurement to build a better multiangle EIS for teaching quality. To manage fuzzy indexes, a teaching quality assessment model was developed using both quantitative and qualitative studies. Practical results show that the use of teaching quality computer synthesis as the evaluation method can efficiently achieve the expected evaluation goal and obtain satisfactory results. For future we have planned to increase the efficiency of teaching quality evaluation. Furthermore, we have planned to use different AI techniques to improve the teaching quality and to create smart teacher technique which will increase teaching quality.

Data Availability

The data used to support the findings of this study are included within the article.

Conflicts of Interest

The author declares that there are no conflicts of interest.

References

[1] M. Zhao and W. Zhan, "Teaching quality evaluation system based on deep learning algorithm," *Modern Electronic Technology*, vol. 43, no. 13, pp. 143–146, 2020.

[2] C. Yu, "Research on innovative teaching of basic courses of computer application in the big data era," *Talent*, vol. 12, no. 18, p. 135, 2020.

[3] H. Jin, Z. Li, M. Qi, and F. Jian, "Research on comprehensive ability evaluation model of computer professionals," *Software Guide*, vol. 19, no. 6, pp. 257–260, 2020.

[4] Li Pei, "Research on the evaluation index system of computer network technology practice teaching quality based on big data," *Network Security Technology and Application*, vol. 5, pp. 99-100, 2020.

[5] X. Zhong and R. Li, "Research on the process control of student evaluation on teaching quality of university teachers," *Education Review*, vol. 2, pp. 61–65, 2020.

[6] Q. Yang, Y. Lian, T. Zhao, and H. Yuan, "Research on the improvement of teaching quality of computer mathematics courses," *Education Modernization*, vol. 7, no. 17, pp. 51-52, 2020.

[7] M. Veeramanickam and M. Mohanapriya, "IOT enabled futurus smart campus with effective E-learning: i-campus," *GSTF Journal of Engineering Technology (JET)*, vol. 3, no. 4, p. 81, 2016.

[8] H. F. Elyamany and A. H. AlKhairi, "IoT-academia architecture: a profound approach," in *Proceedings of the 2015 16th IEEE/ACIS International Conference on Software Engineering, Artificial Intelligence, Networking and Parallel/Distributed Computing (SNPD)*, June 2015.

[9] S. Gul, M. Asif, S. Ahmad, M. Yasir, M. Majid, and M. Arshad, "A survey on role of internet of things in education," *IJCSNS*, vol. 17, no. 5, pp. 159–165, 2017.

[10] J. Marquez, J. Villanueva, Z. Solarte, and A. Garcia, "IoT in education: integration of objects with virtual academic communities," in *Proceedings of the 2016 World Conference on New Advances in Information Systems and Technologies*, Recife, Brazil, March 2016.

[11] J. Chin and V. Callaghan, "Educational living labs: a novel internet-of-things based approach to teaching and research," in *Proceedings of the 2013 9th International Conference on Intelligent Environments (IE)*, July 2013.

[12] Y. Wang, "English interactive teaching model which based upon internet of things," in *Proceedings of the 2010 International Conference on Computer Application and System Modeling (ICCASM)*, October 2010.

[13] H.-C. Cheng and W.-W. Liao, "Establishing an lifelong learning environment using IOT and learning analytics," in *Proceedings of the 2012 14th International Conference on Advanced Communication Technology (ICACT)*, IEEE, PyeongChang, South Korea, February 2012.

[14] A. P. Castellani, N. Bui, P. Casari, M. Rossi, Z. Shelby, and M. Zorzi, "Architecture and protocols for the internet of things: a case study," in *Proceedings of the 2010 8th IEEE International Conference on Pervasive Computing and Communications Workshops (PERCOM Workshops)*, March 2010.

[15] Y. Chen and X. Dong, "The development and prospect of new technology in modern distance education," in *Proceedings of the 2013 International Conference on Information Science and*

Computer Applications (ISCA 2013), Tel Aviv, Israel, October 2013.

[16] M. Bagheri and S. H. Movahed, "The effect of the internet of things (IoT) on education business model," in *in Proceedings of the 2016 12th International Conference on Signal-Image Technology and Internet-Based Systems (SITIS)*, November 2016.

[17] K. Mershad and P. Wakim, "A learning management system enhanced with internet of things applications," *Journal of Education and Learning*, vol. 7, no. 3, p. 23, 2018.

[18] Z. Tianbo, "The Internet of things promoting higher education revolution," in *Proceedings of the Fourth International Conference on, Multimedia Information Networking and Security (MINES)*, pp. 790–793, IEEE, Nanjing, China, November 2012.

[19] B. D. Ralhan, "6 ways the internet of things is transforming the education sector: Featurephilia," 2017, http://indiatoday.intoday.in/education/story/internet-ofthings-transforming-education/1/870592.html.

[20] C. Benson, "The Internet of things, IoT systems, and higher education," *Educause Review*, vol. 51, pp. 34–43, 2016.

[21] S. Mishra, "12 modern learning practices with internet of things," 2017, http://www.clickonf5.org/internet/modern-learning-practices-iot-education/126745.

[22] I. Asseo, M. Johnson, B. Nilsson, C. Neti, and T. J. Costello, "The internet of things: riding the wave in higher education," *Educause Review*, vol. 51, pp. 11–33, 2016.

[23] F. De Arriba-Pérez, M. Caeiro-Rodríguez, and J. M. Santos-Gago, "Towards the use of commercial wrist wearables in education," in *Proceedings of the 2017 4th Experiment@International Conference (exp. at'17)*, June 2017.

[24] M. Ben-Ari, "Constructivism in com-puter science education," *Journal of Computers in Mathematics and Science Teaching*, vol. 20, no. 1, pp. 45–73, 2001.

[25] D. Traynor, S. Bergin, and J. P. Gibson, "Automated assessment in CS1,"vol. 52, pp. 223–228, in *Proceedings of the 8th Australian Conference on Computing Education*, vol. 52, pp. 223–228, Australian Computer Society, Inc., Darlinghurst, Australia, January 2006.

[26] K. M. Ala-Mutka, "A survey of automated assessment approaches for programming assignments," *Computer Science Education*, vol. 15, no. 2, pp. 83–102, 2005.

Hindawi
Mobile Information Systems
Volume 2023, Article ID 9875791, 1 page
https://doi.org/10.1155/2023/9875791

Retraction

Retracted: Intelligent Sports Training System Based on Artificial Intelligence and Big Data

Mobile Information Systems

Received 8 August 2023; Accepted 8 August 2023; Published 9 August 2023

Copyright © 2023 Mobile Information Systems. This is an open access article distributed under the Creative Commons Attribution License, which permits unrestricted use, distribution, and reproduction in any medium, provided the original work is properly cited.

This article has been retracted by Hindawi following an investigation undertaken by the publisher [1]. This investigation has uncovered evidence of one or more of the following indicators of systematic manipulation of the publication process:

(1) Discrepancies in scope
(2) Discrepancies in the description of the research reported
(3) Discrepancies between the availability of data and the research described
(4) Inappropriate citations
(5) Incoherent, meaningless and/or irrelevant content included in the article
(6) Peer-review manipulation

The presence of these indicators undermines our confidence in the integrity of the article's content and we cannot, therefore, vouch for its reliability. Please note that this notice is intended solely to alert readers that the content of this article is unreliable. We have not investigated whether authors were aware of or involved in the systematic manipulation of the publication process.

Wiley and Hindawi regrets that the usual quality checks did not identify these issues before publication and have since put additional measures in place to safeguard research integrity.

We wish to credit our own Research Integrity and Research Publishing teams and anonymous and named external researchers and research integrity experts for contributing to this investigation.

The corresponding author, as the representative of all authors, has been given the opportunity to register their agreement or disagreement to this retraction. We have kept a record of any response received.

References

[1] C. Li and J. Cui, "Intelligent Sports Training System Based on Artificial Intelligence and Big Data," *Mobile Information Systems*, vol. 2021, Article ID 9929650, 11 pages, 2021.

Hindawi
Mobile Information Systems
Volume 2021, Article ID 9929650, 11 pages
https://doi.org/10.1155/2021/9929650

RETRACTED

Research Article

Intelligent Sports Training System Based on Artificial Intelligence and Big Data

Chunguang Li[1] and Jianbiao Cui[2]

[1]*Institute of Physical Education, Dezhou University, Dezhou 253023, Shandong, China*
[2]*College of Physical Education, Hunan First Normal University, Changsha 410006, Hunan, China*

Correspondence should be addressed to Jianbiao Cui; cuijianbiao2021@163.com

Received 10 March 2021; Revised 24 April 2021; Accepted 7 May 2021; Published 24 May 2021

Academic Editor: Muhammad Usman

Copyright © 2021 Chunguang Li and Jianbiao Cui. This is an open access article distributed under the Creative Commons Attribution License, which permits unrestricted use, distribution, and reproduction in any medium, provided the original work is properly cited.

All activities in training fields are for the improvement of athletes' competitive abilities. A sports training system is an organizational system to achieve common goals. Competitive ability is one of the main manifestations of the evolution of the training system. With the rapid development of computer technology, people have begun to combine virtual reality and other technologies to achieve scientific sports-assisted training to eliminate traditional sports training that relied purely on experience. Pose estimation obtains the position, angle, and additional information about the human body in the image in a two-dimensional plane or three-dimensional space by establishing the mapping relationship between the human body features and the human body posture. This article demonstrates a golf-assisted training system to realize the transformation from an experience-based sports training method to a human motion analysis method, using artificial intelligence and big data. The swing posture parameters of the trainer and the coach are obtained using the posture estimation of a human body. Based on this information, an auxiliary training system is built. The two parameters of the joint angle trajectory and the posture similarity are used as auxiliary indicators to compare the trainers. The joint angle trajectory is analyzed, and the coach is guided based on the similarity of the posture.

1. Introduction

Modern training theory believes that the training process of athletes is a systematic project, which is a process of multidisciplinary integration of the "best" combination of factors. Therefore, to grasp the athlete's competitive career process [1], it is necessary to clearly understand the athlete's growth process and the conditions under which the athlete's training system [2–4] forms and evolves. It is one of the essential prerequisites for the athlete's multiyear systematic training to become "scientific" [5–7].

The diversification and professional development of today's competitive sports have made sports training [8, 9] a unique human activity, increasingly rich and complex. With the development of sports training practice and the deepening of people's understanding of the connotation and extension of sports training, more and more people have gradually realized that modern sports training is a process of specialized training for athletes, which continuously improves their performance. It is a process in which competitive ability is its primary objective [10, 11]. For an athlete to engage in competitive training to reach the peak of individual competitive training through systematic training, it is a phased, continuous, and complete training process. This training process usually lasts more than ten years or even more. Then, in this perennial system training, to improve the athletic performance of athletes at a particular stage, not only many people are involved but also many disciplines are involved. The cooperation and operation of these factors constitute the athlete training system. Among them, personnel include coaches, scientific research personnel, management personnel, and service personnel. The personnel regulate athletes' sleeping style, diet and wearable kits, training methods, and training frequency. They may be involved in the design and construction of facilities on which athletes complete training [12]. The competition in modern

competitive sports is becoming increasingly fierce, and athletes' success often depends on "details." It requires different personnel to be careful in their areas of responsibility to ensure the smooth improvement of athletes' competitive abilities so that multidisciplinary knowledge can be fully penetrated into the sports training process, forming a complex system with multiple factors. A multidisciplinary system is an organizational system that achieves common goals, and any such system has certain organizational goals and organizational management problems. It aims to make the athletes' competitive abilities develop to the ideal state [13].

In traditional sports training [14, 15], training methods based on visual observation are usually adopted. With the development of computer vision [1, 2], people begin to use cameras to capture and analyze the athletes' movements. In sports training, the movements of athletes are analyzed and tracked from the video image sequence. A comparison of the athletes' postures is made through scientific quantitative analysis of athletes' movement characteristics and then combines human physiology and physics principles to propose improvements in sports movements. The method assists athletes in training to get rid of traditional sports training purely relying on experience, realize intuitive exercise analysis and guidance, and scientifically improve the level and performance of athletes.

Human-centered technology [16–18] and product design have always been the focus of scientific research personnel and scientific research institutions. The application of computer vision technology in sports training has just started. This article is dedicated to applying artificial intelligence [19–21] and big data technology in the field of sports training. Various training suggestions are provided to detect and track the moving human body in the video and analyze sports posture. We use the human motion analysis based on computer vision. Based on the analysis of this paper, it can be seen that the research of auxiliary sports training systems has substantial theoretical research value and practical engineering significance and has broad application prospects. Following are the main contributions of this paper:

(1) This paper uses the Kinect sensor plug-in OpenNI code to automatically extract the three-dimensional data of 15 joint points of the human body. Finally, the manually extracted posture data are compared with the posture data obtained based on the Kinect three-dimensional sensor to complete its accuracy verification.

(2) This paper proposes a background modeling algorithm based on ViBe modeling, which uses neighborhood pixels to create a background model. Experiments show that this method overcomes the shortcomings of traditional methods and can achieve better detection results for dynamic backgrounds.

(3) Based on the model-based human pose estimation algorithm and the model-free pose estimation algorithm, this paper proposes a human pose estimation method based on contour features combined with image processing. The edge detection is performed on the binary contour map obtained by target detection, and the horizontal scanning is performed. Image processing methods such as human body length ratio constraint have realized the posture estimation of human joints. Experiments show that this method can more accurately extract the main joint data of the human body.

This paper is organized as follows. The related work is discussed in Section 2. The proposed methodology is discussed in Section 3. The experimental results are elaborated in Section 4. Finally, we conclude the paper and provide future research direction in Section 5.

2. Related Work

In this section, we discuss the related work pertaining to our approach. First, we discuss the concept of the athlete training system followed by the impact of competition on athletes' training system, auxiliary training system, and human body pose estimation. We believe the comprehensive review will provide a solid foundation for our proposed work.

2.1. Concept of Athlete Training System. There are three main differences between the athlete training system and the conventional training system. First, the athlete training system is part of the entire training system, and in terms of resources, environment, and other factors, the two are the same to some extent. Still, the factors involved in the athlete training system are part of the entire training system. However, not all these factors are contained in the training system during the training of athletes. The second is that the existence of the athlete training system is based on the presence of the athlete's competitive ability. For example, consider the case when the athlete quits a competitive sports career [22]. In that case, the training system surrounding the athlete will no longer exist, and the training system always exists because of competitive sports. Finally, the athlete training system is a part of the entire competitive sports training system. The athlete training system highlights the athlete's prominent position in training and takes the athlete's competitive ability as the state parameter of the evolution of the training system [23].

2.2. The Impact of Competition on Athletes' Training System. In the athlete training system, all training activities are organized around improving athletes' competitive ability. All athletes participate in competitions to create ideal sports performance. Competitive ability is the ability that athletes must possess to participate in competitive contests. Having a competition inevitably requires athletes to have specific competitive abilities. Only in this way can they show the concept of higher, faster, and stronger competitive sports. Therefore, the emergence and development of the athlete training system must be closely related to the competition

RETRACTED

and continue to evolve and sort out with the competition level changes. The competition plays a guiding role in the development of the athlete's training system [24].

2.3. Auxiliary Training System. As golf has become more popular and valued by people, many auxiliary training devices related to golf have appeared in recent years. With the application of computer technology in sports training, a group of companies dedicated to the research of assisted golf training systems has emerged worldwide and has achieved significant results. The main methods currently used are the image method, graph analysis method, and portable sensor method. The imaging method captures the athletes' movements during the swing through image acquisition equipment and then analyzes and evaluates the movements based on past experience. The video method used in the assisted golf training system is the use of golf motion analysis software "MotionCoach" developed by the Canadian software development company Media Vention. The golf swing analysis system was researched by the American sports software development company Gary Brooks and the DartGoffer developed by the Swiss software development company DartFish [25]. MotionCoach processes video manual calibration and combines the training opinions of golf experts in the calibration and classification assessment process and provides more scientific and meaningful training guidance for the trainees.

The graph analysis method reprocesses the graph information. It extracts the physical parameters based on collecting the image information of the athlete's swing process and compares them with the standard template parameters to realize the digitization of classification evaluation. The graph analysis method used in the golf-assisted training system mainly includes the golf-assisted swing motion analyzer developed by the Korean sports software development company GOLFZON, the golf motion analysis and teaching system MATT-T developed by the North American company TaylorMade, and the auxiliary developed by the Canadian software company Focaltron. The MATT-T teaching system uses a high-speed camera to capture the physical parameters of each joint point during the athlete's swing and uses a computer to draw the physical parameters of these joint points, analyze the data with analysis software, and give the athlete reasonable suggestions.

The portable sensor method is a particular sensor device carried by the athlete. The device captures key posture data in real-time during the swing and combines the data analysis algorithm to give scientific guidance. Zepp Technology Co. launched the world's first portable golf action-assisted training system, Ltd. called GolfSense. The company's combination of advanced image capture equipment and data classification algorithms enables GolfSense to obtain key swing data of several golf swings accurately. It can also provide trainees with more accurate results based on its robust database and scientific motion analysis. It fully understands your swing and gets intuitive visual feedback and training suggestions with the most reference value.

2.4. Human Body Pose Estimation. Singh et al. [26] proposed a solution to estimate the two-dimensional frontal pose of the upper body. This method is mainly aimed at the human body with only the upper body visible, such as standing among flowers, sitting on a sofa, and being blocked by a yacht. This method can also be used to extend to the estimation of the whole body posture. Based on the literature mentioned above, Ibrar et al. optimized the detection process of various parts of the human body and simplified some initialization requirements by adding some constraining conditions [27]. The skin color of the hands is similar to the skin color of the face. The legs are identical to wearing pants and so on, thereby improving the speed of human body posture estimation and the algorithm's accuracy. Andriluka used the existing single-frame image two-dimensional posture estimation as a transition to estimate the three-dimensional human posture in the sequence image. They established a human joint tree model in a single frame of the image and estimated the posture and position of the joint tree model based on the structural model of the image. Finally, based on the Bayesian maximum posterior probability, the two-dimensional posture information in the joint tree model was evaluated. A back-projection operation was used to estimate the three-dimensional posture data. Daubney used a method based on the image structure model to restore the three-dimensional posture of the human body. They established the mapping relationship between the human body features in the image and the three-dimensional space. According to this mapping relationship, the posture of the human body can be estimated directly in the three-dimensional space without the two-dimensional posture estimation. Sinh et al. used the segmentation plus pose matching method to realize the local pose estimation of the hand and leg limbs in the image.

3. Methodology

In this section, we discuss our proposed methodology. First, a brief overview is provided about the image acquisition and data extraction from the posture followed by our algorithm that estimates the human body poses. Finally, we discuss the auxiliary training system that relies on our proposed algorithm.

3.1. Image Acquisition and Posture Data Extraction

3.1.1. Kinect Sensor for Image Acquisition. In this section, Kinect three-dimensional sensor coding is used to realize image acquisition and data extraction of 15 joint points of the human body. The development environment is Win10x86 + VS2018 + Kinect + OpenNI 1.5.2 + OpenCV 4.2.4, and the driver of Kinect is written on this platform. When used in Xbox software, the Kinect sensor has an actual distance range of 1.2 meters to 3.5 meters. Kinect can capture images with a plane range of 6 per square meter, a horizontal field of view of 57°, and a vertical field of view of 43°. Kinect can capture 30 frames of data per second, and a swing is completed in about 2 seconds. The color image data and depth data can be obtained by calling the

RETRACTED

ColorMageSteam function and the DepthMageStream function, respectively, and the real-time image acquisition interface generated is shown in Figure 1.

3.1.2. Kinect Sensor for Joint Data Capture. To obtain the human skeleton in the OpenNI environment, it is necessary to use the UserGenerator generator in the program. This function detects the departure or appearance of the character by registering the two callback functions of NewUser and LostUser. Once the character appears in the above two situations, the state of the person's departure or appearance is detected and the callback functions will be called. Two callback functions such as NewUser and LostUser correspond to the appearance and disappearance of characters, respectively. SkeletonCapability is an ability of the generator UserGenerator, which can be used to store character skeleton information. CalibrationStar and CalibrationEnd are used as the two callback functions in SkeletonCapability in the calibration work of obtaining the human skeleton, and they are used at the beginning and end of the calibration, respectively. The coordinate information obtained through the above steps is based on the Kinect camera coordinate system, and the coordinate projection needs to be converted to the screen coordinate system by the ControlRealWorldToProjective method so that it can be displayed more intuitively. The coordinate data converted by the ConvertRealWordToProjective0 method are stored in the skeletonPointsOut array.

In order to verify the accuracy of the Kinect sensor, two sets of data are used for comparison. One group is based on the horizontal and vertical coordinates of the 15 joint points captured by the Kinect sensor. One frame is used for analysis, as shown in Figure 2. Based on the human joint points captured by Kinect, the picture on the right is based on the manually marked joint points.

3.2. Human Body Pose Estimation Algorithm

3.2.1. Model-Based Human Pose Estimation. The model-based human pose estimation method is related to the constructed human model and the prior knowledge of related motions; that is, the system state at each moment is determined by the system state at the previous moment, and the projection of the human body model and the characteristics of each part of the human body in the image are measured. Between the likelihoods, find the optimal matching method to obtain the human body pose parameters. The process of model-based pose estimation methods is generally "prediction, matching, and update"; that is, first establish a human body model (skeleton model, tree diagram model, dynamic model, and so on) and then pass the previous frame of the human body based on the knowledge of the dynamic model. The posture estimation result assumes the posture of the human body in the current frame. Since the initial frame does not have the prediction of the previous frame, the posture needs to be initialized first and finally the postulated human posture result is projected into the actual image plane, and the posture evaluation function is used as the result of revising the hypothesis. The following will specifically introduce the three important components of the model-based method: building a human body model, selecting an observation matching function, and designing a prediction model.

The establishment of a human body model is based on the preparation stage of the model. The human body model established, based on prior knowledge, can effectively constrain the feature change space, thereby improving the calculation efficiency and reducing the search range for matching. Human body structure models are divided into one-dimensional, two-dimensional, and three-dimensional models. In the process of human body modeling, commonly used models include skeleton models, silhouette models, three-dimensional skeleton models, and graphic structure models. The skeleton model is the simplest way to represent the structure of the human body. It is mainly composed of points and line segments, representing joint points and bones, respectively, as shown in Figure 3. The skeleton model is mainly composed of points and lines, representing the joint points and bones of the human body, respectively. It is the simplest representation method of the human body structure, as shown in Figure 3(a).

In the model-based human body pose estimation method, the observation process is to project a three-dimensional human body model onto the image plane and find the optimal human body poses (parameters) by measuring the likelihood between the projected model and the real image. Commonly used image features in the observation process include optical flow, color, texture, edge, and contour.

In the model-based human pose estimation method, the purpose of the prediction process is mainly to reduce the feasible and search space of the pose. Model-based human pose estimation is a process of searching and solving in a space containing a large number of poses to obtain the pose that best matches the current image pose. However, since the three-dimensional pose of the human body is mostly a high-dimensional continuous variable, what is the current challenge? Dense searching, sampling, and solving are realized in the high-dimensional pose space. Many researchers use Gaussian processes to build dynamic models based on the theory that human motion is a continuous change process with time-series relationships and finally realize predictive search in a low-dimensional space. The specific process is to use low-dimensional subspaces to represent a large number of constraints in the process of human movement and use various dimensionality reduction methods to achieve the purpose of reducing the dimensionality of the posture vector.

3.2.2. Human Pose Estimation Based on Contour Edge Features. The use of model-based human pose estimation methods must search in high-dimensional space. The optimization speed is slow, and it is difficult to achieve real-time processing. It has strong adaptability to the model-free human pose estimation methods based on statistical learning, and the results are accurate. However, the algorithm is more complicated, and the time cost of modeling

RETRACTED

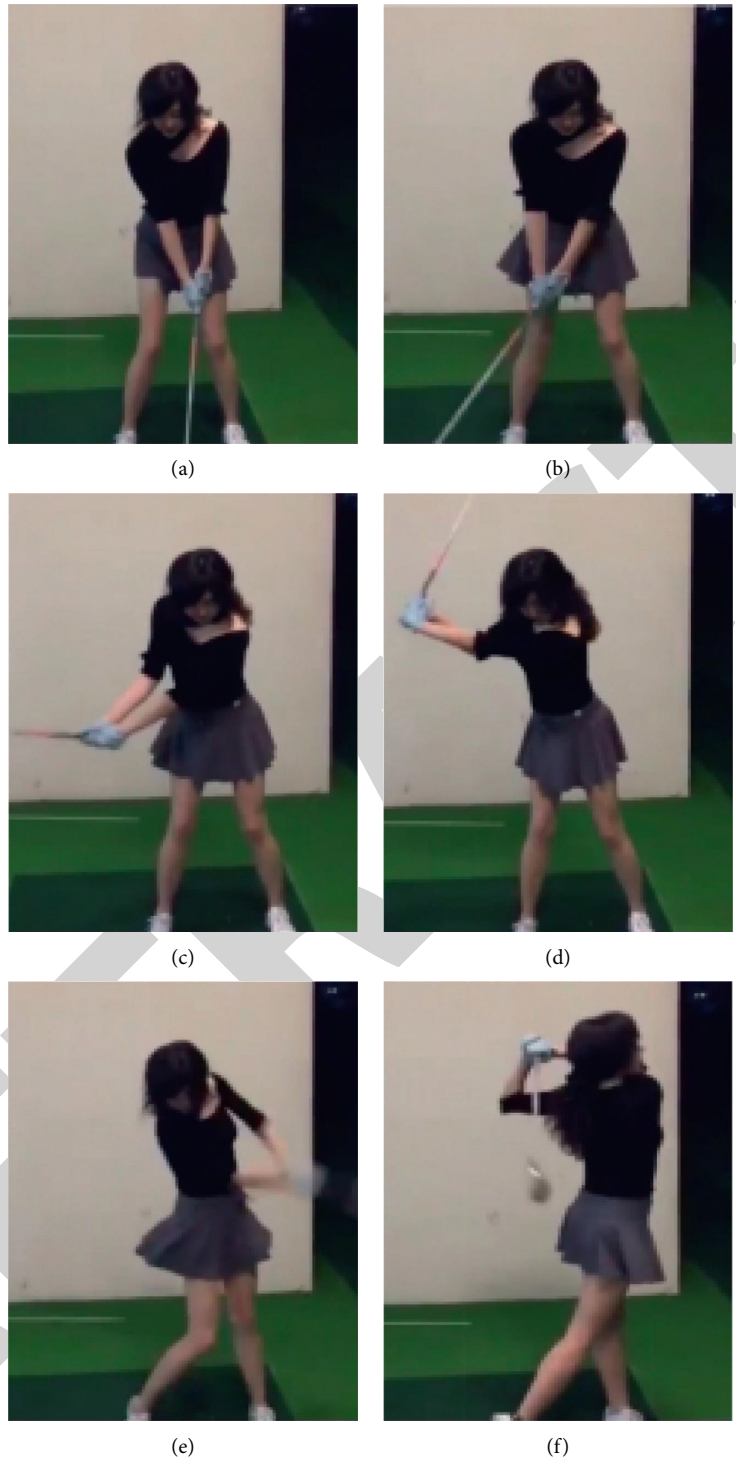

Figure 1: Trainer swing process diagram.

and the labor cost of training samples are relatively high. Based on the matching model-free human body pose estimation method, it is greatly affected by the capacity of the sample set, and the selection of image features is relatively dependent, and the accuracy is not too high, so in combination with the subject of golf sports objects, this paper proposes a human body pose estimation algorithm based on edge contour combined with image processing. Through this algorithm, the joint points of the human body in the picture can be automatically labeled, and the posture data can be obtained. The schematic diagram is shown in Figure 4.

Firstly, the Canny edge detection algorithm is used to obtain its contour edge, and then rough image processing methods such as horizontal line scanning and human body

(a) (b)

Figure 2: Joint point map based on (a) Kinect sensor and (b) manual marking.

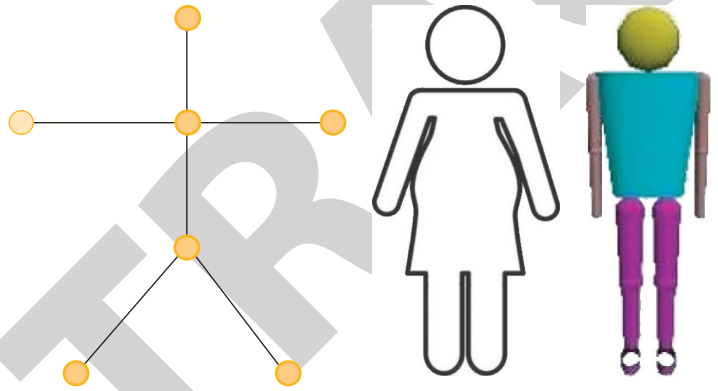

(a) (b) (c)

Figure 3: Human structure model diagram.

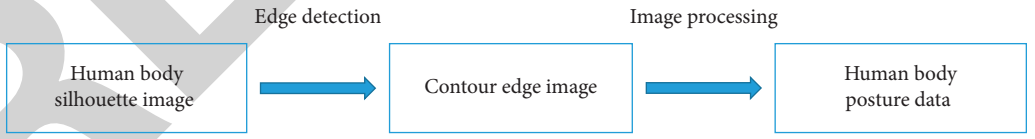

Figure 4: Schematic diagram of attitude estimation based on the image processing method.

length ratio constraints are used so that the coordinates of the human body joint points are obtained to achieve the purpose of posture estimation. The specific content includes the following parts. First, Gaussian filter is used to smooth the image. Image Gaussian filtering can be implemented in two ways: two one-dimensional Gaussian kernels are weighted twice, respectively, and one two-dimensional Gaussian kernel is convolved once. The equation of the one-dimensional Gaussian kernel function is as follows:

$$K = \frac{1}{\sqrt{2\pi\sigma}} e^{(x^* x/2\sigma^* \sigma).} \quad (1)$$

The parameters are determined to get a one-dimensional kernel vector. The equation of the two-dimensional Gaussian kernel function is as follows:

$$K = \frac{1}{\sqrt{2\pi\sigma^* \sigma}} e^{((x^* x + y^* y)/2\sigma^* \sigma).} \quad (2)$$

The parameters are determined to get a two-dimensional kernel vector. Next, the two matrices of the partial derivatives in the x and y directions of the image can be calculated by the finite difference of the first-order partial derivative, and the first-order difference can be used to approximate the

RETRACTED

gradient of the image gray value. The equation of the image gray value gradient (including amplitude and direction) is shown as follows:

$$H_1 = \begin{bmatrix} -1 & -1 \\ & \\ 1 & 1 \end{bmatrix},$$

$$H_2 = \begin{bmatrix} 1 & -1 \\ & \\ 1 & -1 \end{bmatrix},$$

$$\begin{aligned} \phi_1(m,n) &= f(m,n)^* H_1(x,y), \\ \phi_2(m,n) &= f(m,n)^* H_2(x,y), \\ \phi(m,n) &= \sqrt{\phi_1^2(m,n) + \phi_2^2(m,n)}, \\ \theta_\phi &= \tan^{-1}\frac{\phi_2(m,n)}{\phi_1(m,n)}. \end{aligned} \tag{3}$$

The convolution operator used in the Canny algorithm is relatively simple. For example, in the expression, H_1 and H_2 and ϕ and θ represent the magnitude and direction of the edge gradient, respectively.

The position of the edge cannot be completely determined based on the global gradient alone, and nonmaximum suppression of the gradient amplitude is needed to highlight the true edge. This process is an important step for edge detection. The principle of nonmaximum suppression is described as follows (as shown in Figure 5).

The gradient direction of point C is shown by the blue line, and its maximum local gray scale is on this line. The intersection of the eight-valued field of point C and the gradient direction is d_1 and d_2. Comparing the gray value of point C in its eighth whether there is a local maximum in the value field, it can be judged whether point C is an edge point. If the gray value of point C is less than any one of d_1 and d_2, it means that point C is not a local maximum and point C is not an edge point. Set its gray value to 0.

Finally, the double threshold method can reduce the number of false edges. Choose two thresholds: a high threshold and a low threshold. According to the two thresholds, two threshold images are obtained, respectively. The high threshold image obtains an edge image with few false edges, and then the low threshold image is used to connect the high threshold processed edge images into contours so that all edge gaps are closed.

3.3. Auxiliary Training System Based on Human Body Pose Estimation Algorithm. Traditional sports training often relies on manual experience guidance and unable to give accurate numerical analysis of key movements. This article will build an auxiliary training system based on the method of human posture estimation for golf. The system takes the swing big data of the trainer and the coach as input and uses the five joint angle trajectory comparison graphs and the posture similarity of the trainer and the coach as input. Auxiliary training indicators are combined with artificial intelligence technology [3, 4] to output posture prediction results. The frame diagram of the auxiliary sports training system built in this paper is shown in Figure 6.

Auxiliary sports training system function takes the big data image sequence of the trainer and the coach's swing as input and takes the 5 joint angle trajectory comparison chart of the trainer and the coach and the posture similarity change chart of each frame as the auxiliary training index, compares the difference between the joint angles of the trainer and the coach, and at the same time uses artificial intelligence technology to modify the trainer's movements according to the similarity of the posture so as to achieve the purpose of analyzing the sports posture and providing training suggestions.

4. Experiments

In this section, first, we discuss our experimental environment that involves real-time deployment followed by the implementation steps and the obtained experimental results.

4.1. Experimental Environment. The hardware and software components along with the deployed environment are shown in Table 1.

4.2. Implementation Steps.

Step 1. The big image data or other training images collected by the Kinect sensor are used as the input of the auxiliary training system

Step 2. The swing posture data of the trainer and the coach are obtained through the target detection based on artificial intelligence and the human body posture estimation method based on the edge feature of the human body combined with image processing

Step 3. 5 joint angles Angel (head, neck, and chest), Angel2 (left shoulder, left elbow, and left wrist), Angel3 (right shoulder, right hour, and right wrist), Angel4 (left marrow, left knee, and left foot), and Angle5 (right hip, right knee, and right foot) are adopted and are used as the system index, and Euclidean distance is selected as the similarity measure of attitude

4.3. Experimental Results. The 48 frames of swing images of the trainer and the coach are selected as the input of the system, and the output is the trajectory comparison of the joint angles and the similarity of each frame. The following is a demonstration of auxiliary training based on the joint angle trajectory. Figure 7 shows a movement trajectory diagram of five joint angles. Here, the blue line represents the joint angle change diagram of the coach, and the red line represents the joint angle change diagram of the athlete. It can be seen from Figure 7 that the algorithm in this paper has achieved gratifying results. We also have compared with the gc-lstm method. Figures 8 and 9 show the effect of dropout on our model performance and reflect the comparison results of the learning curve. In Figure 8, the loss is plotted against the impact of using dropout on model performance,

RETRACTED

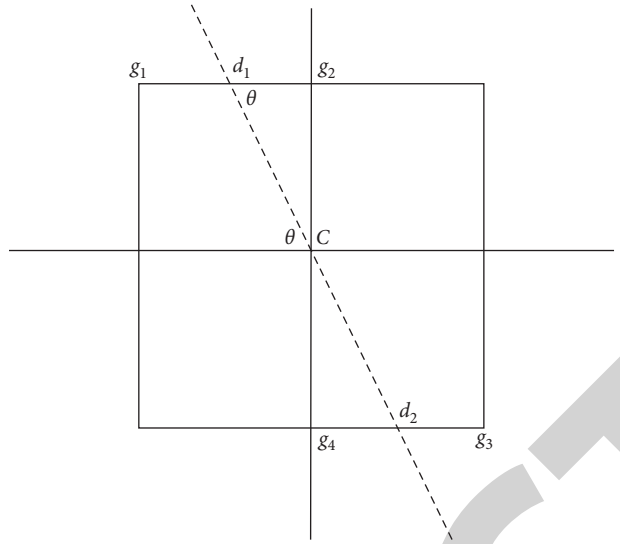

Figure 5: Schematic diagram of nonmaximum suppression.

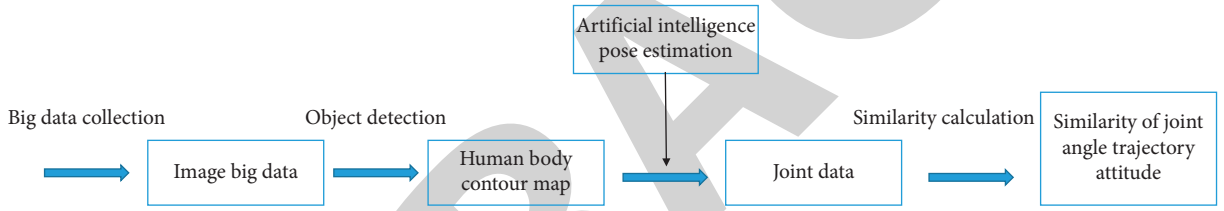

Figure 6: Auxiliary training system frame.

Table 1: Experimental hardware platforms and software simulation environment.

CPU	Intel(R) Core(TM) i5-4200M CPU @ 2.50 GHz
RAM	16.00 GB
Operating system	Windows10
Development environment	VS2018
Development tools	OpenCV + MATLAB

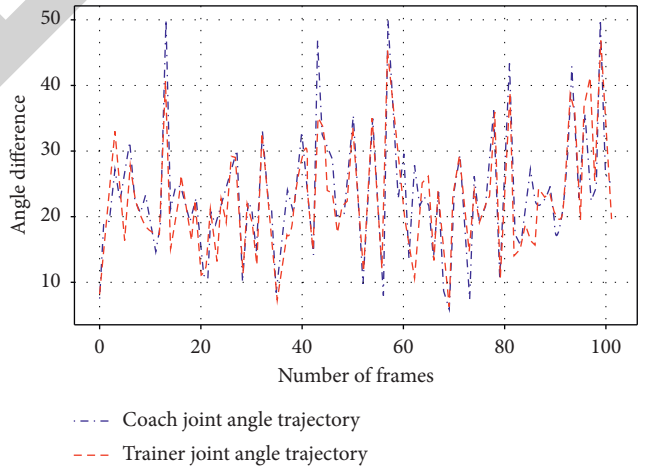

Figure 7: Experimental comparison results.

RETRACTED

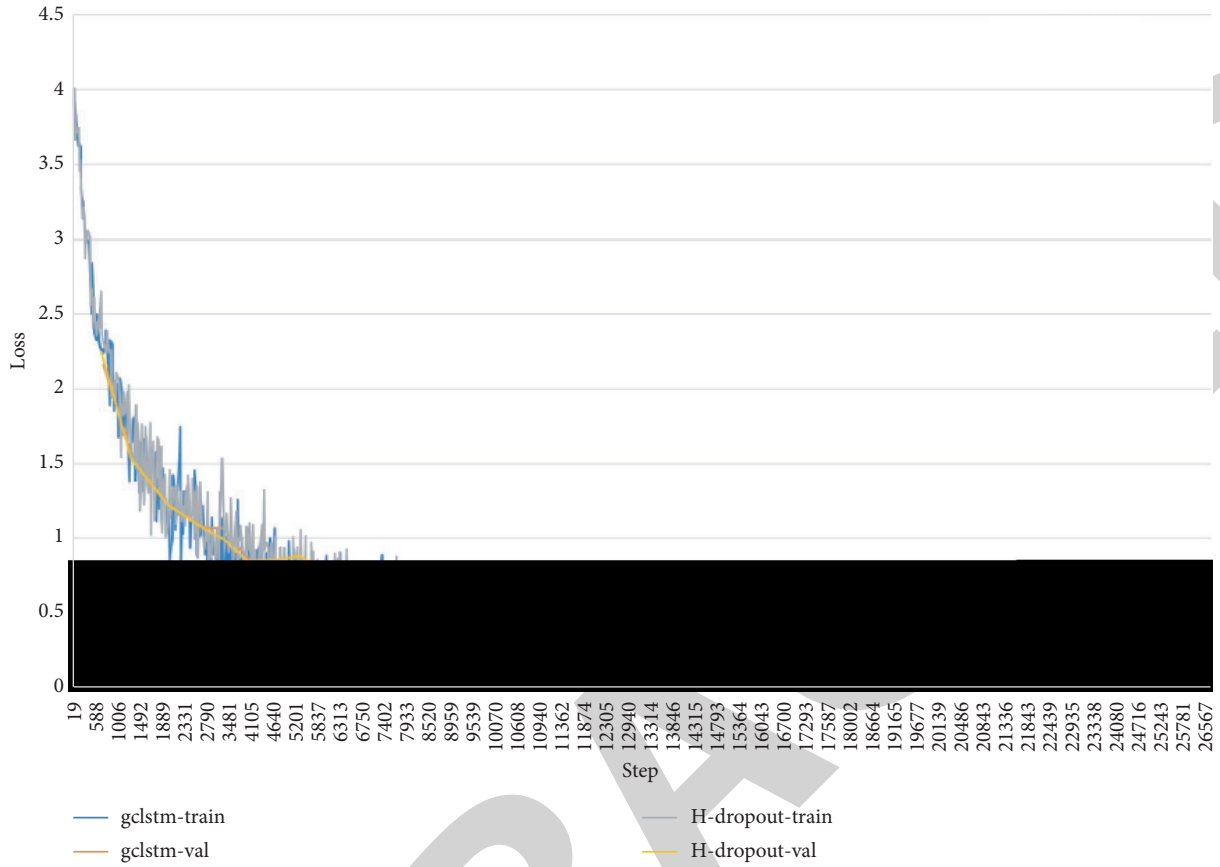

Figure 8: The impact of using dropout on model performance.

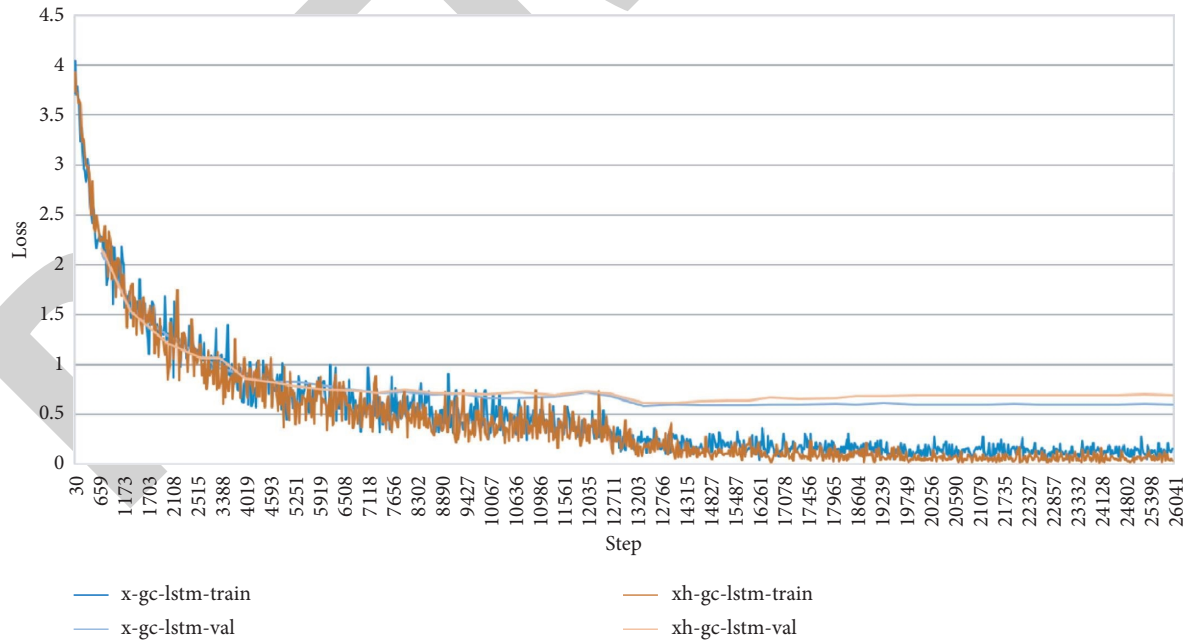

Figure 9: Comparison of learning curve results.

whereas in Figure 9, the loss is computed for different learning curves.

5. Conclusion

Based on artificial intelligence and big data technology, in this paper, the human body posture estimation algorithm is applied to the auxiliary training system. We considered golf as the case study for this purpose. The method of human body posture estimation has completed the construction of the golf auxiliary training system, which brings standardized analysis and quantification to sports training guide. The big data image collected by the Kinect sensor is used as the input of the auxiliary training system, and the swing posture data of the trainer and the coach are obtained through methods such as target detection based on artificial intelligence and posture estimation based on the edge feature of the human body combined with image processing. Finally, the system uses two auxiliary indicators of five joint angle trajectories and posture similarity as output. By comparing the joint angle trajectories of the trainer and the coach, numerous intuitive analyses are performed on the posture similarity. In the future, we aim to apply our algorithm for various sport events to see its performance on large scale with dynamic having diversified nature.

Data Availability

The data used to support the findings of this study are included within the article.

Conflicts of Interest

The authors declare that they have no conflicts of interest.

Acknowledgments

This work was supported by the Project of Dezhou University Scientific Research Fund (2019xgrc55) and Social Science Planning Project of Shandong Province (16CTYJ210).

References

[1] H. K. Behr and L. P. Kuhn, "Key factors in career development and transitions in German elite combat sport athletes," *Martial Arts Studies*, vol. 7, pp. 19–35, 2018.

[2] T. A. Buckley, B. A. Munkasy, and B. P. Clouse, "Sensitivity and specificity of the modified balance error scoring system in concussed collegiate student athletes," *Clinical Journal of Sport Medicine*, vol. 28, no. 2, pp. 174–176, 2018.

[3] A. E. Jeukendrup, "Training the gut for athletes," *Sports Medicine*, vol. 47, no. 1, pp. 101–110, 2017.

[4] O. A. Volodchenko, L. V. Podrigalo, S. S. Iermakov, M. T. Żychowska, and W. Jagiełło, "The usefulness of performing biochemical tests in the saliva of kickboxing athletes in the dynamic of training," *BioMed Research International*, vol. 2019, Article ID 2014347, 7 pages, 2019.

[5] F. Sessa, G. Messina, A. Valenzano et al., "Sports training and adaptive changes," *Sport Sciences for Health*, vol. 14, no. 3, pp. 705–708, 2018.

[6] S. J. McLaren, T. W. Macpherson, A. J. Coutts, C. Hurst, I. R. Spears, and M. Weston, "The relationships between internal and external measures of training load and intensity in team sports: a meta-analysis," *Sports Medicine*, vol. 48, no. 3, pp. 641–658, 2018.

[7] D. Li, C. Yi, and Y. Gu, "Research on college physical education and sports training based on virtual reality technology," *Mathematical Problems in Engineering*, vol. 2021, Article ID 6625529, 8 pages, 2021.

[8] A. Nässi, A. Ferrauti, T. Meyer, M. Pfeiffer, and M. Kellmann, "Psychological tools used for monitoring training responses of athletes," *Performance Enhancement & Health*, vol. 5, no. 4, pp. 125–133, 2017.

[9] N. Vysochina, A. Vorobiova, M. Vasylenko, and F. Vysochin, "Volitional qualities of athletes and their influence on competitive activities," *Journal of Physical Education and Sport*, vol. 18, no. 1, pp. 230–234, 2018.

[10] N. Wan and L. Wan, "Training method for amateur sports in schools dependent on time series data," in *Proceedings of the 2019 11th International Conference on Measuring Technology and Mechatronics Automation (ICMTMA)*, pp. 606–609, IEEE, Qiqihar, China, April 2019.

[11] M. Filchenko, *A Comparison Between Esports and Traditional Sports*, San Jose State University, San Jose, CA, USA, 2018.

[12] P. Maurice, L. Allienne, A. Malaisé, and S. Ivaldi, "Ethical and social considerations for the introduction of human-centered technologies at work," in *Proceedings of the 2018 IEEE Workshop on Advanced Robotics and its Social Impacts (ARSO)*, pp. 131–138, IEEE, Genova, Italy, September 2018.

[13] W. Xu, "Toward human-centered AI: centered AI: a perspective from human-computer interaction," *Interactions*, vol. 26, no. 4, pp. 42–46, 2019.

[14] J. E. Muñoz, A. Gonçalves, É. Rúbio Gouveia, M. S. Cameirão, and S. Bermúdez I Badia, "Lessons learned from gamifying functional fitness training through human-centered design methods in older adults," *Games for Health Journal*, vol. 8, no. 6, pp. 387–406, 2019.

[15] C.-C. Chan, "Social support, career beliefs, and career self-efficacy in determination of Taiwanese college athletes' career development," *Journal of Hospitality, Leisure, Sport & Tourism Education*, vol. 26, Article ID 100232, 2020.

[16] M. S. Messo and S. K. Messa, "Evolution of examination and training system to produce teachers capable to face 21st century educational challenges," *Grassroots*, vol. 51, no. 1, 2017.

[17] M. Roztorhui, A. Perederiy, Y. Briskin, and O. Tovstonoh, "The training system of athletes with disabilitiesstrength-sports," *Sportlogia*, vol. 14, no. 1, 2018.

[18] T. Guzsvinecz, V. Szucs, and C. Sik-Lanyi, "Suitability of the Kinect sensor and leap motion controller-a literature review," *Sensors*, vol. 19, no. 5, Article ID 1072, 2019.

[19] X. Zhang, Y. Yang, Z. Li, X. Ning, Y. Qin, and W. Cai, "An improved encoder-decoder network based on strip pool method applied to segmentation of farmland vacancy field," *Entropy*, vol. 23, no. 4, p. 435, 2021.

[20] Y. Zhang, W. Li, L. Zhang, X. Ning, L. Sun, and Y. Lu, "AGCNN: adaptive gabor convolutional neural networks with receptive fields for vein biometric recognition," *Concurrency and Computation: Practice and Experience*, Article ID e5697, 2020.

[21] L. Zhang, X. Wang, X. Dong, L. Sun, W. Cai, and X. Ning, "Finger vein image enhancement based on guided tri-Gaussian filters," *ASP Transactions on Pattern Recognition and Intelligent Systems*, vol. 1, no. 1, pp. 17–23, 2021.

RETRACTED

Hindawi
Mobile Information Systems
Volume 2021, Article ID 9920751, 8 pages
https://doi.org/10.1155/2021/9920751

Research Article

Intelligent Decision-Making System for Martial Arts Competition Using Deep Learning

Shisen Li,[1] Shenglu Huo ,[2] and Wei Ke[3]

[1]*Department of Physical Education, North China University of Science and Technology, Tangshan 063210, Hebei, China*
[2]*School of Economic and Management, Shanghai University of Sport, Shanghai 200438, China*
[3]*College of Physical Education, HengShui University, Hengshui 053000, Hebei, China*

Correspondence should be addressed to Shenglu Huo; huoshenglu83@126.com

Received 10 March 2021; Revised 24 April 2021; Accepted 27 April 2021; Published 20 May 2021

Academic Editor: Mian Ahmad Jan

Copyright © 2021 Shisen Li et al. This is an open access article distributed under the Creative Commons Attribution License, which permits unrestricted use, distribution, and reproduction in any medium, provided the original work is properly cited.

In the field of martial arts, athletes can win the initiative in the competition if they can correctly and timely acquire the field knowledge, evaluate the situation efficiently, and formulate a suitable strategy. In this paper, we use fuzzy mathematics, mathematical statistics, and artificial intelligence learning algorithms to carry out systematic and in-depth research on the selection of Wushu competition scene decision-making. The fuzzy mathematics theory is combined with the intelligent design theory for decision-making based on a multiagent, case-based reasoning selection, and adaptability evaluation analysis. The Wushu competition scene decision system is constructed based on artificial intelligence learning algorithms. Our approach outperforms the existing approaches in terms of accuracy, sensitivity, specificity, and Matthew's correlation coefficient (MCC). The results of our proposed model can be anticipated to have the potential for better flexibility and scalability in martial arts competition.

1. Introduction

Wushu is a unique traditional project in China and a treasure in the Chinese nation's cultural heritage. As a sport, the Wushu routine is composed of different styles of technical movements. It has the connotation of attack and defense philosophy and high ornamental value, which gives people reasonable enjoyment [1]. Besides, the Wushu routine is highly praised for its rich and diverse cultural forms. Combining competitive Wushu routine and western competitive sports culture makes daily activities more effective. With the increasing influence of Wushu routines globally, more and more international players begin to practice Wushu routines and participate in international competitions. The combination of Wushu routines and the Olympic concept of higher, faster, and stronger makes the routine competition more accumulated. Therefore, it is necessary to improve the technical level of athletes through scientific training.

In the past, the research on the development of the Wushu routine mainly focused on the situation analysis, qualitative analysis, developing direction discussion, and future developmental trend prediction, among others. However, there is little research on the influencing factors of competitive Wushu routine competition performance, and there is almost no research on the factors influencing athlete's competition performance from the perspective of exercise level [2, 3]. Therefore, the athlete's movement requires measures that improve the classification of movement patterns into significant groups and support specialists in their decisions at the training.

In this context, the increasing importance of artificial intelligence learning algorithms has led to a substantial contribution. Artificial intelligence learning can simulate and extend human intelligence. These algorithms allow the development of theory, methods, and application systems for simulating and expanding human intelligence. One of its main goals is to enable machines to perform complex tasks that usually require human intelligence. Its rapid development is widely used in military, financial, management, and other fields. The objective of this paper is to build an artificial intelligence assistant system that is suitable for martial arts

competition decision-making through expert system platform, data mining, online analysis, and virtual reality [4–6]. The artificial intelligence decision support system (IDSS) is a computer intelligent system with special knowledge and inherited experience. It combines artificial intelligence methods and a decision support system (DSS) [7–11]. Numerous researchers have carried out a lot of research on IDSS. In [12], the authors put forward the Web Intelligent Decision Support System framework, which provides effective decision support for decision-makers. In [13], the authors constructed data management, decision-making, and modeling based on a rough set theory that combines an artificial neural network with an expert system to generate new rule's knowledge and realize a fuzzy decision support system. In [14], the authors integrated the agent into an intelligent decision support system and proposed a new coordination engine and information interaction algorithm based on multiagent. Based on multiagent tasking, intelligent decision support system architecture was proposed that improved the intelligent decision-making system's reliability and effectiveness [15]. In [16], an intelligent decision support system for the drilling process based on case-based reasoning was proposed to solve information inaccuracy [16].

However, there is little research on the influencing factors of competitive Wushu routine competition performance, and there is almost no research on the factors influencing athlete's competition performance from the perspective of exercise level [2, 3]. The major contributions of this paper are as follows:

(1) We comprehensively use fuzzy mathematics, mathematical statistics, and artificial intelligence learning algorithms to carry out systematic and in-depth research on the selection of Wushu competition's scene decision-making.

(2) The fuzzy mathematics theory is combined with the intelligent design theory for decision-making based on a multiagent, case-based reasoning selection, and adaptability evaluation analysis. Finally, the Wushu competition scene decision system is constructed based on artificial intelligence learning algorithms.

The rest of this paper is organized as follows. Section 2 discusses the preliminary concept of the system by focusing on different methods followed by artificial intelligence decision-making method for adaptability evaluation of Wushu competition in Section 3. Section 4 presents performance measurement metrics. Results and discussions are presented in Section 5. Finally, Section 6 concludes the paper with a summary and future research direction.

2. The Preliminary Conception of the System

The preliminary conception system of the Wushu competition scene decision is divided into three levels, i.e., database layer, processing layer, and display layer. The database layer is the basic support platform, which provides data support for the processing layer. The processing layer is the core executive organization. It is responsible for the logic processing between martial arts tactics. The display layer aims to transform the processed data into decision-making [17]. The library at this layer mainly completes the collection of Wushu tactical data and constructs the Wushu tactical data warehouse. Data warehouse refers to the effective integration of multiple heterogeneous data sources. After integration, it is reorganized according to the theme. It is mainly used to support decision-making and analysis-oriented data processing. Through the collection of martial arts tactical data, the artificial intelligence assistant system completes the collection and storage of basic data, training data, field data, and image document data, including the feature database of Wushu athletes, the feature database of coaches, and the case database of tactics. The martial arts tactics analysis chart is shown in Figure 1.

It can be observed from the figure that the data of martial arts tactics analysis are collected from different angles and levels through statistical reports and tactical deduction. These include the individual data of athletes, coaches, and sports researchers and all kinds of conventional statistical data and field statistics. The decision analysis in the display layer is to establish various topics, analyze the data of different topics, obtain the optimal scheme, and assist the coach in decision-making. The tactical deduction at the performance layer refers to the simulation and display of position and attack and defense routes at your side and the other side in the competition field by electronic means. It reflects the tactics adopted by your side and the other side and analyzes your side's best attack route and defensive line.

3. Artificial Intelligence Decision-Making for Adaptability Evaluation of Wushu Competition

The adaptability evaluation of complex Wushu competition involves numerous factors, which are difficult to choose. Due to the complexity of Wushu movements, the competitions are often faced with multiple uncertain factors. The artificial intelligence method can analyze the influence of complex factors and can be used to evaluate the adaptability of the Wushu competition effectively. Based on the theory and practice of fuzzy multiagent and case-based reasoning, the artificial intelligence decision-making of Wushu competition scene adaptability evaluation is proposed here.

3.1. Evaluation Method of Wushu Competition Adaptability Based on Fuzzy Mathematics. Fuzzy theory can simulate human thinking, and it is feasible for human decision-making. The characteristics of a fuzzy membership relationship in fuzzy theory can be applied to many decision-making fields. At present, fuzzy subordinate decision-making has been successfully obtained in considerable scientific research. The field adaptability evaluation of Wushu competition under complex conditions is affected by various quantitative and qualitative uncertain factors, such as Wushu action design, routine design, field performance status, and equipment problems. Due to these factors' different units and attributes, it is not easy to compare them. Besides, it is one of the complex problems in adaptability

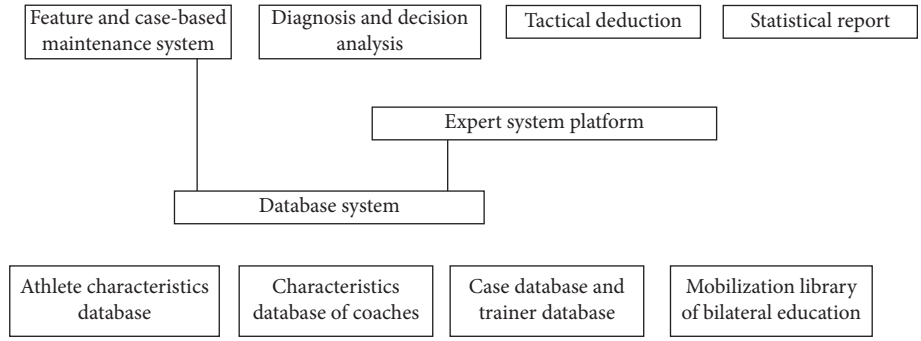

Figure 1: A system for analyzing martial arts tactics.

evaluation to select the main or critical influencing factors from so many factors and then use some measurable indicators to describe them. For the problem of commensurability of the evaluation index, the fuzzy mathematics method can be effectively solved. Because of these factors affecting the adaptability evaluation of the Wushu competition scene, the results obtained by using the fuzzy comprehensive evaluation method are more accurate and applicable [18].

3.2. The Fuzzy Comprehensive Evaluation Model. Assuming that the evaluation target set $O = \{O_1, O_2, \ldots, O_m\}$ and the evaluation index set factory is equal to network $U = \{U_1, U_2, \ldots, U_m\}$, then the basic model of a fuzzy comprehensive evaluation is as follows:

$$D = \{w_1, w_2, \ldots, w_m\} \times \begin{bmatrix} r_{11} & r_{12} & \cdots & r_{1n} \\ r_{21} & r_{22} & \cdots & r_{2n} \\ \vdots & \vdots & \ddots & \vdots \\ r_{m1} & r_{m2} & \cdots & r_{mn} \end{bmatrix}, \quad (1)$$

where D is the set of comprehensive evaluation values and O_i is the fitness of evaluation objectives. The weight of the evaluation index is determined by the analytic hierarchy process (AHP). AHP is a multiobjective decision analysis method combining quantitative and qualitative analysis. It combines mathematical processing with human experience and subjective judgment and can effectively analyze the nonsequential relationship between the levels of objective criteria system, the judgment, and decision-making of comprehensive measurement evaluation. The method to determine the weight of the evaluation index is as follows [19].

According to the evaluation, objectives are achieved based on the mutual influence and subordination relationship among evaluation indexes. The hierarchy of indicators is divided into the target layer, criterion layer, and index layer from high to low (Figure 2). The indicators of the upper level play a dominant role in the indicators of the next level.

For the difference of the influence of pairs of indicators, the judgment matrix constructed according to the above method can objectively reflect. Still, when analyzing and comparing all the results of the indicators, there will inevitably be some degree of inconsistency. To eliminate the inconsistency, the elements in the judgment matrix A should satisfy the following conditions:

$$a_{ij}a_{jk} = a_{ik}, \quad \forall i, j, k = 1, 2, 3, \ldots, n. \quad (2)$$

3.3. Fuzzy Membership Function of Evaluation Index. The relationship between fuzzy set and element set can be expressed by any interval value, i.e., 0, 1. When the fuzzy set completely contains the element, it is expressed as "1"; when the fuzzy set does not contain the element, it is expressed as "0". Similarly, the membership degree indexes the uncertainty of the membership relationship between element sets and fuzzy sets. Generally, when solving a practical problem, the first thing is to determine the membership function, which is usually approximately determined by the reasoning method. The connotation of the subordinate function is to reflect the objective law into the function formula and to synthesize, process, reorganize, and transform people's subjective consciousness. Therefore, the determination of membership function should conform to objective law and have a certain degree of subjectivity and experience, not through subjective imagination. The membership function can be determined by the intuitionistic method, fuzzy statistical method, preferred comparison method, binary comparison method, and absolute comparison method.

3.4. The Intelligent Decision Support System. An intelligent decision support system (DSS) makes use of the advantages of machine learning and expert system technology in qualitative analysis and uncertain reasoning, makes full use of human experience and knowledge in problem-solving, and provides a new way to solve the above problems. The expert system establishes a domain expert knowledge base and problem-solving base system. The expert system can make the machine intelligence reach or even surpass the human expert level in some aspects. The application of unified technology in management often aims at the decision-making problems in specific fields. Applying expert system technology to decision support system and establishing an intelligent decision support system (DSS) can overcome the limitations of expert system and decision support system. Better support management decision service

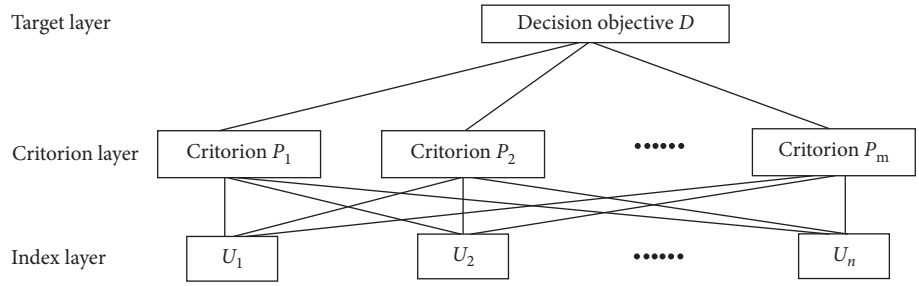

Figure 2: Hierarchical model.

artificial intelligence and expert system technology not only have a profound impact on the technology and structure of decision support system but also have a profound impact on the concept of decision support system in recent years. Almost all the research studies on DSS are based on the application of machine learning technology, and the combination of expert system and decision support system is a direct body. Now, the intelligence of all parts of DSS, such as the combination of man-machine dialogue components, the combination of solving methods, the combination of database model base, method base, and their management system. The combination of expert system technology and decision support component improves the function of each component, which will undoubtedly greatly improve the decision supportability [20–23].

With the deepening of research, expert system technology has penetrated all aspects of DSS, such as architecture and problem-solving, which has an important impact on decision-making methods and processes. The research of intelligent decision support system has gradually developed from the expansion of the function of decision-making components in the past to the comprehensive integration of components and from the past quantitative model to the intelligent decision-making method based on knowledge, and it makes the theory and method of intelligent decision support system mature gradually. Turbo has studied the implementation of a decision support system 1%, but the intelligent system implementation method cannot guarantee that the developed system is an intelligent decision support system.

The intelligent decision support system (IDSS) is a kind of computer intelligent program system with special knowledge and experience. It is the combination of an expert system (ES) and a Wushu competition scene decision support system (DSS). Combining the characteristics of both qualitative and quantitative analysis can be organically combined, and the ability and scope of solving problems can be improved. As shown in Figure 3, it is the structure diagram of the integration of the expert system and decision support system of the Wushu competition scene.

It can be seen from the figure that the combination of DSS and ES in IDSS is mainly reflected in the following three aspects:

(1) The overall combination of DSS and ES

(2) The combination of KB and MB

(3) The combination of the static database (DB) and dynamic database

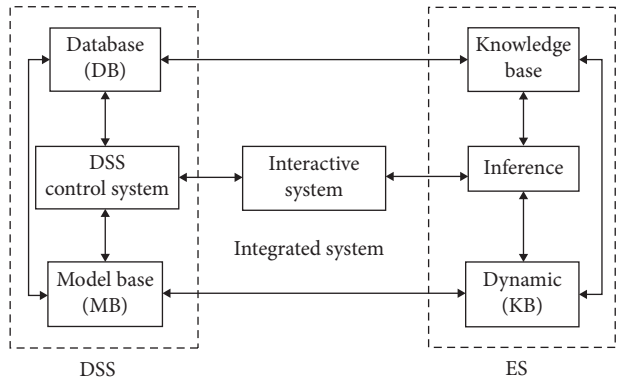

Figure 3: Structural chart for integrating expert system and decision support system.

3.5. Deep Neural Network Model. A deep neural network model is a multilayer network of processing nodes and is most widely used in industries, simulation games, robotics, and many other different fields. A deep neural network model needs to be built based on the huge amount of data. The deep model can be established based on various relationships and laws analyzed by data mining and can also be established by combining martial arts professional knowledge and the experience of coaches and experts. Valuable information can be obtained from a large number of data through the model, and this information can be displayed in an intuitive form so that the data can play an effective role, and the model can be dynamically increased and improved through practical application. Besides, tactical deduction, virtual arena, virtual exhibition hall, and other performance methods are gradually mature.

The basis of the deep neural network assistant system of Wushu competition decision-making is also a large amount of data. It is precisely because of the large amount of data and information accumulated in the daily training and actual competition, which has laid a solid foundation for the system. Also, the rich knowledge and on-the-spot command experience of the coaches provide reliable support for the adjustment and optimization of the system. The data mining, online analysis, and virtual technology involved in this system are relatively mature technologies and are widely used in military, economic, management, and other fields, and achieved success.

4. Formulation of Measurement Scales

To evaluate the performance of a machine learning algorithm, four parameters are commonly used to check the

model reliability and validity. These parameters include overall accuracy of the model, specificity as true-negative rate, sensitivity as true-positive rate, and MCC as Mathew's correlation coefficient. These four metrics calculation formulas are as follows:

$$\begin{aligned}
\mathrm{ACC} &= 1 - \frac{m_-^+ + m_+^-}{m^+ + mP^-}, \quad 0 \le \mathrm{ACC} \le 1, \\
\text{specificity} &= 1 - \frac{m_+^-}{m^-}, \quad 0 \le \mathrm{Sp} \le 1, \\
\text{sensitivity} &= 1 - \frac{m_-^+}{m^+}, \quad 0 \le \mathrm{Sn} \le 1, \\
\mathrm{MCC} &= \frac{1 - \left(m_-^+ + m_-^+/m^+ + mm^-\right)}{\sqrt{\left(1 + m_+^- - m_-^+/m^+\right)\left(1 + m_-^+ - m_+^-/m^-\right)}}, \quad -1 \le \mathrm{MCC} \le 1,
\end{aligned} \tag{3}$$

where m^+ represents true positive, m^- represents the total true negative, m_-^+ represents the false positive, and m_+^- represents the false negative.

In the field of machine learning, the entity that can work independently and has the interactive ability is generally defined as an agent. Independent traditional agents are limited in enjoying resources and solving problems. When they encounter complex and huge practical decision-making problems, they often cannot solve them effectively. Based on this, scholars at home and abroad put forward a multiagent system. The traditional multiagent system is a kind of distributed multiagent system. It can effectively solve complex and huge practical decision-making problems, which are not possessed by independent traditional agents. Through multiple in different hosts or locations, the traditional multiagent can complete more complex decision-making tasks through the interaction and cooperation between the independent traditional multiagents running on.

5. Experimental Results and Discussion

In this section, we evaluate and discuss the performance of our proposed model in detail. There are a lot of professional data in martial arts teaching and scientific research, such as daily training data, competition data, teaching data, and experience data of domestic and foreign counterparts. With the help of deep neural network (DNN), these data are effectively classified and sorted out to form a data warehouse, and an artificial intelligence assistant system for decision-making on the spot of Wushu competition is constructed.

5.1. Interindividual Classification. The establishment of the model needs to be based on the experience of teaching and training level experts; on the other hand, it is to model through the association relationship obtained by data mining. The model includes a static model and a dynamic model. The static model is mainly composed of the individual ability model of the players and the overall ability model of the players on the field. The dynamic model needs to take the field parameters as the input conditions and then carry out the field operation model as shown in Table 1. For example, the formation influence model of both sides can analyze the attack and defense of the current formation by comparing the positions of the players on the field and the positions of the opposing team members. By inputting the field data of both players in real time, it can analyze which position of the team needs to be strengthened and which position of the other side is the weakest. Using artificial intelligence algorithm [24, 25] for self-learning and self-improvement of the model, on the one hand, can optimize and adjust various models through self-learning ability; on the other hand, according to the feedback data in practical application, the key parameters are modified to make the model more in line with the actual situation.

5.2. Individuality of Movement Patterns Multiple Agents. Multiple agents in the system will produce a variety of different decision-making schemes. Before making decisions on the schemes, they must be ranked first; then, the cooperation and cooperation among multiple agents in the system are needed to obtain a higher reliable solution. At present, a large number of studies on the priority of decision schemes have been carried out, and fruitful results have been obtained. For example, some scholars have applied scientific research on the area of fuzzy numbers to the order of the pros and cons of decision-making schemes; some scholars have combined the Minkowski function with grey number theory and put forward the corresponding ranking method. Some scholars use the local rough set to sort the decision schemes in the stochastic control model. However, all of the above methods have their limitations. On the problem of ranking the advantages and disadvantages of the decision-making schemes, the system has not been fundamentally and effectively solved in the application process, and there are still many problems in the ranking of schemes, which makes the evaluation results to lack of scientific rationality, as shown in Table 2. Figures 4–7 show the comparative experimental results of different methods on accuracy (ACC), sensitivity (Sn), specificity (Sp), and Matthew's correlation coefficient (MCC).

At the same time, different from the independent traditional agent, the traditional multiagent system can complete the adaptive adjustment according to the change of environment, which makes it with a strong adaptability feature. The traditional multiagent system is a network system composed of several loosely coupled agents. The traditional multiagent system provides a new framework and model for solving complex problems. It has the performance that other systems cannot match. It has the advantages of distribution, learning and reasoning ability, independence, cooperation, and self-organization ability.

Table 1: Performance of the individual ability model of the players.

Classification task	ACC (%)	Sn (%)	Sp (%)	MCC
Strikes ground	92.81	91.72	94.12	0.821
Strikes body	93.23	92.4	96.3	0.879
Distance time	94.65	93.3	95.52	0.831
Strikes kicks attempts	92.07	91.1	93.7	0.812
Strikes attempts	93.49	90.6	95.91	0.799

Table 2: Performance of the individual movement patterns multiple agents.

Classification task	ACC (%)	Sn (%)	Sp (%)	MCC
Kicks attempts	92.81	91.72	93.12	0.851
Punches attempts	93.23	92.4	93.88	0.838
Side control time	92.65	91.08	93.64	0.825
Leg kicks	94.07	93.76	94.4	0.812
Head kicks	94.49	94.44	95.16	0.891

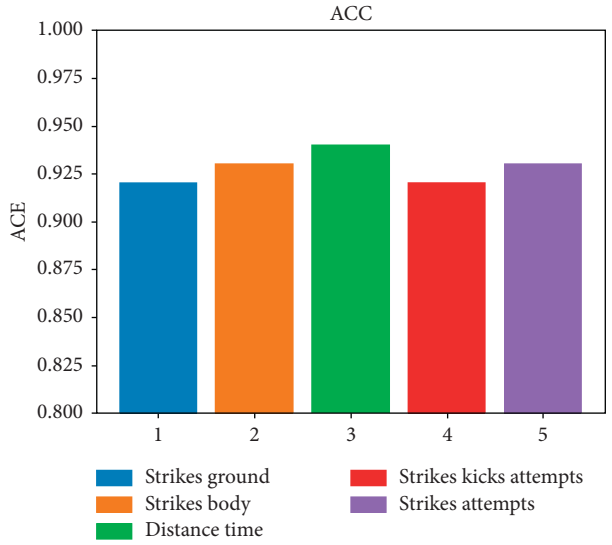

Figure 4: Comparative experimental results of different methods on accuracy.

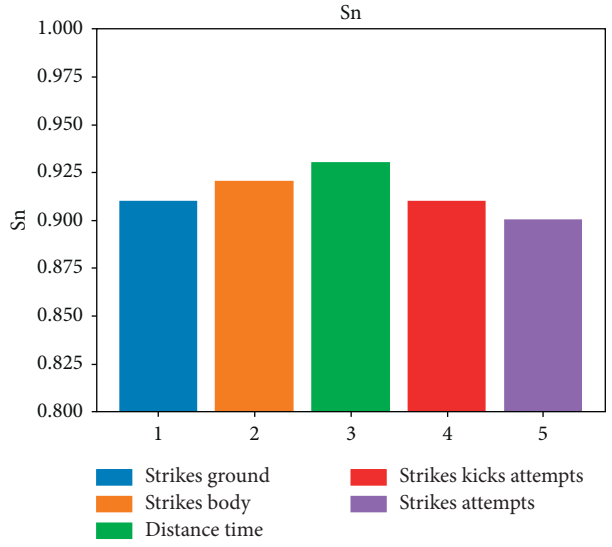

Figure 5: Comparative experimental results of different methods on sensitivity.

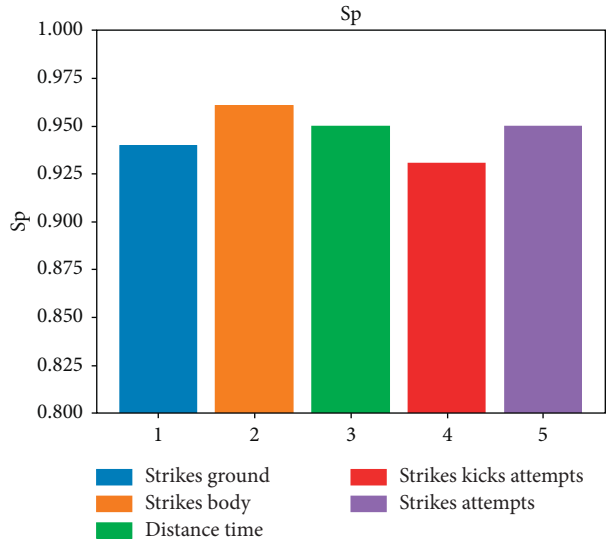

Figure 6: Comparative experimental results of different methods on specificity.

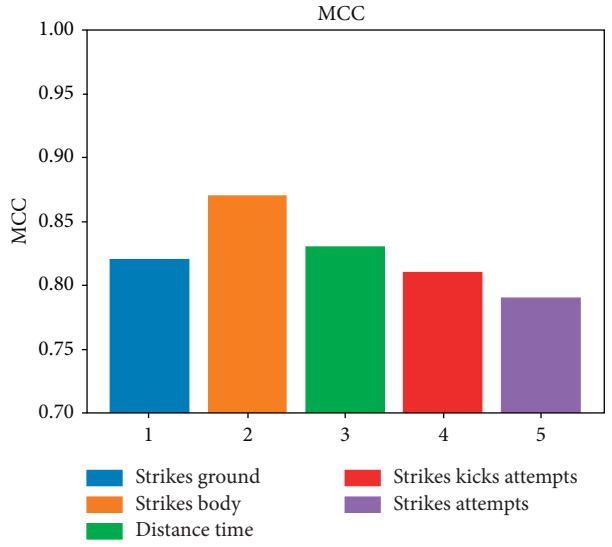

Figure 7: Comparative experimental results of different methods on MCC.

6. Conclusion

With abundant data and multiple analysis tools, the machine learning-assisted system of Wushu competition can display the real-time data of Wushu competition. It can assist the coaches in analyzing and making decisions on the spot and put forward targeted training objectives for daily training, which has substantial application value. On this basis, it can also build and establish numerous application systems. In this research, we have proposed a special system for martial arts experts to collect and accumulate the experience and knowledge of experts and scholars in martial arts to improve the competitive level, teaching level, and scientific research level of Chinese martial arts. Moreover, large-scale distributed control is adopted in a multiagent system which does not affect the operation of the whole multiagent. Our model has much better accuracy, sensitivity, specificity, and Matthew's correlation coefficient (MCC) in comparison with the existing schemes which shows its applications in Wushu competition. The proposed model results can be anticipated to have the potential for better flexibility and scalability in martial arts competition.

Data Availability

The data used to support the findings of this study are included within the article.

Conflicts of Interest

The authors declare that they have no conflicts of interest.

References

[1] K. Wang, "An empirical analysis of the popularization development of Taijiquan based on the concept of national

fitness," *Journal of Wuxi Vocational and Technical College*, vol. 16, no. 1, pp. 70–73, 2017.

[2] C. Wang, *Research on the Development of Bengbu Martial Arts under the Background of National Fitness*, Huaibei Normal University, Huaibei, China, 2018.

[3] L. Zhang, *Research on the Current Situation and Countermeasures of Taijiquan Teaching at Jilin University*, Jilin University, Changchun, China, 2014.

[4] J. Shi and Y. Xue, "Research on the development of Taijiquan in Chengdu I—taking the 13th Taijiquan championship in Chengdu in 2016 as an example," *Sichuan Sports Science*, vol. 36, no. 2, 2017.

[5] X. Chai, C. Gao, and Y. Jing, *The Promotion and Development Status of Taiji Aerobics under the National Fitness Program [Chuan]*, Vol. 10, China Good University, Beijing, China, 2017.

[6] Z. Shi, *Advanced Artificial Intelligence*, Science Press, Beijing, China, 2011.

[7] R. He, L. Chen, B. Wan et al., "Research on DSS oriented model base system based on agent," *Computer and Digital Engineering*, vol. 39, no. 12, pp. 54–57, 2011.

[8] J. Zhu and Y. Liu, "The construction method of an intelligent decision support system based on multi-agent," *Journal of Beijing University of Technology*, no. 1, pp. 6–10, 2001.

[9] S. Zhang, B. Li, and X. Zhao, "Application of intelligent decision support system in ventilation system optimization of Zhaozhuang mine," *Modern Mining*, vol. 34, no. 8, pp. 118–122, 2018.

[10] X. Li, "Analysis of Taijiquan fitness in China from the perspective of national fitness," *Foreign Teachers of China*, no. 6, pp. 46-47, 2018.

[11] G. Xu, "Exploration and research on the cultivation of ways of teenagers' Wushu enlightenment training interest," *Contemporary Sports Science and Technology*, vol. 7, no. 2, pp. 43-44, 2017.

[12] Y. Xu, X. Han, and L. Yang, "Research on the development path of traditional Wushu into the campus," *Chinese Wushu. Research*, no. 7, pp. 61–63, 2018.

[13] Y. Qiu, "On the inheritance of traditional martial arts to confucian spiritual cultivation methods," *Sports Science Research*, vol. 18, no. 5, pp. 15–18, 2014.

[14] B. Liu, "The development of martial arts under the guidance of new era thoughts. Chinese martial arts," *Research*, vol. 7, no. 8, pp. 45–48, 2018.

[15] Y. Zhang and J. Huang, "The influence of martial arts novels and film and TV works on young people's learning martial arts," *Sports Research and Education*, vol. 30, no. 2, pp. 98–100, 2015.

[16] X. Su, P. Li, and W. Shi, "On the characteristics of Chinese Wushu development during the cultural revolution," *Journal of Wuhan Institute of Physical Education*, vol. 33, no. 6, pp. 29–32, 1993.

[17] S. Xiong, *Research on Fuzzy Portfolio Optimization and Application*, Harbin Institute of Technology, Harbin, China, 2014.

[18] A. Dai, *Children's Sensitive Period Diagnosis System Based on Axiomatic Fuzzy Decision Tree*, Jiangxi University of Finance and Economics, Nanchang, China, 2017.

[19] T. Satty, *The Analytic Hierarchy Process*, McGraw-Hill, New York, NY, USA, 1980.

[20] X. Wang, Y. Hong, J. Huang, and Z. P. Jiang, "A distributed control approach to a robust output regulation problem for multi-agent linear systems," *IEEE Transactions on Automatic Control*, vol. 55, no. 12, pp. 2891–2895, 2010.

[21] X. Wang, M. Yang, Y. Jiang et al., "On self-tuning networks-on-chip for dynamic network-flow dominance adaptation," *ACM Transactions on Embedded Computing Systems (TECS)*, vol. 13, no. 2, pp. 1–21, 2014.

[22] J. Li, *Research on Some Problems of Multi-Agent System Unification*, School of automation, Nanjing University of Technology, Nanjing, China, 2011.

[23] W. Liu, *Coordinated Control and Optimization of Complex Multi-Agent Networks*, School of automation, Huazhong University of science and technology, Wuhan, China, 2011.

[24] W. Cai, B. Liu, Z. Wei, M. Li, and J. Kan, "TARDB-net: triple-attention guided residual dense and BiLSTM networks for hyperspectral image classification," *Multimedia Tools and Applications*, vol. 80, no. 7, pp. 11291–11312, 2021.

[25] X. Zhang, Y. Yang, Z. Li, X. Ning, Y. Qin, and W. Cai, "An improved encoder-decoder network based on strip pool method applied to segmentation of farmland vacancy field," *Entropy*, vol. 23, no. 4, p. 435, 2021.

Hindawi
Mobile Information Systems
Volume 2021, Article ID 9938325, 9 pages
https://doi.org/10.1155/2021/9938325

Research Article

E-Commerce Enterprise Supply Chain Financing Risk Assessment Based on Linked Data Mining and Edge Computing

Qiao Qu,[1] **Cheng Liu**,[1] **and Xinzhong Bao**[2]

[1]*School of Economics and Management, University of Science and Technology Beijing, Beijing 100083, China*
[2]*School of Management, Beijing Union University, Beijing 100101, China*

Correspondence should be addressed to Qiao Qu; b20170399@xs.ustb.edu.cn

Received 27 March 2021; Revised 28 April 2021; Accepted 7 May 2021; Published 19 May 2021

Academic Editor: Muhammad Usman

Copyright © 2021 Qiao Qu et al. This is an open access article distributed under the Creative Commons Attribution License, which permits unrestricted use, distribution, and reproduction in any medium, provided the original work is properly cited.

In recent years, the rapid development of information technology has affected the way the world economy operates. The emergence of e-commerce has greatly shortened the time and space distance between economic participants and maximized the sharing of resources. However, the financial management and risk assessment capabilities of the existing supply are insufficient to adapt to the rapidly developing new environment. This article uses a combination of normative analysis and empirical analysis to analyze the status quo of the supply chain of small and medium e-commerce companies. First, this article establishes an evaluation framework for the supply chain of e-commerce companies based on edge computing. Second, according to the distribution of the supply chain, this article adds the member's predetermined quota, reputation, execution time, and other indicators as parameters to establish a fuzzy neural network model. On this basis, combined with the price regression model, the pricing plan is evaluated. The results show that the financing risk obtained by this model differs very little from the actual risk. The above-mentioned model constructs an e-commerce enterprise supply chain financing risk management model that adapts to the environment of the new era.

1. Introduction

Nowadays, with the rise of the network economy environment, e-commerce companies have gradually become the mainstream of domestic and foreign business activities, and they are in a period of rapid development [1, 2]. E-commerce companies can realize information exchange faster and more conveniently and provide more detailed resource information for both parties for the transaction as much as possible, which greatly shortens the time for transaction decision-making. This e-commerce model improves the success rate of transactions and plays an integrated role in the resources of the entire society [3–5]. The e-commerce enterprise platform is open and shared, and it has strong advantages for both enterprises and academia in research on consumer behavior and information control [6]. At present, there are still many problems and shortcomings, and they cause the relatively lagging development of the enterprise [7]. Therefore, studying the financial management mode has important theoretical and practical significance in this period [8–10].

In the aspect of enterprise supply chain management, Hameed et al. [11] pointed out that, due to the relatively flat and simple organizational structure, the main problem affecting the performance of SMEs is the lack of funding sources for purchasing complex and expensive software and hiring competitive intelligence experts. The market when continuously optimizing the financial management mode is to adapt to the constantly changing business environment [12, 13]. Dutta et al. [14] believes that what enterprises in the new era need is a new type of financial management model, so the financial management model should also be innovated and reformed in time to adapt to the development of the times. Jensen pointed out that the information system in enterprise management under e-commerce needs to be updated continuously. Tan et al. [15] pointed out that the contribution of SMEs to a country's economic growth is widely recognized. In the context of e-commerce, the

comprehensive evaluation of supply chain financing risks and the determination of a scientific and reasonable performance evaluation system are the most important. Consumers' consumption habits have shifted from offline to online, which requires SMEs to adopt more e-commerce models for business operations [16].

However, the financial management and risk assessment capabilities of the existing supply are insufficient to adapt to the rapidly developing new environment [17, 18]. Therefore, studying the financial management mode that is suitable has important theoretical and practical significance in this period [19]. This article uses a combination of normative analysis and empirical analysis to analyze the status quo of the supply chain of small and medium e-commerce companies. In the second chapter, we introduced an overview of edge computing and enterprise supply chain management. In the third chapter, we discuss the selection model of e-commerce enterprise supply chain evaluation indicators based on cluster analysis and associated data mining. In the fourth chapter, we discuss the financing model of e-commerce enterprise supply chain based on fuzzy neural network. Finally, we summarize the methods and shortcomings of this article in the fifth chapter.

2. Overview of Related Technology Research

2.1. Edge Computing. In the field of intelligent computing, based on the development of cloud computing, edge computing is applied to the Internet service environment, and mobile edge computing (MEC) technology is born. MEC is a new type of network structure, running and providing information technology services and cloud computing capabilities [20, 21]. Now, this method has become a standardized technology. The basic framework of mobile edge computing is shown in Figure 1.

The actual value of edge computing continues to increase. With the explosive growth of the demand for Internet of Things device access, the demand for analysis and computing power on the MEC side will double [22, 23]. MEC, which has the characteristics of low latency and low energy consumption, can fully meet the needs of users adaptively, so as to achieve the goal of rapid response and agile deployment [24, 25]. In accordance with the trend, MEC will not only mobilize and integrate resources according to the needs of different scenarios in the development of terrestrial communications but also bring about major changes to future maritime communications.

2.2. E-Commerce Enterprise Supply Chain Evaluation. The emergence of e-commerce has greatly shortened the time and space distances between economic participants and maximized the sharing of resources [26–28]. However, nowadays, most of the small- and medium-sized e-commerce companies in our country have low financial management and backward financial management models, which are unable to adapt to the new competition and new challenges brought about by rapid development [29]. E-commerce companies can realize information exchange faster and more conveniently and provide transaction parties with more detailed resource information as much as possible, which greatly shortens the time for transaction decision-making, improves the success rate of transactions, and also plays a significant role in the resources of the whole society. In the context of e-commerce, the comprehensive evaluation of supply chain financing risks and the determination of a scientific and reasonable performance evaluation system are the most important [30].

According to the characteristics of the supply chain financing of e-commerce enterprises and following the ideas and principles of the evaluation index system design, this paper will gradually carry out the relevant construction of the supply chain financing performance evaluation system under the background of e-commerce. In the context of e-commerce, the comprehensive evaluation of supply chain financing risks and the determination of a scientific and reasonable performance evaluation system are the most important. Consumers' consumption habits have shifted from offline to online, which requires SMEs to adopt more e-commerce models for business operations. At present, there are still many problems and shortcomings, and they cause the relatively lagging development of the enterprise. Therefore, studying the financial management mode has important theoretical and practical significance in this period.

3. E-Commerce Enterprise Supply Chain Evaluation Index Selection Model

3.1. The Establishment of Cluster Analysis Model. When goods or labor is treated as commodities and exchanged to meet our own needs, we need to set prices for them [31]. When a commodity has no value, the price no longer exists, because its value corresponds to the corresponding price. The task pricing in this article first follows the basic principles of the law of value, and, secondly, the price cluster analysis is a multivariate statistical analysis to quantitatively study the classification problem according to the characteristics of the thing itself [32, 33]. The basic idea is to divide the data into several categories according to the distance, so that the "difference" of the data within the category is as small as possible, and the "difference" between the categories is as large as possible [34]. The clustering of sample individuals is usually called type clustering.

Use Euclidean distance to measure the closeness between indicators. Euclidean distance is the straight-line distance between two points in space [35]. In the context of e-commerce, the comprehensive evaluation of supply chain financing risks and the determination of a scientific and reasonable performance evaluation system are the most important. The weight of each feature parameter is equal, and the weight represents the distance between two indices. The calculation formula is as follows:

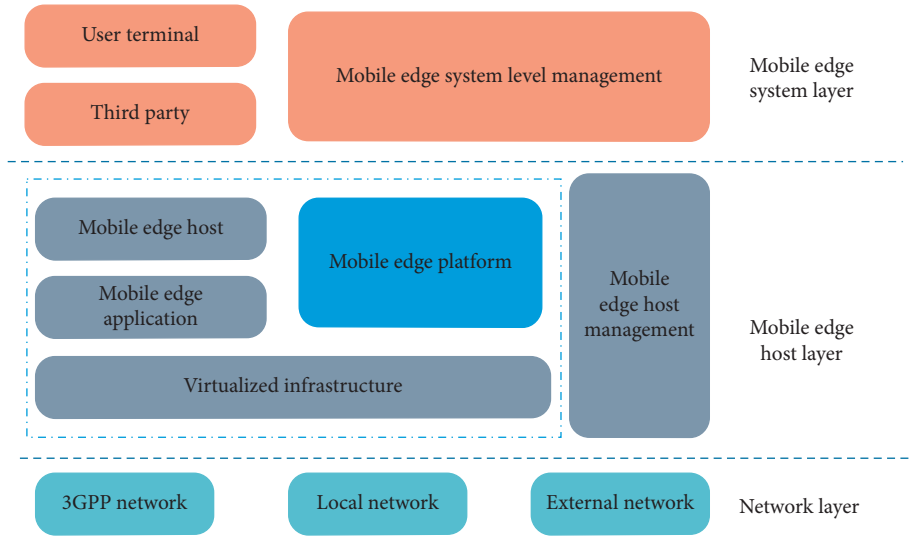

Figure 1: The basic framework of mobile edge computing.

$$d_{ij(2)} = \sqrt{\left(\sum_{k=1}^{p} \left|v_{ik} - v_{jk}\right|^2\right)}. \quad (1)$$

In the above formula, $i, j = 1, 2, \ldots, p$.
The specific process of cluster analysis is as follows:

(1) Combine the two closest units into one category to form a category, and calculate the distance between the newly generated category and the other categories to form a new distance matrix [36].

(2) According to the same principle as the second step, merge the two categories with the closest distance. If the number of categories is still greater than 1, the model continues to repeat this step until all the data is merged into one category.

The task points in Annex 1 are firstly clustered [37, 38]. Figure 2 shows pedigree diagram of the supply chain indicators of the e-commerce enterprise.

As shown in Figure 2, the 835 task points in Annex 1 can be divided into 3 clusters according to latitude and longitude. Each cluster represents a task area point in a different range of latitude and longitude [39, 40]. E-commerce companies can realize information exchange faster and more conveniently and provide transaction parties with more detailed resource information as much as possible, which greatly shortens the time for transaction decision-making, improves the success rate of transactions, and also plays a significant role in the resources of the whole society. The three clusters have large differences; that is, they are far apart [41–43]. Next, the center positions of the three clusters are obtained by this method. Then, the distance between the component and the center of the area can also be obtained. Then the distance between the member and the center of the region can be obtained. At present, there are still many problems and shortcomings, and they cause the relatively lagging development of the enterprise [44]. Therefore, studying the financial management mode has important theoretical and practical significance in this period.

3.2. Establishment and Solution of K-Means Algorithm Model. The optimal clustering result is obtained through iterative optimization of the divided mean.

Algorithm steps are as follows:

$$c^{(i)} = \arg\min_j \left\|x^{(i)} - \mu_j\right\|^2,$$
$$\mu_j = \frac{\sum_{i=1}^{m}\left\{c^{(i)} = j\right\}x^{(i)}}{\sum_{i=1}^{m}\left\{c^{(i)} = j\right\}}. \quad (2)$$

Here, we substitute the data of the three classes obtained by the Q-type clustering analysis into the calculations and obtain the cluster centers of each class after 20 iterations [45]. The basic idea is to divide the data into several categories according to the distance, so that the "difference" of the data within the category is as small as possible, and the "difference" between the categories is as large as possible. The latitude and longitude coordinates of the cluster centers are shown in Table 1.

Next, use the data in Annex 1 to obtain the average value of task pricing in the 3 regions. Combine Annex 2 to obtain the distance from each member to the 3 cluster centers and then to obtain the average distance from all members to the 3 cluster centers. The distance from the member to the cluster center and the average price of various cluster tasks are shown in Table 2.

The specific data of the number of corresponding members and the number of tasks in each cluster area is shown in Table 3.

According to Table 3, analyzing the relationship between supply and demand and pricing, the results show that all three regions can meet the supply and demand ratio <1 [46]. The clustering of sample individuals is usually called type clustering, and the clustering of research variables is called

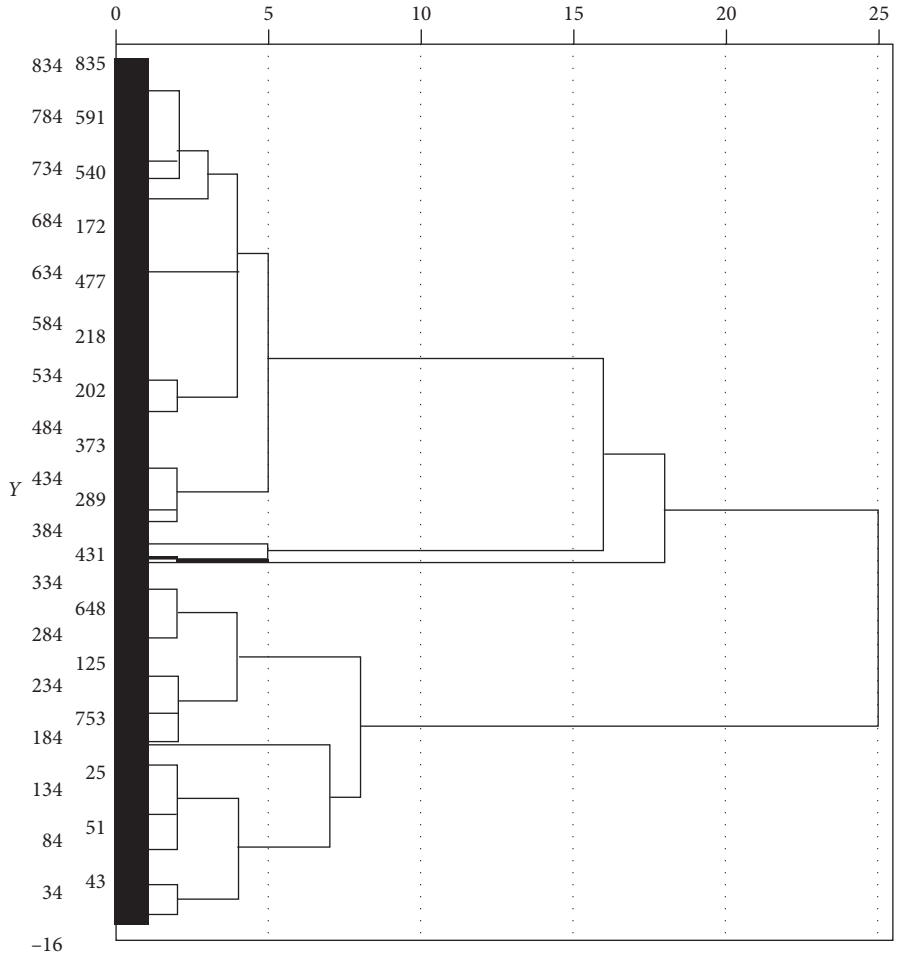

Figure 2: A pedigree diagram of supply chain indicators for e-commerce companies.

Table 1: The latitude and longitude coordinates of the cluster centers.

	Final cluster center		
	Clustering		
	1	2	3
Latitude	22.67	23.02	23.11
Longitude	114.04	113.73	113.23

type clustering; that is, the number of tasks is less than the number of members, so there will be no overtasking or understaffing.

3.3. Determination of Weights-Establishment and Solution of Analytic Hierarchy Process Model. By pairwise comparison, the method of establishing a pairwise comparison matrix is used to compare the influences of factors [47]. E-commerce companies can realize information exchange faster and more conveniently and provide transaction parties with more detailed resource information as much as possible, which greatly shortens the time for transaction decision-making, improves the success rate of transactions, and also plays a significant role in the resources of the whole society. According to the meaning of the question, the following judgment matrix can be constructed:

$$A = \begin{bmatrix} 1 & 6 \\ 0.15 & 1 \end{bmatrix}. \tag{3}$$

P_2 is the supply-demand ratio, and $w_i (i = 1, 2)$ is the corresponding weight of the influence of the two factors on the task completion rate. Finally, we get the comprehensive index of task pricing:

$$P = 0.137 \times P_1 + 0.863 \times P_2. \tag{4}$$

Because the dimensions of P_1 and P_2 are different, large errors will occur in the calculation.

$$L_i' = \frac{L_i' - (1/3)\sum_{i=1}^{3} L_i'}{L_{i\max}' - L_{i\min}'}. \tag{5}$$

According to formula (5), the two types of data are normalized, and then the result is obtained by drawing the image. The relationship between comprehensive indicators and task pricing is shown in Figure 3.

It can be judged that the curve in Figure 3 fits well; that is, the relationship curve between the obtained comprehensive indicators and task pricing is more reasonable. Within the

Table 2: The distance from the member to the cluster center and the average price of various cluster tasks.

	Clustering		
	1	2	3
Task pricing average	69.07	68.04	68.11
Average distance between members and cluster center (km)	1.546	1.602	1.825

Table 3: The number of corresponding members and the number of tasks in each clustering area.

	Clustering		
	1	2	3
Number of members	538	451	988
Number of tasks	202	190	443

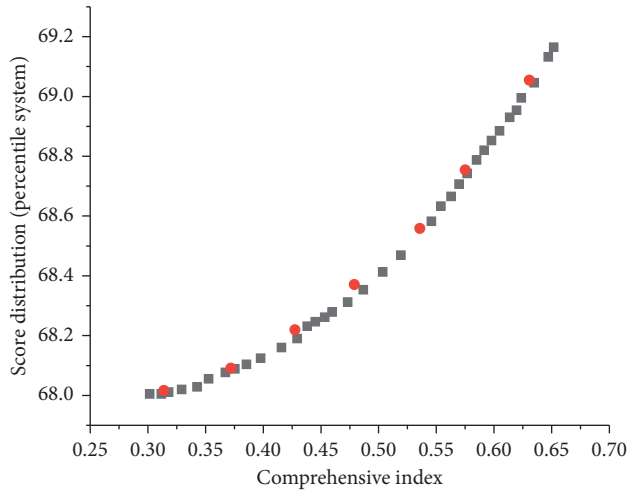

Figure 3: The relationship between comprehensive indicators and task pricing.

scope of the question data, the task pricing increases with the increase of the comprehensive index.

4. E-Commerce Enterprise Supply Chain Financing Model

4.1. Supply Chain Task Packaging Plan. If the tasks are concentrated and the members are also concentrated in this area, then, in this area, members will compete to choose the task, which may lead to malicious snatching, resulting in a low task completion rate. Therefore, we can consider a scheme of jointly packaged and released tasks; that is, several tasks are bundled and handed over to one user to complete. Since the task points are not very far apart, the neighboring task points can be packed [48]. Here, by drawing the scatter diagram of the task point distribution in Annex 1, 100 task point centers are selected, and the task points with a radius of 16 km from the task center point are packaged and released as a task package. The task executor will comprehensively consider the time when the member gets the task release status and the quota situation to obtain the final result. At present, there are still many problems and shortcomings, and they cause the relatively lagging development of the enterprise. Therefore, studying the financial management mode has important theoretical and practical significance in this period. The scatter diagram of the supply chain task point distribution is shown in Figure 4.

4.2. Establishment of Fuzzy Neural Network Model. The neural network that uses nonlinear prediction is usually a backpropagation neural model (BP model). Each represents the impact task. There are 7 factors related to price. The output layer has a node to build the relationship with the model. The neurons in the middle layer are not connected to each other, while the neurons in the adjacent layer are connected by weights. The structure of the fuzzy neural network model is shown in Figure 5.

The task is packaged; that is, several tasks are bundled and released, so that the tasks that originally need to be assigned to multiple members are completed by the same member. The basic idea is to divide the data into several categories according to the distance, so that the "difference" of the data within the category is as small as possible, and the "difference" between the categories is as large as possible. The clustering of sample individuals is usually called type clustering, and the clustering of research variables is called type clustering. The packaged task package will be priced slightly lower than the sum of the single pricing when it is not packaged.

After packaging, the task with the smallest number in the package is a relative single-package task. The number of tasks

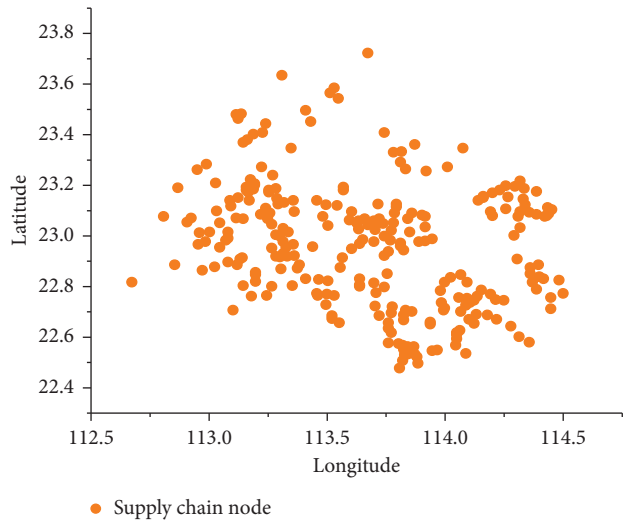

Figure 4: Scatter diagram of the distribution of supply chain task points.

in other packages is a multiple of this relative to the actual number of single-package tasks as the relative number. Suppose that F_x is the price of the commodity, p is the price when it is not packaged, and C is the relative cost coefficient of the relative single-package task.

$$F(x) = \left[C + (A + Bx)^{-\alpha}\right]px. \tag{6}$$

When formula (7) satisfies the above conditions, there are

$$\left(\frac{F(x)}{x}\right)' = \left[Cp + (A + Bx)^{-\alpha}p\right]' = \left[p(A + Bx)^{-\alpha}\right]' = (-\alpha pB)\left[(A + Bx)^{-(1-\alpha)}\right] < 0,$$
$$\lim_{x\longrightarrow\infty}\left(\frac{F(x)}{x} - Cp\right) = \lim_{x\longrightarrow\infty}\left[p(A + Bx)^{-\alpha}\right] = 0, \tag{7}$$
$$(A + Bx)^{-(1-\alpha)} > 0, p > 0, B > 0, \alpha > 0.$$

In the second search, the parameter A^* obtained in the first search is searched again in its neighborhood. The sum of the relative error squares between actual and theoretical relative pricing is calculated and its minimum value is used as the objective function.

$$\widehat{J} = \min \widetilde{J} = \min\left\{\sum\left(\frac{(y_i - y)}{y_i}\right)^2\right\}. \tag{8}$$

At this time, the relative error squared sum of the relative pricing is $\sum_{i=1}^{n}[(y_i - \widetilde{y}_i)/y_i]^2 \approx 0.0010375$, and the relative error value is small.

The basic idea is to divide the data into several categories according to the distance, so that the "difference" of the data within the category is as small as possible, and the "difference" between the categories is as large as possible. The clustering of sample individuals is usually called type clustering, and the clustering of research variables is called type clustering. The evaluation of the supply chain level of e-commerce companies is shown in Figure 6.

The pricing obtained through the model is established by the fuzzy neural network. Therefore, it can be shown that the model established by this question is reasonable and can be used for packaging.

In this article, we will influence the new pricing parameters. Related parameters include the salary level of the employee where the task is located, the complexity of the task, the reputation value of the member, the member's scheduled task limit, and the member's scheduled task start time. For changes that affect the pricing parameters, 0 is not affected. The knowledge base of some rules of the e-commerce supply chain is shown in Table 4.

E-commerce companies can realize information exchange faster and more conveniently and provide transaction parties with more detailed resource information as much as possible, which greatly shortens the time for transaction decision-making, improves the success rate of transactions, and also plays a significant role in the resources of the whole society. All possible combinations of rules are obtained from the given rules after repeated learning, and the factors that affect pricing and the data that lead to price changes are input into the system, and the learning rate is $\alpha = 0.7$. This chapter first designs a scale to

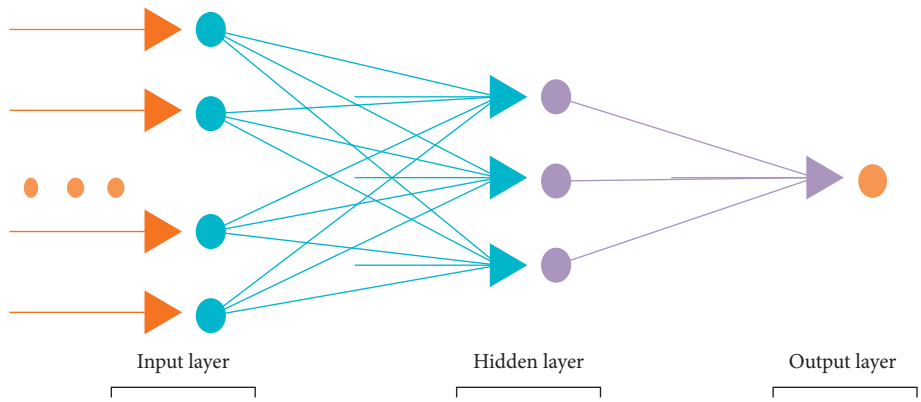

Figure 5: BP fuzzy neural network model structure.

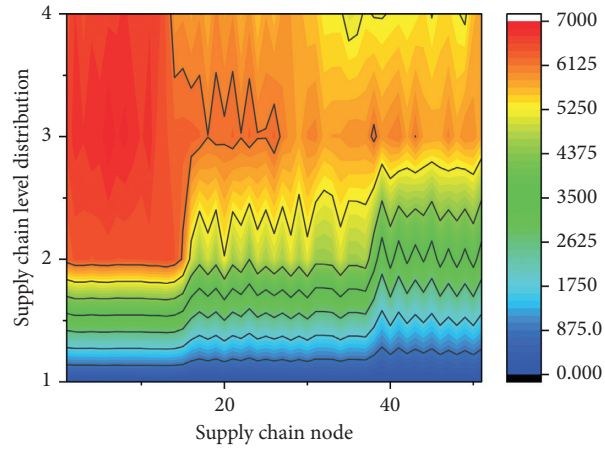

Figure 6: E-commerce company supply chain rating evaluation.

Table 4: Knowledge base of some rules of e-commerce supply chain.

	If							Then
Serial number	x_1 $\lambda_1 = 1$	x_2 $\lambda_2 = 1$	x_3 $\lambda_3 = 1$	x_4 $\lambda_4 = 1$	x_5 $\lambda_5 = 1$	x_6 $\lambda_6 = 1$	x_7 $\lambda_7 = 1$	
1	1							1
2		1						1
3			1					−1
4				1				−1
5					1			−1
6						1		1
7							1	−1

test the credibility and validity of the questionnaire and do a factor analysis on the survey data. The analysis shows the benefits of capital and the degree of decentralization of financial management. Play a major role in the above three submodes. Through the structural equation test, it is concluded that the three hypotheses all pass the test, and the empirical model fits well with the survey data. Studies have shown that the capital management, accounting information disclosure, and financial organization of SMEs are mutually reinforcing and complementary.

At this stage, in the e-commerce environment, the core of financial management of SMEs in our country is the allocation of financial rights, capital operation, and information. It is disclosed that the three submodels can be the main content of the SME financial management model under the current environment. Therefore, the new model should integrate the above three submodels and make them an organic unity. At present, there are still many problems and shortcomings, and they cause the relatively lagging development of the enterprise. Therefore, studying the financial management mode has important theoretical and practical significance in this period. The three submodels restrict and cooperate with each other in function and can effectively play positive influence.

5. Conclusion

At present, there are still many problems and shortcomings, which hinder the good development of the enterprise and cause the relatively lagging development of the enterprise, and it is difficult to adapt to the current increasingly competitive market environment. Therefore, studying the financial management mode that is suitable under the e-commerce has important theoretical and practical significance in this period. In the context of e-commerce, the comprehensive evaluation of supply chain financing risks and the determination of a scientific and reasonable performance evaluation system are the most important. Consumers' consumption habits have shifted from offline to online, which requires SMEs to adopt more e-commerce models for business operations. E-commerce companies can realize information exchange faster and more conveniently and provide transaction parties with more detailed resource information as much as possible, which greatly shortens the time for transaction decision-making, improves the success rate of transactions, and also plays a significant role in the resources of the whole society. However, the financial management and risk assessment capabilities of the existing supply are insufficient to adapt to the rapidly developing new environment. Therefore, studying the financial management mode that is suitable under the e-commerce has important theoretical and practical significance in this period. This article uses a combination of normative analysis and empirical analysis to analyze the status quo of the supply chain of small and medium e-commerce companies. This paper conducts innovative research on the financial management mode under the environment of e-commerce enterprises and proposes a new financial management mode. Although some progress has been made, there are still some limitations in the research, and there are still many contents related to the paper which need to be studied.

Data Availability

The datasets used and/or analyzed during the current study are available from the corresponding author upon reasonable request.

Conflicts of Interest

The authors declare that there are no conflicts of interest.

References

[1] O. Durowoju, H. K. Chan, and X. Wang, "Investigation of the effect of e-platform information security breaches: a small and medium enterprise supply chain perspective," *IEEE Transactions on Engineering Management*, vol. 73, no. 3, pp. 1–16, 2020.

[2] H. Lu, "Analysis of economic benefit of e-commerce business in oceangoing enterprises," *Journal of Coastal Research*, vol. 106, no. 1, p. 217, 2020.

[3] B. Zhang, R. Tan, and C. J. Lin, "Forecasting of e-commerce transaction volume using a hybrid of extreme learning machine and improved moth-flame optimization algorithm," *Applied Intelligence*, vol. 51, pp. 1–14, 2020.

[4] S. Gao, X. Chen, Z. Ren, D. Zhao, and R. Yan, "Meaningful answer generation of e-commerce question-answering," *ACM Transactions on Information Systems*, vol. 39, no. 2, pp. 1–26, 2021.

[5] A. Vinsensius, Y. Wang, E. P. Chew et al., "Dynamic incentive mechanism for delivery slot management in e-commerce attended home delivery," *Transportation Science*, vol. 54, 2020.

[6] W. Xuan and T. N. Chi, "New retail versus traditional retail in e-commerce: channel establishment, price competition, and consumer recognition," *Annals of Operations Research*, vol. 291, 2020.

[7] M. Mao, J. Lu, J. Han, and G. Zhang, "Multiobjective e-commerce recommendations based on hypergraph ranking," *Information Sciences*, vol. 471, pp. 269–287, 2019.

[8] I. M. Gee, B. R. Heard, M. E. Webber, and S. A. Miller, "The future of food: environmental lessons from e-commerce," *Environmental Science & Technology*, vol. 54, no. 23, pp. 14776–14784, 2020.

[9] S. Liu, C. Newman, C. D. Buesching et al., "E-commerce promotes trade in invasive turtles in China," *Oryx*, vol. 55, pp. 1–4, 2020.

[10] A.-A. Guindon and D. J. Wright, "Analytical approach to quantitative risk assessment for solar power projects," *Renewable and Sustainable Energy Reviews*, vol. 133, Article ID 110262, 2020.

[11] H. B. Hameed, Y. Ali, and A. Petrillo, "Environmental risk assessment of e-waste in developing countries by using the modified-SIRA method," *Science of the Total Environment*, vol. 733, Article ID 138525, 2020.

[12] J. Leivo, E. Anttonen, S. S. Jolly et al., "3037The prognostic significance of grade of ischemia in patients with STEMI: a substudy of the randomized trial of primary PCI with or without routine manual thrombectomy (total trial)," *European Heart Journal*, vol. 40, no. 1, 2019.

[13] B. G. Reguero, M. W. Beck, D. Schmid et al., "Financing coastal resilience by combining nature-based risk reduction with insurance," *Ecological Economics*, vol. 169, 2020.

[14] S. Dutta, G. Pregartner, F. G. Rücker et al., "Functional classification of tp53 mutations in acute myeloid leukemia," *Blood*, vol. 134, no. 1, p. 2725, 2019.

[15] R. R. Tan, K. B. Aviso, and D. K. S. Ng, "Optimization models for financing innovations in green energy technologies," *Renewable and Sustainable Energy Reviews*, vol. 113, Article ID 109258, 2019.

[16] P. Zhang, M. Durresi, and A. Durresi, "Multi-access edge computing aided mobility for privacy protection in Internet of Things," *Computing*, vol. 101, no. 7, pp. 729–742, 2019.

[17] A. Boukerche and V. Soto, "Computation offloading and retrieval for vehicular edge computing," *ACM Computing Surveys (CSUR)*, vol. 53, 2020.

[18] S. Kim, T. Choi, S. Song et al., "Special issue on 5G & B5G enabling edge computing, big data and deep learning technologies," *ETRI Journal*, vol. 42, no. 5, 2020.

[19] L. Lin, W. Zhou, and Z. Zhao, "Analytical modeling of noma-based mobile edge computing systems with randomly located users," *IEEE Communications Letters*, vol. 24, no. 12, 2020.

[20] L. Zhou, Y. Hong, S. Wang et al., "Learning centric wireless resource allocation for edge computing: algorithm and experiment," *IEEE Transactions on Vehicular Technology*, vol. 70, no. 1, 1 page, 2020.

[21] X. Xiong, K. Zheng, L. Lei et al., "Resource allocation based on deep reinforcement learning in iot edge computing," *IEEE Journal on Selected Areas in Communications*, vol. 38, no. 6, 1 page, 2020.

[22] X. Hong, L. Liang, X. Jie et al., "Joint task assignment and resource allocation for d2d-enabled mobile-edge computing," *IEEE Transactions on Communications*, vol. 67, no. 6, 2019.

[23] M.-P. Hosseini, T. X. Tran, D. Pompili, K. Elisevich, and H. Soltanian-Zadeh, "Multimodal data analysis of epileptic EEG and Rs-fMRI via deep learning and edge computing," *Artificial Intelligence in Medicine*, vol. 104, Article ID 101813, 2020.

[24] Y. Dai, D. Xu, K. Zhang et al., "Deep reinforcement learning and permissioned blockchain for content caching in vehicular edge computing and networks," *IEEE Transactions on Vehicular Technology*, vol. 69, no. 4, 2020.

[25] O. Laureniu, D. Norbert, C. Octavian et al., "Edge computing in space: field programmable gate array-based solutions for spectral and probabilistic analysis of time series," *The Review of Scientific Instruments*, vol. 90, no. 11, Article ID 114501, 2019.

[26] A. Mehrabi, M. Siekkinen, Y-J. Antti et al., "Edge computing assisted adaptive mobile video streaming," *IEEE Transactions on Mobile Computing*, vol. 18, 2019.

[27] W. Zhang, Z. Zhang, S. Zeadally et al., "Efficient task scheduling with stochastic delay cost in mobile edge computing," *IEEE Communications Letters*, vol. 23, 2019.

[28] A. Gumaei, M. Al-Rakhami, M. M. Hassan et al., "Deep learning and blockchain with edge computing for 5g-enabled drone identification and flight mode detection," *IEEE Network*, vol. 35, no. 1, pp. 94–100, 2021.

[29] W.-J. Chang, L.-B. Chen, C.-Y. Sie, and C.-H. Yang, "An artificial intelligence edge computing-based assistive system for visually impaired pedestrian safety at zebra crossings," *IEEE Transactions on Consumer Electronics*, vol. 67, no. 1, pp. 3–11, 2021.

[30] B. Hu and J. Li, "An edge computing framework for powertrain control system optimization of intelligent and connected vehicles based on curiosity-driven deep reinforcement learning," *IEEE Transactions on Industrial Electronics*, vol. 68, 2020.

[31] S. G. Chen, F. J. Lin, C. H. Liang et al., "Intelligent maximum power factor searching control using recurrent Chebyshev fuzzy neural network current angle controller for Synrm drive system," *IEEE Transactions on Power Electronics*, vol. 36, no. 3, 2020.

[32] H. Li, C. Li, D. Ouyang, S. K. Nguang, and Z. He, "Observer-based dissipativity control for t-s fuzzy neural networks with distributed time-varying delays," *IEEE Transactions on Cybernetics*, vol. 16, no. 99, pp. 1–11, 2020.

[33] Y. D. Koo, H. Seon Jo, M. G. Na, K. H. Yoo, and C.-H. Kim, "Prediction of the internal states of a nuclear power plant containment in LOCAs using rule-dropout deep fuzzy neural networks," *Annals of Nuclear Energy*, vol. 156, no. 3, Article ID 108180, 2021.

[34] R. M. Wang, Y. N. Zhang, Y. Q. Chen et al., "Fuzzy neural network-based chaos synchronization for a class of fractional-order chaotic systems: an adaptive sliding mode control approach," *Nonlinear Dynamics*, vol. 100, no. 4, 2020.

[35] A. Cz, C. Skob, and B. Zf, "Design of stabilized polynomial-based ensemble fuzzy neural networks based on heterogeneous neurons and synergy of multiple techniques," *Information Sciences*, vol. 542, pp. 425–452, 2021.

[36] G. Yangyong and W. Juan, "Modeling of false information on microblog with block matching and fuzzy neural network," *International Journal of Modern Physics C*, vol. 32, 2020.

[37] K. H. Tan, F. J. Lin, C. M. Shih et al., "Intelligent control of microgrid with virtual inertia using recurrent probabilistic wavelet fuzzy neural network," *IEEE Transactions on Power Electronics*, vol. 35, no. 7, 2019.

[38] H. Zhou, H. Zhao, and Y. Zhang, "Nonlinear system modeling using self-organizing fuzzy neural networks for industrial applications," *Applied Intelligence*, vol. 50, no. 5, pp. 1657–1672, 2020.

[39] V. Nasir, S. Nourian, S. Avramidis, and J. Cool, "Stress wave evaluation for predicting the properties of thermally modified wood using neuro-fuzzy and neural network modeling," *Holzforschung*, vol. 73, no. 9, pp. 827–838, 2019.

[40] S. Hou and J. Fei, "Finite-time adaptive fuzzy-neural-network control of active power filter," *IEEE Transactions on Power Electronics*, vol. 34, 2019.

[41] Y. Xu, D. Zhan, L. Liu, H. Lv, L. Xu, and J. Du, "A privacy-preserving cross-domain healthcare wearables recommendation algorithm based on domain-dependent and domain-independent feature fusion," *IEEE Journal of Biomedical and Health Informatics*, vol. 14, no. 5, 2021.

[42] T. Rao and S. Srivastava, "Analyzing stock market movements using twitter sentiment analysis," in *Proceedings of the IEEE International Conference on Advances in Social Networks Analysis and Mining(ASONAM 2012)*, pp. 1–5, Washington, DC, USA, August 2012.

[43] D. Enke, M. Grauer, and N. Mehdiyev, "Stock market prediction with multiple regression, fuzzy type-2 clustering and neural networks," *Procedia Computer Science*, vol. 6, pp. 201–206, 2011.

[44] M. Qasem, R. Thulasiram, and P. Thulasiram, "Twitter sentiment classification using machine learning techniques for stock markets," in *Proceedings of the IEEE International Conference on Advances in Computing, Communications and Informatics (ICACCI)*, pp. 834–840, Kochi, India, August 2015.

[45] A. Feinberg and D. Genethliou, "Load forecasting," in *Applied Mathematics for Restructured Electric Power Systems*, J. Chow, F. Wu, and J. Momoh, Eds., pp. 269–285, Springer, Berlin, Germany, 2005.

[46] R. Rostamzadeh, M. K. Ghorabaee, K. Govindan, A. Esmaeili, and H. B. K. Nobar, "Evaluation of sustainable supply chain risk management using an integrated fuzzy TOPSIS- CRITIC approach," *Journal of Cleaner Production*, vol. 175, pp. 651–669, 2018.

[47] M. Yu, T. Quan, Q. Peng, X. Yu, and L. Liu, "A model-based collaborate filtering algorithm based on stacked AutoEncoder," *Neural Computing and Applications*, vol. 6, no. 12, 2021.

[48] X. Yu, F. Jiang, J. Du, and D. Gong, "A cross-domain collaborative filtering algorithm with expanding user and item features via the latent factor space of auxiliary domains," *Pattern Recognition*, vol. 94, pp. 96–109, 2019.

Hindawi
Mobile Information Systems
Volume 2021, Article ID 9919992, 10 pages
https://doi.org/10.1155/2021/9919992

Research Article

An Action Recognition Algorithm for Sprinters Using Machine Learning

Fengqing Jiang[1] **and Xiao Chen**[2]

[1]*Institute of Science, Jiangxi University of Science and Technology, Ganzhou, Jiangxi 341000, China*
[2]*Physical Education Department, Zhongnan University of Economics and Law, Wuhan, Hubei 430073, China*

Correspondence should be addressed to Xiao Chen; chenxiaozhongnan@sohu.com

Received 9 March 2021; Revised 14 April 2021; Accepted 5 May 2021; Published 19 May 2021

Academic Editor: Xingwang Li

Copyright © 2021 Fengqing Jiang and Xiao Chen. This is an open access article distributed under the Creative Commons Attribution License, which permits unrestricted use, distribution, and reproduction in any medium, provided the original work is properly cited.

The advancements in modern science and technology have greatly promoted the progress of sports science. Advanced technological methods have been widely used in sports training, which have not only improved the scientific level of training but also promoted the continuous growth of sports technology and competition results. With the development of sports science and the gradual deepening of sport practices, the use of scientific training methods and monitoring approaches has improved the effect of sports training and athletes' performance. This paper takes sprint as the research problem and constructs the image of sprinter's action recognition based on machine learning. In view of the shortcomings of traditional dual-stream convolutional neural network for processing long-term video information, the time-segmented dual-stream network, based on sparse sampling, is used to better express the characteristics of long-term motion. First, the continuous video frame data is divided into multiple segments, and a short sequence of data containing user actions is formed by randomly sampling each segment of the video frame sequence. Next, it is applied to the dual-stream network for feature extraction. The optical flow image extraction involved in the dual-stream network is implemented by the system using the Lucas–Kanade algorithm. The system in this paper has been tested in actual scenarios, and the results show that the system design meets the expected requirements of the sprinters.

1. Introduction

Scientific and reasonable sports training [1–3] is a sports training mode based on the feedback information of functional monitoring indicators and technical monitoring indicators to regulate the intensity of sports training. At present, the main application for monitoring sports training from the perspective of technical monitoring is the sports video analysis system [4–7]. However, the motion video analysis system still has serious shortcomings, mainly due to the inability of timely feedback and complicated operations. The test data can be obtained only one or two months or probably three or four months after the image is taken. Hence, the real-time monitoring cannot be realized as the obtained data has no practical guiding value. The bottleneck of rapid feedback of kinematics research lies in the method of data collection and processing. The traditional analytical method is to manually interpret the joints of the human body. The workload is huge, which seriously affects the speed of feedback. Moreover, the manual recognition operation is boring and often affected by errors experienced during fatigue and various operations along with poor repeatability. The operation of motion video analysis system is also relatively complicated, and it requires certain basic knowledge and strict training to operate it. For busy coaches, the operability is very poor.

In order to solve the problem of slow information feedback and poor operability of the sports video analysis system, this article takes sprint as the research problem, uses computer as the tool, and adopts the literature and expert interviews into account for measurement, software engineering modeling of sports [8–10], and human body construction. Research methods such as simulation and mathematical modeling transform the video into a jitter-free

digital image and automatically recognize the joint points of the human body. Typically, this is achieved by extracting the contour line of the moving human body, dividing the movement phase, determining the length of the scale, tracking the area, determining the joint point, performing special judgment, and processing of the situation. At the end, a computer application program "automatic recognition software system for human body joint points in sprint [11, 12]" is generated. The computer automatically recognizes the human body joint points in the sprint motion image, so that the motion video analysis system can accurately and timely feed back the motion information with good operability.

The method of using motion recognition technology to analyze the technical actions of sprinters during the exercise to improve the quality of training has gradually attracted people's attention. Through the recognition of exercise videos during the training process, people's motion status can be grasped, and computer analysis and recognition are used at the same time. The related parameters which are obtained reflect more intuitively the degree of standardization of the athletes' training movements and help coaches and athletes to analyze technical movements and find problems, thereby improving the quality of athletes' training.

The system designed in this article adopts a client/server design architecture. The client data acquisition module acquires and displays real-time video and transmits it to the server synchronously. After the server receives the data, it performs action recognition and feeds back the recognition result. The client and server use multithreading technology for data synchronization. The main contributions of this paper are as follows:

(1) Aiming at the shortcomings of traditional dual-stream convolutional neural networks in processing long-term video information, the time-segmented dual-stream network based on sparse sampling used in this paper can better express the characteristics of long-term motion. First, the continuous video frame data is divided into multiple segments, and a short sequence of data containing user actions is formed by randomly sampling each segment of the video frame sequence, which is then applied to the dual-stream network for feature extraction.

(2) This paper uses the Lucas–Kanade algorithm to extract the optical flow image because it contains the movement and time information of the target, which can effectively represent the movement of the pixels in different areas of the continuous frame image.

(3) This paper proposes a variety of data enhancement methods and network pretraining strategies to alleviate the risk of overfitting in the network training process.

(4) Analyzing the feature fusion methods of multiple dual-stream networks, network fusion at the convolutional layer is adopted and a three-dimensional convolution and pooling operation is used to perform feature aggregation operations, so that the network can express the spatiotemporal characteristics of actions more efficiently. Hence, it ensures higher recognition accuracy.

The rest of the paper is organized as follows. In Section 2, the background information is provided. In Section 3, the research methodology of our proposed work is explained. In this section, first, we discuss the system design followed by video action recognition. In Section 4, we provide comprehensive experimental results. Finally, we conclude the paper with future research directions in Section 5.

2. Background

In recent years, in the field of motion recognition, commercial institutions and scientific research institutes have achieved extremely important results. According to the data acquisition method for classification, the commonly used action recognition methods can be divided into two types based on wearable devices and vision. In sports such as table tennis, since it is a ball game dominated by arm movements, long-term exercise monitoring and analysis using wearable devices will not be conducive to the training effect of athletes. Therefore, the motion recognition method based on machine vision [9] is more suitable for this application' system development.

One of the important sources of human perception about the external environment is visual information. Human action recognition involves many fields such as machine vision, feature selection, and pattern recognition. It is a challenging advanced processing method for motion visual analysis [10]. In recent years, video-based action recognition technology has important research significance both in scientific research and in practical applications. Despite the efforts of researchers worldwide, though the use of machine learning to model and analyze human behavior has made great progress, they are also aware at the same time that the development of behavior recognition technology is still arduous and there are many problems that need to be solved urgently, which mainly include the following:

(1) The influence of the background factors of video environment: It is often difficult to avoid having a more complicated background in a video. The cluttered background factors will have varying degrees of influence on the subject of the action. Therefore, it is more difficult to identify and analyze the action in this case. In addition, factors such as changes in lighting in the video, whether there is occlusion, and the deviation of the viewing angle will also affect the feature performance of behaviors to varying degrees. The feature extraction and analysis of behaviors will become more complicated, resulting in the final recognition result getting difficult to achieve the desired accuracy.

(2) Differences in data within and between classes: Different subjects are doing the same behavior, and there are still certain differences in posture and scale. Therefore, for more complex actions, the data difference within the class makes the action recognition more difficult. In order to effectively improve the effect of behavioral action recognition, it is necessary to fully consider the impact of data changes within and between classes.

(3) Difference between the video action database and the real video data: At present, in order to facilitate effective training and effect verification of various research methods, most of the research is carried out based on some public video action databases. However, compared with various types of video data collected in real life, the video size, the quality, and other aspects are different, and there is a lack of rich changes.

In recent years, research community has poured a lot of enthusiasm for exploration around the abovementioned issues. With the rapid development of machine vision technology, the recognition and analysis of human actions has moved from a pioneering method of artificial representation to a research field based on deep learning methods. It has been able to learn from millions of videos and is applicable to almost advanced solutions for all daily activities. Looking at the research and development of video behavior and action recognition algorithms [11] in recent years, it can be divided into two categories according to the nature of the extracted behavior and action features, i.e., learning methods based on shallow features and methods based on deep learning.

In addition, because the convolutional neural network [13–16] only has a good expression of the two-dimensional features of the image, it is difficult to meet the extraction of the timing information in the video action. It can effectively combine the features of the previous moment to ensure that the network is able to understand the timing information. Since the video behavior can be regarded as a set of continuous and related image sequences, a dual-stream network model framework of CNN [17–19] combined with LSTM is produced. The main objective is to use the convolutional neural network to extract the spatial characteristics of the video frame image, to capture the timing information between actions through the RNN network, and to combine the temporal and spatial information [12] to recognize the video actions. In addition, the movement of the human body can be described by the movement of the skeleton joint points. Hence, a dual-stream RNN is used for spatial position and time dynamic characteristics of the human skeleton joint points for modeling. The RNN-based method can directly pass video frames as input to the network to realize an end-to-end action recognition.

3. Methodology

In this section, first, we discuss our system design in Section 3.1 followed by video action recognition of the athlete (sprinter in this case) in Section 3.2. Finally, we discuss the network model of our action recognition for the sprinter in Section 3.3.

3.1. System Design. Our system design is based on the client–server (C/S) architecture. The client and server are connected through a local area network, and the socket is used to realize the data communication between the front and back ends. The system assigns the data calculation and processing to the algorithm server to complete, and the client is mainly used as the carrier of display and control. This design method reduces the overhead of the client's storage and computing capabilities and effectively improves the real-time performance of the system. In addition, the design concept of multiclient sharing algorithm server is helpful for the expansion of system cluster design. The overall structure of the system is shown in Figure 1.

In this figure, the client program is mainly responsible for the display and collection of action video data. The real-time video stream is captured by the video data acquisition module (as shown in Figure 2). The data transceiver module transmits real-time video data to the server and receives the results of the data recognition processing on the server side. The display module is responsible for displaying the athletes' real-time training actions, videos, and corresponding recognition results. The server-side program is mainly responsible for recognizing the video data of the Ping-Pong ball receiving and serving action and synchronizing the recognition results. The data transceiver module on the server side receives the collected video data and synchronizes the results to the client. The action recognition module is responsible for feature extraction and action recognition of the video data. At the same time, the display module on the server side synchronizes the working status of the server in real time.

The detailed workflow of the system is shown in Figure 3. A thread is opened through the system client to monitor user control instructions and parse them. When receiving the instruction to start training, call the web camera to capture a real-time video stream containing the act of receiving and serving the ball. The client's data transceiver module sends the synchronization instructions and data to the server, notifies it to receive the video data, and calls the identification module for processing and identification. At the same time, the client program will also monitor and display the training video captured by the camera in real time. During user training, the client uses this thread to receive user instructions. If the thread receives an instruction to stop training before the end of the training, the client will stop the acquisition of the video stream and synchronize the message to the server. After the data transceiver module of the system server receives the video data transmitted by the client, it calls the algorithm program of the action recognition module to process the data and finally feeds back the recognition result to the client. At the same time, the server-side display interface will monitor the running status of the server in real time. The client data transceiver module will always monitor the server port and wait to receive the recognition result feedback by the server, call the training pattern in the database for comparison with the recognition

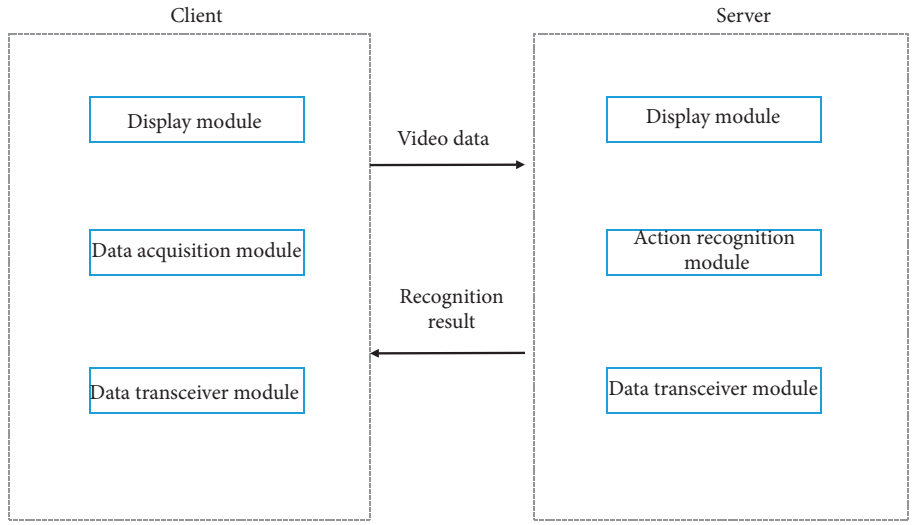

Figure 1: The overall structure of the system.

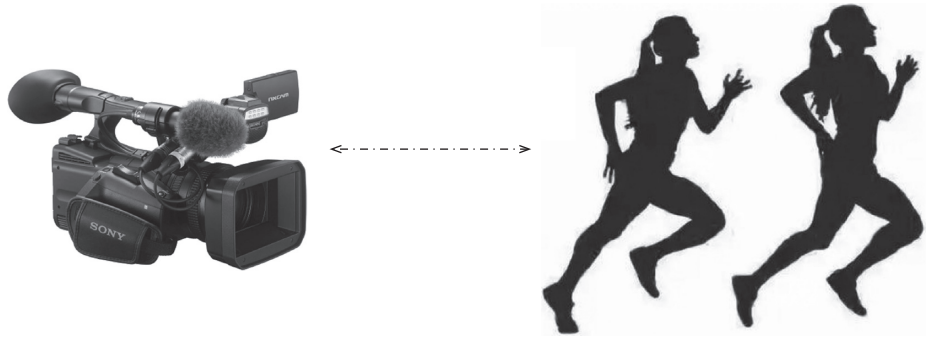

Figure 2: Real-time sprint video data collection.

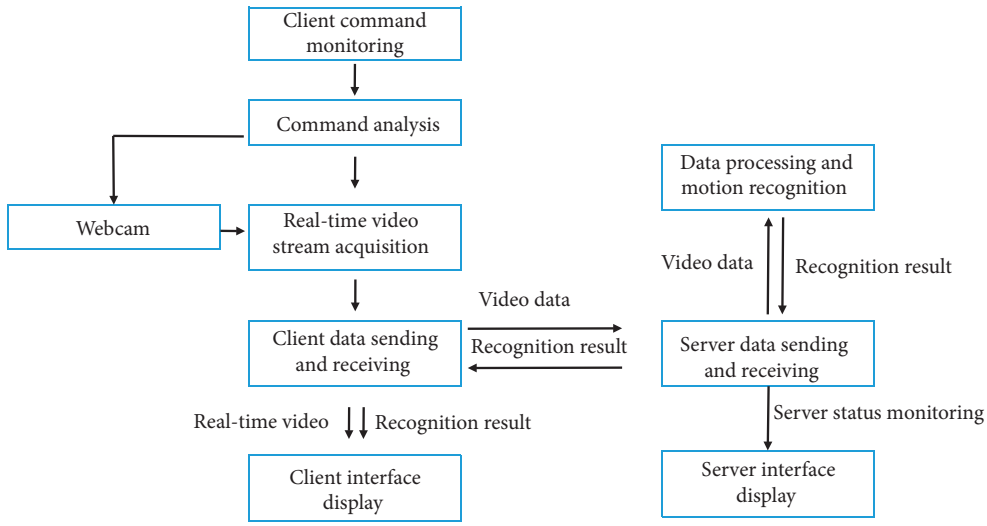

Figure 3: Detailed workflow of the system.

result, and display the completion of the training plan in real time on the interface, and the result will be displayed. It is stored in the database and used as a reference basis for coaches to guide and make training plans in the future.

3.2. Video Action Recognition. In this section, first, we discuss the dual-stream convolutional neural network (CNN) followed by optical flow feature extraction of sprinter's action video data.

3.2.1. Dual-Stream Convolutional Neural Network. In recent years, most of the research work has been inspired by the dual-stream convolutional neural network, which combines the spatiotemporal information extracted from the RGB image and the optical flow image of the video and extracts two types of features through two separate convolutional neural networks. We need to identify and produce the final prediction result. Video information contains two parts: space information and time information. Compared with static images, the time sequence component of video provides additional motion information that represents time for action recognition. The spatial information in the video is the position on each frame of the image, which represents the spatial information such as the target and the scene in the video; the time information refers to the change between video frames and carries the target movement information between consecutive video frames, including the movement of the camera or movement information of the target object, etc. The idea of realizing video action recognition mainly includes two categories, namely, the method of extracting video spatiotemporal features for video recognition and the method of retraining by using human skeleton node information as network input data. In this paper, the system uses ordinary camera equipment to collect motion video for recognition, so the dual-stream convolutional neural network is mainly used to extract video spatiotemporal features for action recognition and analysis.

As shown in Figure 4, the dual-stream convolutional neural network is composed of a convolutional network that expresses two-dimensional information of spatial flow and temporal flow and is used to process the spatiotemporal information of video data. This dual-stream network design architecture comes from biological vision. The spatial-stream network takes a single-frame RGB image of the video as input. The decoupling of the spatial stream and the temporal stream network also enables the use of image data on large image data sets. The pretraining of the spatial-stream network is used to recognize the surface features related to the action and realize the feature description in the spatial domain of the video. The spatial flow network is the same as the common static image recognition network, while the time flow network is to input multiframe stacked optical flow images into the network for training. It is used to learn the time features contained in the action, such as the movement and deformation of the target. For feature description of the video action in the time domain, we use the method of multitask training, which provides two softmax output layers for fusion. The output of the softmax layer is the probability of identifying the action category. Providing two softmax outputs is equivalent to the process of regularization. There are two main fusion methods: averaging and retraining an SVM classifier using the softmax layer for recognition. In short, the processing method of decoupling spatiotemporal features of dual-stream convolutional neural network better describes the movement information of sprinters.

The dual-stream convolutional neural network actually draws on the dual-stream pathway of information processing in the human brain's visual system, which can effectively capture the local motion information of the target in the video and improve the single-stream convolutional neural network's ability to solve the action recognition problem. However, there are also some shortcomings. First, because the prediction of the action video is obtained by the average prediction of the sampled video clips, the medium- and long-term time information is still lacking in the learned features. Secondly, since the training data samples are obtained by randomly sampling video clips, there may be a problem of incorrect assignment of labels for each category of data. Finally, the use of dual-stream convolutional neural networks requires the optical flow image to be precalculated and saved as the input of one of the networks. The network training requires separate training for single-frame RGB images and multiframe stacked optical flow images, so the network is difficult to achieve an end-to-end training.

3.2.2. Optical Flow Feature Extraction of Sprinter's Action Video Data. Optical flow represents the speed vector of the object in the video, including the instantaneous motion direction and speed of the pixel information. It can be used to represent the motion information of the sprinter in the video. The optical flow feature combines the static information and motion information of the image and is a good feature performance for describing the behavior of sprinters. This section will describe the optical flow feature extraction algorithm in detail by introducing the design ideas of the client real-time video data acquisition module. After the data is synchronized to the server through network communication, the optical flow image is extracted from it for sprinter action feature extraction and data processing process. Data preprocessing performed by data enhancement technology can effectively avoid the risk of overfitting during network training due to the small action dataset.

The essence of object movement is the relative positional movement between the object and the scene. When the observer observes the moving object, the scene of the moving object will form a continuously changing image on the retina of the eye, which seems to flow through the retina of the eye; hence, it is called optical flow. Optical flow expresses the instantaneous velocity field of image pixels, including the position, instantaneous velocity, direction, and other pieces of information of a certain pixel of the moving target in the video. The optical flow method is used to extract the motion information of the foreground target in the video, and the motion foreground can be monitored independently without knowing any information of the scene in advance. Optical flow is calculated mainly to determine the change of the same pixel in two adjacent frames by estimating the time domain changes of pixels in different areas of the two frames of images and the correlation between pixels. Next, the vector of the moving target in a single image field is obtained to realize the motion estimation of objects in the image.

The two most famous methods for calculating optical flow are the Hom–Schunck algorithm and the Lucas–Kanade algorithm. The Hom–Schunck algorithm is based on the fact that the gray level of the object image

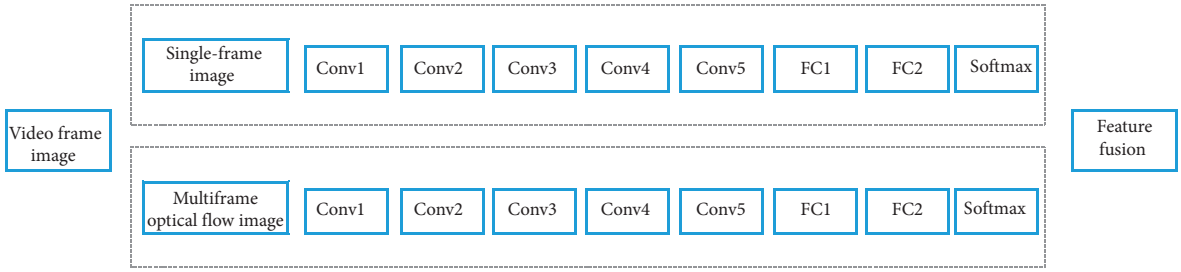

Figure 4: Dual-stream convolutional neural network model.

remains unchanged within a short time interval, assuming that the velocity vector field changes slowly in a given neighborhood, and the global smoothness constraint of the optical flow field is proposed. However, due to the smoothness assumption that the algorithm is based on, there may be large errors in the vector estimation of the optical flow in the edge area of the image or in the presence of occluded areas. The Lucas–Kanade algorithm uses local smoothness constraints, i.e., by assuming that all pixels in a small neighborhood have similar motions, and then realizes the estimation of optical flow. Compared with the previous algorithm, the Lucas–Kanade algorithm is simpler to implement and has lower computational complexity. Therefore, the system uses the Lucas–Kanade algorithm for the calculation and estimation of optical flow. The realization of this algorithm first needs to satisfy several assumptions:

(1) The outside has a constant intensity of light to avoid the intensity of the outside light from causing changes in the pixel value of the same point in the image.

(2) The time between adjacent frames of images is short enough so that the pixel difference between frames can be ignored when considering motion changes.

(3) The image pixels of the moving target perform similar movements in the same neighborhood.

Assuming that the brightness of the pixel at the point (x, y) at time$t$ is $I(x, y, t)$, the pixel point moves to the position $(x + \Delta x, y + \Delta y)$ at time $t + \Delta t$. The brightness at time t is $I(x + \Delta x, y + \Delta y, t + \Delta t)$. Based on the above assumption, the brightness of the pixel at the same point is constant; hence,

$$I(x, y, t) = I(x + \mathrm{d}x, y + \mathrm{d}y, t + \mathrm{d}t). \tag{1}$$

According to the assumption that the movement time of the target object is very short, the above equation can be Taylor-expanded to obtain the following equation:

$$\frac{\partial I}{\partial x}\Delta x + \frac{\partial I}{\partial y}\Delta y + \frac{\partial I}{\partial t}\Delta t + \Delta = 0. \tag{2}$$

Ignoring the higher-order term Δ and deriving the above formula to Δt, the constraint formula for optical flow can be obtained as follows:

$$I_x\mu + I_y v + I_t = 0, \tag{3}$$

where I_x, I_y, and I_t can be calculated directly from the image, and (μ, v) is the optical flow of $I(x, y, t)$, which is an unknown quantity, and the optical flow value cannot be obtained only by the optical flow equation. Therefore, the selected Lucas–Kanade algorithm will solve the equation by attaching various optical flow constraints. This method is based on local smoothness constraints; that is, it is assumed that the pixels of the image have small displacements between adjacent frames and maintain approximate motion in the neighborhood. Then, the basic optical flow equation of the pixels in the neighborhood can be solved by the least square method.

According to the assumption of the Lucas–Kanade algorithm, all pixels in a small local area have similar motions. Based on the basic optical flow equation, an overdetermined equation can be obtained as follows:

$$I_x(X_i)\mu + I_y(X_i)v + I_t(X_i) = 0. \tag{4}$$

The optical flow estimation error is defined as

$$E = \sum_{X_i \in \theta} \left(I_x(X_i)\mu + I_y(X_i)v + I_t(X_i)\right)^2. \tag{5}$$

The optical flow calculation equation can be obtained by fitting by the least square method:

$$A^T A\vec{v} = A^T(-b), \tag{6}$$

where A is the coefficient matrix and $b = -(I_t(X_1), \ldots, I_t(X_n))^T$ is the constant term. When $A^T A$ is a nonsingular matrix, the solution of the above equation is

$$\begin{bmatrix} \mu \\ v \end{bmatrix} = \begin{bmatrix} \sum_i I_x(X_i)^2 & \sum_i I_x(X_i)I_y(X_i) \\ \sum_i I_x(X_i)I_y(X_i) & \sum_i I_x(X_i)^2 \end{bmatrix}^{-1} \begin{bmatrix} -\sum_i I_x(X_i)I_t(X_i) \\ -\sum_i I_x(X_i)I_t(X_i) \end{bmatrix}. \tag{7}$$

From this, the value of μ,v can be obtained.

3.3. Action Recognition Network Model. This paper uses a time-segmented convolutional neural network based on a sparse sampling strategy. Its structure is shown in Figure 5. The time-segmentation convolutional neural network used is to segment the entire video and sparsely sample short segments as the network input and extract the temporal characteristics of the optical flow image and the spatial characteristics of the RGB image to perform action recognition tasks. The time segmentation convolutional neural network first divides a video containing an action into several equal parts and then randomly extracts a short sequence from it that can effectively express the motion information in the entire video. For each sampled segment, feature extraction is performed through a dual-stream convolutional neural network. The temporal stream network captures the temporal structure information of the video and the spatial appearance information of the image captured by the spatial-stream network. Next, a corresponding dual-stream network prediction is generated for each short segment. Finally, an aggregation function is used to fuse the characteristics of time flow and spatial flow network as the recognition result of the entire video. This method can effectively extract the long-term information of the entire video, which is more accurate and effective than the recognition method of densely sampling the entire video segment; also, it no longer increases the computation cost. In the learning process, the loss value of the entire video prediction is optimized through the iterative update parameter calculation to realize the end-to-end network training process.

For a given action video frame data, first, divide it into N video frame sequences of equal length $\{S_1, S_2, \ldots, S_N\}$, and then randomly sample a short-term video sequence from each part S_N. The network models the short-term sequences $(T_1, T_2, \ldots, T_N)$ extracted from each part as the input number, corresponding to the equation below:

$$T(T_1, T_2, \ldots, T_N) = H(G(F(T_1, W), F(T_2, W), \ldots, F(T_N, W))). \tag{8}$$

4. Experimental Setup and Results

In this section, we discuss the experimental environment followed by the dataset that is used in this research. Moreover, we also talk about the training process of the model and the preliminary simulation we have obtained so far.

4.1. Experimental Environment. Since the experiment in this article needs to train a deep neural network, hence the scale is large, the structure is more complex, and the calculation scale is massive. The neural network training process needs to use GPU to accelerate the calculation. The experimental environment configuration is shown in Table 1.

In our experimental work, the data set is a 100-meter short film project, with a total of 5000 videos, each video action lasts about 2–10 seconds, the resolution is $320 * 240$, and the frame rate is 30 frames per second.

4.2. Training. The learning of network parameters is achieved by a small batch of gradient descent algorithm, with the batch size set to 256 and the momentum set to 0.9. Gradient descent in small batches can be accelerated by calculation of matrices and vectors, and the variance of updated parameters can be reduced to obtain more stable convergence. Using a batch, each time can reduce the number of iterations of convergence and at the same time make the result of convergence closer to the effect of gradient descent. For traditional gradient descent algorithms, if the actual objective function plane is a partially concave surface, then a negative gradient will make it point to a steeper position. This situation near the local optimal value of the objective function will cause the convergence rate to slow. At this time, it is necessary to give the gradient a momentum, so that it can jump out of the local optimum and continue to optimize in the direction of gradient descent, so that the network model can more easily converge to the global optimum.

For the time segmentation dual-stream network used in this system, set the initial weight of the spatial stream convolutional neural network to 1 and the initial weight of the time stream convolutional network to 1.5. The learning rate of the network training is set smaller: set the initial value of the spatial flow convolutional neural network to 0.01 and adjust it to one-tenth every 2000 iterations; set the initial value of the time flow convolutional neural network to 0.005; adjust it to one-tenth after 12000 and 18000 iterations of network parameters. In addition, the total time-consuming data training is as follows: the spatial streaming network requires about 2 hours and the time streaming network requires about 11 hours.

4.3. Experimental Results. The value of spatial flow convolutional neural network is set to 0.01 and adjusted it to one-tenth after 2000 iterations. Next, we set the initial value of the time flow convolutional neural network to 0.005 and adjust it to one-tenth after 12000 and 18000 iterations of network parameters. In addition, the total time-consuming data training is as follows: the spatial streaming network requires about 2 hours and the time streaming network requires about 11 hours.

In Figure 6 and Table 2, the accuracy for action sprint is computed. It can be seen from these results that separate spatial stream and time stream convolutional neural networks are far less effective in recognition of actions than the dual-stream fusion network model, and the recognition accuracy is about 5% to 19% lower. For different training methods, due to the small data set of the action category, the dual-stream network trained from scratch has the problem of overfitting. Hence, the performance is the worst, and the pretraining of the spatial-stream network and the cross mode of the time-stream network is time consuming. The dual-stream convolutional neural network initialized by pretraining has a better recognition effect, and the recognition rate can reach 94.3%, which also means that this pretraining method can effectively reduce the risk of overfitting.

Figures 7 and 8 show the recognition results on different frames and the impact of different input resolutions on model performance.

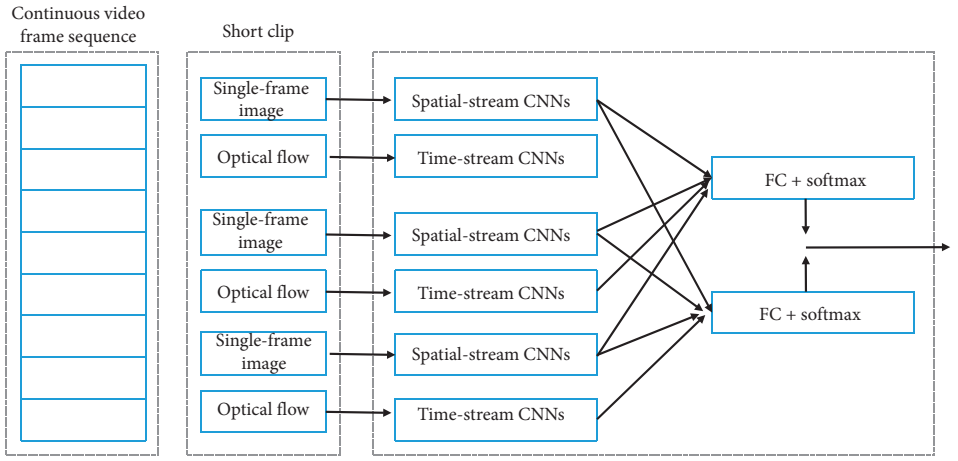

Figure 5: Action recognition network model.

Table 1: Experimental hardware platform and software simulation environment.

CPU	Intel® Core™ i5-4200M CPU @ 2.50 GHz
RAM	16.00 GB
Operating system	Centos 8.0
Development environment	PyCharm 2020.2
Programming language	Python 3.6.5

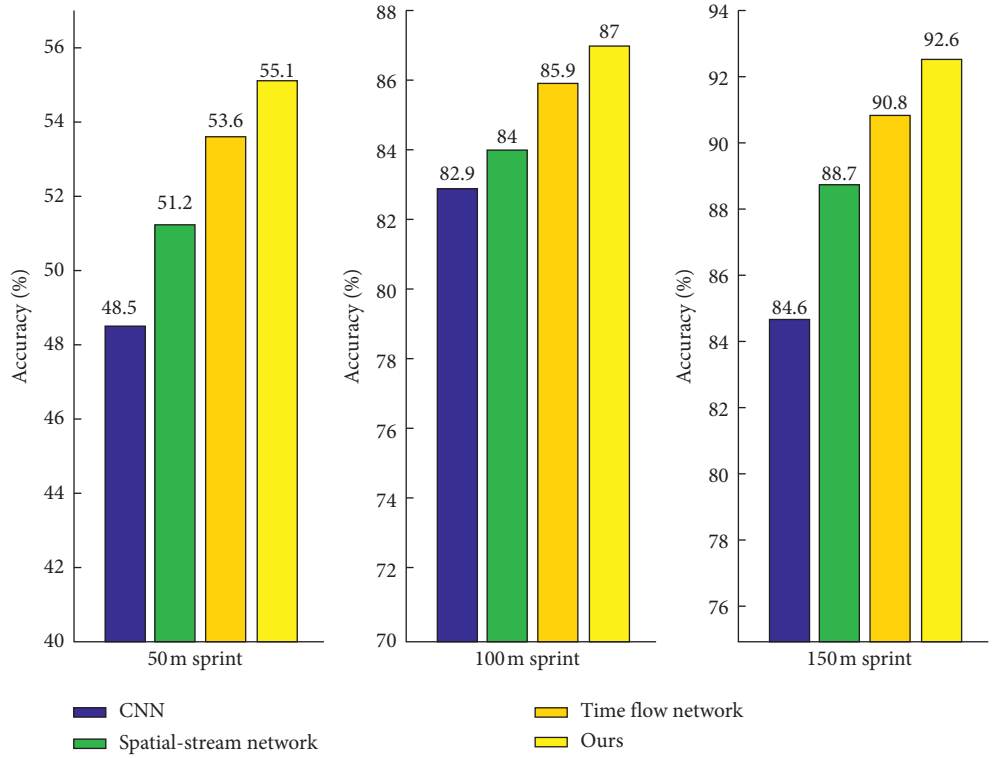

Figure 6: Action recognition network model.

Table 2: Experimental results.

Type	Spatial-stream network (%)	Time flow network (%)	Dual stream (%)
Classic	72.6	73.5	85.6
Spatial flow	75.2	81.6	88.7
Cross mode	77.1	82.6	92.6

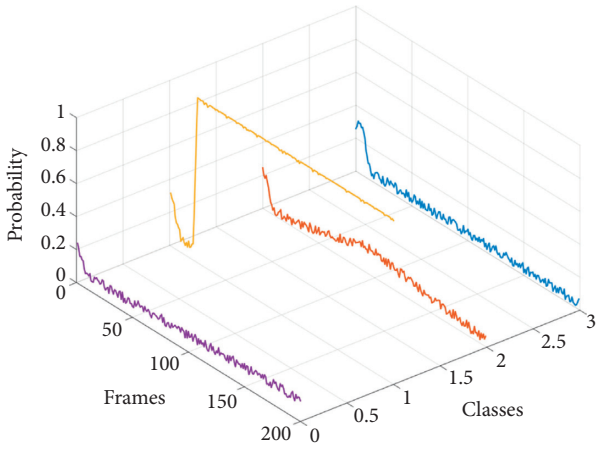

Figure 7: Recognition results on different frames.

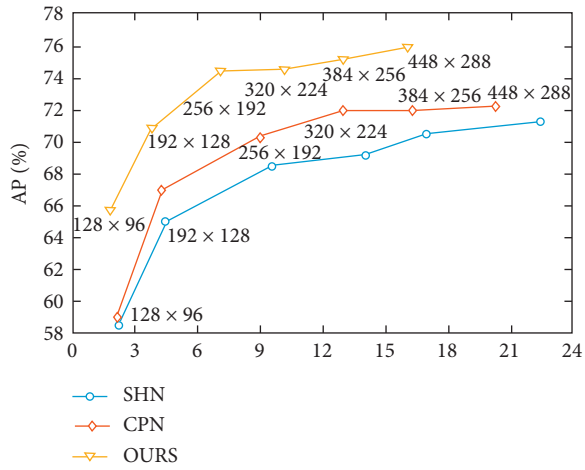

Figure 8: The impact of different input resolutions on model performance.

5. Conclusion

This paper takes sprint as the research object and constructs the image of sprinter's action recognition based on machine learning. Then, in view of the shortcomings of the traditional dual-stream convolutional neural network for processing long-term video information, the time-segmented dual-stream network based on sparse sampling is used that can better express the characteristics of long-term motion. First, the continuous video frame data is divided into multiple segments, and a short sequence of data containing user actions is formed by randomly sampling each segment of the video frame sequence, and then it is applied to the dual-stream network for feature extraction. The optical flow image extraction involved in the dual-stream network is implemented using the Lucas–Kanade algorithm. Optical flow contains the mobility information of the target, which can effectively represent the movement of pixels in different areas of the continuous frame of image. Due to the small amount of action video data (test data), this paper adopts numerous data enhancement methods and network pre-training strategies during data processing to alleviate the risk of overfitting in the network training process. The system in this paper has been tested in actual scenarios, and the results show that the system design meets the expected requirements.

Data Availability

The data used to support the findings of this study are included within the article.

Conflicts of Interest

All the authors declare no conflicts of interest.

Acknowledgments

This work was supported by Jiangxi University of Science and Technology Philosophy and Social Science Prosperity Plan Cultivation Project "Research on the Construction of Mountain Sports Town in Jiangxi Province" (Grant no. FZ18-YB-18).

References

[1] T. Haugen, S. Seiler, Ø. Sandbakk, and E. Tønnessen, "The training and development of elite sprint performance: an integration of scientific and best practice literature," *Sports Medicine-Open*, vol. 5, no. 1, pp. 1–16, 2019.

[2] H. Liang, "Evaluation of fitness state of sports training based on self-organizing neural network," *Neural Computing and Applications*, vol. 33, pp. 1–13, 2021.

[3] C. M. Fairman, M. C. Zourdos, E. R. Helms, and B. C. Focht, "A scientific rationale to improve resistance training prescription in exercise oncology," *Sports Medicine*, vol. 47, no. 8, pp. 1457–1465, 2017.

[4] A. Lopatiev, O. Ivashchenko, O. Khudoliy, Y. Pjanylo, S. Chernenko, and T. Yermakova, "Systemic approach and mathematical modeling in physical education and sports," 2017.

[5] S. Subhash, T. Obafemi-Ajayi, D. Goodman, D. Wunsch II, and G. R. Olbricht, "Predictive modeling of sports-related concussions using clinical assessment metrics," in *Proceedings of the 2020 IEEE Symposium Series on Computational Intelligence (SSCI)*, pp. 513–520, IEEE, Canberra, Australia, December 2020.

[6] A. Laredo, L. P. Concepcion, and N. Mamani-Macedo, "A proposal for modeling of the management of talent recruitment and training in Peruvian sports centers," in *Proceedings*

of the 5th Brazilian Technology Symposium, pp. 505–513, Lima, Peru, November 2021.

[7] A. L. Clouthier, G. B. Ross, and R. B. Graham, "Sensor data required for automatic recognition of athletic tasks using deep neural networks," *Frontiers in Bioengineering and Biotechnology*, vol. 7, p. 473, 2020.

[8] K. Choroś, "Highlights extraction in sports videos based on automatic posture and gesture recognition," in *Proceedings of the Asian Conference on Intelligent Information and Database Systems*, pp. 619–628, Kanazawa, Japan, April 2017.

[9] G. Thomas, R. Gade, T. B. Moeslund, P. Carr, and A. Hilton, "Computer vision for sports: current applications and research topics," *Computer Vision and Image Understanding*, vol. 159, pp. 3–18, 2017.

[10] A. Filgueiras, E. F. Quintas Conde, and C. R. Hall, "The neural basis of kinesthetic and visual imagery in sports: an ALE meta–analysis," *Brain Imaging and Behavior*, vol. 12, no. 5, pp. 1513–1523, 2018.

[11] Y. Kong and Y. Fu, "Human action recognition and prediction: a survey," 2018, http://arxiv.org/abs/06.11230.

[12] P. E. Martin, J. Benois-Pineau, R. Péteri, and J. Morlier, "Sport action recognition with siamese spatio-temporal cnns: application to table tennis," in *Proceedings of the 2018 International Conference on Content-Based Multimedia Indexing (CBMI)*, pp. 1–6, IEEE, La Rochelle, France, September 2018.

[13] H. C. Shih, "A survey of content-aware video analysis for sports," *IEEE Transactions on Circuits and Systems for Video Technology*, vol. 28, no. 5, pp. 1212–1231, 2017.

[14] L. I. U. Ziyu, "Application of college basketball training teaching based on sports video analysis under Network Multimedia," *Solid State Technology*, vol. 64, no. 1, pp. 170–181, 2021.

[15] C. Ning, "Design and research of motion video image analysis system in sports training," *Multimedia Tools and Applications*, pp. 1–19, 2019, In Press.

[16] Y. Li, "Research on sports video image analysis based on the fuzzy clustering algorithm," *Wireless Communications and Mobile Computing*, vol. 2021, Article ID 6630130, , 2021.

[17] W. Cai, B. Liu, Z. Wei et al., "TARDB-Net: triple-attention guided residual dense and BiLSTM networks for hyperspectral image classification," *Multimedia Tools and Applications*, vol. 80, pp. 11291–11312, 2021.

[18] X. Zhang, Y. Yang, Z. Li, X. Ning, Y. Qin, and W. Cai, "An improved encoder-decoder network based on strip pool method applied to segmentation of farmland vacancy field," *Entropy*, vol. 23, no. 4, p. 435, 2021.

[19] X. Ning, X. Wang, S. Xu et al., "A review of research on co-training," *Concurrency and Computation: Practice and Experience*, Article ID e6276, 2021.

Hindawi
Mobile Information Systems
Volume 2021, Article ID 5520079, 9 pages
https://doi.org/10.1155/2021/5520079

Research Article

A Classification Method of Tourism English Talents Based on Feature Mining and Information Fusion Technology

Xin Wei [1,2]

[1]*Graduate School, Nueva Ecija University of Science and Technology, Cabanatuan, Nueva Ecija 3100, Philippines*
[2]*English Language Teaching Unit, Lu'an Vocational and Technical College, Lu'an 237100, China*

Correspondence should be addressed to Xin Wei; xin615290@lvtc.edu.cn

Received 26 February 2021; Revised 10 April 2021; Accepted 10 May 2021; Published 19 May 2021

Academic Editor: Muhammad Usman

Copyright © 2021 Xin Wei. This is an open access article distributed under the Creative Commons Attribution License, which permits unrestricted use, distribution, and reproduction in any medium, provided the original work is properly cited.

With the rapid development of the Internet, text data has become one of the major formats of big data tourism and improves the quality and promotes the optimization and upgradation of tourism English talents. This paper proposes a model of tourism English talent resources based on data mining techniques using a big data framework. The characteristic distribution structure model is built to identify and blend the characteristics of tourism English talent resources. Connection feature mining and information fusion are combined to share data and schedule resources during the talent training process. Initially, the proposed research work uses a cloud storage system for developing intercultural communicative competence of tourism English talents. Next, the optimal scheduling design of tourism English talent training resource's big data is carried out. Finally, the fuzzy clustering method deals with the adaptive clustering of tourism English talent resource distribution big data. The simulation findings show that the proposed method has high precision and big data computation efficiency. Moreover, it can successfully mentor the development of a new framework of tourism English talent training.

1. Introduction

The training goal of tourism English talents is located in the technical application of the tourism industry and the compound management talents to cultivate the middle level of the tour guide industry, the hotel industry and the middle level, and the management talents above the middle level. Therefore, the training target of the Higher Vocational Tourism English talents is the technical nature of the talent type, the professionalism of knowledge ability, and the graduate's direction [1]. At present, a lot of travel agencies and hotel enterprises urgently need strong English listening, speaking, reading, writing, translation comprehensive ability, familiarity with the tourism industry-related policies, policies, good tourism, hotel management, and other professional knowledge and skills, with cross-cultural interdisciplinary talents. Tourism English majors must be closely integrated into the market because the professional orientation of the students is suitable for the needs of the current society; it depends highly on whether the orientation of the majors and the arrangement of the courses are reasonable and whether they have the current travel agency and the knowledge structure required by the hotel. Direct trade relations are established with many countries and regions. The number of the top five hundred multinational companies in the world has been increasing. Also, the number of multinational corporations and the amount of outbound tourism in the world ranks are increasing [2]. Therefore, there is a strong ability to express English, the managers who are familiar with the tourism knowledge and tour guide business, the tour guides, and the market demand. To improve tourism English, the quality of talents needs to optimize the training mode of tourism English talents and promote the improvement of the quality of tourism English talents [3].

Given the strong practical characteristics of a tourism English major, the most effective way to train its talents can only be the combination of production and learning. Therefore, in addition to strengthening the construction of training rooms, internships, outside schools, and training

bases, big data scheduling and integration of tourism English talent resources should also be carried out according to the requirements of the quality, knowledge, and ability of social posts. The data mining methods for tourism English talents mainly include blind convolution algorithm, feature extraction method, time-frequency analysis method, and statistical analysis method. These methods cannot eliminate the convolution effect of the mining channel to singular features. There are several data mining tools that companies can use to translate raw data into actionable insights. These include statistics, artificial intelligence, hidden Markov models, metalearning, genetic algorithm, machine learning, and decision tree. It affects the accuracy of big data features mining in the distribution of big tourism English talent resources. In [4], a new information mining and scheduling algorithm for tourism English talent resources based on differential cumulate function feature mining is proposed. To improve the ability of information collection and feature analysis of tourism English talent resources, the distributed resources information of tourism English talent resources under a big data environment is fused and processed. However, the algorithm has high computational complexity and a big implementation cost [5–7].

In this research work, an effective and intelligent computational model is proposed. In view of the above problems, a new model of tourism English talents training is proposed based on big data, and it constructs a big data mining model of tourism English talents. Data mining is widely used in the field of artificial intelligence (AI), marketing, government intelligence (GI), services, and advertising. There are some other industries like crime agencies, retail healthcare, e-commerce, telecom, biological data analysis, and information retrieval like communication systems. Data mining is used to examine or explore the data using queries. These queries can be fired on the data warehouse. In the cloud storage system, the optimal scheduling design of tourism English talent training resource big data is carried out, and the fuzzy clustering method is used to deal with the adaptive clustering of tourism English talent resource distribution big data. This research work adopts the attribute distribution structure model to classify and fuse the features of tourism English talent resources, and it combines the methods of association feature mining and information fusion to share data and schedule resources in the process of talent training. Finally, the performance test is carried out through the simulation experiment, which shows the superior performance of this method in improving the big data analysis ability of tourism English talents training.

The rest of the paper is organized as follows: tourism English talent resource distribution model is explained in Section 2; big data feature extraction is discussed in Section 3, and, in Section 4, experimental results and discussion are discussed. Finally, we demonstrate a conclusion and future work in Section 5.

2. Tourism English Talent Resource Distribution Model

In this section, we elaborate the new cross-cultural communicative competence model that is proposed in the book titled "Intercultural Communication in Context" and the elements of cross-cultural communicative competence of tourism English talents.

2.1. The Formation of Cross-Cultural Communication Ability Elements. The formation of cross-cultural communication ability elements includes four elements, that is, knowledge factors, emotional factors, mental activity characteristics, and situational characteristics. Cross-cultural communication elements of tourism English talents are shown in Figure 1. The knowledge in the cross-cultural communication skills mentioned in the figure refers to the degree of understanding of the target's culture in the party of communication, and the cross-cultural communication ability is directly proportional to its understanding. Among them, knowledge factors include cultural values, beliefs and behaviors, verbal and nonverbal scripts, simplified and rigid cognition, and ethnocentrism. These factors can have a positive or negative impact on the communicators. Emotional factors refer to the attitudes adopted by the communicators in dealing with communicative objects from different cultural groups, that is, approaching or alienating. In the intercultural communication activities, inevitably there will be fear or anxiety. Therefore, if they are willing to communicate, the motivation of their communication is a more important emotional factor in cross-cultural communication. The ability to deal with stress and tolerance is positively related to intercultural communicative competence, and knowledge and affective factors in cross-cultural communicative competences interact with and support each other. The more knowledge, the less anxiety, and the more cross-cultural, the more arguments. The stronger the communicative motivation is, the stronger the communicative motivation is, and the more chances of obtaining relevant experience are, the more intercultural communication knowledge becomes more and more abundant.

Similarly, mental activity factors are a comprehensive manifestation of knowledge and emotional factors, including verbal and nonverbal communication and role play. Having more opportunities to practice using the target language is an important factor to enhance their abilities, and attention should also be paid to a series of auxiliary nonlanguage symbols such as body language, spatial language, and time language of the communication partner in communication. Role play is related to context. It is the use of verbal and nonverbal symbols in the destination culture according to their role identities. Moreover, for situational characteristics, the environment has a great influence on both sides of the communication. Situational characteristics

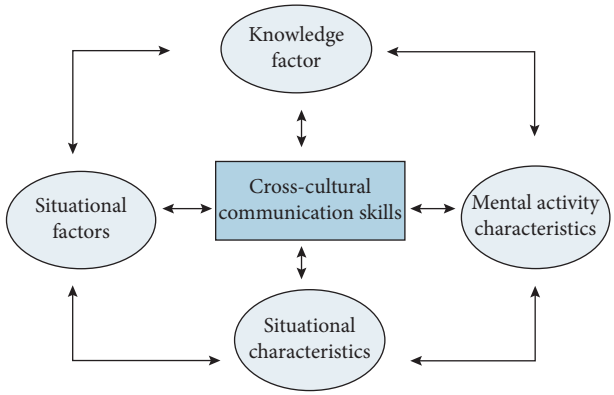

Figure 1: Cross-cultural communication elements of tourism English talents.

mean the real context of cross-cultural communication. The situational characteristics affecting their communicative competence are environmental context, prior contact, status differences, and third-party interference. Therefore, individuals have increased knowledge and experience in cross-cultural communication, and, as a result, their motivation has increased and they have actively participated in communicative activities, and vice versa, forming a learning cycle of good success.

2.2. The Elements of Cross-Cultural Communicative Competence of Tourism English Talents. The cross-cultural communicative competency elements constitute the first element of the domestic study's cross-cultural communicative competencies and are summarized into four communicative competence systems: basic communicative competence systems, emotional and relational competence systems, plot competence systems, and strategic capacity system. The elements of cross-cultural communicative competence of tourism English talents are shown in Figure 2.

From Figure 2, basic communicative competence system refers to the communicative ability that an individual needs to have in order to achieve communicative purposes, including language competence, and wants to connect with social cultural norms. These include verbal skills, nonverbal abilities, cultural abilities, interpersonal skills, and cognitive abilities, where the tourism English talent cultivation model believes that emotional competence refers to the communicator's recognition and understanding of the other party. Empathy needs to recognize the differences between individuals and cultures fully understand the self, suspend the self, eliminate the separation of oneself from the environment, conceiving for others, and finally preparing for empathy go through these six stages. Relational ability refers to the communication strategies used by the communicating parties in the process of communication. For example, the need for mutual communication between the two parties should be the basis for establishing relationships. The generation of consensus is the prerequisite for communication, and it is also related to cultural orientation and values.

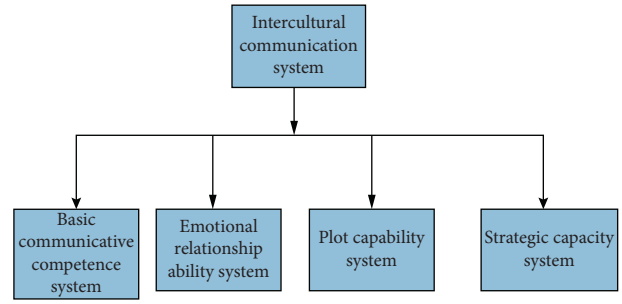

Figure 2: The elements of cross-cultural communicative competence of tourism English talents.

Similarly, the plot ability system comes to the plot competence system; it generally refers to the fixed sequence of interactions in a particular cultural environment. There are unique verbal and nonverbal rules in each plot. It proposes four aspects of ability, that is, common sense in communication, and also refers to the ability of a script communicator who directs behaviors to strive to achieve communicative purposes. The ability to follow the rules of communication in a particular context is appropriate to handle social scene responses. Moreover, strategy capability system proposed by the tourism English talent training model is different from the general communication strategy, but it is the remedial measures adopted by the communicators in the face of language barriers or verbal skills and clearly shows that strategic competence is an important part of the communicative competence.

3. Big Data Feature Extraction

In this section, we elaborate the big database model of tourism English talent resources distribution and the principles of big data mining for big-scale tourism English talent resources distribution. The feature fusion of tourism English talent resources optimized by big data fusion has good information mining capabilities.

3.1. Big Database Model of Tourism English Talent Resources Distribution. The big data characteristic information of tourism English talent resources distribution is usually expressed as a set of nonstationary broadband time series. The big-scale tourism English talent database big data resource information mining and scheduling is realized by using the method of time series detection [8]. Firstly, a big database model of tourism English talent resource distribution is constructed. In the construction of big data flow model of tourism English talent resource distribution, the task code is distributed to a number of data nodes by using distributed code execution mode, and the result is returned to the client after execution. It can effectively avoid the movement and transmission of cached data in the big database of tourism English talent resources distribution and use single computer or network computer to access the big amount of data and realize the evaluation and prediction of

tourism resources information amount. The big database of tourism English talent resources distribution uses I/O, USB, and disk and other devices to achieve efficient read-write access [9]. Thus, the access and management model of tourism English talent resources distribution database is shown in Figure 3.

According to the analysis of Figure 2, suppose that the big database data set of tourism English talent resources distribution is the number of big data sets $X = \{x_1, x_2, \ldots, x_n\}$ of tourism English talent resources distribution, and the joint distribution feature vectors in n are all N-dimensional vector X containing c big data classes of resource distribution. The clustering center of the big data class of $v_i = \{v_{i1}, v_{i2}, \ldots, v_{ip}\}$ resource distribution is big data. If the joint distribution function of nonstationary time sampling $\{x(t_1), \ldots, x(t_n)\}$ and the joint distribution function of $\{x(t_1 + \tau), \ldots, x(t_n + \tau)\}$ are autocorrelation in the big database of tourism English talent resources distribution, the big data features of tourism English talent resource distribution are expressed as follows:

$$\theta_1(k+1) = \theta_1(k) - \mu \mathrm{Re}[y(k)\varphi^*(k)]. \tag{1}$$

The spectral features of the big database of tourism English talent resources distribution are analyzed by using aliasing spectrum ambiguity function, and the function relationship between the response variable and the forecast variable $\mathrm{X} = (\mathrm{x}_1, \ldots, \mathrm{x}_n, \ldots, \mathrm{x}_{n+m})$ is determined. $\langle R_1, +, \times \rangle$ and $\langle R_2, \oplus, \otimes \rangle$ are closed loop of the two eigenvector sets. Because the big data features of tourism English talent resource distribution database are combined with probability distribution function mapping $f: R_1 \mapsto R_2$, for any $m_i \in R_1$, the big data information feature extraction equation of tourism English talent resource distribution can be obtained as follows:

$$\begin{aligned}
\dot{x} &= V \cos\theta \cos\psi_V, \\
\dot{y} &= V \sin\theta, \\
\dot{z} &= -V \cos\theta \sin\psi_V, \\
\dot{\vartheta} &= \omega_y \sin\gamma + \omega_z \cos\gamma, \\
\dot{\psi} &= \frac{(\omega_y \cos\gamma - \omega_z \sin\gamma)}{\cos\vartheta}, \\
\dot{\gamma} &= \omega_x - \tan\vartheta(\omega_y \cos\gamma - \omega_z \sin\gamma),
\end{aligned} \tag{2}$$

where x, y, and z indicate the initial frequency of big data in the big database of tourism English talent resources distribution, ψ_V indicates the big data training set of tourism English talent resources distribution, θ denotes the solution vector Q in the space of the talent resource distribution variable, ϑ is the instantaneous amplitude of the complex signal $z(t)$ of the big tourism English talent resource distribution database, and γ represents the statistical characteristics in the big tourism English talent database [10].

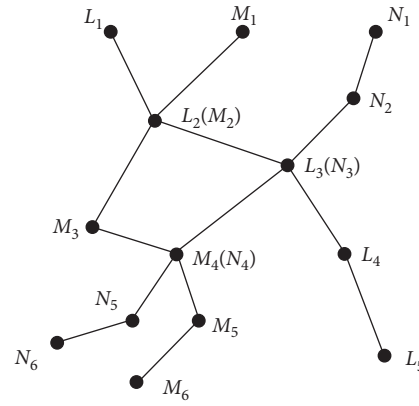

Figure 3: Distribution structure model of tourism English talent resources.

3.2. Principles of Big Data Mining. Based on constructing the distributed data structure model of tourism English talent training resources, the big data mining process is carried out and the big data distributed structure model of tourism time series algorithm provides regression algorithms that are used for optimizing and forecasting of continuous values like sales, overtime, and temperature. This algorithm can predict the trends that are based only on the original data set that is used to create a model. English talent resources distribution is designed. The computer data set under the condition of source distribution big data is fused and analyzed [11]. The schematic block diagram of big data mining for big-scale tourism English talent resources distribution is shown in Figure 4.

Fast data and resource information mining and scheduling are carried out in the big database of tourism English talent resources distribution to realize the integration of resource distribution big data [12]. Let R be the trust relation with quaternion (E_i, E_j, d, t) in the big data feature data of big-scale tourism English talent resources distribution. The information state equation of data classification attribute $A = \{A_1, A_2, \ldots, A_m\}$ and the information state equation of big data feature data integration of big-scale tourism English talent resources distribution are obtained as follows:

$$\begin{aligned}
P_i(t) &= \sum_{n=1}^{N} \frac{A}{r} e^{-jkr} R_{in} \frac{1}{r} e^{-ikr}, \\
P_i(t) &= \frac{A}{r^2} \sum_{n=1}^{N} e^{-j2kr} a_{in} e^{j\psi_{in}}.
\end{aligned} \tag{3}$$

The time-frequency characteristics of the big database signal of tourism English talent resource distribution are calculated, and the big data structural model of the talent training information base resource distribution is constructed [13]. The big data model of resource distribution is obtained as follows:

$$x(t) = \sum_{i=0}^{p} a(\theta_i) s_i(t) + n(t). \tag{4}$$

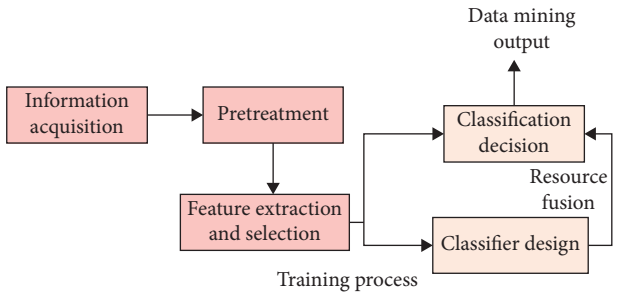

Figure 4: Principles of big data mining for big-scale tourism English talent resources distribution.

The big data characteristic data of tourism English talent resource distribution are sampled and updated in sequence, and the spectrum of nonstationary broadband signal $z(t)$ in the big database of tourism English talent resource distribution is obtained. Furthermore, time-frequency analysis is used to carry out transient analysis [14]. According to the estimation of time frequency, the probability function density expression of the accuracy of big data characteristic data for the distribution of big tourism English talent resources is as follows:

$$p(y|\alpha,\theta) = \sum_{k=1}^{K} \alpha_k p_k\left(y|\mu_k, \sum k\right). \tag{5}$$

Big tourism English talent resource distribution big data is a sample set composed of n samples. There are m indexes in each big data sample of tourism English talent resource distribution; then the index characteristic vector of j sample is $x_j = \left\{x_{1j}, x_{2j}, \ldots, x_{mj}\right\}^T$, tourism English. The a posteriori probability of big data is estimated as $p(x_0)$:

$$P_{ij}(k) = \frac{\left(l_j(k) - l_i(k)\right)\eta_{ij}(k)}{\sum_{j\in N_i(k)}\left(l_j(k) - l_i(k)\right)\eta_{ij}(k)}. \tag{6}$$

According to the results of big data mining, data sharing and resource scheduling in the process of talent training are carried out by combining association feature mining and information fusion methods.

3.3. Optimization of Cross-Cultural Communicative Competence. Constructing English for tourism in the context of big data is not exactly equivalent to the Basic English content. It has its uniqueness, except listening, speaking, reading, writing, and translation of Basic English training. In addition to their abilities, they must also develop their professional English skills, relevant cross-cultural thinking skills, and communication skills. Therefore, in the tourism English curriculum, student's cross-cultural communication skills should be cultivated to meet the requirements of the current society, disciplines, and students themselves. From the study of intercultural communicative competence by various scholars at home and abroad, cross-cultural communicative competence is a comprehensive, multidimensional system such as knowledge system, relationship system, and behavior system. Based on these researches on the elements of intercultural communication, and combining the characteristics of the curriculum of tourism English under the big data environment, a cross-cultural communicative competence framework for tourism English teaching in the context of big data is constructed. The framework of cross-cultural communicative competence of English tourism talents is shown in Figure 5.

From Figure 5, we can observe that, for a student majoring in tourism management, English communication skills have become a core skill. Compared with other professional students, English communication ability is a requirement within the category of professional competence. Therefore, colleges and universities pay great attention to tourism English teaching in the context of big data. However, in practice, students find that they have a high level of enthusiasm for learning professional English, but the results are not obvious. The bigger reason is that travel professional English is different. Basic English requires global awareness and industry awareness, which is the basis for developing cross-cultural communication skills. The global awareness mentioned here includes cross-cultural awareness and cross-cultural thinking. Cross-cultural awareness can also be called cultural awareness [15]. Similarly, In the process of cross-cultural communication, cultural conflicts occur everywhere. In order to shorten the conflict period, it is necessary to adapt to the rapid recovery period. This is a process of entering a steady state through a series of adjustments from a relatively unstable state [16]. The theory of adaptation to cross-cultural adaptation process can be summarized as a model curve [17]. The adaptability plays an important role in the exchange process. This is a turning point from uncertainty decision rather than acceptance. Adaptability includes two elements: psychological adaptability and cultural adaptability [18, 19].

Moreover, in the reform of foreign language classroom teaching, cultivating student's communicative application ability is the focus of foreign language circles in recent years. The University English Classroom Requirements with a target meaning also highlights language knowledge and application capabilities. For the purpose of tourism English, language knowledge and cultural knowledge are the basic teaching contents of the teacher's class. In addition, the ability of the first three media is in communication practice. Communicative practice ability is the highest level of intercultural communication ability. It includes communicative competence, nonverbal communication, and communication skills. The communicative practice ability emphasizes the use of linguistic, nonverbal, and related strategies in practical situations to solve practical cross-cultural communication problems. The ability of a large communication strategy is the core competitiveness of tourism services.

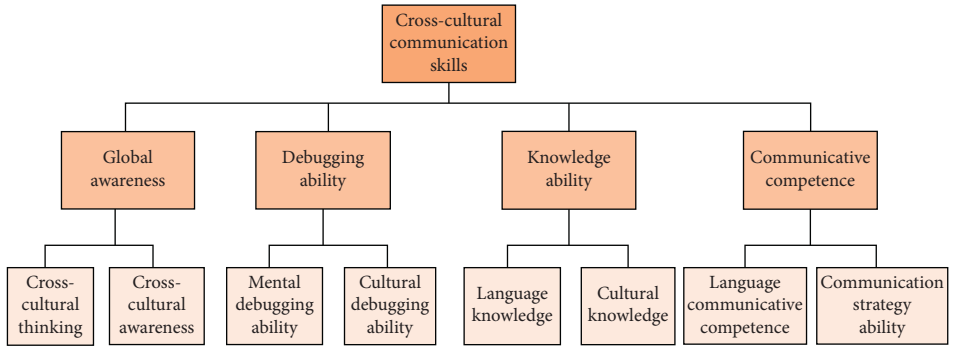

Figure 5: Framework of cross-cultural communicative competence of English tourism talents.

3.4. Feature Classification and Information Fusion of Tourism English Talent Resources. The fuzzy clustering method is used to deal with the adaptive clustering of tourism English talent resources distribution, the attribute distribution structure model is used to classify the features and information fusion of tourism English talent resources, and the time-frequency analysis method is adopted. By extracting the big data feature of resource distribution, the information state function of big data feature data of tourism English talent resource distribution is presented as follows:

$$\begin{aligned}\dot{x}_i &= f_i(x_i, u_i)D\big(x_i, A_j(L)\big)\\ &= \min\big\{D\big(x_i, A_j(L)\big)\big\},\end{aligned} \tag{7}$$

where $x_i \in R^n$, and the state vector of big data feature data representing the distribution of tourism English talent resources is presented. Based on the above analysis, the feature extraction of resource distribution big data in the big database of tourism English talent resources distribution is realized, and the big scale is extracted. The big data training sample of tourism English talent resource distribution in the database, the time-frequency feature of the extracted tourism English talent resource distribution big data is rearranged by sliding time window, and the tourism English talent database distribution big data is carried out. The expression of the frequency domain model is as follows:

$$x_n = [x(0), x(1), \ldots, x(N-1)]^T. \tag{8}$$

The big data fusion algorithm of tourism English talents training is improved by phase spectrum compensation, and the attribute weights of random linear access channel for resource big data fuzzy decision fusion of tourism English talent training are obtained as follows:

$$F = \begin{bmatrix} \omega^0 & \omega^0 & \omega^0 & \cdots & \omega^0 \\ \omega^0 & \omega & \omega^2 & \cdots & \omega^{k-1} \\ \omega^0 & \omega^2 & \omega^4 & \cdots & \omega^{2(k-1)} \\ \vdots & \vdots & \vdots & \vdots & \vdots \\ \omega^0 & \omega^{k-1} & \omega^{2(k-1)} & \cdots & \omega^{(k-1)^2} \end{bmatrix} = \prod_{0 \le j < i \le k-1} \left(\omega^i - \omega^j\right). \tag{9}$$

The vector model structure of big data fuzzy decision fusion for tourism English talents training is expressed as follows:

$$\begin{cases} \dot{m}_i(t) = -a_i m_i(t) + b_i\big(p_1(t-\sigma), p_2(t-\sigma), \ldots, p_n(t-\sigma)\big), \\ \dot{p}_i(t) = -c_i p_i(t) + d_i m_i(t-\tau). \end{cases} \tag{10}$$

Combined with the association feature mining and information fusion method, data sharing and resource scheduling are carried out in the training process, so that the data fusion capacity is improved [15, 16].

3.5. Big Data Fusion and Optimization Mining of English Talent Resource Distribution. In the tourism English talent database, the prediction of packet information can be as follows: $\{\lambda_i: 1 \le i \le S\}$, criterion $\{R_j: 1 \le j \le L\}$, and density prior information sliding time window rearrangement of big data for tourism English talent resources distribution calculation is expressed as follows:

$$
\begin{aligned}
N_{i,j} &= \left(f(A)_{i,1} \otimes f(B)_{1,j}\right) \oplus \left(f(A)_{i,2} \otimes f(B)_{2,j}\right) \oplus \cdots \oplus \left(f(A)_{i,h} \otimes f(B)_{h,j}\right) \\
&= \left(\left(K_A \cdot \left(A_{i,1} + rp\right) \cdot k_A^r \bmod n\right) \cdot \left(K_B \cdot \left(B_{1,j} + rp\right) \cdot k_B^r \bmod n\right)\right) \oplus \cdots \oplus \\
&\quad \left(\left(K_A \cdot \left(A_{i,h} + rp\right) \cdot k_A^r \bmod n\right) \cdot \left(K_B \cdot \left(B_{h,j} + rp\right) \cdot k_B^r \bmod n\right)\right) \\
&= \sum_{u=1}^{h} \left(\left(K_A \cdot \left(A_{i,u} + rp\right) \cdot k_A^r \bmod n\right) \cdot \left(K_B \cdot \left(B_{u,j} + rp\right) \cdot k_B^r \bmod n\right)\right) \bmod n \\
&= \sum_{u=1}^{h} \left(\left(\frac{s \cdot l}{k_A^r} \cdot \left(A_{i,u} + rp\right) \cdot k_A^r \bmod n\right) \cdot \left(\frac{s \cdot l}{k_B^r} \cdot \left(B_{u,j} + rp\right) \cdot k_B^r \bmod n\right)\right) \bmod n \\
&= (s \cdot l)^2 \sum_{u=1}^{h} \left(\left(A_{i,u} + rp\right) \cdot \left(B_{u,j} + rp\right)\right) \bmod n \\
&= (s \cdot l)^2 \sum_{u=1}^{h} \left(A_{i,u} \cdot B_{u,j} + \left(A_{i,u} + B_{u,j}\right) \cdot rp + r^2 p^2\right) \bmod n.
\end{aligned} \tag{11}
$$

It can be seen that the nearest-neighbor matching method using the time-frequency eigenvector can find out the potential matching of the big data features of the tourism English talent resources:

$$
\begin{aligned}
&\left(V(a_1, \ldots, a_m)^{(\alpha_1, \ldots, \alpha_m)}\right)^{-1} V(b_1, \ldots, b_m)^{(\beta_1, \ldots, \beta_m)} \\
&= \left(\left(V(a_1, \ldots, a_m)^{-1} V(b_1, \ldots, b_m)\right)^{\left(\alpha_1^{-1}, \ldots, \alpha_m^{-1}\right)^T}\right)^{(\beta_1, \ldots, \beta_m)}.
\end{aligned} \tag{12}
$$

The fuzzy feature balance metric of the differences between j and c categories in the big data sample of tourism English talent resources distribution can be expressed as follows:

$$
f_j(u_j, s, w) = \sum_{h=1}^{c} \left\{ u_{hj}^2 \left[\sum_{i=1}^{m} \left[w_i \left(r_{ij} - s_{ih} \right) \right]^2 \right]^{\alpha/2} \right\}. \tag{13}
$$

The big data signal analysis of tourism English talent resources distribution is extended to the disturbed environment. For the time series of tourism English talent resources $\{x(t_0 + i\Delta t)\}$, $i = 0, 1, \ldots, N-1$, the fast resource information of the big database of tourism English talent resources distribution is established. The mining and scheduling model objective function is,

$$
\min\{f(u, s, w) = f_1(u_1, s, w), f_2(u_2, s, w), \ldots, f_n(u_n, s, w)\}. \tag{14}
$$

4. Result Analysis and Discussion

In this section, we compare the performance and utility of the proposed model. The efficiency of the proposed model was initially tested using the optimization of tourism English talent training mode is realized. In order to improve the ability of fast resource information mining and scheduling, a sliding time window rearrangement of big data prior information of tourism English talent resource distribution in big tourism English talent database is carried out.

4.1. Experimental Setup. In this paper, each algorithm was evaluated through experiments, and broad data computational approaches were used, that is, the open-source Apache Hadoop and the Apache Spark platform. First of all, we created a Spark cluster that uses physical nodes, that is, 80 nodes. To determine the basic software and hardware specifications for the experiment, all computing nodes have been simplified, and their configuration is shown in Table 1. For example, operating systems Ubuntu 18, Spark 3.01, and Hadoop 3.2 are used in experimental configurations. In all 80 nodes, one node was used as a master node or as a processing node, and the remaining 79 nodes were used as slaves in the cluster. Apache Hadoop's software library is a tool used in basic programming models to spread vast data collection through computer clusters. For each local server calculation and storage, it is scheduled to reach multiple computers. Apache Spark is a hierarchical programming engine for large-scale data processing that provides high-level APIs for Java, Python, R, and Scala and is used as an advanced map driver. Apache Spark enables a wide range of high-level tools, including SQL Spark for structured data analysis, MLlib for apprenticeships, and GraphX for graphics processing.

4.2. Simulation Experiment and Result Analysis. In order to test the application performance of this algorithm in realizing the big data mining of tourism English talent resource distribution and the optimization of training mode, the simulation experiment is carried out. In the experiment, 100 pieces of big data sample data of tourism English talent resource distribution are selected, the number of talent attribute samples is 50, and the dimension of time-frequency

Table 1: Configuration detail of cluster.

Hardware	Number of cluster nodes	80
	Hard disk	500 GB
	No. of CPU cores	8
	Processor	3.0 GHz × 4
	Connectivity	100 Mbps ethernet LAN
	RAM size	30 GB
	Data block size	256 Mb
Software	Operating system	Ubuntu 18
	Java-JDK	V-1.8
	Hadoop	V-3.0
	Spark	V-3.0.1
	Open-PDC	V-1.5
	Python	V-3.8

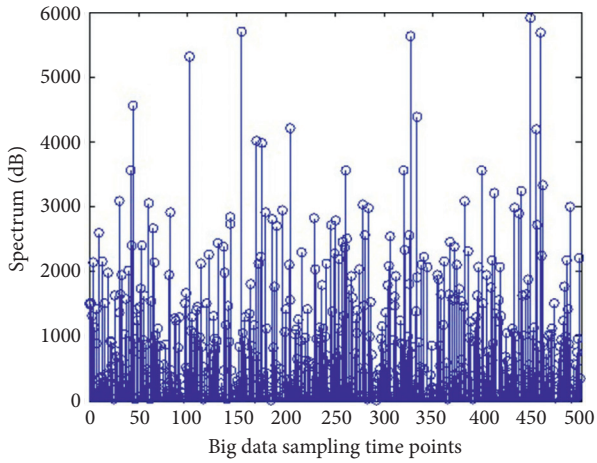

Figure 6: Big data mining results of tourism English talent training.

feature state space of the big database of tourism English talent resource distribution is 10, which is sampled according to the characteristic data. According to the above simulation experimental environment design and parameter design, the big data feature extraction and resource information mining of tourism English talent resource distribution are carried out, and the data mining is obtained. The effect of some parameters, that is, learning rate and activation functions, on accuracy is summarized in Table 1, that is, performance of different phenotype. We have optimized the parameters settings for all the learning algorithms for accuracy-based analysis. The result is shown in Figure 6.

The results of the analysis of Figure 6 show that the data mining of tourism English talent training resource distribution using this method is of high accuracy. The fast resource information mining of big data for tourism English talent resources distribution can be realized. SQL Server Data Mining offers Office 2007 data mining additives for the detection of data patterns and relationships. This is also helpful in improving the analysis. The add-in called Data Mining Client for Excel is used first to plan, compile, analyze, handle, and forecast data. In order to compare the performance of scheduling, different methods are used to mine the big data of tourism English talent

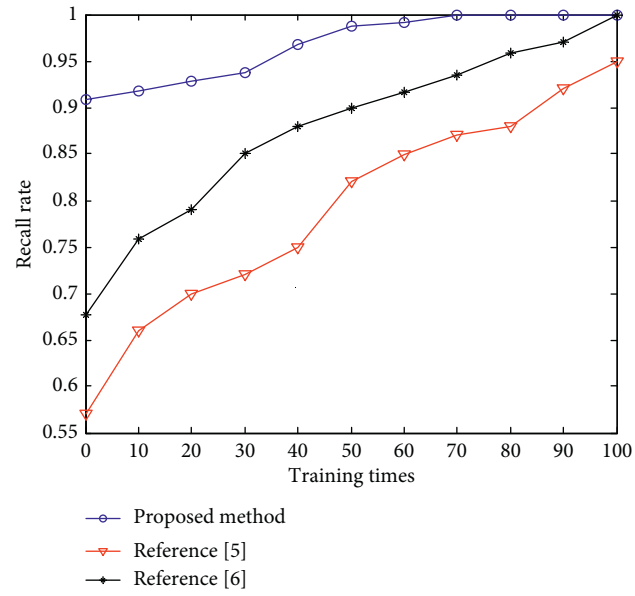

Figure 7: Big data analysis performance test.

resources distribution, and the recall test results are shown in Figure 7.

The results of the analysis in Figure 7 show that this method has good accuracy and big data clustering ability for tourism English talent resource data mining, which can effectively guide the construction of a new model for tourism English talent training.

5. Conclusions

In this paper, a new model of tourism English talent training based on big data is proposed, and the big data mining model of tourism English talents is constructed. Traditional methods use basic algorithms to predict the future. However, it does not provide reliable findings as compared to data mining. In the cloud storage system, the optimal scheduling design of tourism English talent training resource big data is carried out, and the fuzzy clustering method is used to deal with the adaptive clustering of tourism English talent resource distribution big data.

Moreover, the attribute distribution structure model is constructed to classify and fuse the features of tourism English talent resources, and the methods of association feature mining and information fusion are combined to share data and schedule resources in the process of talent training. Time-frequency features of tourism English talent resource distribution big data are extracted to realize the fast mining and positioning of the data. The simulation results show that this method has good accuracy and big data clustering ability, which can effectively guide the construction of a new model of tourism English talent training. This model has a good application value in promoting the promotion of tourism English talent training model. In the future, big data research needs to deal with the relationship between data and theory. The combination of data driving

and theoretical driving is conducive to the benign development of the mutual promotion of theory and data.

Data Availability

The data used to support the findings of this study are included within the article.

Conflicts of Interest

The author declares that there are no conflicts of interest regarding the publication of this paper.

Acknowledgments

The paper was supported by Anhui Province Overseas Study Visiting Project of Universities Excellent Talents Cultivation in 2017 (Grant no. GXFX2017237); Internet-Based Teaching Management Model Innovation Research, Anhui Vocational and Adult Education Association Education Scientific Research Planning Project (Grant no. AZJXH17156); Provincial Quality Engineering Practical English Excellent Open Course of Anhui Provincial Education Department (Grant no. 2017KFK136); Research on the Professional Development of Public English Teachers from the Perspective of Innovative Development of Higher Vocational Education, Key Project of Humanities and Social Sciences in Universities of Anhui Province (Grant no. SK2018A0832); Research on the Construction and Development of "2 + 2 + 2" Practical English Mixed Teaching Curriculum System in Higher Vocational Colleges (Grant no. SK2018A1170); Provincial Quality Engineering Teaching Research Project of Anhui Provincial Department of Education: Higher Vocational English Teaching Research Based on EOP + PE Ability Cultivation from NA Perspective (Grant no. 2019JYXM0613); and Provincial Quality Engineering Teaching Research Project of Anhui Provincial Education Department in 2020: Study on Practical English Course Ideological and Political Construction from the Perspective of "Taoism" (Grant no. 2020KCSZYJXM228).

References

[1] T.-z. Wen, A.-q. Xu, and G. Chneg, "Multi-fault diagnosis method based on improved ENN2 clustering algorithm," *Control and Decision*, vol. 30, no. 6, pp. 1021–1026, 2015.

[2] A. Kumar, R. Pooja, and G. K. Singh, "Design and performance of closed form method for cosine modulated filter bank using different windows functions," *International Journal of Speech Technology*, vol. 17, no. 4, pp. 427–441, 2014.

[3] N. Rajapaksha, A. Madanayake, and L. T. Bruton, "2D space-time wave-digital multi-fan filter banks for signals consisting of multiple plane waves," *Multidimensional Systems and Signal Processing*, vol. 25, no. 1, pp. 17–39, 2014.

[4] Y. Jiang, F. L. Chung, S. Wang, Z. Deng, J. Wang, and P. Qian, "Collaborative fuzzy clustering from multiple weighted views," *IEEE Transactions on Cybernetics*, vol. 45, no. 4, pp. 688–701, 2015.

[5] A. Bi and S. Wang, "Transfer affinity propagation clustering algorithm based on kullback-leiber distance," *JEIT*, vol. 38, no. 8, pp. 2076–2084, 2016.

[6] B. N. Alahmad and S. Gopalakrishnan, "Energy efficient task partitioning and real-time scheduling on heterogeneous multiprocessor platforms with QoS requirements," *Sustainable Computing: Informatics and Systems*, vol. 1, no. 4, pp. 314–328, 2011.

[7] H. Wang, H. Jin, J. Wang, and W. Jiang, "Optimization approach for multi-scale segmentation of remotely sensed imagery under k-means clustering guidance," *Acta Geodaetica et Cartographica Sinica*, vol. 44, no. 5, pp. 526–532, 2015.

[8] O. Shi-feng, Y. Gao, and Z. Xiao-hui, "Adaptive combination algorithm and its modified scheme for blind source separation," *Journal of Electronics & Information Technology*, vol. 33, no. 5, pp. 1243–1247, 2011.

[9] G. Tian, H. E. Ke-qing, J. Wang et al., "Domain-oriented and tag-aided web service clustering method," *Chinese Journal of Electronics*, vol. 43, no. 7, pp. 1266–1274, 2015.

[10] W. Tao, C. Lifei, and G. Gongde, "High-dimensional data clustering algorithm with subspace optimization," *Journal of Computer Applications*, vol. 34, no. 8, pp. 2279–2284, 2014.

[11] Y. Lei, X. Yu, S. Yue et al., "Research on PSO-based intuitionistic fuzzy kernel clustering algorithm," *Journal of Communication*, vol. 4, no. 5, Article ID 2015099, 2015.

[12] B. Zhang, H. Jie, G. Ma et al., "Mixture of probabilistic canonical correlation analysis," *Journal of Computer Research and Development*, vol. 52, no. 7, pp. 1463–1476, 2015.

[13] C. Sun, C. Yang, S. Fan et al., "Energy efficient distributed clustering consensus filtering algorithm for wireless sensor networks," *Information and Control*, vol. 44, no. 3, pp. 379–384, 2015.

[14] X.-y Guo, "Simulation and analysis on uncertain attenuation property of underwater acoustic signal for oil field pipe," *Computer Simulation*, vol. 31, no. 3, pp. 118–121, 2014.

[15] W. Zhang and Q. Chen, "Network intrusion detection algorithm based on HHT with shift hierarchical control," *Computer Science*, vol. 41, no. 12, pp. 107–111, 2014.

[16] H. Luo, Y. Qu, and Y. Yu, "Oscillation criteria of second order neutral delay emden-fowler equations with positive and negative coefficients," *Acta Mathematicae Applicatae Sinica*, vol. 40, no. 5, pp. 667–675, 2017.

[17] Z. Duo, G. Xu, X. Chen, and K. Yuan, "Rational non-hierarchical quantum state sharing protocol," *Computers, Materials & Continua*, vol. 58, no. 2, pp. 335–347, 2019.

[18] Q. He, S. Yu, H. Xu et al., "A weighted threshold secret sharing scheme for remote sensing images based on chinese remainder theorem," *Computers, Materials & Continua*, vol. 58, no. 2, pp. 349–361, 2019.

[19] F. Guo, P. Liu, W. Ren et al., "Research on the relationship between garlic and young garlic shoot based on big data," *Computers, Materials & Continua*, vol. 58, no. 2, pp. 363–378, 2019.

Hindawi
Mobile Information Systems
Volume 2021, Article ID 9989237, 20 pages
https://doi.org/10.1155/2021/9989237

Research Article

Identification of Pneumonia Disease Applying an Intelligent Computational Framework Based on Deep Learning and Machine Learning Techniques

Yar Muhammad,[1] **Mohammad Dahman Alshehri**,[2] **Wael Mohammed Alenazy**,[3] **Truong Vinh Hoang**,[4] **and Ryan Alturki**[5]

[1]*Department of Computer Science, Abdul Wali Khan University Mardan, Mardan, Khyber Pakhtunkhwa, Pakistan*
[2]*Department of Computer Science, College of Computers and Information Technology, Taif University, P.O. Box 11099, Taif 21944, Saudi Arabia*
[3]*Department of Self Development Skills, CFY Deanship King Saud University, Riyadh, Saudi Arabia*
[4]*Department of Information Technology Specialization, FPT University, Hoa Lac High Tech Park, Hanoi, Vietnam*
[5]*Department of Information Science, College of Computer and Information Systems, Umm Al-Qura University, Makkah, Saudi Arabia*

Correspondence should be addressed to Mohammad Dahman Alshehri; alshehri@tu.edu.sa

Received 23 March 2021; Revised 30 April 2021; Accepted 7 May 2021; Published 18 May 2021

Academic Editor: Muhammad Usman

Copyright © 2021 Yar Muhammad et al. This is an open access article distributed under the Creative Commons Attribution License, which permits unrestricted use, distribution, and reproduction in any medium, provided the original work is properly cited.

Pneumonia is a very common and fatal disease, which needs to be identified at the initial stages in order to prevent a patient having this disease from more damage and help him/her in saving his/her life. Various techniques are used for the diagnosis of pneumonia including chest X-ray, CT scan, blood culture, sputum culture, fluid sample, bronchoscopy, and pulse oximetry. Medical image analysis plays a vital role in the diagnosis of various diseases like MERS, COVID-19, pneumonia, etc. and is considered to be one of the auspicious research areas. To analyze chest X-ray images accurately, there is a need for an expert radiologist who possesses expertise and experience in the desired domain. According to the World Health Organization (WHO) report, about 2/3 people in the world still do not have access to the radiologist, in order to diagnose their disease. This study proposes a DL framework to diagnose pneumonia disease in an efficient and effective manner. Various Deep Convolutional Neural Network (DCNN) transfer learning techniques such as AlexNet, SqueezeNet, VGG16, VGG19, and Inception-V3 are utilized for extracting useful features from the chest X-ray images. In this study, several machine learning (ML) classifiers are utilized. The proposed system has been trained and tested on chest X-ray and CT images dataset. In order to examine the stability and effectiveness of the proposed system, different performance measures have been utilized. The proposed system is intended to be beneficial and supportive for medical doctors to accurately and efficiently diagnose pneumonia disease.

1. Introduction

Chronic diseases and epidemics have taken the lives of a large number of people and created numerous crises in the countries, which takes a long time for a country to recover from the loss caused by both of these major outbreaks. Some diseases that ascend in a specific time period within a population are termed outbreaks and epidemics [1]. Epidemic means the incidence of more cases of a disease at a particular period of time than expectations in an area, country, or group of people. The term outbreak is considered to be local and does not cause people to be panic.

Pneumonia is an infective disease that inflames the air sacs in a single or both lungs caused by fungi, bacteria, and viruses [2]. In addition, the pulmonary alveoli are affected very badly by the lung infection, the small balloon shape bags at the bottom of the bronchioles as shown in Figure 1. Pneumonia has several types including mycoplasma

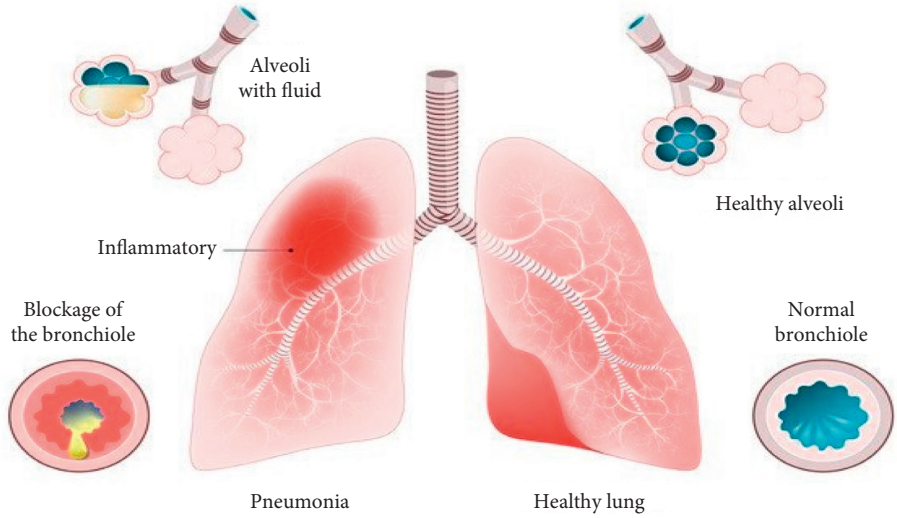

Figure 1: Pneumonia infected and normal lung.

pneumonia, viral pneumonia, bacterial pneumonia, and other types of pneumonia. Bacterial pneumonia occurs due to bacteria or fungi. Various symptoms are associated with the occurrence of bacterial pneumonia such as weakness of the body, old age, illness, poor nutrition, and weakened immune system. It is dangerous for people of all ages, but more dangerous for smokers, alcoholics, recent surgical patients, asthma, viral infection, and people having a frail immune system. Different viruses cause viral pneumonia such as flu and are accountable for almost 1/3 of all pneumonia cases. The chances of bacterial pneumonia increase with viral pneumonia, and one is at more risk to have bacterial pneumonia as well when attacked by viral pneumonia. Mycoplasma pneumonia is also called atypical pneumonia and is caused by bacterium and generally affects all age people. Lobar pneumonia is one in which it usually affects one or more lobe/section out of the five lobes/section of the lungs (2 lobes in the left and 3 lobes at the right). Bronchopneumonia is one in which the pneumonia reaches the bronchial tubes. It is considered to be the most important and dangerous type of pneumonia all over the world, mostly found in children younger than 5 years, and causes death (approximately 12.9% of annual child deaths) [3, 4]. Pneumonia has several symptoms including fever, cough which produces mucus (greenish, yellowish, or bloody), squatness of breath, heavy sweating, tiredness, trembling, chest pain (which incurs with coughing and breathing), loss of appetite, turning color of lips and nails to blue, and confusion (in old age people). It is considered to be more dangerous for adults as well and is one of the leading causes of sickness and expiry across the world particularly in China [5–7].

In 2017, more than 850,000 people died from pneumonia. The death ratio due to pneumonia is very high in South Asia and Sub-Saharan Africa. According to a report published in 2017, the death ratio in five countries, i.e., Pakistan, India, Ethiopia, Nigeria, and the Republic of Congo, was more than half of the deaths from childhood pneumonia and was called the ultimate disease of poverty [8]. This shows that the mortality rate due to pneumonia has a strong correlation with the income of a country. In Japan, pneumonia is the third leading reason of expiry in elder people with age ≥80 years [9]. Approximately 1 million people are diagnosed with pneumonia disease and around 50 k people die from this disease in a country like United States (US) every year. In Portugal, after lung cancer, pneumonia is the second most dangerous disease that leads to mortality due to respiration problems [10]. The list of the mortality rate due to pneumonia disease from 1990 to 2017 in all ages of people is shown in Figure 2. Pneumonia is a curable disease and does not spread from one country to another; its transmission is generally across local communities and can be controlled through basic health measures [11].

At the beginning of the 21st century, several coronaviruses have passed through the species fence to produce lethal pneumonia in human beings. In order to know the origin and development of these fatal pandemics, the experts need to inspect the structure of the virus and the method of how this virus causes infection. Furthermore, doing so will help the specialists in finding the right solution and providing proper treatment and possibly developing vaccines [13]. A short summary of the past epidemics and history of various types of coronavirus (MERS, SARS, and COVID-19) which have occurred over time are represented in Table 1.

Severe Acute Respiratory Syndrome Coronavirus (SARS-CoV) [14] is a serious breathing sickness problem that occurs due to coronavirus and has several indications like squatness of breath, temperature, coughing, and generally pneumonia. SARS appeared firstly in 2002 in China at Guangdong province and spread across the world. About 8 to 8.5 k people got affected by this disease which results in 750–800 deaths [10, 15], with a fatal rate of about 10%. It is anticipated that this disease originated from bats [16]. The symptoms of SARS and flu are almost the same like headache, fever, chills, tiredness, and sometimes diarrhea.

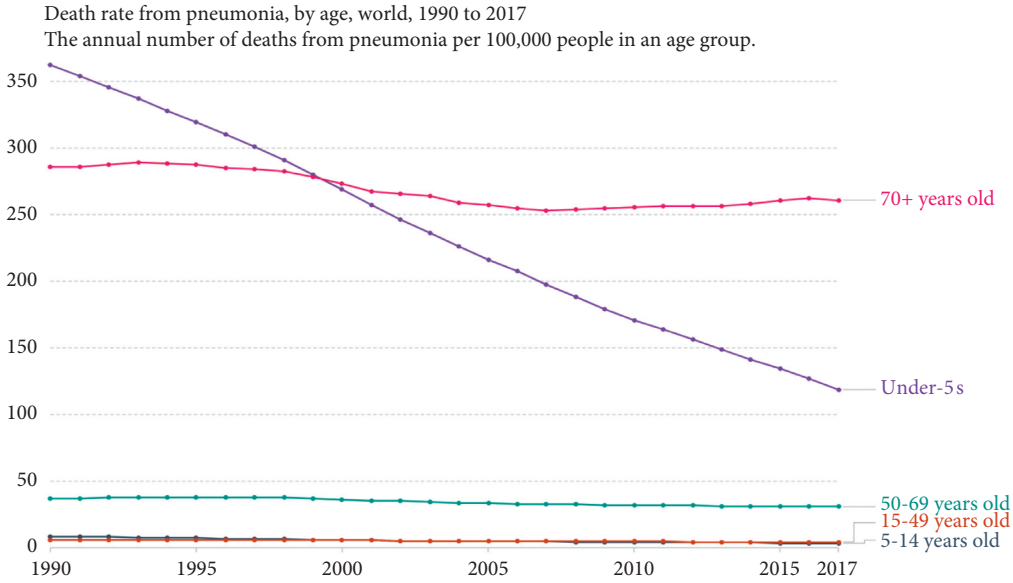

Figure 2: Death rate from pneumonia across the world by age from 1990 to 2017 [12].

Table 1: Past epidemics occurred over time.

Epidemic name	Duration	Approximate deaths
Antoine plague	170–180	5.0 million
Prague of Justinian	541–543	35–50 million
Japanese smallpox outbreak	734–736	1.2 million
Black death	1349–1353	200 million
Smallpox outbreak	1520+	56–60 million
Italian plague outbreak	1628–1630	1.0 million
Yellow fever (US)	1886–1891	1.5 million
Spanish flu	1918–1920	45–50 million
Third plague (China and India)	1985+	12 million
Asian flu	1959–1960	1.2 million
HIV/AIDS	1980–to present	30–35 million
SARS	2002-03	700–800
Swine flu	2009-10	0.2 million
Ebola	2014–2017	10,000–11,000
MERS	2015–to present	860
COVID-19	2019–(12/04/2021)	2.94 million

After a few days, some other symptoms like higher temperature fever, shortness of breath, and dry cough begin to appear as well [17].

The Middle East Respiratory Syndrome Coronavirus (MERS-Cov) is a viral respirational infection produced by a virus [18], which appeared for the first time in 2012 in the Middle East, Saudi Arabia [19, 20]. Some other cases of MERS disease were found in Jordan [21] and Qatar [22] and spread across the world. MERS is a zoonotic virus that was found mostly in camels and can be transmitted between humans and camels. According to the WHO report, humans are affected due to contact with the affected dromedary camels [23, 24]. MERS has various symptoms which include dumpiness of breath, temperature, diarrhea, coughing, headache, vomiting, nausea, chest pain, and throat infection [22, 25, 26].

Nowadays, the world is facing a hazardous pandemic which occurred due to a virus and is named COVID-19, acknowledged in December 2019, for the first time in China, Wuhan Province, and lead to the death of many people [27–30]. COVID-19 is a type of coronaviruses which is found to be more dangerous and lethal than the other types [31]. The earlier cases of this disease were related to a seafood market in Wuhan, China, where live animals were kept for selling, and are considered to be a zoonotic origin of this pandemic [32]. The virus is transmitted from one person to another in three ways: (a) touching each other, (b) close contact (person-to-person), and (c) vaporizer transmission [33]. The most dangerous thing about COVID-19 is that it remains in incubation for up to two weeks (incubation period of 2 weeks) without any symptoms. COVID-19 has various symptoms such as shortness of breath, high temperature, fever, tiredness, pains, dry cough, sore throat, nausea, and flu, and some people will also have diarrhea [34]. Various techniques are investigated to identify this disease which include chest X-ray, CT scan, blood culture, sputum culture, fluid sample, bronchoscopy, and pulse oximetry.

Medical image analysis plays a vital character in the diagnosis of various ailments like MERS, Covid-19, pneumonia, etc., and is considered to be one of the auspicious approaches [35, 36]. Therefore, to detect pneumonia, chest X-ray images are used by various researchers. In addition, to analyze chest X-ray images accurately, there is a need for an expert radiologist who possesses expertise and experience in the desired domain. According to the World Health Organization (WHO) report, about 2/3 persons in the world still do not have access to the radiologist, in order to diagnose their disease. In order to overcome the issues mentioned above, this study proposes an intelligent computational framework based on ML and DL to detect

pneumonia disease in an efficient and effective manner. We used various Deep Convolutional Neural Network (DCNN) transfer learning techniques such as AlexNet, SqueezeNet, VGG16, VGG19, and Inception-V3 for extracting useful features from the image dataset. Six ML classifiers such as K-Nearest Neighbours (KNN), Logistic Regression (LR), Support Vector Machine (SVM), Naïve Bayes (NB), Adaboost (AB), and Artificial Neural Network (ANN) have been investigated to diagnose whether a person has pneumonia or not. The proposed models have been trained and tested on chest X-ray and CT image dataset [37]. The performance of the proposed framework is tested on numerous performance measures such as accuracy, specificity, sensitivity, *F*1-measure, AUC-score, Mathew Correlation Coefficient (MCC), and ROC curve. It is expected that the suggested system will support the medical practitioners in order to diagnose pneumonia disease efficiently.

The remaining paper is organized as follows. Section 2 represents the review of the literature. The material and methods used in this study are discussed in Section 3. Section 4 demonstrates the results and discussion, and finally, we conclude our paper in Section 5.

2. Literature Review

Pneumonia is one of the fatal diseases, which is more dangerous for children and old age people. Toğaçar et al. [38] have used X-ray images of lungs for the identification of pneumonia. They have used CNN as a feature extractor by utilizing the existing models of CNN such as VGG-16 and AlexNet. These models extract a large number of features from images; for the reduction of the number of deep features, they used feature selection algorithms. Furthermore, they applied classical ML classifiers like, DT, LDA, and Linear regression for the diagnosis of pneumonia and achieved good results which show the importance of DL and classification algorithms. Liang and Zheng [39] have developed a framework based on DL for the diagnosis of child pneumonia using an image dataset and achieved satisfactory results. Jaiswal et al. [40] have proposed a DL-based method for the diagnosis of pneumonia using chest X-rays images. Their proposed classification/detection model was based on Mask-RCNN and achieved some good results which show the robustness and effectiveness of the model. Ge et al. [41] have investigated the prediction of pneumonia disease through ML (SVM, KNN, and DT) and DL (MLP and RNN) models and achieved promising results in terms of accuracy. Sirazitdinov et al. [42] have proposed an automated system for the forecasting of pneumonia on chest X-rays using ML algorithms. They used two types of CNN, i.e., Mask R-CNN and RetinaNet, and achieved satisfactory results.

Behzadi-Khormouji et al. [43] have presented a method based on DL and, specifically, CNN by using chest X-ray images and produced good results in terms of accuracy. To enhance the accuracy of the model, they used DCNN which was pretrained on the ImageNet data. In addition, they proposed a three-step preprocessing technique in order to enhance the generality of the model. Bhandary et al. [44] have proposed another healthcare framework based on DL for the diagnosis and detection of cancer and pneumonia. They have used two DL approaches, where the first one is a modified AlexNet. It was envisioned to separate and classify the chest X-rays (image dataset) into normal and abnormal classes by using SVM, and the performance of the proposed scheme was validated on pretrained DL transfer functions (VGG16 and AlexNet). On the other hand, the second approach implements a synthesis of handcrafted and the learned features in a person in order to increase the accuracy of lung cancer during valuation.

Medical imaging plays a significant part in the identification of numerous diseases [45, 46]. Classification of medical images is a significant and critical task to be accomplished. In order to classify the chest X-rays images and to diagnose pneumonia, this study depicts an extensive study of the fine-tuned versions of the latest Deep Convolutional Neural Network (DCNN) architectures (CNN, AlexNet, SqueezeNet, VGG16, VGG19, and Inception V3) for feature extraction and ML classification algorithms for the classification of pneumonia patients from a normal person.

3. Material and Methods

The following subsection describes the resources used and the approaches followed in carrying out this research study.

3.1. Dataset. The development of an automated and intelligent system extensively depends on the problem-related dataset. It means that a problem-specific dataset has a very high influence on the efficiency of an intelligent model. Considering the significance of the dataset, a chest X-ray and CT image dataset was used which is available online in the UCI Kaggle databases. The dataset consists of a total of 5856 images of two categories/classes, i.e., pneumonia and normal images. The dataset contains 1583 normal and 4273 pneumonia images. The dataset is distributed in two parts (training and testing), where 70% of the data is used to train the models while 30% of the data is used to test and validate the model. Figure 3 demonstrates an example of both categories/classes of chest X-ray images, where Figure 3(a) represents a normal image while Figure 3(b) represents the chest X-ray of a person having pneumonia.

3.2. Proposed System Methodology. The main goal and objectives of the proposed system are to diagnose whether a person has pneumonia or not at the early stages through their chest X-ray images in order to prevent them from more damage. In this study, the recent DCNN architectures based on the fine-tuned versions of (CNN, AlexNet, SqueezeNet, VGG16, VGG19, and Inception V3) are used to extract useful features from the images. Several preprocessing techniques are used, in order to present the data in a normalized form to the classification models. Various ML classification models such as KNN, SVM, LR, NB, AB, and ANN are used in this study. Different performance assessment metrics are computed to measure and track the performance of each utilized ML model. Keras deep learning framework is deployed which uses TensorFlow at the

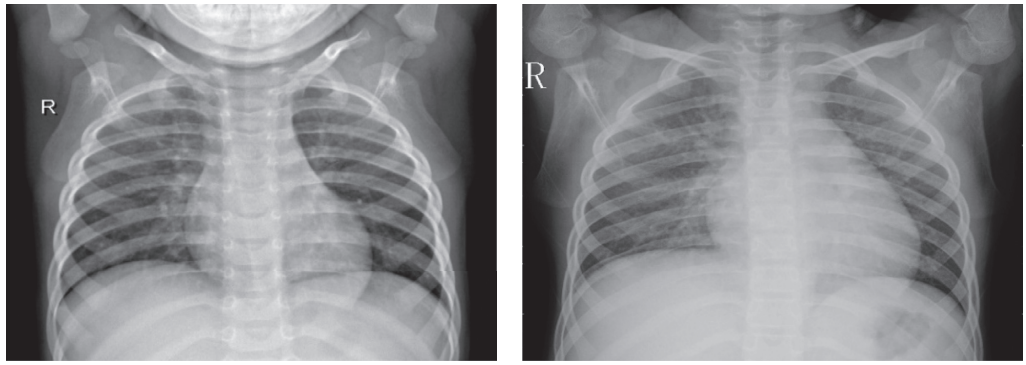

(a) (b)

Figure 3: An example of chest X-ray images (a) Normal, (b) Pneumonia.

backend for building and training our proposed system. The libraries and packages used in the implementation of the work include TensorFlow, Keras, Sklearn, Matplotlib, Seaborn, and NumPy. All the experiments were performed using the Jupyter NoteBook of the Anaconda integrated development environment (IDE). Figure 4 represents the framework of the proposed system.

3.3. Data Preprocessing. Data preprocessing is a vital technique used to provide data to the classification models in a well-organized manner, which are then trained and tested while using the normalized data. For the improvement of visual information quality (removal of noise, increasing contrast, deletion of high or low frequencies, etc.) of each input image, these images are preprocessed with the help of numerous techniques before being used in the classifiers. Preprocessing techniques such as intensity normalization, Contrast Limited Adaptive Histogram Equalization (CLAHE), and Min-Max normalization have been investigated in this study. Intensity normalization, CLAHE, and Min-Max normal distribution are interesting and important preprocessing techniques in image processing applications. Figure 5 represents the normal and images after applying the preprocessing techniques.

Looking at the dataset which represents two classes, i.e., pneumonia and normal images, almost 75% of the images represent pneumonia and the remaining 25% describe normal images which means that the dataset is imbalanced. To resolve the issue of unbalanced dataset and overfitting and to increase the accuracy of the models, various augmentation techniques have been used. The data augmentation techniques used include geometric transformations like rotations, zooms, rescale, shift, flips, and shears.

3.4. CNN Basic Architecture. CNN is a popular deep learning model particularly used for image classification problems. It normally consists of five layers which include the input layer, convolution layer, pooling layer, fully connected layer, and output layer. The practical assistance of CNN is having fewer parameters which significantly decrease the time it takes to learn and reduce the amount of data needed for training the model. In addition, CNN can be trained end-to-end for the extraction and selection of features from an image and, at last, can be used to predict or classify the images. It seems a bit difficult to know how a network understands or processes an image, but features conquered at various layers of a network perform better as compared to human-built features [47]. Figure 6 represents the basic architecture of the used CNN model.

The CNN architecture used for the experimental work in this study has the following properties:

(1) Input layer: X-ray images are used as input and are provided at the input layer. The image dimensions are kept to $244 * 244$.

(2) Convolutional layer: we have used 3 convolution layers having $3 * 3$ filter sizes and padding is set to zero.

(3) Pooling layer: we have used max pooling for calculating the maximum value at every patch for each feature map. The max-pooling size is set to 2×2 while the stride value used is 2.0.

(4) Fully connected layer: this layer used in the proposed architecture utilized the sigmoid activation function at the outer layer.

(5) Output layer: the output layer gives us the predicted result that whether the person has pneumonia or not.

3.5. Deep Learning (DL) Architectures. DL architectures are extensively used in image processing specifically in healthcare for diagnosing various diseases. These DL techniques extract useful features from the images and present them to the models for further investigation. Here, in our study, we have used five important DL architectures such as AlexNet, VGG16, VGG19, Inception-V3, and SqueezeNet. A brief description of the investigated DL architectures is given hereinafter.

3.5.1. AlexNet. AlexNet is a type of CNN, which comprises various layers such as input, convolution, max pooling, dense, and output layers that are its basic building blocks. In 2012, it won the ILSVRC competition. It solves the problem

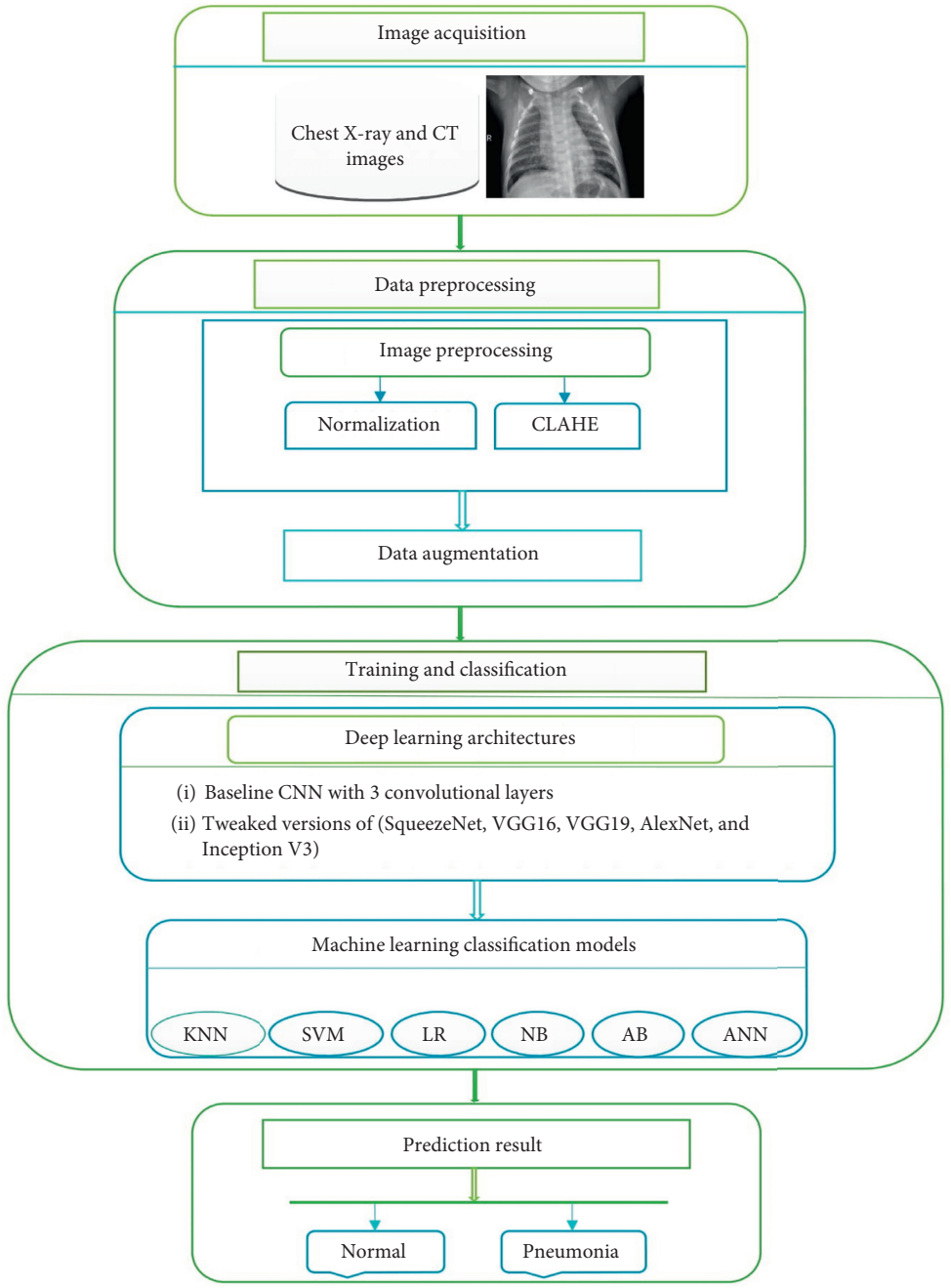

Figure 4: Proposed framework for pneumonia identification.

of image classification where the input image is one of 1000 different classes and the output is a vector of those classes. The kth element of the output vector is considered to be the likelihood that the input image belongs to the kth class. It may be noted that the sum of probabilities of the entire output vector is always equal to 1. AlexNet takes an RGB image as input having the size of $256 * 256$, which means that all the images in the training and testing set need to have the size of $256 * 256$. If the input image fails in matching the standard image size, then it needs to be converted to the standard size, i.e., $256 * 256$ before using to train the network. If the input image used is a gray-scale image, then it is converted to RGB by replicating the single channel into a 3-channel RGB image. The architecture of AlexNet is changed from the CNN model which was used for computer vision problems and is much larger than CNN. AlexNet has 60 million parameters and 650,000 neurons which take a very long time for training.

3.5.2. VGG-16 and VGG-19. VGG (Visual Geometry Group) is a type of CNN architecture proposed for the first time by two researchers Simonyan and Zisserman in 2014 [48]. The VGG architecture won the ILSVR (ImageNet) competition in 2014. This architecture improves the AlexNet architecture by substituting the large kernel-sized filters, i.e.,

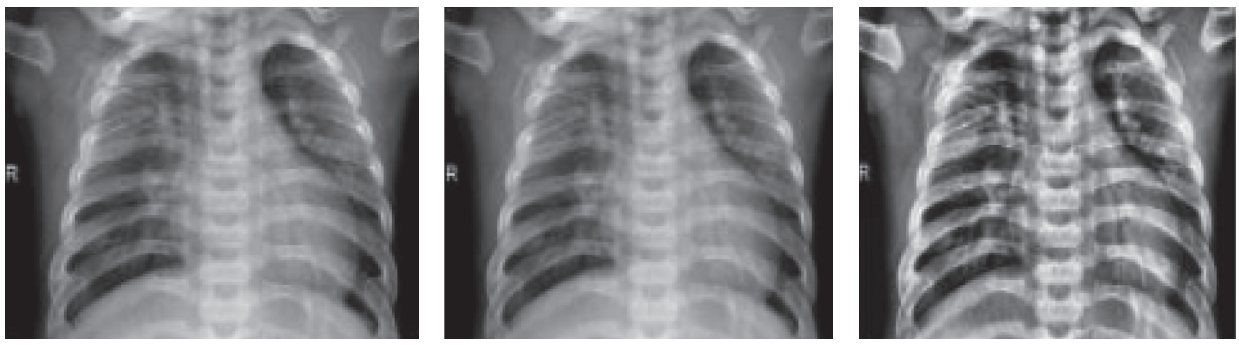

(a) (b) (c)

Figure 5: Images before and after applying preprocessing techniques: (a) original, (b) normalize, and (c) CLAHE.

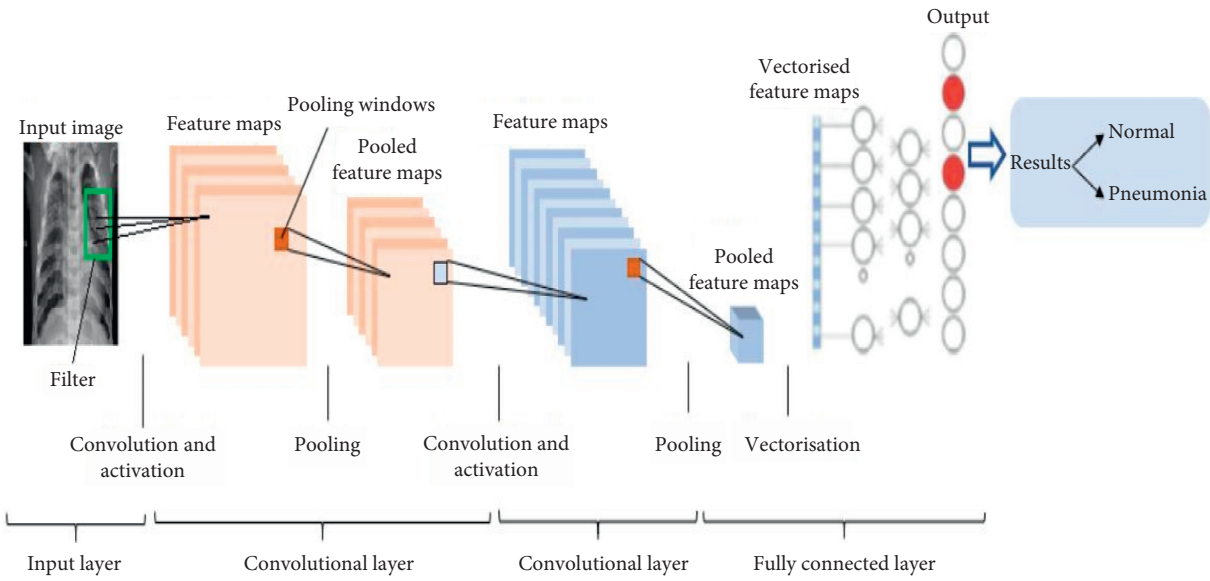

Figure 6: Basic architecture of CNN model.

(11 in the first convolutional layer and 5 in the second convolutional layer) with multiple small $3 * 3$ kernel-sized filters at the convolutional layer one after another and $2 * 2$ in the max-pooling layer. At last, it has two fully connected layers followed by the activation function softmax/sigmoid for the output. The well-known VGG models are VGG-16 and VGG-19. The VGG-16 model consists of 16 layers while the VGG-19 model contains 19 layers. The main difference between both models is that VGG-19 contains one more layer at each of the three convolutional blocks.

3.5.3. Inception-V3. Inception models are a type of deep neural network (DNN) architecture developed by a researcher named Szegedy et al. for the first time in 2014, and the model was named as inception model [49]. The structures of inception models and the conventional CNN model are different from each other in such a way that inception models are inception blocks which means lapping the same input tensor with multiple filters and concatenating their results. There are various versions of the inception models. In 2015, Szegedy et al. [50] proposed a new version of the inception models named Inception-V3, which is an improved version of the previous versions of inception models, i.e., Inception-V1 and Inception-V2, and possesses more parameters. Inception-V3 contains a total of 24M parameters. The advancement in Inception-V3 was as follows: (a) it factorizes the "$n \times n$" convolution into asymmetric convolutions, i.e., $1 \times n$ and $n \times 1$, (b) it factorizes the 5×5 convolutions into two 3×3 convolutions, and (c) it replaces 7×7 convolutions to a series of 3×3 convolutions. Actually, it consists of a block of convolutional layers which are arranged in a parallel manner and each layer consists of different sizes of filters 1×1, 3×3, and 5×5, respectively. Furthermore, 3×3 max pooling is also performed. The outputs are concatenated and sent to the next inception module.

3.5.4. SqueezeNet. SqueezeNet is a type of deep neural network developed by the researchers of Stanford University and was released on 22nd February 2016 for the first time. It is a type of CNN architecture consisting of 18 layers, particularly used in computer vision and image processing. The

main objectives and goal of the authors from developing SqueezeNet were to create a smaller neural network, which consists of fewer parameters, can fit into computer memory easily (requires less memory), and can be easier to transmit over a computer network (requires less of bandwidth). Firstly, the original version of this architecture was implemented on top of a DL framework named Caffe. After a short period of time, the researchers started the use of this architecture in a number of open-source DL frameworks. SqueezeNet was firstly labeled in a paper in which it was compared with the AlexNet and was mentioned that it achieves AlexNet level accuracy with "50X" fewer parameters. AlexNet contains 240 MB parameters while SqueezeNet consists of only 5 MB parameters. Both the SqueezeNet and AlexNet are two different DNN architectures, and they have just one thing in common, i.e., their accuracy when evaluated on the ImageNet image dataset.

3.6. Machine Learning (ML) Classification Algorithms. Various ML classification algorithms have been investigated for the diagnosis of whether a person has pneumonia disease or not. Each classification algorithm has its own importance, and its significance varies from application to application. In this paper, 6 distant natures of classification algorithms, namely, KNN, SVM, LR, NB, AB, and ANN, are applied in order to select the best and generalized prediction model.

3.7. Performance Measures. In order to track the performance of each classifier used in this study, several performance measures have been utilized such as accuracy, specificity, sensitivity, $F1$-measure, Mathew Correlation coefficient (MCC), AUC-score, and ROC curve. All the performance metrics are calculated by using the confusion table as shown in Table 2.

$$\begin{aligned}
\text{accuracy} &= \frac{\text{TP} + \text{TN}}{\text{TP} + \text{TN} + \text{FP} + \text{FN}} * 100,\\
\text{specificity} &= \frac{\text{TN}}{\text{TN} + \text{FP}} * 100,\\
\text{sensitivity} &= \frac{\text{TP}}{\text{TP} + \text{FN}} * 100,\\
F1 - \text{measure} &= \frac{2 * (\text{precision} * \text{recall})}{\text{precision} + \text{recall}},\\
\text{MCC} &= \frac{(\text{TP} * \text{TN}) - (\text{FP} * \text{FN})}{\sqrt{(\text{TP} + \text{FP})(\text{TP} + \text{FN})(\text{TN} + \text{FP})(\text{TN} + \text{FN})}}.
\end{aligned} \tag{1}$$

All of the abovementioned formulas are carried out from the confusion matrix which consists of the following basic components:

True positive (TP): it means that the model prediction is positive and in actual fact the person has pneumonia. So, a pneumonia subject is diagnosed correctly by the model.

Table 2: Confusion matrix.

	Predicted (−)	Predicted (+)
Actual (−)	TN	FP
Actual (+)	FN	TP

True negative (TN): it means that the model prediction is negative and in actual fact the person does not have the pneumonia disease. Hence, a healthy person is diagnosed correctly by the classification model.

False positive (FP): it means that the model did a wrong prediction by classifying a healthy person as a pneumonia patient. This is also known as type-1 error.

False negative (FN): it means that the model did a wrong prediction by classifying a pneumonia patient as healthy. This is also known as type-2 error.

4. Results and Discussion

The simulation results of various ML classification algorithms by using different DL architectures such as AlexNet, SqueezeNet, VGG-16, VGG-19, and Inception-V3 are discussed in this section. These DL architectures, also called transfer learning techniques, extract useful features from the images which are very useful in classifying the normal and pneumonia patients in an efficient way. The performance of all utilized ML classifiers, i.e., KNN, SVM, LR, NB, AB, and ANN, was checked on the pneumonia chest X-ray dataset on full feature space generated by the transfer learning techniques. For measuring the performance of ML classifiers, different performance measures are used. In addition, preprocessing techniques are also applied to all features before being used by the classification algorithms.

4.1. Performance of Convolutional Neural Network (CNN) Classification Algorithm. This subsection represents the experimental results attained by the CNN classification algorithm. We performed multiple experiments on the basic CNN model by using various epoch numbers. First, we used 100 epochs and then 150 epochs, and at last, we used 200 epochs and got that the accuracy was increasing from epoch 0 to epoch 10, and after, that it becomes stable and remained 92.30%. Figure 7 represents the ROC curve obtained through the CNN classifier.

4.2. Performance of all Classifiers Using AlexNet Architecture. This section represents the simulation results carried out through all the utilized ML classification algorithms using the AlexNet transfer learning technique. Table 3 shows the experimental results attained through all the utilized 6 ML classification models.

Table 3 reveals that ANN outclassed all the other classifiers in terms of each performance measure. ANN attained the classification accuracy of 96.44%, specificity of 92.62%, and sensitivity of 96.82% as shown in Table 3. LR performed very well and achieved an accuracy of 95.94%, specificity of 91.40%, and sensitivity of 96.98% and stood second in

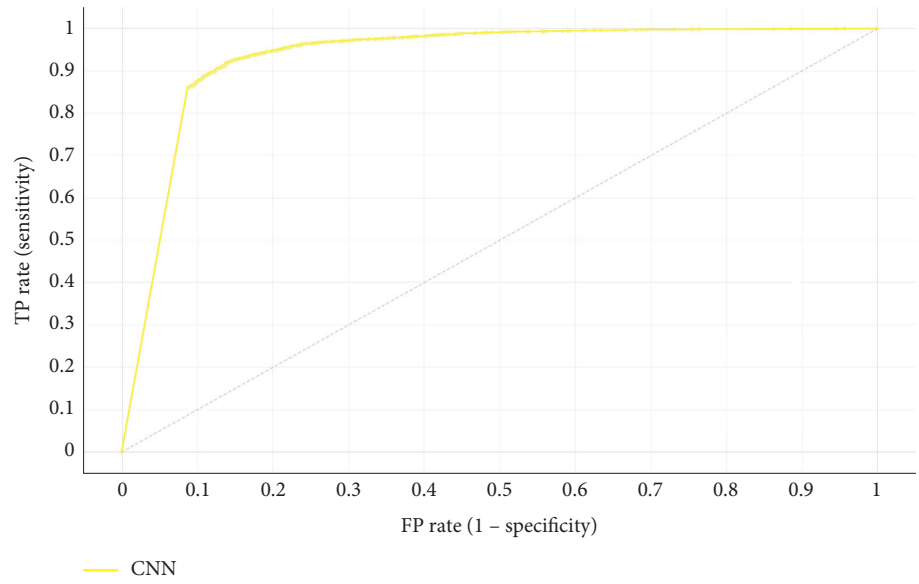

Figure 7: ROC curve of the Convolutional Neural Network (CNN) classification algorithm.

Table 3: Performance of all classifiers using the AlexNet transfer learning architecture.

Classification model	Accuracy	Sensitivity	Specificity	AUC	*F*1-score	MCC
KNN ($k = 5$)	94.10	95.40	90.08	96.76	0.94	0.73
SVM (rbf)	51.13	54.52	50.98	53.45	0.54	0.51
SVM (linear)	88.65	92.98	72.53	88.94	0.85	0.70
AB	89.72	92.63	80.74	86.62	0.89	0.73
NB	87.89	87.56	88.62	92.68	0.88	0.72
LR	95.94	96.98	91.40	98.42	0.95	0.89
ANN	96.44	96.82	92.62	98.84	0.96	0.91

performance competition as shown in Table 3. SVM with kernel = "rbf" stood last in this regard as compares to other classification algorithms by achieving the classification accuracy of 51.13% as shown in Table 3.

Figure 8 shows the performance of all 6 ML classification algorithms using the features extracted through DL AlexNet architecture from the image dataset. From Figure 8, it is obvious that ANN outclasses other classification algorithms in terms of all performance measures where SVM with kernel = "rbf" performs poorly and stood last in the performance competition.

Figure 9 shows the *F*1-score and MCC score of all the utilized 6 ML classification algorithms using AlexNet DL architecture.

Figure 10 illustrates the ROC curves of all the utilized ML classifiers using AlexNet transfer learning architecture.

From Figures 9 and 10, it is observed that ANN produced good results and beats the rest of the classifiers in terms of all performance measures.

4.3. Performance of All Classifiers Using SqueezeNet Architecture. The experimental results and performances of all the utilized 6 ML classifiers, using the SqueezeNet transfer learning technique, are discussed here in this subsection. The transfer learning techniques are used to extract valuable features from the images and then present them to the classifiers to classify it. Table 4 shows the performances of all 6 ML classification algorithms.

Table 4 demonstrates that ANN performs excellently in terms of all performance measures as compared to the rest of the classification models. ANN conquered the classification accuracy of 96.97%, specificity of 92.99%, and sensitivity of 97.52% as shown in Table 4. LR performs very well and achieved a classification accuracy of 96.24%, specificity of 92.99%, and sensitivity of 97.52% and stood second in performance competition as shown in Table 4. SVM with kernel = "linear" stood last in this regard as compared to other classifiers by achieving the accuracy of 52.03% as mentioned in Table 4.

Figure 11 signifies the performance of all utilized 6 ML classification algorithms using the features extracted through DL SqueezeNet architecture from the image dataset. From Figure 11, it is obvious that ANN outclasses other classification algorithms in terms of all performance measures where SVM with kernel = "rbf" performs poorly as compared to the rest of the classifiers.

Figure 12 shows the *F*1-measure and MCC score of all the utilized ML classification models using SqueezeNet transfer learning architecture. From Figure 12, it is observed that ANN beats all the other models in terms of *F*1-measure and MCC score by achieving the *F*1-score of 0.97 and MCC score of 0.92, respectively.

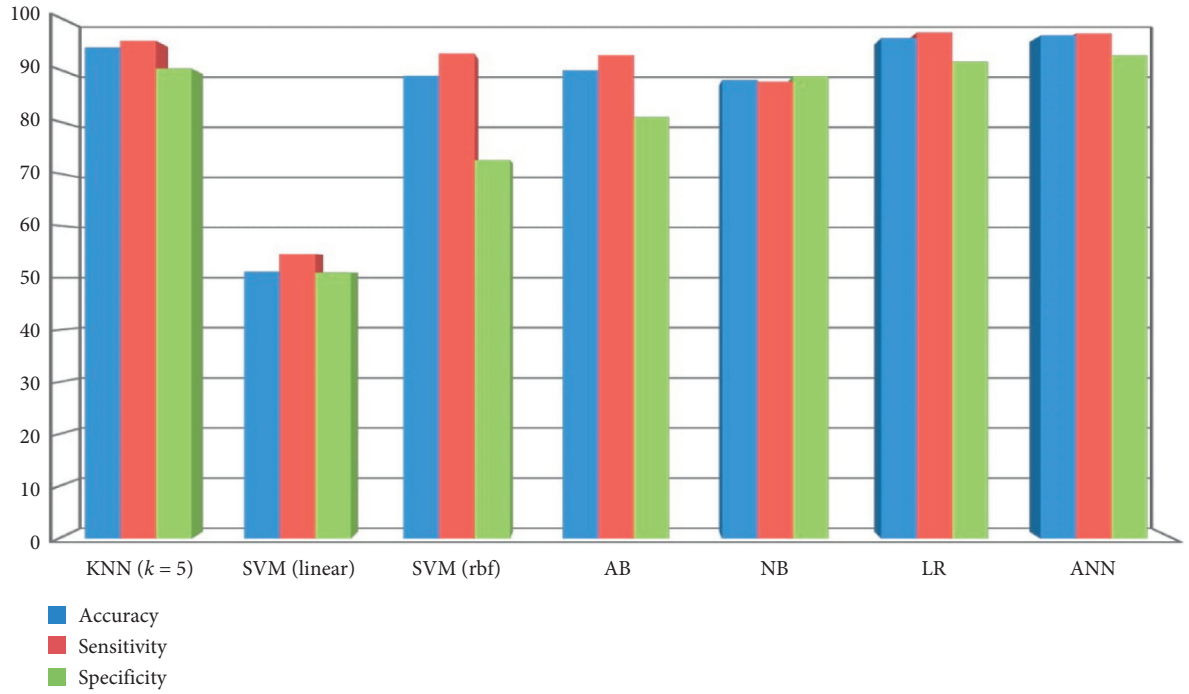

Figure 8: Performance of all classifiers using the AlexNet transfer learning technique.

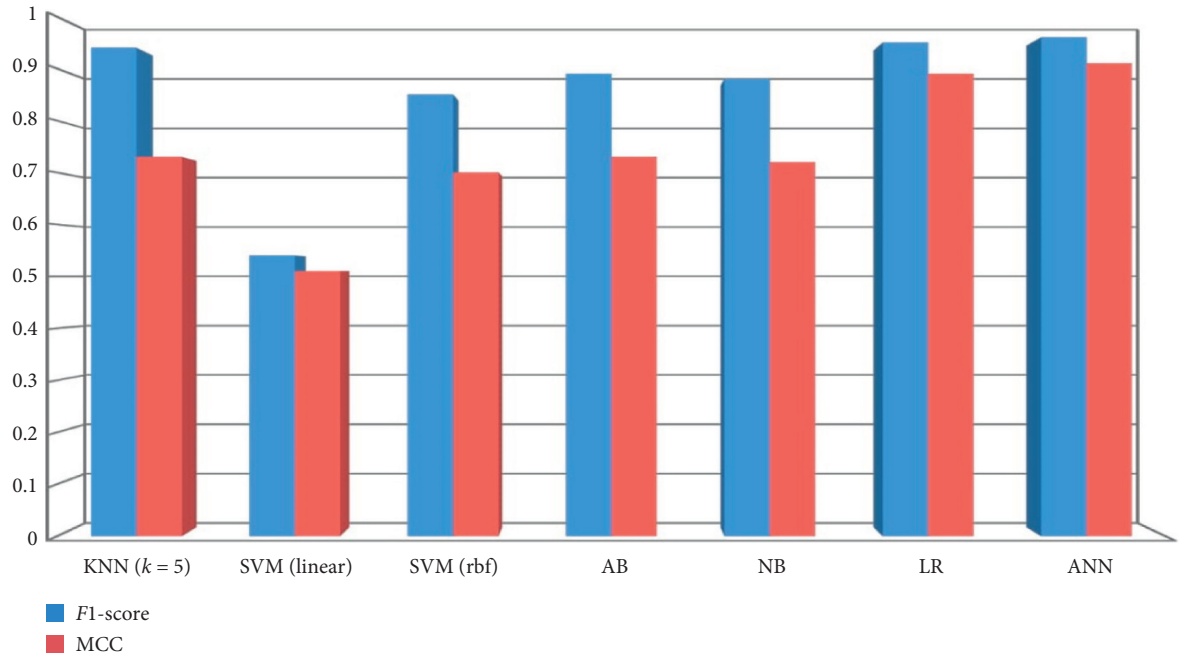

Figure 9: *F*1-score and MCC of all classifiers using the AlexNet transfer learning technique.

Figure 13 illustrates the ROC curves of all 6 ML classification algorithms on chest X-ray and CT image dataset using SqueezeNet transfer learning techniques.

4.4. Performance of All Classifiers Using VGG16 Architecture. The experimental results and performances of all 6 ML classification algorithms using VGG-16 transfer learning techniques are described in this subsection. Table 5 notifies the performances of all 6 classifiers using VGG-16 architecture.

From Table 5, it is obvious that LR performs brilliantly in terms of the entire performance as compared to other classification models. LR attained an accuracy of 96.82%, sensitivity of 97.80%, and specificity of 94.03% as shown in Table 5. The second best model while using VGG16 architecture is ANN which attained an accuracy of 96.56%, specificity of 93.28%, and sensitivity of 97.52%. Again, SVM

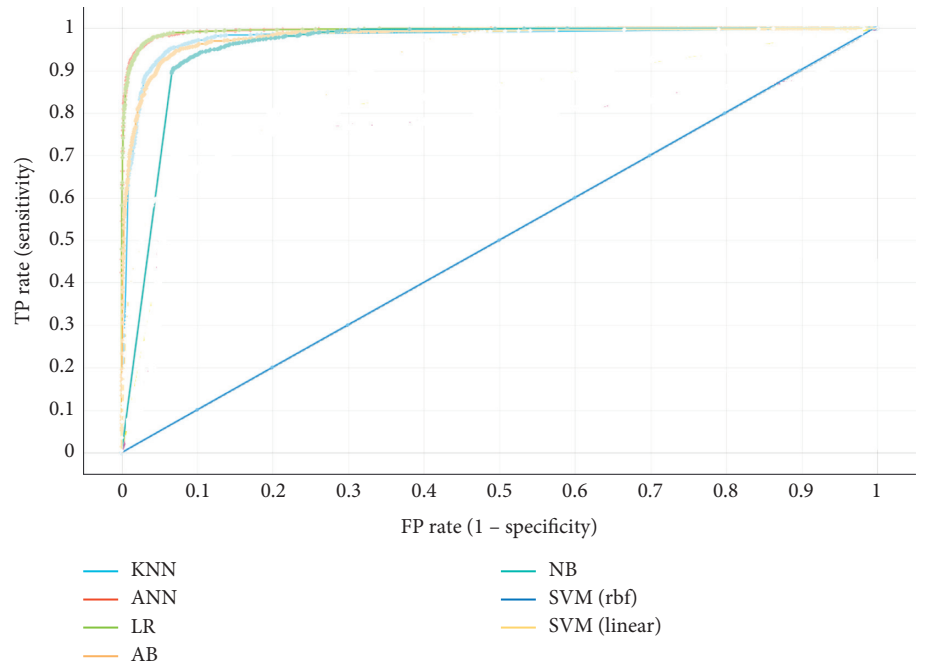

Figure 10: ROC curves of all 6 ML classifiers using the AlexNet transfer learning technique.

Table 4: Performance of all classifiers using the SqueezeNet transfer learning architecture.

Classification model	Accuracy	Sensitivity	Specificity	AUC	*F*1-score	MCC
KNN ($k = 5$)	95.16	96.44	91.05	97.80	0.95	0.73
SVM (rbf)	52.03	55.43	51.88	54.33	0.55	0.52
SVM (linear)	88.71	93.96	73.37	89.85	0.86	0.70
AB	90.12	93.13	81.43	87.34	0.90	0.74
NB	88.51	88.23	89.26	93.20	0.89	0.73
LR	96.24	97.62	91.94	99.20	0.96	0.90
ANN	96.97	97.52	92.99	99.40	0.97	0.92

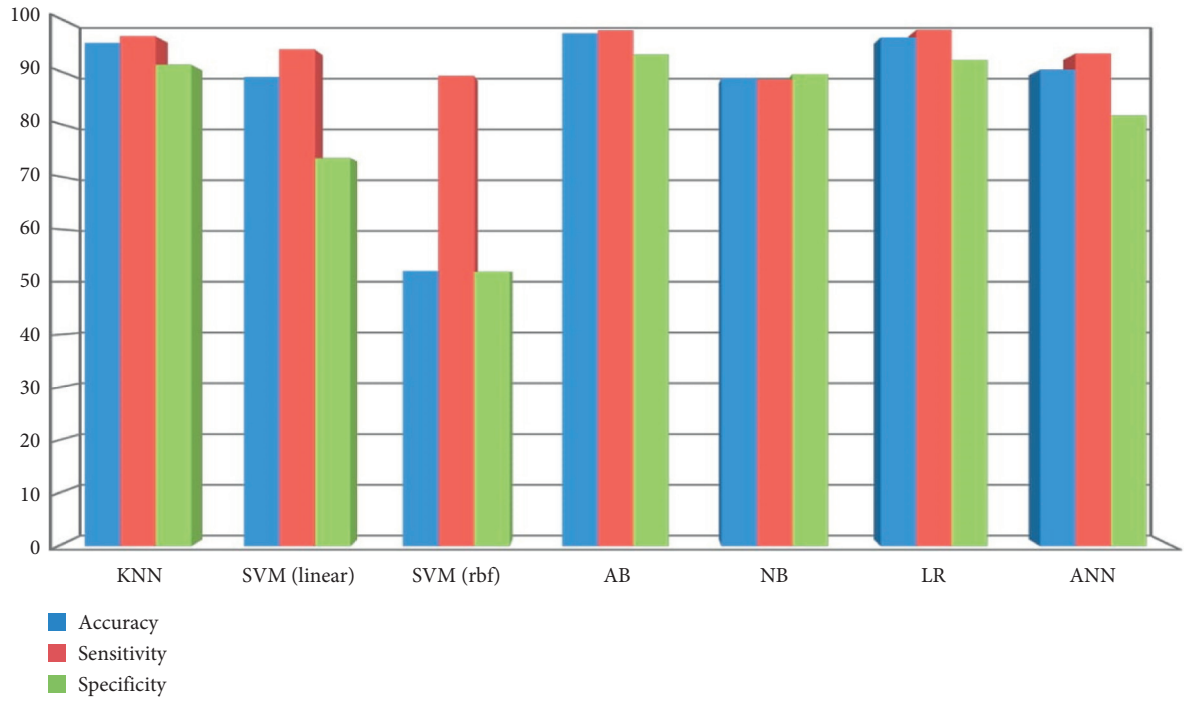

Figure 11: Performance of all classifiers using the SqueezeNet transfer learning technique.

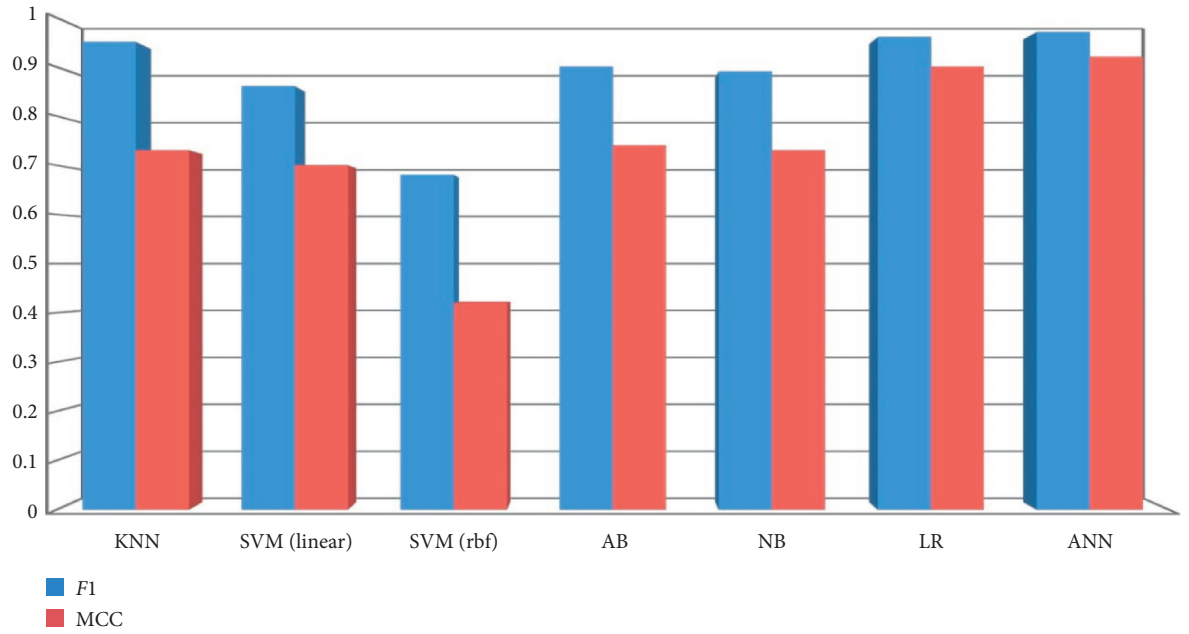

Figure 12: $F1$-score and MCC of all classifiers using the SqueezeNet transfer learning technique.

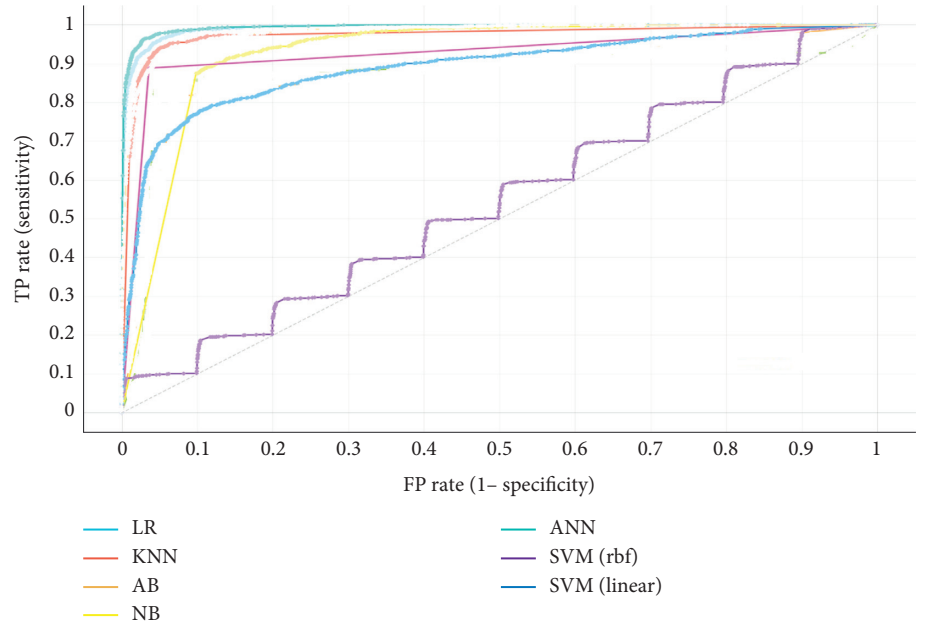

Figure 13: ROC curves of all 6 ML classifiers using the SqueezeNet transfer learning technique.

with kernel = "rbf" performed poorly as compared to other classification models and achieved an accuracy of 50.30% as shown in Table 5.

The performances of all 6 ML classification models, using VGG-16 transfer learning techniques, are shown in Figure 14.

Figure 15 shows the $F1$-score and MCC results of all 6 ML classification algorithms using VGG-16 transfer learning architecture while the ROC curves of all the utilized ML classification models are represented in Figure 16. It is observed from both Figures 15 and 16 that LR performed excellently in terms of these measures as compared to the other classifiers. The lowest performance was observed for SVM with kernel = "rbf" and stood last in this competition.

4.5. Performance of All Classifiers Using VGG19 Architecture. This subsection demonstrates the performance and experimental results obtained through all 6 ML classification models using the VGG-19 transfer learning technique. The transfer learning techniques extract useful features from the images and then present them to the classifiers for further processing. The performance of all 6 ML classification models is presented in Table 6.

Table 5: Performance of all classifiers using the VGG16 transfer learning techniques.

Classification model	Accuracy	Sensitivity	Specificity	AUC	*F*1-score	MCC
KNN ($k = 5$)	95.41	96.00	93.66	98.32	0.95	0.88
SVM (linear)	81.72	81.23	82.99	87.33	0.83	0.59
SVM (rbf)	50.30	86.24	47.42	69.30	0.70	0.35
AB	90.12	93.57	80.01	86.82	0.90	0.74
NB	86.50	84.41	92.69	94.10	0.87	0.70
LR	96.82	97.80	94.03	99.51	0.97	0.92
ANN	96.56	97.52	93.28	99.22	0.97	0.91

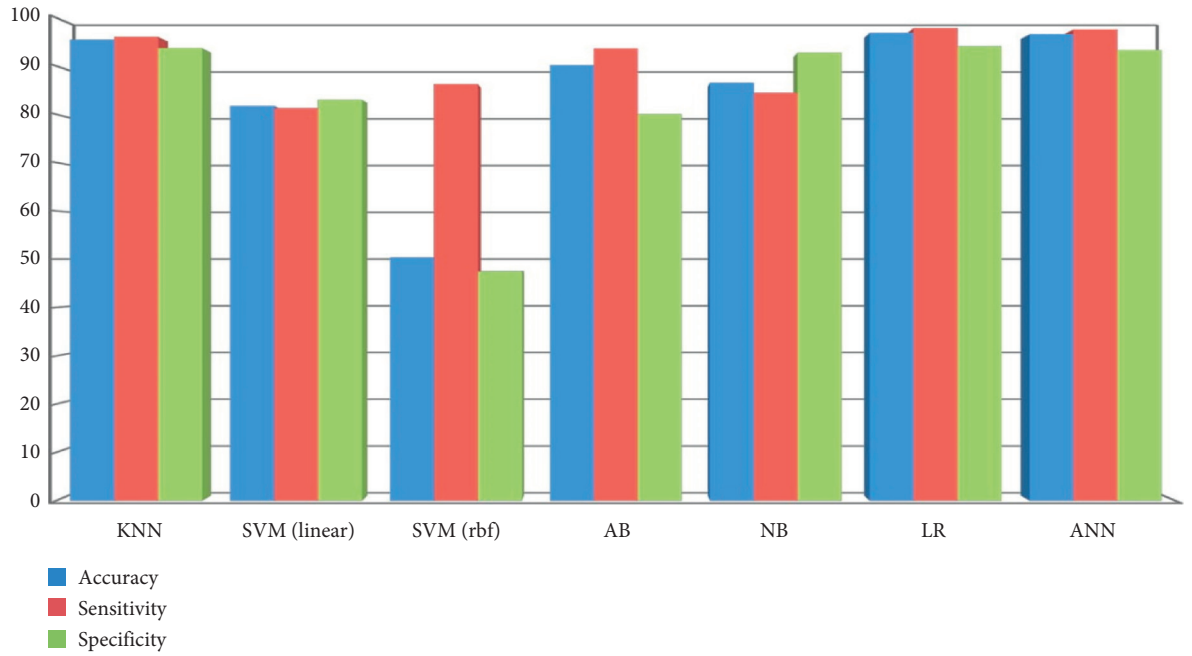

Figure 14: Performances of all classifiers using the VGG16 transfer learning technique.

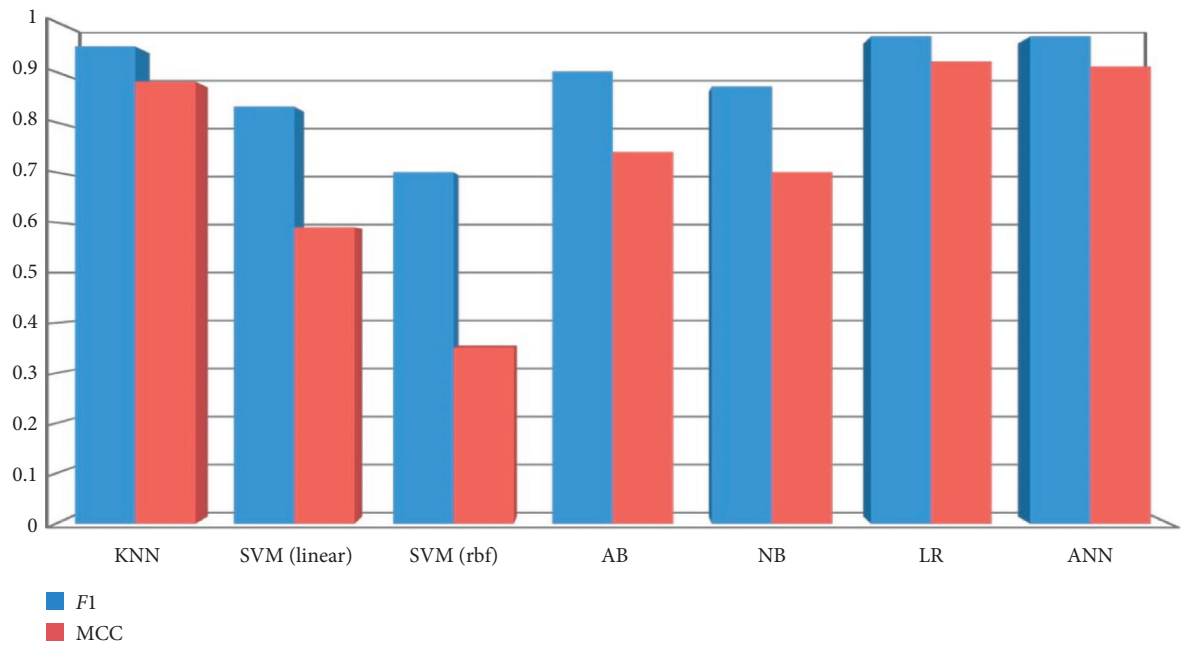

Figure 15: *F*1-score and MCC of all classifiers using the VGG16 transfer learning technique.

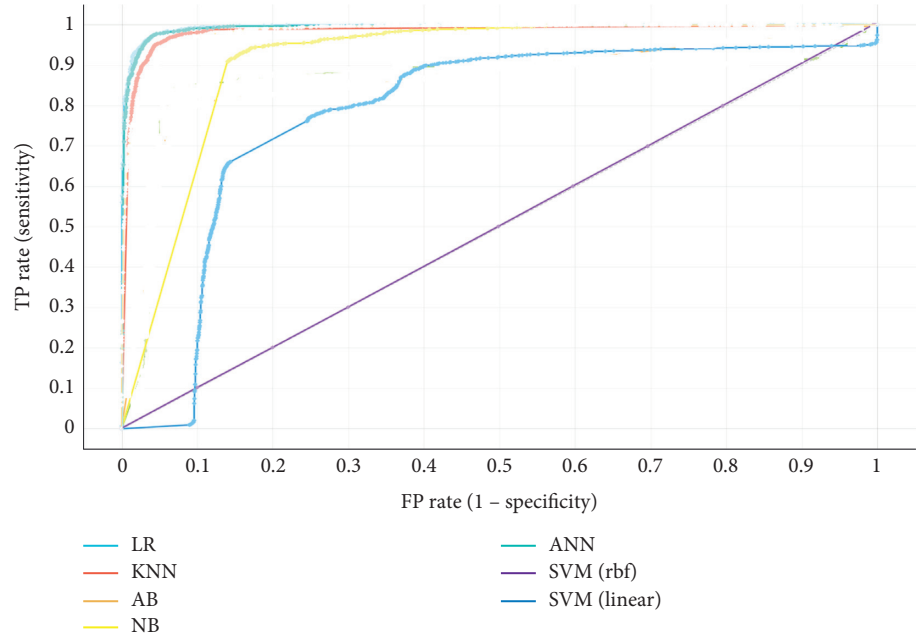

Figure 16: ROC curves of all 6 ML classifiers using the VGG16 transfer learning technique.

Table 6: Performance of all classifiers using the VGG19 transfer learning techniques.

Classification model	Accuracy	Sensitivity	Specificity	AUC	*F*1-score	MCC
KNN ($k = 5$)	96.10	96.09	94.11	97.89	0.96	0.89
SVM (linear)	84.70	82.20	84.89	87.55	0.85	0.61
SVM (rbf)	50.32	84.30	48.80	69.60	0.69	0.36
AB	92.42	90.27	82.10	86.92	0.91	0.75
NB	88.40	86.33	93.09	94.60	0.89	0.72
LR	96.92	97.60	94.79	98.91	0.97	0.91
ANN	97.01	97.62	93.80	99.12	0.97	0.92

Table 6 shows that the ANN classification model gives good performance while comparing it with the other models. ANN attained 97.01% classification accuracy, 97.62% sensitivity, and specificity of 93.80%. Sensitivity illustrates that the analytical test was positive and the person has pneumonia while the specificity shows that the diagnostic test was negative and the person does not have pneumonia and is healthy. LR also performed well and achieved good results, i.e., an accuracy of 96.92%, sensitivity of 97.60%, and specificity of 94.79%. Again, SVM with kernel = "rbf" shows the lowest performance by attaining the accuracy of 50.32%, specificity of 48.80%, and sensitivity of 84.30% as represented in Table 6.

Figure 17 demonstrates the performance of all 6 ML classification models using VGG-19 transfer learning architecture. ANN outclasses all the other classifiers in terms of accuracy, specificity, and specificity. SVM with kernel = "rbf" shows the lowest performance as shown in Figure 17. The MCC and *F*1-score results of all 6 ML classification algorithms using VGG-19 transfer learning architecture are described in Figure 18. From Figure 18, it is obvious that ANN performed brilliantly while SVM with kernel = "rbf" performed poorly.

Figure 19 demonstrates the ROC curves of all 6 ML classification algorithms on chest X-ray and CT image dataset using VGG-19 transfer learning techniques.

4.6. Performance of All Classifiers Using Inception-V3 Architecture. The performance and experimental results attained through all 6 ML classifiers using Inception-V3 DL architecture are discussed here in this subsection. The performance of all 6 ML classification models using Inception-V3 architecture is illustrated in Table 7.

Table 7 demonstrates that the ANN classification model performed really well in terms of the utilized performance measures as compared to the other models. ANN attained the classification accuracy of 97.19%, 97.88% sensitivity, and specificity of 94.92%. LR also showed good performance and achieved 97.08% classification accuracy, sensitivity of 97.90%, and specificity of 94.33%. Again, SVM with kernel = "rbf" shows the lowest performance as compared to the other classification models as shown in Table 7.

The performance of all 6 ML classification models using the Inception-V3 transfer learning technique is demonstrated in Figure 20. ANN classification model outperformed all the other classifiers in terms of accuracy, specificity, and specificity. SVM with kernel = "rbf" performed poorly and remained at the last position in the classifier performance competition.

The MCC and *F*1-score of all classification algorithms using Inception-V3 DL architecture are described in Figure 21, while the ROC curves of all classification algorithms

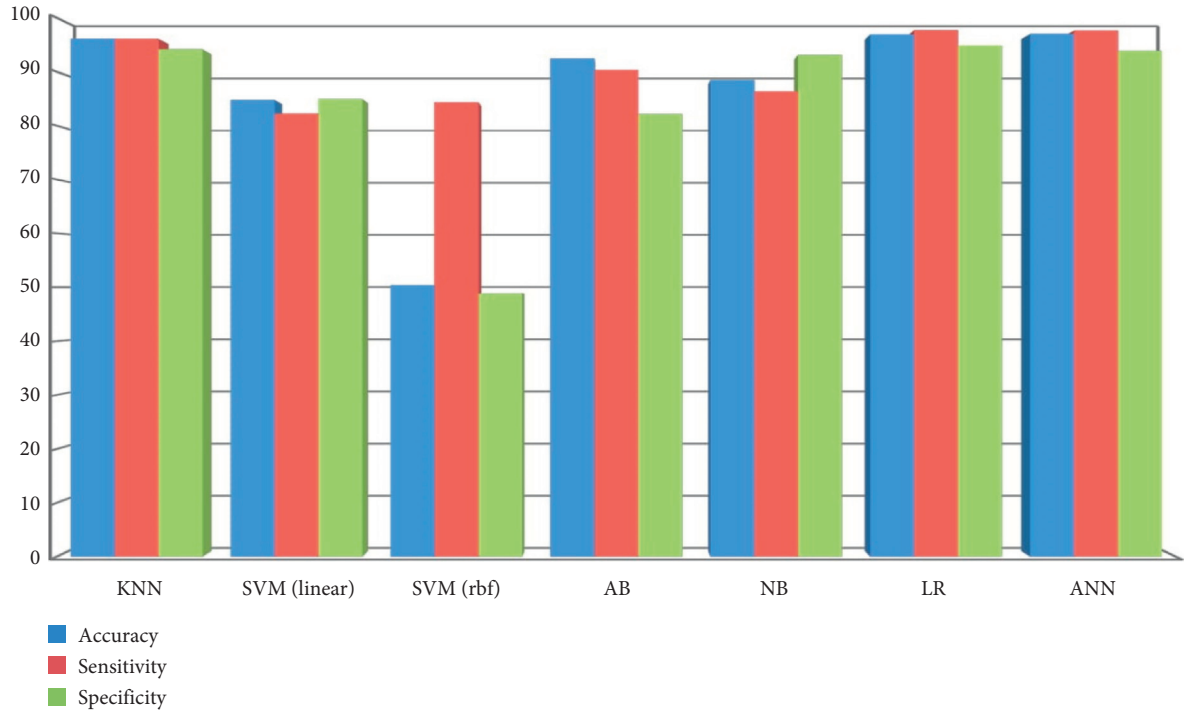

Figure 17: Performances of all classifiers using the VGG19 transfer learning technique.

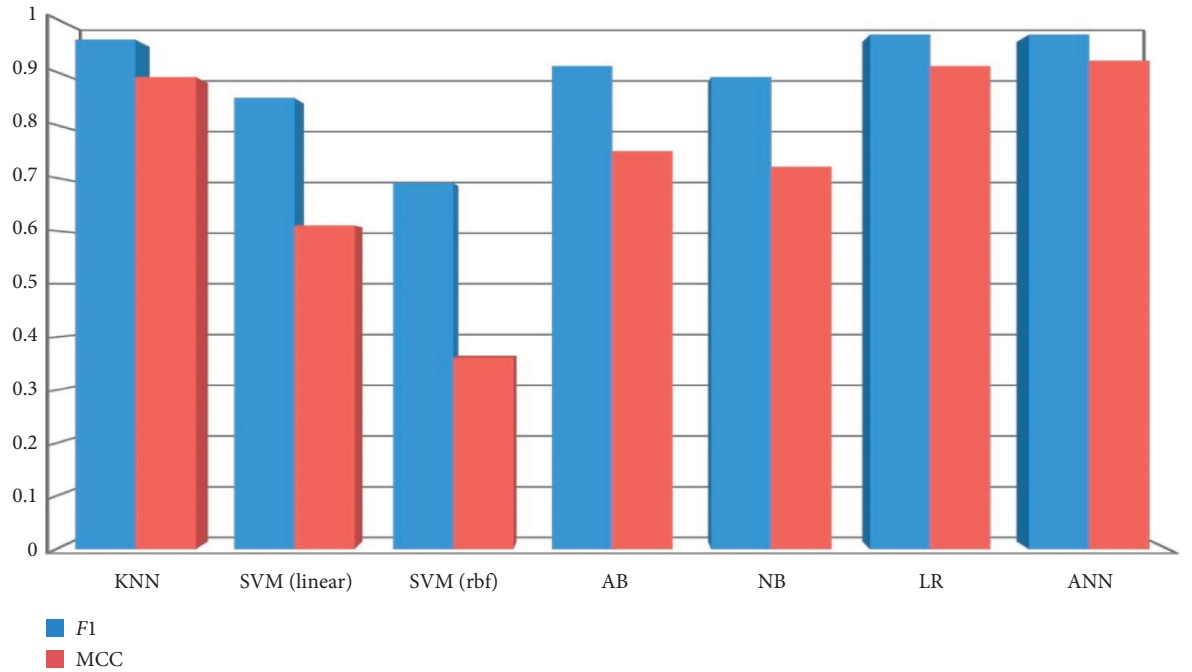

Figure 18: *F*1-score and MCC of all classifiers using the VGG19 transfer learning technique.

using Inception-V3 DL architecture on chest X-ray images are demonstrated in Figure 22.

The performance of all five utilized DCNN transfer learning techniques and 6 ML classification algorithms have been evaluated by using various performance evaluation metrics as discussed above. From the abovementioned results, it is obvious that Inception-V3 and ANN performed brilliantly by attaining the classification accuracy of 97.19%, sensitivity of 97.92%, specificity of 94.92%, AUC of 99.53%, *F*1-measure of 0.97, and MCC of 0.92. LR along with Inception-V3 performs very well by gaining the classification accuracy of 97.08%, sensitivity of 97.90%, specificity of 94.33%, AUC of 99.52%, *F*1-measure of 0.97, and 0.92 of MCC score and stood second in this regard. The

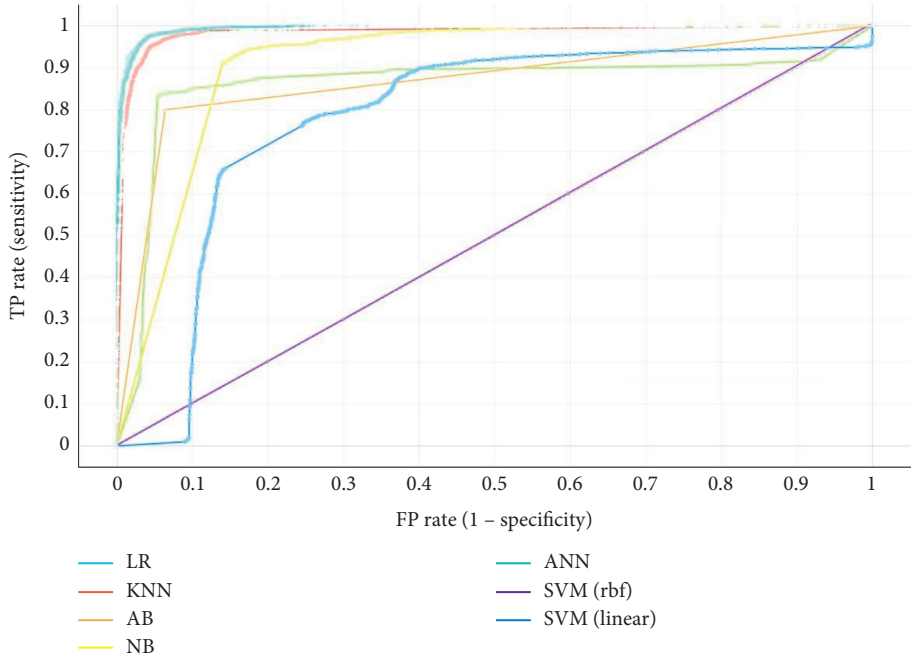

Figure 19: ROC curves of all 6 ML classifiers using the VGG19 transfer learning technique.

Table 7: Performance of all classifiers using the Inception-V3 transfer learning techniques.

Classification model	Accuracy	Sensitivity	Specificity	AUC	*F*1-score	MCC
KNN ($k = 5$)	94.20	94.24	94.03	97.80	0.94	0.85
SVM (linear)	85.02	92.03	86.41	87.33	0.85	0.78
SVM (rbf)	50.30	84.23	48.39	50.20	0.74	0.33
AB	87.40	91.33	78.91	83.62	0.87	0.67
NB	91.50	90.89	93.13	95.90	0.92	0.80
LR	97.08	97.90	94.33	99.52	0.97	0.92
ANN	97.19	97.88	94.92	99.53	0.97	0.92

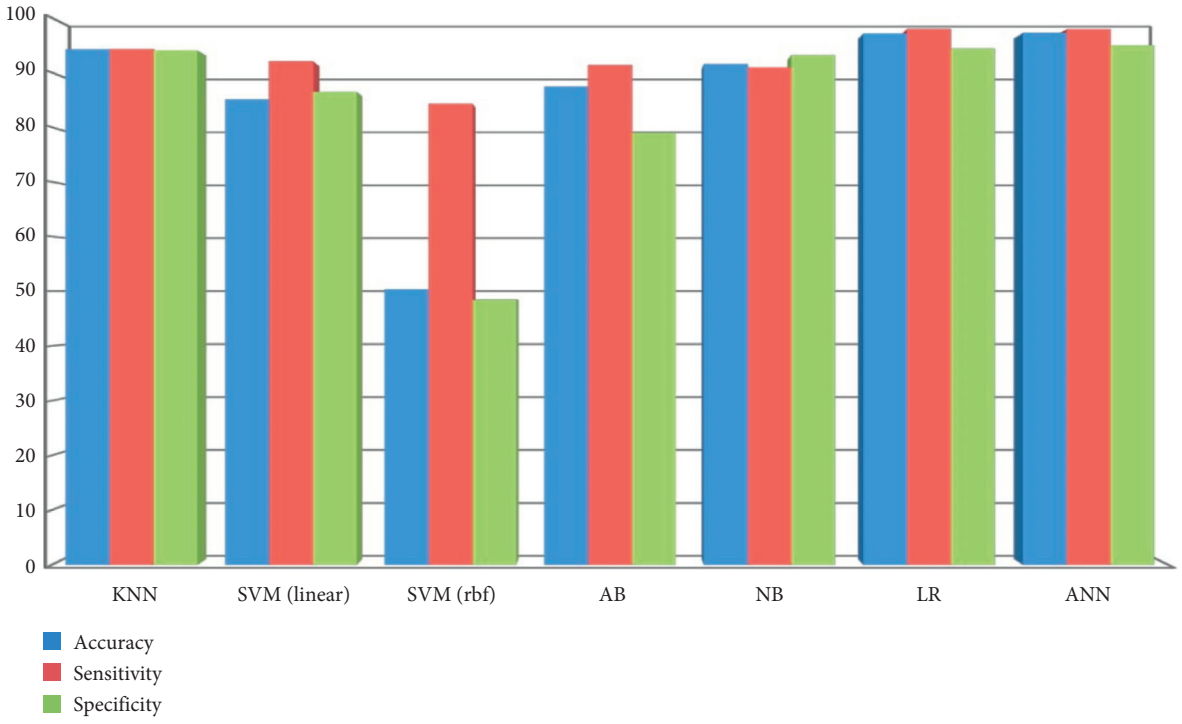

Figure 20: Performances of all classifiers using the Inception-V3 transfer learning technique.

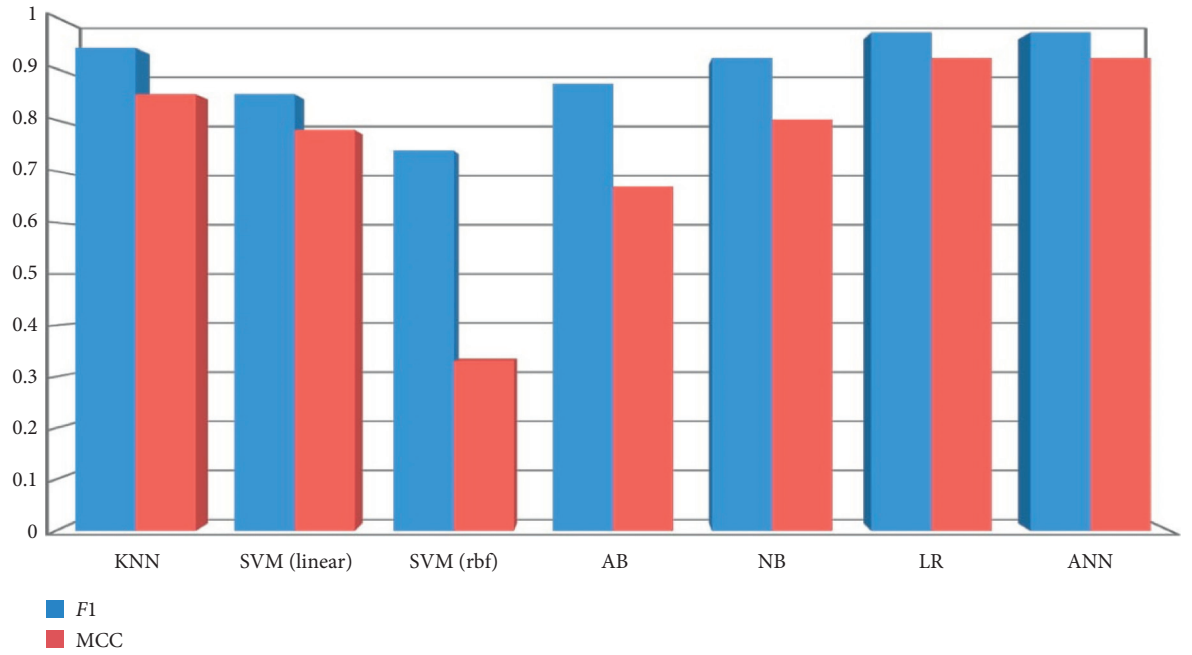

Figure 21: $F1$-score and MCC of all classifiers using the Inception-V3 transfer learning technique.

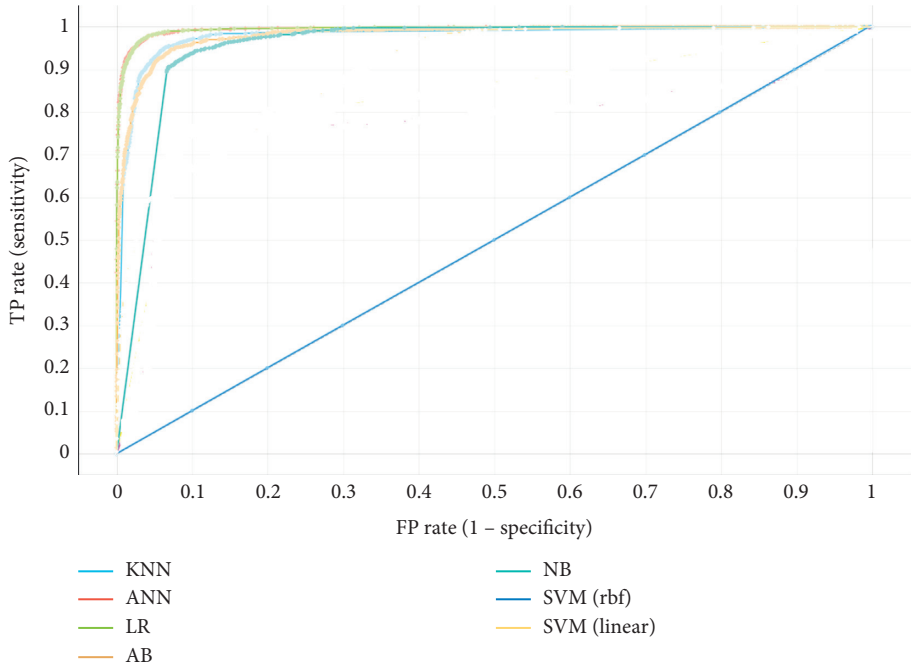

Figure 22: ROC curves of all 6 ML classifiers using the Inception-V3 transfer learning technique.

Table 8: A comparative study of the proposed system and previous approaches.

Publications	Approach	Accuracy (%)
Kermany et al. [51]	Convolutional neural network (CNN)	92.81
Stephen et al. [52]	DL model with 4 conv-layers and 2 dense layers	93.71
Saraiva et al. [53]	DL model with 6 conv-layers and 3 dense layers	95.29
Liang and Zheng [39]	DL model with 48 conv-layers and 2 dense layers	96.01
Wu et al. [54]	CNN + random forest	96.70
Proposed method	Intelligent framework (Inception-V3 + ANN)	97.19

performance of SVM with kernel = "rbf" is the worst among all the classification algorithms.

In addition, a comparative study of the proposed system is conducted with the previous ML and DL methods used in the past [39, 51–59]. A brief description of those approaches and the accuracies attained while using those approaches are demonstrated in Table 8.

Table 8 demonstrates a short summary of the previous approaches and classification accuracies attained via those techniques.

5. Conclusion

Pneumonia is an infective disease and is very hazardous for all ages and is more dangerous specifically for smokers, alcoholics, recent surgical patients, asthma patients, people with weakened immune systems, and children having an age of less than 5 years. The death ratio caused by pneumonia can be condensed if the patients are diagnosed at the initial stages and on-time medication and treatment is provided to them. This study proposes an ML- and DL-based intelligent predictive system for the diagnosis of pneumonia. Chest X-ray and CT image dataset was utilized for both training and testing of the proposed system. In order to improve the quality of visual information of each input image, various preprocessing methods such as intensity normalization, CLAHE, and Min-Max normalization have been utilized in this study. Five fine-tuned versions of DL transfer learning techniques such as AlexNet, SqueezeNet, VGG-16, VGG-19, and Inception-V3 were utilized to extract useful features from the X-ray images and then present them to the classifiers for further processing. Six imperative ML classification algorithms such as KNN, NB, ANN, SVM, LR, and AB were used to examine the efficiency of the proposed system. Numerous performance evaluation measures including classification accuracy, sensitivity, specificity, $F1$-score, AUC, MCC, and ROC were used to measure the performance of the proposed system. From the experimental results, it is observed that the Inception-V3 transfer learning technique and ANN performed brilliantly and attained the highest classification accuracy of 97.19%. Future work of this study includes the development of more optimized ML and DL algorithms that can significantly enhance the classification results. Further, developing an IoT-based real-time diagnosis of pneumonia disease is also one of the future works of this study.

Data Availability

All data is available in this paper.

Conflicts of Interest

The authors declare that they have no conflicts of interest.

Acknowledgments

This paper was supported by the Taif University Researchers Supporting Project Number TURSP-2020/126, Taif University, Taif, Saudi Arabia.

References

[1] C. Orbann, L. Sattenspiel, E. Miller, and J. Dimka, "Defining epidemics in computer simulation models: how do definitions influence conclusions?" *Epidemics*, vol. 19, pp. 24–32, 2017.

[2] J. H. Bates, G. D. Campbell, A. L. Barton et al., "Microbial etiology of acute pneumonia in hospitalized patients," *Chest*, vol. 101, no. 4, pp. 1005–1012, 1992.

[3] The Pneumonia Etiology Research for Child Health (PERCH), "Causes of severe pneumonia requiring hospital admission in children without HIV infection from Africa and Asia: the PERCH multi -country case-control study," *Lancet*, vol. 394, no. 10200, pp. 757–779, 2019.

[4] L. Liu, S. Oza, D. Hogan et al., "Global, regional, and national causes of under-5 mortality in 2000–15: an updated systematic analysis with implications for the sustainable development goals," *The Lancet*, vol. 388, no. 10063, pp. 3027–3035, 2016.

[5] Y. Tian, Y. Wu, H. Liu et al., "The impact of ambient ozone pollution on pneumonia: a nationwide time-series analysis," *Environment International*, vol. 136, Article ID 105498, 2020.

[6] E. Prina, O. T. Ranzani, and A. Torres, "Community-acquired pneumonia," *The Lancet*, vol. 386, no. 9998, pp. 1097–1108, 2015.

[7] T. Welte, A. Torres, and D. Nathwani, "Clinical and economic burden of community-acquired pneumonia among adults in Europe," *Thorax*, vol. 67, no. 1, pp. 71–79, 2012.

[8] K. Watkins and D. Sridhar, "Pneumonia: a global cause without champions," *Lancet*, vol. 392, pp. 718-719, 2018.

[9] K. Kondo, K. Suzuki, M. Washio et al., "Effectiveness of 23-valent pneumococcal polysaccharide vaccine and seasonal influenza vaccine for pneumonia among the elderly—selection of controls in a case-control study," *Vaccine*, vol. 35, no. 36, pp. 4806–4810, 2017.

[10] K. E. Asnaoui, Y. Chawki, and A. Idri, "Automated methods for detection and classification pneumonia based on X-ray images using deep learning," 2020, https://arxiv.org/abs/2003.14363.

[11] The Lancet Global Health, "The disgraceful neglect of childhood pneumonia," *The Lancet. Global Health*, vol. 6, no. 12, p. e1253, 2018.

[12] https://ourworldindata.org/grapher/pneumonia-mortality-by-age.

[13] Y. Yang, F. Peng, R. Wang et al., "The deadly coronaviruses: the 2003 SARS pandemic and the 2020 novel coronavirus epidemic in China," *Journal of Autoimmunity*, vol. 109, Article ID 102434, 2020.

[14] T. G. Ksiazek, D. Erdman, C. S. Goldsmith et al., "A novel coronavirus associated with severe acute respiratory syndrome," *New England Journal of Medicine*, vol. 348, no. 20, pp. 1953–1966, 2003.

[15] A. C. Walls, Y.-J. Park, M. A. Tortorici, A. Wall, A. T. McGuire, and D. Veesler, "Structure, function, and antigenicity of the SARS-CoV-2 spike glycoprotein," *Cell*, vol. 181, no. 2, 2020.

[16] B. Hu, L.-P. Zeng, X.-L. Yang et al., "Discovery of a rich gene pool of bat SARS-related coronaviruses provides new insights into the origin of SARS coronavirus," *PLoS Pathogens*, vol. 13, no. 11, 2017.

[17] C. Wu, Y. Liu, Y. Yang et al., "Analysis of therapeutic targets for SARS-CoV-2 and discovery of potential drugs by computational methods," *Acta Pharmaceutica Sinica B*, vol. 10, no. 5, pp. 766–788, 2020.

[18] World Health Organization, "Middle East respiratory syndrome coronavirus (MERS- CoV)," 2018, https://www.who.int/emergencies/mers-cov/en/.

[19] S. Van Boheemen, M. De Graaf, C. Lauber et al., "Genomic characterization of a newly discovered coronavirus associated with acute respiratory distress syndrome in humans," *MBio*, vol. 3, no. 6, Article ID e00473, 2012.

[20] A. M. Zaki, S. Van Boheemen, T. M. Bestebroer, A. D. M. E. Osterhaus, and R. A. M. Fouchier, "Isolation of a novel coronavirus from a man with pneumonia in Saudi Arabia," *New England Journal of Medicine*, vol. 367, no. 19, pp. 1814–1820, 2012.

[21] B. Hijawi, M. Abdallat, A. Sayaydeh et al., "Novel coronavirus infections in Jordan, April 2012: epidemiological findings from a retrospective investigation," *Eastern Mediterranean Health Journal*, vol. 19, no. 1, pp. S12–S18, 2013.

[22] H. Z. Farooq, E. Davies, S. Ahmad et al., "Middle East respiratory syndrome coronavirus (MERS-CoV)-surveillance and testing in north England from 2012 to 2019," *International Journal of Infectious Diseases*, vol. 93, 2020.

[23] World Health Organization, "Middle East respiratory syndrome coronavirus (MERS-CoV)," 2019, https://www.who.int/news-room/fact-sheets/detail/middle-east-respiratorysyndrome-coronavirus-(merscov).

[24] H. A. Mohd, J. A. Al-Tawfiq, and Z. A. Memish, "Middle East respiratory syndrome coronavirus (MERS-CoV) origin and animal reservoir," *Virology Journal*, vol. 13, no. 1, p. 87, 2016.

[25] N. Wang, O. Rosen, L. Wang et al., "Structural definition of a neutralization-sensitive epitope on the MERS-CoV S1-NTD," *Cell Reports*, vol. 28, no. 13, pp. 3395–3405, 2019.

[26] R. Aguanno, A. ElIdrissi, A. A. Elkholy et al., "MERS: progress on the global response, remaining challenges and the way forward," *Antiviral Research*, vol. 159, pp. 35–44, 2018.

[27] G. Lippi, M. Plebani, and B. M. Henry, "Thrombocytopenia is associated with severe coronavirus disease 2019 (COVID-19) infections: a meta-analysis," *Clinica Chimica Acta*, vol. 506, 2020.

[28] A. Cortegiani, G. Ingoglia, M. Ippolito, A. Giarratano, and S. Einav, "A systematic review on the efficacy and safety of chloroquine for the treatment of COVID-19," *Journal of Critical Care*, vol. 57, 2020.

[29] S. Tian, N. Hu, J. Lou et al., "Characteristics of COVID-19 infection in Beijing," *Journal of Infection*, vol. 80, no. 4, pp. 401–406, 2020.

[30] A. Wilder-Smith, C. J. Chiew, and V. J. Lee, "Can we contain the COVID-19 outbreak with the same measures as for SARS?" *The Lancet Infectious Diseases*, vol. 20, 2020.

[31] World Health Organization, "Novel coronavirus (2019-nCoV) situation report—28," 2020, https://www.who.int/docs/default-source/coronaviruse/situation-reports/20200217-sitrep-28-covid-19.pdf?sfvrsn=a19cf2ad_2.

[32] K. Roosa, Y. Lee, R. Luo et al., "Real-time forecasts of the COVID-19 epidemic in China from February 5th to February 24th, 2020," *Infectious Disease Modelling*, vol. 5, pp. 256–263, 2020.

[33] J. Yang, Y. Zheng, X. Gou et al., "Prevalence of comorbidities in the novel Wuhan coronavirus (COVID-19) infection: a systematic review and meta-analysis," *International Journal of Infectious Diseases*, vol. 94, 2020.

[34] R. Simcock, T. V. Thomas, C. E. Mercy et al., "COVID-19: global radiation oncology's targeted response for pandemic preparedness," *Clinical and Translational Radiation Oncology*, vol. 22, 2020.

[35] Y. Muhammad, M. Tahir, M. Hayat, and K. T. Chong, "Early and accurate detection and diagnosis of heart disease using intelligent computational model," *Scientific Reports*, vol. 10, pp. 1–17, 2020.

[36] M. Elkhodr, B. Alsinglawi, and M. Alshehri, "A privacy risk assessment for the internet of things in healthcare," *Applications of Intelligent Technologies in Healthcare*, Springer, Berlin, Germany, 2019.

[37] D. Kermany, K. Zhang, and M. Goldbaum, "Labeled optical coherence tomography (oct) and chest X-ray images for classification," *Mendeley Data*, vol. 2, 2018.

[38] M. Toğaçar, B. Ergen, Z. Cömert, and F. Ozyurt, "A deep feature learning model for pneumonia detection applying a combination of MRMR feature selection and machine learning models," *IRBM*, vol. 41, 2019.

[39] G. Liang and L. Zheng, "A transfer learning method with deep residual network for pediatric pneumonia diagnosis," *Computer Methods and Programs in Biomedicine*, vol. 187, Article ID 104964, 2019.

[40] A. K. Jaiswal, P. Tiwari, S. Kumar, D. Gupta, A. Khanna, and J. J. P. C. Rodrigues, "Identifying pneumonia in chest X-rays: a deep learning approach," *Measurement*, vol. 145, pp. 511–518, 2019.

[41] Y. Ge, Q. Wang, L. Wang et al., "Predicting post-stroke pneumonia using deep neural network approaches," *International Journal of Medical Informatics*, vol. 132, Article ID 103986, 2019.

[42] I. Sirazitdinov, M. Kholiavchenko, T. Mustafaev, Y. Yixuan, R. Kuleev, and B. Ibragimov, "Deep neural network ensemble for pneumonia localization from a large-scale chest X-ray database," *Computers & Electrical Engineering*, vol. 78, pp. 388–399, 2019.

[43] H. Behzadi-khormouji, H. Rostami, S. Salehi et al., "Deep learning, reusable and problem-based architectures for detection of consolidation on chest X-ray images," *Computer Methods and Programs in Biomedicine*, vol. 185, Article ID 105162, 2020.

[44] A. Bhandary, G. A. Prabhu, V. Rajinikanth et al., "Deep-learning framework to detect lung abnormality—a study with chest X-ray and lung CT scan images," *Pattern Recognition Letters*, vol. 129, pp. 271–278, 2020.

[45] M. D. Alshehri and F. K. Hussain, "A fuzzy security protocol for trust management in the internet of things (fuzzy-IoT)," *Computing*, vol. 101, no. 7, pp. 791–818, 2019.

[46] M. D. Alshehri, F. Hussain, M. Elkhodr, and B. S. Alsinglawi, "A distributed trust management model for the internet of things (DTM-IoT)," *Recent Trends and Advances in Wireless and IoT-Enabled Networks*, Springer, Berlin, Germany, 2019.

[47] O. Mohamed, O. Mohammed, A. Brahim, and E. A. Khalid, *Content-Based Image Retrieval Using Convolutional Neural Networks*, Springer, Berlin, Germany, 2018.

[48] K. Simonyan and A. Zisserman, "Very deep convolutional networks for large-scale image recognition," 2014, https://arxiv.org/abs/1409.1556.

[49] C. Szegedy, W. Liu, Y. Jia et al., "Going deeper with convolutions," Technical report, Cornell University, New York, NY, USA, 2014.

[50] C. Szegedy, V. Vanhoucke, S. Ioffe, and J. Shlens, "Rethinking the inception architecture for computer vision," 2015, https://arxiv.org/abs/1512.00567.

[51] D. S. Kermany, M. Goldbaum, W. Cai et al., "Identifying medical diagnoses and treatable diseases by image-based deep learning," *Cell*, vol. 172, no. 5, pp. 1122–1131, 2018.

[52] O. Stephen, M. Sain, U. J. Maduh et al., "An efficient deep learning approach to pneumonia classification in healthcare,"

Journal of Healthcare Engineering, vol. 2019, Article ID 4180949, 7 pages, 2019.

[53] A. Saraiva, N. Ferreira, L. Sousa et al., "Classification of images of childhood pneumonia using convolutional neural networks," in *Proceedings of the 12th International Joint Conference on Biomedical Engineering Systems and Technologies*, pp. 112–119, Prague, Czech Republic, February 2019.

[54] H. Wu, P. Xie, H. Zhang et al., "Predict pneumonia with chest X-ray images based on convolutional deep neural learning networks," *Journal of Intelligent & Fuzzy Systems*, vol. 39, no. 12, pp. 1–15, 2020.

[55] A. Conversano, F. Melillo, A. Napolano et al., "Renin-angiotensin-aldosterone system inhibitors and outcome in patients with SARS-CoV-2 pneumonia," *Hypertension*, vol. 76, no. 2, pp. e10–e12, 2020.

[56] F. Mei, J. Fan, J. Yuan et al., "Comparison of venous thromboembolism risks between COVID-19 pneumonia and community-acquired pneumonia patients," *Arteriosclerosis, Thrombosis, and Vascular Biology*, vol. 40, no. 9, pp. 2332–2337, 2020.

[57] L. Nicolai, A. Leunig, S. Brambs et al., "Immunothrombotic dysregulation in COVID-19 pneumonia is associated with respiratory failure and coagulopathy," *Circulation*, vol. 142, no. 12, pp. 1176–1189, 2020.

[58] S. Salomaa, E. Cardis, S. D. Bouffler, M. J. Atkinson, and N. Hamada, "Low dose radiation therapy for COVID-19 pneumonia: is there any supportive evidence?" *International Journal of Radiation Biology*, vol. 96, no. 10, pp. 1224–1227, 2020.

[59] B. Van Ginneken, "The potential of artificial intelligence to analyze chest radiographs for signs of COVID-19 pneumonia," *Radiological Society of North America*, vol. 299, 2021.

Hindawi
Mobile Information Systems
Volume 2023, Article ID 9803212, 1 page
https://doi.org/10.1155/2023/9803212

Retraction

Retracted: Prediction of College Students' Psychological Crisis Based on Data Mining

Mobile Information Systems

Received 8 August 2023; Accepted 8 August 2023; Published 9 August 2023

Copyright © 2023 Mobile Information Systems. This is an open access article distributed under the Creative Commons Attribution License, which permits unrestricted use, distribution, and reproduction in any medium, provided the original work is properly cited.

This article has been retracted by Hindawi following an investigation undertaken by the publisher [1]. This investigation has uncovered evidence of one or more of the following indicators of systematic manipulation of the publication process:

(1) Discrepancies in scope
(2) Discrepancies in the description of the research reported
(3) Discrepancies between the availability of data and the research described
(4) Inappropriate citations
(5) Incoherent, meaningless and/or irrelevant content included in the article
(6) Peer-review manipulation

The presence of these indicators undermines our confidence in the integrity of the article's content and we cannot, therefore, vouch for its reliability. Please note that this notice is intended solely to alert readers that the content of this article is unreliable. We have not investigated whether authors were aware of or involved in the systematic manipulation of the publication process.

Wiley and Hindawi regrets that the usual quality checks did not identify these issues before publication and have since put additional measures in place to safeguard research integrity.

We wish to credit our own Research Integrity and Research Publishing teams and anonymous and named external researchers and research integrity experts for contributing to this investigation.

The corresponding author, as the representative of all authors, has been given the opportunity to register their agreement or disagreement to this retraction. We have kept a record of any response received.

References

[1] J. Liu, G. Shi, J. Zhou, and Q. Yao, "Prediction of College Students' Psychological Crisis Based on Data Mining," *Mobile Information Systems*, vol. 2021, Article ID 9979770, 7 pages, 2021.

Hindawi
Mobile Information Systems
Volume 2021, Article ID 9979770, 7 pages
https://doi.org/10.1155/2021/9979770

RETRACTED

Research Article

Prediction of College Students' Psychological Crisis Based on Data Mining

Jingjing Liu,[1] Guangyuan Shi,[2] Jing Zhou,[1] and Qiumei Yao[3]

[1]*HebeiWomen's Vocational College, Shijiazhuang 050091, Hebei, China*
[2]*Cangzhou Vocational and Technical College, Cangzhou 061017, Hebei, China*
[3]*Hebei Normal University, Shijiazhuang 050024, Hebei, China*

Correspondence should be addressed to Guangyuan Shi; yaoqm7707@stu.hebtu.edu.cn

Received 9 March 2021; Revised 24 April 2021; Accepted 8 May 2021; Published 17 May 2021

Academic Editor: Mian Ahmad Jan

Copyright © 2021 Jingjing Liu et al. This is an open access article distributed under the Creative Commons Attribution License, which permits unrestricted use, distribution, and reproduction in any medium, provided the original work is properly cited.

The development of a college students' psychological management system has become an essential indicator to monitor and prevent the psychological crisis. University student management databases accumulate massive data, but the conventional data processing tasks are restricted to simple statistical analysis, storage, and query management. This paper discusses the application of big data technology for the current psychological management system by investigating psychological crisis screening indicators. Data mining techniques are used to realize the dynamic management of psychological early warning data, real-time monitoring of high-risk groups' psychology, and improvement of the accuracy and effectiveness of early identification and warning of students' psychological crisis. Based on a combination of qualitative and quantitative analysis, we conduct a series of studies on three typical types of network public opinions, i.e., Internet rumors, online public opinions of college students, and emergent public health incidents in terms of the transmission mechanism, early warning, and decision-making mechanism, as well as the evolution mechanism of the network public opinion.

1. Introduction

College students are a representative group of netizens. They are highly educated and have a much higher utilization rate of the Internet. They are a powerful force in the network public opinion and have a significant influence within various groups. The way students are organized determines the nature of problems and confusions that exist and are often revealed and disseminated through the Internet. Compared with the general public's online opinion, college students' opinion contains more content and spreads faster. Therefore, it is of significant interest to study specific network public opinion judgment by taking college students as the representatives. Considering the characteristics of college students' online public opinion, using intuitionistic fuzzy reasoning judgment, analytic hierarchy process, and expert scoring method, a set of network public opinion theory model is constructed to provide theoretical basis and data support for college students' online public opinion management.

In recent years, college students' mental health has aroused the general concern of the whole society. The in-depth study of college student's mental health and the exploration of college students' psychological intervention mode are the hotspots of scholars worldwide. Data mining technology is incomparable to other technologies in mining hidden rules in business data and solving specific problems. With the maturity of data mining technology, many scholars continue to research methods and apply data mining techniques to universities' teaching and management fields. The authors of this paper studied sufficient literature by conducting in-depth research and study on data mining technology and tried to apply it to the data of college students' psychological problems. This paper discusses the basic principles and concepts of data mining technology. The tasks, methods, and application fields of data mining are discussed to analyze its feasibility for solving college students' psychological problems by making a detailed analysis of fuzzy mathematics. This paper uses a decision tree

algorithm to calculate which attribute is most relevant to psychological issues (i.e., the attribute with the most significant information gain value) as the decision tree's root node. Next, it uses an iterative, recursive method to classify the remaining attributes with the same algorithm to form a decision tree. It establishes a classification tree model to predict and analyze the psychological problems of college students. The Apriori algorithm is used to analyze the internal relationship between students' psychological problems and students' attributes to provide decision-making support information for the school psychological counseling center and make mental health education more targeted and purposeful. The author independently developed an excellent performance, simple, and practical data mining system for psychological problems. The system has a friendly interface and has data file access, data preprocessing, decision tree generation, association rules generation, rule interpretation, and rule preservation. With this data mining system, some knowledge of classification rules and association rules is obtained successfully. Considering students' psychological problems in our university as an example, the function verification experiment of data mining of students' psychological problems is carried out. Finally, it points out the shortcomings of this paper and the direction of future efforts.

The rest of this paper is organized as follows. In Section 2, the related work is discussed. In Section 3, the intuitionistic fuzzy early warning model of college students' opinion is presented. In Section 4, a dynamic method based on bootstrap estimation is proposed for prediction of college students' psychological crisis based on data mining. In Section 5, the experimental results and analysis are discussed. Finally, the paper is concluded with future research directions in Section 6.

2. Related Work

Fuzzy mathematics is a branch of mathematics that studies and deals with ambiguity in mathematical problems. The basis of modern mathematics is Cantor's set theory. This theory defines that each set consists of explicit elements that either belong to or do not belong to a certain set and cannot be ambiguous. However, many words in the objective world have no clear quantitative boundaries, such as youth, tallness, and heat. The phenomena that exist in these objective worlds are also called ambiguity. Probability has been used in traditional uncertainty studies. The classical inductive probability logic assumes that the parties can exhaust all experiments' possible outcomes and know the probability of any event outcome. They cannot express ignorance, discord, distrust, and lack of trust. Zadeh believes that elements only belong to or do not belong to a specific set in Cantor's set theory [1]. Such binary logic has little place. In 1965, fuzzy set theory was proposed, which created fuzzy mathematics and applied mathematical methods to study ambiguity. In fuzzy set theory, for any element $u \in U$ in a given universe U, a corresponding real number $u_A(u) \in [0, 1]$ belonging to the interval [0, 1] is given. This corresponding number is called the membership of u to A and is used to describe the extent to which u belongs to $\underline{A}$ so that precise mathematical tools can be used to describe inaccurate ambiguities.

Fuzzy evaluation deals with fuzzy evaluation objects through precise mathematical means and can make scientific, reasonable, and close-to-the-actual quantitative assessment of the data with vague information. The evaluation result is a vector, not a point value, and the information contained is rich. It can accurately describe the object to be evaluated and further process and obtain reference information. However, the fuzzy comprehensive evaluation method is computationally complex, and the subjectivity of the index weight vector is strong. When the index set U is large, i.e., the number of index sets is large, under the conditional constraint that the weight vector is 1 (the relative membership weight), then the coefficients tend to be too small, and the weight vector does not match the fuzzy matrix. Moreover, the result is superfuzzy, and the resolution is very poor. It is impossible to distinguish who has a higher degree of membership or even can cause the judgment to fail. Dempster-Shafer [2, 3] proposed a trust and likelihood function to apply it to uncertainty measurement. It generalizes the classical probability and proposes a method to describe the parties' insufficient ignorance in determining the probability. It has been widely studied and applied in different fields. However, fuzzy set theory only contains the membership degree of the element, that is, it can only be used to describe the evidence of support and unsupported elements, while ignoring that the element may not support or oppose, that is, the nature of neutrality.

To solve this problem better, Atanassov [4] first proposed an intuitionistic fuzzy concept in 1986. He proved that the fuzzy set is only a special case of the intuitionistic fuzzy set. The intuitionistic fuzzy set uses the nonmembership function to represent the neutral state of the element for the set, which can more accurately describe the object's ambiguity. Intuitionistic fuzzy sets have better inference accuracy and description ability than fuzzy sets. Intuitionistic fuzzy set theory has been developed and applied to various problems. Several scholars have performed significant studies [5–9] on this theory by presenting the algorithms of intuitionistic fuzzy sets. By combining intuitionistic fuzzy sets with L-fuzzy sets and interval-valued fuzzy sets, straight L-fuzzy sets and interval values were proposed. For this purpose, the author in [10] first proposed two theorems about modular operators but did not explicitly point out these theorems' meaning. Until 2003, Atanassov [11] revisited these two theorems in the literature, used them to discuss the separation conditions of intuitionistic fuzzy sets, and finally applied them to the decision-making process. Other scholars have performed a lot of research on the theory of intuitionistic fuzzy sets. Hu et al. [12] defined the concepts of expansion and concentration of intuitionistic fuzzy sets and discussed their properties. Various examples show that these concepts are very useful for dealing with linguistic variables. Bustince and Burillo [13–16] proved that the vague set is an intuitionistic fuzzy set and studied some functional properties of the intuitionistic fuzzy relation and the entropy of the S-intuitionistic fuzzy set. The authors in [17]–19] proposed a very close relationship between D-S theory and fuzzy set theory and offered a new likelihood function intuitionistic fuzzy set reasoning. At present,

RETRACTED

people's research on fuzzy reasoning continues to deepen and promote the development of theory.

3. Intuitionistic Fuzzy Early Warning Model of School Students' Internet Public Opinion

In this paper, the research on the network public opinion of colleges and universities is carried out. The analysis mode of college students' online public opinion is used to express the public opinion situation. The purpose is to explain the evolution law of college students' network public opinion from a deeper level. We use the intuitionistic fuzzy set theory and the analytic hierarchy process to construct a mathematical model to monitor the college students' network public opinion and determine the network public opinion warning level.

3.1. Intuitionistic Fuzzy Set of College Students' Online Public Opinion Warning Level. We adopt a linear mapping method for mapping the regional distribution of audience, the number of people participating in the discussion, the speed of the network sensation of the university, the source of the network grievances of the university, the way of its dissemination, the public's emotional tendency, attention, and hotspots to the values in the interval [0, 1].

For calculating the membership degree of each factor, the intuitionistic fuzzy comprehensive evaluation method is used. The factors involved in the reasoning include the analysis of the topic itself, the audience's analysis, and the analysis of the connection between the audience and the topic. Correspondingly, their respective domains are the domain of importance of a particular topic, the audience's reflection domain, and the domain of contact between the audience and the topic.

3.1.1. Judging the Network Public Opinion Warning Level. The warning level is determined using the following factors.

(1) Intuitionistic fuzzy subsets reflecting the importance of a particular topic

The importance of a particular topic can be derived from the method described above for calculating the importance of the topic. Let $X_1 \in [0,1]$ be the normalized importance, and record the corresponding domain $A = [0, 1]$. The membership functions constructing the intuitionistic fuzzy subsets $A_1 = \{\text{general}\}$ and $A_2 = \{\text{general}\}$ and their intuition indices are each

$$\begin{aligned} u_{A_1} &= 0.9\ \exp\left(-\frac{x_1^2}{2\delta_u^2}\right), \\ u_{A_2} &= 0.9\ \exp\left(-\frac{(1-x_1)^2}{2\delta_u^2}\right), \\ \pi_{A_1} &= 0.1\ \exp\left(-\frac{(0.5-x_1)^2}{2\delta_\pi^2}\right), \\ \pi_{A_1}(x_1) &= 0. \end{aligned} \tag{1}$$

Let $\delta_u = 0.1416$ and $\delta_\pi = 0.035$, then the intuitionistic fuzzy set subsets constructed under the domain W can be written separately as $(x_1, u_{A_1}, \gamma_{A_1})$ and $(x_1, u_{A_2}, \gamma_{A_2})$.

(2) Intuitive fuzzy subsets representing audience responses

Audience response can be obtained through the combination of the number of audiences participating in the discussion and the speed of the spread of college students' online public opinion. The membership function of the intuitionistic fuzzy set representing the audience response can be calculated by weighted average using intuitionistic fuzzy comprehensive evaluation. Let $X_2 \in [0,1]$ be the number of normalized audiences, $X_3 \in [0,1]$ be the speed of normalization, the domain that the audience reflects $B = [0,1] \times [0,1]$, and the intuitionistic fuzzy subsets under the domain are $B_1 = \{\text{slow}\}$ and $B_2 = \{\text{fast}\}$. The subset of intuitionistic fuzzy sets that describe the audience response can be written as $((x_2, x_3), u_{B_1}, \gamma_{B_1})$ and $((x_2, x_3), u_{B_2}, \gamma_{B_2})$. Construct the membership function and the intuitionistic index of the intuitionistic fuzzy subsets, respectively:

$$\begin{aligned} uB_1(x_2, x_3) &= 0.45\left[\exp\left(-\frac{x_2^2}{2\delta_u^2}\right) + \exp\left(-\frac{x_3^2}{2\delta_u^2}\right)\right], \\ uB_2(x_2, x_3) &= 0.45\left[\exp\left(-\frac{(1-x_2)^2}{2\delta_u^2}\right) + \exp\left(-\frac{(1-x_3)^2}{2\delta_u^2}\right)\right], \\ \pi B_1(x_2, x_3) &= 0.05\left[\exp\left(-\frac{(0.5-x_2)^2}{2\delta_u^2}\right) + \exp\left(-\frac{(0.5-x_3)^2}{2\delta_u^2}\right)\right], \\ \pi B_1(x_2, x_3) &= 0. \end{aligned} \tag{2}$$

(3) An intuitionistic fuzzy subset describing the interrelationship between the audience and the topic

Analyze the sentimental tendency of the public in expressing speech, the public's attention to the college's online public opinion, and whether the topic is a hot topic, using the weighted average operation in the intuitionistic fuzzy comprehensive evaluation to construct a description of the relationship between the audience and the topic. For the intuitionistic fuzzy subset membership of the relationship, let $X_4 \in [0,1]$ be the normalized attitude bias, $X_5 \in [0,1]$ be the normalized attention, $X_6 \in [0,1]$ be the normalized increase in concern, and $X_7 \in [0,1]$ be the normalized duration of concern. The corresponding intuitionistic fuzzy subset $C_1 = \{\text{sparse}\}$ and $C_2 = \{\text{tight}\}$; the intuitionistic fuzzy subset describing the interrelationship between the audience and the topic is $((x_4, x_5, x_6, x_7), u_{C_1}, \gamma_{C_1})$ and $((x_4, x_5, x_6, x_7), u_{C_2}, \gamma_{C_2})$. Construct the membership function and the intuitionistic index of two intuitionistic fuzzy subsets, respectively:

RETRACTED

$$
\begin{aligned}
uC_1(x_4, x_5, x_6, x_7) &= 0.225\left[\exp\left(-\frac{x_4^2}{2\delta_u^2}\right) + \exp\left(-\frac{x_5^2}{2\delta_u^2}\right) + \exp\left(-\frac{x_6^2}{2\delta_u^2}\right) + \exp\left(-\frac{x_7^2}{2\delta_u^2}\right)\right],\\
uC_2(x_4, x_5, x_6, x_7) &= 0.225\left[\exp\left(-\frac{(1-x_4)^2}{2\delta_u^2}\right) + \exp\left(-\frac{(1-x_5)^2}{2\delta_u^2}\right) + \exp\left(-\frac{(1-x_6)^2}{2\delta_u^2}\right) + \exp\left(-\frac{(1-x_7)^2}{2\delta_u^2}\right)\right],\\
\pi C_1(x_4, x_5, x_6, x_7) &= 0.225\left[\exp\left(-\frac{(0.5-x_4)^2}{2\delta_\pi^2}\right) + \exp\left(-\frac{(0.5-x_5)^2}{2\delta_\pi^2}\right) + \exp\left(-\frac{(0.5-x_6)^2}{2\delta_\pi^2}\right) + \exp -\left(\frac{(0.5-x_7)^2}{2\delta_\pi^2}\right)\right],\\
\pi C_2(x_4, x_5, x_6, x_7) &= 0.
\end{aligned}
\tag{3}
$$

(4) Early warning level of college students' online public opinion

According to the four types of college students' online public opinion, the level of urgency is different. The intuitionistic fuzzy subsets under the early warning domain are $Z_1 = \{\text{levelIV}\}$, $Z_2 = \{\text{level III}\}$, $Z_3 = \{\text{levelII}\}$, and $Z_4 = \{\text{levelI}\}$. Constructing the membership function and intuitionistic fuzzy index of each of the four subsets as follows:

$$
\begin{aligned}
u_{Z_1}(z) &= 0.9\ \exp\left(-\frac{z^2}{2\delta_u^2}\right),\\
u_{Z_2}(z) &= 0.9\ \exp\left(-\frac{(1/3-tz)^2}{2\delta_u^2}\right),\\
u_{Z_3}(z) &= 0.9\ \exp\left(-\frac{(2/3-tz)^2}{2\delta_u^2}\right),\\
u_{Z_4}(z) &= 0.9\ \exp\left(-\frac{(1-z)^2}{2\delta_u^2}\right),\\
u_{Z_4}(z) &= 0.9\ \exp\left(-\frac{(1-z)^2}{2\sigma_u^2}\right),\\
\pi_{Z_1}(z) &= 0.1\ \exp\left(-\frac{(1/6-tz)^2}{2\sigma_\pi^2}\right),\\
\pi_{Z_2}(z) &= 0.1\ \exp\left(-\frac{(1/2-tz)^2}{2\sigma_\pi^2}\right),\\
\pi_{Z_3}(z) &= 0.1\ \exp\left(-\frac{(5/6-tz)^2}{2\sigma_\pi^2}\right),\\
\pi_{Z_4} &= 0,
\end{aligned}
\tag{4}
$$

where $z \in [0, 1]$, $\sigma_u = 0.07$, and $\sigma_\pi = 0.035$.

4. A Method Based on Bootstrap Estimation

In order to obtain the robustness estimation of the unknown coefficient β and the nonparametric main part $g(\cdot)$, we use the bootstrap estimation method to improve the penalty. First, the fitted values $\overline{\beta}, \overline{g}$, and $\{\overline{\varepsilon_t}\}$ are the unknown coefficients, nonparametric functions, and residuals from the penalty least squares estimate of y_i to x_i. For the existing m samples, a random sample is recorded. The bootstrap residual is $\overline{\varepsilon_1}, \ldots, \overline{\varepsilon_m}$. Next, generate a new bootstrap sample based on the model $y_i = x_i\overline{\beta} + \overline{g}(t_i) + \overline{\varepsilon_m}$, and then, estimate based on the newly generated bootstrap sample $y = (y_1, \ldots, y_i)$, thus obtaining the unknown coefficient β and the nonparametric main $g(\cdot)$ parameter estimation. Finally, repeat the above steps B times to get the final bootstrap parameters and corresponding probability intervals. The multistep probability density prediction method proposed is shown in Figure 1.

5. Empirical Analysis and Simulation

From the lyric topics collected by Sina Microblog, Baidu Post Bar, and other channels, several college students' online youth topics were selected: (1) postgraduate fee reform; (2) Fudan poisoning case; (3) college poverty health assessment methods; (4) overseas anticorruption; (5) discrimination of university growth and death; (6) the aunt comics to discourage uncivilization; (7) Shanghai Bund. The data collected by these topics is normalized, as shown in Table 1.

For the first college student network lyric topic, the input detection vector is (0.23, 0.92, 0.53, 0.02, 0.71, 0.69, 0.15). First, the vector is blurred, and the output is (0.67, 0.82, 0.59, 0.77); it is obvious that the topic has the highest degree of closeness with the warning level (Z2 level), and it is known that Z2 is a media level (medium type). The same reason can be obtained to judge the results of the early warning level of college students' online public opinion topics. The results are shown in Table 2.

As can be seen from Table 2, the early warning levels of the abovementioned seven college students' online public opinion topics are moderate, extraheavy, light, heavy, light, light, and heavy. For the special heavy and severe lyric events, for the sake of social harmony and stability, the government needs to take some necessary measures to control the direction of public opinion and prevent the general turmoil caused by the public sentiment. The results of this study are consistent with the actual discussion of the

RETRACTED

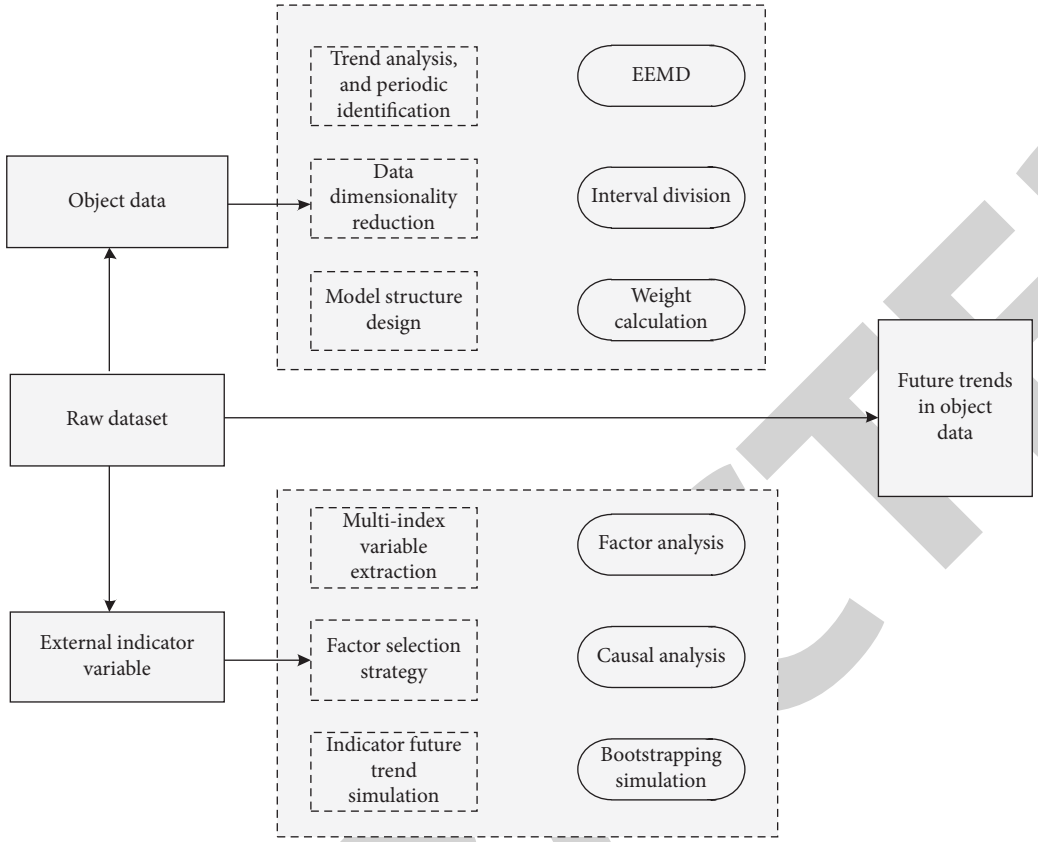

Figure 1: The proposed semiparametric additive modeling prediction framework.

Table 1: College lyric topics collecting data.

Topic	x_1	x_2	x_3	x_4	x_5	x_6	x_7
1	0.23	0.92	0.53	0.02	0.71	0.69	0.15
2	0.65	0.71	0.68	0.97	0.60	0.58	0.37
3	0.48	0.84	0.43	0.65	0.33	0.45	0.47
4	0.57	0.89	0.36	0.78	0.39	0.35	0.28
5	0.32	0.25	0.61	0.54	0.18	0.24	0.30
6	0.41	0.25	0.36	0.75	0.12	0.14	0.15
7	0.58	0.87	0.37	0.80	0.34	0.37	0.25

Table 2: Research results of lyric topics in colleges and universities.

Topic	σ_1	σ_2	σ_3	σ_4	Warning level
1	0.67	0.82	0.59	0.77	III
2	0.73	0.67	0.70	0.82	I
3	0.76	0.68	0.75	0.64	iv
4	0.73	0.65	0.78	0.73	II
5	0.81	0.74	0.63	0.70	iv
6	0.85	0.71	0.64	0.69	iv
7	0.75	0.66	0.79	0.71	II

event. The actual social impact and trend of the event are basically consistent with the model prediction results.

From January 26th to January 30th, related news such as "Hunan University Transfer Order Cancellation" became a hot topic. Around the relevant public opinion set up in education news, 36,765 positive information, 19,346 negative information, and 26,322 neutral information were recorded. The more the audience, the greater the influence of public opinion. Normalize the number of public opinion audiences to get the value x^2. The higher the x^2, the higher the risk level. In this case, the x^2 value is 0.87. The trend of attention on the PC side and the mobile site is shown in Figure 2.

The main information dissemination platform was news, and it reached the peak of event dissemination on January 26. The number of information dissemination was 458. The incident began to spread from January 21, and the first time the Huda responded was on the January 22, and hence, the attention began to rise sharply. On the 2nd, the official responded for the second time. Due to the inconsistency of its statements, the media and netizens were triggered. With the focus on continuous fermentation, its attention reached its first peak on the 24th. Subsequently, the dissemination and attention of the event began to gradually slow down. By January 30, the Ministry of Education's investigation results and treatment opinions were announced. As the netizens were dissatisfied with the results of their disposal, the degree of attention rose again, once reaching a secondary peak, and as time went on, attention degree gradually slows down, as shown in Figure 3. After the outbreak of the illegal transfer of postgraduate students in Hunan University, it caused widespread concern. Take Sina Microblog as an example, the topic titled "Hunan University Transfer Event" once jumped to the top of the real-time topic list, with about 6.9 million topic readings, comprehensive analysis, x6

RETRACTED

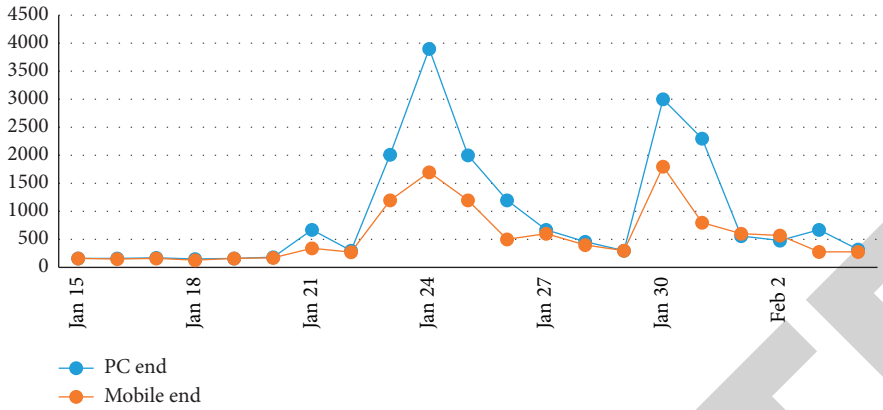

Figure 2: The trend of attention on the PC side and the mobile side.

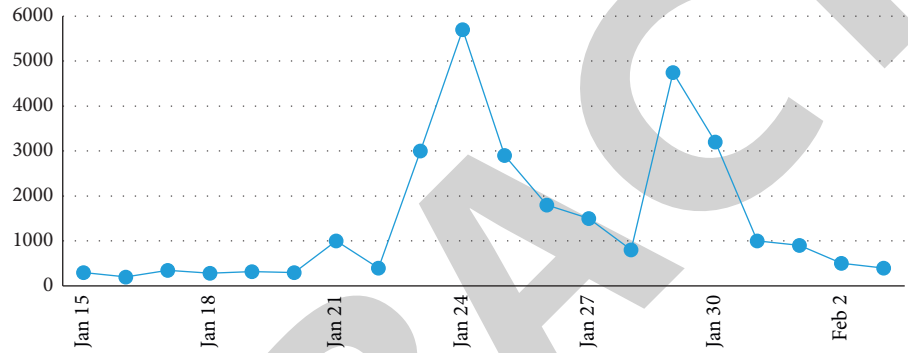

Figure 3: Variation curve.

sensitivity and focus degree, and x7 value of topic hotspot sensitivity 0.36 and 0.29. The higher the value of x6 and x7, the higher the danger level. Therefore, the input detection vector is (0.56, 0.87, 0.38, 0.65, 0.35, 0.36, 0.29); first, blur the vector; the output is (0.7368, 0.6814, 0.7925, 0.7136); judging the network public opinion warning level is level II.

6. Conclusion

This paper mainly constructs a qualitative and quantitative theoretical model to evaluate college students' network public opinion warning level. The model is constructed using intuitionistic fuzzy reasoning and a hierarchical analytical process. While using intuitionistic fuzzy reasoning to judge the network public opinion warning level, the topic importance, public reaction, and topic relevance are used as the participation factors. The degree of membership of each factor is calculated by the intuitionistic fuzzy comprehensive evaluation method. The closest intuitionistic fuzzy set is used as the network alert level. The analytic hierarchy process is used for decomposing the target into multiple indicator levels. An expert scoring method is introduced to determine each level of indicators' weight to determine the final indicator system. After the consistency check of the indicators' specific weight values at various levels, the network public opinion's index value can be calculated according to the constructed model, and the warning level to be activated is determined according to the threshold interval corresponding to the index value. At the same time, the model was tested empirically by the stampede event in Shanghai. Empirical studies show that the topic's importance can be obtained through the membership function and the intuitional real number calculation. The audience reflection can be obtained through the joint result of the number of audiences participating in the discussion and the public opinion's speed. The weighted average of the intuitionistic fuzzy evaluation is constructed to describe the relationship between the audience and the topic. The analytic hierarchy process can decompose the factors affecting the development of public opinion into 25 indicators that can be observed and measured. By comparing the importance of different levels of elements, each indicator's specific scores are obtained. The public opinion research index value S is used to predict the degree of attention. The closer the value of S is to 1, the more serious the whole situation's development will be.

Data Availability

The data used to support the finding of this study are included within the article.

Conflicts of Interest

The authors declare that they have no conflicts of interest.

RETRACTED

Hindawi
Mobile Information Systems
Volume 2021, Article ID 9956593, 10 pages
https://doi.org/10.1155/2021/9956593

Research Article

Cross-Cultural Communication of Regional Images Based on Multimodal Discourse Analysis and Network Security

Qing Xu[1] **and Guangming Wang**[2]

[1]*Wenzhou University College of Foreign Studies, Wenzhou University, Wenzhou, Zhejiang Province 325035, China*
[2]*Zhengzhou University, School of Politics and Public Administration, Zhengzhou, Henan Province 450001, China*

Correspondence should be addressed to Qing Xu; xuqing@wzu.edu.cn

Received 23 March 2021; Revised 15 April 2021; Accepted 25 April 2021; Published 7 May 2021

Academic Editor: Mian Ahmad Jan

Copyright © 2021 Qing Xu and Guangming Wang. This is an open access article distributed under the Creative Commons Attribution License, which permits unrestricted use, distribution, and reproduction in any medium, provided the original work is properly cited.

Numerous evaluation methods are used as effective indicators for the cross-cultural communication of a regional image. However, because these indicators are primarily in a foreign cultural situation, it is challenging to measure their attitudes and cognitions across geographic distances and cultural differences. This challenge motivated us to combine cultural communication methods and modern location service technology to carry out regional image communication research. First, this article examines the basic process of cross-cultural communication and the generation of regional images from an information transmission and network security perspective. It combines multimodal discourse to analyze influencing factors and establishes a hierarchical model of the cross-cultural communication indicator system. Secondly, based on the location-based service (LBS), this article adds scene information to develop a user tendency model. This model effectively handles the conversion between two-dimensional scoring space and three-dimensional tendency space and can adapt to the short-term changes of users' tendency. The experimental results verify that the location-based e-commerce recommendation algorithm proposed in this paper can better solve information overload and obtain a significant recommendation effect.

1. Introduction

The division of physical space makes it possible to produce a regional image, and it also creates a space of different ideas for the researchers [1, 2]. The cross-cultural communication path aims to explore how to bridge the division of physical space through the construction of information space and adjust the conceptual space solidified by different communication subjects with the provisioning of network security [2]. After the spatialization of philosophical and sociological research, the academic circles have been lacking in studying foreign land's image from the perspective of space, which is precisely a critical issue that is indispensable in the study of foreign images [3, 4]. The problem of the foreign image was initially the problem of space and then the image [4].

In recent years, relevant scholars have carried out research around the aforementioned issues [4]. Wan-Shilu Yang and Hung-Chi Chen [5] compared the information keywords by initially calculating the similarity between the content of each web page and the user's interest, then introduced the location information, and constructed the utility function. Finally, they calculated the result and sort the web recommendation list. In [6], the authors have carried out research on the application of dynamic user analysis in mobile services by providing relevant services and information based on a new user's preferences. In [7], the authors incorporated location and other contextual attributes into the common user interest model, further enriching the user interest model. For each scenario, an associated user interest needs to be generated [8, 9]. Therefore, the provision of services is suitable for the user's interest and can be better applied to the user's current scenario [10]. Reasonable evaluation indicators and methods are an effective indicator of the cross-cultural communication elements of a regional image. However, because the

survey subjects are in a foreign cultural situation, it is extremely difficult to measure their attitudes and cognitions across geographic distances and cultural differences. Hence, this article combines cultural communication methods and modern location service technology to carry out regional image communication [11–13].

The main contributions of this work are as follows:

(1) First, this article introduces the research overview of location services and cross-cultural communication of geographical image

(2) Next, we discuss the evaluation index analysis methods based on location services and analytic hierarchy from network security viewpoint

(3) Finally, we conduct a simulation test on the location-based and service-based cross-cultural communication model, which will be established in this paper

The rest of this paper is organized as follows. In Section 2, a detailed literature review of related studies is provided. In Section 3, image evaluation based on location service and level analysis is discussed. In Section 4, the simulation test results on the proposed approach are discussed. Finally, we conclude the paper and provide future research directions in Section 5.

2. Related Work

In this section, first, we discuss the existing literature pertaining to location-based service (LBS) followed by cross-cultural communication of geographical images. This will lay a solid foundation for our proposed work and objectives.

2.1. Location-Based Service. Location-based service (LBS) technology integrates Internet, wireless communication, mobile positioning, and GIS [14–16]. As mobile phones become an indispensable part of our lives, the mobile service market has an increasingly urgent need for using mobile phones to implement location information. An example of a recommendation algorithm combining location and network security is shown in Figure 1.

LBS can use the software and hardware resources of the telecommunication operator to obtain the geographic location information of the mobile terminal user. For example, LBS can be used for obtaining geographic location coordinates. Next, collaborative filtering is used at each layer (where the user is located) to obtain multiple recommendation lists. Finally, LBS weighs the recommendation lists of each layer to obtain the final recommendation list. With the support of GIS (geographic information system) platform, it can bring about economic growth of corresponding services.

2.2. Cross-Cultural Communication of Geographical Image. The cognition of the external world is inseparable from the division of interior and exterior centered on the environment in which the cognition subject lives [17, 18]. The problem of image actually involves the issue of the space between the cognition subject and the image itself. One of the sources of people's cognition of space problems is caves. One of the most primitive forms of human settlements is caves. In Chinese myths and legends, primitive humans before the Chao family lived in naturally formed caves [19, 20]. The cave separates two completely heterogeneous spaces inside and outside with solid objects and possesses the most primitive functions of all spaces: belonging and separation. Physical separation also means separation in culture, identity, and cognitive norms. This separation treats the subject's culture and norms as authentic, conceals a certain truth, and establishes the subject's cognitive hegemony through the establishment of rules for the inhabitants of the space to understand the outside world [21–23]. The existence of this hegemony strengthens the spiritual space of the subject and makes it possible to separate all the spiritual activities of the subject (including the construction of the images) from the original face of the world. In other words, after geographical space divides the "old and dead" foreign country into two isolated and closed entities, imagine it as the only way to fill the "picture in the mind." The information spaces interact with physical space to continuously adjust the cognitive space of human beings [24]. Therefore, the route of cross-cultural dissemination of regional images is to study how the communication media, which is the connection link, create an information space and use their respective conceptual spaces as the scale of communication to build a cognitive relationship between the interacting parties.

3. Image Evaluation Based on Location Service and Cross-Cultural Communication

In this section, first, we discuss the location service model of our proposed approach followed by the cross-cultural communication of regional images based on multimodal discourse analysis and network security.

3.1. Location Service Model. In order to satisfy the different preferences of users in different regions, various researchers have made attempts, and the most famous one is the LARS model, which uses traditional collaborative filtering at different spatial levels to recommend users with spatial attributes [25, 26]. Projects without spatial attributes have the characteristics of high recommendation accuracy and high system stability. However, the user's spatial location distribution affects the recommendation system. Moreover, from the perspective of a larger spatial scale, the interests of users are different in different countries and regions. For each scenario, an associated user interest will be generated [8, 9]. Therefore, the provision of services is suitable for the user's interest and can be better applied to the user's current scenario [10]. Reasonable evaluation indicators and methods are an effective indicator of the cross-cultural communication elements of a regional image. It is subdivided into spatial scale of the city level; users in different regions also have different interests and tastes, and they will also show different preferences for different regional images [27, 28].

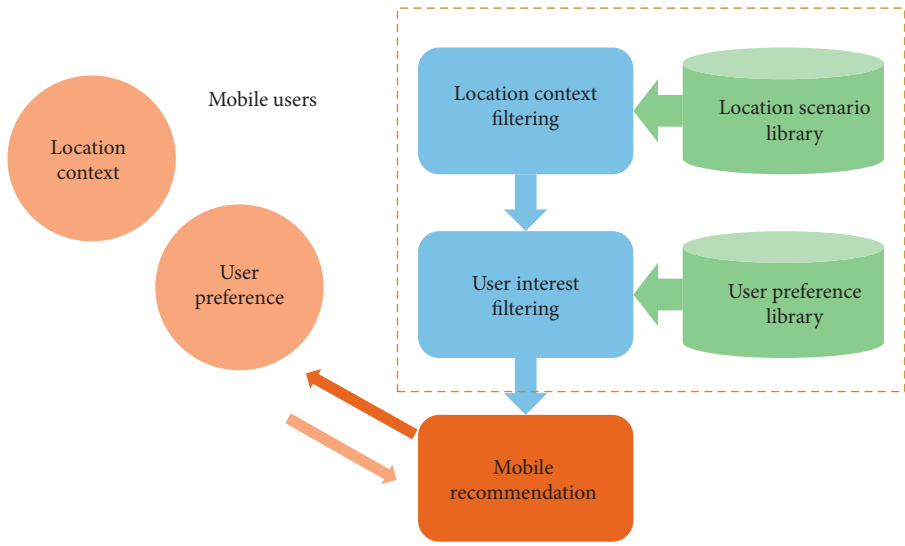

Figure 1: An example of a recommendation algorithm combining location and network security.

In this paper, we consider the similarity of the user distribution of the project based on the idea that if two projects are similar, then their user distributions are similar to each other. We propose an indicator called the distance distribution coefficient to measure the user distribution of a given project. This article selects the best degree of competition for tasks in different locations. The minimum positioning objective function corresponding to the optimal radius is

$$\min_{w,b,e} \varphi(a,b,e) = \frac{1}{2}\omega^T\omega + \frac{1}{2}\gamma\sum_{k=1}^{N} e_k^2. \tag{1}$$

The constraints are

$$y_k\left[\omega^T\phi(x_k) + b\right] = 1 - e_k, \quad k = 1,2,\ldots,N. \tag{2}$$

The LaGrange function is defined as

$$L(w,b,e,\alpha) = \phi(w,b,e) - \alpha_k\sum_{k=1}\left\{\alpha_k y_k\left[\omega^T\phi(x_k) + b\right] - 1 - e_k\right\}. \tag{3}$$

The above equation is optimized, and the matrix equation can be finally obtained as follows:

$$\begin{bmatrix} 0 & -Y^T \\ Y & ZZ^T + \gamma^{-1}I \end{bmatrix}\begin{bmatrix} b \\ \alpha \end{bmatrix} = \begin{bmatrix} 0 \\ I \end{bmatrix}. \tag{4}$$

Bringing in the Mercer condition, the final decision function is obtained as

$$y(x) = \operatorname{sgn}\left[\sum_{k=1}^{N}\alpha_k y_k \psi(x_k, x_l)\right]. \tag{5}$$

After the user distance distribution coefficient is obtained, the similarity calculation between items can be similar based on the network structure:

$$\max_{\{p_i,y_i\}} \pi(p,y,x) = \sum_{j=1}^{M}\sum_{i=1}^{K_{B(I)}}(p_i - c_i)x_{ij}y_i. \tag{6}$$

In this paper, the similarity using the distance distribution coefficient is called geographic similarity, and the cosine-like similarity calculation method of geographic similarity is as follows:

$$\begin{aligned} &\text{s.t. } p_i > c_i, \\ &\quad y_i > x_{ij}, \\ &\quad y_i = 0 \text{ or } 1 \quad \left(i = 1,2,\ldots,K_{B(I)},\ j = 1,2,\ldots,M\right). \end{aligned} \tag{7}$$

After obtaining the mixed similarity of the fusion location factors, the users are divided into levels of different heights by using a hierarchical structure according to the user's location coordinate information, as shown in equations (8) and (9):

$$\max_{\{x_{ij}\}} \mu_j(x) = \sum_{i=1}^{K_{B(I)}} r_{ij}x_{ij}, \tag{8}$$

$$\begin{aligned} &\text{s.t. } \left(r_{ij} - p_i\right)x_{ij} \geq 0, \\ &x_{ij} \leq y_i, \\ &x_{ij} = 0 \text{ or } 1 \quad (i = 1,2,\ldots,K_{B(I)};\ j = 1,2,\ldots,M). \end{aligned} \tag{9}$$

Next, we perform collaborative filtering at each layer (where the user is located) to obtain multiple recommendation lists; finally, weigh the recommendation lists of each layer to obtain the final recommendation list [29]. After the spatialization of philosophical and sociological research, the academic circles have been lacking in the study of the image of foreign land from the perspective of space, and this is precisely an important issue that is indispensable in the

study of foreign image. However, because the survey subjects are in a foreign cultural situation, it is very difficult to measure their attitudes and cognitions across geographic distances and cultural differences. Based on this, this article combines cultural communication methods and modern location service technology to carry out regional image communication research. The problem of the foreign image is firstly the problem of space and then the problem of the image. The specific process of the recommendation list will be shown in Figure 2.

In order to improve the accuracy of the recommendation system, this paper adds the user distribution of the item as a feature parameter to the calculation of the recommendation algorithm on the basis of the traditional method that only relies on the score data to calculate the similarity. After the hybrid similarity is obtained through the improved similarity calculation, the clustering idea is used to divide and generate the geographical user clusters, and then, the collaborative filtering recommendation is performed. The main contributions are as follows. After the first division is completed, traverse the user data in the area to obtain the user item score matrix of each layer of the area, and calculate the mixed similarity of the fusion geographic factors according to the similarity calculation method introduced above degree. Finally, a global recommendation list and several local recommendation lists are obtained.

3.2. Cross-Cultural Communication Evaluation Based on Analytic Hierarchy Process. After the hybrid similarity is obtained through the improved similarity calculation, the clustering idea is used to divide and generate the geographical user clusters, and then, the collaborative filtering recommendation is performed. Therefore, the provision of services is suitable for the user's interest and can be better applied to the user's current scenario. Reasonable evaluation indicators and methods are an effective indicator of the cross-cultural communication elements of a regional image. Subdivided into the spatial scale of the city level, users in different regions also have different interests and tastes, and they will also show different preferences for different regional images.

3.2.1. The Establishment of Hierarchical Analysis Structure. First, perform collaborative filtering in each layer where the user is located to obtain multiple recommendation lists; finally, weigh the recommendation lists of each layer to obtain the final recommendation list. By exploring the potential impact of cross-cultural communication assessment, this article has identified eight influencing factors, and the established hierarchical analysis structure is shown in Figure 3.

3.2.2. The Construction of the Judgment Matrix. After the first division is completed, the user data of the area is traversed to obtain the user item score matrix of each layer in the area, and the similarity calculation method is introduced based on the above degree. We can find that the geographical similarity value in the average ranking score is smaller than the cosine similarity, and the accuracy and recall rate are higher than the cosine similarity. This shows that the recommendation effect of the geographical similarity is better than the traditional cosine similarity, which shows that the user location distribution can play an effective role in project-based collaborative filtering. Table 1 shows the matrix results based on the data items.

3.2.3. Matrix Consistency Check.

$$M_i = \prod_{j=1}^{n} a_{ij}, \quad i = 1, 2, \ldots, n. \tag{10}$$

(1) Calculate the n^{th} root:

$$\overline{W}_i = \sqrt[n]{M_i},$$
$$W_i = \frac{\overline{W}_i}{\sum_{j=1}^{n} \overline{W}_j}. \tag{11}$$

(2) Calculate the largest characteristic root of the judgment matrix:

$$\lambda_{\max} = \sum_{i=1}^{n} \frac{(AW)_i}{nW_i}. \tag{12}$$

Through the calculation of each level of the judgment matrix, Table 2 shows the judgment matrix results based on the data items.

4. Model Effect and Simulation Test Results

In this section, first, we provide the evaluation index of our model followed by model test data and the ultimate experimental results.

4.1. Model Evaluation Index. Earlier, we discussed the evaluation index analysis methods based on location services and analytic hierarchy. This study uses precision to measure the prediction accuracy of the generated recommendation list [30]. The accuracy is defined as follows:

$$\text{Precision} = \frac{\sum_{u \varepsilon U} |R(u) \cap T(u)|}{\sum_{u \varepsilon U} |T(u)|}. \tag{13}$$

At the same time, we have also carried out the calculation and comparison of the recall rate (recall), which is defined as follows:

$$\text{Recall} = \frac{\sum_{u \varepsilon U} |R(u) \cap T(u)|}{\sum_{u \varepsilon U} |R(u)|}, \tag{14}$$

where $T(u)$ is the list of items that the user actually likes in the test set.

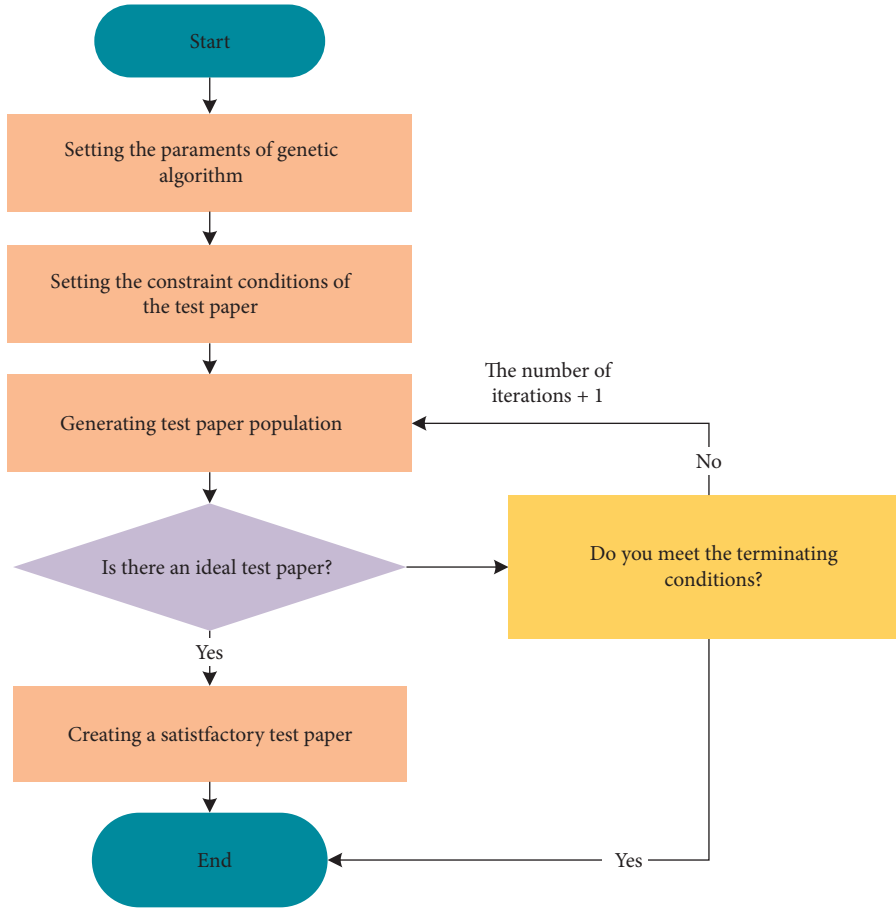

Figure 2: The specific process of the recommendation list.

$$r_i = \frac{L_i}{N}. \tag{15}$$

In order to satisfy the broad interests of users, this study uses diversity indicators, namely, internal diversity and external diversity. Interuser diversity is measured by hamming distance, which is defined as follows:

$$H_{ut}(L) = 1 - \frac{Q_{ut}(L)}{L}. \tag{16}$$

Take the average of all users to get $H(L)$ of the system. As $H(L)$ increases, the diversity of the recommendation system increases.

And, the internal diversity of user u (intrauser diversity) is defined as

$$I_u(L) = \frac{1}{L(L-1)} \sum_{\alpha \neq \beta} \text{sim}(\alpha, \beta). \tag{17}$$

4.2. Model Test Data. In the system testing phase, this article will conduct a simulation test on the location-based service-based cross-cultural communication model established in this article. The dataset uses Gowalla data in the public database. Gowalla is a website that provides location check-in. This article uses the Gowalla dataset, which contains 30,367 geographic reference points in a certain area, as well as information about 357,753 visits by 19,183 users of Gowalla. We selected at least 20 users to visit each location, and each user visited at least 20 locations and finally obtained 85,862 times of 1962 users to 2063 locations [31]. Figure 4 shows a schematic diagram of partial location information of the database.

In the experiment designed in this article, each dataset is randomly divided, 80% of which is used for training. The training set is regarded as known information, and the test set does not allow any information to be used for prediction. According to the test set, the performance of this algorithm is evaluated from various aspects.

4.3. Model Test Results. This paper compares the three different similarity calculation forms, namely, cosine similarity, Jaccard similarity, and Sorensen similarity, under the combination of geographic similarity and traditional similarity under the change of the balance factor. The LARS introduced in paper is used for comparison. Although the LARS algorithm is not the best algorithm in the location-aware recommendation system, it takes into account the accuracy of the recommendation system and the stability in the actual system application. It is still a very practical algorithm.

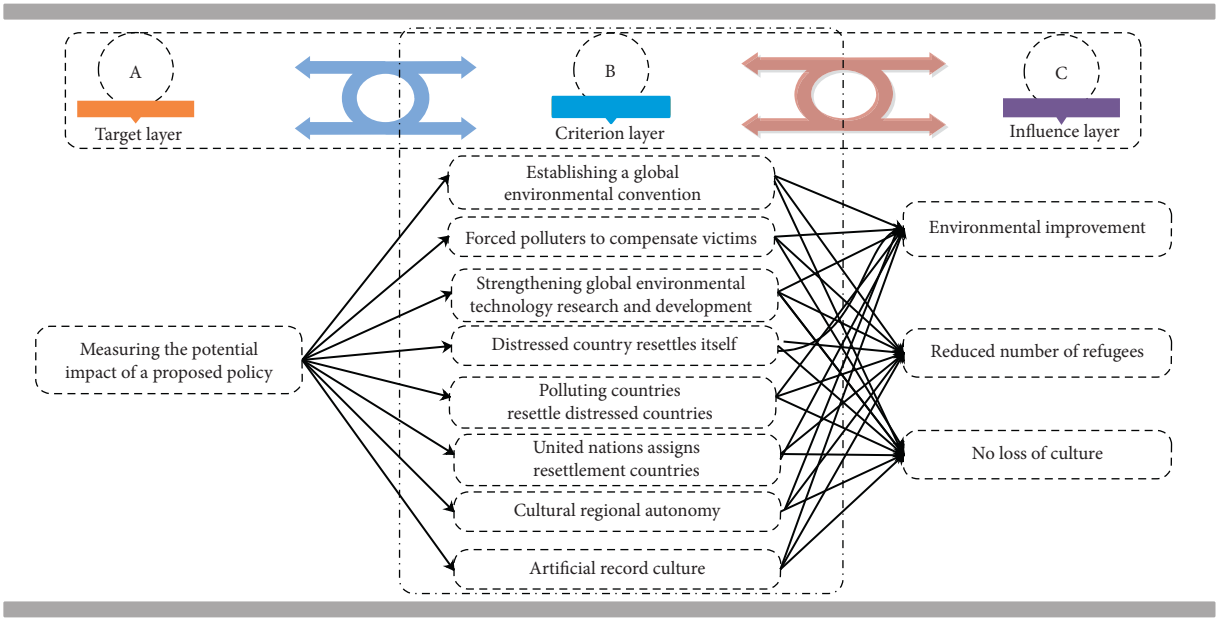

Figure 3: A hierarchical analysis structure for measuring the potential impact of cross-cultural communication assessment.

Table 1: The matrix results based on the data items.

A	B_1	B_2	B_3	B_4	B_5	B_6	B_7	B_8
B_1	1	1/3	1/3	1/3	1/4	1/5	1/3	1/4
B_2	3	1	2	1/3	1/4	1/5	1/3	1/3
B_3	3	½	1	1/3	1/4	1/5	1/2	1/3
B_4	3	3	3	1	1/3	¼	3	3
B_5	4	4	4	3	1	1/3	3	3
B_6	5	5	3	4	3	1	3	3
B_7	3	3	2	1/3	1/3	1/3	1	3
B_8	4	3	3	1/3	1/3	1/3	1/3	1

Table 2: The judgment matrix results based on the data items.

Calculation result of judgment matrix					λ_{max}	CI	RI	CR
$AW = \begin{bmatrix} 0.0328 \\ 0.0542 \\ 0.0478 \\ 0.1465 \\ 0.2142 \\ 0.3071 \\ 0.1083 \\ 0.0891 \end{bmatrix}$	B_1 $W = \begin{bmatrix} 0.6144 \\ 0.2684 \\ 0.1172 \end{bmatrix}$	B_5 $W = \begin{bmatrix} 0.1365 \\ 0.6250 \\ 0.2385 \end{bmatrix}$	B_1	3.0735	0.0368	0.5200	0.0707
			B_2	3.0536	0.0268	0.52	0.0515
	B_2 $W = \begin{bmatrix} 0.5278 \\ 0.3325 \\ 0.1396 \end{bmatrix}$	B_6 $W = \begin{bmatrix} 0.1168 \\ 0.6833 \\ 0.1998 \end{bmatrix}$	B_3	3.0618	0.0197	0.100	0.0478
			B_4	3.0037	0.0018	0.5000	0.0036
	B_3 $W = \begin{bmatrix} 0.5469 \\ 0.3445 \\ 0.1085 \end{bmatrix}$	B_7 $W = \begin{bmatrix} 0.1220 \\ 0.3196 \\ 0.5584 \end{bmatrix}$	B_5	3.0183	0.0091	0.5300	0.0176
			B_6	3.0246	0.0123	0.5200	0.0236
	B_4 $W = \begin{bmatrix} 0.1095 \\ 0.5816 \\ 0.3090 \end{bmatrix}$	B_8 $W = \begin{bmatrix} 0.0936 \\ 0.2797 \\ 0.6267 \end{bmatrix}$	B_7	3.0183	0.0091	0.4900	0.0178
			B_8	3.0857	0.0428	0.4900	0.0825

C-CF, J-CF, and S-CF appearing below are collaborative filtering based on user-item score data for cosine similarity, Jaccard similarity, and Sorensen similarity calculations. C-LARS, J-LARS, and S- LARS use three similarities for collaborative filtering calculations under the LARS algorithm. DC-CF, DJ-CF, and DS-CF are algorithms that calculate the hybrid similarity under three similarity forms and then perform collaborative filtering. DC-LARS, DJ-LARS, and DS-LARS are algorithms based on user location distribution proposed in this paper. In the case of similarity calculation, NBI is a recommendation algorithm based on a bipartite graph network. Accuracy of cosine-like form in cosine similarity and geographic similarity are shown in Figures 5–7.

In Figure 5–7, Method A is the cosine-like method of geographic similarity, and Method B is the traditional cosine

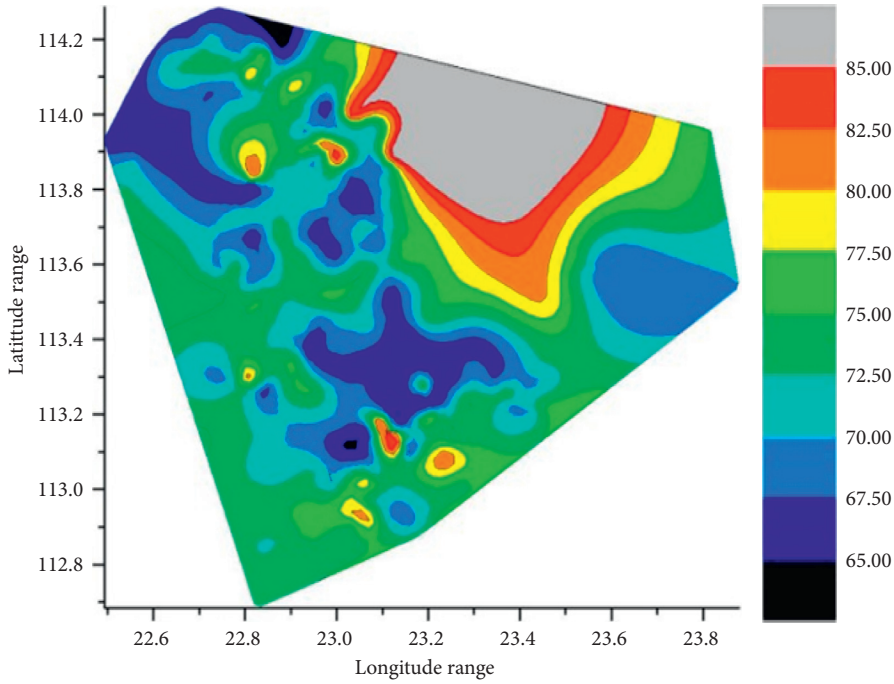

Figure 4: Schematic diagram of partial location information of the database.

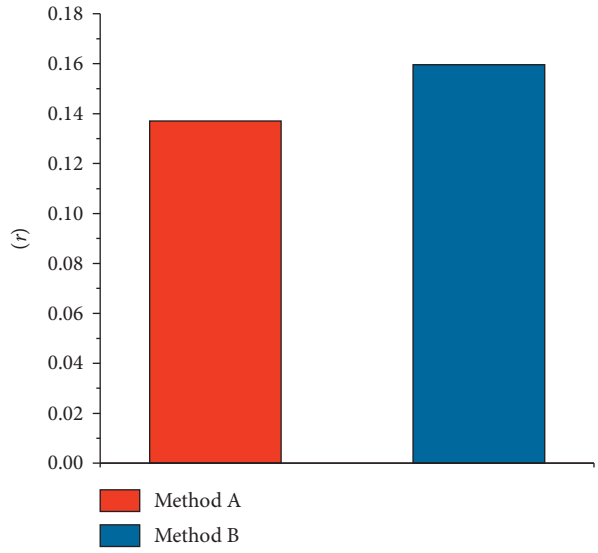

Figure 5: Accuracy of cosine-like form in cosine similarity and geographic similarity (r).

similarity method. The ordinate in the figure is the algorithm index; from left to right are the average ranking score, accuracy, and recall rate. As shown in Figure 5–7, we compared the performance of the cosine form of item-based collaborative filtering and the cosine-like form of geographic similarity in the dataset under the three indicators of average ranking score, accuracy, and recall rate. We can find that the geographical similarity value in the average ranking score is smaller than the cosine similarity, and the accuracy and recall rate are higher than the cosine similarity. This shows that the recommendation effect of the geographical similarity is better than the traditional cosine similarity, which reflects that the user location distribution can play an effective role in project-based collaborative filtering.

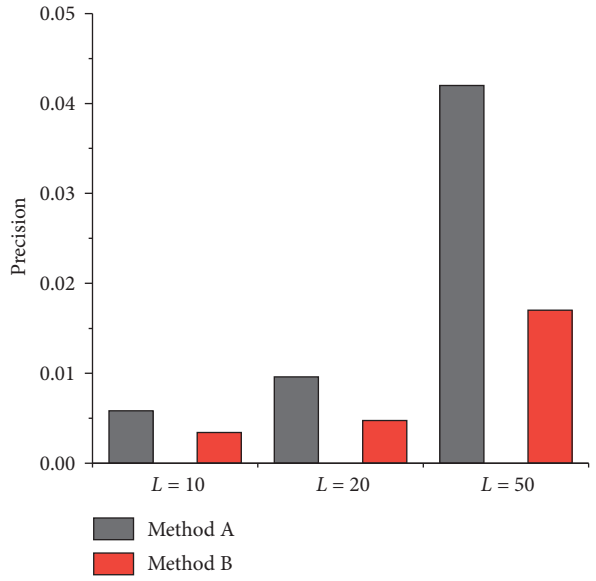

Figure 6: Accuracy of cosine-like form in cosine similarity and geographic similarity (Precision).

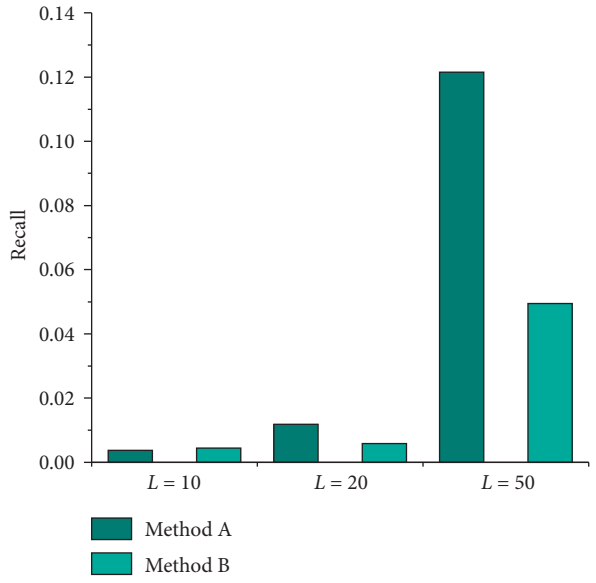

Figure 7: Accuracy of cosine-like form in cosine similarity and geographic similarity (Recall).

5. Conclusion

After the spatialization of philosophical and sociological research, the academic circles have been lacking in the study of the image of foreign land from the perspective of space, and this is precisely an important issue that is indispensable in the study of the foreign image. The problem of foreign image is firstly the problem of space and then the problem of the image. Reasonable evaluation indicators and methods are an effective indicator of the cross-cultural communication elements of a regional image. However, because the survey subjects are in a foreign cultural situation, it is very difficult to measure their attitudes and cognitions across geographic distances and cultural differences. This article combines cultural communication methods and modern location service technology to carry out regional image communication research. Due to the limited research conditions of this article, the research on the geographical image communication based on location services is not perfect. In the future, we will continue to devote ourselves to related research and to improve the progress of cross-cultural communication of regional image.

Data Availability

The data used to support the findings of this study are available from the corresponding author upon request.

Conflicts of Interest

The authors declare that they have no conflicts of interest.

Acknowledgments

This study was supported by the project of Zhejiang Education Department: Regional Images in the MOOC and Multimodal Construction and Cross-cultural Communication (Y201941084).

References

[1] Z. Liu, "A study on English translation of tourism publicity in coastal cities from the perspective of cross-cultural communication," *Journal of Coastal Research*, vol. 115, no. sp1, p. 87, 2020.

[2] D. Warad, V. Rodriguez, and A. Nageswara Rao, "Cross-cultural communication in pediatric oncology: catch them when they're young," *Cancer*, vol. 124, no. 7, pp. 1516-1517, 2018.

[3] M. F. Ilowite, T. I. Kang, and J. W. Mack, "Reply to Cross-cultural communication in pediatric oncology: catch them when they're young," *Cancer*, vol. 124, no. 7, p. 1517, 2018.

[4] S. H. Kim, N. Petard and J. H. Hong, What is lost in translation: a cross-cultural study to compare the concept of nuttiness and its perception in soymilk among Korean, Chinese, and Western groups," *Food Research International*, vol. 105, pp. 970–981, 2018.

[5] K. Würth, W Langewitz, S Reiter-Theil, and S Schuster, "Their view: difficulties and challenges of patients and physicians in cross-cultural encounters and a medical ethics perspective," *Bmc Medical Ethics*, vol. 19, no. 1, p. 70, 2018.

[6] L. R. Koenig, M. Li, L. A. Zimmerman et al., "Associations between agency and sexual and reproductive health communication in early adolescence: a cross-cultural, cross-sectional study," *Journal of Adolescent Health*, vol. 67, no. 3, pp. 416–424, 2020.

[7] H. Haragus, R. Prejbeanu, J. Patrascu et al., "Cross-cultural adaptation and validation of the Romanian oxford shoulder score," *Medicine*, vol. 97, no. 23, p. e10926, 2018.

[8] Z. Wang, L. Gao, and J. Huang, "Location-flexible mobile data service in overseas market," *IEEE Transactions on Mobile Computing*, vol. 99, 2020.

[9] R. S. Thoma, A. Schwind, P. Wendland et al., "Cooperative passive coherent location: a promising 5G service to support road safety," *IEEE Communications Magazine*, vol. 57, no. 9, pp. 86–92, 2019.

[10] D. C. Turkoglu and M. E. Genevois, "A comparative survey of service facility location problems," *Annals of Operations Research*, vol. 292, 2020.

[11] I. Averbakh and W. Yu, "Multi-depot traveling salesmen location problems on networks with special structure," *Annals of Operations Research*, vol. 286, 2020.

[12] L. Navarro, "Injury frequency and characteristics (location, type, cause and severity) differed significantly among athletics ('track and field') disciplines during 14 international championships (2007–2018): implications for medical service planning," *British Journal of Sports Medicine*, vol. 54, no. 3, p. 159, 2020.

[13] J. H. Park, "Location of arrest and effect of prehospital advanced airway management after emergency medical service-witnessed out-of-hospital cardiac arrest: nationwide observational study," *Emergency Medicine Journal*, vol. 36, no. 9, pp. 541–547, 2019.

[14] H. Andersson, "Using optimization to provide decision support for strategic emergency medical service planning - three case studies," *International Journal of Medical Informatics*, vol. 133, pp. 103975.1–103975.10, 2020.

[15] C. Hansen, C. Mena, and E. Aktas, "The role of political risk in service offshoring entry mode decisions," *International Journal of Production Research*, vol. 57, 2019.

[16] B. Sarasola and K. F. Doerner, "Adaptive large neighborhood search for the vehicle routing problem with synchronization constraints at the delivery location," *Networks*, vol. 75, 2020.

[17] K. S. J. Glew, S. Wanless, M. P. Harris et al., "Moult location and diet of auks in the North Sea inferred from coupled light-based and isotope-based geolocation," *Marine Ecology Progress Series*, vol. 599, 2019.

[18] S. Saeed, M. Asim, T. Baker, and Z. Maamar, "A location-sensitive and network-aware broker for recommending web services," *Computing*, vol. 101, no. 5, pp. 455–475, 2019.

[19] J.-H. Huh and T.-J. Kim, "A location-based mobile health care facility search system for senior citizens," *The Journal of Supercomputing*, vol. 75, no. 4, pp. 1831–1848, 2019.

[20] J. D. Oa, "Service quality, satisfaction and behavioral intentions towards public transport from the point of view of private vehicle users," *Transportation*, vol. 12, no. 2, pp. 134–148, 2021.

[21] B. A. Chang, "Impact of a short-term domestic service-learning program on medical student education," *Annals of Global Health*, vol. 85, 2019.

[22] S. Z. Ali and L. Tiziana, "Service utilization patterns for childbirth and neonatal mortality in the Occupied Palestinian Territory during conflict," *European Journal of Public Health*, vol. 30, no. 5, pp. 856–860, 2020.

[23] N. Wang, "A two-stage charging facilities planning method for electric vehicle sharing systems," *IEEE Transactions on Industry Applications*, vol. 99, 2020.

[24] B. Luo, X. Li, J. Weng, J. Guo, and J. Ma, "Blockchain enabled trust-based location privacy protection scheme in VANET," *IEEE Transactions on Vehicular Technology*, vol. 69, no. 2, pp. 2034–2048, 2020.

[25] L. A. Kuehn, S. L. Casperson, J. D. Derner et al., "23 Current progress in the Agricultural Research Service Beef Grand Challenge: a large-scale genetics by environment by management evaluation project," *Journal of Animal Science*, vol. 98, no. Supplement_4, pp. 13-14, 2020.

[26] C. Zhang, "Geographic image management system based on Silverlight," *Haematologica*, vol. 99, no. 11, pp. 1057–1062, 2014.

[27] J. Poor, *Geographic Image Storage, Transmission and Display System*, 2006.

[28] J. A. Santiváñez and E. Melachrinoudis, "Reliable maximin-maxisum locations for maximum service availability on tree networks vulnerable to disruptions," *Annals of Operations Research*, vol. 286, no. 1-2, pp. 669–701, 2020.

[29] D. Mao, J. Tan, and J. Wang, "Location planning of PEV fast charging station: an integrated approach under traffic and power grid requirements," *IEEE Transactions on Intelligent Transportation Systems*, vol. 99, pp. 1–10, 2020.

[30] Y. Wang, "Preserving location privacy in UASN through collaboration and semantic encapsulation," *IEEE Network*, vol. 99, no. 7, pp. 316–327, 2020.

[31] B. M. Carius, M. D. April, C. S. Pedersen, and S. G. Schauer, "Historical alternans in the emergency department (H.A.t.E.D.) for pain: an analysis of patient pain descriptors to attending and trainee clinicians," *Southern Medical Journal*, vol. 114, no. 1, pp. 23–27, 2021.

Hindawi
Mobile Information Systems
Volume 2021, Article ID 9934090, 8 pages
https://doi.org/10.1155/2021/9934090

Research Article

Application of Data Envelopment and Internet of Things Technology for Asset Value Evaluation

Lunsheng Wang,[1] Mingwu Gao,[2] and Zhenlu Liang[3]

[1]*Information Center, Shandong Institute of Commerce and Technology, Jinan 250103, Shandong, China*
[2]*Publicity Department, Information Center, Shandong University of Arts, Jinan 250014, Shandong, China*
[3]*Network Information Center, Qilu University of Technology, Jinan 250353, Shandong, China*

Correspondence should be addressed to Zhenlu Liang; lzl@qlu.edu.cn

Received 1 April 2021; Revised 19 April 2021; Accepted 26 April 2021; Published 4 May 2021

Academic Editor: Mian Ahmad Jan

Copyright © 2021 Lunsheng Wang et al. This is an open access article distributed under the Creative Commons Attribution License, which permits unrestricted use, distribution, and reproduction in any medium, provided the original work is properly cited.

Assets are an essential part of an enterprise's production and an indispensable economic entity for production and operation. The valuation of assets is one such area that has received significant attention in recent years. However, there exist numerous issues from various perspectives. These issues require us to study and explore them further. This article discusses the role of Internet of Things (IoT) and data envelopment methods to improve and develop asset evaluation. Based on the concept of asset evaluation, this paper designs an asset evaluation framework using the IoT. This framework can provide an all-weather and no-delay preparation basis for the asset appraisal work. Moreover, this paper uses data envelopment and particle swarm optimization (PSO) algorithm to clean and reclassify asset data. The objective of this algorithm is to solve the nonlinear function optimization problems associated with asset value evaluation. Finally, we verify the effectiveness and practicability of the model by comparing experimental simulation and manual evaluation.

1. Introduction

In the context of the rapid development of contemporary science and technology in microeconomic activities worldwide, intangible assets show much more vitality than tangible assets [1]. The amount of intangible assets generally reflects the scientific and technological capabilities and intellectual and cultural capabilities possessed by these assets' owners. Intangible assets are an essential part of an enterprise and indispensable in its production and operation [2, 3]. The country's long-term asset management practices under the conditions of a market economy provide a basis for evaluating intangible assets. The existing economic knowledge and mathematical methods provide a means to establish an evaluation system that can offer intangible assets' value [4, 5]. With the continuous deepening of reform and opening up and the rapid development of the socialist market economy, intangible assets and their assessment issues have attracted significant attention from relevant state departments. Especially, in the recent period, articles calling for attention and strengthening intangible assets' assessment are not uncommon [6–8]. Through the development of intangible assets' evaluation, the role, status, and value of intangible assets will be recognized and valued by the society. However, this work still has many problems in many aspects [9].

With the advent of globalization and the era of knowledge economy, the profoundly changing domestic and international environment on the one hand provides extensive development space for the asset appraisal industry, but also brings a lot of new problems to the healthy development of asset appraisal industry. The evaluation business has begun to transform from traditional business to emerging business [10]. The types and scope of evaluation have gradually expanded, and the market's requirements for evaluation and quality have become higher and higher [11, 12]. However, many asset appraisal agencies still adopt the old business philosophy, blindly pursue economic

benefits, and neglect the control of appraisal risks [13]. Frederick M. Babcock pointed out that it is necessary to determine which evaluation method to choose based on its purpose and the specific asset status [14]. It is necessary to define the purpose of the evaluation before starting the evaluation work. Jaffe and Lush pointed out that a correct understanding of the meaning of value in economic theory can help improve the quality of evaluation results [15]. With the further development of measurement technology and measurement tools, evaluators' evaluation results will be more accurate [16]. The cornerstone of asset appraisal research is the theoretical basis of appraisal. The research on appraisal theoretical basis mainly discusses the problem of value concept and the relationship between appraisal theory and economic theory [17].

The significance of asset evaluation is not to know how much a company's asset brand is worth, but to help companies find the advantages and weaknesses of brand equity, to achieve the benefits of further enhancing brand equity. With the continuous deepening of reform and opening up and the rapid development of the socialist market economy, intangible assets and their assessment issues have attracted significant attention from relevant state departments [18]. The studies mentioned above have many problems and challenges that need to be addressed. These issues require us to study and explore them in practice. This article discusses the use of Internet of Things (IoT) technology, data envelopment methods, and particle swarm optimization (PSO) algorithm to further improve and develop asset evaluation methods to carry out related work on asset evaluation [19]. Data envelopment and PSO algorithm ensure the cleaning and reclassification of asset data. On the other hand, IoT provides the adaptation of the latest technological trends used for asset evaluation within the manufacturing industry.

The rest of this paper is organized as follows. In Section 2, we will give an overview of related technologies, i.e., asset evaluation and Internet of Things. In Section 3, we will introduce the asset evaluation data analysis based on data envelopment and particle swarm. In Section 4, we will perform the performance and simulation tests of the model built in Section 3. Finally, we summarize and discuss the methods of this paper and give future research directions in Section 5.

2. Related Work

In this section, first we provide a brief overview and the latest technological trends in IoT followed by the existing studies for asset evaluation.

2.1. Internet of Things Technology. The productive social forces are constantly developing, and the subsequent demands for various intelligent applications are also being affected by this development. In an environment where multiple technologies collide and blend, the IoT with the goal of "intelligence" has begun to emerge [20]. The IoT's communication range can cover the world, and data can be exchanged between real objects, and all data sent by real objects can be reflected in real time through legal means [21]. IoT's perception layer is like the nerve endings of the human body's sensory organs, which can connect data in the information space with those in the physical space [22]. The perception layer can obtain the environmental information for various applications, e.g., the manufacturing industry. The information obtained through the built-in special equipment processing responds according to the agreed procedure and transmits the reaction result to the transmission layer through a special channel [23]. The collection devices in the perception layer are called perception devices or perception nodes. Standard devices such as RFID, two-dimensional codes, sensor nodes, and smart terminals can be embedded into mobile communication terminals [24]. From the above description of IoT, in a narrow sense, the automatic identification function and intelligent operation of the IoT are smart networks that are connected based on objects and people. The IoT uses numbers and networks to represent all things, achieves the transmission between people and the transmission in objects, and finally integrates the data transmitted between them.

2.2. Asset Valuation. Asset appraisal method is the general term for a series of technical means implemented by appraisers in the asset appraisal business for the purpose of assessing and estimating the assets' value. At present, the three basic evaluation methods commonly used in the world are the cost method, the market method, and the income method [25]. They apply the technical methods in financial management, accounting, engineering technology, statistics, and other disciplines in accordance with the inherent requirements of asset evaluation to the practice of asset evaluation. They are the three major components of the asset evaluation method system [26]. These three basic methods are actually to judge the value of assets from different time points. Based on the value at different time points, the current value of the assessed object is obtained after analysis and calculation. The schematic diagram of asset evaluation methods and characteristics is shown in Figure 1.

From the perspective of asset appraisal, value and price belong to two different conceptual categories. Value belongs to the category of exchange value [27]. It reflects the monetary relationship between the goods and services to be exchanged and their buyers and sellers. It is the estimate of the value of goods and services in a specific time by professional appraisers based on a specific value definition. Price refers to the amount of currency actually paid or received by the buyer and seller for the goods or services traded in a specific transaction [28]. The result of asset appraisal is a reflection of the value of the appraised object, not the actual transaction price of the appraised object.

3. Asset Evaluation Data Analysis Based on Data Envelopment and Particle Swarm

This article uses the IoT, PSO, and data envelopment methods to improve and develop asset evaluation plans. Since the PSO was proposed, it has received a lot of attention. Numerous research results related to PSO have

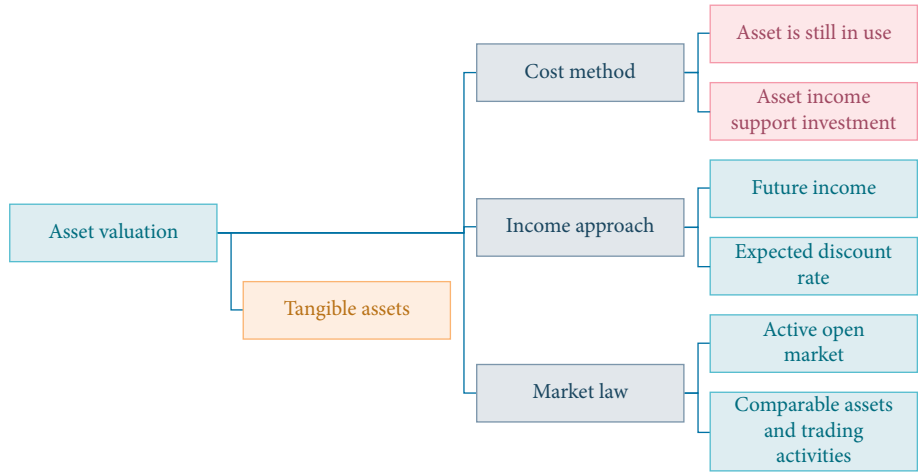

Figure 1: Schematic diagram of asset evaluation methods and characteristics.

appeared constantly [29, 30]. The PSO's application field has gradually expanded from the initial function optimization to a broader area, which has promoted this algorithm. PSO is mainly used in the following aspects. Function optimization is the earliest and most common application field of PSO. It applies the technical methods in financial management, accounting, engineering technology, statistics, and other disciplines according to the inherent requirements of asset evaluation to the practice of asset evaluation. They are the three major components of the asset evaluation method system. These three primary methods are actually to judge the value of assets from different time points. Based on the value at different time points, the assessed object's current value is obtained after analysis and calculation.

Based on existing research, it is found that, in some common function optimization problems, including some typical nonlinear function optimization problems, PSO has shown outstanding performance. According to bionics, PSO adopts a predator strategy. The particle of PSO is analogous to a flock of birds, and each particle is an individual among them [31, 32]. During the foraging process, individual birds constantly adjust their foraging process based on their own experience and other birds' behavior, that is, adjusting the individual bird's speed and position in the foraging process (optimization). In this process, the individual bird's individual optimal solution can be obtained, but the bird group's optimal solution, that is, the optimal global solution, can be obtained. For the optimal solution, the following equation is used:

$$\begin{cases} v_{ij}(t+1) = v_{ij}(t) + c_1 r_1(t)\left(p_{ij}(t) - x_{ij}(t)\right) \\ \quad + c_2 r_2(t)\left(p_{gj}(t) - x_{ij}(t)\right), \\ m_{ij}(t+1) = m_{ij}(t) + v_{ij}(t+1). \end{cases} \tag{1}$$

PSO is used to optimize the combined algorithm to search for the minimum value more accurately [33, 34], as shown in the following equation:

$$h_j = \frac{\sum_{r=1}^{s} u_r y_{rj0}}{\sum_{i=1}^{m} v_i x_{ij0}}. \tag{2}$$

The use of PSO greatly reduces the computational complexity, makes the adjustment of the inertia weight of the wavelet basis function more rapid, and avoids being trapped locally. In this algorithm, the selection of individual position vector elements is the key to optimize the algorithm combined with the wavelet and neural network.

The wavelet analysis of the expansion parameters, translation parameters, and the combination of weights between the layers in the neural network model are used as the position vector of the particle swarm, which has good results [35, 36]. At the same time, the particle fitness function can select the error function of the wavelet neural network, as shown in the following equation:

$$\max h_{j0} = \frac{\sum_{r=1}^{s} u_r y_{rj0}}{\sum_{i=1}^{m} v_i x_{ij0}}. \tag{3}$$

The algorithm will perform a random initialization at the very beginning, and the initial position of the particles often affects the quality of the result and, sometimes, directly determines the accuracy of the final result of the algorithm, as shown in the following equation:

$$\begin{aligned} &\max h_{j0} = t\sum_{r=1}^{s} u_r y_{rj0} = \sum_{r=1}^{s} \mu_r y_{rj0}, \\ &\text{st.} \quad \begin{cases} \sum_{i=1}^{m} w_i x_{ij} - \sum_{r-1}^{s} \mu_r yrj \geq 0 \ (j = 1, \ldots, n), \\ \sum_{i=1}^{m} w_i x_{ij0} = 1, \\ w_i \geq 0 \ (i = 1, \ldots, m), \\ \mu_r \geq 0 \ (r = 1, \ldots, s). \end{cases} \end{aligned} \tag{4}$$

In PSO, the shared information contains the best information of the entire population. All particles update their next position based on their own experience and the best information of the entire population. Generally, they try their best to the current global optimal direction found in the group runs, as shown in the following equation:

$$\min \theta,$$
$$\text{st.} \begin{cases} \sum_{j=1}^{n} \lambda_j x_{ij} \le \theta x_{ij} \, (i = 1, \ldots, m), \\ \sum_{j=1}^{n} \lambda_j y_{ij} \ge y_{rj0} \, (r = 1, \ldots, m), \\ \lambda_j \ge 0 \, (j = 1, \ldots, n). \end{cases} \tag{5}$$

When solving some complex functions such as multimodality, the algorithm often falls into a local optimal solution, and it is difficult to escape this area, causing particles to stagnate in this area and appear premature, and the accuracy cannot meet the expected requirements. It can be depicted using the following equation:

$$\text{st.} \begin{cases} \frac{\sum_{r=1}^{s} u_r y_{rj}}{\sum_{i=1}^{m} v_i x_{ij}} \le 1 \ (j = 1, \ldots, n), \\ v_i \ge 0 \, (i = 1, \ldots, m), \\ u_r \ge 0 \, (r = 1, \ldots, s). \end{cases} \tag{6}$$

Using equation (3), equation (2) is transformed into an equivalent linear programming problem, as shown in the following equation:

$$\begin{aligned} t &= \frac{1}{\sum_{i=1}^{m} v_i x_{ij}}, \\ w_i &= t v_i, \\ \mu_r &= t u_r. \end{aligned} \tag{7}$$

The last step is to iteratively search for the optimized value by repeating the above procedure until the best solution is found by the particle swarm to meet the requirements, or has reached the maximum number of iterations set by the PSO.

4. Model Simulation and Testing Process

In this section, first we analyze the efficiency of asset valuation in Section 4.1 followed by test results of the asset evaluation system in Section 4.2.

4.1. Analysis of Asset Evaluation Efficiency. If the task is not completed, it can be analyzed from different aspects such as geographic location, task price, and member psychology. Since there are many uncertain factors in the psychological situation of members, it is difficult to carry out qualitative analysis here. Therefore, this article chooses to analyze the low task completion rate from two aspects: the spatial matching degree between the task point and the member, and the reasonableness of the pricing strategy. IoT can facilitate this scenario as it has the ability to bridge the gap between spatial matching degree and reasonableness of the pricing strategy. IoT allows the data to exchange between real objects in real time, which can be reflected in real time through legal means. Its role for asset evaluation can be realized through its perception layer. This layer is like the nerve endings of the human body's sensory organs, which can connect data in the information space with those in the physical space, i.e., asset evaluation of the communicating entities.

For asset evaluation, we make a scatter diagram of the distribution of mission points and the distribution of members. It can be seen from Figure 2 that tasks are clustered in areas with high membership density. Therefore, the spatial matching degree between the number of tasks in each area and the number of members is high, and there will be no overtasking and understaffed situations, that is, task pricing and the correlation between the spatial matching degrees is not strong. Hence, the spatial matching degree is not the main reason for the low task completion rate. The wavelet analysis of the expansion parameters, translation parameters, and the combination of weights between the layers in the neural network model are used as the position vector of the particle swarm, which has good results. At the same time, the particle fitness function can select the error function of the wavelet neural network. The scatter diagram of asset distribution and mission completion is shown in Figure 2.

The results are obtained by choosing a step size of 0.1; use MATLAB programming to obtain 20 sets of optimized solutions:

$$Z_1 = -0.002Z_2 - 0.0869Z_3 + 1.6Z_4 + 0.385Z_5. \tag{8}$$

The completion of the 100 tasks extracted from the processing data under the new evaluation scheme is shown in Table 1.

It can be seen from Table 1 that, under the new pricing plan, the completion rate is significantly higher than that of the original plan. Therefore, it can be considered that the new pricing plan is more reasonable than the original plan, and the user acceptance is also higher. From the above, the automatic identification function and intelligent operation of the IoT achieve much higher completion rate. Broadly speaking, the IoT uses numbers and networks to represent all things, achieves not only the transmission between people but also the transmission among objects, and finally integrates the data transmitted between them.

4.2. Asset Evaluation System Test Results. The valuation of assets is an area that has received more attention in recent years. However, this work still has numerous challenges from various aspects. In order to better verify the effectiveness of the asset evaluation system established in this article, we conducted a further system performance test process on the system. The encryption time test results of the asset evaluation system are shown in Figure 3.

It can be seen from Figure 3 that when the number of plaintext bytes is less than 1 byte, the algorithm with the anonymity design has a smaller gap with the former. Please note that, in this figure, the x-axis represents the number of bytes and the y-axis represents the time in millisecond (msec). The

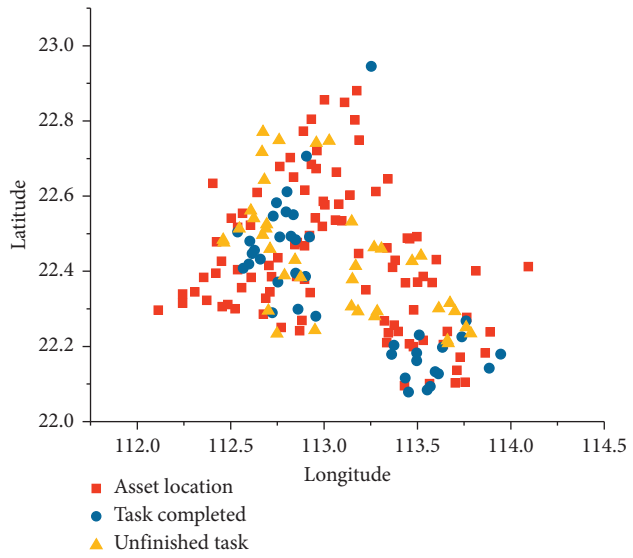

Figure 2: Scatter diagram of asset distribution and task completion.

Table 1: Comparison of the completion rate of asset evaluation tasks.

	Completed	Uncompleted	Completion rate (%)
New evaluation plan	74	26	74.00
Original evaluation plan	835	1042	44.49

time difference is caused by the instability of the system's encryption time when the number of plaintext bytes is small. Due to the increase in the number of cyclic groups participating in the initialization algorithm, the anonymous CIBE algorithm is at a disadvantage as a whole, but the time difference required for encryption algorithm encryption is small, so it can be said that the anonymous CIBE algorithm does not increase the computational burden on the encryption time. This algorithm can be applied to the technical methods in financial management, accounting, engineering technology, statistics, and other disciplines in accordance with the inherent requirements of asset evaluation to the practice of asset evaluation. There are three major components of the asset evaluation method system. These three basic methods are actually to judge the value of assets from different time points. Based on the value at different time points, the current value of the assessed object is obtained after analysis and calculation. Figure 4 shows the change process of the extreme value of the asset evaluation system in the evaluation process.

It can be seen from Figure 4 that the asset evaluation system has shown better results and performance in the extreme value test. This shows that the system can effectively carry system fluctuations under different conditions. The wavelet analysis of the expansion parameters, translation parameters, and the combination of weights between the layers in the neural network model are used as the position vector of the particle swarm, which has good results. At the same time, the particle fitness function can select the error function of the wavelet neural network.

For the asset evaluation system established in this article, we test the score distribution of the system for different assets. Therefore, this article chooses to analyze the low task completion rate from two aspects: the spatial matching degree between the task point and the member, and the reasonableness of the pricing strategy. The distribution of the scores of different assets at the time of evaluation is shown in Figure 5.

It can be seen from Figure 5 that the asset evaluation system has shown better results and performance for the score distribution of different assets during evaluation. The comparison is first made based on longitudinal comparison, which uses multiple sets of data to test how the optimized algorithm compares with the preoptimized algorithm and whether the similar optimized algorithms have changed, and whether the performance is more suitable for the edge environment of the IoT.

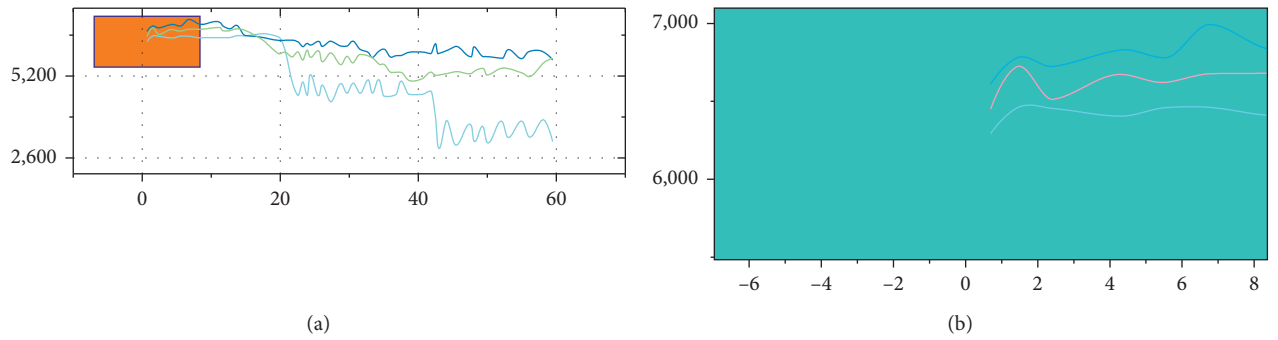

Figure 3: The encryption time test chart of the asset evaluation system.

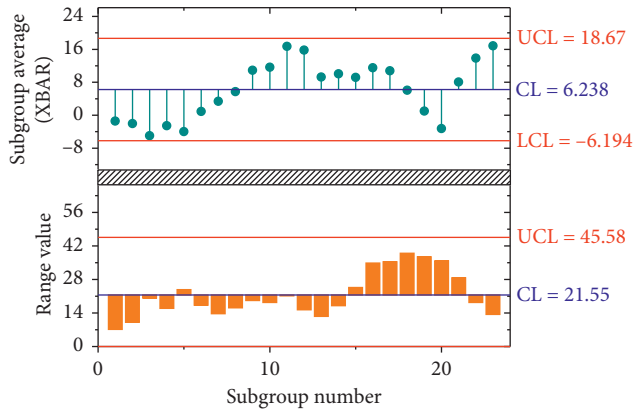

Figure 4: Changes in the range of the asset appraisal system during the appraisal process.

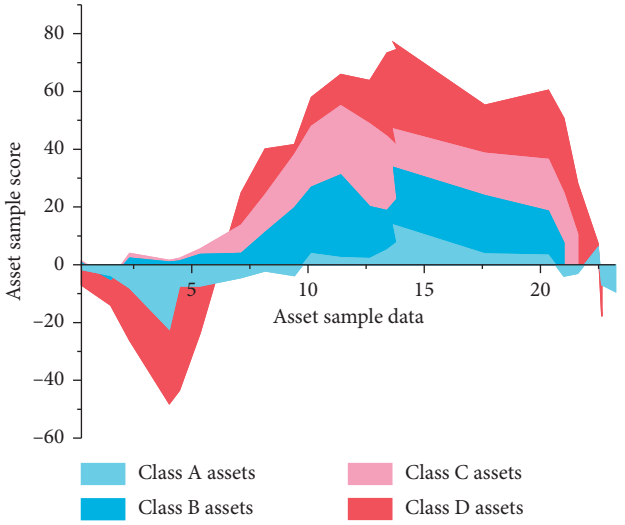

Figure 5: The distribution of scores of different assets at the time of evaluation.

5. Conclusions

With the advent of globalization and the era of knowledge economy, the profoundly changing domestic and international environment, on the one hand, provides extensive development space for the asset appraisal industry but also brings a lot of new challenges to the healthy development of the asset appraisal industry on the other hand. Business evaluation has begun to transform from traditional businesses to emerging businesses due to the technological

trends and the emergence of the Internet of Things (IoT). However, there are numerous challenges for effective asset evaluation from a technology perspective. In this article, an asset evaluation framework was designed to use the data envelopment methods, IoT, and particle swarm optimization (PSO) algorithm. This framework can provide an all-weather and no-delay preparation for asset appraisal. Data envelopment and PSO algorithm ensure the cleaning and reclassification of asset data. We verify the effectiveness and reasonable practicability of the model by comparing experimental simulation and manual evaluation. Although this article has carried out a more in-depth study of asset evaluation, it still has numerous gaps to be filled due to the limitation of personal knowledge level. In the future, we will further research asset appraisal and provide scientific advice for the asset appraisal industry's healthy development.

Data Availability

The data used to support the findings of the study are available from the corresponding author upon request.

Conflicts of Interest

The authors declare that they have no conflicts of interest.

References

[1] B. J. Wu, A. X. He, A. Y. Le et al., "How earthquake-induced direct economic losses change with earthquake magnitude, asset value, residential building structural type and physical environment: an elasticity perspective," *Journal of Environmental Management*, vol. 231, pp. 321–328, 2019.

[2] H. Masset, M. Z. Esteki, E. Dimitriadou et al., "Multi-centre evaluation of a comprehensive preimplantation genetic test through haplotyping-by-sequencing," *Human Reproduction*, vol. 34, no. 8, 2019.

[3] P. Lin and X.-X. Yuan, "A two-time-scale point process model of water main breaks for infrastructure asset management," *Water Research*, vol. 150, no. 1, pp. 296–309, 2019.

[4] F. Chasset and C. Francès, "Current concepts and future approaches in the treatment of autaneous lupus trythematosus: a comprehensive review," *Drugs*, vol. 79, no. 11, 2019.

[5] D. P. Bigelow and T. Kuethe, "A tale of two corders: use value assessment, land development, and irrigation envestment," *American Journal of Agricultural Economics*, vol. 102, no. 4, pp. 1404–1424, 2020.

[6] J. Abreu-Gomez, D. Walker, T. Alotaibi, M. D. F. McInnes, T. A. Flood, and N. Schieda, "Effect of observation size and apparent diffusion coefficient (ADC) value in PI-RADS v2.1 assessment category 4 and 5 observations compared to adverse pathological outcomes," *European Radiology*, vol. 30, no. 8, pp. 4251–4261, 2020.

[7] F. Lais, G. Navarro, S. M. Leite et al., "Pathways linking environmental risks, polygenic risk score to schizophrenia and psychotic experiences," *A Brazilian Cohort of Children and Adolescents Schizophrenia Bulletin*, vol. 120, no. 1, p. S24, 2020.

[8] K. Kaddoura, T. Zayed, Z. Chen et al., "Optimized maintenance model for wastewater treatment plants," *Canadian Journal of Civil Engineering*, vol. 30, pp. 1–47, 2020.

[9] S. Sannigrahi, S. Chakraborti, P. K. Joshi et al., "Ecosystem service value assessment of a natural reserve region for strengthening protection and conservation," *Journal of Environmental Management*, vol. 244, no. 15, pp. 208–227, 2019.

[10] A. Aslam, U. Mehmood, M. H. Arshad et al., "Dye-sensitized solar cells (DSSCs) as a potential photovoltaic technology for the self-powered internet of things (IoTs) applications," *Solar Energy*, vol. 207, pp. 874–892, 2020.

[11] B. M. Elhalawany, R. Ruby, and K. Wu, "D2D communication for enabling internet-of-things: outage probability analysis," *IEEE Transactions on Vehicular Technology*, vol. 1, no. 99, 2019.

[12] S. Gupta, E. M. Johnson, J. G. Peacock et al., "Radiology, mobile devices, and internet of things (IoT)," *Journal of Digital Imaging*, vol. 33, no. 12, 2020.

[13] Y. Qian, L. Ma, and X. Liang, "The performance of chirp signal used in LEO satellite internet of things," *IEEE Communications Letters*, vol. 23, no. 8, 2019.

[14] B. Pourghebleh, V. Hayyolalam, and A. A. Anvigh, "Service discovery in the Internet of Things: review of current trends and research challenges," *Wireless Networks*, vol. 26, no. 7, 2020.

[15] A. C. Faleye, A. A. Adegoke, K. Ramluckan et al., "Everything you wanted to know about smart cities: the internet of things is the backbone," *Science of the Total Environment*, vol. 5, no. 3, pp. 60–70, 2019.

[16] C. Michie, I. Andonovic, C. Davison et al., "The internet of things enhancing animal welfare and farm operational efficiency," *Journal of Dairy Research*, vol. 87, no. S1, pp. 1–8, 2020.

[17] U. Tariq, A. Ibrahim, T. Ahmad, Y. Bouteraa, and A. Elmogy, "Blockchain in internet-of-things: a necessity framework for security, reliability, transparency, immutability and liability," *IET Communications*, vol. 13, no. 19, pp. 3187–3192, 2019.

[18] M. Usman, A. Jolfaei, and M. A. Jan, "RaSEC: an intelligent framework for reliable and secure multilevel edge computing in industrial environments," *IEEE Transactions on Industry Applications*, vol. 56, no. 4, pp. 4543–4551, 2020.

[19] Y. Yang, W. J. Xue, and J. Liu, "Efficiency evaluation of county-level public hospitals in Hainan, China: a four-stage data envelope analysis model based on panel data," *Chinese Medical Journal*, vol. 134, pp. 876–878, 2021.

[20] H. Khan, M. A. Jan, M. Alam, and W. Dghais, "A channel borrowing approach for cluster-based hierarchical wireless sensor networks," *Mobile Networks and Applications*, vol. 24, no. 4, pp. 1306–1316, 2019.

[21] Y. J. Chen and S. E. Chang, "CMOS cook modulator with fast envelope transient," *Electronics Letters*, vol. 55, no. 17, 2019.

[22] G. N. Eastep, R. H. Ghanam, T. J. Green, and J. S. Saad, "Structural characterization of HIV-1 matrix mutants implicated in envelope incorporation," *Journal of Biological Chemistry*, vol. 296, no. 2, Article ID 100321, 2021.

[23] W. Yao, F. Khan, M. A. Jan et al., "Artificial intelligence-based load optimization in cognitive internet of things," *Neural Computing and Applications*, vol. 32, pp. 1–11, 2020.

[24] X. Li and Y. Liu, "A quick algorithm for evaluation of minimum zone circles from polar coordinate data," *Review of Scientific Instruments*, vol. 90, no. 12, Article ID 125114, 2019.

[25] M. Ibrar, A. Akbar, R. Jan et al., "ARTNet: AI-based resource allocation and task affloading in a reconfigurable internet of vehicular networks," *IEEE Transactions on Network Science and Engineering*, vol. 44, p. 1, 2020.

[26] S. Pollmann, A. Springer, S. Rustgi et al., "Substrate channeling in oxylipin biosynthesis through a protein complex in

the plastid envelope of *Arabidopsis thaliana*," *Journal of Experimental Botany*, vol. 70, no. 19, pp. 1483–1495, 2019.

[27] H. W. Yen, S. Takakuwa, P. G. Gu et al., "Signs of outflow feedback from a nearby young stellar object on the proto-stellar envelope around HL tau," 2019.

[28] L. Doan, S. Ramstedt, W. Vlemmings et al., "The extended molecular envelope of the asymptotic giant branch star $\pî {1}$ gruis as seen by ALMA II. the spiral-outflow observed at high-angular resolution," *Astronomy and Astrophysics*, vol. 20, pp. 1–10, 2019.

[29] B. Miszalski and V. Manick, "The post-common-envelope binary nucleus of the planetary nebula IC 4776: neither an anomalously long orbital period nor a wolf–rayet binary," *Monthly Notices of the Royal Astronomical Society*, vol. 14, no. 1, p. 1, 2019.

[30] M. Bertagnolli and J. Tabernero, "Value assessment frameworks in oncology: championing concordance through shared standards," *Annals of Oncology*, vol. 30, pp. 505-506, 2019.

[31] C. V. Gonzalez, I. Herraiz, J. Delgado et al., "OP10.05: oetal growth assessment and perinatal outcomes associated with extremely high sFlt/PlGF value," *Ultrasound in Obstetrics and Gynecology*, vol. 54, no. S1, pp. 116-117, 2019.

[32] A. Pichon-Riviere, S. Garcia-Marti, W. Oortwijn, F. Augustovski, and L. Sampietro-Colom, "Defining the value of health technologies in latin America: cevelopments in value frameworks to inform the cllocation of healthcare sesources," *International Journal of Technology Assessment in Health Care*, vol. 35, no. 1, pp. 64–68, 2019.

[33] P. Bahri, D. R. Morales, A. Inoubli et al., "Proposals for engaging fatients and healthcare professionals in risk minimisation from an analysis of dtakeholder input to the EU ialproate assessment using the novel analysing stakeholder hafety engagement tool (ASSET)," *Drug Safety*, vol. 10, pp. 1–44, 2021.

[34] D. Schlicke, N. V. Tue, J. Gomes, C. Sousa, and M. Azenha, "Analytical assessment of restraint forces and crack widths in end-restrained building slabs," *Engineering Structures*, vol. 224, Article ID 111218, 2020.

[35] M. N. Scheu, L. Tremps, U. Smolka, A. Kolios, and F. Brennan, "A systematic failure mode effects and criticality analysis for offshore wind turbine systems towards integrated condition based maintenance strategies," *Ocean Engineering*, vol. 176, no. 15, pp. 118–133, 2019.

[36] V. Kunniyoor, P. Singh, and K. Nadella, "Value of closed-cycle gas turbines with design assessment," *Applied Energy*, vol. 269, Article ID 114950, 2020.

Hindawi
Mobile Information Systems
Volume 2021, Article ID 9993019, 9 pages
https://doi.org/10.1155/2021/9993019

Research Article

Systematic Study on Expression of Vocal Music and Science of Human Body Noise Based on Wireless Sensor Node

Yifei Xu

Yulin University School of Art, Yulin 719000, Shaanxi, China

Correspondence should be addressed to Yifei Xu; xuyifei@yulinu.edu.cn

Received 11 March 2021; Revised 7 April 2021; Accepted 21 April 2021; Published 29 April 2021

Academic Editor: Mian Ahmad Jan

Copyright © 2021 Yifei Xu. This is an open access article distributed under the Creative Commons Attribution License, which permits unrestricted use, distribution, and reproduction in any medium, provided the original work is properly cited.

In this paper, we use a wireless sensor node to investigate the relationship between vocal art composition and human body noise. For the vocal music, the suggested predictor created a wireless sensor node convergence link model and the HART graph routing model is used to systematically design the human noise science. The wireless sensor node optimizes the acquisition of information on vocal art and analyzes the acoustic signal characteristics. The optimally balanced scheduling model has been used to scientifically and distributedly regulate vocal art performance and human body noise. The proposed model enhances the signal detection ability and raises the performance level of vocal art, music art, and human body noise signal. The results of the simulation demonstrate that the proposed model enhances the signal acquisition capability of vocal music and the analysis of human noise. It has a powerful ability to generate vocal signal characteristics and a stronger ability to handle interference with noise.

1. Introduction

The vocalist's performance, like all musical works, is dependent on the singer or performer's ability to reproduce the composer's work. The goal of singing is to use powerful vocal abilities to effectively convey the ideological content of songs, to infect the audience with haunting melodies, and to make the audience enjoy the art [1]. The human body is a marvelous human organ for the singer; its interpretation, expression, representation, and embodiment of human musical art is unmatched in any musical instrument in the world. Master the correct breathing technique as well as the correct voice. The sound's high position relates to complete headspace resonance, which we stress as mask resonance [2]. A focused, bright, relaxed, and penetrating sound resonates with the entire cavity of the head. Singing is more relaxing, and it sounds brighter and more wonderful [3]. Humming practice should help you achieve a high position sound. It seems to be that human body noise and transcription have a systemic connection with vocal music art expression, and it is useful to research the relationship model between vocal music art expression and the science of body noise in a person [4]. The Vocal Art Performance Network is suggested in conjunction with wireless sensors to capture artistic information of vocal music and gain control over the improvement of human body noise [5]. Network channel equation design and optimization of path detection algorithms, as well as path conflict avoidance design, are the fundamental technologies of vocal art expression and systemic control of human body noise science [6].

Wireless sensors are scientific and systemic ways of monitoring the expression of sound and noise art in the human body [7]. The optimization of the network causation node was governed through the design of routing protocol optimization and control of the wireless sensor route of the Internet of Things. Some research findings were discovered, including a network activation node that suggested a scientific and systemic control method for the human voice of wireless sensors without sound and performance [8]. To increase human body noise position, adaptive modulation coding has been used. Maximum sensor power management is used, and as a result, network node coverage capacity is increased [9]. This procedure, however, has issues with low stability and consistency in gathering voice art information

from wireless sensors and systemic monitoring of human body science. A scientific and systematic method of human noise control and data collection based on wireless sensors with a strong and appealing understanding of node communication load is proposed in [10]. Wireless sensor nodes constructed the topological model of the routing graph of the voice information distribution route, checked the combined load and power of the wireless Internet sensor of things, and performed network routing conflict prevention design. There are other problems with the control mechanism, such as less interference and less autonomous deployment capability [11]. It also investigates noise settings, noise extraction facilities, sound sampling quality, storage format, age of recorded items, number of recorded items, vocal music, and other topics and is of high standard and seriousness [12]. The study meets the standards by distinguishing between men and women, but the sound portion of the recorded object is unclear, and the kinds of sound signal collection and singing range are not defined. The preceding content is one of the most important factors determining the performance of Sound Music Art [13].

This research presents a mathematical framework for vocal expression and the science of human noise based on wireless sensors and a wireless node of convergence sensor model of vocal art. The HART graph routing model is used to create a structured design for vocal art and noise science. The wireless sensor is designed to make the best use of node models, and the convergent connection gain control technique is used to control wireless sensor vocal art performance. Furthermore, the adaptive balanced scheduling model is used for scientific and distributed tracking of vocal art performance as well as human body noise. The network of wireless sensors for acquiring information about vocal art is intended to better acquire information on vocal art and understand sound signal characteristics. We also enhance our ability to voice and detect the signal. Finally, simulation experiments are conducted in order to demonstrate the best performance of this technique in scientific and systemic performance and human noise analysis.

2. Methodology

In this section, we introduce vocal data using wireless sensors in order to control human corporal noise on a scientific and systematic level. Additionally, we develop an artistic expression of vocal music and a distribution model of human noise control nodes in wireless sensor and vocal performance, as well as a convergence link model for human noise control nodes.

2.1. Voice Signal Preprocessing. The extraction of acoustic parameters is critical to the objective assessment of the body voice. The voice signal must be processed in advance, including digital, preaccentuation, framing, and window addition, regardless of the procedure used to extract and evaluate the parameters [14, 15]. Supplementation is an important step in analyzing voice signals and extracting acoustic parameters. People's speech signals are analog, so the analog signals must be converted to digital signals before the digital signals can be processed and analyzed [16]. In this paper, a valuable and digitized voice data file is obtained by recording the singing voice signal with a microphone and a computer sound card and collecting it for later use [17]. After receiving the data file of the human voice signal, the signal is reweighted, and frame and window preprocessing is performed, which allows the signal after processing to satisfy the real needs; it is critical to increasing the accuracy of the subsequent data processing. Figure 1 depicts a noise signal that has been preconditioned [18].

2.2. Frame and Window. The generation of speech signals is related to various movements of the organs of speech, and the random movement of the organs causes the signal itself to be unstable. However, the state of vocal organ changes is much slower than that of sound vibration [19]. Therefore, it is considered that the speech signal is stable within 10–30 ms, and there is no obvious change in the characteristics of the speech spectrum and some physical properties in the short term. Therefore, only the speech signal is divided into a few short speech segments, the processing method of the stationary signal can be introduced into the speech signal processing, and each segment here is called a short speech analysis frame. Each frame signal is regarded as a stationary process, which overcomes the difficulty of the speech signal analysis and processing, and the processing of each frame is equal to the long signal with invariant features. N sampling points are combined into one observation unit, called frame length. Usually, the frame length is 256 or 512, and the time is about 20–30 ms.

The framing should be continuous; that is, it is not possible to replicate the frame, and the information is not presented and not processed between frames. The solution to this issue is to overlap the components so that frame and structure can maintain a smooth transition, which includes samples M, called frameshifts, usually 0–1/2 frame lengths. The signal is altered after framing from the original signals as the frames at start and end are stopped and need a window to be attached. Adding windows to the signal can not only effectively solve the problem of the discontinuity of the position signal at the beginning of the frame, but also make the original nonperiodic speech signal present the part of the periodic function. In the process of signal windowing, window functions are usually selected according to the nature and processing requirements of the signal being analyzed. The main part of the rectangular window is more concentrated, but the side lobe is high and there is a side lobe, which will transform the high-frequency interference and the leakage into the transform. It is suitable for the precise readout of the main lobe frequency but does not consider the signal processing of the amplitude accuracy. The peak value of the main lobe and the first side lobe peak decay to 40 dB, which is suitable for the analysis of the narrowband signals with strong interference noise as shown in Figure 2 for the preprocessed noise signal.

The voice demands the involvement and collaboration of power bodies, vibrational organisms, resonance organisms,

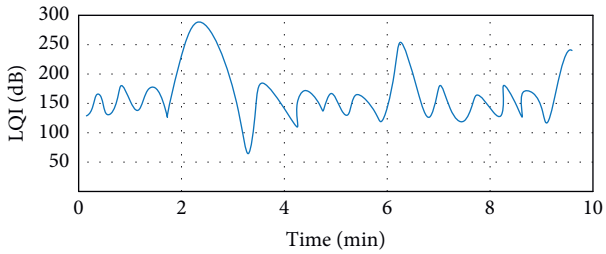

Figure 1: Preconditioning noise signal [18].

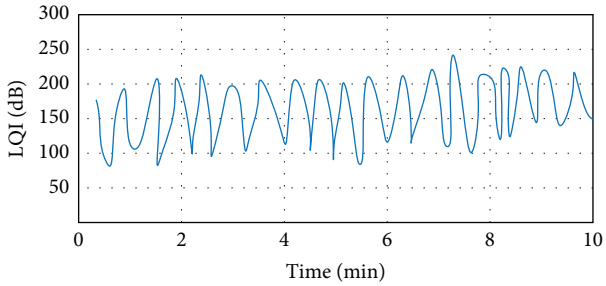

Figure 2: Preprocessed noise signal [19].

and the nervous system. Due to the incredibly intricate process, the voice function is a multidimensional and multiparameter evaluation of your voice with a complete and impartial assessment of your creative voice. It is important to have multidimensional acoustic signal parameters: selection and proper extraction of the technical signals of the voice utilizing vocal analysis, observation of the person's state in a pronunciation, assessment of whether the voice is normal and its regularity, and opening the doctor's diagnosis for an unbiased evaluation of the subsequent technique [20].

2.3. Vocal Performance and Human Noise Control Nodes Convergence Link Model. To realize the information collection of vocal art based on wireless sensors and the scientific and systematic control of human body noise, firstly, the convergence link model of vocal art expression and human noise control node of a wireless sensor is constructed. The wireless sensor vocal art monitoring area is a square area with a side length of M, and there are N vocal art sensor routing relay nodes, assuming that the base station has sufficient energy. In the process of scientific and systematic control of vocal art and human noise, the energy balance control is carried out through the adaptive allocation of laser sensor routing nodes [21]. The information acquisition node of wireless sensor vocal music art is defined as$i$, based on the number of neighbor nodes, the number of hops and sampling interval T_f between source and cluster head node is determined. The power consumed by cluster head node to transmit L bit data is set as $T_s = N_f T_f$, and the equilibrium game between cluster head node and transmission link is carried out by using the game analysis method of node transmit power. The energy consumption of each node is obtained as follows:

$$T_c = \mathrm{ent}\left(T_f / N_c\right). \tag{1}$$

The distributed routing detection algorithm is used to analyze the coverage of nodes through the shortest path deployment. When$c_j T_c < T_f \forall j \in [0, N_f - 1]$, the base station of the wireless sensor network with vocal performance and human noise is located at the top of the monitoring area of the network at the initial moment [8]. The data packet forwarding of wireless sensor dominating point set is$\sum_{j\in S, j\neq i} x_j r_j(x) p_j^i(x)$. The characteristics of output power spectral density of vocal performance and human noise wireless sensor network converging link are obtained by using the conflict coordination control method:

$$p_i = \frac{\sigma^2}{1 - \sum_{j=k+1}^{n} \gamma_i / \gamma_j + G} \frac{\gamma_i}{h_i(\gamma_i + G)}, \tag{2}$$

where $\gamma_i = \gamma_{th}$, and the sensor coefficient representing the artistic performance of the wireless sensor and the energy saving distribution of the nodes of the human noise control node estimates the minimum variance of the wireless sensor node η at any position and obtains the triggered node. The objective function of energy balance control is described as follows:

$$\arg\max_{p_i \in P_i} u_i = \arg\max_{p_i \in P_i} \gamma_i = \frac{\gamma_{th}\sigma^2}{h_i[G - (n-k-1)\gamma_{th}]}, \tag{3}$$

where $\mathrm{argmax}_{p_i \in P_i} u_i$ is the frame head length of cluster head node i. The maximum likelihood estimation results of the convergence link model for the stability control of the vocal art performance sensor can be expressed as follows:

$$\sigma_\eta^2 = E[\hat{x}(\eta) - x(\eta)]^2, \quad \eta \in \Omega_\eta, \tag{4}$$

where $\hat{x}(\eta)$ is the coverage of the sensor network based on the equivalent model of the vocal performance of the wireless sensor and the convergence link gain control of the human noise control node is constructed, and the trigger control between the vocal art performance and the human noise control node is carried out [22].

2.4. HART Graph Routing Algorithm and Routing Detection Protocol Design. The HART graph routing model is used to design the route detection protocol for vocal performance and human noise wireless sensor networks. The HART map routing detection protocol is constructed based on the IEEE 802.3 EFM protocol, and $M_1\, M_2 \cdots M_N$ are the human body noise distribution under the wireless sensor. In the optimal network topology, the network transmission channel $K\{r_i\}$ is a two-way channel wireless transceiver channel, which is represented as$r_i(x)$, where $mu(i, x) + np$ is the network node distribution density of the noise coverage area of the human body, and the network transmission channel $mu(i, \mathbf{x}) + np > 0$ is the wireless transceiver channel of a two-way channel [9]. According to the HART graph routing model, the difference characteristic function of node output is obtained:

$$Es(j) = \{(u, v) \in E | u \in Vs(j), v \in Vs(j)\}. \quad (5)$$

The trigger node of the vocal art expression and the human body noise wireless sensor network is transformed into the link holomorphic analytical model, and the trigger node is repaired to obtain the relationship between the vocal music art expression and the human body noise wireless sensor network. The 2D coordinate system of the routing node is represented by (x_u, y_u), and the artistic representation of vocal music is equivalent to the gain control model of the convergence link of the human noise control node in the following form:

$$\max_{p_i \in P_i} u_i(p_i, p_{-i}) = \ln(1 + \gamma_i) - \beta_i \gamma_i, \quad i \in N. \quad (6)$$

Based on the two-way link model (k, i), the vocal art expression of wireless sensor, and the design of human noise acquisition routing detection protocol model, the accuracy percentage of cluster head emission data is obtained:

$$\eta_{\text{comm}} = \frac{k_1 \cdot l}{E_{\text{comm}}} \cdot \left(1 - p_{\text{drop}}\right). \quad (7)$$

The cluster head node transmit data packet is$CH_i (i \in C_1)$, the channel equalization control method is used to calculate the average communication time interval of the first node [10]. For a given link gain coefficientγ_{th}, when$\beta_{c_1} = u_i'(\gamma_{th})$, vocal performance and human noise wireless sensor network, the overlay gain transfer function of the complex is described as

$$\frac{\partial u_i}{\partial p_i} = \frac{G h_i}{\sum_{j \neq i} h_j p_j + \sigma^2} \left(\frac{1}{1 + \gamma_i} - \frac{1}{1 + \gamma_{th}}\right). \quad (8)$$

The average amount of mutual information for the j reference node is

$$R_i(k) = \text{diag}\left\{r_{(i-1)q+1}(k), r_{(i-1)q+2}(k), \ldots, r_{(i-1)q+q}(k)\right\} \quad (i = 1, 2, \ldots, N). \quad (9)$$

From this, the correlation matching function between the artistic expression of vocal music and the root node and trigger node of the human body noise wireless sensor network is described as follows:

$$\begin{aligned} \breve{B}(k) &= E\left[w(k)\breve{V}^T(k)\right], \\ &= E\left[w(k)V^T(k)\right]\left[L^{-1}(k)\right]^T, \\ &= \left[\breve{B}_1(k) \;\; \breve{B}_2(k) \;\; \cdots \;\; \breve{B}_N(k)\right], \end{aligned} \quad (10)$$

where

$$\begin{cases} \Phi(k) = [A(k) - J(k)\breve{H}(k)], \\ \breve{w}(k) = \Gamma(k)w(k) - J(k)\breve{V}(k). \end{cases} \quad (11)$$

According to the above processing, a routing detection protocol based on the HART model and wireless network sensors is established.

3. Control Optimization Realization

In this section, we will discuss the collection of vocal music art information, as well as the performance of vocal music art and the realization of scientific systemic control optimization for human noise. In addition, we will also analyze and control the convergence link between vocal performance and the human noise control node.

3.1. Analysis and Gain Control of Convergence Link. Vocal music is conducted by using a vocal art format convergence model and the wireless sensor network human noise control node, as well as a routing detection protocol between vocal art expression and the wireless body noise sensor network. It optimizes the art of vocal music and the research and systematic management of human noise. The human noise science systematic control approach is used to control the wireless sensor's vocal art performance, as well as the convergent link control for the node of human noise control and the path between the vocal art expression and the human noise wireless sensors.

The numbers of conflicts and the delay are $\alpha_l$and τ_l, respectively, where $l \in [0, L-1]$ $\tau_0 < \tau_1 < \ldots \tau_{L-1}$, and the robust sexy radius $GNInter_i(n)$ of trigger node can be expressed as

$$N\text{Inter}_i(n) = N\text{Inter}_i(n) + 1, \quad \text{if } j \notin N_i \cup t_{ij} \geq T_h. \quad (12)$$

If $CIntra_i(n)$ is used to represent the energy overhead of the transmission of F-bit packets by node i and the maximum threshold for transmission packets of node $CInter_i(n)$, then the allocated power and time chips for each cluster head node are

$$\begin{aligned} \text{CIntra}_i(n) &= \frac{N\text{Intra}_i(n)}{T}, \\ \text{CInter}_i(n) &= \frac{N\text{Inter}_i(n)}{T}. \end{aligned} \quad (13)$$

Based on this, the routing conflict avoidance mechanism of the Internet of things is designed, and the maximum probability density function of sensor node i effectively covering the monitoring area $U_i(n)$ in the$t(n)$ time window is obtained as follows:

$$U_i(n) = \alpha \text{CIntra}_i(n) + (1 - \alpha)\text{CInter}_i(n), \quad \alpha \in (0, 1). \quad (14)$$

By optimizing the topology design of the routing diagram of the vocal art expression and the human body noise wireless sensor network, the robustness coefficient of the vocal art expression and the human body noise wireless sensor network routing graph topology is obtained.

$$E_{\text{Rx}}(l) = lE_{\text{elec}}. \quad (15)$$

Among them, d is the artistic representation of vocal music and the routing transfer probability of the

transmission node of the human noise wireless sensor network is the residual energy r of the cluster head, which is the current communication cycle of vocal art expression and human body noise wireless sensor network. Therefore, the convergent link gains control of vocal performance, and the human noise control node is realized. The optimized control objective function is as follows:

$$T(n) = \begin{cases} \dfrac{P}{1 - P[r \bmod (1/P)]} \cdot \left\{ c\left[\dfrac{E_{res}}{E_{init}} + \left(r_u di\ v \dfrac{1}{p} \right) \left(1 - \dfrac{E_{res}}{E_{init}} \right) \right] + (1-c) \dfrac{d_{\max} - d_i}{d_{\max} - d_{\min}} \right\} n \in G, \\ 0, \end{cases} \tag{16}$$

where when vocal art performance and human body noise wireless sensor network trigger node election as cluster head, set ru is 0; when there is a routing conflict, set the sensor transmission node connectivity cost coefficient equal to threshold d0; the residual energy of the triggered node gradually decreases; and vocal performance and human noise control node convergence link gain control matrix BN×1 are as follows:

$$\begin{aligned} r(t) &= \sum_i \sum_{j=0}^{N_f - 1} \sum_{l=0}^{L-1} b_i \alpha_l p\left(t - iT_s - jT_f - c_j T_c - \tau_l \right) + \omega(t), \\ &= \sum_i \sum_{j=0}^{N_f - 1} b_i p_h\left(t - iT_s - jT_f - c_j T_c - \tau_0 \right) + \omega(t). \end{aligned} \tag{17}$$

Multiplying the vocal performance with the node link matrix $\mathrm{SN} \times L$ of the human body noise wireless sensor network and the energy matrix $\mathrm{TL} \times 1$ consumed by the node to receive the l bits data, thus realizing the expression of the vocal music art of the wireless sensor and the human body. Route detection and link gain control of noise control nodes.

3.2. Cluster Head Transmit Power Equalization Control and Adaptive Equalization Scheduling. A control model equalizes voice performance and human noise with cluster head power. Wireless sensor networks are installed to implement the wireless sensor; the node is used for the optimal wireless sensor deployment and as an approach to the convergent link gain control. A balanced adaptive planning model is used to regulate vocal art and the noise of the human body scientifically. The communication load between wireless sensor vocal art performance and human noise control node is as follows:

$$\begin{aligned} r(t) &= \sum_i \sum_{j=0}^{N_f - 1} \sum_{l=0}^{L-1} b_i \alpha_l p\left(t - iT_s - jT_f - c_j T_c - \tau_l \right) + \omega(t), \\ &= \sum_i \sum_{j=0}^{N_f - 1} b_i p_h\left(t - iT_s - jT_f - c_j T_c - \tau_0 \right) + \omega(t), \end{aligned} \tag{18}$$

where

$$p_h(t) = \sum_{l=0}^{L-1} \alpha_l p\left(t - \tau_{l,0} \right). \tag{19}$$

In addition, $\omega(t)$ is the weight of routing conflict avoidance for intracluster nodes and $p_h(t)$ is the power attenuation of l bits data sent by wireless sensor vocal art information acquisition nodes. The payload overhead of the routing topology for the vocal performance and human noise wireless sensor network cluster heads and trigger nodes is obtained as follows:

$$P_{\mathrm{AOMDV}} = (1 - P_d)^2 \left\{ 1 - \left[1 - (1 - P_e)^n (1 - P_d)^{n-1} \right]^m \right\}. \tag{20}$$

The routing conflict avoidance mechanism of the Internet of things is constructed and the RMS error of node robustness control is obtained by using the maximum likelihood estimation model. The calculation formula is expressed as follows:

$$\begin{aligned} \mathrm{MSE} = \xi &= E\left[\varepsilon_k^2 \right], \\ &= E\left[d_k^2 \right] - 2W^T P + W^T R W. \end{aligned} \tag{21}$$

The message coverage of the triggering node has been strengthened because of the performance of the vocal music, the load of the human noise wireless sensor network, and the robustness perception coefficient from the source to the sink. The game model for robustness control of the information acquisition node of the wireless sensor sound music art is achieved as follows, following an autoadaptable rotation schedule:

$$\begin{aligned} E_{Tx}(L, d) &= \begin{cases} LE_{\mathrm{elect}} + L\varepsilon_{fs} d^2, & d < d_0, \\ LE_{\mathrm{elect}} + L\varepsilon_{mp} d^4, & d < d_0, \end{cases} \\ E_{Rx}(L) &= LE_{\mathrm{elect}}. \end{aligned} \tag{22}$$

4. Analysis of Simulation Experiment

In this section, we examine and evaluate the performance and effectiveness of the proposed model and test the application apprehending wireless sensor's network for the vocal music art and also acquisition node optimization control and the human body noise scientific systematic

analysis. The experiment analysis is carried out; the experiment is carried out with MATLAB 7 simulation tool.

4.1. Experimental Setup. We have set up a wireless sensing network cluster with default configurations. The C/C++ network is used to build the related graphical model of vocal art expression and body noise. The message link model and control of the wireless sensing vocal music node are also built on the same configuration. The initial location of wireless sensor network transmission is set at 200 to 200, the radius of communication coverage in a single node is 2 m, the bit sequence of vocal data is 24 Mbit, and network topology occurs. There are 6 activate nodes and 12 sink nodes, with a link output delay of 20 80 s, and an estimated completion possibility is set to Pe = 0.98 with false alarm chance, that is, Pd = 0. 04. The node transmission data simulation time is 100 s with the SNR of 3 dB, and the acquisition results of vocal and human noise signals are shown in Figure 3.

The signal model of Figure 3 is taken as the research object, the artistic expression of vocal music and the detection of human noise signal are carried out, and the detection results are shown in Figure 4.

4.2. Detection of Human Noise Signal. To increase the control robustness of vocal music information acquisition nodes, the cluster head transmit power equalization control technique is used to implement adaptive equalization scheduling of wireless sensor nodes. The wireless sensor vocal art information collection vocal art performance and the human body noise scientific systemic control performance test simulation analysis result is shown in Table 1.

According to the analytical results in Table 1, the proposed method increases the signal collection of vocal music and the system analysis ability of the human body's noise signal. It has a robust ability to extract sound signal characteristics, a stronger ability to withstand noise interference, and a high test detection probability. Figure 5 demonstrates a performance test comparison that illustrates how this procedure can increase the accuracy of vocal and human noise detection.

In addition, Table 2 shows the medians and standard variations of diverse acquisition procedures. From Table 2, the current study's findings show that various types of data measurement techniques achieve comparable results for the chosen number of elements. In f0, F1, and F3 measures, as well as the associated statistical significance and variance factors, acquisition methods were observable. Furthermore, there were no significant changes in some time measures, such as the number of pauses and percentage pauses. Remarkably, there was some frequency and strength variability in the recording devices that remained constant.

4.3. Subjective Auditory Perception Evaluation. Individual auditory evaluation is affected by personal measures and there are issues with precision and stability. It is undeniable that subjective auditory perception assessment is the only

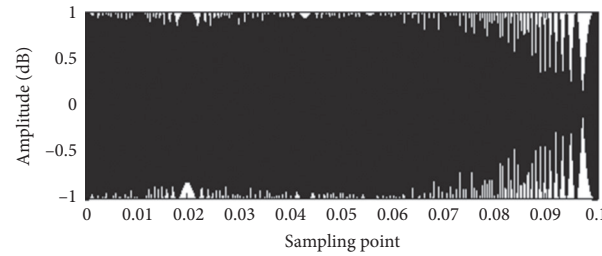

Figure 3: Acquisition results of vocal and human noise signals.

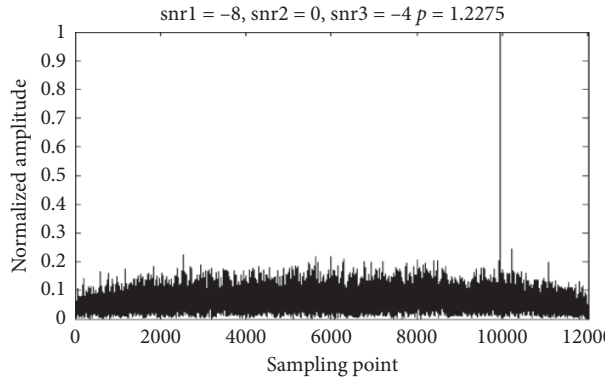

Figure 4: Detection result of vocal art signal based on the wireless sensor.

Table 1: Comparison of performance testing.

SNR (dB)	Proposed method	Reference [4]	Reference [6]
−10	89.94	82.34	83.98
−5	94.35	89.65	85.33
0	98.43	93.21	92.94
5	99.54	94.39	95.4
10	95.63	96.89	97.83

standard for testing and evaluating the performance of vocal music art as well as the validity of objective test parameters of human noise and sound function to provide directed signals for voice input training samples. The subjective auditory perception assessment of vocal voice and human noise is carried out to validate the efficacy of the human noise detection procedure. We invited two vocal music teachers and vocal professionals to listen to 41 sound recording materials individually to examine the audible perception. The score was scored by ten points and was higher than 8.5, based on the quality, the volume, the color, and the range of the sound signals. The results were excellent with a 7.5–8.5 split. There is a mild distinction between 6.5 and 7.5 and less than 6.5. In the XLS (F0), the first resonance peak (F1, and third resonance peak (F3) is sampled for the experiment and the subjective assessment results are stored. The acoustic parameters and subjective evaluation results of each art voice signal are shown in Table 3. The subjective appraisal findings are 7, 19, 5, and 10, respectively, among the 41 samples of the Art Vocals Signal. In Table 3 are shown the acoustic

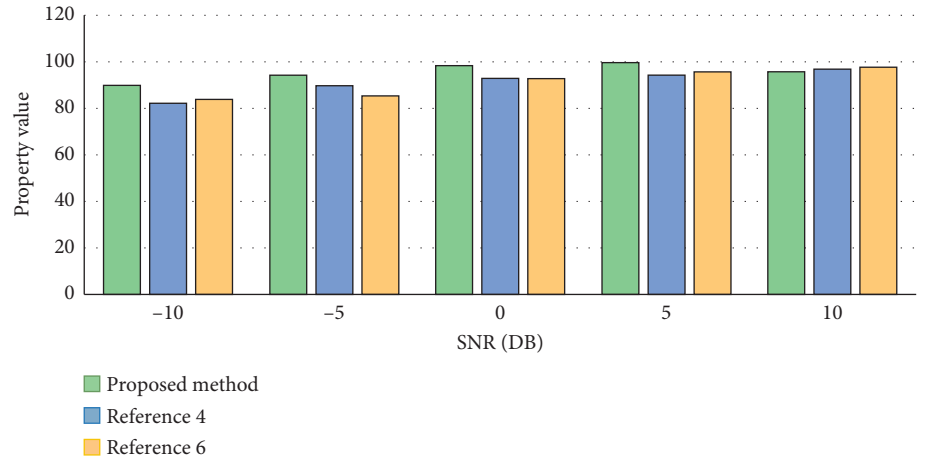

Figure 5: The performance test comparison.

Table 2: Medians and standard variations of diverse acquisition procedures.

Measure	PC		SSR		HDD	
	Medians	SD	Medians	SD	Medians	SD
Number of pauses	35.6	15.04	43.97	17.18	42.33	19.76
Pauses (%)	0.22	0.1	0.21	0.08	0.32	0.2
F3-HZ	1, 361.34	113.88	1, 315.03	117.01	1, 321.75	112.03
F1-HZ	752.78	175.21	695.82	173.38	721.38	146.08
F0-HZ	141.85	40.38	139.43	38.32	141.31	39.59
Medians of pause length in sec	0.31	0.08	0.27	0.07	0.39	0.17

Table 3: Subjective auditory perception evaluation.

Number	Sex	F1 (HZ)	F3 (HZ)	F0 (HZ)	Subjective evaluation results
1	M	578.5	2147.6	516.2008	Poor
2	M	621	2440.8	518.3619	Poor
3	M	548.8	2109	496.7788	Poor
4	M	562.5	2145.6	506.2008	Poor
5	M	611	2430.8	515.3679	Poor
6	M	544.8	2139	486.7788	Poor
7	M	453.1	2547.7	388.8746	Good
8	M	531	2543.3	483.3791	Good
9	M	576.9	2592.1	517.8078	Good
10	M	527.8	2914.2	476.5466	Good
11	M	568.6	2547.2	474.2042	Good
12	M	433.1	2647.7	384.8746	Good
13	M	521	2546.3	473.3791	Good
14	M	575	2692.1	527.8078	Good
15	M	527.9	2814.2	466.5466	Good
16	M	558.6	2546.2	472.2042	Good
17	M	558.6	2546.2	472.2042	Good
18	M	400.8	2909	358.2	Excellent
19	M	408.8	2845.4	308.256	Excellent
20	M	410.8	2809	350.2	Excellent
21	M	691	3289	514.1546	Secondary
22	M	358.5	2308	246.155	Secondary
23	FM	288.5	2138.8	260.6958	Poor
24	FM	364.9	2152.6	250.7011	Poor
25	FM	261.5	2135.8	270.6958	Poor
26	FM	354.9	2172.6	250.7011	Poor
27	FM	297.8	2454.6	258.8196	Good
28	FM	335.4	2592.3	130.0283	Good
29	FM	291.2	2418.2	226.6648	Good
30	FM	386.2	2585.7	258.7824	Good

Table 3: Continued.

Number	Sex	F1 (HZ)	F3 (HZ)	F0 (HZ)	Subjective evaluation results
31	FM	392.5	2998.9	164.2512	Good
32	FM	296.5	2453.6	255.8196	Good
33	FM	338.4	2598.3	168.0283	Good
34	FM	287.2	2518.2	225.6648	Good
35	FM	402.8	2885.4	308.9557	Excellent

parameters and the subjective results of the evaluation for each voice signal.

5. Conclusion

This paper provides an acquisition methods framework for systematic analysis of vocal art and human body noise performance based on wireless sensors and constructs the convergence of vocal music node wireless sensor models. The HART graph routing model is used to design the vocal art and human noise sciences continuously, to create a node-optimal deployment model for the wireless sensor, and to control the performance of the wireless sensor's vocal art using a converging link gain control approach. The adaptive equilibrated scheduling model is used to regulate vocal performance and human body noise scientifically and distributedly. The network of wireless sensors for acquiring information about vocal art is intended to better acquire information on vocal art and understand sound signal characteristics and improve the ability to speak and detect signals. The findings of the simulation show that the method proposed must improve the ability to acquire the vocal musical signal and to analyze human noise. The teachings and instructions of vocal music performers have a high application value.

Data Availability

The datasets used and/or analyzed during the current study are available from the corresponding author on reasonable request.

Conflicts of Interest

The author declares that he has no conflicts of interest.

References

[1] Y. Pan, Z. Yan, W. Guo et al., "Pulse laser injection seeded state detector and experimental research," *Laser Technology*, vol. 40, no. 2, pp. 153–156, 2016.

[2] X. Lu, "Anti-interference control algorithm for UAV based on attitude fusion filter," *Transducer and Microsystem Technologies*, vol. 35, no. 7, pp. 116–119, 2016.

[3] C. Sun, C. Yang, S. Fan et al., "Energy efficient distributed clustering consensus filtering algorithm for wireless sensor networks," *Information and Control*, vol. 44, no. 3, pp. 379–384, 2015.

[4] S. Chao-xuan, P. Wang, H. Zhuang-zhi et al., "Feature-level fusion recognition algorithm based on analogy decision tree classification," *Control and Decision*, vol. 31, no. 06, pp. 1009–1014, 2016.

[5] I. A. Kareem and M. G. Duaimi, "Improved accuracy for decision tree algorithm based on unsupervised discretization," *International Journal of Computer Science and Mobile Computing*, vol. 3, no. 6, pp. 176–183, 2014.

[6] A. Hu, R. Zhang, and D. Yin, "Image quality assessment using a SVD-based structural projection," *Signal Processing: Image Communication*, vol. 29, no. 3, pp. 293–302, 2014.

[7] L. C. Manikandan and D. R. K. Selvakumar, "A new survey on block matching algorithms in video coding," *International Journal of Engineering Research*, vol. 3, no. 2, pp. 121–125, 2014.

[8] Y. Zhan, H. Dai, and S. Wang, "Image quality assessment scheme with topographic independent components analysis for sparse feature extraction," *Electronics Letters*, vol. 50, no. 7, pp. 509-510, 2014.

[9] Z. Li, M. Song, G. Yin, X. Ma, and H. Song, "Cross deployment networking and systematic performance analysis of underwater wireless sensor networks," *Sensors*, vol. 17, no. 7, p. 1619, 2017.

[10] H. Zhong, K. Ma, and Y. Zhou, "Modified BM3D algorithm for image denoising using nonlocal centralization prior," *Signal Processing*, vol. 106, pp. 342–347, 2015.

[11] Z. C. Qin, Z. Zhou, and X. C. Zhao, "Energy efficient beamforming scheme for wireless sensor networks," *Journal on Communications*, vol. 34, no. 4, pp. 19–27, 2013.

[12] W. Wang, R. Wang, H. MEHRPOUYAN, and G. Zhang, "Beamforming for simultaneous wireless information and power transfer in two-way relay channels," *IEEE Access*, vol. 5, no. 5, pp. 9235–9250, 2017.

[13] C. Du, X. Chen, and L. Lei, "Energy-efficient optimisation for secrecy wireless information and power transfer in massive MIMO relaying systems," *IET Communications*, vol. 11, no. 1, pp. 10–16, 2017.

[14] J. R. A. Wang, L. Sboui, and Z. Rezki, "Power minimization of a wireless sensor node under different rate constraints," *IEEE Transactions on Signal Processing*, vol. 64, no. 13, pp. 3458–3469, 2016.

[15] R. J. Alouini, J. Kim, Z. Xie et al., "A skin-attachable, stretchable integrated system based on liquid GaInSn for wireless human motion monitoring with multi-site sensing capabilities," *Npg Asia Materials*, vol. 9, no. 10, p. e443, 2017.

[16] L. Sun, P. Ren, and Q. Du, "Fountain-coding aided strategy for secure cooperative transmission in industrial wireless sensor networks," *IEEE Transactions on Industrial Informatics*, vol. 12, no. 1, pp. 291–300, 2016.

[17] A. Wang, H. Meng, Y. F. A. Gaus et al., "Artificial intelligent system for automatic depression level analysis through visual and vocal expressions," *IEEE Transactions on Cognitive & Developmental Systems*, no. 99, p. 1, 2017.

[18] A. S. Cohen, T. L. Renshaw, and K. R. Mitchell, "A psychometric investigation of "macroscopic" speech measures for clinical and psychological science," *Behavior Research Methods*, vol. 48, no. 2, pp. 475–486, 2016.

[19] F. Kim, S. Marguerat, and V. Shahrezaei, "Division rate, cell size and proteome allocation: impact on gene expression noise

and implications for the dynamics of genetic circuits," *Royal Society Open Science*, vol. 5, no. 3, p. 172234, 2018.

[20] H. Bdi and L. J. WilliamS, "Principal component analysis," *Wiley Interdisciplinary Reviews: Computational Statistics*, vol. 2, no. 4, pp. 433–459, 2010.

[21] Y. Zhao and R. Zhang, "Full-duplex wireless-powered relay with self-energy recycling," *IEEE Wireless Communications Letters*, vol. 4, no. 2, pp. 201–204, 2015.

[22] H. Dai, Y. Huang, C. Li, and L. Yang, "Energy-efficient resource allocation for device-to-device communication with WPT," *IET Communications*, vol. 11, no. 3, pp. 326–334, 2017.

Hindawi
Mobile Information Systems
Volume 2021, Article ID 9995980, 9 pages
https://doi.org/10.1155/2021/9995980

Research Article

Moving Object Detection Technology of Line Dancing Based on Machine Vision

Liyun Liu

College of Physical Education, Changsha University of Science & Technology, Changsha, Hunan 410114, China

Correspondence should be addressed to Liyun Liu; llyun@csust.edu.cn

Received 8 March 2021; Revised 6 April 2021; Accepted 20 April 2021; Published 27 April 2021

Academic Editor: Muhammad Babar

Copyright © 2021 Liyun Liu. This is an open access article distributed under the Creative Commons Attribution License, which permits unrestricted use, distribution, and reproduction in any medium, provided the original work is properly cited.

In this paper, line dancing's moving object detection technology based on machine vision is studied to improve object detection. For this purpose, the improved frame difference for the background modeling technique is combined with the target detection algorithm. The moving target is extracted, and the postmorphological processing is carried out to make the target detection more accurate. Based on this, the tracking target is determined on the time axis of the moving target tracking stage, the position of the target in each frame is found, and the most similar target is found in each frame of the video sequence. The association relationship is established to determine a moving object template or feature. Through certain measurement criteria, the mean-shift algorithm is used to search the optimal candidate target in the image frame and carry out the corresponding matching to realize moving objects' tracking. This method can detect the moving targets of line dancing in various areas through the experimental analysis, which will not be affected by the position or distance, and always has a more accurate detection effect.

1. Introduction

The development of human action recognition can be summarized as movement, action, and activity. So far, human action is in the research stage of action recognition, that is, by extracting some features from the training data, using supervised or unsupervised training as a classification model, extracting features from the new data, and sending them to the model to get the classification results. Human action recognition has developed from human action recognition in the image to human action recognition in the video [1] using input data. Video action recognition is to process and analyze the original graphics or image sequence data collected by sensors and learn and understand the human action and behavior. Generally, based on motion detection and feature extraction, the human motion pattern is obtained through analysis. The mapping relationship between video content and action type description is established so that the computer can understand the video [2, 3].

In recent years, for video action recognition, the primary type of action videos includes daily human actions such as walking, running, waving, and clapping; sports actions such as diving, skating, and riding; and life actions such as cutting vegetables and washing vegetables. In numerous research studies on human action recognition, few universities and institutions have studied dance actions. Dance is a way of emotional expression to the public through body movements, which is more complex in expression and has a wide variety of movements. There are many dance actions with their own characteristics [4–6]. Therefore, the research of dance action is still in the stage of dance action analysis. In most cases, it is through the posture analysis of the collected dance action, and then it is applied to the performance of animated characters by using animation processing software. Various universities and enterprises have continuously studied human action recognition due to applying action recognition technology in numerous fields. Human action recognition can help the public life to be more colorful and facilitate human beings' production and energy significantly [7].

Due to the disappearance of intangible cultural heritage (because of the lack of inheritors), human action's key information can be preserved through action recognition

technology to preserve intangible cultural heritage relevant actions. For example, dance actions have national characteristics in many areas of China. Critical information of dance actions is obtained and preserved through action recognition technology, which reduces the possibility of interruption of dance inheritance [8]. For dance action recognition, Pan et al. used zero crossings' angular velocity to realize video motion sequence segmentation [9]. Zheng et al. developed a more complex technology and used linear dynamic system output to represent low-level segments (primitives) [10]. Gao showed that motion segmentation is implied in state machine or motion graph representation [11]. However, the low-level segmentation cannot represent a complete action sequence. Talaat proposed three methods to long segment sequences into action subsequences [12] automatically. The first two methods were applied in practice video, which meant that the algorithm traversed all frames from the beginning to the end and created segmentation when breakpoints appear. The first algorithm allocated a cut when the intrinsic dimension of the local model suddenly increases. The second algorithm allocated the cut when the posture of the observed distribution changed. The third algorithm is a batch segmentation process and used the clustering method to form a simple action cluster for the continuous frame sequence of Gaussian mixture model belonging to different elements. Moemen et al. proposed to use the time structure of the vital pose set for modeling [13]. By comparison, the third method proposed by authors in [14] is more flexible (the speed change that allows gaps between adjacent postures is more robust). It is expected that the time structure would be learned automatically rather than designed manually [14].

Machine vision is an emerging and rapidly developing discipline. It is a broad area involving digital signal processing, graphics and image processing, human-computer interaction, pattern recognition, mathematical statistics, computer science, and other fields [15]. It has become an irresistible trend to use machine vision instead of traditional radar, infrared, and other means to capture external information through image and video technology [16]. Object tracking technology is an important research direction in machine vision, which has great practical value in real life. Moving object tracking technology is mainly used to process the video's continuous images, which contains more information about the moving object. Through the analysis of the scene spatial position change information between dynamic sequence images on the time axis, the moving target is extracted from the background, and then the target position is tracked. The target behavior can be analyzed further and understood by calculating the target motion information, such as the centroid position, motion mode, and trajectory route, to achieve a higher-level task. Moving object detection and tracking research is closely related to real life, bringing great convenience to people's lives. Using computer instead of human eyes and brain, people do not have to operate the computer all day to work easily and save workforce and material resources for the company. This technology has high practical value in intelligent transportation, important units, densely populated public areas, banks with high-security requirements, monitoring and detection of museums, medicine, military, and other aspects. With the continuous improvement of science and technology and computer technology's continued development, video image acquisition and storage costs are significantly reduced, and the processing speed is constantly improved. These are the platform support for the development of video tracking technology. Video tracking technology is in line with the future trend of automation, information, and intelligence. On the other hand, the tracking technology based on machine vision can solve the complex work of processing many video information for a long time, saving workforce and material resources, and bringing convenience to people. Moving object tracking technology is closely related to people's lives, bringing comfort to people's lives. Moreover, target tracking technology is widely used in military science and technology, a broad field related to science and technology and people's livelihood [17]. With the advancement of science and technology, the research in this field will be more mature and perfect. Based on machine vision, this paper studies the moving object detection of line dancing and judges the detection and tracking accuracy and effect of this method.

The rest of this paper is organized as follows. In Section 2, we discuss our proposed moving object detection of line dancing using machine vision. In Section 3, we comprehensively evaluate our proposed work. Finally, the paper is concluded and future research directions are provided in Section 4.

2. Moving Object Detection Method of Line Dancing Based on Machine Vision

The moving object detection of line dancing based on machine vision has two integral parts: background subtraction method and adaptive tracking of moving target. First we discuss the background subtraction method for moving objection detection in line dancing in Section 2.1 followed by adaptive tracking of moving target based on mean-shift in Section 2.2.

2.1. Background Subtraction Method for Moving Object Detection in Line Dancing. After understanding the basic methods of moving object detection, analyzing the applicable scene and the advantages and disadvantages of each method, this paper decided to use the moving object detection method based on background subtraction. Various methods of background modeling are deeply studied, and the advantages and disadvantages of various algorithms are compared. Considering the real-time and accuracy of the system, the improved frame difference background modeling method is adopted.

2.1.1. Improved Frame Difference Background Modeling Method. In this paper, based on the traditional frame difference background modeling, a new initialization method is proposed and its feasibility is proved by experiments. The

steps of improved frame difference background modeling are as follows:

Get Initial Image. This step involves the following methods to get the initial image.

Choosing the Average Method. The principle of choosing the average method is proposed based on the original average method. Two adjacent images are selected. The region with variable pixel value is the moving target region, and the region with stable pixel value is the background region. The traditional adjacent frame difference method is used to distinguish the background region and the foreground region through threshold selection. The pixel of the moving object is set to 0, and the pixel of the background part remains unchanged.

The selection of threshold T can be selected through experiments. Generally, the change of background pixels is small, but it is not completely unchanged. The threshold T can be obtained through experiments according to the actual situation. In order to get a complete background image, we can select N frames in a video and use the adjacent frame difference method to compare the two images before and after to get a continuous background sequence. The process of selecting the average method is as follows:

(1) The background sequence is obtained by frame difference method. The target region is set to 0, and the background region remains unchanged.

$$b_i(x,y) = \begin{cases} 0, & \text{if } |f_i - f_{i-1}| > T, \\ f_i(x,y), & \text{if } |f_i - f_{i-1}| \le T. \end{cases} \quad (1)$$

(2) The number $m(x,y)$ of times that the pixel in $B_i(x,y)$ in the background sequence image is not zero is obtained.

(3) The average of the sum of background sequence images is as follows:

$$b(x,y) = \frac{1}{m(x,y)} \sum_{i=1}^{N-1} b_i(x,y). \quad (2)$$

(4) Let iteration parameters be $i = 1$.

(5) Frame difference method:

$$BW_i = \begin{cases} 1, & \text{if abs}(I_i - I_{i-1}) \ge T, \\ 0, & \text{if abs}(I_i - I_{i-1}) < T. \end{cases} \quad (3)$$

The selection of threshold T: T is determined manually, which can be obtained through practical experience. I_i and I_{i-1} are the i-th and $i-1$-th images, respectively, and BW_i is the difference image.

Background Update. After the initial background image is obtained by selecting the average value method, the background area and the moving target area of the current image are distinguished according to the frame difference method. The background part of the moving target area does not need to be updated, and the background area of the previous image remains unchanged. The background region is updated by adding the weights of the background of the previous frame and the image of the current frame.

$$B_i(x,y) = \begin{cases} B_{i-1}(x,y), & \text{if } BW_i(x,y) = 1, \\ (1-\alpha)B_i(x,y) + \alpha I_i, & \text{if } BW_i(x,y) = 1, \end{cases} \quad (4)$$

(1) $i = i + 1$, return to step (3), and perform iterative operation.

The average method is selected to segment the moving object, and then the background area is averaged, which reduces the influence of the moving object on the background, and the extracted background effect is more accurate. A few prior video sequences are needed.

When the initial background image is obtained, the appropriate number of frames should be selected for modeling. If the number of selected frames is too small, holes will appear in the results obtained by the average method [18]. If it chooses too many frames, it will not only waste resources but also increase the burden of calculation. Moreover, if the time is too long, factors such as illumination and environmental changes will affect the accuracy of the results. Generally, it can be selected according to the speed of the object and the size of the target, so that all areas in the video image can display the background [19].

2.1.2. Moving Target Recognition. The principle of moving object recognition is that the background image obtained by the improved frame difference background modeling method is combined with the background difference method to obtain the moving object and realize the detection of the moving object. The binary image of the moving target is processed by morphological operation to remove the small target irrelevant to the moving target, fill the holes in the target, and connect the broken part of the target after threshold segmentation to make the image more complete. The main steps of moving target recognition are as follows:

(1) The improved frame difference background modeling method obtains the background image $B_i(x,y)$.

(2) Background difference: the difference operation is performed between the current frame image $f_i(x,y)$ and the background image $B_i(x,y)$.

$$D_i(x,y) = |f_i(x,y) - B_i(x,y)|. \quad (5)$$

(3) Image binarization: the experiment obtains the appropriate threshold T, set "1" if it is greater than the threshold, and set "0" if it is less than the threshold.

$$R_i(x,y) = \begin{cases} 1, & D_i(x,y) \ge T, \\ 0, & D_i(x,y) < T. \end{cases} \quad (6)$$

(4) For the binary image, the irrelevant pixels are removed by morphological operation to make the target more complete. Flow chart of moving target recognition is shown in Figure 1.

2.2. Adaptive Tracking of Moving Target Based on Mean Shift. After obtaining the moving object image, in order to realize the moving object detection and tracking of line dancing, the mean-shift algorithm is used to carry out the follow-up research. In recent years, mean-shift algorithm is widely used in target tracking. Some scholars use the Bhattacharyya coefficient as the similarity measure between target model and candidate target and use mean-shift algorithm to search the optimal candidate target, to obtain good tracking effect. Target tracking based on mean shift is a template-based tracking method [20].

2.2.1. Basic Principle of Mean Shift. In the field of machine vision, data analysis is usually carried out in multidimensional space. To estimate the nonparametric density of multidimensional sampled data sets, it needs to know the kernel function used in multidimensional space, that is, the multivariate kernel function.

In d-dimensional space, n points $x_i = R^d$, $i = 1$ are given; Λ, n and a positive definite $d * d$ bandwidth matrix H, the multivariable kernel density of kernel $K(x)$ are estimated as

$$\widehat{f}_{H,K}(x) = \frac{1}{n|H|^{(1/2)}} \sum_{i=1}^{n} K\left(H^{-(1/2)}(x - x_i)\right). \tag{7}$$

Generally, the bandwidth matrix H has two forms: one is diagonal matrix, that is, $H = \text{diag}[h_1^2 \Lambda h_d^2]$; the other is proportional unit matrix, that is, $H = h^2 I$. In this case, (7) can be written as follows:

$$\widehat{f}_{h,K}(x) = \frac{1}{nh^d} \sum_{i=1}^{n} K\left(\frac{x - x_i}{h}\right). \tag{8}$$

If $K(x)$ is centrosymmetric, $K(x) = C_{k,d} k(\|x\|^2)$ and $K(x)$ is defined in the interval of $x \geq 0$; then $K(x)$ is called the contour function of $K(x)$ and $C_{k,d}$ is the normalized constant coefficient.

After introducing the contour function, the kernel density estimation can be rewritten as follows:

$$\widehat{f}_{h,K}(x) = \frac{c_{k,d}}{nh^d} \sum_{i=1}^{n} k\left(\left\|\frac{x - x_i}{h}\right\|^2\right). \tag{9}$$

This expression is commonly used in mean-shift algorithm to calculate the probability density of eigenvalues. If it wants to know the location of the highest density data in the data set, it can estimate the standard density gradient. Let $g(x) = -k'(x)$, and calculate the error covariance gradient. After simplification, it can get the mean-shift vector $m_{hG}(x)$.

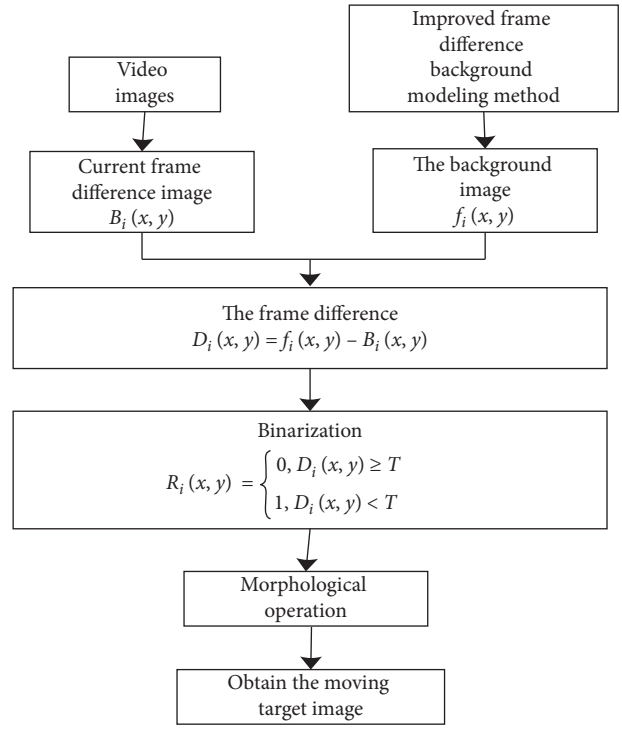

Figure 1: Flow chart of moving target identification.

$$m_{hG}(x) = \frac{\sum_{i=1}^{n} x_i g\left(\left\|x - x_i/h\right\|^2\right)}{\sum_{i=1}^{n} g\left(\left\|x - x_i/h\right\|^2\right)}. \tag{10}$$

2.2.2. Practical Application of Mean Shift in Moving Target Tracking. In this section, we discuss the practical application of mean shift in moving target tracking. We mainly focus on the description of target model in this section.

Because the histogram of the target image records the probability of color appearance, which is not affected by the shape change of the target, mean shift selects the color histogram as the feature description of the target. Suppose the center of the target region is y_0 and the pixel position of the target in the image is represented by $\{x_i\}_{i=1\Lambda n}$. If the target model is a histogram of m values, the normalized color distribution can be expressed as

$$\widehat{q}_u = C \sum_{i=1}^{n} \delta[b(x_i) - u], \tag{11}$$

where function b: $R^2 \longrightarrow \{1\Lambda M\}$ is the image of the pixel at x_i to the color index, $\delta(x)$ is the delta function, and C is the normalization coefficient.

According to the above frame difference method, the background area and the moving target area of the current image are distinguished, so that the pixels near the center of the target model are more reliable than other pixels. Therefore, different weights can be given to the pixels at different positions of the target, the pixels near the center are given a large weight, and the pixels far away from the center are given a small weight. By introducing kernel estimation

into the objective density function, the probability density estimation of the objective model can be expressed as

$$\widehat{q}_u = C\sum_{i=1}^{n} k\left(\left\|\frac{y_0 - x_i}{h}\right\|^2\right)\delta[b(x_i) - u], \tag{12}$$

where $k(x)$ is the contour function of the kernel function, and $\|y_0 - x_i/h\|$ in function $k(x)$ is used to eliminate the influence of different sizes of targets. Using condition of $\sum_{u=1}^{m}\widehat{p}_u = 1$, it can get the following results:

$$C = \frac{1}{\sum_{i=1}^{n}\left(\left\|y_0 - x_i/h\right\|^2\right)}. \tag{13}$$

In subsequent frames, the region that may contain the moving target is called the candidate region, and its center coordinate is y, which is also the center coordinate of the kernel function. The pixels in the region are represented by $\{x_i\}_{i=1\Lambda n_h}$. The description of the candidate region is called target candidate model. The probability density of the eigenvalue $u = 1\Lambda m$ of the candidate model is as follows:

$$\sum_{u=1}^{m}\widehat{p}_u(y) = C_h\sum_{i=1}^{nk} k\left(\left\|\frac{y - x_i}{h}\right\|^2\right)\delta[b(x_i) - u], \tag{14}$$

where $C_h = (1/\sum_{i=1}^{nk} k(\|y - x_i/h\|^2))$ is the normalized constant coefficient.

The similarity function describes the degree of similarity between the target model and the candidate target, and the probability distributions of the two models are exactly the same in ideal cases. In the mean-shift algorithm, Bhattacharyya coefficient is selected as the similarity function. The Bhattacharyya coefficient is defined as follows:

$$\widehat{p}(y) = p(\widehat{p}(y), \widehat{q}) = \sum_{u=1}^{m}\sqrt{\widehat{p}_u(y)\widehat{q}_u}. \tag{15}$$

The value of P is between 0 and 1. The larger the value of $\widehat{p}(y)$ is, the more similar the two models are. In the current frame, the candidate model is calculated by calculating different candidate regions, so that the candidate region with the largest $\widehat{p}(y)$ is the position of the target in the current frame.

2.2.3. Implementation Process of Moving Object Detection and Tracking. The most likely position of the target in the current frame is the candidate region that makes $\widehat{p}(y)$ maximum. In order to maximize $\widehat{p}(y)$, the position y_0 of the target center of the previous frame in the current frame is the starting position, and the optimal matching position is found, whose center is y. Firstly, the target candidate model $\widehat{p}(y_0)$ is calculated, and the Taylor expansion of (15) is performed at $\widehat{p}(y_0)$. The Bhattacharyya coefficient can be approximately expressed as

$$\rho(\widehat{p}(y), \widehat{q}) \approx \frac{1}{2}\sum_{u=1}^{m}\sqrt{\widehat{p}_u(y_0)\widehat{q}_u} + \frac{C_h}{2}\sum_{i=1}^{nk}\omega_i k\left(\left\|\frac{y - x_i}{h}\right\|^2\right), \tag{16}$$

where

$$\omega_i = \sum_{u=1}^{m}\delta[b(x_i - u)]\sqrt{\frac{\widehat{q}_u}{\widehat{p}_u(\widehat{y}_0)}}. \tag{17}$$

It can be seen from (16) that only the second term changes with y, so that

$$f_{h,k} = \frac{C_h}{2}\sum_{i=1}^{n_k}\omega_i k\left(\left\|\frac{y - x_i}{h}\right\|^2\right). \tag{18}$$

To maximize $\rho(\widehat{p}(y), \widehat{q})$ is equivalent to maximizing $f_{h,k}$.

By analyzing (17), it can see that this expression is similar to the kernel density estimation function, but with one more weight ω_i, it can make $f_{h,k}$ take the maximum value by means shift iteration. The specific steps are as follows:

(1) Suppose the distribution of the target model is $\{\widehat{q}_u\}_{u=1\Lambda m}$ and the estimated position of the target is $\widehat{y}_0$.

(2) Initialize the target position of the current frame with $\widehat{y}_0$, calculate the distribution $\{\widehat{p}_u(\widehat{y}_0)\}_{u=1\Lambda m}$, and estimate the Bhattacharyya coefficient: $\rho[\widehat{p}(y_0), \widehat{q}] = \sum_{u=1}^{m}\sqrt{\widehat{p}(\widehat{y}_0), \widehat{q}}$.

(3) Calculate the weight according to (17).

(4) Calculate the new position of the target according to the mean-shift vector: $\widehat{y}_1 = \sum_{i=1}^{n_h} x_i w_i g\ (\|\widehat{y}_0 - \widehat{x}_i/h\|^2)/\sum_{i=1}^{n_h} w_i g(\|\widehat{y}_0 - \widehat{x}_i/h\|^2)$.

(5) Update $\{\widehat{p}_u(\widehat{y}_0)\}_{u=1\Lambda m}$ and estimate $\rho[\widehat{p}(y_1), \widehat{q}] = \sum_{u=1}^{m}\sqrt{\widehat{p}(\widehat{y}_1), \widehat{q}}$.

(6) When $\rho[\widehat{p}(y_1), \widehat{q}] < \rho[\widehat{p}(y_0), \widehat{q}]$, $\widehat{y}_1 \leftarrow (1/2)\ (\widehat{y}_0 + \widehat{y}_1)$.

(7) If $\|\widehat{y}_1 - \widehat{y}_0\| < \varepsilon$, end; otherwise $\widehat{y}_0 \leftarrow \widehat{y}_1$, go to step 1.

The process of target tracking is to get the maximum Bhattacharyya coefficient through the gradient descent search of mean-shift vector, so as to find the best matching position of the target in the next frame.

3. Experimental Results and Discussion

Taking a dance troupe in a certain city as the research object, 10 dance performers from the dance troupe are invited to cooperate with the experiment. They are asked to carry out dance performance and use cameras to collect images of their dance actions.

The background effect obtained by the proposed method is compared with that obtained by traditional unimproved frame difference background modeling. The results are shown in Figure 2.

Figure 2(a) is the background of traditional frame difference background modeling method, and Figure 2(b) is the image of improved frame difference background modeling. It can be seen that the initial image of the traditional method contains the target information, and the shadow of the object motion is obvious when modeling the background, so the modeling is not accurate. The improved modeling method

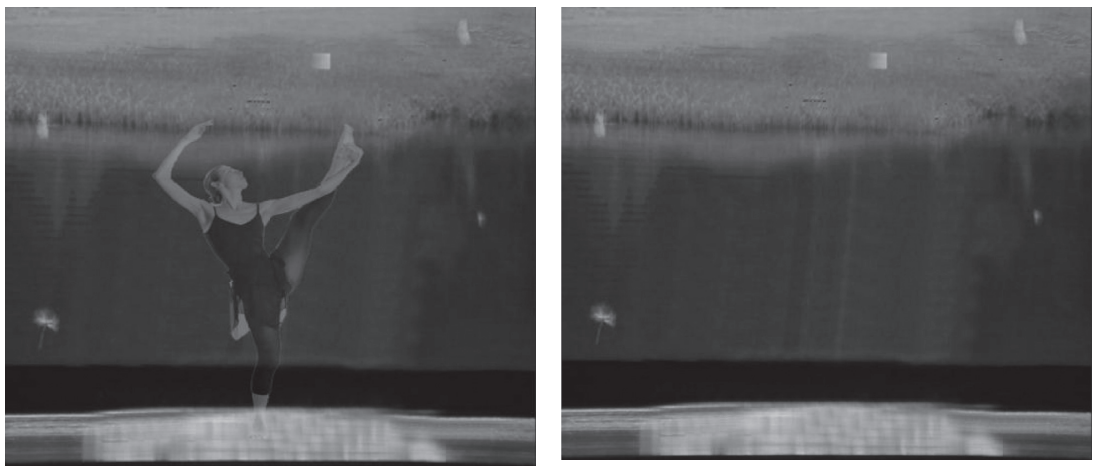

(a) (b)

Figure 2: Background modeling results. (a) Traditional methods of background modeling. (b) The method of background modeling in this paper.

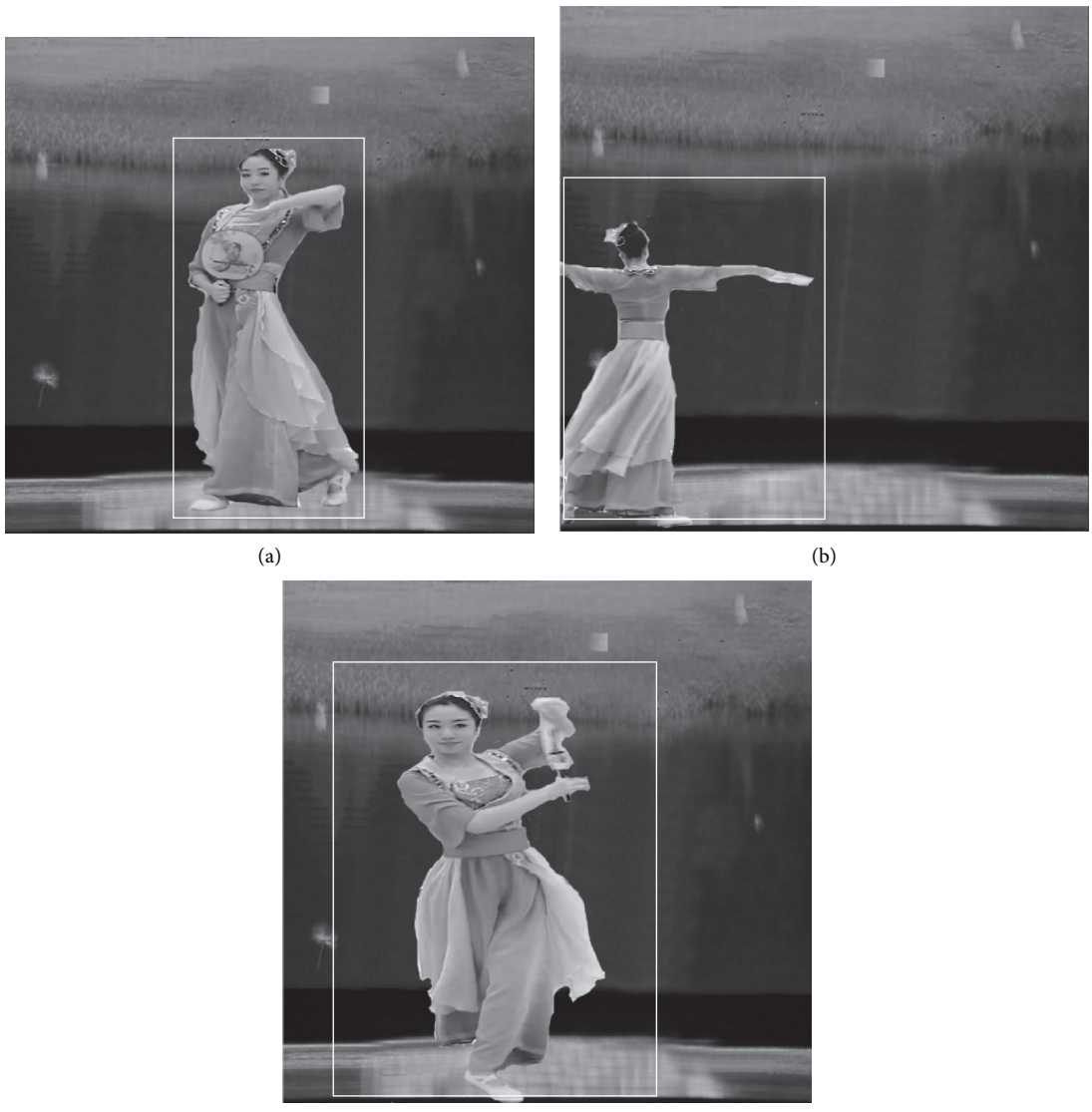

(a) (b)

(c)

Figure 3: Detection effect of moving target in line dancing under simple background. (a) Starting test. (b) The dancer is on the edge of the picture. (c) The dancer approaches the camera.

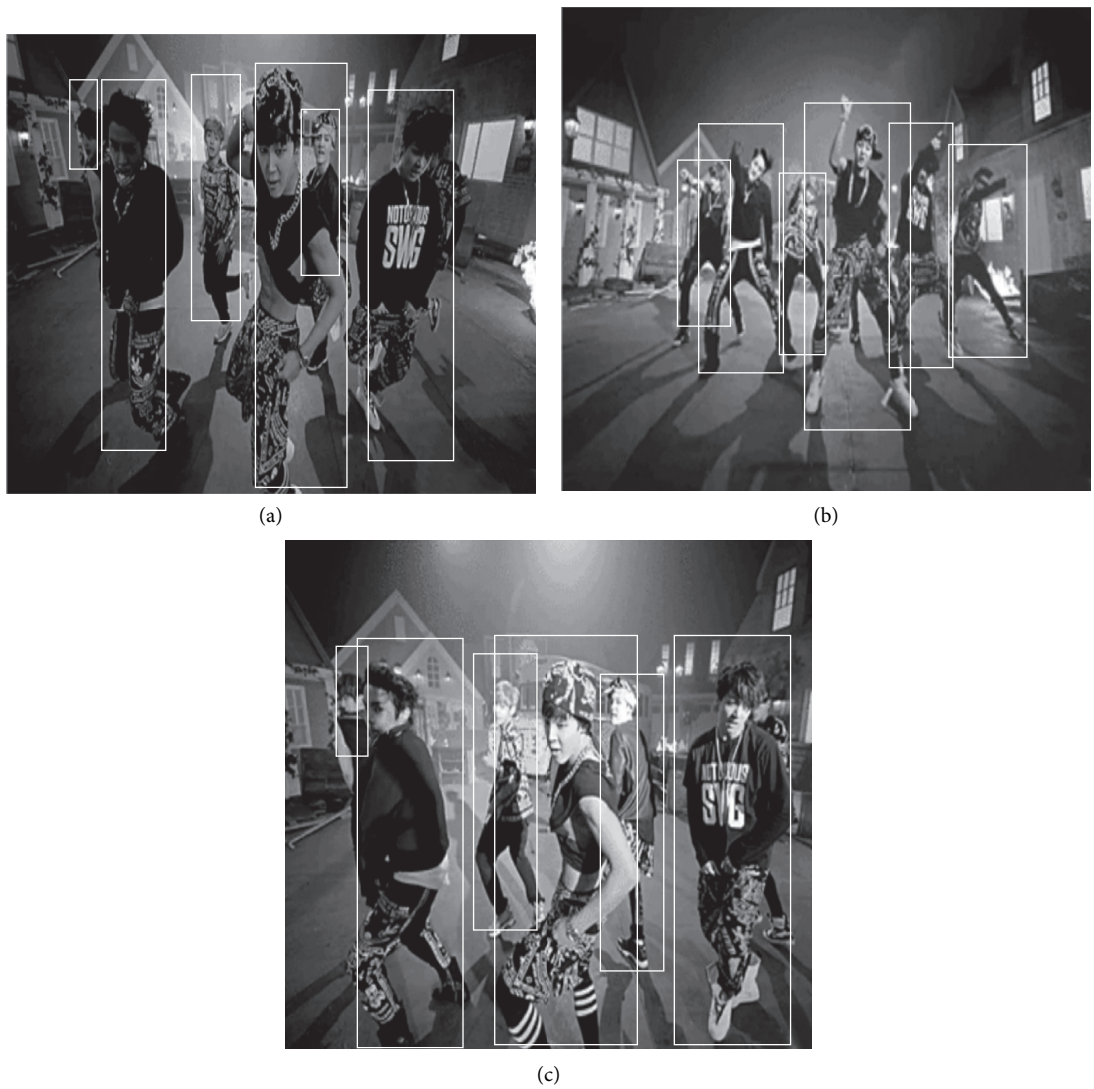

(a) (b) (c)

Figure 4: Detection results of moving objects in line dancing under complex background. (a) Camera lens nearly. (b) Camera pulls away. (c) Actor displacement.

reduces the influence of motion information, and the background effect is ideal.

A simple stage background is selected; the dancers are invited to make different dance actions and are required to be in the normal position, the edge of the screen, and the position close to the camera, respectively, so as to verify the effect of moving object detection and tracking of line dancing by the proposed method. The test results are shown in Figure 3.

It can be seen from Figure 3 that when the line dancing target moves, the proposed method can predict the centroid position of the target and search and match the target in a window neighborhood of the prediction point in the next frame. It can be seen from Figure 3(a) that the method in this paper can accurately locate the object of line dancing. As can be seen from Figure 3(b), when the target object is at the edge of the field of view of the camera, a part of the target object can still be located. As can be seen from Figure 3(c), when the moving object is close to the camera and the size changes, the detection and tracking window will also change.

Under the influence of complex background, the moving target detection results of line dancing select the complex stage background with bright color. The webcam is fixed, and the proposed method is used to detect and track the line dancing movement of each dancer. The results are shown in Figure 4.

It can be seen from Figure 3 that the proposed method can detect the moving object of line dancing in complex background and obtain more accurate detection and tracking results.

The experimental results show that in the case of obstacles, the detection and tracking of moving objects in line dancing are improved. The experimental results are shown in Figure 5.

It can be seen from Figure 5 that when the detected object is partially occluded, even if only a few parts are not occluded, moving object detection of line dancing can still be

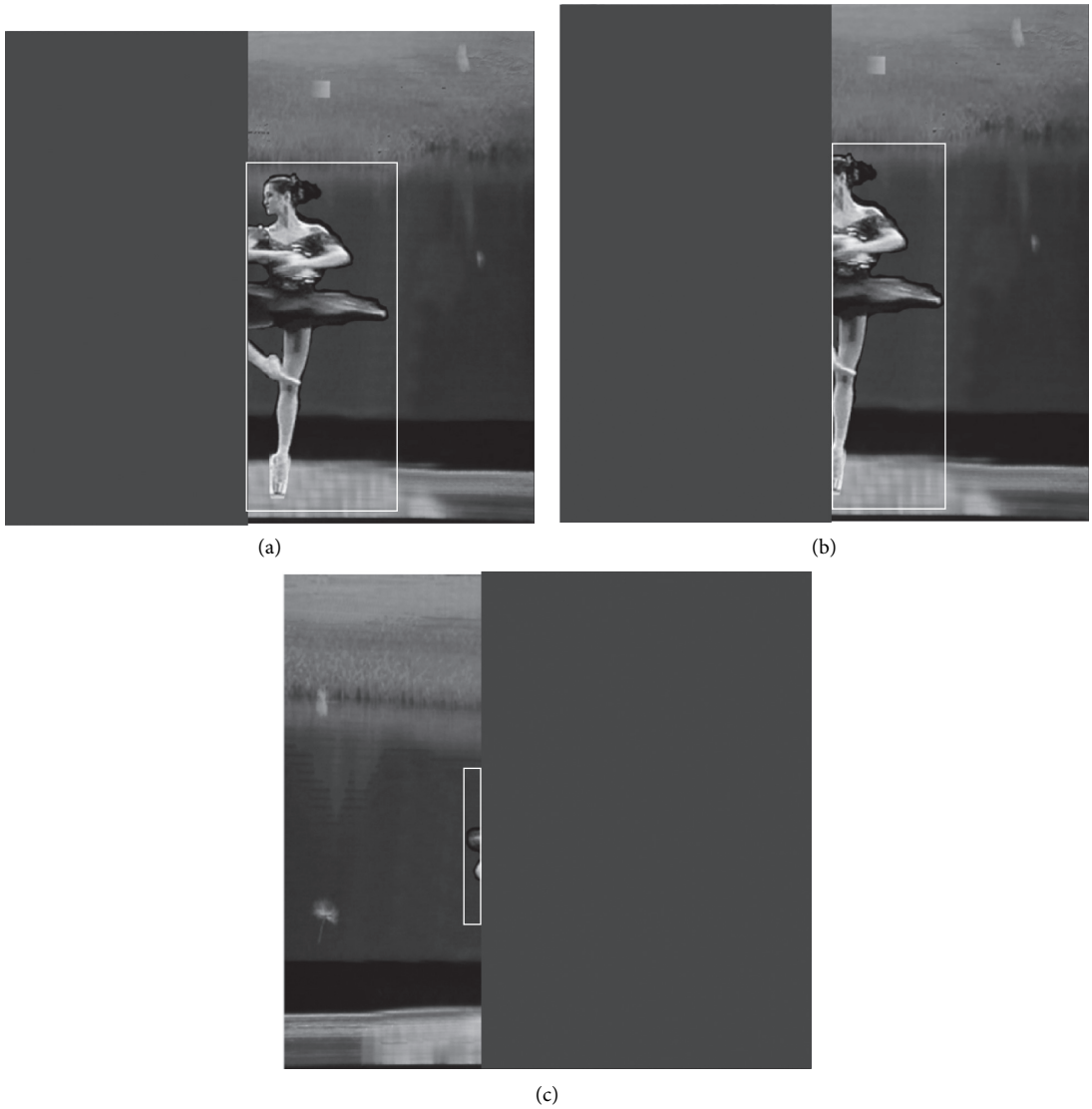

(a) (b) (c)

Figure 5: Detection results in the case of obstacle occlusion. (a) 1/3 Keep out. (b) 2/3 Keep out. (c) Remove the cover.

Table 1: Recognition rate of different human body regions (%).

Detection method	The upper part of the body	The lower part of the body	The upper part of the body + the lower part of the body	Hold body
RGB methods	72.31	71.58	84.54	79.15
Flow methods	85.05	84.24	90.66	85.46
This paper's methods	96.99	96.42	98.51	97.34

realized. When the detected object is completely occluded, the detection and tracking frame will be reduced to a small point. Once the target to be detected is exposed, an edge will be detected immediately, which shows that the detection efficiency of the proposed method is high.

In this paper, the recognition rate of RGB recognition method, flow recognition method, and the proposed method are used to compare the different parts of the upper body, lower body, and the whole body. From the recognition rate obtained by different methods, it can be seen that the recognition rate of the upper body or the lower body is relatively close, but the recognition rate of the lower body is slightly higher. The recognition rate of the combination of human body regions is the highest. The recognition rate of the direct recognition of human body regions is lower than that of the combination of human body regions. The reason is that the number of upper body or lower body movements is close, and the lower body movements are more. In the application of the whole-body region of the human, when the movement is only the upper body region or the lower

body region, the two regions will affect each other, and the dance action naming often uses the lower body and upper body action naming, respectively, and the separate training can improve the accuracy of recognition. The recognition effect of different features extracted from different human regions is shown in Table 1.

4. Conclusion

This paper mainly studies the moving object detection method of line dancing based on machine vision. We used two approaches to achieve this objective. An improved frame difference background modeling is used to attain moving object detection, and the mean-shift method is used to achieve moving object tracking. We took the real-life choreographer as an example for our experimental results to verify our approach and prove that both our approaches can detect the moving objects in any area of the camera lens and not receive the restriction of occlusion or distance camera. It can be seen that the method can obtain good detection results of moving objects of line dancing [19, 20].

Data Availability

The data used to support the findings of this study are available from the corresponding author upon request.

Conflicts of Interest

The authors declare that there are no conflicts of interest regarding the publication of this paper.

Acknowledgments

This study was supported by the Project of the Ideological and Political Research of University Course in Hunan Province: Research and Practice of the Ideological and Political Teaching of the Course "Line Dance" and the study result of the Project of the Hunan Educational Science Plan: Study on the Optimizing of Physical Education in University under the Impact of Epidemic Situation (XJK20CGD012).

References

[1] W. Huang and H. Xu, "Development of six-dof welding robot with machine vision," *Modern Physics Letters B*, vol. 32, no. 5, Article ID 1840079, 2018.

[2] X. Pan, Z. Liu, and G. Zhang, "Line structured-light vision sensor calibration based on multi-tooth free-moving target and its application in railway fields," *IEEE Transactions on Intelligent Transportation Systems*, vol. 99, pp. 1–10, 2020.

[3] C. Guo, J. Qian, and D. Reynaerts, "Deterministic removal strategy for machine vision assisted scanning micro electrochemical flow cell," *Journal of Manufacturing Processes*, vol. 34, no. 08, pp. 167–178, 2018.

[4] P. Trsli, A. Weir, J. Riordan, E. Omerdic, and G. Dooly, "Vision-based localization system suited to resident underwater vehicles," *Sensors*, vol. 20, no. 2, p. 529, 2020.

[5] M. F. Seyed, M. M. Reza, and N. Mahdi, "Flying small target detection in ir images based on adaptive toggle operator," *IET Computer Vision*, vol. 12, no. 4, pp. 527–534, 2018.

[6] P. Hai-Hong, V. Ngoc-Son, N. Vu-Lam, and Q. Mathias, "Action recognition based on motion of oriented magnitude patterns and feature selection," *IET Computer Vision*, vol. 12, no. 5, pp. 735–743, 2018.

[7] B. Zhong, H. Huang, and E. Lobaton, "Reliable vision-based grasping target recognition for upper limb prostheses," *IEEE Transactions on Cybernetics*, vol. 99, pp. 1–13, 2020.

[8] Y. T. Chang, L. F. Sun, J. X. Pu, and H. F. Yu, "Air target identification using multiple sensors based on modified evidence support," *Computer Simulation*, vol. 37, no. 07, pp. 394–398, 2020.

[9] M. Pan, A. Liu, Y. Yu et al., "Radar hrrp target recognition model based on a stacked cnn-bi-rnn with attention mechanism," *IEEE Transactions on Geoscience and Remote Sensing*, vol. 99, pp. 1–14, 2021.

[10] J. Zheng, H. Fan, Q. Zhang, G. Yin, and Z. Li, "Magnetic anomaly target recognition based on svd and svms," *IEEE Transactions on Magnetics*, vol. 55, no. 9, pp. 1–8, 2019.

[11] X. Gao, "Design and implementation of marine automatic target recognition system based on visible remote sensing images," *Journal of Coastal Research*, vol. 115, p. 277, 2020.

[12] M. Talaat, I. Arafa, and H. M. B. Metwally, "Advanced automation system for charging electric vehicles based on machine vision and finite element method," *IET Electric Power Applications*, vol. 14, no. 13, pp. 2616–2623, 2020.

[13] M. Y. Moemen, H. Elghamrawy, S. N. Givigi, and A. M. Noureldin, "3-d reconstruction and measurement system based on multi-mobile robot machine vision," *IEEE Transactions on Instrumentation and Measurement*, vol. 99, p. 1, 2020.

[14] A. I. Khalyasmaa, M. D. Senyuk, and S. A. Eroshenko, "High-voltage circuit breakers technical state patterns recognition based on machine learning methods," *IEEE Transactions on Power Delivery*, vol. 34, no. 4, pp. 1747–1756, 2019.

[15] S. Abouzahir, M. Sadik, and E. Sabir, "Bag-of-visual-words-augmented histogram of oriented gradients for efficient weed detection," *Biosystems Engineering*, vol. 202, no. 3, pp. 179–194, 2021.

[16] J. Zhang, J. Zhu, H. Deng, Z. Chai, M. Ma, and X. Zhong, "Multi-camera calibration method based on a multi-plane stereo target," *Applied Optics*, vol. 58, no. 34, p. 9353, 2019.

[17] Z. Gao, Y. Gu, Y. Lv, Z. Xu, and Q. Wu, "A monocular vision measurement system of three-degree-of-freedom air-bearing test-bed based on fccsp," *Photonic Sensors*, vol. 8, no. 2, pp. 119–126, 2018.

[18] G. Maier, F. Pfaff, M. Wagner et al., "Real-time multitarget tracking for sensor-based sorting," *Journal of Real-Time Image Processing*, vol. 16, no. 6, pp. 2261–2272, 2019.

[19] Y. Wang, H. Liu, M. Guo, X. Shen, B. Han, and Y. Zhou, "Image recognition model based on deep learning for remaining oil recognition from visualization experiment," *Fuel*, vol. 291, no. 3, Article ID 120216, 2021.

[20] Z. Wang, G. Yu, B. Zhou, P. Wang, and X. Wu, "A train positioning method based-on vision and millimeter-wave radar data fusion," *IEEE Transactions on Intelligent Transportation Systems*, vol. 99, pp. 1–11, 2021.

Hindawi
Mobile Information Systems
Volume 2021, Article ID 9955988, 8 pages
https://doi.org/10.1155/2021/9955988

Research Article

Fatigue Load Spectrum of Highway Bridge Vehicles in Plateau Mountainous Area Based on Wireless Sensing

Li Rui, Xie Xiaoyu, and Duan Xueyan

The Faculty of Civil Engineering and Mechanics, KunMing University of Science and Technology, Kunming 650500, China

Correspondence should be addressed to Li Rui; liruiking@kust.edu.cn

Received 4 March 2021; Revised 30 March 2021; Accepted 15 April 2021; Published 26 April 2021

Academic Editor: Muhammad Usman

Copyright © 2021 Li Rui et al. This is an open access article distributed under the Creative Commons Attribution License, which permits unrestricted use, distribution, and reproduction in any medium, provided the original work is properly cited.

In Yunnan and other plateau mountainous areas, hydropower and mineral resources are abundant, and there are relatively many vehicles used for the transportation of large hydropower facilities. The widespread phenomenon of vehicle overload causes severe fatigue among the drivers. However, there is no reference vehicle load spectrum for fatigue analysis in the existing research. The application of wireless sensing technology to bridge health monitoring is favorable for the entire monitoring system's low-cost and intelligent development. In this study, wireless sensors are used to collect sensing data in the measured area and perform preliminary filtering processing. The data collected by the sensing layer is aggregated at the TD gateway layer to realize local short-term storage of monitoring data, and 3G wireless transmission is used for the effective processing of the data. The clustering method is used to classify the vehicle models based on investigating the most representative expressway traffic flow information in Yunnan Province. Moreover, the weighted probability distribution model of different vehicle models is established through statistical analysis, which simplifies the composition's fatigue intensity spectrum model. The selection of five vehicles of the equivalent model followed by a six-axle vehicle has the most significant impact on bridge damage as the standard fatigue vehicle. The research results establish a basis for the fatigue design of highway bridges in plateau and mountainous areas and provide data to establish vehicle fatigue load spectra in national highway regions.

1. Introduction

In recent decades, with the rapid growth of China's economy, quantity and weight of road traffic vehicles grow with each passing day. Bridge accidents caused by fatigue damage of vehicles increase year by year, and fatigue problem attracts more and more attention of the public. Because moving traffic is the major fatigue load for bridge structure, proper selection of fatigue load spectrum of vehicle is the key to rational prediction of fatigue life of bridge structures.

There is fatigue load spectrum of vehicle or standard fatigue vehicle model available for fatigue analysis a long time ago in foreign countries, for example, Specification for Fatigue Implementation, part 10 of BS5400 Bridge Criterion [1] issued by United Kingdom in 1978. This model formulates load frequency spectrum applicable to highway steel bridges in England in the view of statistical data of vehicles on truck highway bridges. AASHTO Load and Resistance Factor Design (LRFD) formulates the first edition of steel bridge fatigue specification on basis of Goodman diagram of American Welding Society and standard fatigue vehicle model applicable to American highway bridges is raised in the specification [2]. The six-axle vehicle weighing 445 kilo newton (kN) in total is selected as standard fatigue vehicle for making fatigue design is raised in General Code for Design of Highway Bridges and Culverts (JTG D60—2015) [3] in China. At the same time, many scholars in China conduct studies on fatigue load spectrum of vehicle. Wang et al. carried out an investigation and studied traffic volume of Hengfu road section on the inner-ring road in Guangzhou City and build fatigue-loaded vehicle model for viaducts in Guangzhou City. Su et al. carried out an investigation and statistical analysis on traffic volume of outer-ring road in Tianjin City and work out fatigue load spectrum applicable to highway bridges in Tianjin City. Le et al. took the bridge on a certain road section in Shanghai City as object of study to conduct a statistical analysis through investigation into vehicular traffic at site and formulate fatigue load spectrum

for fatigue design of road bridges in Shanghai City. Shao et al.'s research results provide anti-fatigue design of bridges and evaluation of fatigue life with reliable vehicle load spectrum on basis of investigation into vehicle load at the site of Jiujiang Yangtze River Bridge [4]. Jiang et al. took Aizhai Bridge on Jicha Highway as engineering background and conducted a random load investigation and study to obtain the load spectrum of random vehicle on Aizhai Bridge [5]. Wang et al. established fatigue load spectrum of beam bridges in road freight passage with mass flow and heavy load. However due to China's vast territory, economic development varies from region to region and traffic operation conditions of all regions are quite different. Fatigue load spectrum obtained from results of investigation into different regions does not have general applicability. Thus, plateau mountainous areas such as Yunnan Province cannot directly apply the fatigue load spectrums of other regions. Specific regional traffic situation shall be combined to formulate the vehicle fatigue load spectrum with regional representativeness [6].

In order to establish the load spectrum of fatigue vehicles on the highway, the major contributions of this work are as follows:

Conducting an investigation into traffic flow information of G56 highway (Kunming to Baoshan road section on Hangzhou-Ruili Highway), and obtaining random distribution characteristic of traffic flow by statistical analysis.

Secondly, a T-beam bridge with a span of 30 meters, which is the most representative bridge type on highway of Yunnan Province, is adopted for fatigue life analysis.

Finally, the load spectrum of fatigue vehicles is established through the principle of equivalence. Meanwhile, a six-axle truck with maximum contribution to fatigue damage was determined as the fatigue standard vehicle model for simplified fatigue analysis [7].

2. Traffic Investigation and Statistics

In this work, wireless sensors network (WSN) is used to accumulate traffic flow data. WSN is a group of dedicated wireless sensors for monitoring and recording the physical conditions of the environment and organizing the collected data at a central location. WSNs measure environmental conditions like temperature,, humidity, wind, and so on. WSN is similar to wireless ad hoc networks in the sense that they rely on wireless connectivity. WSNs are spatially distributed autonomous sensors that cooperatively pass their data through the network to a main location [8].

In virtue of dynamic weighing wireless network sensing system on G56 highway (Kunming to Baoshan road section), observation of vehicular traffic on January 1, 2015, has been made for 24 hours to obtain traffic flow data of 9440 automobiles. Data information includes traffic flow, vehicle model, and weight. In general, all-day traffic flow information obeys a certain rule. Traffic flow has gradually risen from 4 o'clock in the morning and reaches the first peak at 11 o'clock in the morning. Traffic flow falls slightly after lunchtime but begins to recover at about 14 o'clock at noon. It reaches the second peak until 18 o'clock in the afternoon. Numerical values of two peaks have no big gap, about 600 vehicles. Night falls after the second peak and traffic flow falls gradually and then reaches the minimum value at 3 o'clock in the morning of the next day [9].

With reference to automotive models [10] and in view of parameters including number of axles, number of wheels, wheelbase, and vehicle weight, statistics of vehicular traffic data, statistics finds that there are mainly 26 vehicle models. Afterwards, vehicles are classified into 5 typical vehicle models by clustering methodology [11]. Clustering indexes, respectively, select number of axles, number of wheels, overall volume, gross weight, damage coefficient, minimum ground clearance, and vehicle conversion factor. Classification result is shown in Table 1.

In Table 1, there are 6087 type 1 vehicles taking up 64.5% of total vehicles; there are 501 type 2 vehicles taking up 5.3% of total vehicles; there are 1516 type 3 vehicles taking up 16.1% of total vehicles; there are 107 type 4 vehicles taking up 1.1% of total vehicles; there are 1227 type 5 vehicles taking up 13% of total vehicles.

3. Fatigue-Loaded Vehicle Model

3.1. Proportion of Vehicle Models. In order to make proportions of traffic flow more practical in simulative environment, statistical results are computed as shown in Table 2. The idea was based on statistical number of vehicles in each model and exclusion from small vehicles (weighing 3 tons on experience) [6] as with relatively little fatigue damage to bridges. Percent in the bracket represents the proportion of that vehicle model to total number of traffic flow. Proportion of gross vehicles is included in the classification and is 86.4%.

3.2. Vehicle Weight. Random distribution of vehicle weight data of traffic flow has several patterns including normal distribution, logarithmic normal distribution, Weibull distribution, Gamma distribution, and Gaussian mixture distribution. This text, respectively, assumes that vehicle weight data obeys the above-mentioned five distribution patterns. In addition, it utilizes maximum like parameter estimation method such as likelihood method or other approximate formulas to estimate relative parameters of each distribution. It also makes distribution fit tests of all distribution according to Kolmogorov-Smirnov test-related theory in hypothesis testing to find the suitable distribution pattern and to obtain the probability density function of vehicle weight distribution for each vehicle model at last. The Kolmogorov-Smirnov (K-S) test [12] is used to decide if a sample comes from a population with a specific distribution. The K-S test is based on the empirical distribution function (ECDF). Statistical analysis on vehicle weight data is made to obtain the distribution pattern and its probability distribution parameters for each vehicle model in random traffic flow. Please check specific numerical values in Table 3. πi, μi,

Table 1: Classification of typical vehicles.

Vehicle model	Model car	Number of axles	Wheelbase (m)	Axle weight (kN)	Total weight (kN)	Proportion in classification (%)
Type 1	V1–V4	2	—	—	≤30	76
	V5–V7	2	3.3	22, 53	75	6
	V10–V15	2	4.7	40, 60	100	17.9
Type 2	V8-V9	3	4.65, 1.25	50, 64, 64	178	68.4
	V16–V17	3	3.55, 1.32	45, 54, 55	154	6
	V18-V19	3	4.325, 1.35	24, 72, 71	167	25.4
Type 3	V20	4	3.3, 6, 1.35	53, 60, 67, 67	247	69.2
	V21	4	3.4, 7.6, 3	60, 80, 70, 70	280	30.7
Type 4	V22-V23	5	3, 1.35, 7, 1.3	51, 85, 85, 63, 63	347	53.7
	V24	5	3.3, 1.32, 6, 1.35	60, 105, 73, 73, 73	384	47.2
Type 5	V25	6	3.3, 1.32, 6, 1.3, 1.3	51, 85, 85, 79, 79, 79	458	0.4
	V26	6	3.3, 1.32, 6, 1.3, 1.3	45, 65, 90, 67, 60, 60	387	99.5

Table 2: Proportion of various fatigue-loaded vehicle models.

	Type 1	Type 2	Type 3	Type 4	Type 5
Proportion					
	M1: (50.9%)	M2: (5.32%)	M3: (16.07%)	M4: (1.13%)	M5: (13%)

Table 3: Weight distribution of various models of vehicles.

Vehicle model	Distribution pattern	Weight			Distribution parameter I			Distribution parameter II		
Type 1	Lognormal				μ:1.56			σ:0.80		
Type 2	Triple-normal	π_1: 0.50	π_2: 0.46	π_3: 0.04	μ_1: 14.14	μ_2: 24.78	μ_3: 68.85	σ_1: 6.09	σ_2: 18.17	σ_3: 10.73
Type 3	Triple-normal	π_1: 0.49	π_2: 0.46	π_3: 0.05	μ_1: 16.61	μ_2: 38.22	μ_3: 74.88	σ_1: 5.82	σ_2: 15.98	σ_3: 4.27
Type 4	Triple-normal	π_1: 0.32	π_2: 0.39	π_3: 0.29	μ_1: 16.63	μ_2: 39.05	μ_3: 47.69	σ_1: 4.54	σ_2: 7.74	σ_3: 34.79
Type 5	Triple-normal	π_1: 0.22	π_2: 0.31	π_3: 0.47	μ_1: 17.88	μ_2: 39.3	μ_3: 51.47	σ_1: 3.83	σ_2: 10.39	σ_3: 14.05

and σi in the table represent weight function, mean value, and variance at No. i peak, respectively. Shown in Table 3, except type 1 vehicle model obeying logarithmic normal distribution, the remaining four types of vehicle models obey mixed normal distribution.

3.3. Wheelbase. Wheelbase data is obtained by measuring samples of the above types of vehicle models obtained from on-site traffic investigations. The mean value and standard deviation (in bracket) of wheelbases of different vehicle models are shown in Table 4. Axle 1 represents the distance from the second vehicle axle to the first vehicle axle in the direction from vehicle head to tail. The rest of the data is in a similar fashion.

3.4. Axle Weight. According to Chen's study, axle weight has linear approximate relationship [13] with vehicle weight.

$$w_i = a_i W + b_i, \tag{1}$$

where W represents vehicle weight, w_i represents the weight of No. i axle, and a_i and b_i are the coefficients. In this paper, the linear relation between axle weight and vehicle weight is inherited, and the coefficients of the linear relationship are estimated based on the measured vehicle data. The coefficients for different vehicle models are shown in Table 5.

3.5. Fatigue Analysis Based on Measured Vehicle Models. In order to verify the applicability of the above measured fatigue-loaded vehicle models, a representative prestressed concrete simply supported T-shaped beam bridge on the section from Kunming to Baoshan on G56 highway is selected to make the fatigue analysis. This test makes relevant fatigue analysis by means of random flow loading.

3.6. Random Traffic Simulation. Based on the above measured fatigue-loaded vehicle models, this text utilizes Monte Carlo method to make simulation of random traffic flow by means of Fortran language programming. The flow chart of random vehicle flow simulation program is shown in Figure 1.

3.7. Analysis of Fatigue Response. The above-mentioned random traffic flow simulation program is utilized to load the influence line of mid-span moment of simple supported T-shaped beam to obtain the history of load response under the

Table 4: Statistical parameters of wheelbase data.

Vehicle model	Mean value ± standard deviation of wheelbase (m)				
	Axle 1	Axle 2	Axle 3	Axle 4	Axle 5
Type 1	4.2 ± 0.936				
Type 2	4.325 ± 1.534	1.35 ± 1.773			
Type 3	3.3 ± 1.213	6 ± 2.703	1.35 ± 0.756		
Type 4	3.3 ± 1.187	1.32 ± 0.465	6 ± 2.703	1.35 ± 0.65	
Type 5	3.3 ± 1.144	1.32 ± 0.465	6 ± 2.703	1.3 ± 0.33	1.3 ± 0.335

Table 5: Parameter in a linearity fitting of axle load and vehicle weight.

Vehicle model	Fitting parameter	w_1	w_2	w_3	w_4	w_5	w_6
Type 1	a	0.23	0.77				
	b	0.58	−0.58				
Type 2	a	0.18	0.41	0.41			
	b	2.36	−1.18	−1.18			
Type 3	a	0.05	0.23	0.36	0.36		
	b	2.23	0.85	−1.54	−1.54		
Type 4	a	0.03	0.22	0.25	0.25	0.25	
	b	2.45	1.12	−1.19	−1.19	−1.19	
Type 5	a	0.03	0.14	0.14	0.23	0.23	0.23
	b	2.53	0.79	0.79	−1.37	−1.37	−1.37

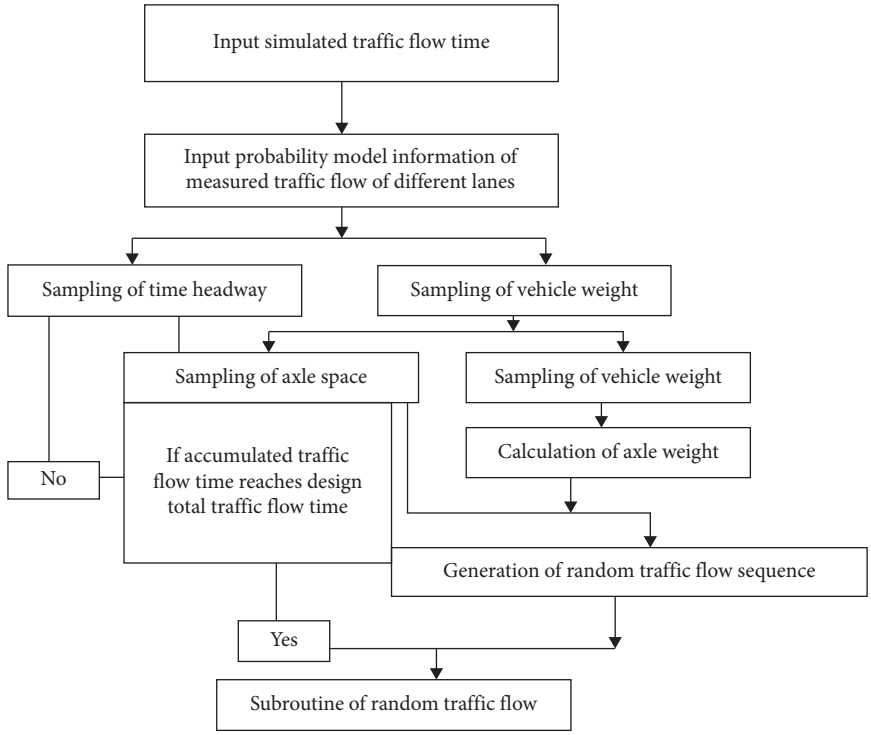

Figure 1: Flow chart of random vehicle flow simulation program.

effect 24-hour random traffic flow in Figure 2. "Drainage method" [14] is utilized to make counting statistics of the response history. Please check the statistical histogram of load amplitude distribution in Figure 3. Effective cycle index of total load amplitude is 2357 times. Response of mid-span moment of T beam under random vehicle is shown in Figure 2.

3.8. Fatigue Damage Accumulation. Fatigue load caused by random traffic flow passing through bridge belongs to variable fatigue load amplitude and is usually transformed into equivalent fatigue load amplitude for calculation [9] in the project. According to the definition, fatigue accumulating damage generated by equivalent load amplitude ΔSeq

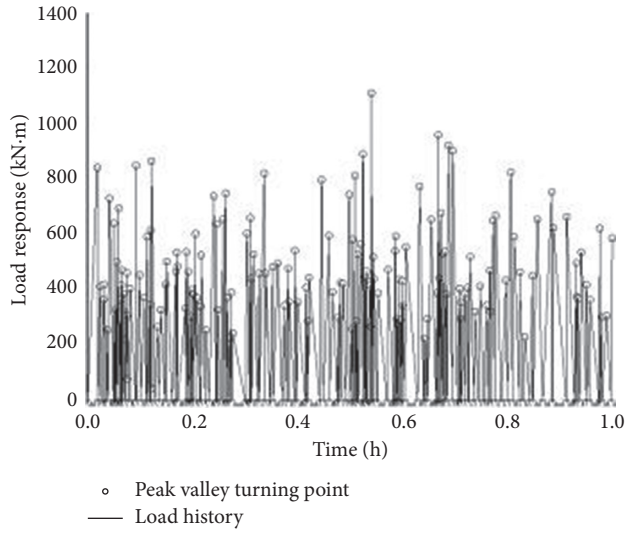

Figure 2: Response of mid-span moment of T beam under random vehicle flow.

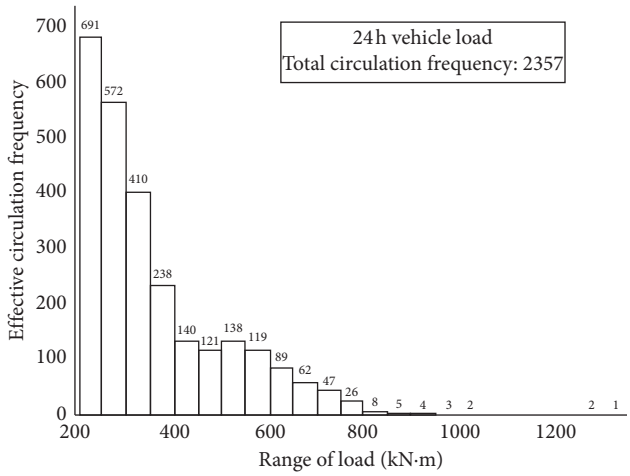

Figure 3: Statistical histogram of load amplitude distribution.

and that by variable load amplitude are equal in case of cycle indexes with the same function, which is shown below.

$$D = \sum \frac{n_i}{N_i} = \frac{\sum n_i}{N_{\text{eq}}}. \quad (2)$$

In the formula, D represents the degree of damage to component under the effect of fatigue load. That its value is 1 represents component fatigue failure. ni represents the action times of component load amplitude ΔS_i, N_i represents fatigue life of component under the effect of load amplitude ΔS_i, N_{eq} represents fatigue lift of component under the effect of equivalent load amplitude ΔS_{eq}, and $\sum n_i$ represents total action times of variable amplitude load. Approximation relation between fatigue life N and load amplitude is usually described by $N = C\Delta S^{-m}$ in component fatigue analysis and C and m are two fatigue curve parameter. If N_i and N_{eq} are represented by ΔS_{i} and ΔS_{eq}, respectively, the formula for calculating equivalent load amplitude will be as follows:

$$S_{\text{eq}} = \left(\sum \frac{n_i}{\sum n_i} \Delta S_i^m \right)^{1/m}. \quad (3)$$

In analysis of the text, load amplitude ΔS_i refers to ΔM, the mid-span moment amplitude of T-shaped beam. According to the hypothesis on force analysis of reinforced concrete structure, the equivalent stress amplitude of main tensile reinforcement in mid-span of bridge $\Delta\sigma_{\text{eq}}$ [15] is as follows:

$$\Delta\sigma_{\text{eq}} = \frac{E_s}{E_c} \frac{\Delta M_{\text{eq}} y}{I}. \quad (4)$$

In the formula, E_s and E_s are elasticity module of reinforced concrete; ΔM_{eq} is the equivalent bending moment amplitude in mid-span of T-shaped beam; y is the distance between reinforcement position and mid-span section centroid; and I is mid-span second moment of area.

With reference to *S-N* Curve put forwarded by Mason, this text makes an analysis on fatigue damage accumulation of reinforcements in concrete bridges. *S-N* Curve is as follows.

When span is over 10 m (in consideration of main reinforcement welding), the formula below is adopted for calculation.

$$\lg N = 12.7160 - 3.2599 lg\Delta\sigma. \quad (5)$$

Formulas (3)–(5) are utilized to calculate the equivalent stress amplitude of bridge reinforcements and fatigue life corresponding to effective stress amplitude. Assume that traffic flow has no obvious change within the entire design basis period. It can be calculated according to daily traffic volume and the above-mentioned fatigue life of equivalent stress amplitude that degree of fatigue damage to bridge reinforcements is 0.1045 within 100-year design basis period.

3.9. Formulation of Practical Frequency Spectrum of Fatigue Vehicle Load Model. Equivalence of each vehicle model in Table 1 is made through classic equivalence principle (equivalence of axle weight and equivalence of wheelbase) [16, 17] to transform Table 1 into practical frequency spectrum of fatigue vehicle load model for 5 vehicle models. Please check the spectrum in Table 6.

4. Determination of Standard Fatigue Vehicle

For convenience of engineering calculation, damage equivalence is made towards the above-obtained fatigue vehicle load spectrum containing 5 vehicle models to simplify it to the model of a stand fatigue vehicle. Random traffic flow simulation program that is previously compiled is slightly adjusted now to make random traffic flow become the motorcade with the same weight and wheelbase for only 1 type and to calculate the degree of fatigue damage caused by each type of fatigue vehicle model in Table 6 to mid-span concrete and reinforcement of T-shaped beam. Comparison is made between the above degree of fatigue damage and that caused by actual traffic flow in Section 3.3 to select 1 type

Table 6: Practical frequency spectrum of fatigue vehicle load model.

Vehicle model	Number of axle (piece)	Diagram	Total weight (kN)	Proportion in total traffic volume (%)
*V*1	2	40 kN 40 kN; 4.2 m	80	50.9
*V*2	3	50 kN 64 kN 64 kN; 4.325 m 1.35 m	178	5.32
*V*3	4	53 kN 60 kN 67 kN 67 kN; 3.3 m 6 m 1.35 m	247	16.07
*V*4	5	40 kN 71 kN 100 kN 73 kN 73 kN; 3.3 m 1.32 m 6 m 1.35 m	357	1.13
*V*5	6	45 kN 65 kN 90 kN 67 kN 60 kN 60 kN; 3.3 m 1.32 m 6 m 1.3 m 1.3 m	387	13

Table 7: Comparison of damage degree between different vehicles and actual traffic flow.

Vehicle model	Proportion of vehicle	*N*	Range of equivalent stress	100-year injury tolerance	Contrast percentage
*V*2	5.32%	514	21.4	0.0783	−25.0%
*V*3	16.07%	1494	15.03	0.0720	−31.1%
*V*4	1.13%	110	26	0.0316	−69.7%
*V*5	13.00%	1338	17.47	0.1052	0.1%
Actual traffic flow	—	2357	14.65	0.1045	—

Proportion of vehicle in the table represents the ratio of the quantity of this vehicle model to actual traffic flow. *N* and range of equivalent stress are both calculation results under 24 hours. Contrast percentage is the percentage of difference from the damage degree of actual traffic flow.

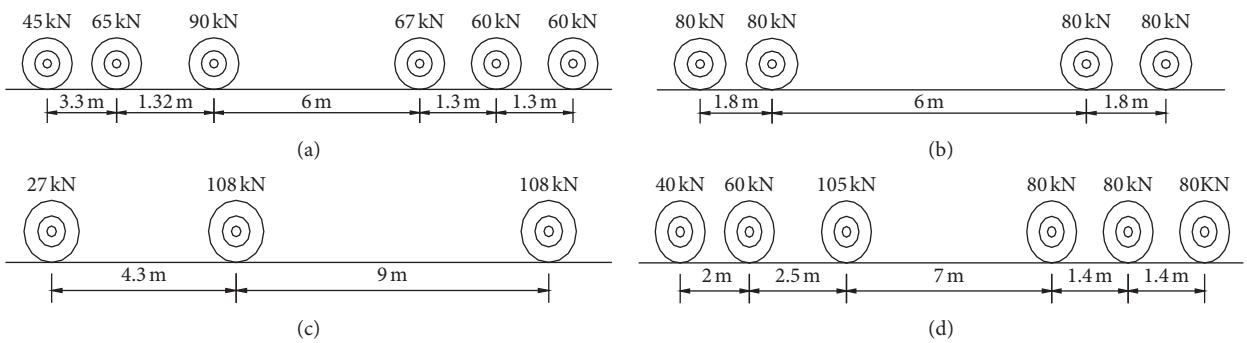

Figure 4: Standard fatigue vehicle layout. (a) Standard fatigue vehicle layout in this paper. (b) Standard fatigue vehicle layout in BS5400. (c) Standard fatigue vehicle layout in AASHTO. (d) Standard fatigue vehicle layout in General code of China.

with minimum difference in damage as standard fatigue vehicle. Comparison results are shown in Table 7.

Seen from comparison results in Table 7, damage degree under *V*5 fatigue vehicle model and damage degree caused by actual traffic flow have minimum deviation so *V*5 is regarded as standard fatigue vehicle whose specific arrangement is shown in Figure 4(a). At the same time, Figure 4 also gives specific arrangement for standard fatigue vehicles in different specifications. "General Code" in the figure identifies General Code for Design of Highway Bridges and Culverts. Standard fatigue vehicle layout is shown in Figure 4.

Each standard vehicle is loaded to the influence line of T-shaped beam through traffic flow program and its degree of fatigue damage is calculated. Calculation result and degree of fatigue damage caused by actual traffic flow to T-shaped beam are compared and comparison results are shown in Table 8.

Table 8: Comparison of fatigue damage caused by different standard fatigue vehicles.

	Proportion of vehicle	N	Range of equivalent stress	100-year injury tolerance	Contrast percentage
Traffic flow	13%	2357	14.650	0.1045	—
"General Code"	13%	1339	20.340	0.1730	65.53%
BS5400	13%	1337	18.998	0.1383	32.35%
AASHTO	13%	1333	16.095	0.0832	−20.41%
This text	13%	1338	17.472	0.1052	0.66%

Proportion of vehicle in the table represents the ratio of the quantity of this vehicle model to actual traffic flow. N and range of equivalent stress are both calculation results under 24 hours. Contrast percentage is the percentage of difference from the damage degree of actual traffic flow.

As Seen from Table 8, standard fatigue vehicles mentioned in "General Code" and BS5400 Specification both overestimate the fatigue damage to bridges in Yunnan Province caused by actual traffic on highways, but AASHTO Specification underestimates the fatigue damage to bridge. However, standard vehicle raised in this text is relatively closer to the fatigue damage to bridges in Yunnan Province caused by actual traffic on highways. Thus, standard vehicle raised in this text is more applicable to the fatigue design of highway bridges in Yunnan Province.

5. Conclusion

This paper makes an investigation and analysis on the traffic volume of G56 highway in Yunnan Province. Wireless sensors network is used to collect traffic flow data on the highway. The data collected by the wireless sensor layer is analyzed to realize local short-term storage of monitoring data and then effective processing of the data. Based on the investigation of the most representative expressway traffic flow, the clustering method is applied to classify the vehicle models. In addition, the weight probability distribution model of different vehicle models is developed through statistical analysis, which simplifies the fatigue intensity spectrum model of composition. It was observed that the selection of five vehicles of equivalent model followed by six-axle vehicle has the greatest impact on bridge fatigue damage as the standard fatigue vehicle. The research results provided a basis for the fatigue design of highway bridges in plateau and mountainous areas and provided data for the development of vehicle fatigue load spectra in national highway regions.

Data Availability

The analysis data are included in the manuscript.

Conflicts of Interest

The authors declare that there are no conflicts of interest regarding the publication of this paper.

Acknowledgments

This work was financially supported by the National Natural Science Foundation of China (No. 51568029).

References

[1] AASHTO LRFD, *Bridge Design Specifications*pp. 14–36, Texas Department of Transportation, Austin, TX, USA, 6th edition, 2012.

[2] CCCC Highway Consultants Co., Ltd., "JTG D60-2015," *General Specifications for Design of Highway Bridges and Culverts*, pp. 115–126, China Communication Press, Beijing, China, 2016.

[3] C.-H. Chen, F. Song, F.-J. Hwang, and L. Wu, "A probability density function generator based on neural networks," *Physica A: Statistical Mechanics and Its Applications*, vol. 541, Article ID 123344, 2020.

[4] Y. H. Shao and P. M. Lv, "Fatigue load spectrum for Jiujiang Yangtze River bridge," *Journal of Chang'an University: Natural Science Edition*, vol. 35, no. 5, pp. 50–56, 2015.

[5] T. Y. Jiang, "Investigation on the random vehicle load spectrum of the highway," *Bridge Journal of Changsha University of Science and Technology: Natural Science*, vol. 12, no. 3, pp. 56–62, 2015.

[6] C. Wang, "Study on load spectrum and fatigue performance of the fatigue vehicle in the small-span PC girder bridge on heavy-load highway," pp. 12–16, Beijing Jiaotong University, Beijing, China, 2015, Master's Thesis.

[7] B. Chen, X. Li, X. Xie, Z. Zhong, and P. Lu, "Fatigue performance assessment of composite arch bridge suspenders based on actual vehicle loads," *Shock and Vibration*, vol. 2015, no. 5, 13 pages, Article ID 659092, 2015.

[8] J. F. Zhao, "Study on loads of regular vehicles and extra heavy vehicles on multi regional highway bridges," pp. 3–11, Chang'an University, Xi'an, China, 2014, Master's Thesis.

[9] R. Li, "Study on joint fatigue life of concrete filled steel tubular truss arch bridge," pp. 37–49, Kunming University of Science and Technology, Kunming, China, 2012, Doctor's Thesis.

[10] H. Wang, Q. Chen, and Y. Zhang, "On the LLR criterion based shortening design for LDPC codes," in *Proceedings of the IEEE 2016 Annual Conference on Information Science and Systems*, Princeton, NJ, USA, March 2016.

[11] A. Wongsriwor, V. Imtawil, and P. Suttisopapan, "Design of rate-compatible LDPC codes based on uniform shortening distribution," *Engineering and Applied Science Research*, vol. 45, no. 2, pp. 140–146, 2018.

[12] M. Baldi, N. Maturo, E. Paolini, and F. Chiaraluce, "On the use of ordered statistics decoders for low-density parity-check codes in space telecommand links," *EURASIP Journal on Wireless Communications and Networking*, vol. 6, p. 272, 2016.

[13] M. Beermann, T. Breddermann, and P. Vary, "Rate-compatible LDPC codes using optimized dummy bit insertion," in *Proceedings of the 8th International Symposium on Wireless Communication Systems*, pp. 447–451, Aachen, Germany, November 2011.

[14] CCSDS, "Short block length LDPC codes for TC synchronization and channel coding," *Orange Book. CCSDS*, vol. 231, 2015.

[15] W. Sun, S. Yu, W. Lou, Y. T. Hou, and H. Li, "Protecting your right: verifiable attribute-based keyword search with fine-grained owner-enforced search authorization in the cloud,"

IEEE Transactions on Parallel and Distributed Systems, vol. 27, no. 4, pp. 1187–1198, 2016.

[16] Y. Miao, J. Ma, X. Liu, J. Weng, H. Li, and H. Li, "Lightweight fine-grained search over encrypted data in fog computing," *IEEE Transactions on Services Computing*, vol. 12, no. 5, pp. 772–785, 2019.

[17] M. Ibrar, A. Akbar, R. Jan et al., "ARTNet: AI-based resource allocation and task offloading in a reconfigurable internet of vehicular networks," *IEEE Transactions on Network Science and Engineering*, vol. 7, 2020.

Hindawi
Mobile Information Systems
Volume 2021, Article ID 9994050, 10 pages
https://doi.org/10.1155/2021/9994050

Research Article

Interactive Teaching System of Basketball Action in College Sports Based on Online to Offline Mixed Teaching Mode

Wenbo Guo and Yunjie Niu

Institute of Physical Education, Henan University, Kaifeng 475001, China

Correspondence should be addressed to Yunjie Niu; toutou2020@qztc.edu.cn

Received 8 March 2021; Revised 8 April 2021; Accepted 18 April 2021; Published 22 April 2021

Academic Editor: Muhammad Babar

Copyright © 2021 Wenbo Guo and Yunjie Niu. This is an open access article distributed under the Creative Commons Attribution License, which permits unrestricted use, distribution, and reproduction in any medium, provided the original work is properly cited.

The mixed teaching mode can be used to improve students' academic performance. In this study, an interactive teaching system of basketball action in college sports based on online to offline mixed teaching mode is developed. The system is mainly comprised of teacher function module, student function module, and system analysis module. In the teacher function module, online to offline mixed teaching mode is introduced to realize the interactive teaching of basketball action in college sports in the form of organic combination of microclass, massive open online course, and traditional classroom teaching. The student function module is mainly used to manage the information related to students learning basketball actions. The system analysis module uses the data mining model based on multiant colony clustering combination algorithm to obtain the learners' behavior data and then designs a targeted interactive teaching course for basketball action. After testing, it was concluded that the designed system can improve the students' mastery of basketball movement in sports and can be applied to improve student's academic performance.

1. Introduction

In the tide of higher education reform, a series of reforms and innovations have been carried out in ideology, theory, teaching materials, and practice system of physical education. The traditional teaching methods cannot meet the needs of teaching development. With the in-depth reform of physical education, the implementation of the new curriculum system, and the scientific management of work, the management content of physical education has greatly increased [1]. This requires physical education administrators to constantly improve their management level. This includes the ability to understand sports management activities, seriously understand and master the scientific teaching methods and management content, and actively explore new ways of physical education management.

The teaching management system of basketball action in college sports is composed of the main body, object, and means of sports teaching management and has some similarities and differences compared with the teaching management of other courses [2]. Therefore, in addition to the general rules of teaching management, the management of basketball action in college sports teaching should also follow the rules of human body function adaptability, action formation, and changes of human physiological function. Only by following these scientific rules of human activities to manage physical education, can the management task of basketball action teaching in college be completed more smoothly [3]. From the perspective of work arrangement, the teaching management of basketball action in college sports is composed of several different and interrelated stages, such as midterm management and final management. Its characteristics are that there are few managers and more management contents. It needs to work in an orderly way in multiple stages, with a large amount of work and complicated management tasks. In addition, the teaching management of basketball action in colleges and universities has the characteristics of repetition, circulation, and indirect coordination. It includes term circulation, academic year circulation, and irregular circulation. The management personnel should not only do their own job of organizing and managing physical education, but also carry out

teaching work to the leaders of higher authorities and teaching management organizations at the same level. It has a wide range of work contacts, including both vertical contact and horizontal coordination. It can coordinate and deal with the relationship at all levels and solve all kinds of problems in the teaching process in time; basketball action teaching management in college sports needs to be in line with the overall teaching order, subject to the school's teaching decision-making. But because it is a relatively independent teaching mode, it has its own management object and scope. Therefore, basketball actions in college sports teaching management and school teaching management have both subordination and relative independence. Managers of basketball action teaching in college sports keep close contact with students and teachers in the process of specific management, coordination, and organization of teaching activities. This is accomplished to ensure a good teaching environment and teaching order through this teaching management mode, to create necessary preconditions for serving the students and teachers [4].

The rapid development of modern education technology and Internet communication technology has affected many aspects of life. The emergence of Taobao online store has curbed the monopoly of physical stores in the industry. Didi taxi has broken the situation of no competition in the taxi industry, prompting taxi drivers to improve their service quality. Compared with the conservatism and closeness of traditional physical education, openness and cooperation are the most significant characteristics of the "Internet +" era. The application of new classroom teaching modes, methods, and resources with stronger interactivity and visibility, such as microclass and massive open online course (MOOC), has developed rapidly in China's Curriculum Teaching Reform [5]. As the medium of transforming theory into practice, the innovation of the teaching mode of physical education plays an important role in teaching. At present, the demand for interdisciplinary talents is increasing with the development of society, and the goal of school education is no longer limited to the cultivation and investigation of students' single professional courses and professional ability. The development of teaching content and teaching form has enriched a lot [6, 7]. Therefore, blended teaching mode is more and more popular among educators and students, and O2O teaching mode is one of them [8].

O2O mode was initially used in commercial marketing, which is expressed as online to offline (O2O) in English. It refers to a marketing mode that drives offline operation and consumption through online marketing purchase or reservation. It is also called offline business mode. It is applied in the field of education and teaching, which is called the O2O teaching mode. At this time, great changes have taken place in the meaning of O2O mode, which mainly refers to the sharing of teaching and learning resources through network information technology, the change of traditional learning methods and teaching methods, and the creation of an open, interactive, personalized, efficient, and comfortable teaching environment [9–11]. Through a certain teaching design, the teaching mode flexibly combines network with traditional classroom education and effectively makes up for the defects of single online learning and traditional classroom learning. It is not only the mixture of autonomous learning, collaborative learning, acceptance learning, and discovery learning but also the mixture of real classroom environment and virtual network environment or the mixture of offline communication and online communication between teachers and students [12].

The main contribution of this work is as follows:

This paper designs an interactive teaching system of basketball action in college sports based on O2O mixed teaching mode

The system provides an interactive teaching system and can meet the design requirements

2. The Interactive Teaching System of Basketball Action in College Sports Based on O2O Mixed Teaching Mode

2.1. Design of System Architecture. Based on the O2O mixed teaching mode, all the functions of the interactive teaching system for basketball action in college sports are realized according to the user's browser and the interaction of basketball action's interactive teaching server. The database server of the system can organize store and maintain all the data related to the system. The Internet is used to connect the interactive teaching server of basketball action. Students, teachers, and administrators section of the system send their access requests to the server through the browser. The interactive teaching server of basketball action is applied to the interactive teaching course of basketball action on the database server. Figure 1 represents the architecture of basketball action in college sports interactive teaching system based on O2O mixed teaching mode.

This system is comprised of three parts: teacher function module, student function module, and system analysis module. The overall functional structure of the interactive teaching system of basketball action in college sports based on O2O mixed teaching mode is shown in Figure 2.

2.1.1. Physical Education (PE) Teaching Management. The PE teaching management part of the teacher management module consists of curriculum management, performance management, teaching resources, teaching analysis, question answering and discussion, class hour statistics, and system management. In the course management, O2O mixed teaching mode is mainly used to realize the interactive teaching of basketball action. The architecture of the O2O mixed teaching mode is shown in Figure 3.

Microclass, MOOC, and traditional classroom complement each other. The emergence of microclass makes the teaching method of physical education more flexible, and the construction of MOOC broadens the coverage of traditional knowledge dissemination [13]. Making accurate microclass and massive MOOCS can provide indispensable online resources for basketball action classroom teaching, thus organically integrating with traditional classroom teaching and fundamentally subverting the existing teaching mode.

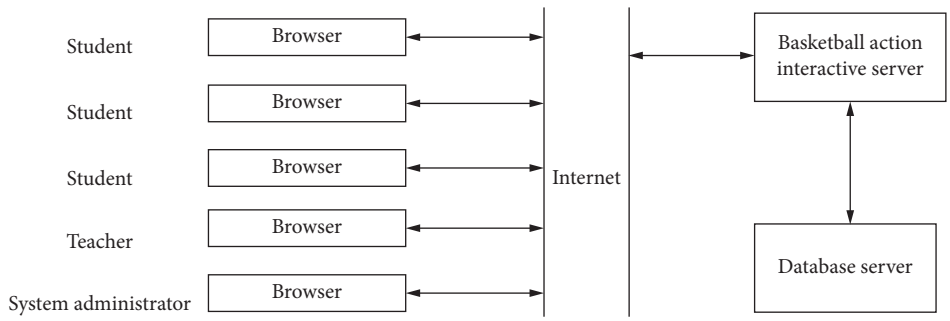

Figure 1: Architecture of basketball action in college sports interactive teaching system based on O2O mixed teaching mode.

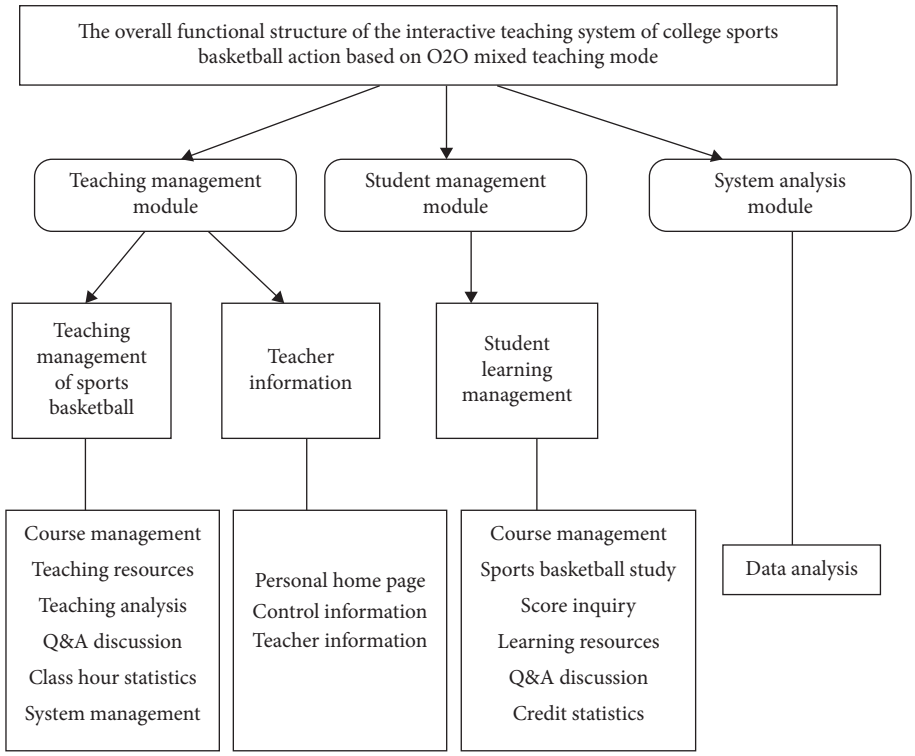

Figure 2: The overall functional structure of the interactive teaching system of basketball action in college sports based on O2O mixed teaching mode.

Combined with the successful experience of microclass and MOOC in classroom teaching, this paper constructs a three-dimensional O2O sports teaching mode based on micro-class-MOOC-traditional classroom.

Basketball technology in sports is different from the teaching of other disciplines. The introduction of microclass and MOOC cannot completely replace the traditional classroom teaching. The integration of microclass and MOOC into traditional sports classroom teaching is not simple addition. It should combine the characteristics and needs of basketball teaching course to study the three-dimensional teaching mode of the organic combination of microclass, MOOC, and traditional classroom teaching. The microclass embedded in the interactive teaching of basketball actions can shorten the time spent by teachers in explaining the essentials of basketball technical actions. MOOCS and microclasses are not limited by time and space. Before classroom teaching, students can complete the preview of new courses and review of learned courses. After class, no matter when and where students can watch the video of microclass, they can learn and imitate basketball actions repeatedly to deepen their understanding and mastery, so as to realize the organic combination of sports basketball inside and outside class and save a lot of time for basketball teaching in classroom of teachers' to make differentiated instruction.

The O2O basketball action teaching mode of "micro-class-MOOC-traditional classroom" includes four parts: interactive teaching course construction, classroom teaching, after class learning, and evaluation feedback. The construction of interactive teaching course is to create valuable microclass resources in a moody class platform. Firstly, it should conduct detailed research on basketball action, decompose the contents of basketball action, extract

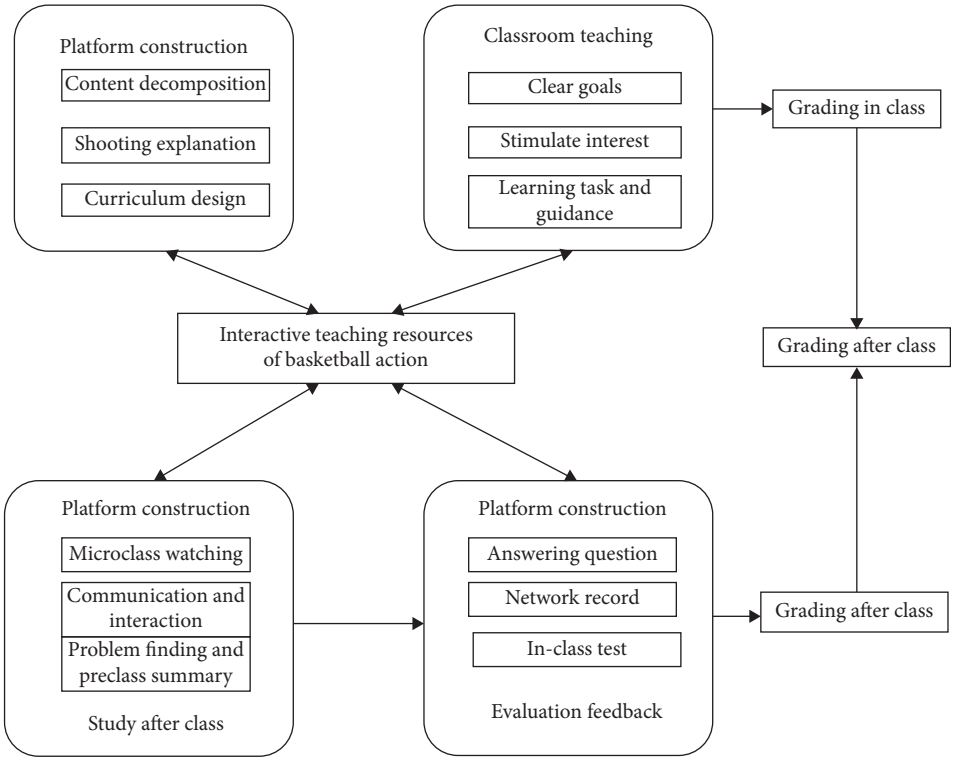

Figure 3: Architecture of O2O mixed teaching mode.

the essence of basketball action, prepare for the shooting of microclass, open the moody class platform, provide high-quality online course resources, and provide corresponding text teaching materials, self-test summary, learning tasks, and so on. Through the MOOC platform, students can have targeted and repeated learning difficulties knowledge points and can also consolidate and master basketball action knowledge points through online Q and A, so as to build an independent learning support system for students. Before classroom teaching, students can preview the course through the MOOC platform. The preview task is designed to be interesting, so as to stimulate learning interest and solve the knowledge learning beyond the key and difficult points of teaching. The key and difficult points of teaching are the important problems to be solved in basketball action classroom teaching. Classroom teaching focuses on solving students' problems and improving vulnerable learning groups. It also gives corresponding measures for students' feedback and evaluation of online testing exercises. After class learning, students can flexibly control the time and place of autonomous learning, skip what they have mastered, and focus on consolidating their own unskilled knowledge points. Feedback evaluation is not only a link between online and offline but also a booster to promote the continuous development of teaching. Feedback evaluation includes two aspects: basketball performance evaluation and students' periodic evaluation feedback on MOOC platform and microclass video. Performance evaluation includes evaluation of old teachers, mutual evaluation of students, and evaluation of offline activities. Through the analysis and combined with the results of students' feedback, teachers can optimize and adjust the course content. Each link of this mode influences and promotes each other, which is a kind of teaching mode of learning initiative, integration diversification, teaching diversification, and three-dimensional support [14, 15].

2.1.2. Teacher Information. The teacher information section of the teacher management module consists of the following modules: personal home page, teacher information, and contact information.

(a) Personal home page: teachers' personal home page used to publish some teachers' personalized information

(b) Teacher information: the age, professional title, curriculum vitae, and other pieces of basic information of the teacher

(c) Contact information: the contact information of teachers

2.1.3. Student Learning Management. The student learning management part of the student management module is mainly composed of the following modules: curriculum management, sports technology learning, score query, learning resources, question answering and discussion, and class hour statistics.

(a) Course management: students can conduct interactive teaching of basketball actions, course query, course selection, and other operations

(b) Sports technology learning: after students choose the interactive teaching course of basketball action, they can learn the project

(c) Score query: after the teacher publishes the scores, students can query their basketball test scores online through the login system

(d) Learning resources: some necessary learning resources, such as courseware and software

(e) Q&A and discussion: in the process of learning, students can communicate with teachers or classmates online when they encounter difficult problems

(f) Credit statistics: make statistics on the credits of courses taken by students

2.1.4. System Analysis Module. The system analysis module is mainly based on the relationship between the data in the database, and then a data warehouse is built to analyze the data. This system introduces data mining model based on multiant colony clustering combination algorithm, which can find the information hidden in learners' behavior data and then guide PE teaching [16].

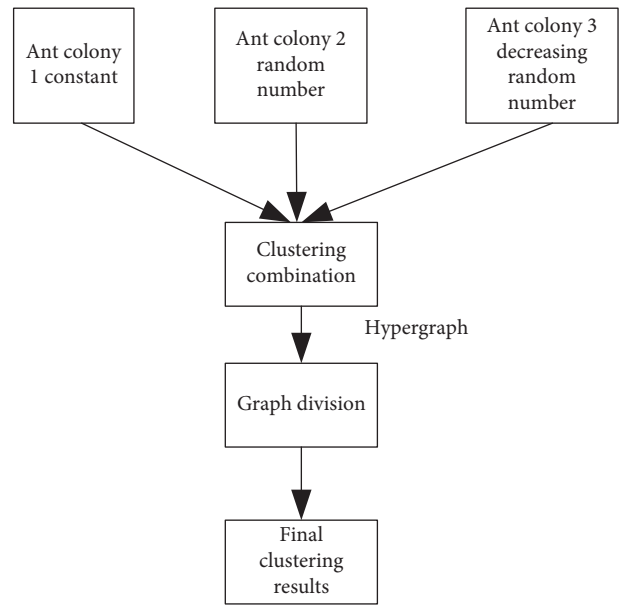

Figure 4: Structure diagram of data mining model based on multiant colony clustering combination algorithm.

2.2. Data Mining Model Based on Multiant Colony Clustering Algorithm. One of the difficulties in network teaching is how to monitor the learning process of students, so as to realize the effective combination of teaching and learning based on network teaching platform. In this paper, data mining technology is applied to establish the corresponding data mining model and to mine the association between learner behavior data. According to the mining data, different teaching objectives and teaching content organization strategies are used for different student groups to realize the hierarchical teaching of students' network [17, 18].

2.2.1. Model Structure. Figure 4 shows the structure of the data mining model based on multiant colony clustering combination algorithm. Ant colony algorithm is inspired by the foraging behavior of ants. At the core of this behavior is the indirect communication between the ants with the help of chemical pheromone trails, which enables them to find short paths between their nest and food sources.

The first layer of the proposed model is composed of three ant colony modules with different speed types, and the middle layer is composed of clustering module, which combines the preliminary clustering results into a hypergraph. The last layer is the graph partition module, which uses the graph partition algorithm based on ant colony algorithm to divide the hypergraph twice to get the final clustering results of learner behavior data.

2.2.2. Clustering Combination. The clustering results of a known group of learners' behavior data are expressed as a hypergraph. Assuming that $O = \{o_1, o_2, \ldots, o_n\}$ represents a set of learners' behavior data, the n learners' behavior data are divided into k classes, which can be expressed as a label vector $\lambda \in I^n$. In the r cluster results, the known q-th learner behavior data $\lambda^{(q)}$ is divided into $k^{(q)}$ categories, and then it can get a binary member matrix $H^{(q)} \in I$. In this matrix, each cluster is represented as a superedge (corresponding to the column of the matrix). By combining these member matrices, an adjacency matrix of a hypergraph with n vertices and $\sum_{q=1}^{r} k^{(q)}$ hyperedges is obtained.

$$H = \left(H^{(1)}, \ldots, H^{(r)}\right). \tag{1}$$

Each row of the matrix H represents a vertex (learner behavior data), and each column represents a superedge. The value of the vertex belonging to the same superedge is 1; otherwise, it is 0. So far, the clustering results of a group of learner behavior data have been mapped into the critical matrix of hypergraph.

Here is a simple example to illustrate the above concept. Table 1 shows three cluster marker vectors with seven learner behavior data $o_i\,(i = 1, 2, \ldots, 7)$, among which clusters 1 and 2 are logically consistent, while cluster 3 has some disputes on the classification of objects 3 and 5. The adjacency matrix H of the hypergraph is shown in Table 2, where seven vertices $v_i\,(1, 2, \ldots, 7)$ of hypergraph correspond to seven objects. Each cluster is represented as a hyperedge, and there are nine hyperedges.

Next, the adjacency matrix H of a hypergraph with n vertices and $\sum_{q=1}^{r} k^{(q)}$ hyperedges can be determined by the following formula:

$$S = HH^T. \tag{2}$$

It is transformed into a symmetric adjacency matrix S of $n \times n$, where H^T is the transpose matrix of H. Each row and column of S correspond to a vertex in the hypergraph, and the value on the nondiagonal line reflects the weighted value of the hyperedge. If two vertices belong to the same superedge more times, the weight of the superedge is larger.

Table 1: Cluster marker vector.

	$\lambda^{(1)}$	$\lambda^{(2)}$	$\lambda^{(3)}$
o_1	1	2	1
o_2	1	2	1
o_3	1	2	2
o_4	2	3	2
o_5	2	3	3
o_6	3	1	3
o_7	3	1	3

Table 2: Adjacency matrix of hypergraph.

H	1			2			3	
1	1	0	0	0	1	0	1	0	0
2	1	0	0	0	1	0	1	0	0
3	1	0	0	0	1	0	0	1	0
4	0	1	0	0	0	1	0	1	0
5	0	1	0	0	0	1	0	0	1
6	0	0	1	1	0	0	0	0	1
7	0	0	1	1	0	0	0	0	1

2.3. Graph Partition Algorithm Based on Ant Colony Algorithm. The main idea of the second partition of hypergraph is that the operation of the learner behavior data object o_i is changed to the operation of the vertex v_i, and the distance $d(o_i, o_j)$ between the learner behavior data is changed to the distance $d(v_i, v_j)$ between the vertices. Therefore, the graph partition algorithm based on ant colony algorithm is a dynamic clustering algorithm by moving vertices on the plane [19,20].

Suppose $G(V, E)$ is a graph, $V = \{v_i, i = 1, 2, 3, \ldots, n\}$ is the set of vertices, and E is the set of edges. The adjacency matrix of graph $A = [a_{ij}]$. Where $\begin{cases} a_{ij} \neq 0 & \text{if and only if } (v_i, v_j) \in E \\ a_{ij} \neq 0 & \text{if and only if } (v_i, v_j) \notin E \end{cases}$, the distance $d(v_i, v_j)$ between any two vertices is defined as

$$d\left(v_i, v_j\right) = \frac{\left|D\left(\rho\left(v_i\right), \rho\left(v_j\right)\right)\right|}{\left|\rho\left(v_i\right)\right| + \left|\rho\left(v_j\right)\right|}, \tag{3}$$

where $\rho(v_i)$ is the set of all vertices adjacent to vertex v_i, including v_i itself; $\rho(v_j)$ is the set of all vertices adjacent to vertex v_j, including v_j itself; D is the symmetry difference between the two sets.

If two vertices v_i and v_j have a large number of common adjacent nodes, that is, $\rho(v_i) \cup \rho(v_j) - \rho(v_i) \cap \rho(v_j)$ is a small set, then $d(v_i, v_j)$ is smaller, that is, v_i and v_j will eventually come together and fall into one category. On the contrary, if there are only a few or no adjacent edges between the two vertices v_i and v_j, that is, $\rho(v_i) \cup \rho(v_j) - \rho(v_i) \cap \rho(v_j)$ is a large set, then $d(v_i, v_j)$ is larger. In other words, v_i and v_j will eventually be far apart and belong to different classes.

3. Results

In order to test the application effect of the system, the experimental environment is designed to ensure the normal operation of the system. Table 3 shows the details.

Table 3: System experimental environment design.

Project	Content
Operating system	Microsoft Windows 10
Database	MySQL server
Browser	Internet Explorer
CPU	Intel i5
Memory	8 GB
Hard disk	600 GB

3.1. The Rationality Test of the System. The rationality of the system in this paper is tested. Taking the support and confidence as the test index, the rationality of the basketball action course taught by the system to students is analyzed. The details of the interactive teaching course of basketball action are shown in Table 4. The rationality test results of the system are shown in Figures 5 and 6 .

Through the analysis of the above table, we can know that, in the interactive teaching of five kinds of basketball actions, such as passing and catching the ball + dribbling, holding the ball breakthrough, personal defense, grabbing the ball, grabbing the basket, and pitching, the support degree and confidence degree of the basketball action course displayed by the system in this paper for students are as high as 0.99, so the rationality of the basketball action course displayed by this system for students is very high, and it matches the students' learning progress very well. The reason is that the data mining model based on multiant colony clustering algorithm is used in this system to mine the learning behavior data of student groups. According to the mining model, different teaching objectives and teaching content organization strategies are used for different student groups to realize the hierarchical teaching of student network.

3.2. The Application Satisfaction Test of the System. Through the form of a questionnaire survey, this paper analyzes the application satisfaction of users after using the system, and the test content is shown in Table 5.

The test results are shown in Figure 7.

From the above table, it can be seen that, after the application of the system in this paper, the user's satisfaction with this system is higher than 98%. Therefore, this system is deeply loved by users, and the application feedback is good.

3.3. The Teaching Effect Test of the System. In order to test the teaching effect of the system in this paper, this paper tests the students' mastery of basketball action before and after using this system and after interactive teaching of basketball action in college sports, as well as the examination results of basketball action in college sports. The types of basketball action in college sports are moving, passing and catching, dribbling, shooting, holding breakthrough, personal defense, grabbing, breaking, and grabbing. The test results are shown in Table 6. Among them, the full score is 10. More than 6 points are qualified, and less than 6 points are unqualified.

Table 4: Interactive teaching course of sports basketball action.

Action type	Course details
1	Pass and catch + dribble
2	Breakthrough with the ball
3	Individual defense
4	Grab the ball
5	Grab the basket and throw the ball

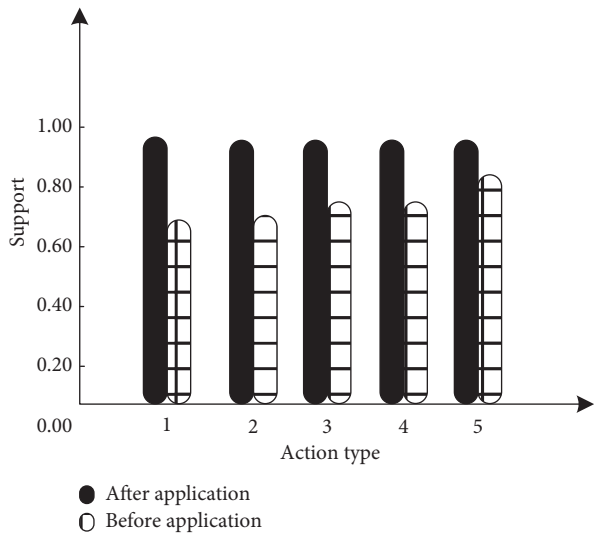

Figure 5: Support test results.

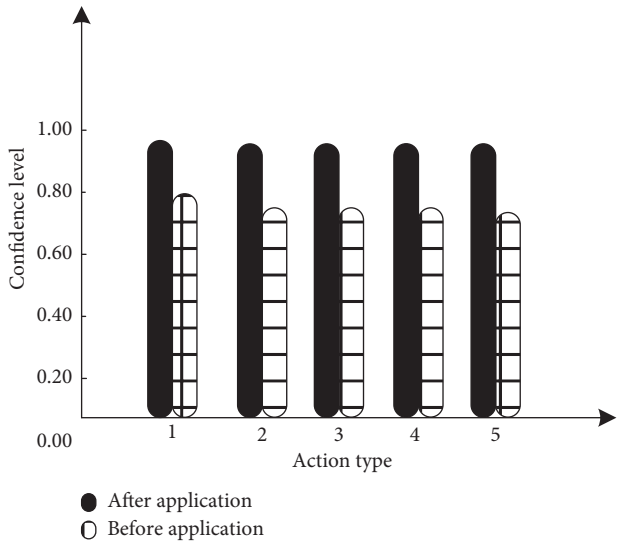

Figure 6: Results of confidence test.

According to the data in Table 6, when the types of basketball action in college sports are moving, passing and catching, dribbling, shooting, breakthrough with the ball, personal defense, grabbing the ball, breaking the ball, grabbing the basket, and pitching, before using the system in this paper, the students' mastery of basketball action in college sports is poor, and the test score of sports basketball action is less than 6 points, with an average score of 5 points. After using this system, the students have a good grasp of basketball action in college sports, and the test score of basketball action is more than 6 points, with an average of 9 points. In contrast, this system can effectively improve the students' mastery of basketball action and improve their sports performance.

3.4. The Data Mining Effect of Students' Group Learning Behavior of the System. The data mining effect of the system in this paper is tested on five students' learning behavior, and the interactive teaching course of two kinds of basketball actions is taken, namely, holding the ball breakthrough and personal defense, as an example to test the mining effect of this system. The mining effect is mainly reflected by precision P and recall R. The test results are shown in Figures 8 and 9 .

$$P = \frac{N_{ij}}{N_i},$$
$$R = \frac{N_{ij}}{N_j}, \tag{4}$$

where N_{ij} is the number of classification i in cluster j; N_j is the number of all objects in cluster j; N_i is the number of all objects in cluster i.

As shown in Figures 8 and 9, this system has a good effect on the data mining of five students' learning behavior. In the interactive teaching course of holding the ball breakthrough and personal defense, after the data mining of five students' learning behavior, the maximum precision rate is 0.98, and the maximum precision rate is 0.98. The mining performance is significant, which has a positive impact on the setting of interactive teaching course of basketball action.

3.5. The Concurrency Test of the System. At present, in the application performance test of all the systems, it needs to pay attention to its concurrency resistance. The concurrency resistance reflects whether the system can carry concurrent user access. The number of concurrent users of this system is set to 10, 20, 30, and 40 in turn. Taking the interactive teaching course of three kinds of basketball actions, such as grabbing the ball, breaking the ball, grabbing the basket, and pitching, as an example, under the condition of a different number of users, the system in this paper is running smoothly. Whether the screen gets stuck in the interactive teaching of basketball action is mainly reflected by the utilization rate of CPU. The test results are shown in Figure 10.

As shown in Figure 10, when the number of concurrent users of this system is 10, 20, 30, and 40, under the condition of a different number of users, although the CPU utilization rate of this system is gradually increasing, the maximum value is less than 40%, the CPU utilization rate is low, and there is no significant interference to the interactive teaching screen of this system. Therefore, the concurrency of this system is low. The test is passed, and the performance remains the same under different concurrent users.

Table 5: The content of the system application satisfaction test.

Evaluation item code	Evaluation content	Option
A	Views on the interactive teaching course of basketball action setup in this paper	Approve/disapprove
B	Is the teaching of this system reasonable	Reasonable/unreasonable
C	This paper discusses the effect of the system on students' practical ability	Positive/negative

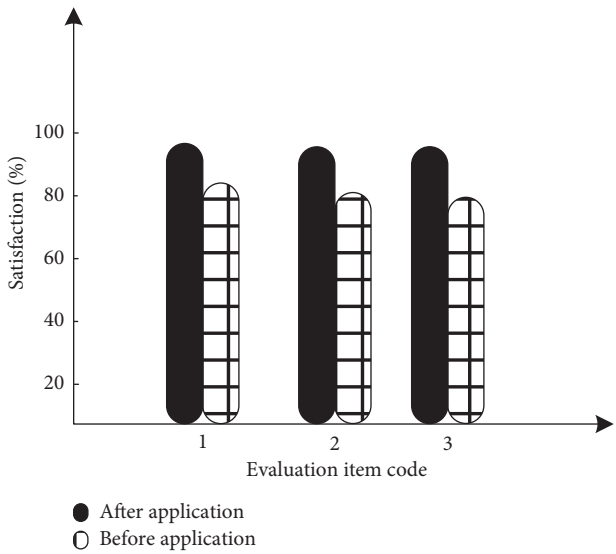

Figure 7: Test results of application satisfaction of this system.

Table 6: Teaching effect test of this system.

Action type	Score before use	Score after use
Move	5	9
Pass and catch	5	8
Dribble	5	9
Shoot	5	9
Breakthrough with the ball	5	9
Individual defense	4	9
Grab the ball	4	8
Break the ball	4	8
Blue bowling	5	9
Average	5	9

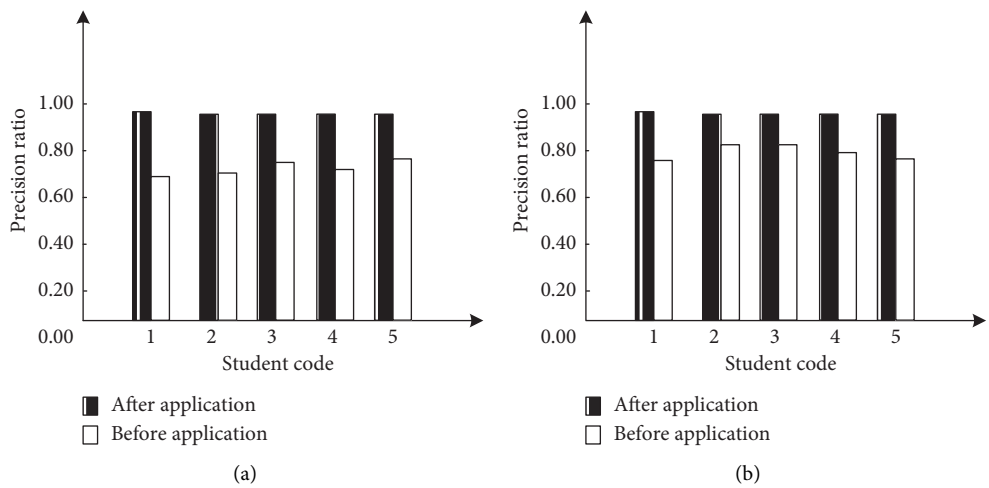

Figure 8: Precision test results. (a) Breakthrough with the ball. (b) Individual defense.

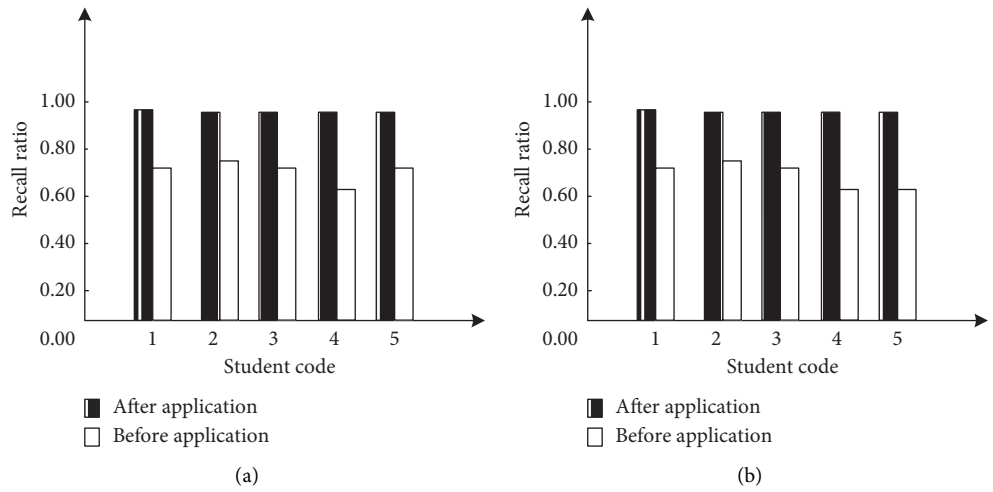

Figure 9: Recall test results. (a) Breakthrough with the ball. (b) Individual defense.

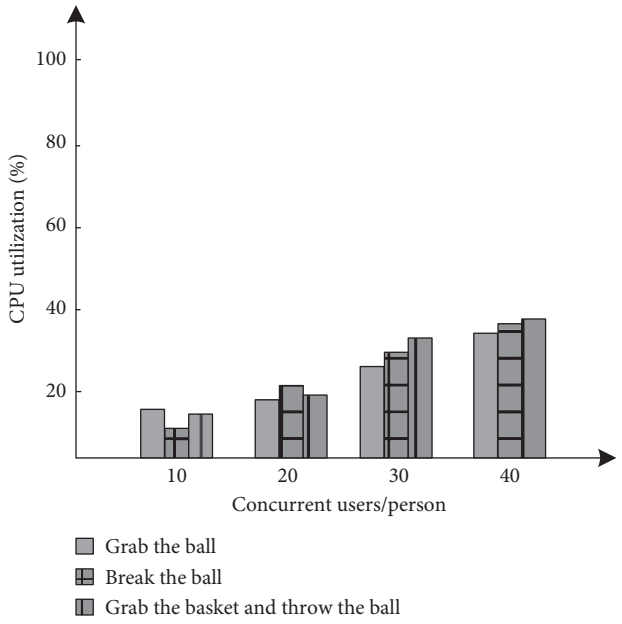

Figure 10: Concurrency test results of the system.

4. Conclusions

With the information technology, distance education system based on network has made great progress. Moreover, at this stage, multimedia technology has been fully integrated with network communication technology, and teaching work is more carried out in the network environment, so that the teaching mode has been completely changed. The networked teaching system has the characteristics of autonomy and interaction, which makes the communication between students and students and teachers more convenient. This paper designs an interactive teaching system of basketball action in college sports based on O2O mixed teaching mode and verifies its availability in the experiment. PE is one of the compulsory courses, which can enhance the system and health of students. Networked teaching solves the time and space constraints of PE, meets the requirements of interaction between students and teachers in the process of PE, and promotes the development of PE. Therefore, the application of networked technology in PE has a great role in promoting PE. However, due to the practicality of PE teaching activities, it cannot be separated from the traditional way of PE. Therefore, for networked PE teaching, it is a beneficial supplement to the traditional PE teaching and cannot replace the traditional PE teaching.

Data Availability

The data used to support the findings of this study are available from the corresponding author upon request.

Conflicts of Interest

The authors declare that they have no conflicts of interest.

References

[1] J.-H. Ahn, "The interaction effect of autonomy and self-control on exercise adherence intention in university's general physical education class students," *Korean Journal of Sports Science*, vol. 29, no. 2, pp. 353–367, 2020.

[2] A. Nova, A. R. Sinulingga, and A. Syahputra, "The level of parents anxiety on physical education activity at lintang city elementry school," *Jp. jok (Jurnal Pendidikan Jasmani, Olahraga Dan Kesehatan)*, vol. 3, no. 2, pp. 156–164, 2020.

[3] Z. Zhang and H. Min, "Analysis on the construction of personalized physical education teaching system based on a cloud computing platform," *Wireless Communications and Mobile Computing*, vol. 2020, no. 3, 8 pages, 2020.

[4] Y. Ma, "Cultivation of the ability of creating and arranging aerobics in physical education majors," *World Scientific Research Journal*, vol. 5, no. 9, pp. 88–93, 2019.

[5] Z. Zhong, "Design and application of university physical education system based on computer aided system," *IPPTA: Quarterly Journal of Indian Pulp and Paper Technical Association*, vol. 30, no. 8, pp. 681–686, 2018.

[6] T. Yue and Y. Zou, "Online teaching system of sports training based on mobile multimedia communication platform,"

International Journal of Mobile Computing and Multimedia Communications, vol. 10, no. 1, pp. 32–48, 2019.

[7] S. Ryan, M. Maina, and J. Maina, "Effects of a sound field amplification system on teacher movement in physical education settings," *The Physical Educator*, vol. 75, no. 4, pp. 569–581, 2018.

[8] H. Li, H. Zhang, and Y. Zhao, "Design of computer-aided teaching network management system for college physical education," *Computer-Aided Design and Applications*, vol. 18, no. S4, pp. 152–162, 2021.

[9] L. Yanru, "An artificial intelligence and machine vision based evaluation of physical education teaching," *Journal of Intelligent and Fuzzy Systems*, vol. 40, no. 1, pp. 1–11, 2020.

[10] D. Xu and T. S. Rappaport, "Construction on teaching evaluation index system of track and field general course for physical education major in light of wireless network technology," *Journal of Intelligent and Fuzzy Systems*, vol. 37, no. 7, pp. 1–9, 2019.

[11] A. O. Roliak, "Professional education of teachers in physical training and health: the experience of Denmark," *Pedagogy of Physical Culture and Sports*, vol. 24, no. 3, pp. 143–150, 2020.

[12] L. Yun, W. Ying, L. Yanli, and Y. Xiuying, "Practical experience of mixed teaching mode based on SPOC in physiology experiment course for international students," *Education Study*, vol. 2, no. 4, pp. 304–312, 2020.

[13] A. Li, S. Yu, F. Qinggang, and Z. Yongmei, "Exploration of the mixed teaching mode of "three classes" under the intelligent teaching-based on computer programming course," *Education Study*, vol. 2, no. 1, pp. 33–42, 2020.

[14] Z. Wu, Y. Guo, and J. Wang, "A case study of adoption of a mixed teaching mode in the teaching of English-Chinese translation course," *Chinese Studies*, vol. 10, no. 01, pp. 31–41, 2021.

[15] N. Xu and W. H. Fan, "Research on interactive augmented reality teaching system for numerical optimization teaching," *Computer Simulation*, vol. 37, no. 11, pp. 203–206+298, 2020.

[16] L. Chen, X. Wei, X. Wei, and Y. Du, "Exploration and practice of the "trinity" mixed teaching mode of organic synthetic chemistry," *University Chemistry*, vol. 34, no. 7, pp. 52–59, 2019.

[17] B. G. Masadis and E. Kouli, "Satisfaction of teaching alternative basketball skills on 5 th & 6 th graders," *HuSS International Journal of Research in Humanities and Social Sciences*, vol. 3, no. 9, pp. 61–67, 2020.

[18] Y. Y. Chia, "A study of basketball course teaching quality, sports enjoyment, and learning satisfaction in college students," *Asian Journal of Education and Social Studies*, vol. 1, no. 1, pp. 1–12, 2018.

[19] Z. Fang, "Analysis of the class system reform and innovation form of the public physical health curriculum in higher education institutions," *International Journal for Engineering Modelling*, vol. 31, no. 1, pp. 365–371, 2018.

[20] O. Shkola, V. Zhamardiy, and V. Saienko, "The structure model of methodical system usage fitness-technology in student physical education," *International Journal of Applied Exercise Physiology*, vol. 9, no. 10, pp. 89–96, 2020.

Hindawi
Mobile Information Systems
Volume 2021, Article ID 5521144, 9 pages
https://doi.org/10.1155/2021/5521144

Research Article

Local Cultural IP Development and Cultural Creative Design Based on Big Data and Internet of Things

Wei Bi[1] **and Guangming Wang**[2]

[1]*Art and Design College, Guangdong University of Finance and Economics, Guangzhou 510320, Guangdong, China*
[2]*School of Politics and Public Administration, Zhengzhou University, Zhengzhou 450001, Henan, China*

Correspondence should be addressed to Guangming Wang; zzdxkjb@gs.zzu.edu.cn

Received 2 March 2021; Revised 24 March 2021; Accepted 8 April 2021; Published 20 April 2021

Academic Editor: Mian Ahmad Jan

Copyright © 2021 Wei Bi and Guangming Wang. This is an open access article distributed under the Creative Commons Attribution License, which permits unrestricted use, distribution, and reproduction in any medium, provided the original work is properly cited.

Relying on the development of cultural tourism resources and the development of cultural tourism industry to achieve regional industrial revitalization is an important way of implementing postdisaster reconstruction in areas suffering from major natural disasters. To this end, this article proposes a local cultural IP development and cultural creative design method based on big data and the Internet of Things to explore new ideas for postdisaster reconstruction in such areas. First, we collect traditional and modern cultural element data and carry out data cleaning and processing through the Internet of Things. Second, we use data mining to perform multilayer collaborative processing on regional cultural data based on ontology modeling and tensor decomposition. Based on our approach, local cultural categories can be effectively screened and filtered out. Finally, we establish a cultural IP development model based on the Internet of Things and verify the validity and applicability of the model through system testing and simulation analysis.

1. Introduction

The deep integration and development of cultural tourism have become a major national strategy in the new era [1]. Culture is the soul of tourism, and tourism is an important carrier of culture. From the perspective of theory and industrial practice of culture and tourism research, the simple development and utilization of cultural resources and tourism resources are no longer adapted to the current development trend of the world's cultural tourism industry [2]. Since the 1970s, the in-depth involvement of multiple disciplines and industries represented by management, culture, history, geography, sociology, political science, and economics has made significant development in cultural and tourism industry [3, 4]. Since the 21st century, "promoting tourism with culture, excelling culture with tourism, and integrating culture and tourism" has become an important trend in the development of global cultural tourism industry [5].

It is important to effectively coordinate the development of national cultural undertakings, cultural industries, and tourism and effectively improve the country's cultural soft power and influence [6, 7]. The research on cultural tourism resources in western academia mainly focuses on the constituent elements of cultural tourism resources and their utilization and development. In the aspect of research on the constituent elements of cultural tourism resources, Robert Dodo explained the relationship between the elements of Ashanti cultural resources and the perception and utilization of resources from the perspectives of cultural geography and cultural anthropology [8]. Thomas F King proposed that the evaluation of influence elements of American "cultural resources" should not be limited to archaeological sites or historical buildings, but more widely, effective methods should be used to use more diverse evaluation dimensions [9]. These methods should be used while determining whether a project is implemented or not by considering its impact on cultural resources in accordance with relevant laws and regulations [10]. With the continuous increase in people's leisure time and the vigorous development of tourism, the integration of cultural industry and the tourism

industry continued to deepen. Some scholars have put forward their own views on this deepening of ties between these two industries. Wiener [11] compared and observed the development trends of the cultural industry and tourism in the United States and pointed out that cultural tourism's resources are a key element in strengthening the cooperation between these two industries to cultivate mutually beneficial new markets. Relying on the development of cultural tourism resources and the development of cultural tourism industry to achieve regional industrial revitalization is one of the important ways to implement postdisaster reconstruction in areas suffering from major natural disasters [12]. The postdisaster reconstruction in different regions of the world contains government practices in the development of local cultural tourism resources. More and more regions suffering from natural disasters are developing the cultural tourism industry by designing local cultural tourism resources to revitalize the local economy, politics, society, and culture [13, 14]. As a whole, the rational development of local cultural tourism resources can produce better economic and social benefits to the disaster-stricken areas.

For this purpose, governments at all levels mobilize the available forces by performing their own functions to guide and promote the rational and efficient development of local cultural tourism resources and the healthy development of cultural tourism industry from different perspectives [15]. The major contributions of this paper are as follows:

(i) We propose a local cultural IP development and cultural creative design method based on big data and the Internet of Things to explore new ideas for postdisaster reconstruction in areas suffering from natural disasters.

(ii) We evaluated our work comprehensively by performing experimental results. These results justify the validity and efficiency of our work.

The rest of this paper is organized as follows. In Section 2, we discuss an overview of related research on the Internet of Things and local cultural IP development. In Section 3, we discuss the classification and selection process of local cultural data based on data mining. In Section 4, we discuss the applicability of the model and the comparative testing process. Finally, we discuss the limitations of this article and future research prospects in Section 5.

2. Related Search

In this section, first we provide a comprehensive literature overview on the Internet of Things followed by local cultural IP development. The presentation of literature review on Internet of Things lays a solid basis for the justification of using it for local cultural IP development.

2.1. Internet of Things Technology. The Internet of Things (IoT) edges the gap between real-world and virtual world by connecting physical world devices with the Internet. For example, connecting radio, television, microwave, and similar devices with the Internet enable all ordinary devices to exchange their data [16, 17]. The Internet of Things is generally a wireless network, but because everyone is around, there can be as many as one thousand to five thousand Internet of Things devices, so the Internet of Things system may contain 500 to 1,000 trillion Internet of Things devices. In the Internet of Things system, everyone can use electronic tags to connect real objects to the network, and in the Internet of Things system, owners can find out their specific locations. Central computers for the Internet of Things can be used to centrally manage and control equipment and personnel and can also remotely control related equipment in the home and can also perform location search and item antitheft and so on, similar to an automated operating system, and less through mobile phones, the data can be integrated into big data to realize the connection between objects and objects [18, 19]. In the perception layer, if we need to obtain information about items in the Internet of Things system, we need to read the relevant tags attached to the items through a reader. The privacy of tag data will lead to the leakage of key information of the entire network which has a devastating impact. Therefore, label privacy is one of the important objects for privacy protection in the Internet of Things [20]. Privacy includes information privacy and location privacy. Information privacy means that an attacker cannot obtain private information such as the identity of the tag and the reader and other information related to the user of the tag or the reader [21].

2.2. Local Cultural IP Development. In a broad sense, cultural tourism as an activity experience for people has existed in ancient times. Since the 1980s, cultural tourism has become an important part of the international tourism market [22, 23]. From the perspective of the resource itself, according to the interpretation of the "Modern Chinese Dictionary," resource is a natural source of production and living materials and is the basis for human survival and social development. Marx also pointed out that "Labor and land are the two primitive forming elements of wealth." Engels believed that the creation of wealth requires materials provided by nature and the transformation of human labor, both of which are indispensable. It can be seen that resources refer to substances or materials formed in nature that can be used for human survival and social development. From the perspective of application field, cultural tourism resources, as the name suggests, are the resources used in the cultural tourism field, which can be regarded as natural, cultural, and social resources used in the "cultural creation" behavior of the tourism business main body [24, 25].

From the perspective of resource attributes, cultural tourism resources have the dual nature of both cultural resources and tourism resources [26, 27]. From the perspective of cultural resources, cultural resources include various resources that people can use in cultural production or activities. Cultural tourism activities from the subject "cultural creation" to the object "cultural consumption" all contain the characteristics of cultural resources. The difference between cultural tourism resources and cultural

resources lies in the application of the subject of "cultural production" in the tourism field. From the perspective of tourism resources, foreign countries call tourism resources tourism attractions, that is, "any natural, humanistic object, or other factors that can attract tourists to generate tourism motives and may be used to develop tourism activities can be called tourism attractions [28]. Therefore, the difference between cultural tourism resources and tourism resources is that they can satisfy tourists' pursuit of cultural knowledge and spiritual level to a greater extent and can bring certain economic, social, and cultural benefits to tourist destinations [29]. The "postdisaster" discussed in this article is a broad concept. After the occurrence of natural disasters in the sense of time and space, the impact of natural disasters on Beichuan society, economy, and culture is the state to be reconstructed as shown by the industrial foundation, local culture, and residents' social psychology. Based on this, this article intends to analyze and discuss the development of local cultural IP and the design of cultural creation from the perspective of the development of local cultural tourism resources after the disaster [30].

3. Classification and Screening Process of Local Cultural Data Based on Data Mining

In the process of using machine learning methods to classify cultural data, data preprocessing is an important preprocessing stage, which has an important impact on the back-end classification results. Data preprocessing can transform the initial problem from high-dimensional space to low-dimensional space, thereby reducing computational complexity and improving classification efficiency. Correspondingly, it can eliminate irrelevant or redundant features, prevent the classifier from overfitting, and enhance the quality of the classification algorithm [31].

MultiSURF is an algorithm based on Relief. It is an algorithm that judges the importance of elements by weighting them. Each feature is assigned a different weight according to the degree of association between each attribute and class label, where the weight is less than the setting the elements of the threshold value which will be deleted. MultiSURF pseudocode is given in Figure 1. First, the operator randomly selects a sample of R, from the training set, and then searches for nearest neighbor samples of the same category as R and nearest neighbor samples of different categories from R [32]. It is worth noting that MultiSURF uses the boundary value Tear to determine which instances will be regarded as neighbors, R is the average pairwise distance between other instances, and a is the cost between the target instance R and all other instances. The pseudocode flow chart of the MultiSURF algorithm is shown in Figure 2.

The MultiSURF algorithm is very efficient and does not interfere with the data type. It assigns different weights based on the performance of a single feature in the calculation phase to identify the category and then uses the set weight threshold to select a feature subset:

$$g^i(x, y) = \lambda' f^i(x, y). \tag{1}$$

However, in practical problems, a single feature usually cannot effectively classify categories. Correspondingly, the algorithm does not consider the correlation between features. Therefore, the downside of the algorithm is that it cannot eliminate redundant features well.

$$E = E\left(y_1^l, \ldots, y_n^l\right) = \sum_j^h \left(y_j^l - t_j\right). \tag{2}$$

Since redundant features do not increase data information, they can affect the confidence of model classification, and the effect of redundant features will also be superimposed on the model, making the model effect worse.

Genetic algorithm is one of the most advanced algorithms for classification and screening. It is a type of the search heuristic method, inspired by Charles Darwin's theory of natural evolution, reflecting the process of natural selection. The process of natural selection is to select the most suitable individual from the population. The offspring continuously produced in this process will inherit some of the characteristics of the parents and add some characteristics to the next generation.

$$F\left(X_{n+1} | J_n\right) \neq F\left(X_{n+1} | J_n - Y_n\right),$$

$$\lambda = \max \frac{1}{NM} \left\{ \sum_{k=0}^{L-1} f_k^r(x, y), \sum_{k=0}^{L-1} f_k^d(x, y), \sum_{k=0}^{L-1} f_k^b(x, y) \right\}. \tag{3}$$

If parents have better adaptability, their offspring may be stronger than their parents and have a better chance of survival. This process will be repeated continuously, and finally, the most suitable generation will be found. In this process, as in the case of biological evolution, it has a mechanism to select suitable chromosomes in each generation. In order to simulate the evolutionary process, the selected chromosomes undergo genetic operations, such as crossover and mutation, and finally select the most suitable individuals for reproduction. In order to produce the next generation of offspring, this concept can be used to search for problems, that is, to prepare a set of solutions to the problem and select the best solution from it.

$$\Delta f_r = \left[\frac{\partial f_r}{\partial x_1}, \frac{\partial f_r}{\partial x_2}, \ldots, \frac{\partial f_r}{\partial x_n} \right]. \tag{4}$$

The fitness function determines the survivability of an individual (the ability of an individual to compete with other individuals). Each individual will get a fitness value through calculation, and the probability of an individual being selected for reproduction is based on its fitness score. The main purpose of the selection phase is to select the most suitable individuals and let them pass their genes to the next generation. Figure 1 shows the algorithm flow of the local cultural IP development model based on data mining.

A pair of individuals (parents) is selected based on their fitness scores. Individuals with higher scores have more chances to be selected for reproduction. Crossover is the most important stage in the genetic algorithm. For each pair of parents to mate, an exchange point needs to be randomly

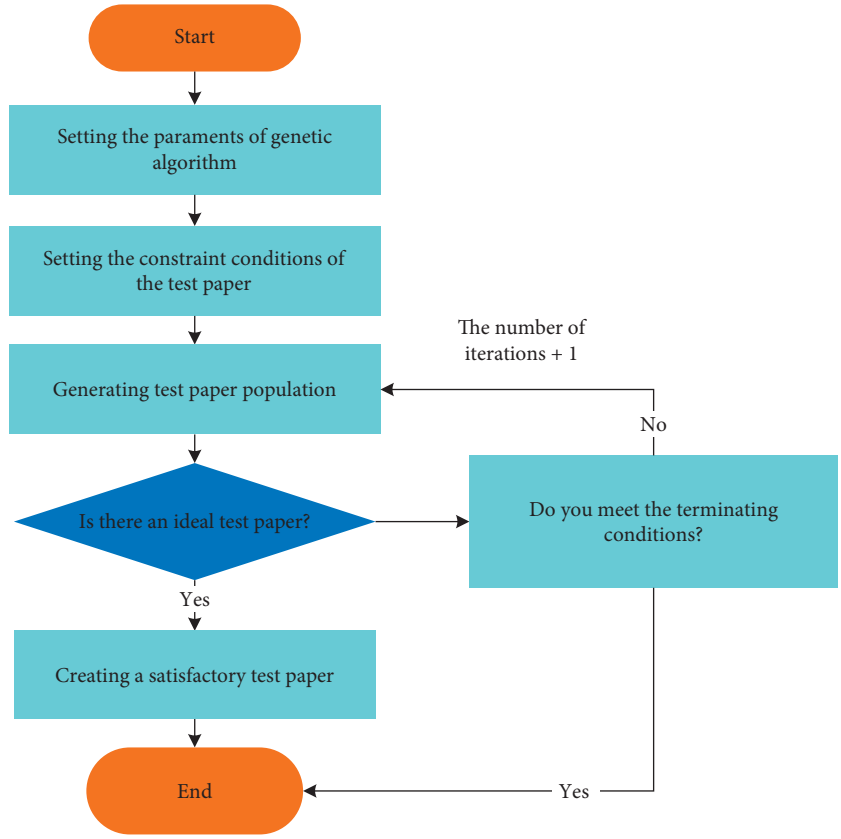

Figure 1: Algorithmic flow of the local cultural IP development model based on data mining.

selected from the genes for exchange. Offspring are created by exchanging parental genes until the exchange point is reached, and then new offspring are added to the population.

$$E\left(X_{n+1}|J_n\right) \neq E\left(X_{n+1}|J_n - Y_n\right). \tag{5}$$

In some of the new offspring formed, some of their genes may be mutated with low random probability. This means that certain bits in the chromosome can be flipped, and the main purpose of mutation is to maintain the diversity within the population and prevent premature fusion. As the algorithm continues to repeat, if the population has converged (the algorithm does not produce offspring that are significantly different from the previous generation), the algorithm terminates.

$$X_t = \sum_{i=1}^{k} \alpha_i X_{t-i} + \sum_{i=1}^{k} \beta_i Y_{t-i} + u_{1t}. \tag{6}$$

As a search heuristic algorithm for solving optimization, the genetic algorithm is one of evolutionary algorithms. When the number of iterations of GA continues to increase, the overall fitness value of each generation will gradually converge to the local optimal solution, so the selected optimal feature subset can be obtained. In addition, GA usually uses the accuracy of the classification learning algorithm as a fitness function.

$$\begin{gathered} x^{(j+1)} = x^{(j)} + s_j d^{(j)}, \\ \left|f^{(j)} - f^{(j-1)}\right| \leq \tau, \\ \left|f^{(j)} - f^{(b)}\right| \leq \tau, \\ F = \frac{\left(\mathrm{SSE}_r - \mathrm{SSE}_u\right)/k}{\mathrm{SSE}_u/(T-2k)} \sim F_{(k,T-2k)}. \end{gathered} \tag{7}$$

In order to facilitate subsequent experiments to compare the pros and cons of the three different classifications in the screening algorithm and to verify the performance of the MSGA feature selection algorithm proposed in this paper, we used the three algorithms to select their respective feature subsets, of which the MultiSURF method selected 8 Features, 10 features were selected based on the GA-wrapped method, and 8 features were selected by MSGA. The 8 features selected using the MultiSURF feature selection algorithm are shown in Table 1.

We use the MultiSURF algorithm to sort all the features and delete some features that are not relevant to the category. The 2 features selected in the first step of random initialization are used as the initial population.

$$\begin{gathered} F\left(X_{n+1}|\Omega_n\right) \neq F\left(X_{n+1}|\Omega_n - Y_n\right), \\ x^{(i)} = \sum_{i<j} o^{(i,j)}\left(x^{(i)}\right)(3). \end{gathered} \tag{8}$$

```
Requirements: For each training instance there are a set of feature vectors and category labels
        n: number of training samples
        a: number of features
Precomputed distance array
for i = 1 to n
        #According to Tneari to identify neighbors and find hits and misses
        Initialize hit and miss counters h = 0.0 and m = 0.0
        for j = 1 to n
         if Ri and Rj distance value < Tneari (use distance array judgment) then
            if Rj is hit then
                h = h + 1 {and mark this instance as hit}
            else if Rj is miss then
                m = m + 1 {and mark this instance as miss}
            end if
         end if
        end for
    #Update feature weight vector W[A]
    for all hits and misses
        for A = 1 to a
          W [A] = W [A] – diff (A, Ri, H)/(n*h) + diff (A, Ri, M)/(n*m)
        end for
    end for
end for
Return feature score vector W the quality of the price feature
```

Figure 2: MultiSURF algorithm pseudocode flow display diagram.

Table 1: Eight features selected using the MultiSURF feature selection algorithm.

Feature name	Feature description
Downlink_avg_acketsize	Downstream packet size average
Downlink_acketsize_ar	Downstream packet size variance
Downlink_packetsize_pdf_entropy	Downstream packet size information
Downlink_rate_packet	Downlink packet rate
Downlinkes_rate_bytes	Downstream byte rate
Uplink_interval_max	Maximum uplink packet arrival time interval
Datalink-avg-packetsize	Overall package size average
Datalink_acketsize_var	Overall package size variance

Calculate the fitness of an individual, that is, first decode the individual, and then use the reduced sample set to calculate the fitness. According to fitness value selection, crossover and mutation population can be calculated using the following equation:

$$\nabla_{\alpha} = \frac{w - \varepsilon \nabla_{w}(w, \alpha)}{L((w^{*})}. \tag{9}$$

We add all the new individuals from the previous step to the population to form a new population.

4. Applicability and Comparative Test of Cultural IP Model

In this chapter, we will conduct practical and comparative tests on the local cultural IP development and cultural and creative design models based on the Internet of Things and data mining established above. The test will further verify that the improved MultiSURF combined with the genetic algorithm can have a more stable and applicable performance. We will mainly analyze the scalability and accuracy

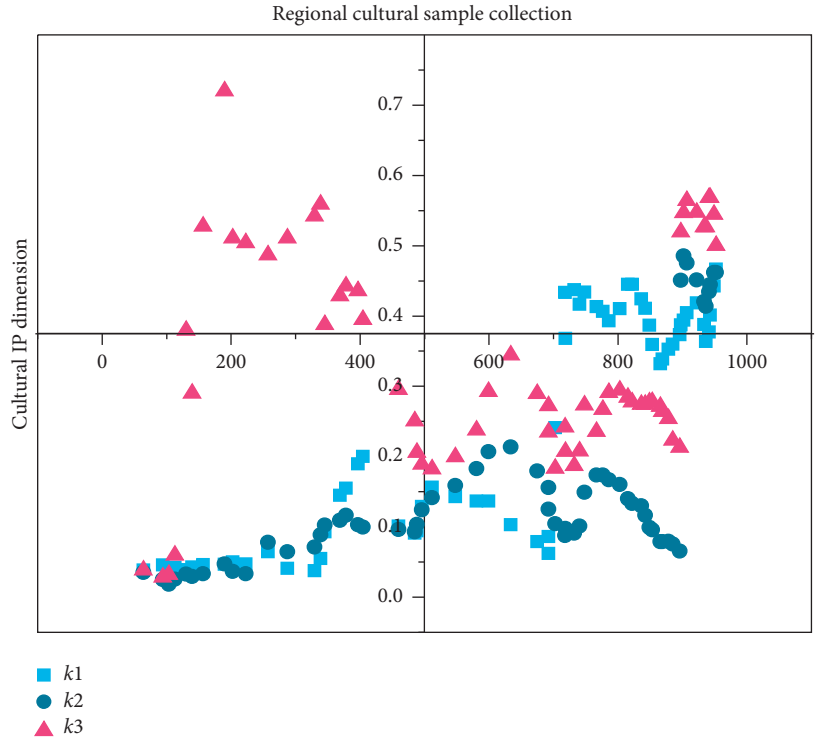

Figure 3: Clustering results of the MultiSURF algorithm under different k values.

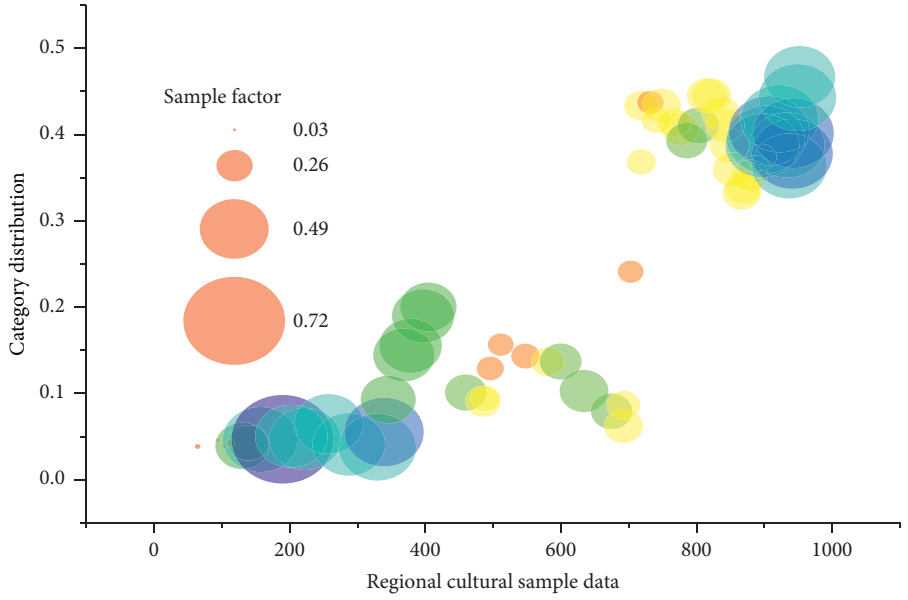

Figure 4: The influence of sample factors on local cultural IP development algorithm.

of the algorithm to verify whether the improved algorithm has good robustness under the Spark cluster.

4.1. Local Cultural IP Development Data Sources. The benchmark dataset used in the experiment in this section is the scoring dataset provided by the Web scope project team. In this section, the experiment extracts a subdataset containing nearly 20,000 scoring records from the scoring dataset, according to the principle of random sampling, and selects 15,000 cultural data as the test set, and its data size is the same as another score provided by the project team. The datasets are comparable.

4.2. Local Cultural IP Development Model Test. The collected data are first classified by the MultiSURF algorithm, and the final clustering result is 9. The classification description of

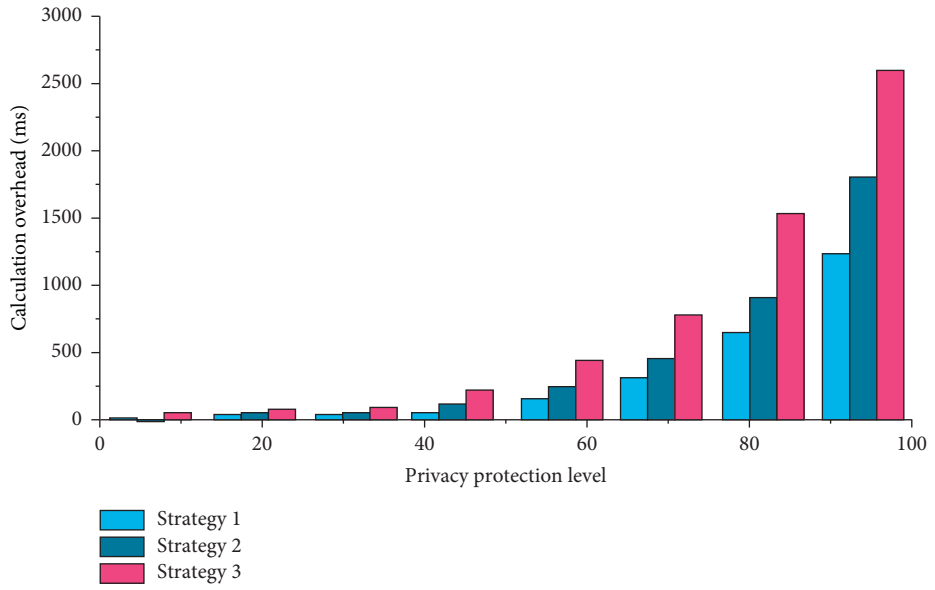

Figure 5: Model performance of the local cultural IP development model under different k values.

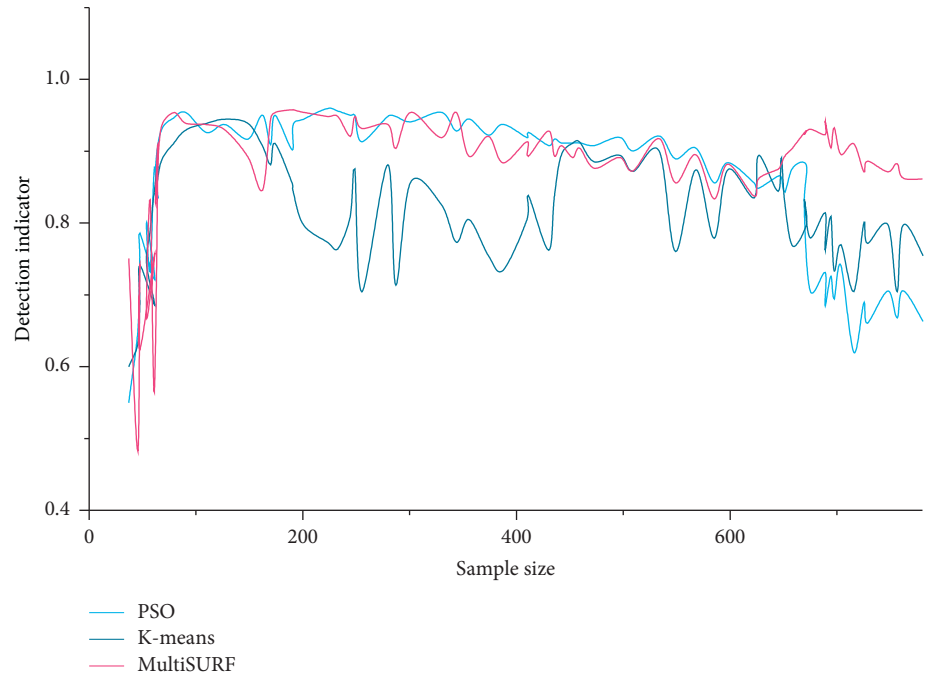

Figure 6: Accuracy analysis of local cultural IP development models with different algorithms.

this algorithm can be divided into 9 categories, namely, geographical resources, ancient texts, historical relics, ethnic education, humanities and economics, social customs, ideology and religion, culture and art, regional news, and other categories. 9 is the clustering center k of the K-means algorithm, and the manually classified data are also 9 categories, indicating that the MultiSURF algorithm classification result is correct. The clustering results of the MultiSURF algorithm under different k values are shown in Figure 3.

For the final clustering results, it can be seen from Figure 3 that the directions of historical cultural relics, social customs, and so on account for a relatively large proportion, and the abovementioned directions are considered to have the potential and value of cultural IP development. In the economic category, there are documents in the category of historical relics. The influence of sample factors on the local cultural IP development algorithm is shown in Figure 4.

When clustering datasets of the same size, as the number of points increases, the time consumed by the algorithm

gradually decreases. Then, perform *K*-means algorithm clustering, input the cluster center value as 9, as the initial cluster center, and obtain the final clustering result. Because the MultiSURF algorithm determines the clustering center, there is no need to repeat iterations, and the time consumed decreases faster. At the same time, as the number of nodes increases, the workload of a single node is reduced, making the overall clustering time less and less. The model performance of the local cultural IP development model under different k values is shown in Figure 5.

The larger the expansion ratio is, the more advantageous the parallel algorithm is. The speedup comparison result of the MultiSURF algorithm, *K*-means, and PSO algorithm is shown in Figure 6.

It can be seen from Figure 6 that as the number of nodes in the cluster increases, the utilization of the cluster becomes higher and higher, but the MultiSURF algorithm increases faster than the *K*-means algorithm, indicating that the improved algorithm is suitable for a distributed environment. Speedup is the ratio of the time required for a single node to the time required for a cluster of r nodes. However, due to the limitation of nodes, the speedup ratio cannot be increased without limit. The expansion ratio can test the efficiency of algorithm parallelization. Figure 6 describes the change trend of the expansion ratio of the *K*-means algorithm and the MultiSURF algorithm under the Data2 dataset as the number of nodes increases. In the same dataset and cluster environment, the expansion ratio of the *K*-means algorithm and the MultiSURF algorithm has the same trend. The difference is that the MultiSURF algorithm is faster than the *K*-means algorithm and approaches a certain fixed value, which shows that the MultiSURF based on Spark algorithm has better scalability.

5. Conclusion

Since the beginning of 21st century, "promoting tourism with culture, commemorating culture with tourism, and integrating culture and tourism" has become an important trend in the development of global cultural tourism industry. This paper combines stakeholder theory along with new public service theory and other related theories, using literature research, field investigation, case analysis, and other research methods to analyze the development of different types of cultural tourism resources before and after the disaster. Limited by the level of personal research ability and objective reality, this paper still has some areas to be improved. First, the literature review is not comprehensive and in-depth, and the materials and data used in the paper may have lags and limitations. Future research may further tend to integrate the above research fields to varying degrees. We will comprehensively use economics, tourism, cultural studies, management, sociology, and other multidisciplinary research perspectives and methods, combined with a specific research object for related research.

Data Availability

The datasets used and/or analyzed during the current study are available from the corresponding author on reasonable request.

Conflicts of Interest

The authors declare that they have no conflicts of interest.

References

[1] S. Zhang, X. Xu, J. Peng, K. Huang, and Z. Li, "Physical layer security in massive internet of things: delay and security analysis," *IET Communications*, vol. 13, no. 1, pp. 93–98, 2019.

[2] X. U. Yi, "Research on security and reliability of smart home system based on internet of things," *Environmental Technology*, vol. 12, no. 3, pp. 324–341, 2019.

[3] W. Xu, C. Varghese, I. P. Bissett, G. O'Grady, and C. I. Wells, "Network meta-analysis of local and regional analgesia following colorectal resection," *British Journal of Surgery*, vol. 107, no. 2, pp. e109–e122, 2020.

[4] S. Yumin, "Research and simulation of large data differentiation classification technology under the internet of things," in *Proceedings of the 2018 International Conference on Intelligent Transportation, Big Data & Smart City (ICITBS)*, Xiamen, China, January 2018.

[5] C. K. Wu, K. F. Tsang, Y. Liu, H. Zhu, H. Wang, and Y. Wei, "Critical internet of things: an interworking solution to improve service reliability," *IEEE Communications Magazine*, vol. 58, no. 1, pp. 74–79, 2020.

[6] S. Venkatraman, B. Surendiran, and P. Arun Raj Kumar, "Spam e-mail classification for the Internet of Things environment using semantic similarity approach," *The Journal of Supercomputing*, vol. 76, no. 1, pp. 756–776, 2020.

[7] C. N. Songer, G. S. Calip, N. Srinivasan, V. Maziero Barbosa, and J. T. Pham, "Factors influencing antibiotic duration in culture-negative neonatal early-onset sepsis," *Pharmacotherapy*, vol. 41, no. 1, 2021.

[8] X. Yu, Q. Hu, H. Li, J. Du, J. Gao, and L. Sun, "Cross-domain recommendation based on latent factor alignment," *Neural Computing and Applications*, vol. 7, no. 2, pp. 215–230, 2021.

[9] J. Shu, M. Deng, and J. He, "Optimization of ship-borne anticollision sounding system based on internet of things and full convolution neural network," *Journal of Coastal Research*, vol. 103, pp. 757–761, 2020.

[10] M. D. Rizzo, R. B. Crawford, A. Bach, S. Sermet, A. Amalfitano, and N. E. Kaminski, "Imiquimod and interferon-alpha augment monocyte-mediated astrocyte secretion of MCP-1, IL-6 and IP-10 in a human co-culture system," *Journal of Neuroimmunology*, vol. 333, Article ID 576969, 2019.

[11] V. Radonjic, M. S. Dogatovic, M. J. Stanojevic, and N. Mladenovic, "Revenue maximization of Internet of things provider using variable neighbourhood search," *Journal of Global Optimization*, vol. 78, 2020.

[12] C. E. Morgan and H. Donald, "IP247: the on-service vascular surgery practice management strategy maintains local productivity while allowing expansion of outreach practice," *Journal of Vascular Surgery*, vol. 67, no. 6, p. e151, 2018.

[13] M. Mayer and A. J. Baeumner, "A megatrend challenging analytical chemistry: biosensor and chemosensor concepts ready for the internet of things," *Chemical Reviews*, vol. 119, no. 13, 2019.

[14] C. Massip, H. Guet-Revillet, M. Grare, A. Sommet, and D. Dubois, "Enhanced culture recovery of campylobacter with modified cary-blair medium: a practical field experience," *Journal of Microbiological Methods*, vol. 149, pp. 53-54, 2018.

[15] I. P. Massad, M. Avila, L. Contreras-Porcia, and C. Bulboa Contador, "Spores re-suspending technology, a new system

improving spore seeding for culture of commercial red seaweeds," *Aquaculture*, vol. 526, 2020.

[16] M. A. Jan, F. Khan, M. Alam, and M. Usman, "A payload-based mutual authentication scheme for internet of things," *Future Generation Computer Systems*, vol. 92, pp. 1028–1039, 2019.

[17] M. Khanipour, K. Niknami, and M. Abe, "Challenges of the fars neolithic chronology: an appraisal," *Radiocarbon*, vol. 63, no. 2, pp. 693–712, 2020.

[18] M. Ke, Z. Gao, Y. Wu, X. Gao, and K. K. Wong, "Massive access in cell-free massive MIMO-based internet of things: cloud computing and edge computing paradigms," *IEEE Journal on Selected Areas in Communications*, vol. 39, no. 3, pp. 756–772, 2021.

[19] F. Ip, G. Lewis, and C. Lefevre, "Author accepted manuscript: carotenoid skin coloration enhances face and body attractiveness: a cross-cultural study," *Quarterly Journal of Experimental Psychology*, vol. 72, no. 2, 2019.

[20] Y. Hasegawa, R. Ishii, Y. Kyutoku, . Dan, and B. Rousseau, "Biases in paired preference tests: cross-cultural comparison of Japanese and American consumers," *Journal of Sensory Studies*, vol. 34, no. 3, 2019.

[21] X. Yu, F. Jiang, J. Du, and D. Gong, "A cross-domain collaborative filtering algorithm with expanding user and item features via the latent factor space of auxiliary domains," *Pattern Recognition*, vol. 94, pp. 96–109, 2019.

[22] E. Hittinger and P. Jaramillo, "Internet of things: energy boon or bane?" *Science*, vol. 364, no. 6438, pp. 326–328, 2019.

[23] B. Comery, W. R. G. Perry, S. Young et al., "Delivery of surgical care in Samoa: perspectives on capacity, barriers and opportunities by local providers," *Anz Journal of Surgery*, vol. 90, no. 10, pp. 1910–1914, 2020.

[24] W.-C. Chen, J.-S. Niu, I.-P. Liu et al., "Study of a palladium (Pd)/aluminum-doped zinc oxide (AZO) hydrogen sensor and the kalman algorithm for internet-of-things (IoT) application," *IEEE Transactions on Electron Devices*, vol. 67, no. 10, pp. 4405–4412, 2020.

[25] J. Chauhan and P. Goswami, "An integrated metaheuristic technique based energy aware clustering protocol for internet of things based smart classroom," *Modern Physics Letters B*, vol. 34, no. 22, Article ID 2050360, 2020.

[26] R. Ceipek, J. Hautz, A. De Massis, K. Matzler, and L. Ardito, "Digital transformation through exploratory and exploitative internet of things innovations: the impact of family management and technological diversification," *Journal of Product Innovation Management*, vol. 38, no. 1, pp. 142–165, 2021.

[27] C. Landa-Solís, A. Olivos, B. Olivos-Díaz et al., "Behavior of multipotent stem cells isolated in mobilized peripheral blood from sheep after culture with human chondrogenic medium," *Tissue & Cell*, vol. 52, pp. 116–123, 2018.

[28] X. Yu, Y. Chu, F. Jiang, Y. Guo, and D. Gong, "SVMs classification based two-side cross domain collaborative filtering by inferring intrinsic user and item features," *Knowledge-Based Systems*, vol. 141, pp. 80–91, 2018.

[29] A. Villa-Henriksen, G. T. C. Edwards, L. A. Pesonen, O. Green, and C. Aage, "Internet of Things in arable farming: implementation, applications, challenges and potential," *Biosystems Engineering*, vol. 191, pp. 60–84, 2020.

[30] H. A. A. Al-Kashoash, H. Kharrufa, Y. Al-Nidawi, and A. H. Kemp, "Congestion control in wireless sensor and 6LoWPAN networks: toward the internet of things," *Wireless Networks*, vol. 25, no. 8, pp. 4493–4522, 2019.

[31] X. Yu, J. Yang, and Z. Xie, "Training SVMs on a bound vectors set based on fisher projection," *Frontiers of Computer Science*, vol. 8, no. 5, pp. 793–806, 2014.

[32] G. Royer, F. Fourreau, B. Boulanger et al., "Local outbreak of extended-spectrum β-lactamase SHV2a-producing *Pseudomonas aeruginosa* reveals the emergence of a new specific sublineage of the international ST235 high-risk clone," *Journal of Hospital Infection*, vol. 104, no. 1, pp. 33–39, 2020.

Hindawi
Mobile Information Systems
Volume 2021, Article ID 9969399, 8 pages
https://doi.org/10.1155/2021/9969399

Research Article

Analysis of Influencing Factors of Social Mental Health Based on Big Data

Yixuan Zhao[1] and Qinghua Tang[2]

[1]*Far East University of the Philippines, Liaocheng, Shandong 252000, China*
[2]*School of Public Health and Management, Guangxi University of Chinese Medicine, Nanning, Guangxi 530200, China*

Correspondence should be addressed to Qinghua Tang; 2019163801@feu.edu.ph

Received 11 March 2021; Revised 25 March 2021; Accepted 9 April 2021; Published 19 April 2021

Academic Editor: Mian Ahmad Jan

Copyright © 2021 Yixuan Zhao and Qinghua Tang. This is an open access article distributed under the Creative Commons Attribution License, which permits unrestricted use, distribution, and reproduction in any medium, provided the original work is properly cited.

Big data is a large-scale rapidly growing database of information. Big data has a huge data size and complexity that cannot be easily stored or processed by conventional data processing tools. Big data research methods have been widely used in many disciplines as research methods based on massively big data analysis have aroused great interest in scientific methodology. In this paper, we proposed a deep computational model to analyze the factors that affect social and mental health. The proposed model utilizes a large number of microblog manual annotation datasets. This huge amount of dataset is divided into six main factors that affect social and mental health, that is, economic market correlation, the political democracy, the management law, the cultural trend, the expansion of the information level, and the fast correlation of the rhythm of life. The proposed model compares the review data of different influencing factors to get the correlation degree between social mental health and these factors.

1. Introduction

Big data mainly refers to the relatively macroscopic network data generated by Internet platforms and has become an important part of big data research. It is different from microscopic big data generated by genes and brain sciences. Social science research based on big data analysis technology is of great significance for mastering political, economic, and social psychology and behavioral laws [1]. Network big data analysis technology has some advantages, that is, sample size and representation, relying on the advantages of the network platform; it can achieve measurement covering large-scale groups. This sample is close to the overall characteristics and advantages and is conducive to solving traditional research. The method represents the problem, timeliness: network big data makes it possible to track large-scale group measurements in a regular, even real-time manner. Its tracking time can be as good as yearly, monthly, daily, and hourly, or even every minute. Objectivity, network big data is based on the objective behavior data of users, such as search engine search and clicks behavior, social network likes, and forwards and publishes content and has good objectivity of evidence. Cost-effectiveness: traditional research methods are often limited by research costs such as human resources and financial resources. It is impossible to achieve regular and real-time measurements of large-scale groups. Network big data analysis is supported by technologies such as web crawling and text analytics. It has been possible to obtain large amounts of data at a relatively low cost [2].

Research methods based on massively big data analysis have led to thinking about scientific methodology. Research does not require direct contact with the research subject, but new research findings can be obtained by direct analysis and mining of massive data, which may have spawned a new research model [3]. To this end, Turing Award winner Gray distinguishes data-intensive science from computational science and depicts the "fourth paradigm" based on data-intensive scientific research [4]. However, some researchers have doubts about big data analysis technology and believe that big data cannot replace the original research methods. It can be seen that there is still controversy about how to treat the big data analysis technology of the network.

In this paper, to overcome the problem we proposed a new framework model based on psychology which is also one of the important areas of the combination of big data and social sciences [5]. Our main contributions to this study are to present big data analysis methods that have been widely used to solve emotional psychology [6]; behavioral economics, personality psychology, and health psychology [7]; political psychology; and many other important psychological issues. So, in combination with other psychological empirical methods and for the effective features set in this study, we treat psychological research based on network big data analysis technology. The proposed model compares the review data of different influencing factors to get the correlation degree between social mental health and these factors. Unfortunately, the current systematic thinking about the methodology of online big data psychology is still very small [8].

The rest of the paper is organized as follows: In Section 2, the methods are discussed in detail. Section 3 includes big data key technologies while in Section 4, the neural network algorithm is discussed. Similarly, in Section 5, experimental results and discussion are discussed. Finally, we demonstrate a conclusion and future work.

2. Methods

In this section, we present the two different research methods that are used in this literature. These research techniques include cognitive neuroscience method technology and traditional research method techniques.

2.1. Cognitive Neuroscience Technology. Compared with modern research techniques, cognitive neuroscience techniques were formed in the 1980s and 1990s. Cognitive neuroscience techniques are formed by the combination of cognitive science and neurology. Cognitive neuroscience research attracted widespread attention from psychologists and reflections based on the perspective of psychological development [9]. Cognitive neuroscience research, mainly through modern cognitive neuroscience research techniques, such as brain wave (EEG), functional magnetic resonance imaging (fMRI), brain magnetic (MEG), transracial magnetic stimulation (TMS), and other technologies, to reveal the law of the occurrence and development of psychology and behavior. Moreover, cognitive neuroscience has become one of the hottest cross-disciplinary fields in recent years. These fields mainly include the research on the neural mechanism of cognitive behavior, the neuroscience research of cognitive behavioral psychology theory, and the research on the theoretical model of cognitive behavioral psychological mechanism based on brain neural stimulation [10]. For example, explore the neural mechanisms of individual psychological perceptions, learning memories, attention, speech, executive control, thinking, emotions, and other psychological activities or behaviors [11].

2.2. Traditional Research Techniques. The traditional research techniques are divided into two main methods, that is, the questionnaire and behavioral method. The questionnaire method is based on the respondent's self-reporting method for a series of self-reported questionnaires and uses this as data evidence to study people's psychological and behavioral patterns [12]. The main advantages of this method are targeted, quick access to data of larger populations. By designing structural, standardization, or open-ended questions directly related to the purpose of the research, the respondent's first-hand data on the problem is collected in a targeted manner. The questionnaire method can obtain data of large-scale populations more quickly through standardized operation procedures. Compared with the high research cost of cognitive neuroscience technology, the cost of the questionnaire survey is relatively low, and the sample coverage is relatively large. However, the questionnaire survey method has certain defects in subjective bias, sample size, and timeliness [13]. Network big data analysis technology has a relatively large advantage in these aspects. Poor objectivity: because the questionnaire survey method adopts a self-reporting method, there is a strong subjective bias in the research results, especially the social approval response is the most typical [14]. Similarly, the behavioral experiment method mainly involves the experimenter manually or designing different experimental conditions and observes the difference of behavioral results of the subjects under different experimental conditions, tests if the experimental conditions affect the outcome significantly [15]. The behavioral experiment method can be 83 degrees of data to explore causality. Since the experimental method controls the influence of other unrelated interference factors, it can be more reliable to judge whether the difference in behavior results is caused by the experimental conditions (i.e., independent variables), thereby causing causal inference. In view of the significance of causality in research, experimental methods also occupy an important position in scientific methodology [16]. In the behavioral experiment, the experimental person's artificial conditional intervention and the laboratory-specific environmental space may cause the experimental situation to differ from the actual environment of the subject; thus, the experiment the result is interference. Therefore, behavioral experiment methods generally face the challenge of low ecological validity. Although natural experiments can improve the authenticity of the environment, there are challenges in terms of operational feasibility and disturbance variable control. The network big data is constructed on the user's real network situation, collects objective data by not intervening in user behavior activities, so it has high ecological validity. The sample size is small and the representativeness is limited [17].

3. Big Data Key Technologies

3.1. Big Data Features. The term big data was born in 1997 and usually denotes a massive and compound collection of data. Big data has four outstanding features. These features include massive data, sparse value, multisource heterogeneity, and exponential growth. The massive data contains full sample data and ultrahigh dimensional complex data, rather than a small amount of sampled data. The sparse value of a single piece of data is extremely low and the correlation between the data is poor. The multisource heterogeneity data

sources are complex, the channels are wide, and most of them are unstructured data mixed structured data, which is difficult to sort and sort. In exponential growth, the amount of data contained in big data will change with the output index, and the traffic can reach terabytes [18].

3.2. Big Data Core Technology. To overcome the information threshold of big data and discover the information value of big data, its key technology is divided into three partial layers [19]. These include data platform, analysis platform, and display platform. The data platform is responsible for the collection and classification storage management of big data. The data gathered must be filtered and remarked. Marking data is always cleaned up and updated, and it contains most of the research value of massive data [9]. The analysis platform is responsible for big data calculation and analysis and is an important way to value the visualization. The transformation process requires strong computing platform support. The commonly used distributed big data computing frameworks are MapReduce, Parameter Server, and so forth. The analysis methods are commonly used for manual modeling or neural network analysis [20, 21]. Display platforms often use big data products to promote big data products, including big data research rules or value research models. The complete analysis: marking and extraction process of big data is shown in Figure 1.

4. Neural Network Algorithm

The NN algorithm is an automatic calculation technique that simulates the brain study mechanism. The study covers NN organization simulation, learning algorithm, memory model, and network communication model. At present, the neural network algorithm models realized by research mainly include the feed-forward neural network, reply neural network, and time series memory neural network. Neural networks are the most efficient network model. Its outstanding feature learning capability can be broadly used in image and speech recognition. The feed-forward neural network is divided into multilayer structures, each layer consists of multiple sets of neurons, and information is input along the feed-forward layer, one-way flow transmission. Based on this feature, the feed-forward neural network can effectively extract the characteristics of data space structure. The most famous implementation methods such as perceptron and deep automatic encoder have made outstanding contributions in the field of artificial intelligence and computer vision development.

4.1. Restricted Boltzmann Machine. In 1986, Hinton and Sejnowski proposed the RBM is a multiplicative stochastic neural network. The network consists of visible units. Visible variables and hidden variables are binary variables, that is, 0, 1. A two-part graph is a whole network. The edges are exclusive to the exposed unit and unseen unit. As seen in Figure 2, there is no boundary relation between the visible and the hidden units:

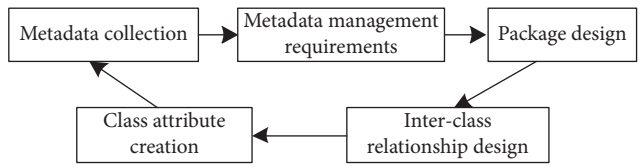

Figure 1: Metadata management under a three-tier architecture.

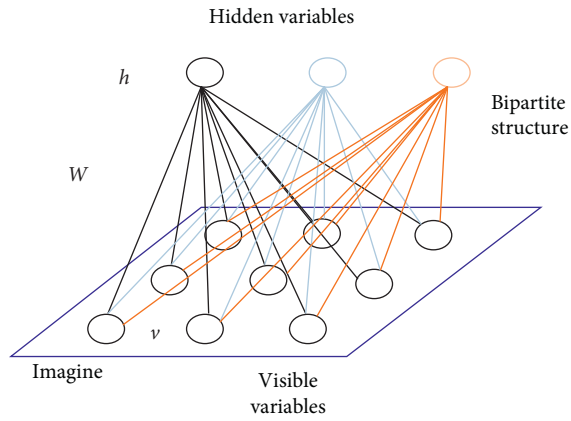

Figure 2: The structure of the restricted Boltzmann machine.

RBM is an energy-based model which shows visible v and hidden h energy from the joint as shown in the following equation:

$$E(v, h; \theta) = -\sum_{ij} W_{IJ} v_i h_j - \sum_i b_i v_i - \sum_j a_j h_j, \quad (1)$$

where θ is the parameter $\{W, a, b\}$ of RBM, W is the edge between the visible and hidden units, and a and b are the bias between the visible and hidden units. Based on the joint configuration of visible variable v and hidden variable h, we can obtain the joint probability between h and v:

$$P_\theta(v, h) = \frac{1}{Z(\theta)} \exp(-E(v, h; \theta)), \quad (2)$$

where $Z(\theta)$ is the normalization factor called partition function; according to function (1), function (2) can be written as

$$P_\theta(v, h) = \frac{1}{Z(\theta)} \exp\left(\sum_{i=1}^{D}\sum_{J=1}^{F} W_{ij} v_i h_j + \sum_{i=1}^{D} v_i b_i + \sum_{j=1}^{F} a_j h_j\right). \quad (3)$$

We hope the likelihood function of the largest observed data $P(v)$ can be obtained by function (3):

$$P_\theta(v) = \frac{1}{Z(\theta)} \sum_h \exp\left[v^T W h + a^T h + b^T v\right]. \quad (4)$$

The RBM parameters we get, by maximizing $P(v)$, is comparable to increasing $\log(P(v)) = L(\theta)$:

$$L(\theta) = \frac{1}{N} \sum_{n=1}^{N} \log P_\theta\left(v^{(n)}\right). \quad (5)$$

Then, according to random gradient descent, we can get

$$(P, v \mid h) = \prod_i P, v_i \mid hP, v_i = 1 \mid h = \frac{1}{1 + \exp\left(-\sum_j W_{ij} h_j - b_i\right)}. \tag{6}$$

Take a sample of data and set the state of the visible variable to this sample data. Randomly initialize W. The state of the hidden variable is updated according to the first formula of equation (6); that is, h_j is set to state 1 with the probability of $P(h_j = 1|v)$; otherwise, it is set to 0. Then, for each side $v_i h_j$, calculate $P_{\text{data}}(v_i h_j) = v_i * h_j$ (note that the states of v_i and h_j are both {0, 1}). v_1 is reconstructed according to the state of h and the second formula of the formula (6), h_1 is obtained from the first formula of v_1 and formula (6), and $P_{\text{model}}(v_i^1 h_i^1) = v_i^1 * h_i^1$ is calculated. The weight W_{ij} of the update edge W_{ij} is $W_{ij} = W_{ij} + L * (P_{\text{data}}(v_i h_j)) = P_{\text{model}}(v_i^1 h_j^1)$. Take the next data sample and repeat steps 1–4. The above process is iterated K times.

4.2. Deep Belief Network. The deep belief network (DBN) consists of a backpropagation (BP) and multilayer restricted Boltzmann machine (RBM) network. Figure 3 shows the over model. In the deep belief network, the learned output of the upper layer RBM network is used as the input of the next layer, so that each layer can better abstract the features of the upper layer and extract the data features layer by layer. The top-level BP network uses the features extracted by the RBM network as input for classification or prediction.

The RBM consists of a visible layer v and a hidden layer h, as shown in Figure 4. The visible layer is used to input feature data and the hidden layer is used for feature detectors. The nodes in the visible layer and the hidden layer have no connection with each other, that is, each node takes values independently of each other. Each node of the hidden layer can only randomly take the value 0 or 1, and the full probability distribution $P(v, h)$ satisfies the Boltzmann distribution. The full probability distribution can be calculated by the conditional distribution $P(v|h)$and$P(h|v)$. When v is input, the hidden layer h can be obtained by$P(h|v)$, and after the hidden layer h, the visible layer can be obtained by $P(v|h)$. By adjusting the parameters, the visible layer v' obtained from the hidden layer is the same as the original visible layer v; that is, the hidden layer is visible, another expression of the layer. Therefore, the hidden layer can be used as a feature of the visual layer input data. The joint distribution of RBM under given model parameters (θ) is

$$E(v, h; \theta) = \frac{\exp(-E(v, h; \theta))}{Z}, \tag{7}$$

where $Z = \sum_v \sum_h \exp(-E, v, h; \theta)$ is the normalization factor, and the energy function is as follows:

$$(E, v, h; \theta) = -\sum_{ij} W_{ij} v_i h_j - \sum_i v_i b_i - \sum a_j h_j, \tag{8}$$

where i, j are nodes; $W_{ij}$is the connection weight between the visible layer unit and the hidden layer unit; and b_i and a_j are offsets. The BP neural network consists of three layers of

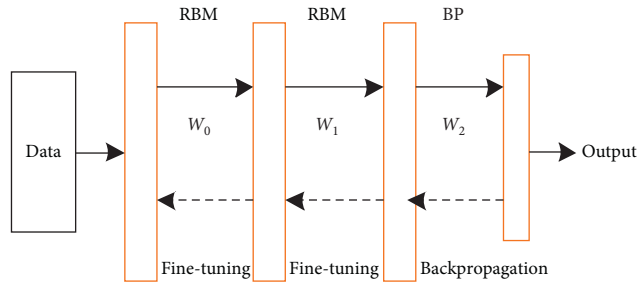

Figure 3: The deep belief network (DBN).

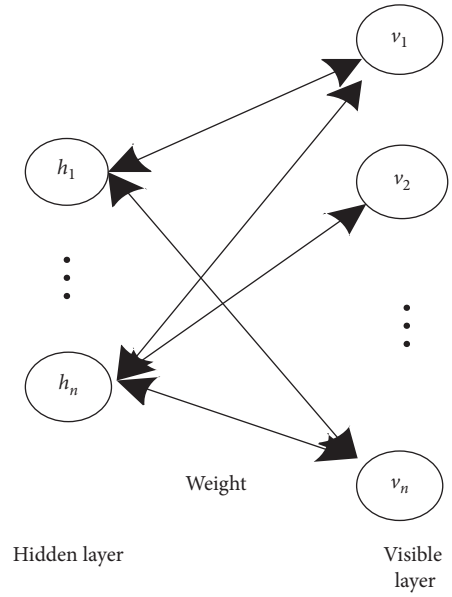

Figure 4: RBM structure.

neurons: input layer, hidden layer, and output layer. The structure of the BP network is shown in Figure 5. BP network in a DBN can be understood as a classifier with supervised learning.

In the BP network, the output of the hidden layer node, $O_j = f(\sum W_{ij} x_i - a_j)$, where a_j is the neuron threshold, and f is the excitation function, generally taking the Sigmoid function. The output of the output node $y_k = f(T_{jk} O_j - b_k)$, where b_k is the neuron threshold and T_{jk} is the strength of the connection between the hidden layer node and the output layer node.

5. Experimental Results and Discussion

In this section, we analyze and discuss the results achieved by our proposed model for the microblog data of 2017 and 2018 from January to September are used as experimental data.

5.1. Evaluation Method. In this section, we demonstrate the measurement of the performance proposed model. The confusion metrics is one of the most widely used techniques used by several researchers for the identification of the performance result. In this paper, the correlation coefficient (Corr) and mean absolute error (MAE) are used as

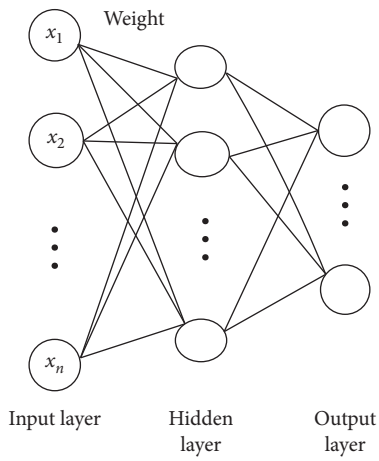

Figure 5: BP network structure.

evaluation indicators. The correlation coefficient is calculated as follows:

$$\text{Corr} = \frac{1}{n}\sum_{i=1}^{n}\left(\frac{R_i - \overline{R}}{\sigma_R} \times \frac{P_i - \overline{P}}{\sigma_P}\right), \tag{9}$$

where n is the predicted sample point; R_i and P_i are the actual mean and predicted mean of the mental health level test sample, respectively; and R is the mean and standard deviation of R_i and P is the mean and standard deviation of P_i, respectively. To calculate the average absolute error, we used the following equation:

$$\text{MAE} = \frac{1}{n}\sum_{i=1}^{n}\left|R_i - P_i\right|. \tag{10}$$

5.2. Model Parameters. The DBN structure is determined by the network depth. These include the number of inputs, the number of outputs, and the number of hidden layer nodes in each layer. The number of nodes in the 1st layer of RBM viewport nodes is determined by the number of input sample features. In this study, social psychology considers many influencing factors, many of the above factors; we take each of the microblog comments, that is, (1) economic market correlation degree; (2) political democracy related degree; (3) management legal system related degree; (4) cultural thoughts diverse degree; (5) degree of information expansion; and (6) rapid correlation of life rhythm. These six main influencing factors are as the characteristics of network learning; all data are manually marked and each influencing factor is also graded in a hierarchical manner so that it can be digitized as the input tensor. Each influencing factor has its own rating according to the criteria.

A major impact on model performance is the depth of the DBN network. Research shows that if the number of RBM layers increases, DBN modeling is enhanced and the hidden layer in the higher layer provides more abstract functional representation and improved network prediction performance. Overfitting may however contribute to several layers. The number of hidden nodes also influences the performance of the model in DBN. The number of nodes is too small, the performance of the data from model mining is not good, and it can be fitted easily when too many nodes are present.

5.3. Model Training. The training of the DBN model is divided into two steps: pretraining and fine-tuning.

Step 1: separately train each layer of RBM networks unsupervised separately, obtain the weights of the generated models through pretraining by unsupervised greedy layer-by-layer method, and ensure that the feature information is retained as much as possible when the feature vectors are mapped to different feature spaces. The RBM training process actually determines the probability distribution that best produces the training samples by determining the weights. That is to say, a distribution is obtained such that the probability of training the sample under this distribution is the greatest.

Step 2: the BP network of the last layer of the DBN receives the output vector of the RBM as the input feature vector and supervises the classifier. Each layer of the RBM network adjusts the weights in its own layer to ensure that the feature vector mapping of the layer is optimal, and the feature vector mapping of the entire DBN is not optimal, so the BP network propagates the error information from top to bottom. Layer RBM fine-tunes a DBN network.

5.4. Training Results. In this paper, the microblog data of 2017 and 2018 from January to September are used as experimental data. All the data is crawled from the Internet, manually labeled, the emotional tendency is graded, and the related aspects are also graded. The grade is divided into 5 levels: 1 is the least relevant and 5 is the maximum correlation. Among them, the data from January to July of 2017 and 2018 is used as training data for the training DBN model, the data for August is used as feasibility verification data, and data of September is used as forecast test data.

In order to reasonably set the DBN's network depth, we study the impact of the DBN layer number {2, 3, 4} on the model prediction performance and set the number of each hidden layer node to 100. The average absolute error MAE is used as the evaluation index, and the research results are shown in Figure 6. It can be seen from Figure 6 that the DBN network depth has little effect on the accuracy of psychological prediction, and the overall three-layer structure model has the best forecast performance. In this study, DBN network depth has little effect on forecast performance, mainly due to a large amount of training data, providing sufficient data information, so that fewer RBM layers can also deeply mine data features.

Based on the above research results, we use the three-layer DBN model to further study the influence of the number of hidden layer nodes on the prediction performance of the model. The number of hidden layer nodes is set to 50, 100, and 200, respectively. MAE is also used as the evaluation index. As shown in Figure 7. It can be seen from Figure 7 that when the number of hidden layer nodes is 100,

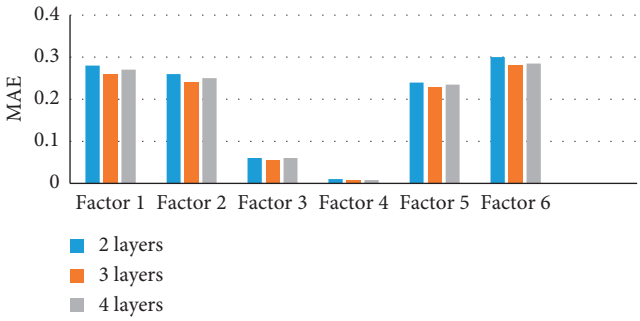

Figure 6: The impact of the number of DBN layers on performance.

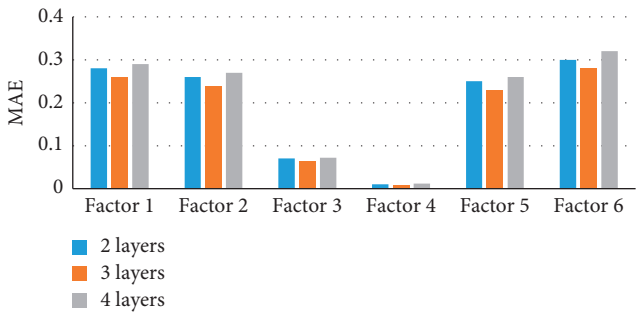

Figure 7: The impact of the number of hidden units of DBN on performance.

the overall prediction performance of the model is optimal. Therefore, this study will eventually adopt a three-tier DBN model with each hidden layer node set to 100.

In order to verify the accuracy of the proposed method, DBN prediction model and classical machine learning prediction model linear regression (LR), neural network (NN), support vector machine (SVM), random forest (random forest, RF), and autoregressive integral moving average model (autoregressive), the integrated moving average model (ARIMA) is compared and the results are shown in Tables 1 and 2. It can be seen from Tables 1 and 2 that the prediction performance of the DBN-based forecasting model is significantly better than other classical prediction models under the two evaluation indexes of correlation coefficient and average absolute error. This indicates that compared with other classical forecasting methods, the deep learning-based forecasting model can deeply mine the input sample features, extract the main factors affecting the mental health level, and reduce the influence of noise in the sample, thus having higher forecast accuracy.

Considering that Weibo has different differences in the hot topics in different time periods, in order to further verify the performance of the deep learning prediction model based on different environments, this paper uses the 2017 data as training data for 2018. The February and July comments were tested for predictive results as shown in Tables 3–6.

Table 1: Correlation coefficient of prediction results of September data.

Model	F1	F2	F3	F4	F5	F6
DBN	0.764	0.726	0.727	0.749	0.743	0.772
ARIMA	0.322	0.041	0.004	0.105	0.289	0.196
NN	0.628	0.588	0.688	0.715	0.702	0.724
RF	0.555	0.584	0.6	0.609	0.552	0.796
LR	0.622	0.684	0.682	0.649	0.604	0.691
SVM	0.524	0.67	0.647	0.579	0.688	0.687

Table 2: Average absolute error of prediction results of September data.

Model	F1	F2	F3	F4	F5	F6
NN	39.146	28.539	6.079	29.494	24.571	0.517
RF	44.024	31.618	6.707	29.603	23.667	0.474
DBN	24.333	27.805	5.811	26.974	22.58	0.403
LR	42.277	31.202	6.686	30.581	23.615	0.424
SVM	43.818	32.799	6.11	32.286	27.03	0.437
ARIMA	125.167	50.023	25.776	90.503	41.952	1.128

Table 3: Correlation coefficient of prediction results of January and February data.

Model	F1	F2	F3	F4	F5	F6
LR	0.652	0.649	0.543	0.631	0.588	0.63
SVM	0.623	0.639	0.623	0.585	0.522	0.538
ARIMA	0.039	0.141	0.222	0.011	0.101	0.386
DBN	0.696	0.744	0.718	0.698	0.712	0.773
NN	0.536	0.683	0.648	0.622	0.652	0.631
RF	0.522	0.654	0.503	0.522	0.522	0.575

Table 4: Average absolute error of prediction results of January and February data.

Model	F1	F2	F3	F4	F5	F6
RF	33.248	0.715	8.246	47.215	52.153	29.234
LR	28.268	0.561	7.363	35.326	45.189	26.404
ARIMA	59.234	1.245	31.244	99.135	132.241	38.281
DBN	24.234	0.491	6.139	28.351	27.333	24.891
SVM	32.971	0.743	8.917	43.726	50.134	30.862
NN	29.184	0.693	7.623	41.257	46.251	27.238

Table 5: Correlation coefficient of prediction results of July data.

Model	F1	F2	F3	F4	F5	F6
LR	0.614	0.674	0.638	0.603	0.671	0.683
RF	0.543	0.597	0.596	0.546	0.572	0.701
ARIMA	0.314	0.005	0.106	0.275	0.031	0.181
DBN	0.752	0.719	0.737	0.732	0.713	0.766
SVM	0.513	0.634	0.568	0.679	0.665	0.679
NN	0.613	0.679	0.707	0.695	0.589	0.715

Table 6: Average absolute error of prediction results of July data.

Model	F1	F2	F3	F4	F5	F6
RF	0.563	45.134	7.105	41.236	26.682	31.019
LR	0.492	42.418	6.782	37.072	25.162	31.28
ARIMA	1.108	124.249	26.023	52.074	43.128	92.105
DBN	0.428	26.291	5.924	28.285	23.297	28.284
SVM	0.537	43.904	7.097	39.287	27.137	33.281
NN	0.526	40.017	6.972	38.186	25.459	30.231

6. Conclusion

In this paper, we proposed a new framework that discusses the application of big data processing technology in social psychology. The proposed method is based on the deep belief network which establishes six major influencing factors that include the degree of economic market relevance of microblog commentary data, political democracy correlation, management legal system, cultural ideological diversification, information expansion, the rapid correlation of life rhythm, and the statistical model. Using the big data of the comments to train the model, fully explore the semantic features in the big data, and realize the mining of emotions and social psychology based on the commentary big data. By comparing with the classical machine learning judgment method based on the correlation and the average absolute error evaluation index, the validity of the DBN model in the mining of social psychological impact is verified. Research shows that a deep learning prediction approach can better overcome the weaknesses of conventional approaches, particularly in the case of big data, which can further explore the importance of big data in the heart and increase the implementation impact of big data comments.

Future big data research needs to deal with the relationship between data and theory. On the one hand, data-driven evidence can validate or correct existing theories, and as data-driven evidence continues to accumulate, it is expected to further refine innovative theories. On the other hand, the new theory can further provide guidance for subsequent empirical research. The combination of data driving and theoretical driving is conducive to the benign development of the mutual promotion of theory and data.

Data Availability

Data sharing is not applicable to this article as no datasets are generated or analyzed during the current study.

Conflicts of Interest

All authors declare that they have no conflicts of interest.

References

[1] J. A. Foley, N. Ramankutty, K. A. Brauman et al., "Solutions for a cultivated planet," *Nature*, vol. 478, no. 7369, pp. 337–342, 2011.

[2] M. Herrero, P. K. Thornton, A. M. Notenbaert et al., "Smart investments in sustainable food production: revisiting mixed crop-livestock systems," *Science*, vol. 327, no. 5967, pp. 822–825, 2010.

[3] P. J. Ericksen, J. S. I. Ingram, and D. M. Liverman, "Food security and global environmental change: emerging challenges," *Environmental Science & Policy*, vol. 12, no. 4, pp. 373–377, 2009.

[4] K. E. Giller, "Can we define the term 'farming systems'? a question of scale," *Outlook on Agriculture*, vol. 42, no. 3, pp. 149–153, 2013.

[5] C. Klapwijk, M. Van Wijk, T. Rosenstock, P. Van Asten, P. Thornton, and K. Giller, "Analysis of trade-offs in agricultural systems: current status and way forward," *Current Opinion in Environmental Sustainability*, vol. 6, pp. 110–115, 2014.

[6] D. Harris and A. Orr, "Is rainfed agriculture really a pathway from poverty?" *Agricultural Systems*, vol. 123, pp. 84–96, 2014.

[7] H. Todd, "Women climbing out of poverty through credit; or what do cows have to do with it?" *Livestock Research for Rural Development*, vol. 10, no. 3, pp. 1–9, 1998.

[8] H. M. J. Udo, H. A. Aklilu, L. T. Phong et al., "Impact of intensification of different types of livestock production in smallholder crop-livestock systems," *Livestock Science*, vol. 139, no. 1-2, pp. 22–29, 2011.

[9] X. Yu, Y. Chu, F. Jiang, Y. Guo, and D. Gong, "SVMs classification based two-side cross domain collaborative filtering by inferring intrinsic user and item features," *Knowledge-Based Systems*, vol. 141, pp. 80–91, 2018.

[10] F. Khan, A. Ur Rehman, J. Zheng, M. A. Jan, and M. Alam, "Mobile crowd sensing: a survey on privacy-preservation, task management, assignment models, and incentives mechanisms," *Future Generation Computer Systems*, vol. 100, pp. 456–472, 2019.

[11] D. Yang, G. Xue, X. Fang, and J. Tang, "Crowdsourcing to smartphones: incentive mechanism design for mobile phone sensing," in *Proceedings of the MobiCom '12: The 18th Annual International Conference on Mobile Computing and Networking*, pp. 173–184, Istanbul, Turkey, August 2012.

[12] X. Hu, "Social drive: a crowdsourcing-based vehicular social networking system for green transportation," in *Proceedings of the ACM MSWiM '13: 16th ACM International Conference on Modeling, Analysis and Simulation of Wireless and Mobile Systems*, pp. 85–92, Barcelona, Spain, November 2013.

[13] M. Usman, M. A. Jan, X. He, and J. Chen, "A survey on big multimedia data processing and management in smart cities," *ACM Computing Surveys*, vol. 52, no. 3, pp. 1–29, 2019.

[14] X. Hu, T. H. S. Chu, H. C. B. Chan, and V. C. M. Leung, "Vita: a crowdsensing-oriented mobile cyber-physical system," *IEEE Transactions on Emerging Topics in Computing*, vol. 1, no. 1, pp. 148–165, 2013.

[15] D. Huang, T. Xing, and H. Wu, "Mobile cloud computing service models: a user-centric approach," *IEEE Network*, vol. 27, no. 5, pp. 6–11, 2013.

[16] X. Ge, T. Han, Y. Zhang et al., "Spectrum and energy efficiency evaluation of two-tier femtocell networks with partially open channels," *IEEE Transactions on Vehicular Technology*, vol. 63, no. 3, pp. 1306–1319, 2014.

[17] S. Y. Sohn and A. S. Lee, "Bayesian network analysis for the dynamic prediction of early stage entrepreneurial activity index," *Expert Systems with Applications*, vol. 40, no. 10, pp. 4003–4009, 2013.

[18] X. Yu, J. Yang, and Z. Xie, "Training SVMs on a bound vectors set based on Fisher projection," *Frontiers of Computer Science*, vol. 8, no. 5, pp. 793–806, 2014.

[19] X. Yu, F. Jiang, J. Du, and D. Gong, "A cross-domain collaborative filtering algorithm with expanding user and item features via the latent factor space of auxiliary domains," *Pattern Recognition*, vol. 94, pp. 96–109, 2019.

[20] N. J. Yuan, Y. Zheng, L. Zhang, and X. Xie, "T-finder: a recommender system for finding passengers and vacant taxis," *IEEE Transactions on Knowledge and Data Engineering*, vol. 25, no. 10, pp. 2390–2403, 2013.

[21] M. Babar, F. Arif, M. A. Jan, Z. Tan, and F. Khan, "Urban data management system: towards Big Data analytics for Internet of Things based smart urban environment using customized Hadoop," *Future Generation Computer Systems*, vol. 96, pp. 398–409, 2019.

Hindawi
Mobile Information Systems
Volume 2021, Article ID 6616284, 11 pages
https://doi.org/10.1155/2021/6616284

Research Article

Evaluation of Potential Correlation of Piano Teaching Using Edge-Enabled Data and Machine Learning

Sibing Sun

School of Music, Harbin Normal University, Harbin 150080, China

Correspondence should be addressed to Sibing Sun; ssb@mail.sdufe.edu.cn

Received 23 December 2020; Revised 15 January 2021; Accepted 1 February 2021; Published 14 April 2021

Academic Editor: Mian Ahmad Jan

Copyright © 2021 Sibing Sun. This is an open access article distributed under the Creative Commons Attribution License, which permits unrestricted use, distribution, and reproduction in any medium, provided the original work is properly cited.

Data science has expanded at an exponential growth with the advancement of big data technology. The data analysis techniques need to delve deeper to find valuable information (Sarac 2017). The notion of edge computing is broadly acknowledged. Edge-enabled solutions provide computing, analysis, storage, and control nearer to the edge of the network, which support the efficient processing and decision-making. Machine learning has also attained significant attention in this context due to its flexibility and its ability to provide a variety of supervised, unsupervised, and semisupervised techniques. This research presents a specific model to evaluate the potential correlation of piano teaching using machine learning. The data analysis is performed at the edges of network for efficient results (Tan et al. 2017). The association rule mining technique of machine learning is utilized with the integration of improved *T*-test method. The improved *T*-test is performed for the measurement of association rules and proposed a new measure and influence degree of association rules. It is evident from the results that the use of the degree of influence as a measure of association rules to find the potential relevance of multimedia-assistant piano teaching evaluation data is extremely feasible. It overcomes shortcomings of existing measurement standards and reduces the generation of redundant rules. The existing literature highlights the concepts of evaluation of potential correlation and evaluates the advantages. However, there is a lack of an effective strategy for piano teaching. The proposed model performs efficient calculation and storage. The feasibility and effectiveness of the proposed framework are verified using the analysis of the actual dataset. The verification results show that it is feasible and valuable to find the potential relevance of multimedia-assisted piano teaching evaluation.

1. Introduction

The emergence of Internet of Things (IoT) and the proliferation of machine learning have improved the way we act and think. Entering the new era of machine learning, an effective strategy for data analysis has become a challenging task. The existing models face challenges to have efficient data analysis and evaluation. Educational technologies (e.g., multimedia technology) improve the popularity of the modern educational system. Multimedia technology improves the quality of teaching in various applications. Among these applications, piano teaching is one such application that has benefitted from using multimedia technology. The use of modern educational technologies in piano teaching has been popularized in recent years. In fact, these technologies have promoted the application of modern education to a new horizon. Due to the continuous development of multimedia technology, various educational theories and teaching models have been put forward, so that multimedia piano teaching also faces some new problems. The intersection of these aspects is the need to scientifically evaluate and analyze the quality and effectiveness of multimedia piano teaching. At present, the existing evaluation system can realize the functions of data entry, query, and statistics but cannot discover the relationships and rules existing in the data and cannot predict the future development trend based on the existing data. Therefore, the big data mining technology based on machine learning is applied to the analysis of multimedia piano teaching evaluation data, which provides decision support for teaching managers, which is of great significance to the improvement of multimedia piano teaching quality [1].

The idea of edge computing is gaining prominence with the rise of complex data analysis. Edge-enabled solutions provide efficient processing and control nearer to the edge for scalability and latency management. Edge computing offloading technology uses computing-intensive that is hard to handle by mobile devices. The relocation of jobs to the servers nearby the edge device not only advances the processing capability of the devices. This paper proposes a multimedia-assisted piano teaching model based on big data machine learning. The data analysis is performed at the edges of network for efficient results. The association rule mining technique of machine learning is utilized with the integration of improved T-test method. The improved T-test is performed for the measurement of association rules and proposed a new measure and influence degree of association rules. The paper proposes an improved T-test-based model using the traditional support degree, confidence framework, validity, and relevance. The influence degree model analyzes the influence degree measurement and verifies its effectiveness using a specific case study [2].

2. Data Analysis and Evaluation of Multimedia-Aided Piano Teaching

The evaluation of multimedia-assisted piano teaching is not the purpose of evaluation activities. The ultimate goal of evaluation is to improve the work, scientific management, and research decision-making by evaluating the information obtained. This evaluation can be improved by using the edge-commuting. The edge-enabled analysis will improve the efficiency of the data analysis process. The evaluation information data do not spontaneously play a role. It is necessary to properly process the evaluation information along with its feedback. The feedback evaluation information exerts its comprehensive role as much as possible to make the evaluation activity effective. The data analysis factors are described in the coming sections.

2.1. The Factors Affecting the Quality of Multimedia-Assisted Piano Teaching. The development of multimedia-assisted piano teaching is a complex systematic project, which is closely related to the corresponding theoretical research, technological progress, teaching practice, and so forth. Its teaching effect is influenced by many factors such as the information literacy of teachers and students, the quality of teaching courseware, and the teaching support platform. At present, multimedia-assisted piano teaching is still in the exploration stage in terms of teaching mode, teaching methods, and teaching strategies. Therefore, through the big data and machine learning technology to analyze the factors affecting the effect of multimedia teaching, it provides various links for improving multimedia-assisted piano teaching. Valuable information is of great significance to improve the quality of multimedia teaching.

2.2. Feedback on Evaluation, Analysis, and Timely Adjustment in Teaching Methods and Processes. In this information society, the efficiency of information transmission and the timeliness of feedback accelerate the process of social development. In the evaluation process, we must allow the advantage of using computer network technology in data processing and information transmission. The computer processing is made more efficient with the help of edge computation where the processing unit is provided with the network edges. The collected data are sorted and analyzed to obtain the distribution state of the data. The characteristics, rules, and relationship of the data is utilized at the edges and useful information is extracted for improving the quality of multimedia-assisted piano teaching and contributing to teaching management. According to the evaluation feedback information, solve various problems in the teaching in time, further optimize various aspects of multimedia-assisted piano teaching, give full play to the advantages of multicoal-assisted piano teaching, and lay the foundation for improving the quality of piano teaching.

2.3. Teachers' Information Literacy and Teachers' Self-Improvement Promotion. Multimedia-assisted piano teaching combines the advantages of multimedia teaching and traditional teaching and plays a big role in improving teaching quality. However, at the same time, it also puts forward higher requirements for the quality and ability of teachers engaged in multimedia piano teaching. In the evaluation process, we must strive to provide teachers with useful information through the orientation, diagnosis, and timely feedback of the evaluation system with the help of edge computing. Through the analysis of the evaluation data, we find out the problems and deficiencies of teachers in all aspects of multimedia piano teaching and help teachers improve their multimedia information, emergency technology, and classroom integration ability to promote the self-improvement and improvement of piano teachers. The evaluation index of multimedia-assisted piano teaching model is shown in Figure 1.

2.4. Guarantee the Reliability of the Evaluation Data. Evaluation is a subjective activity, and the evaluator's attitude is direct or not, which has a direct impact on the evaluation results. Scientific processing of the obtained evaluation data is important and an important issue to ensure the quality of the evaluation. Since the evaluation indicators are derived from the same target, there must be an intrinsic link between various indicators, which also leads to some correlation between the evaluation data of different evaluation indicators. We can find out that through the association rules. The correlation between the evaluation data is used, and it is checked whether the obtained evaluation data are reliable based on the correlation.

3. Machine Learning-Based Association Rule Metrics

In this section, the machine learning-based association rule metrics are designed. The overall process is applied to the multimedia-aided piano teaching techniques considered as

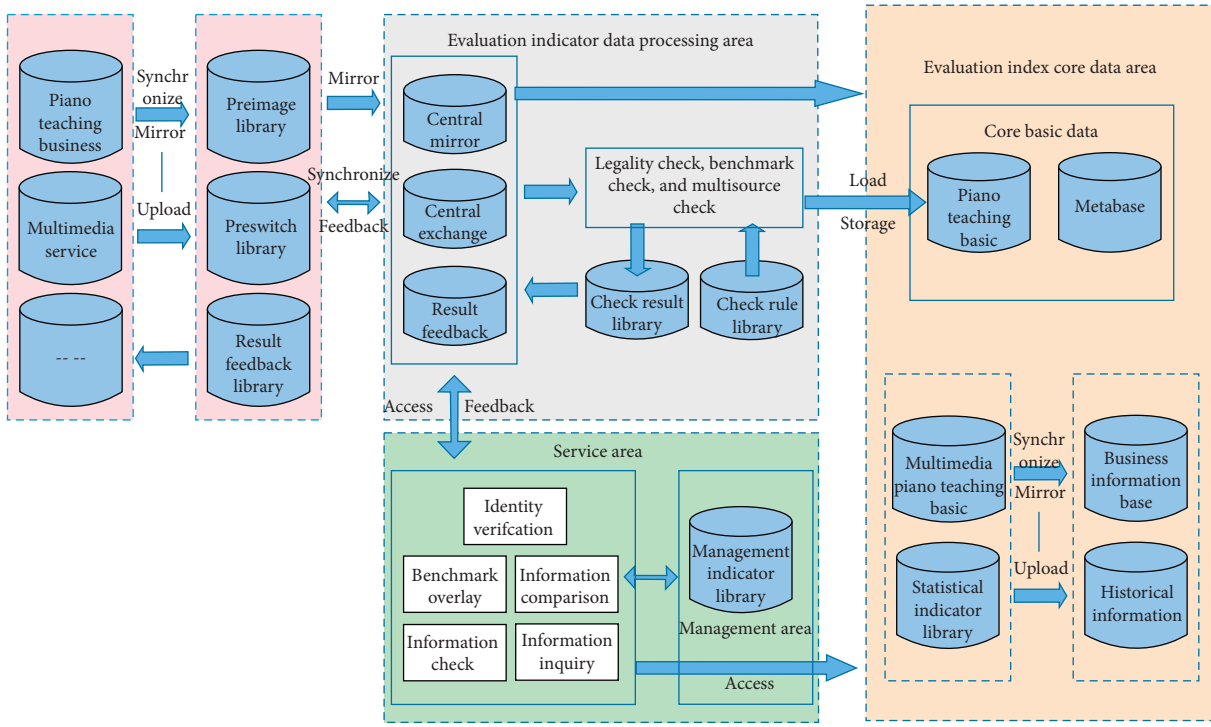

Figure 1: Evaluation index of multimedia-assisted piano teaching model.

the edge of the networks. Initially, the standard is discussed in the context of association rules. A detailed description is provided in the subsection.

3.1. Machine Learning Association Rule Standard. In the past few years, there have been many controversies about the problems of traditional support and credibility models, and many improvements have been proposed. Various new rule evaluation criteria have been proposed and added to the mining algorithm. The generation of association rules is restricted and constrained to obtain more novel and effective association rules. There are broadly two different categories. The first category is to try to find alternatives to the measure of credibility and to improve the objective evaluation method of extending the support threshold limit. The second category is to try to increase the subjective measure. Multimedia-assisted piano teaching data mining process diagram is shown in Figure 2.

Data mining of multimedia-assisted piano teaching data is first performed. The data mining process can be divided into the following steps:

(1) Data cleansing: eliminating noise and data not related to the mining theme.

(2) Data integration: integrating data from multiple data sources.

(3) Data selection: selecting data related to mining topics.

(4) Data transformation: using data such as normalization to transform data into a form suitable for data mining.

(5) Data mining: the core steps to mine knowledge using methods such as classification, fusion, and association rules.

(6) Mode evaluation: evaluation of the effect of the model, the commonly used indicators have accuracy, recall rate, and so on.

(7) Knowledge representation: the model represented by a technically understandable model and the knowledge obtained by the mining presented to the user.

3.2. Relativity. Relativity [3–5] is the ratio of confidence to expected confidence, and its expression is defined as

$$\text{relativity}\ (X \Rightarrow Y) = \frac{P(Y|X)}{P(Y)} = \frac{P(XY)}{P(X)P(Y)}, \tag{1}$$

where $P(Y)$ is the expected confidence of the rule $X \Rightarrow Y$, indicating that the transaction in D contains the percentage of Y. The relevance of the rule $X \Rightarrow Y$ describes the influence of the item set X on the item set Y. When the degree of correlation is equal to 1, it indicates that X has no effect on the Y; that is, X and Y are independent, and the rule is called an irrelevant rule. At 1 o'clock, it indicates that the occurrence of X is lower than the possibility of occurrence of Y, and the rule is said to be a negative correlation rule; when it is greater than 1, it indicates that the appearance of X increases the possibility of occurrence of Y, which is called a positive correlation rule [6]. Through the analysis of the correlation, the misleading strong association rules can be effectively filtered out. The relevance definition of association rules $X \Rightarrow Y$ fully considers the directionality of the rules.

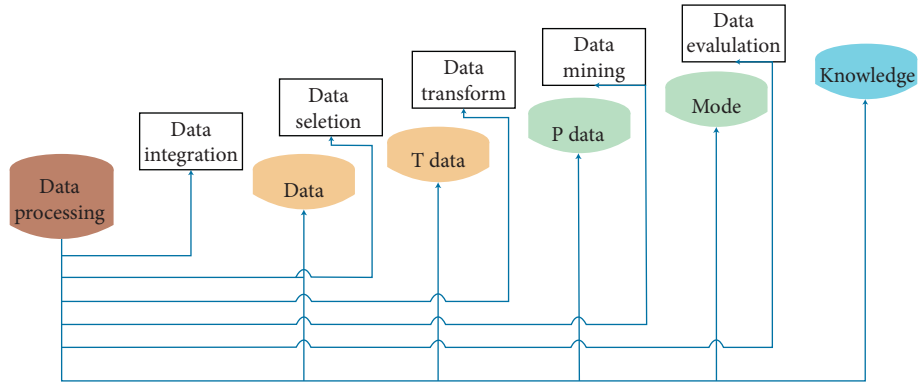

Figure 2: Data mining process workflow.

The greater the correlation, the greater the positive correlation between Y and X and the greater the positive effect of X on Y; the lesser the correlation (less than 0), the greater the intensity of negative correlation between Y and X; and the greater the inhibition of X to Y, the bigger the effect. This correlation is utilized in the proposed model for data analysis of piano teaching evaluation. In addition, the relativity is computed at the edges of the computing [7].

3.3. Interest Level. The interest of the basis difference is defined as follows:

$$\text{Interest}\ (X \Rightarrow Y) = P(Y|X) - P(Y). \tag{2}$$

According to the definition of interest, there are three possible scenarios for the metric of interest $(X \Rightarrow Y)$:

(1) If the degree of interest is > 0, then X and Y are positively correlated.

(2) If the degree of interest is <0, then X and Y are negatively correlated.

(3) If the degree of interest $= 0$, then X and Y are irrelevant and independent of each other.

In fact, there are many definitions of the interestingness of the rules. The interestingness is defined in the literature [8–11]:

$$\text{Interest}\ (X \Rightarrow Y) = \frac{P(Y|X)/P(X) - P(Y)}{\max(P(Y|X)/P(X), P(Y))}. \tag{3}$$

This definition makes the interest level between -1 and 1, and the interestingness of a rule is greater than 0, indicating that the more interested in the rule (the greater its practical value), the more unreasonable the rule, and the more interested people are in the negative rule of the rule (that is, the greater the actual use value of the reverse rule). Among the factors influencing the quality of rules, in addition to the three factors that affect the degree of interest, such as coverage, implementation, and confidence, there are also rule complexity factors. In addition, Alex also analyzed several other factors that may affect the quality and interestingness of the rules, including the size of the rule front, the imbalance of class distribution, the influence of rule attributes, the cost of misclassification, and the classification rules.

3.4. Relative Confidence. The literature [8] introduces the concept of relative confidence. If the probability $P(X)$ is used to represent the percentage of transactions in D containing X, $P(\overline{X})$ is used to indicate that the transaction in D does not contain the percentage of X, $P(Y|X)$, which means that Y appears in transaction D when D appears. In the calculation of conditional probability, $P(Y|\overline{X})$, when transaction X does not appear, the conditional probability of appearing in D is Y. If X is a frequent item set, then $\min \sup \le P(X) \le 1$. The definition of $X \Rightarrow Y$ relative confidence is as follows: if $\min \sup \le P(X) \le 1$, relative confidence is $P(Y|X) - P(Y|\overline{X})$.

If $P(X) = 1$ or $P(\overline{X}) = 0$ and $P(Y) = 1$, relative confidence is 1.

If $P(X) = 1$ or $P(\overline{X}) = 0$ and $P(Y) < 1$, relative confidence is 0.

If $P(X) = 1$, this means that each transaction in D contains X. If each transaction contains Y at the same time, the relative confidence is defined as 1; otherwise, the relative confidence is defined as 0. Confidence due to strong association rules $P(Y|X) \ge \min$ confidence. Therefore, the value range of relative confidence is $[-1 + \min$ confidence, $1]$.

Introducing a threshold of relative confidence R_1 and R_2, they are all positive numbers greater than 0 and less than one. The relative confidence of strong association rules must be one of the following three situations:

$R_1 \le$ relative confidence ≤ 1

$-R_2 <$ relative confidence $< R_1$

$-1 <$ relative confidence $\le -R_2$.

According to the value of relative confidence, strong association rules can be divided into three categories: positive association rules, invalid association rules, and negative association rules [12].

3.5. Effectiveness. The concept of validity is introduced in [13]. If $P(X)$ is used to indicate the probability of occurrence of transaction X, $P(\overline{X})$ is the probability that transaction X does not occur. The support and confidence of association rules $X \Rightarrow Y$ can be expressed as $P(XY)$ and $P(XY)/P(X)$, respectively. The validity of defining $X \Rightarrow Y$ is

$$\text{Validity} = \frac{P(XY)}{P(X)^* P(X)} - \frac{P(\overline{X}Y)}{P(\overline{X})^* P(\overline{X})}. \quad (4)$$

The intuitive meaning of the above formula is as follows: validity = (probability of simultaneous occurrence of X and Y in the D database) – (probability of simultaneous occurrence of Y in the D database). Since the value intervals of $P(XY)$ and $P(\overline{X}Y)$ are both at (0, 1), it is obvious that the value range of the validity is (–1, 1) [14].

It can be seen from the definition of validity that if the validity of X and Y is less than zero, it means that the probability of occurrence in the D database is less than the probability of occurrence; if the validity of $X \Rightarrow Y$ is equal to zero, the probability of occurrence in the D database is equal to the probability of occurrence [15]. Therefore, when mining association rules, if the validity of $X \Rightarrow Y$ is less than or equal to zero, even if the support and confidence are satisfactory, the extracted association rules are still useless association rules [15].

3.6. Suitability. Considering the possibility of Y appearing when X does not appear and whether X and Y are related, the concept of matching is proposed, which is defined as follows.

For example, $P(X)$ denotes the probability of occurrence of X, $P(Y)$ denotes the probability of Y, $P(XY)$ denotes the probability of simultaneous occurrence of X and Y, $P(\overline{X}Y)$ denotes the probability of simultaneous occurrence of $\overline{X}Y$, and $P(\overline{X})$ denotes the probability that X does not appear; then, the matching degree of $X \Rightarrow Y$ is defined as follows: (the confidence of $X \Rightarrow Y$) – (confidence of $X \Rightarrow Y$); namely,

$$\text{match} = \frac{P(Y|X)}{P(X)} - \frac{P(Y|\overline{X})}{P(\overline{X})}. \quad (5)$$

If match >0, then $P(XY) > P(X)P(Y)$, explaining that X and Y have positive correlations.

If match = 0, then $P(XY) = P(X)P(Y)$, explaining that X and Y are irrelevant, that is, redundant rules.

If match <0, then $P(XY) < P(X)P(Y)$, declaring that the negative rules of the rules may have research value.

If match = 0, then $P(XY) = P(X) = P(Y)$, noting that X and Y appear simultaneously or not in the record set.

As can be seen from the formula, the definition of matching not only includes the relevance factor but also includes the factor of $P(Y)$. Therefore, the degree of matching can fully reflect the validity of the rule $X \Rightarrow Y$.

3.7. Metric Improvement. The matrices can be improved in two different ways that are (1) insufficient measures of some association rules and T-test. A detailed description is provided as follows [16].

3.7.1. Insufficient Measures of Some Association Rules. In the pattern of generating association rules, the classic support and confidence framework are generally used to generate association rules. However, when the framework is used to generate rules, a large number of redundant and irrelevant rules are generated, which affects the user's choice of rules and even misleads the judgment [17]. Many researchers now use a variety of metrics to filter the association rules they have acquired to obtain effective rules. As illustrated in the example shown in the following table, this is a project set of length 2. The well has minimum support and confidence of 0.2 and 0.5, respectively. A set of transaction data are shown in Table 1 [18, 19].

From the table, it can be said that I and J always appear or do not appear at the same time, which is a valid association rule. When $I \Rightarrow J$, the support and confidence are 0.4 and 1, respectively. In the network sample, when $G \Rightarrow E$, support and confidence are also 0.4 and 1. $I \Rightarrow J$ and $G \Rightarrow E$ have the same support and confidence and should be valid association rules. However, as can be seen from the table, E always appears regardless of whether G appears [20]. Obviously, $G \Rightarrow E$ is not a valid association rule [21].

3.7.2. T-Test. The idea of the T-test can be introduced into the measurement of association rules. The test can be introduced in the following ways.

(a) One-Sample T-Test. A one-sample T-test tests if there is a difference between the mean of a single variable and a given constant. For example, the researcher wants to know the difference between the average score of a group of students and the score of 85. If the population mean is known, the difference significance test between the sample mean and the population mean is also a single sample T-test.

Let the overall X obey the normal distribution $N(\mu, \sigma^2)$, where σ^2 is unknown, from which the sample $(X_1, X_2, X_3, \ldots, X_n)$) is extracted; it is now necessary to test the hypothesis H_0: $_{\mu} = \mu_0, H_1$: $_{\mu} \neq \mu_0$, where μ_0 is a known constant. When making a hypothesis test on the population mean and when the variance $^2_{\sigma}$ is known, choose the statistic:

$$U = \frac{(\overline{X} - \mu_0)}{(\sigma/\sqrt{n})}. \quad (6)$$

But now $_{\sigma}$ is unknown, so you cannot directly use U as the test statistic. Usually when the standard deviation $_{\sigma}$ is unknown, the subsample standard deviation S is used instead of the overall standard deviation to get a new statistic.

$$T = \frac{(\overline{X} - \mu_0)}{(S/\sqrt{n})}. \quad (7)$$

It can be known from the sampling distribution theorem that if H_0 is established, the statistic T obeys the t distribution with a degree of freedom of $n - 1$. For a given a, the

Table 1: A set of transaction data.

TID	Items
1	*E, G, I, J, M*
2	*E, F, H, K, L, M, J*
3	*E, F, G, L, I*
4	*E, I, J, M*
5	*E, L, M, K*
6	*E, F, H, K, L, I, J*
7	*E, G, I, L, M*
8	*E, G, L, M*
9	*E, F, H, I, J, K, L*
10	*E, F, H, K, L, M, J*

critical value $t_a(n-1)$ that can be checked by the t distribution table makes

$$P\{|T| > t_a(n-1)\} = a. \tag{8}$$

(b) Independent Sample T-Test. The independent sample T-test compares the two-sample means, requiring the two samples to be independent of each other, the samples are all from the normal population, and the mean is a descriptive statistic that is meaningful for the test.

The first case: when the two population variances are unknown and equal, $\sigma_1 = \sigma_2$, the combined variance is used as an estimate of the two population variances, mathematically defined as

$$S_{P^2} = \frac{(n_1-1)s_1^2 + (n_2-1)s_2^2}{n_1+n_2-2}, \tag{9}$$

where s_1^2, s_2^2 are the variance of the first and second sets of samples, respectively; n_1, n_2 are the number of samples of the first and second sets of samples, respectively. At this time, the variance σ_{12}^2 of the sampling distribution of the difference between the two samples is

$$\sigma_{12}^2 = \frac{S_{P^2}}{n_1^2} + \frac{S_{P^2}}{n_2^2}. \tag{10}$$

The second case: when the two population variances are unknown and unequal, that is, $\sigma_1 \neq \sigma_2$, respectively, the respective variances are used, and the variance σ_{12}^2 of the sample distribution of the two-sample mean difference is

$$\sigma_{12}^2 = \frac{S^2}{n_1^2} + \frac{S^2}{n_2^2}. \tag{11}$$

Thus, the test statistic of the two population mean difference test is t statistic, and the mathematical definition is

$$t = \frac{\overline{X}_1 - \overline{X}_2 - (\mu_1 - \mu_2)}{\sqrt{\sigma_{12}^2}}. \tag{12}$$

(c) Paired Sample T-Test. In practice, some data are naturally related in pairs. In order to be necessary, it is sometimes necessary to design experiments so that the data become related pairs. Innocent is naturally related or artificially designed. The variance between the two samples is not equal. At this time, the test of the two population averages with no significant difference is to use the paired sample T-test process, and the T-test of the paired sample is required to make the two samples compared have a pairing relationship. Both samples are required to come from a normal population, and the mean is a descriptive statistic that is meaningful for the test.

The paired sample T-test can be considered as an extension of the one-sample T-test, but the test object is the difference between a group of observations from a normal assignment independent sample to a two-group paired sample. If the difference between the two paired samples x_{1i} and x_{2i} is $d_i = x_{1i} - x_{2i}$ independent and comes from the normal allocation, whether the maternal expected value μ of d_i is μ_0 can be obtained by the following statistics.

Among them $i = 1,2, \ldots\ldots, n$, X, Y, and Z all follow a normal distribution, where $\mu_z = E(Z)$ constructs a new statistic:

$$T = \frac{Z}{S_i\sqrt{n-1}}. \tag{13}$$

If the assumption is true, according to the sampling distribution theorem, the statistic T obeys the t distribution with a degree of freedom of $n = 1$. For a given a, a critical value can be obtained from the t distribution $t_{a/2}(n-1)$; then

$$P\{|T| > t_{a/2}(n_1+n_2-2)\} = a. \tag{14}$$

4. Instance Simulation

The evaluation of multimedia-assisted piano teaching is not the purpose of evaluation activities. The ultimate goal of evaluation is to improve the work, scientific management, and research decision-making by evaluating the information obtained. The evaluation information data do not spontaneously play a role, and it is necessary to appropriately process the evaluation information, give feedback on the evaluation information, and exert its comprehensive role as much as possible to make the evaluation activity effective. This is also the purpose of multimedia-assisted piano teaching evaluation data analysis. This chapter uses the LIBSVM toolkit and modifies it accordingly and then uses MATLAB to perform multimedia-assisted piano teaching modeling on real datasets.

4.1. Proposed Multimedia-Assistant Piano Teaching (MAPT) Model. The model mainly uses the association rule algorithm in data mining to sort and analyze the data and related data in the teaching evaluation database to obtain the distribution state of the data, the characteristics of the data, the change law of the data, and the model between the data. Provide useful information to improve the quality of teaching and provide decision support to managers. The model function diagram is shown in Figure 3.

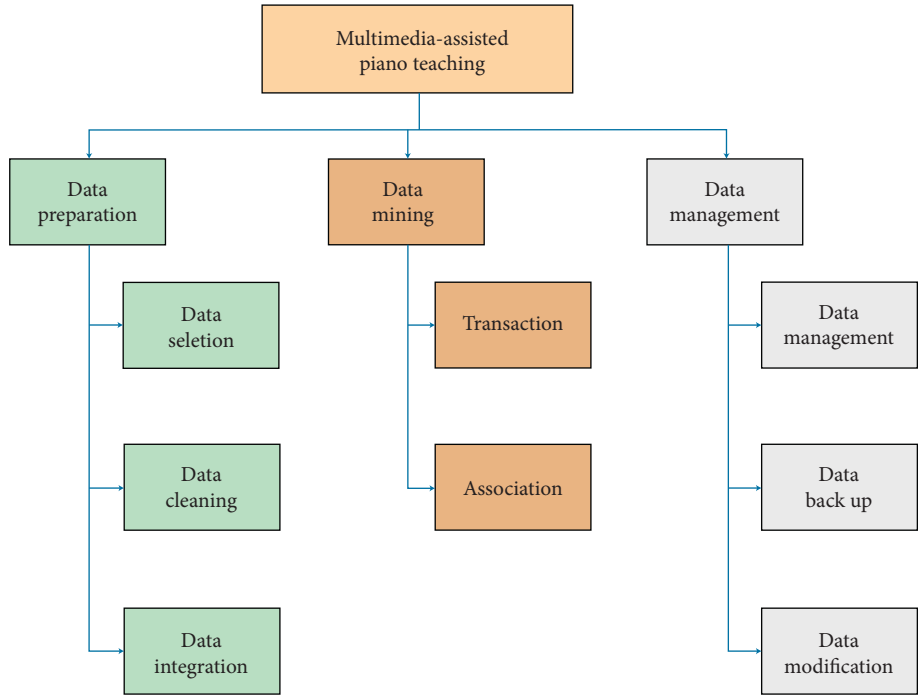

Figure 3: Model function diagram.

4.2. Implementation of Proposed MAPT Model. The model adopts an association rule mining (ARM) algorithm. ARM is a rule-based technique for identifying fascinating relations among variables. The relationship is discovered in the huge dataset. It is envisioned to recognize robust rules. The model adopts Apriori algorithm as the ARM algorithm of the system and adds the function of attribute selection based on Apriori algorithm. Then, in the association rule generation algorithm, the influence measure based on T-test is added to the traditional confidence measure, in order to provide more interesting and useful association rules. In the execution process, the algorithm first opens the database, reads the original data in the database, and converts the original data into an instance object by calling the application. Initialize the instance object, and display the attributes in the instance object in the form of a table. The user can select the item of interest and reedit the instance object according to the item selected by the user. Items that are not of interest and records are deleted, and the instance class object is reformed as in Algorithm 1.

4.3. Results Analysis and Discussion. This section provides the detail about results of the proposed model. The data collected at the edges of the network are analyzed using the machine learning approach. The mining algorithm of the above association rules is applied to the evaluation system of MAPT in a university. According to the existing evaluation result data of the school, some association rules can be obtained. Taking all the data of the multimedia-assisted piano teaching effect evaluation of the university from 2005 to 2007 as an example, the association rules of the teacher's title, the teacher's highest age, the teacher's age, and the teacher's multimedia-assisted piano teaching evaluation results are used. Association rule analysis result 1 is shown in Table 2.

(1) Minimum support: 0.3
(2) Number of iterations: 9
(3) The generated large item set:
(4) Size of the big data item $L(1)$: 11
(5) The size of the big data item $L(2)$: 11
(6) The size of the big data item $L(3)$: 1
(7) The best rules have been found.

If we set the minimum confidence level to 80% and the minimum impact degree to 4, we can get the association rules "professor, doctoral ⇒ excellence" and "professor ⇒ excellent." The data of the association rule show that the higher the title, the higher the education and the student evaluation, the better the result, and the quality of the teacher's multimedia-assisted piano teaching has a lot to do with the academic qualifications and professional titles, which shows that the school's teacher training is very important.

The data of the piano teaching effect from 2005 to 2007 are considered as a case study. The evaluation of the multimedia auxiliary piano teaching effect is considered in the case study. The first-level indicators of the multimedia classroom teaching evaluation standard in the multimedia-assisted piano teaching effect evaluation system are adapted. The major attributes are teacher quality, teaching design, and teaching process. Then the association rules between the teaching environment and the teacher's multimedia-assisted piano teaching evaluation results are extracted. Before the analysis of association rules, we quantified the evaluation

```
Produce Get_ValidRuls (min_effect)
Begin
   ValidRules = null;
   For each rule in A
      begin
         effect_i=(confidence_rule = P_y)/SQRT(P_y)/n)
            if effect > min_effect
               then add rule to ValidRules
            return ValidRules;
      end
End
```

Algorithm 1: Proposed algorithm.

Table 2: Association rule analysis result 1.

Association rules	Confidence	Influence degree
Professor, doctor ⟶ excellent	0.88	4.87
Professor ⟶ excellent	0.83	4.32
Elderly ⟶ professor, excellent	0.67	9.98
Doctor ⟶ professor, excellent	0.52	2.16
lecturer ⟶ master	0.69	6.87
Doctor, excellent ⟶ professor	0.56	3.57

scores of teacher quality, teaching design, teaching process, teaching courseware, and teaching environment. There are four grades of excellent, good, medium, and poor. Association rule analysis result 2 is shown in Table 3.

(1) Minimum support: 0.3

(2) Number of iterations: 7

(3) The generated large item set:

(4) Size of the big data item $L(1)$: 12

(5) The size of the big data item $L(2)$: 27

(6) The size of the big data item $L(3)$: 6

If we set the minimum confidence level to 70% and the minimum impact degree to 4, we can get the association rules "teacher quality (excellent), teaching process (excellent) ⇒ excellent" and "teacher quality (excellent) ⇒ excellent." The data of the association rule show that the quality of multimedia-assisted piano teaching has a lot to do with the quality of teachers and the teaching process. It should be noted that the "teaching environment" does not appear in the excavated rules. There are two possibilities. The construction of multimedia-assisted piano teaching environment has little effect on the quality of multimedia-assisted piano teaching. Secondly, the score of "teaching environment" is too low, which does not promote the quality of multimedia-assisted piano teaching. We believe that the second possibility is very likely to occur, indicating that the construction of multimedia-assisted piano teaching environment is now a weak link, and construction should be stepped up to provide good support for multimedia-assisted piano teaching. Practice has shown that, in the analysis of multimedia-assisted piano teaching evaluation data, the use of association rules technology to dig can obtain useful

Table 3: Association rule analysis result 2.

Association rules	Confidence	Influence degree
Teacher quality (excellent), teaching process (excellent) ⟶ excellent	0.78	9.87
Teacher quality (excellent) ⟶ excellent	0.63	6.32
Instructional design (excellent) ⟶ teaching courseware (excellent)	0.57	5.98
Teacher quality (excellent) ⟶ teaching process (excellent)	0.42	3.16

information for teachers' own quality improvement and teaching management decision-making.

The exhaustive and comprehensive experiments are carried out. The dataset of the year 2005 to 2007 of the local university is considered. Experiments were conducted on the validity of the impact of the multimedia teaching evaluation. It is verified whether the use of influence can reduce the generation of redundant rules. The experiment was carried out in Lenovo computer 8g memory, 3G frequency, Win XP, MATLAB environment. The degree of influence is used to filter the association rules generated under the traditional support and confidence framework. When the minimum confidence is set to 0.5, the total number of association rules generated before and after filtering will be tested with the support threshold. The support degree verification diagram is shown in Figure 4. The scatter plot of support is shown in Figure 5. The scatter diagram of the confidence association rules is shown in Figure 6.

After filtering from the above figure, it can be seen that the number of effective association rules measured by the degree of influence to the association rules generated under the support and confidence framework has been significantly reduced. This shows that the use of influence can effectively negate irrelevant rules and filter out redundant rules. In order to reflect the superiority of the model, the more popular model based on traditional correlation and effectiveness is selected. In order to increase the contrast, the same set of experimental data is selected. Comparison of traditional relevance validity models is shown in Table 4.

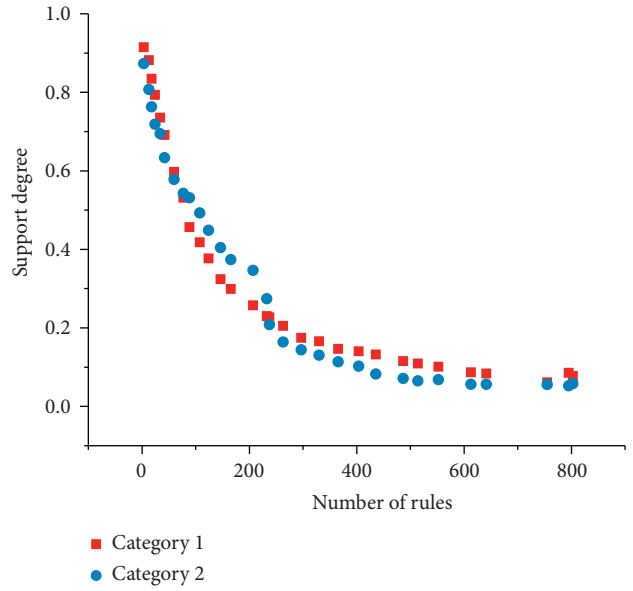

Figure 4: Support degree verification diagram.

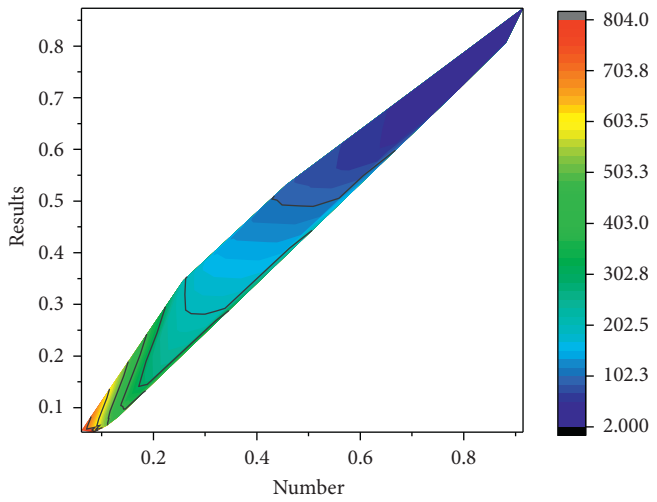

Figure 5: Scatter plot of support degree and confidence association rules.

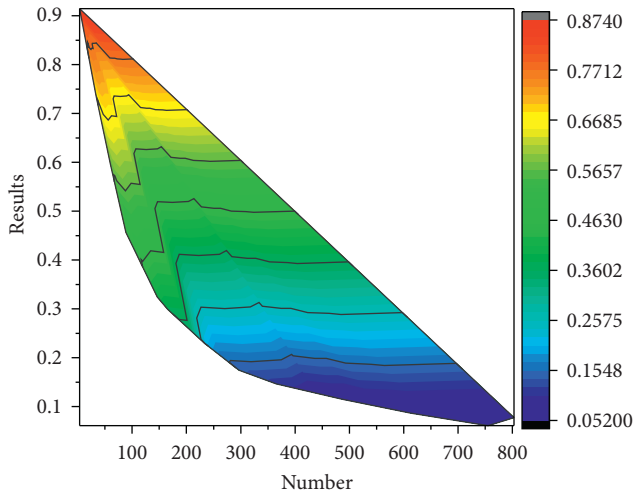

Figure 6: The scatter diagram of the confidence association rules.

Table 4: Comparison of traditional relevance validity models.

Influence degree	Detected influence	Correct number	False detection	Precision rate
8.23	8.29	8.09	0.2	0.982989064
8.28	8.34	8.14	0.2	0.983091787
8.33	8.39	8.19	0.2	0.983193277
8.38	8.44	8.24	0.2	0.983293556
8.43	8.49	8.29	0.2	0.983392645
8.48	8.54	8.34	0.2	0.983490566
8.53	8.59	8.52	0.07	0.998827667
8.58	8.88	8.81	0.07	1.026806527
8.63	8.93	8.86	0.07	1.026651217
8.68	8.98	8.91	0.07	1.026497696
8.98	9.28	9.21	0.07	1.025612472
9.28	8.78	8.71	0.07	0.938577586
9.58	9.08	9	0.08	0.939457203
9.88	9.38	9.3	0.08	0.941295547
9.8	9.3	9.22	0.08	0.940816327
9.72	9.22	9.14	0.08	0.940329218
9.64	9.14	9.06	0.08	0.939834025
9.56	9.06	8.98	0.08	0.939330544
9.48	8.98	8.9	0.08	0.938818565

Table 4 describes the detail of the traditional relevance in the context of validity. The validation is achieved and depicted in Table 4.

The experimental results show that the use of influence can not only obtain effective association rules but also divide the obtained rules into strong association rules and weak association rules and overcome some deficiencies of relevance and validity, making the rules more objective, reasonable, and convenient for users to choose. The verification results show that it is feasible and valuable to find the potential relevance.

5. Conclusion

This paper studies and analyzes the traditional support and confidence framework based on edge-enabled data analysis. The metrics such as relevance and validity indicate the shortcomings. On this basis, the T-test is introduced into the measurement of association rules of machine learning, and a new measure of the relevance of association rules is proposed. The model is utilized to assess the potential correlation of piano teaching using machine learning techniques. The ARM technique of machine learning is utilized with the integration of improved T-test method. The data analysis is performed at the edges of network for efficient results. While the theoretical and visual analysis of the impact metric is carried out, its effectiveness is verified by an example. The machine-related association rule metric impact is applied to the analysis of multimedia-assisted piano teaching quality evaluation data. Effectively improve the reliability, scalability, reusability, and maintainability of the model. The feasibility and effectiveness of the proposed framework are verified using the analysis of the actual dataset. The verification results show that it is feasible and valuable to find the potential relevance of multimedia-assisted piano teaching evaluation data by using the degree of influence as the measure of association rules. It is evident from the results that the use of the degree of influence as a measure of association rules to find the potential relevance of multimedia-assistant piano teaching evaluation data is extremely feasible.

Data Availability

The data used to support the findings of this study are available from the corresponding author upon request.

Conflicts of Interest

The authors declare that they have no conflicts of interest.

Acknowledgments

This study was supported by 2019 Key Projects of Art and Science Planning in Heilongjiang (2019A003).

References

[1] H. Sarac, "Effect of multimedia assisted 7e learning model applications on academic achievement and retention in students," *European Journal of Educational Research*, vol. 6, no. 3, pp. 299–311, 2017.

[2] L. Tan, C. Chen, Z. F. Fang et al., "Exploration of multimedia-assisted and bilingual teaching model in analytical chemistry experiments," *Laboratory Science*, vol. 8, no. 5, pp. 221–235, 2017.

[3] O. Ji-Won, O. S. Nam, I. Choi Joon et al., "Does the gadoxetic acid-enhanced liver MRI impact on the treatment of patients with colorectal cancer? comparison study with18F-FDG PET/CT," *BioMed Research International*, vol. 1, pp. 841–857, 2016.

[4] R. S. Florêncio, M. S. B. Meira, M. V. D. Cunha et al., "Plasmatic estradiol concentration in the mid-luteal phase is a good prognostic factor for clinical and ongoing pregnancies, during stimulated cycles of in vitro fertilization," *Jbra Assisted Reproduction*, vol. 22, no. 1, pp. 8–14, 2018.

[5] A. Moglia, V. Perrone, V. Ferrari et al., "Influence of videogames and musical instruments on performances at a

simulator for robotic surgery," *Minimally Invasive Therapy & Allied Technologies*, vol. 26, no. 3, pp. 129–134, 2017.

[6] M. Bartoli, L. Rosi, A. Giovannelli et al., "Production of bio-oils and bio-char from Arundo donax, through microwave assisted pyrolysis in a multimode batch reactor," *Journal of Analytical & Applied Pyrolysis*, vol. 122, 2016.

[7] J. Lv, "Research of Japanese translation teaching based on multimedia network technology," *Journal of Computational and Theoretical Nanoscience*, vol. 13, no. 12, pp. 10375–10379, 2016.

[8] P. Zhou, Y. Zhou, D. Wu, and H. Jin, "Differentially private online learning for cloud-based video recommendation with multimedia big data in social networks," *IEEE Transactions on Multimedia*, vol. 18, no. 6, pp. 1217–1229, 2016.

[9] L. I. Mei and X. N. University, "Teaching reform research based on assisted multimedia of tourism management major," *Education Teaching Forum*, vol. 19, no. 2, pp. 122–135, 2017.

[10] E. Akin, "Observation of multimedia-assisted instruction in the listening skills of students with mild mental deficiency," *Educational Research & Reviews*, vol. 11, no. 5, pp. 182–193, 2016.

[11] N. Zaranis, "The use of ICT in kindergarten for teaching addition based on realistic mathematics education," *Education and Information Technologies*, vol. 21, no. 3, pp. 589–606, 2016.

[12] J. Li, R. Singh, and R. Singh, "A novel large-scale multimedia image data classification algorithm based on mapping assisted deep neural network," *Multimedia Tools & Applications*, vol. 76, no. 18, pp. 1–24, 2017.

[13] H. Tambunan and E. Napitupulu, "Effectiveness of interactive multimedia based learning model in engineering mechanics," *International Education Studies*, vol. 9, no. 10, p. 155, 2016.

[14] Y. Bai, Z. Chen, J. Xie, and C. Li, "Daily reservoir inflow forecasting using multiscale deep feature learning with hybrid models," *Journal of Hydrology*, vol. 532, pp. 193–206, 2016.

[15] J. Yang, B. Champagne, Y. Zou, and L. Hanzo, "Joint optimization of transceiver matrices for MIMO-aided multiuser AF relay networks: improving the QoS in the presence of CSI errors," *IEEE Transactions on Vehicular Technology*, vol. 65, no. 3, pp. 1434–1451, 2016.

[16] F. Wang, J. Liu, M. Chen, and H. Wang, "Migration towards cloud-assisted live media streaming," *IEEE/ACM Transactions on Networking*, vol. 24, no. 1, pp. 272–282, 2016.

[17] K.-H. Chiang, C.-Y. Fan, H.-H. Liu, and G.-D. Chen, "Effects of a computer-assisted argument map learning strategy on sixth-grade students' argumentative essay reading comprehension," *Multimedia Tools and Applications*, vol. 75, no. 16, pp. 9973–9990, 2016.

[18] D. Fan, L. Wei, and M. Cao, "Extraction of target region in lung immunohistochemical image based on artificial neural network," *Multimedia Tools & Applications*, vol. 75, no. 19, pp. 1–18, 2016.

[19] F. Korur, S. Toker, and A. Eryılmaz, "Effects of the integrated online advance organizer teaching materials on students' science achievement and attitude," *Journal of Science Education and Technology*, vol. 25, no. 4, pp. 628–640, 2016.

[20] S. Kim, "Behavioral learning game for socio-physical IoT connections," *Eurasip Journal on Wireless Communications & Networking*, vol. 2016, no. 1, pp. 1–11, 2016.

[21] R. Boateng, S. L. Boateng, R. B. Awuah et al., "Videos in learning in higher education: assessing perceptions and attitudes of students at the University of Ghana," *Smart Learning Environments*, vol. 3, no. 1, pp. 1–13, 2016.

Hindawi
Mobile Information Systems
Volume 2023, Article ID 9819581, 1 page
https://doi.org/10.1155/2023/9819581

Retraction

Retracted: Real-Time Data Scheduling of Flexible Job in Papermaking Workshop Based on Deep Learning and Improved Fuzzy Algorithm

Mobile Information Systems

Received 8 August 2023; Accepted 8 August 2023; Published 9 August 2023

Copyright © 2023 Mobile Information Systems. This is an open access article distributed under the Creative Commons Attribution License, which permits unrestricted use, distribution, and reproduction in any medium, provided the original work is properly cited.

This article has been retracted by Hindawi following an investigation undertaken by the publisher [1]. This investigation has uncovered evidence of one or more of the following indicators of systematic manipulation of the publication process:

(1) Discrepancies in scope

(2) Discrepancies in the description of the research reported

(3) Discrepancies between the availability of data and the research described

(4) Inappropriate citations

(5) Incoherent, meaningless and/or irrelevant content included in the article

(6) Peer-review manipulation

The presence of these indicators undermines our confidence in the integrity of the article's content and we cannot, therefore, vouch for its reliability. Please note that this notice is intended solely to alert readers that the content of this article is unreliable. We have not investigated whether authors were aware of or involved in the systematic manipulation of the publication process.

Wiley and Hindawi regrets that the usual quality checks did not identify these issues before publication and have since put additional measures in place to safeguard research integrity.

We wish to credit our own Research Integrity and Research Publishing teams and anonymous and named external researchers and research integrity experts for contributing to this investigation.

The corresponding author, as the representative of all authors, has been given the opportunity to register their agreement or disagreement to this retraction. We have kept a record of any response received.

References

[1] S. Dang and W. Tang, "Real-Time Data Scheduling of Flexible Job in Papermaking Workshop Based on Deep Learning and Improved Fuzzy Algorithm," *Mobile Information Systems*, vol. 2021, Article ID 9930740, 12 pages, 2021.

Hindawi
Mobile Information Systems
Volume 2021, Article ID 9930740, 12 pages
https://doi.org/10.1155/2021/9930740

RETRACTED

Research Article

Real-Time Data Scheduling of Flexible Job in Papermaking Workshop Based on Deep Learning and Improved Fuzzy Algorithm

Shihong Dang and Wei Tang

College of Bioresources Chemical and Materials Engineering of Shaanxi University of Science and Technology, Xi'an 710021, China

Correspondence should be addressed to Shihong Dang; bs1301002@sust.edu.cn

Received 5 March 2021; Revised 21 March 2021; Accepted 27 March 2021; Published 10 April 2021

Academic Editor: Mian Ahmad Jan

Copyright © 2021 Shihong Dang and Wei Tang. This is an open access article distributed under the Creative Commons Attribution License, which permits unrestricted use, distribution, and reproduction in any medium, provided the original work is properly cited.

The traditional real-time data scheduling method ignores the optimization process of job data that leads to delayed delivery, high inventory cost, and low utilization rate of equipment. This paper proposes a novel real-time data scheduling method based on deep learning and an improved fuzzy algorithm for flexible operations in the papermaking workshop. The algorithm is divided into three parts: the first part describes the flexible job shop scheduling problem; the second part constructs the fuzzy scheduling model of flexible job data in papermaking workshop; and finally the third part uses a genetic algorithm to obtain the optimal solution of fuzzy scheduling of flexible job data in papermaking workshop. The results show that the optimal solution is obtained in 48 seconds at the 23rd attempt (iteration) under the application of the proposed method. This result is much better than the three traditional scheduling methods with which we compared our results. Hence, this paper improves the work efficiency and quality of papermaking workshop and reduces the operating cost of the papermaking enterprise.

1. Introduction

With the deepening of economic globalization, the users' demand for products has increased. Multiple species and small batch manufacturing is becoming more and more common with the passage of time. This mode of production makes the production environment more and more complex. How to reduce the unnecessary expenses in production is the key for survival and development of enterprises. More and more enterprises need to make the production more intelligent: a concept known as effective production scheduling. In the past fifty years, as an NP difficult problem, the production scheduling has attracted more and more attention from academia and industrial circles due to its significant economic benefits and its own high challenges [1]. However, in order to describe the actual situation in the production process more accurately and improve the quality of scheduling, it is necessary to conduct a comprehensive and in-depth study. Aimed at real workshop flexible scheduling problem in recent years, domestic and foreign scholars have done a lot of research work, but because of the complexity of the scheduling problem, no universal method is suitable for all kinds of scheduling problems.

The existing methods can be summarized into three categories: the traditional operational research, heuristic rules, and swarm intelligence optimization algorithms. The traditional operations research method proposed in literature [2] solves the problem by establishing a mathematical model, which is generally only applicable to small scale scheduling problems, and has a strong dependence on the specific problem to be solved, so it cannot ensure delivery on time. The heuristic rule method proposed in literature [3] is a general term for a class of methods that use heuristic information to solve problems. It defines certain rules in advance, then applies them to the scheduling process, and finally produces a scheduling scheme. This rule has the

characteristics of being simple and intuitive, the cost of calculation is small, and it is generally easier to implement. It can be used alone or conveniently in conjunction with other algorithms. Heuristic rule method is suitable for small scale scheduling problems and is less efficient in solving large scale scheduling problems. Finally, the third category, i.e., swarm intelligence optimization algorithm, proposed in literature [4] belongs to the meta-heuristic algorithm, which uses certain natural phenomena or the living habits of certain groups to model and solve problems. The solution process is usually to randomly generate one or more scheduling solutions and then gradually perform iterative optimization through defined rules, which can converge to the optimal solution more quickly and can be applied to all types of optimization problems. However, the method of equipment utilization rate is low. All these three scheduling methods are based on scheduling environment relying on strict limitations, emphasis on all kinds of restrictions, and production information clearly in advance, but in the real production environment, there are a lot of uncertainty factors. Typically, the required information is often unable to obtain in advance, so with the development of fuzzy technology, the application of fuzzy number to represent dealing with uncertain parameters received wide attention by showing the incomparable superiority to other methods and application prospect. Processing time and delivery date are treated as fuzzy numbers, which are more in line with the actual problem associated with production. This kind of scheduling problem is called fuzzy scheduling problem.

In view of the problems associated with traditional methods, firstly, this article introduces the uncertainty in the scheduling process of flexible production system and then describes the scheduling problem and related concepts of flexible workshop with fuzzy operation time interval. In order to minimize *makespan*, a scheduling model based on fuzzy logic and genetic optimization is proposed. Finally, the feasibility of model is verified by an example. The results show that the optimal solution is obtained at 48 seconds and on the 23^{rd} iteration, which is better than the three traditional methods. Therefore, this method can effectively improve papermaking efficiency and save papermaking cost.

The rest of the paper is structured as follows. In Section 2, the real-time data scheduling for flexible jobs in papermaking workshop using an Improved Fuzzy algorithm is discussed. In Section 3, the experimental results are discussed. Finally, we conclude the paper and research gaps are discussed in Section 4.

2. Real-Time Data Scheduling for Flexible Jobs in Papermaking Workshop Using an Improved Fuzzy Algorithm

The basic idea of scheduling problem is to allocate resources to different tasks in a certain period of time. Its purpose is to optimize one or more objectives. Resources and tasks in organization will be in many forms, such as the machines in workshops, the runways in airports, the work teams in construction sites, the processing units in computers. All of them can be regarded as resources. However, the tasks may be the papermaking processes in production, the takeoff and landing of the airport aircraft, various stages of construction project, and the execution of computer programs. The scheduling is a decision-making process, which plays an important role in most of the manufacturing systems and information processing environments. In addition, it exists in transportation and distribution facilities and other types of service industries [5].

The manufacturing industry is an industry that makes materials, energy, equipment, technology [6–8], capital, information, and human resources, needed by the society. The production workshop is a manufacturing system with the interactive relationship between manufacturing resources and production and processing tasks. It is composed of manufacturing resources and production tasks. The workshop scheduling is the arrangement of processing tasks on the processing time and manufacturing resources for realizing the manufacture process. There are many possibilities for this combination, so it is necessary to optimize the production workshop scheduling [9].

In the process of workshop manufacturing, how to allocate resources for the production and processing tasks and thus to realize the optimization of production scheduling is the problem of workshop scheduling. The problem of workshop scheduling involves the following basic elements: task, resource, time, and performance index of scheduling optimization. Based on these basic elements, the commonly used classification methods are shown in Table 1 [10].

This article mainly focuses on the research of flexible job shop scheduling in task types. The basic research ideas are shown in Figure 1.

Based on the scheduling problems in the workshop, the flexible work system is formulated for fuzzy scheduling in the flexible job shop (Section 2.1). Fuzzy parameters are designed, variables are described, objectives and constraints are set, and the model is optimized to construct a fuzzy scheduling model of flexible job data, and the optimal solution of the model is obtained by genetic algorithm (Section 2.2). Finally, experimental analysis is carried out to verify the effectiveness of the method (Section 2.3).

2.1. Description of Flexible Job Shop Scheduling Problem (FJSP). The idea of job shop scheduling is that each paper in the job set is processed in a fixed order on all machines, and each process corresponds to a machine. In Figure 2(a), the working procedure of paper can only be executed after finishing the last process. In the actual production environment, the machine of a certain process is not unique. In Figure 2(b), the process can be selected from machines and equipment, i.e., the FJSP problem [3].

The flexible job shop scheduling can be described as follows: there are n pieces of paper to be processed, and the aggregation of paper is $(A_1, A_2, \ldots, A_n)$. There are m machines with different functions $(M_1, M_2, \ldots, M_n)$. The completion of paper needs multiple working processes, and there is an ordered constraint between each process. Each process can be conducted on different machines. The goal

RETRACTED

Table 1: Types of shop scheduling problems.

Basic elements	Type	Explanation
Task	Single machine scheduling problem	There is only one machine in the processing system, and there is only one working procedure for the work pieces to be processed. All work pieces are processed on this machine, and each working procedure needs to be optimized. Single machine shop scheduling is the simplest scheduling problem.
	Parallel machine scheduling problem	The processing system has a group of machines with the same function, and there is only one process/task for the work piece to be processed. Each process can be processed by any one of the processing equipments with the same function.
	Job shop scheduling problem	The working system has a group of machines with different functions. The work pieces to be processed include multiple processes. The processing routes of work pieces are different from each other. Each process is processed on a machine that has been uniquely designated in advance.
	Flexible job shop scheduling problem	Flexible job shop scheduling problem is an extension of job shop scheduling problem. Each process may be processed by multiple machines. The processing equipment of each process of the part may not be specified in advance and may be unique. The process can be processed by any one of a group of processing equipment with the same function.
	Flow shop scheduling problem	The machining system has a group of machines with different functions, and the work pieces to be processed include multiple processes. Each process is processed on one machine, and the processing routes of all work pieces are the same.
	Open shop scheduling problem	There are multiple processes for parts, but there is no sequence between them. One process can only be processed on single processing equipment, and single processing equipment can only process one process at the same time.
	Hybrid shop scheduling problem	In the actual production process, we often encounter the combination of the above types of scheduling problems, such as the combination of job shop scheduling and flexible job shop scheduling, and the combination of job shop scheduling and flow shop scheduling.
Resources	Single resource workshop scheduling	There is only one resource that restricts the production capacity of the workshop, the most common one is machine tool equipment resources.
	Double resource shop scheduling	At the same time, there are two kinds of resources that restrict the production capacity of the workshop. In addition to the common machine equipment resources, the other resource may be the operating technicians of the machine equipment, or some type of tools.
	Multiresource shop scheduling	At the same time, there are more than two kinds of resources needed for workpiece processing, which restrict the production capacity of the workshop. These resources include machine tool equipment, operators, material delivery system, and other auxiliary resources. Multiresource workshop scheduling problem is the most complex one.
Time	Deterministic scheduling	The processing time and related parameters of the workpiece are known quantities.
	Uncertain scheduling	The processing time and related parameters of workpiece are uncertain random variables.
Optimization target	Single target workshop scheduling	This kind of job shop scheduling problem has only one optimization objective.
	Multiobjective shop scheduling	This kind of job shop scheduling problem has two or more optimization objectives. For multiobjective scheduling problems, there is usually no optimal solution, so it is necessary to balance and choose the optimal solution among the noninferior solutions.

of scheduling is to select the most appropriate equipment for each process and thus to determine the processing sequence and the optimal scheme of optimizing the specified evaluation index [11]. Finally, it is necessary to draw Gantt chart and optimize a certain performance index. Generally, the method of drawing Gantt chart is to arrange the time of working procedures from starting point to ending point in production activities, so as to calculate the starting time and the earliest completion time and then find out the key path by the constraints. The paper in the machine system generally needs to meet the following constraints, as shown in Table 2.

Due to the influence of numerous factors, the paper processing time and delivery time are not always accurate. The manager or decision-maker can only provide a rough data and the possible range of data change. For this uncertainty, the traditional method is to approximate the imprecise number as an exact number and then solve it by the method of solving the exact problem. This method has two disadvantages. One is that the model may change, leading to the deviation of the solution. The other is that the solution is not in line with the traditional expression and it is not intuitive [12]. The random probability distribution function is used to represent the distribution of parameters. This method requires that the historical data of parameters must be known. In fact, it is very difficult to obtain these data. In addition, the optimization based on random method is also very difficult in processing.

RETRACTED

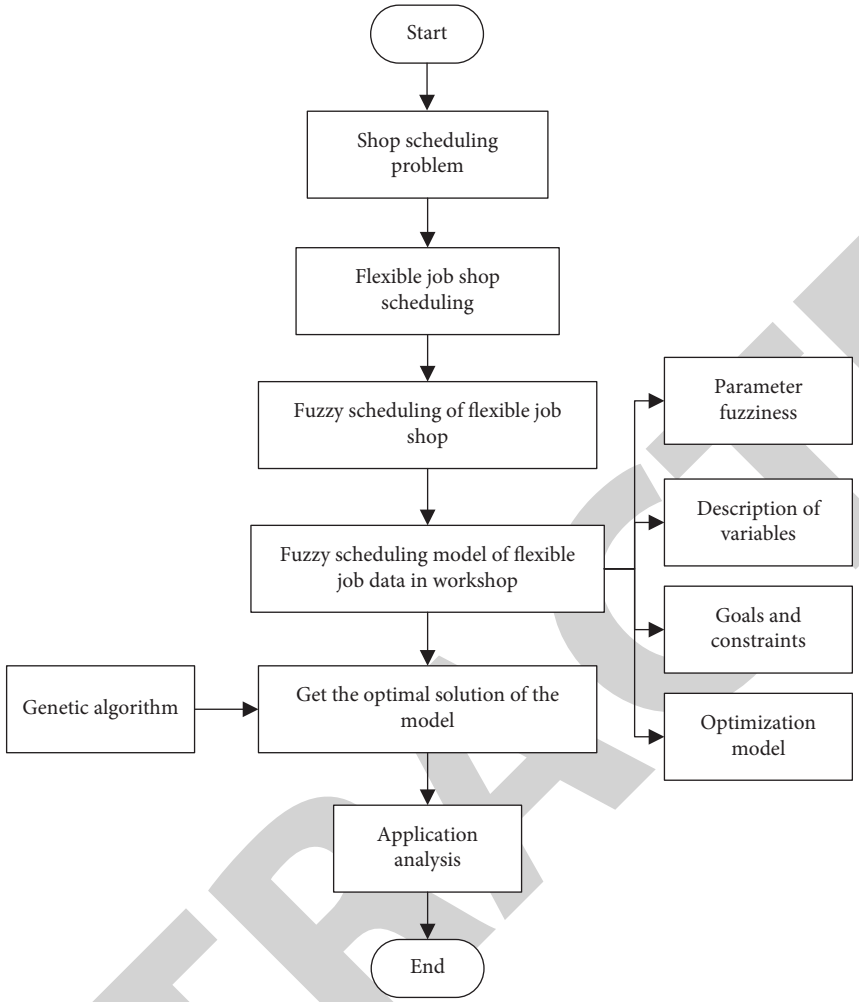

Figure 1: Research ideas of scheduling.

With the development of fuzzy technology, the fuzzy number is used to express and deal with uncertain parameters. This problem has been widely studied, which shows the advantages and its application prospects. The processing time and delivery time processed by fuzzy number are more in line with the actual production. This kind of scheduling problem is called fuzzy scheduling problem [13]. With the development of fuzzy mathematics, the idea of fuzzy mathematical programming is applied to the scheduling field. The fuzzy scheduling has become an important branch of uncertain scheduling problems. The scheduling problem of fuzzy delivery time and fuzzy processing time has become a research hotspot.

2.2. Fuzzy Scheduling Model of Flexible Job Data in Papermaking Workshop

2.2.1. Description of Variables. The variables required by the model are shown in Table 3.

$$R_{ijegk} = \{1, \text{ if } j\text{th process of paper } i \text{ and } g\text{th process } g \text{ of paper } e \text{ are executed on the same machine } k, \text{if process } j \text{ is prior to process } g, \tag{1}$$

$$X_{ijk} = \begin{cases} 1, & \text{if the } j-\text{th process of paper } i \text{ is performed on machine } k, \\ 0, & \text{other.} \end{cases} \tag{2}$$

In this equation, i, j, k, m_{ijk}, D_i, r_i, and w_i are the input variables. S_{ijk}, E_{ijk}, MP_k, and MS are the output variables. R_{ijegk} and X_{ijk} are decision variables. Compared with the traditional job shop scheduling model, the fuzzy job shop

RETRACTED

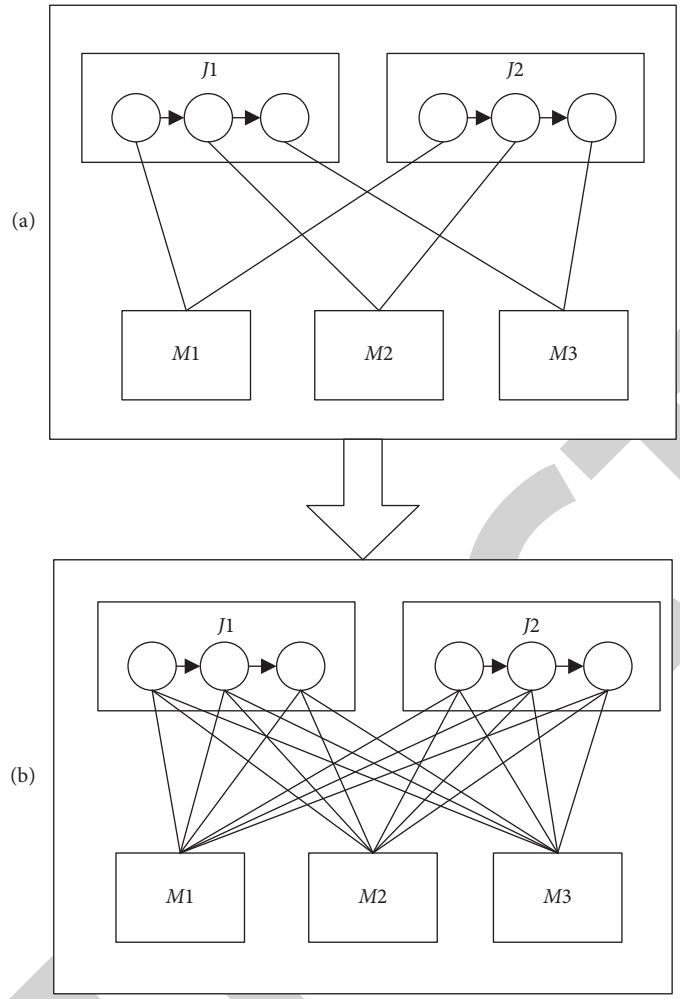

Figure 2: Comparison of JSP problem and FISP problem.

Table 2: Imposed constraints on machine system.

Serial number	Constraint condition
1	The process of machining on a machine at a certain time is unique.
2	Once a process is started, it cannot be stopped unless there is a machine fault, unless all the processes to be processed are finished.
3	There is often no coupling between papers, the sequence of processes is given in advance, and there is no sequence constraint between different processes.
4	When $t = 0$, there are no other constraints, and all of them can be operated on optional machines.
5	All machines are idle at $t = 0$ and can be processed.
6	At a certain time point, the operation equipment that can be selected for a certain process of paper is unique.
7	After one of the working procedures of the paper is processed, it is immediately moved to the machine that processes the next working procedure, and the moving time of the machine can be ignored.

scheduling model adds variables to describe the processing cost, production profit, and other influence factors. These variables improve the practical application ability of scheduling system, which is in line with the objective needs of enterprise. Meanwhile, they greatly improve the complexity of model solution, which is also one of the main difficulties in subsequent algorithm researches [14].

2.2.2. Parameter Fuzzification. The fuzzy scheduling is a scheduling method developed on the basis of workshop scheduling, which is more close to the actual production. In the fuzzy scheduling, the operation time of paper J_i on machine M_i is not determined, but various factors in production are comprehensively considered, such as the proficiency of workers, the operation of equipment, raw

RETRACTED

Table 3: Description of variables.

Variable	Explain
i	Paper serial number, $i = 1, 2, \ldots, N$ (N is the number of paper)
j	Process number of paper i, $j = 1, 2, \ldots, J$ (J is the number of processes)
k	Machine serial number, $k = 1, 2, \ldots, K$ (K is the total number of machines)
m_{ijk}	Processing time of the j-th process of paper i on machine k
S_{ijk}	The start time of the j-th process of paper i on machine k
E_{ijk}	Completion time of the j-th process of paper i on machine k
MP_k	Completion time of all paper on machine k
MS	Final finish time for all paper
D_i	Delivery time of paper i
r_i	Penalty coefficient for early completion of paper i
w_i	Penalty coefficient for delayed completion of paper i

materials, and other uncertain factors that may affect production. Triangular fuzzy numbers $(P_{ij}^1, P_{ij}^2, P_{ij}^3)$ are used to denote the processing time of paper as shown in Figure 3. $P_{ij}^1, P_{ij}^2, P_{ij}^3$ denote the early completion time, on-time completion, and delay in paper processing completion, respectively. A mapping relationship is established between the processing of any paper i in a period of time $x \in [P_{ij}^1, P_{ij}^3]$ and the extent of paper belonging to the completion set in this period. That is the membership function $F_{ij}(x)$. $F_{ij}(x)$ represent the membership degree of paper i belonging to the completion set in the processing time x [15].

The fuzzy delivery time $\widetilde{D}_i$ is represented by the satisfaction of relative completion time of paper, and it is denoted by two tuples (a_i^1, a_i^2). a_i^1 and a_i^2 denote the on-time delivery time and delayed delivery time of paper J_i. If the paper is completed within the window $[0, a_i^1]$ of delivery time, the satisfaction of this paper is 1. If the paper is completed outside the delivery time window, the satisfaction is denoted by a linear membership function (Figure 4).

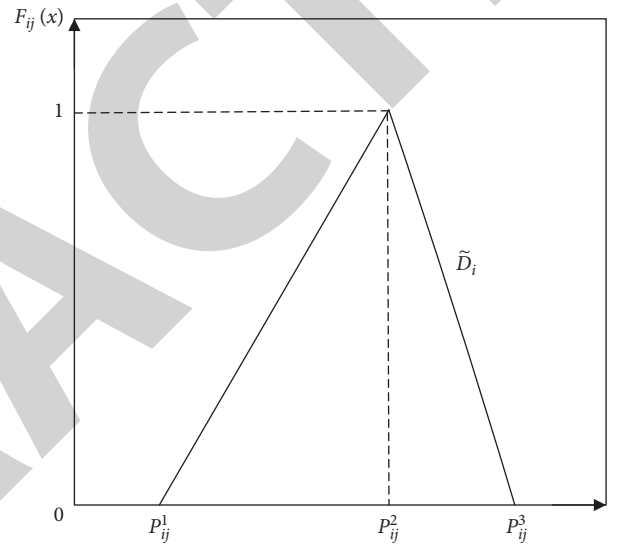

Figure 3: Fuzzy machining time.

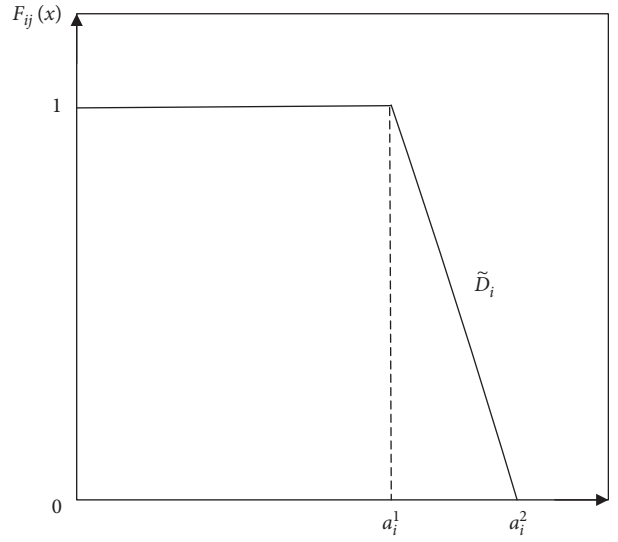

Figure 4: Delivery date of fuzzy number.

2.2.3. Targets and Constraints. Targets and constraints include the objective function, the constraints themselves, and the optimization model. We discuss them here.

(a) Objective Function

Minimize the total cost of paper, or reduce the free-load running time of machine and the actual working time of guarding the machine.

$$\min(HS) = \max_{k=1,\ldots,k} (HP_k). \tag{3}$$

Make the circulation time of paper in the system the shortest; $\min(MS) = \max_{k=1,\ldots,k} (HP_k)$; i.e., the penalty for delayed completion of the paper is zero; $0 = \sum_{i=1}^{N} w_i \cdot \max(0, E_{iJ_ik} - D_i)$; i.e., the penalty for early completion of paper is the minimum value [16].

(b) Constraints

Sequential Constraints. the processing sequence between adjacent working procedures of the same paper:

$$E_{iJ_ik} - E_{i(j-1)_m} \geq m_{ijk}, \tag{4}$$

RETRACTED

which indicates that the j th working procedure of paper i must be started after finishing the $j-1$ th working procedure.

Resource Constraint. after one processing task on the same machine is completed, we can start another task.

$$E_{egk} - E_{ijk} \geq m_{egk}. \tag{5}$$

At any given time, machine k cannot process any two different papers at the same time, and it is unable to process any two different processes at the same time [17].

Cost Constraints. the processing cost per unit time of each machine is different, and the power consumption for startup is different, so the labor intensity of workers is different. After adding the actual weight coefficient, a processing cost constraint condition is formed:

$$HP_k = MP_k \cdot H_k, \tag{6}$$

$$HS = \sum_{k=1}^{K} HP_k. \tag{7}$$

They represent the completion cost of all paper on machine k and the total completion cost of all paper.

Other Constraints. the completion time of any process cannot be less than its processing time.

$$E_{ijk} \geq m_{ijk}, \ \forall j. \tag{8}$$

2.3. Optimization Model. In this paper, two kinds of models for job shop scheduling are built. The first model only considers the fuzzy processing time, and the second model comprehensively considers the fuzzy processing time and fuzzy delivery time. The following two types of models are described in detail [18].

2.3.1. Job Shop Scheduling Model under Fuzzy Processing Time. In the job shop scheduling problem, for a given set of paper, if the processing time of each paper is accurate, according to the processing time, the paper can be arranged from small to large (SPT criterion), so that the optimal scheduling scheme of minimum flow time can be obtained. But if the processing time is fuzzy, because it involves the sum and comparison of fuzzy numbers, scheduling scheme cannot be simply obtained by SPT criterion [19].

In (9), d denotes the feasible scheduling set of the paper. For a given schedule $Q \in d$, let $f(Q)$ represent the corresponding objective function value. The scheduling model of minimum fuzzy process time is

$$\min_{Q \in d} f(Q) = \max_{1 \leq i \leq n} \{\widetilde{D}_i\}. \tag{9}$$

In this equation, $\{\widetilde{D}_i\}$ denotes the comprehensive evaluation index of the i th paper.

2.3.2. Scheduling Model under Fuzzy Processing Time and Fuzzy Delivery Time. The fuzzy delivery time of fuzzy scheduling problem is shown in Figure 4. If the paper is completed in delivery time window, it will not be punished. If the paper is completed outside the delivery window, a penalty is caused. The process meets the following basic assumptions: (1) the paper is waiting for processing at the same time, and the preparation time is 0; (2) the paper is not allowed to be interrupted and it has no priority. The machine can only process one paper; (3) the delivery window is sufficiently small: $(e_i^n - e_i^m)(\min_{i \in n}\{p_i\}, \forall i \in n)$, v is the advanced weight, and z is the delay weight [20].

The penalty function is shown as follows:

$$d(e, Q) = \sum_{1 \leq i \leq n} \left[v \max\left(0, e_i^m - D_i\right) + z \max\right]\left(0, D_i - e_i^n\right). \tag{10}$$

The minimum scheduling model of earliness/tardiness penalty is shown as follows:

$$\min_{Q \in d} f(e, Q) = \min_{Q \in d} f\left(e', Q'\right). \tag{11}$$

The goal is to find the best common delivery time e' and the best order Q', so as to minimize $f(e, Q)$.

2.4. Calculation of Optimal Solution of the Model. After the establishment of the multiobjective fuzzy scheduling model of job shop, the corresponding algorithm should be constructed to optimize and solve the problem. The job shop scheduling problem is the NP difficult problem. How to develop an effective algorithm to solve the scheduling problem has always been an important issue in the field of scheduling and optimization. The job shop fuzzy scheduling problem is more complex than the general scheduling problem. It is not only necessary to arrange the sequence of working procedure, but also to consider the machine selection. The number of feasible solutions is much more than that of traditional scheduling problems. How to find the optimal solution within a large range of feasible solutions is the main problem of genetic algorithm [21].

In the past thirty years, people have simulated the biological system and its behavior characteristics from different perspectives, forming new disciplines which have significant impact on the development of modern science and technology. For example, the fuzzy set theory is generated by the simulation of human thinking mode. The artificial neural network [22–26] theory is generated by the simulation of human brain nerve. The immune algorithm is generated by the simulation of animal and plant immune mechanism in nature. The evolutionary computing theory is generated by the simulation of biological evolution mechanism in nature [27, 28]. Generally, the imitation based on

RETRACTED

biological evolution mechanism forms three typical optimization calculation models, respectively.

(i) Genetic algorithm (GA)

(ii) Evolution strategy (ES)

(iii) Evolutionary programming (EP)

In this article, the genetic algorithm is used to optimize the fuzzy scheduling model. The basic elements of genetic algorithm include chromosome coding, population initialization, selection, crossover, and mutation. The basic flow of general genetic algorithm is described in Figure 5.

The flexibility of job shop scheduling makes the solution more complex. It is not only necessary to sort the working procedures, but also to select a machine for each working procedure. Based on the basic process of genetic algorithm, the fuzzy scheduling model of flexible job shop is solved. The specific steps are shown in Figure 6.

Step 1. Parameter setting: the size of the population is determined as N, and the number of iterations is g.

Step 2. Genetic code: the scheduling problem is encoded as a double chromosome structure.

Step 3. Generation of initial population: N individuals are randomly generated to form the initial population and the initial evolution algebra $t = 0$.

Step 4. Determine the objective function of flexible job shop scheduling problem, and transform the objective function into adaptive fitness function.

Step 5. The fitness value of each chromosome in the population is calculated by the adaptive fitness function. If the fitness value meets the end condition or the number of iterations is $t = G$, the operation is ended and the optimal solution is output. Otherwise, the next step is performed.

Step 6. Select a certain number of individuals by roulette selection, and perform the genetic operation on these individuals.

Step 7. Using deep neural network: calculate the crossover probability and mutation probability, and perform the adaptive genetic evolution operation according to crossover and mutation operation, so that new generation of population is obtained.

Step 8. Let $t = t + 1$, and return to Step 5.

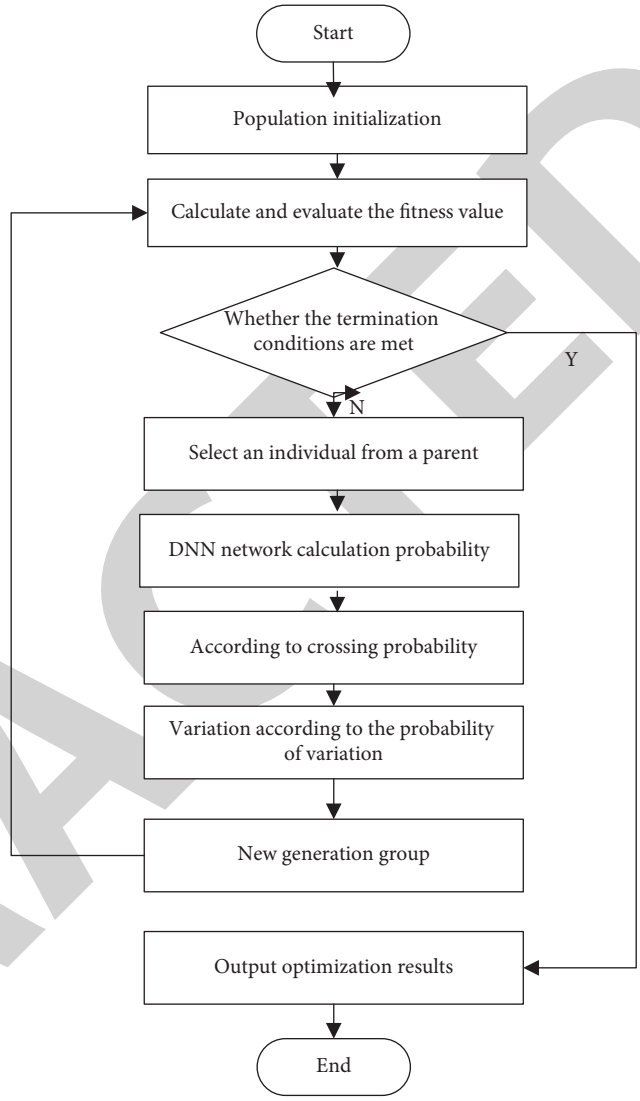

Figure 5: Basic flow chart of genetic algorithm.

3. Experimental Analysis

In order to verify the performance of improved genetic algorithm, a standard example was adopted for testing. The operating system is Windows XP, and the main frequency of CPU is 2.60 GHz. The memory is 2.0 GB. The programming language is Visual Basic. The traditional JSP problem can be regarded as a special case of unique and fixed FJSP of machine selection chain. Therefore, this algorithm can be applied to solve JSP and FJSP problems.

3.1. Parameter Setting. In this example, the simulation parameters include number of paper $N = 4$; number of machines $M = 10$; number of workers $W = 7$; number of individuals $Z = 50$; number of iterations $Y = 100$; selection probability $P_g = 0.9$; cross probability $Pc = 0.8$; and variation probability $\mathrm{Pm} = 0.1$. The paper processing process was repeatedly simulated ten times.

3.2. Evaluation Index. The performance index of workshop scheduling problem is the standard for production managers to evaluate the scheduling scheme. According to the different production demand, the scheduling indexes are different. Based on the summary of workshop scheduling performance indexes by Jia Zhaohong and Zeng Qiang, this article divided the performance indexes of workshop scheduling into the following categories: performance indexes based on completion time, performance indexes based on delivery time, performance indexes based on cost, performance indexes based on machine load and processing quality. Now, the performance indexes based on completion time are selected. The completion time refers to the time of

RETRACTED

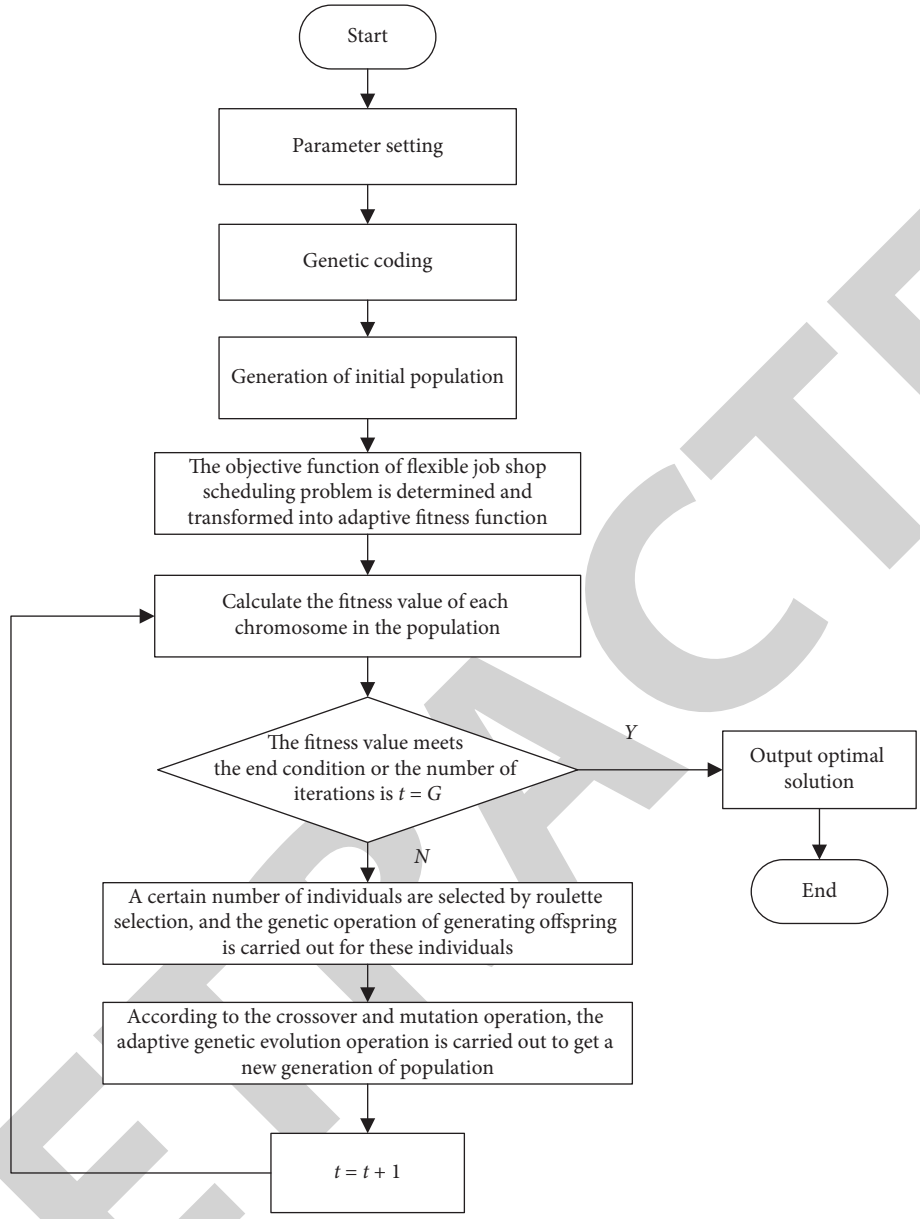

Figure 6: Fuzzy scheduling model solution of flexible job shop based on genetic algorithm.

finishing all the papermaking processes. The performance index based on the completion time is the most fundamental index to measure the scheduling performance, which can reflect the production efficiency of workshop, so it is also the most widely used performance index in the field of workshop scheduling research. It mainly includes maximum completion time, average completion time, maximum passing time, total flow-through time, weighted flow-through time, average flow-through time, and weighted average flow-through time.

3.3. Result Analysis. The experimental results verify that the proposed scheduling method is an optimization method with high quality and fast convergence speed. In order to ensure the reliability of the experimental results, select a workshop real data comparison contrast experiment. The experimental simulations were performed using MATLAB software. The method of this paper is based on operational research method, heuristic rules, and swarm intelligence optimization algorithm of workshop flexible job data scheduling method. The experimental parameters are the same as the improved algorithm.

Table 4 shows that the proposed method can get the optimal solution for 48 sec at the 23rd attempt. Respectively, the other three methods converge to the optimal solution for 52 sec at the 40th attempt, for 50 sec at the 38th attempt, and for 61 sec at the 44th attempt. Through comparison, we can see that the proposed method has many advantages. It not only makes the maximum completion time shorter, but also accelerates the convergence.

Figure 7 shows the change process of the weighted target value in the algorithm. It can be seen from the figure that the

RETRACTED

Table 4: Result analysis.

Project	Optimal algebra	Computing time (s)
Article method	23	48
Operational research method	40	52
Heuristic rule method	38	50
Swarm intelligence optimization algorithm	44	61

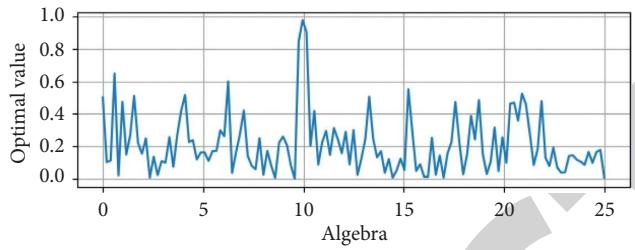

Figure 7: The change process of the optimal value.

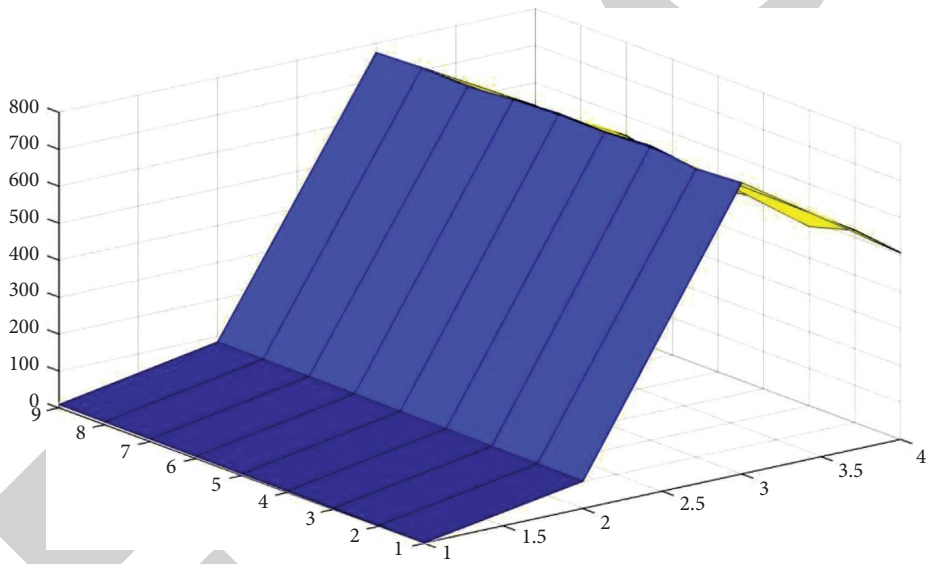

Figure 8: The final Pareto solution set.

overall trend of the optimal value is gradually optimized as the algebra of the algorithm increases, but, locally, the change of the optimal value has more fluctuations.

The Pareto solution set finally solved by the Pareto optimization method has multiple solutions or individuals, which can provide multiple feasible optimization solution sets for comparison for flexible job shop scheduling. The distribution of Pareto solutions in the time-cost-quality space is as follows, highlighted by Figure 8. Optimize the target weights according to the set schedules, and calculate the algorithm fitness value of each individual solution in the Pareto optimization solution set. This value is unique, and the final satisfaction of the decision optimization is done by calculating the fitness value and selecting the smallest value individual or solution. The corresponding scheduling plan Gantt chart is shown in Figure 9.

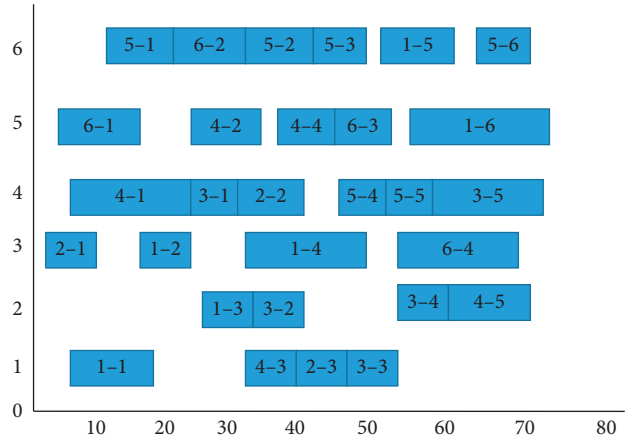

Figure 9: Gantt chart.

REJECTED

4. Conclusions

Job shop scheduling problem (JSSP) is one of the most famous machine scheduling approaches and at the same time extremely difficult combinatorial optimization problems. The main reason is the complexity and dynamic characteristics in the scheduling environment. Meanwhile, a large number of randomness and factors which are difficult to be quantified make the problem more difficult to be solved. With the development of fuzzy mathematics, the idea of fuzzy mathematical programming is applied to the scheduling field, forming an important branch of uncertain scheduling: fuzzy scheduling. The traditional real-time scheduling methods cannot deliver on-time, inventory problem of high cost and low equipment utilization rate; therefore, this paper puts forward an algorithm based on improved fuzzy flexible job real-time data scheduling method of papermaking workshop. On the basis of the scheduling problem in the flexible job shop, a fuzzy scheduling model for flexible job data in papermaking workshop was established. Through the comparison experiment, we can see that the method in this paper has more advantages, which not only makes the maximum completion time shorter, but also speeds up the convergence speed, thus achieving the purpose of this study. In the future, the utilization rate of scheduling equipment will be considered as a research method to further improve the proposed method.

Data Availability

The data used to support the findings of this study are included within the article.

Conflicts of Interest

The authors declare that they have no conflicts of interest.

Acknowledgments

This work was funded through the research and application of networked PLC platform for scientific research project of Xianyang Vocational and Technical College (project number: 2016KYA02); Scientific Research Project of Shaanxi Provincial Department of Education: research on networked PLC platform (project number: 17JK1172); Research Project of Xianyang Vocational and Technical College: The Exploration and Practice of the School-Running Model of the Mixed Ownership of the Public-Run Higher Vocational College (project number: 2017JYA03); and Project of Shaanxi Provincial Science and Technology Co-ordination and Innovation Project: The Technical and Thermal Control System for the Recovery and Utilization of the Waste Heat of the Drying Part of the Paper Machine (project number: 2016 KTCQ01-35).

References

[1] P. R. Ricardo and H. A. Arturo, "A hybrid estimation of distribution algorithm for flexible job-shop scheduling problems with process plan flexibility," *Applied Intelligence*, vol. 48, no. 10, pp. 3707–3734, 2018.

[2] W. H. Xu, Z. C. Ji, and Y. Wang, "A flower pollination algorithm for flexible job shop scheduling with fuzzy processing time," *Modern Physics Letters B*, vol. 32, no. 3, pp. 184–190, 2018.

[3] C. Wang, Z. C. Ji, and Y. Wang, "Multi-objective flexible job shop scheduling problem using variable neighborhood evolutionary algorithm," *Modern Physics Letters B*, vol. 31, no. 19–21, pp. 174–177, 2017.

[4] N. E. H. Tellache and M. Boudhar, "Flow shop scheduling problem with conflict graphs," *Annals of Operations Research*, vol. 261, no. 1-2, pp. 339–363, 2018.

[5] H. Ilani, E. Shufan, and T. Grinshpoun, "Partially concurrent open shop scheduling with integral preemptions," *Annals of Operations Research*, vol. 259, no. 1-2, pp. 157–171, 2017.

[6] X. Ning, P. Duan, W. Li, and S. Zhang, "Real-time 3D face alignment using an encoder-decoder network with an efficient deconvolution layer," *IEEE Signal Processing Letters*, vol. 27, pp. 1944–1948, 2020.

[7] W. Cai and Z. Wei, "PiiGAN: generative adversarial networks for pluralistic image inpainting," *IEEE Access*, vol. 8, pp. 48451–48463, 2020.

[8] X. Ning, K. Gong, W. Li, and L. Zhang, "JWSAA: joint weak saliency and attention aware for person re-identification," *Neurocomputing*, 2020.

[9] S. Zuo, I.-H. Hou, T. Liu, A. Swami, and P. Basu, "Joint rate control and scheduling for real-time wireless networks," *IEEE Transactions on Wireless Communications*, vol. 16, no. 7, pp. 4562–4570, 2017.

[10] V. Rostampour, O. T. Haar, and T. Keviczky, "Distributed stochastic reserve scheduling in AC power systems with uncertain generation," *IEEE Transactions on Power Systems*, vol. 34, no. 2, pp. 1005–1020, 2018.

[11] J. Shima, A. N. Behrouz, and S. T. A. Niaki, "Preemptive multi-skilled resource investment project scheduling problem; mathematical modelling and solution approaches," *Computers & Chemical Engineering*, vol. 96, no. 4, pp. 55–68, 2017.

[12] Z. J. Zhang, F. Hu, and N. Zhang, "Ant colony algorithm for satellite control resource scheduling problem," *Applied Intelligence*, vol. 48, no. 10, pp. 1–11, 2018.

[13] P. Wu, F. Chu, and A. Che, "Bi-objective scheduling of fire engines for fighting forest fires: new optimization approaches," *IEEE Transactions on Intelligent Transportation Systems*, vol. 4, no. 19, pp. 1140–1151, 2018.

[14] G. Li, C. Deng, J. Li, Q. Zhou, and W. Wei, "Deadline and period assignment for update transactions in co-scheduling environment," *IEEE Transactions on Computers*, vol. 66, no. 7, pp. 1119–1131, 2017.

[15] C. Lin, D. Han, J. Deng, and G. Wu, "P2S: a primary and passer-by scheduling algorithm for on-demand charging architecture in wireless rechargeable sensor networks," *IEEE Transactions on Vehicular Technology*, vol. 66, no. 9, pp. 8047–8058, 2017.

[16] X. Yu, J. Yang, and Z. Xie, "Training SVMs on a bound vectors set based on fisher projection," *Frontiers of Computer Science*, vol. 8, no. 5, pp. 793–806, 2014.

[17] L. Wang, J. Cai, and X. Shi, "Multi-objective flexible job shop energy-saving scheduling problem based on improved genetic algorithm," *Journal of Nanjing University of Science & Technology*, vol. 41, no. 4, pp. 494–502, 2017.

[18] X. Yu, Y. Chu, F. Jiang, Y. Guo, and D. Gong, "SVMs classification based two-side cross domain collaborative filtering by inferring intrinsic user and item features," *Knowledge-Based Systems*, vol. 141, pp. 80–91, 2018.

RETRACTED

Hindawi
Mobile Information Systems
Volume 2021, Article ID 5578476, 10 pages
https://doi.org/10.1155/2021/5578476

Research Article

Multimedia Interaction-Based Computer-Aided Translation Technology in Applied English Teaching

Hongxia Wu

Baotou Medical College, Baotou 014040, China

Correspondence should be addressed to Hongxia Wu; 102012078@btmc.edu.cn

Received 2 March 2021; Revised 20 March 2021; Accepted 26 March 2021; Published 10 April 2021

Academic Editor: Muhammad Usman

Copyright © 2021 Hongxia Wu. This is an open access article distributed under the Creative Commons Attribution License, which permits unrestricted use, distribution, and reproduction in any medium, provided the original work is properly cited.

Multimedia interaction-based computer-aided translation (CAT) is an effective method for translating massive multimedia applications. It is an essential English learning tool for college students with majors in multimedia technology. English teachers need to properly guide their students to use CAT technology by improving the students' English translation capabilities via reasonable setting of courses, selection of multimedia materials for teaching, and implementation of learning multimedia assessment. This paper proposes a semiautomatic evaluation method for a machine translation system based on fuzzy mathematics. It first discusses the characteristics of multimedia CAT software, describes its working principle, and proposes an optimization scheme suitable for translating teaching by analyzing its advantages and disadvantages. The author believes that only through the combination of multimedia interaction-based CAT teaching and traditional translation teaching we can better achieve the purpose of translation education to improve the quality and English-speaking talent.

1. Introduction

Multimedia interaction-based computer-aided translation (CAT) is developed from machine translation (MT). Based on MT, it can be translated by flexible human-computer interaction technology (HCI). It can also be called machine-aided translation (MAT) [1]. Broadly speaking, CAT refers to the operation of computer operating systems by interacting with multiple application software. CAT includes specialized translation software, e.g., SDL TRADOS, TransStar, and Yaxin, used to improve translation efficiency. At present, high-end computer-aided translation research and talent cultivation approaches are gathered in some internationally renowned institutions such as the Higher Education Institute of the Third University of Paris and the Translation Department of the Chinese University of Hong Kong [2]. In mainland China, there are not many colleges and universities that have adopted CAT technology, with the exception of Peking University and Beijing University of Aeronautics and Astronautics. The use of CAT technology in teaching is still a relatively new concept for most colleges and universities, and it has not been given enough attention [3].

The translation courses that are currently offered rarely involve the use of translation technology [4]. Therefore, it is necessary to briefly introduce the development of computer-aided translation [5]. Since the 1990s, CAT has experienced an early stage trial (early 40s and early 50s), a highly optimistic phase (mid of the mid-1950s), a decade of silence and stagnation (60–70s), the revival period (70s), and the transition period (80s to 90s). CAT was gradually accepted, and developers begin to provide translators' software operation platforms for professional translators. True CAT development is suitable for the early 1990s, such as SDL text processing, terminology management, and the emergence of translation memories. According to Professor Scott, the core of CAT technology is Translation Memory (TM). When the translator is working efficiently, CAT synchronizes the language database in backstage to complete the so-called translation memory [6]. Once the currently translated sentence has been translated, the computer will automatically provide the stored translation results. For similar sentences, translation references and suggestions will also be provided, and the translator can select, discard, or reedit the recurring according to the actual needs [7]. CAT provides

text that shortens the translation time and improves the translation efficiency. Another important component of CAT is terminology management. Broadly speaking, any vocabulary that appears in a translation can be saved as a term if it is necessary for repeated use and the set of terms that are saved becomes a term base. Term bases can also be reused, not only in this translation but also in future projects or other people's translation work, which not only improves the efficiency but more importantly, addresses translation consistency issues [8].

The rest of this paper is organized as follows. In Section 2, the literature review is provided. In Section 3, the application of multimedia interaction-based computer-aided translation technology along with its application to English translation teaching is discussed. This section also provides a detailed evaluation of the proposed approach. Finally, the paper is concluded, and future research directions are provided in Section 4.

2. Literature Review

Today, in addition to the leader Trados, the well-known CAT software includes DeJa Vu, Wordfast, Idiom, Catalyst, etc. In 1998, for the first time in China, CAT software was introduced from abroad [9]. The first domestic CAT software was known as Yaxin, and then Snowman, Wynn, and other companies have also designed their own versions of CAT software. The history of domestic translation software is only ten years old. With the development of science and technology, the computer operating system began to transition from one Windows to another, and the original command mode was converted to the current mode of graphics that is more convenient for users. The software development industry has also experienced an unprecedented competitive trend. In such a market environment, many old products such as Landau have faded out of people's horizons. At the same time, some new and more competitive translation software such as Kingsoft and Orient Express appeared. In 2014, Yan Yuxi, a computer-aided translation major at Peking University, conducted a network survey on the application of CAT software in the Chinese market. The results showed that there are four main types of software commonly used in China: Trados, Wordfast, Snowman CAT, and Yaxin CAT [10]. In this section, we explain the features and principles of multimedia interaction-based CAT in Section 2.1, the impact of multimedia interaction-based CAT on teaching objectives in Section 2.2, and finally, the impact of multimedia interaction-based computer-aided translation on teaching organizations in Section 2.3.

2.1. Features and Principles of Multimedia Interaction-Based CAT Software. CAT is the use of computer-aided manual translation, creating a translation process of human-computer interaction. Generalized CAT, including the integrated application of various computer operating systems and application software, involve paper text entry, editing, typesetting, storage, printing, backup, transmission, network resources, use of related electronic software, etc. The loosely coupled machine-assisted translation (MAT) is based on the principle of Translation Memory (TM) in the context of computer software [11, 12].

It is the technical core of machine-assisted translation, supplemented by other auxiliary translation methods such as electronic dictionary, terminology management, alignment tools, quality inspection, word count, text analysis, project management, and other application software systems. In actual translation activities, sentences in different documents are more or less duplicated. By recycling these translation resources, the goal of avoiding duplication of labor can be achieved. In order to make use of these resources, the machine first needs to divide the existing corpus into segments (usually sentences or a clause or phrase), align, and then add other information by the translation unit. The form is stored in the database, and the system automatically finds whether there are sentences in the library that are similar to the current segment, i.e., exact match and fuzzy match, through the similarity algorithm. The translation is used as a reference; if not, the translator can also find the translation of words in the sentence by cross-query.

The management of translation projects is also part of the translation of CAT technology [13, 14]. For a large workload and tight time translation, this requires several translators to assist in the division of labor. Inconsistent terminology may cause difficulties and incomprehensibility such as "details," "specifications," "instructions," etc.. When the project manager determines the unified terminology, it will not appear. Establish a matching mechanism for words, phrases, or sentences (matching), use the computer to complete the finished translation or the existing translation resources, and the translator grasps the quality of the translation and stores it in the memory. The most characteristic of CAT is a self-learning function [15]: the system automatically saves the translation result to the translation server. The next time the system encounters the same or similar sentences, it can refer to it or use it directly, saving the time for the translator to search the dictionary and input, thus effectively avoiding the emergence of the translation process. Repeated phenomena ensure the efficiency of translation. In addition, due to the continuous accumulation of translated corpora, it is more efficient to provide services for professional translators.

The essence of MT is to match the original text and the translated language through the corpus. This kind of translation principle makes the decisive factor of translation quality affected by two aspects: First, the richness of the back-end corpus. In other words, is there a translation in the corpus that corresponds to the input text? If not, it will not be translated. Second, whether the translation vocabulary in the translation machine is more suitable for the original text? It will determine the quality of the translation—the main advantage of CAT software results in the aforementioned two aspects. Software is popular among professional translators and is being applied to translation teaching. This kind of computer-assisted translation requires the users to have considerable foreign language knowledge so that the new model can train the English and translation ability of college students. In short, the quality of translation is mainly

controlled by professional translators. Therefore, computer-aided translation tools cannot determine the quality of translation. This translation software has no corpus at the beginning, just like newborn babies. The parallel corpus is the translation of commonly used related vocabulary and sentences as the translation volume of translators' increases.

2.2. Impact of Multimedia Interaction-Based CAT on Teaching Objectives. For a longer period of time, colleges and universities have different understandings of translation teaching, and they insist on different schooling characteristics. Therefore, these colleges and universities have different tasks for the translation curriculum. Undergraduate translation teaching in key institutions such as 211 and 985 (Chinese Projects) is more inclined to focus on students' testing and consolidation of foreign language knowledge, improve language application ability, literary translation ability, and TEM8 translation test. Students go to practice, and their goal is to send undergraduate students to higher education institutions for further study. Figure 1 shows the classic translation model. The undergraduate translation major of higher translation colleges in higher education institutions, in addition to testing and consolidating foreign language knowledge and improving language application ability, is more inclined to enable students to understand the concepts and rules of the translation profession and to master the ability and skills of bilingual transformation. The subject matter is also more focused on practical texts and is used to illustrate the difficulty and skill of text translation in real work environments and to improve students' ability to work in translation jobs. In comparison, the goal of translation teaching based on computer-assisted translation technology is clear, i.e., to cultivate a composite translation practical talent with a certain professional background and a good ability to translate Chinese and English with strong computer translation software application ability. From a professional background, students can choose legal text translation, business text translation, literary text translation, and political text translation according to their own interests and hobbies. They can choose to construct corresponding professional translation terms in the translation practice process. The libraries and translation memory lay a solid foundation for the translation of the relevant translation business after graduation so that students can smoothly enter the job role. Classic translation mode is shown in Figure 1.

2.3. Impact of Multimedia Interaction-Based Computer-Aided Translation on Teaching Organizations. Helping students understand and master various translation skills is one of the primary goals of translation teaching. Its high-level goal is to develop students' ability to analyze and solve problems by applying what they have learned in future translation practice and actual translation work. The teaching content of the translation course, based on computer translation technology, is similar to that of traditional translation teaching. Therefore, when organizing the translation practice course of CAT technology, students must understand the importance of cooperation between human translation and computer translation. Students need to build sound CAT thinking so that they can establish a sense of responsibility as a qualified translator and actively guide other students to clearly understand the translation activities under computer-assisted translation technology. In the process of teaching, students play the role of participants and researchers, while teachers act as pointers and promoters. Under the guidance of teachers, students should actively participate in classroom activities, study problems, analyze problems and apply what they have learned to solve problems. If students only passively and passively accept the knowledge imparted by teachers, they will not be able to understand the used and technical connotation of CAT in a true sense, let alone the actual development of students' translation practice ability. In the practice of translation under computer-aided technology, a qualified translator needs to have translation memory management skills, computer-assisted translation editing skills, translation project management skills, and high translation skills. Therefore, in the translation practice teaching using computer-aided translation technology, teachers should cultivate students' comprehensive translation ability from the following six aspects:

(1) Cognition and use of the CAT translation system, such as SDL TRADOS computer-assisted translation software;

(2) Understanding and acquisition of translation tools, such as corpus indexing software, translation memory entry, and translation corpus;

(3) Chinese and English bilingual language and cultural conversion ability;

(4) Chinese and English editing ability of translation results;

(5) Translation memory translation terms and content translation ability;

(6) Computer, office software, and other operational capabilities: In the process of teaching organization, a combination of theory and practice should be adopted to enable students to master the theoretical basis, operational principles, operational methods, etc., of computer-aided translation systems in a relatively short period of time. In short, theoretical teaching is the guiding and paving, and specific exercises and applications should occupy a larger part of the curriculum. When students are familiar with and use the relevant computer-assisted translation technology system, the teaching organization should focus on the methods that teachers teach and practice with students.

3. The Application of Multimedia Interaction-Based Computer-Aided Translation Technology in Applied English Translation Teaching

In this section, we discuss the application of multimedia interaction-based CAT technology for English translation.

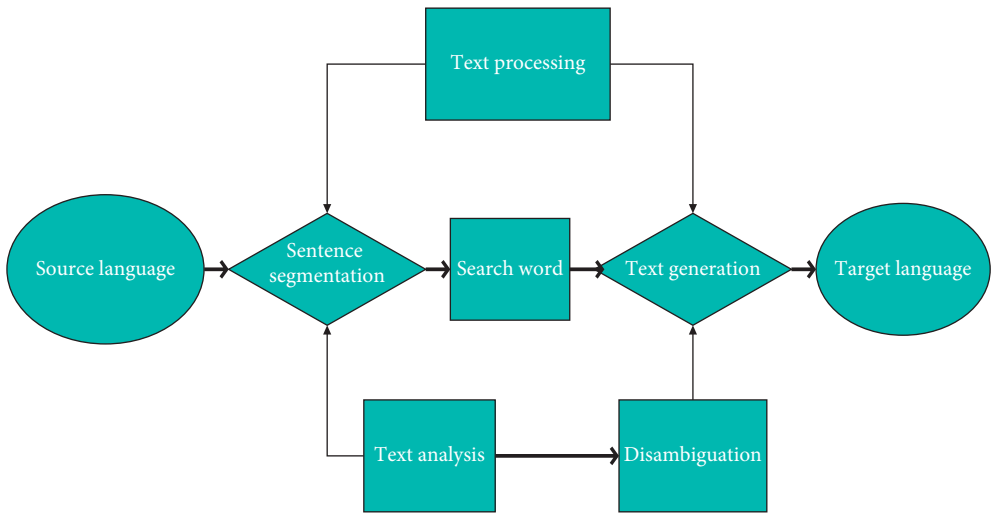

Figure 1: Classic translation mode.

First, we will discuss the translation process in translation teaching followed by curriculum sitting, its preparation before classes, teaching implementation, and assessment of learning effectiveness.

3.1. Multimedia Interaction-Based CAT Software Translation Process in Translation Teaching. CRACIUNESCU believes that the thinking of the human brain is roughly divided into three levels: pragmatic layer, semantic layer, and syntactic layer.

The functions of these three levels are as follows:

(1) *Semantic layer*. There is no simple dictionary translation for the meaning of context and the context of the article.

(2) *Syntactic layer*. Understand the meaning of vocabulary in sentences.

(3) *Pragmatic layer*. It has the meaning of context and the context of the article and understands the human meaning of the vocabulary.

Nowadays, computers can basically understand the semantic layer through simple mechanics. Due to the application of parallel corpora, computer-aided translation software can process large data. Therefore, the translation of the computer also has a certain syntax layer function.

3.1.1. CAT Issues in Applied Teaching. Computer-assisted translation is used for auxiliary translation because the meaning of the language is different in different moods and contexts. Auxiliary translation has studied the following issues.

(1) How to ensure the intelligence and automation of translation in the process of using CAT technology by translators and teachers.

(2) How can I use CAT software to improve the quality and efficiency of manual assisted translation?

(3) How to manage the overall translation process of CAT technology so that the quality of human translation is adequately guaranteed.

In order to solve the above problems, experts began to design computer-aided translation software with the following functions: First, the software translation library is managed to provide translators with more convenient operations, thereby increasing the speed of translation. Secondly, it provides the ability to automatically search the database. Third, in order to achieve better translation quality, the translation results should be tested.

3.1.2. CAT Roles in Applied Teaching. Compared with the traditional translation process, computer-aided translation software is unique because the computer actively participates in the work of landscaping. In the whole process of translation, the role of computer-aided translation software is mainly reflected in the following aspects:

(1) Searching the corpus in the system to provide better choices for translators.

(2) Searching the database of the whole system looking for a similar statement.

(3) The translator's translation results are stored in the parallel corpus corresponding to the term corpus, and the terms specified by the translator are stored in the term corpus.

It can be seen that the computer-assisted translation software mainly helps professional translators to perform "memory" in the whole process of translation, thereby improving the translation efficiency of professional translators. Therefore, this system is also called the TM system-Translation Memory system [9]. Through the translation memory system to establish a matching mechanism of words, phrases, or sentences (Matching, the use of computers to complete the finished translation, or the existing translation resources, the translator grasps the quality of

translation, stored in the memory, the system is the most distinctive). It is a self-learning function of CAT. The system automatically saves the translation result to the translation server. The next time you encounter the same or similar sentences, you can refer to it or use it directly, saving the time for the translator to check the dictionary and entry, thus effectively avoiding the translation process. Repeated phenomena appear to ensure the efficiency of translation.

3.2. Curriculum Setting. There are two types of computer-aided translation technology teaching modes: one is an additional activity type, i.e., students mainly learn computer-aided translation technology through network environment outside the classroom, and the teachers regularly guide. The one is comprehensive type, i.e., the combination of traditional teaching methods and computer-assisted translation technology teaching. Teachers develop computer-aided translation technology learning plans to guide, supervise, and evaluate students' learning outcomes. Teachers use network resources to make reasonable settings for the target course. When choosing a web resource, consider whether the selected material is conducive to improving the student's translation skills and to what extent. Teachers should develop a computer-aided translation technology syllabus, including subject selection, classroom organization, teaching methods, and student English level assessment. The structural diagram of translation classroom teaching mode is shown in Figure 2.

3.3. Preparation before Class. Preparations include browsing the website in advance, selecting translation learning information suitable for students and related task content, and arranging different learning materials according to different learning ability of students.

Before the class, the teacher recorded the language learning knowledge points into the microcourse video, and the corresponding courseware, exercises, and other resources were provided to the learners through the learning cloud space. At the same time, teachers design learning activities based on learning cloud space, students participate in online learning activities, exercise exercises, and summarize learning gains and confusion to prepare for the offline classroom. Teachers provide tutoring to students' online learning activities and design classroom activities in combination with students' preclass learning.

3.4. Teaching Implementation. The teacher should clearly indicate the teaching objectives and teaching contents of this lesson, and then arrange the students to complete the teaching tasks independently or cooperatively according to the actual teaching content.

In the classroom, teachers make breakthroughs in language knowledge points according to the preclass students' learning situation and analyze and discuss students' learning confusion and problems. Communicate, organize students to carry out skills training such as listening, speaking, and reading. Through the teaching activities such as skills training, communication and reporting, problem solving and self-assessment, and mutual evaluation, students will internalize the teaching content of language knowledge, listening, speaking, reading, and writing skills.

3.5. Assessment of Learning Effectiveness. The assessment of the learning outcomes of students can test the learning outcomes of students and test whether students can use computer-assisted translation techniques reasonably and effectively. After class, teachers will provide solid learning based on students' classroom performance. Materials investigate learning effects and improve instructional design and summarize the teaching. Students use the materials provided by the teacher to study, so as to check the lack of knowledge points and at the same time conduct summary and feedback evaluation.

3.5.1. Using the Analytic Hierarchy Process to Construct an Evaluation Model Hierarchy. The evaluation of translation quality considers three main factors: "vocabulary," "grammar," and "discourse." Vocabulary is examined from three aspects: lexical collocation, rhetoric, terminology, and dialect use; grammar mainly examines whether the grammar of the translation is correct; text includes cohesiveness, coherence, intent, and acceptability. The evaluation system structure is shown in Figure 3. As can be seen from Figure 3, A indicates the target layer machine translation evaluation and the criterion layer three indicators. It is represented by C_i ($i = 1, 2, 3$), and each indicator in the criterion layer is set up with its own subindicators. The three indicators can be further divided. Therefore, this paper determines each by establishing an Analytic Hierarchy Process (AHP) model. The weight of indicators in the machine translation evaluation architecture provides a reference for the application of applied English teaching. The evaluation system structure formed by Delphi technology is used to summarize the results of expert consultation, and the following judgment matrices are obtained after processing. Each value in the row represents the relative importance value of the indicator of the row to the index of the column in question and is represented by the quantitative relationship.

3.5.2. Establishing a Judgment Matrix. Prof. Satie's metric method gives quantitative comparisons for different comparisons, as shown in Table 1.

According to the hierarchical structure of Figure 1, applying the method of representation of Prof. Satie, through a questionnaire survey of some teachers and experts of the school, according to the generation method and structural characteristics of the judgment matrix, establishes a comparative judgment matrix for each level of the evaluation system, as shown in Tables 2–5.

3.5.3. Single-Level Sort of Weight. The relative importance value of each factor is determined by a given matrix, and the weight is calculated for each index in its determined weight matrix calculation using the following steps:

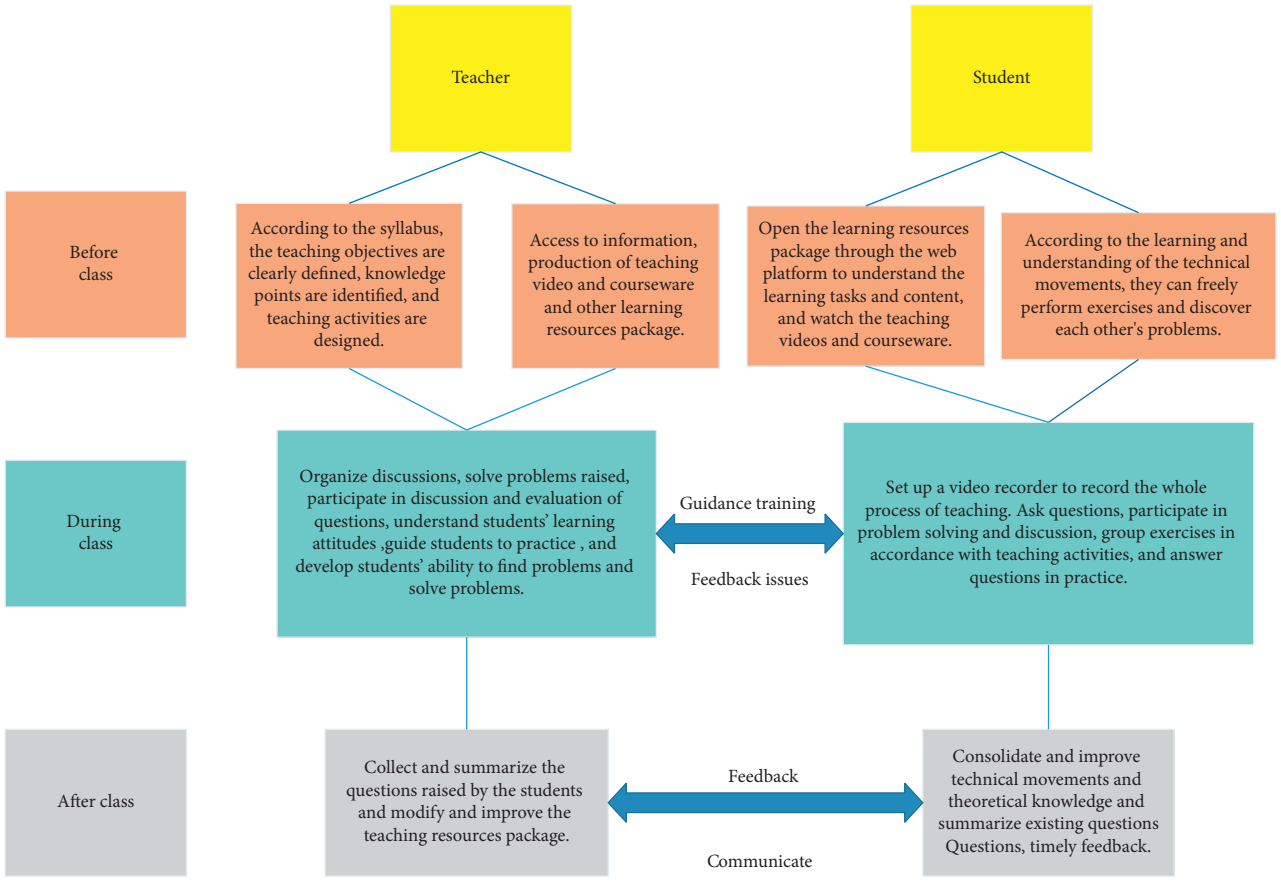

Figure 2: The structural diagram of translation classroom teaching mode.

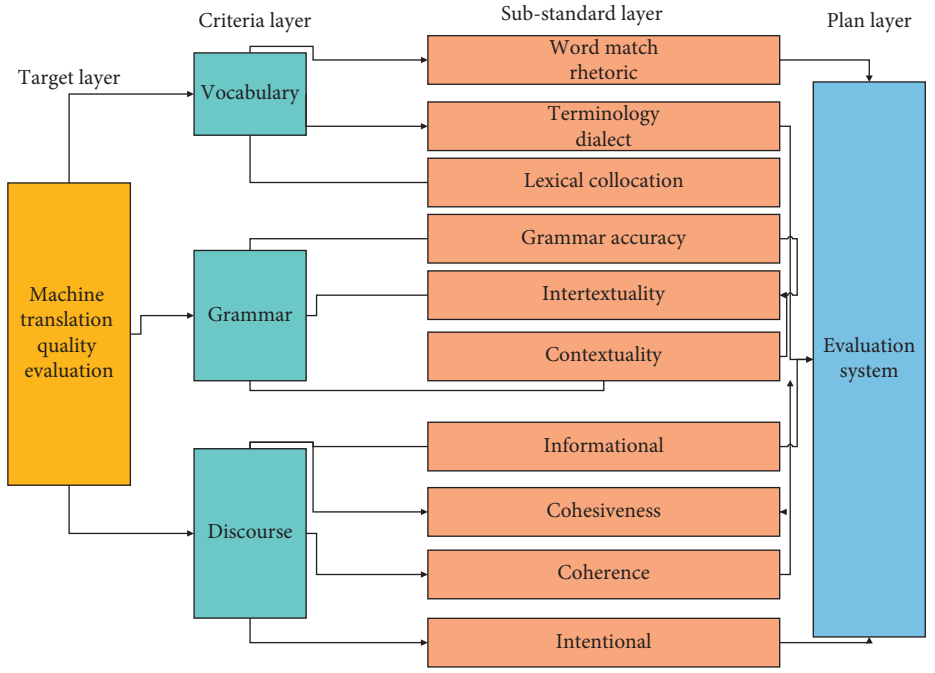

Figure 3: Machine translation evaluation architecture.

(1) Multiplication of matrix elements by rows

$$M_i = \prod_{j=1}^{n} aij, \quad i = 1, 2, \cdots, n. \tag{1}$$

(2) Calculate the weight value

$$W_i = \frac{M_i}{\sum_{j=1}^{n} M_j}, \quad i = 1, 2, \cdots, n. \tag{2}$$

From the judgment matrix A, the weights of B1, B2, and B3 can be calculated. That is, the weights of innovation consciousness, innovation personality, and innovation ability in the criterion layer for the target layer "the translation quality was evaluated" can be determined, and the calculated weight vectors can then be calculated. Fill in Table 2, respectively; get the weight vector of the three criterion factors for the target layer. Similarly, calculate the weight vector of the judgment matrix B1, B2, B3, and fill in the results in Tables 3–5.

3.5.4. Consistency Check of the Judgment Matrix. In order to scientifically reflect the relative importance of each index [15], after the weight vector of the judgment matrix is obtained, the consistency of its validity must be tested. The specific inspection steps are as follows:

(1) Multiply the judgment matrix by its corresponding weight vector.

(2) Calculate the maximum eigenvalue of the judgment matrix.

(3) Calculate the consistency index CI and select the average random consistency index RI. Among them,

$$\mathrm{CI} = \frac{\lambda_{\max} * n}{n - 1}. \tag{3}$$

(4) Calculate the consistency index ratio:

$$\mathrm{CR} = \frac{\mathrm{CI}}{\mathrm{RI}}. \tag{4}$$

The length of the international trade data to be encrypted is defined as n, followed by the standard normal distribution function, the key extension sequence $X = x_1, x_2, ..., x_n$, and the statistics of the binomial and Hof of the encrypted bit sequence $S_n = x_1 + x_2 + ... + x_n$, and the characteristic recombination output of the encrypted data in international trade is obtained as follows:

$$\mathrm{Decrypt}(sk, c^*)AA^{-1} = \begin{pmatrix} t_{1,1} & \cdots & t_{1,m} \\ \vdots & \ddots & \vdots \\ t_{m,1} & \cdots & t_{m,m} \end{pmatrix} = E. \tag{5}$$

The stochastic linear processing model of encrypted data in international trade is constructed by using the MIMO hybrid precoding method. The public key encrypted plaintext sequence of international trade data is obtained by constructing the Hash function.

$$\mathrm{Decrypt}(sk, c^*)A^{(\alpha_1, \cdots, \alpha_m)}\mathrm{Decrypt}(sk, c^*)\left(A^{-1}\right)^{\left(\alpha_1^{-1}, \cdots, \alpha_m^{-1}\right)^T} = \begin{pmatrix} \alpha_1 a_{1,1} & \cdots & \alpha_m a_{1,m} \\ \vdots & \ddots & \vdots \\ \alpha_1 a_{m,1} & \cdots & \alpha_m a_{m,m} \end{pmatrix}\begin{pmatrix} {\alpha_1}^{-1} t_{1,1} & \cdots & {\alpha_1}^{-1} t_{1,m} \\ \vdots & \ddots & \vdots \\ {\alpha_m}^{-1} t_{m,1} & \cdots & {\alpha_m}^{-1} t_{m,m} \end{pmatrix} = E. \tag{6}$$

Gram–Schmidt orthogonal vector quantization method is used to construct the Turbo code model of international trade data. The Turbo code model is obtained as follows:

$$\mathrm{Decrypt}(sk, c^*)\left(A^{(\alpha_1, \cdots, \alpha_m)}\right)^{-1} = \begin{pmatrix} {\alpha_1}^{-1} t_{1,1} & \cdots & {\alpha_1}^{-1} t_{1,m} \\ \vdots & \ddots & \vdots \\ {\alpha_m}^{-1} t_{m,1} & \cdots & {\alpha_m}^{-1} t_{m,m} \end{pmatrix} = \left(A^{-1}\right)^{\left(\alpha_1^{-1}, \cdots, \alpha_m^{-1}\right)^T}. \tag{7}$$

(5) To determine the value of CR is determined based on whether a matrix consistency test by. The conformity test evaluation table is shown in Table 6.

By calculation, the CR values of the judgment matrix A, B1, B2, and B3 are all less than 0.1 and they have satisfactory consistency. It is concluded that they are all valid matrices, and the values of $\lambda_{\max}$, CI, and CR are entered in Tables 2–5.

3.5.5. Hierarchical Total Sorting. Figure 4 shows the development of CAT in recent years. Index System of Quality

Table 1: Correspondence table for quantitative comparison.

Degree a_{ij}	Definition	Explanation
1	Equally important	The i element is as important as the j element
3	Slightly important	The i element is slightly more important than the j element
5	Obviously important	The i element is significantly more important than the j element
7	Much more important	The i element is much more important than the j element
9	Extremely important	The i element is more important than the j element
2 4 6 8	Between the above adjacent judgments	For the above two judgments of the compromise
The above number is reciprocal	Reverse comparison	i and j elements

Table 2: Judgment matrix A.

A	B1	B2	B3	W	Consistency check indicator
B1	1	1/3	1/2	0.16	$\lambda_{max} = 3.001$
B2	3	1	2	0.54	CI = 0.005
B3	2	1/2	1	0.30	CR = 0.0086 < 0.1

Table 3: Judgment matrix B1.

B1	C1	C2	C3	W	Consistency check indicator
C1	1	1/3	1/5	0.11	$\lambda_{max} = 3.000$
C2	3	1	1/2	0.31	CI = 0.002
C3	5	2	1	0.58	CR = 0.0034 < 0.1

Table 4: Judgment matrix B2.

B2	C4	C5	C6	C7	W	Consistency check indicator
C4	1	1/2	2	2	0.26	$\lambda_{max} = 4.000$
C5	2	1	4	4	0.50	CI = 0
C6	1/2	1/4	1	1	0.13	CR = 0.4 < 0.1
C7	1/2	1/4	1	1	0.14	

Table 5: Judgment matrix B3.

B1	C8	C9	C10	W	Consistency check indicator
C8	1	1/3	1/5	0.11	$\lambda_{max} = 3.004$
C9	3	1	1/2	0.31	CI = 0.002
C10	5	2	1	0.58	CR = 0.0034 < 0.1

Table 6: Conformity test evaluation table.

CR	Result
CR = 0	Completely satisfactory consistency
CR < 0.1	With satisfactory consistency
CR > 0.1	Need to reevaluate relative importance until CR < 0.1 is satisfied

Evaluation Model for Innovative Talents Cultivation is shown in Table 7.

The weight of each factor indicator is shown in Figure 5.

It can be seen from Figure 5 that the talent evaluation index changes with the change of factor level, and there is a certain correlation between various factors, which requires us to take into full consideration when translating English, and only after we fully understand the meaning can we translate.

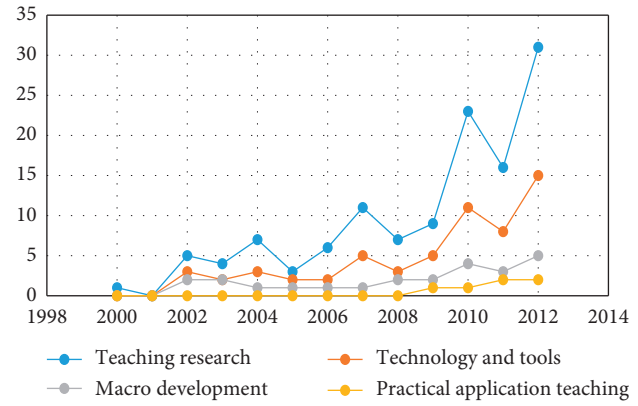

Figure 4: Trend of the number of documents in each theme in China is changing year by year.

Table 7: Index system of quality evaluation model for innovative talents cultivation.

Target layer A	Criterion level B	Factor layer C	The weight of each factor index
The evaluation of translation quality A	Vocabulary B1	Rhetoric C1	0.02
		Dialect use C2	0.05
		Lexical collocation C3	0.10
	Discourse B2	Cohesiveness C4	0.14
		Coherence C5	0.27
		Intentional C6	0.01
		Acceptability C7	0.01
		Contextuality C8	0.03
	Grammar B3	Intertextuality C9	0.10
		Grammar C10	0.18

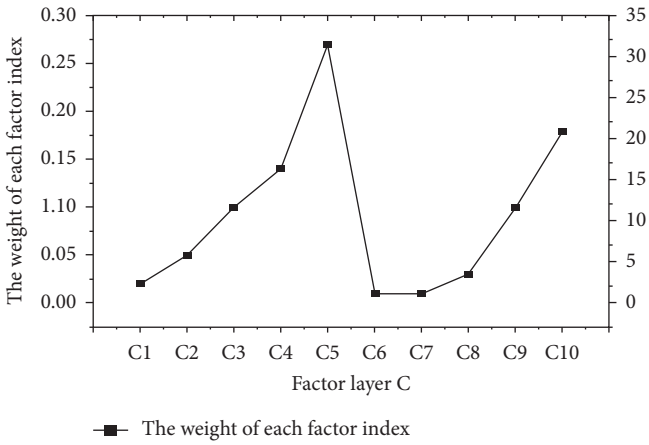

Figure 5: The weight of each factor indicator.

4. Conclusion

Today, with the development of the Internet, our translation and interpretation teaching will inevitably use new tools and technologies. Whoever takes the first step and whoever takes the lead can obtain new resources. English translation trains talents that are technical rather than academic. According to the survey of the translation industry, various types of CAT software have long been the core tools of front line practitioners in translation work. Therefore, CAT enters the translation of this practical professional curriculum system, which can rightly be considered as part of the course. As China becomes more integrated into the process of internationalization and the increasingly close international exchanges and cooperation, it has provided an unprecedented opportunity for the development of the translation market, and the development of the translation market has also fostered the cultivation of talents, especially English undergraduate applicants. The cultivation of typed translation talents raises the requirements for new and higher staff members. A good translator should have not only good translation skills but also be good at using translation techniques to complete translation tasks more efficiently. This paper proposes a semiautomatic evaluation method for a machine translation system based on fuzzy mathematics. Compared with the manual evaluation method, the proposed method is not only fast but also greatly reduces the workload of the evaluation, and the evaluation process is more objective, reducing the influence of subjective factors on the evaluation results. This method can evaluate the quality of a certain aspect of a system and can also compare the quality of different systems. These results can be used as a training sample for another neural network-based machine translation evaluation method. The established neural network evaluation system can evaluate any machine translation system automatically, conveniently, objectively, and quickly.

Data Availability

The data used to support the findings of this study are available from the corresponding author upon request.

Conflicts of Interest

The author declares that she has no conflicts of interest.

References

[1] M. Ivleva and E. Melekhina, "Cloud platform SmartCAT in teaching future translators," *Linguistic and Cultural Studies: Traditions and Innovations*, vol. 20, no. 5, pp. 155–160, 2005.

[2] J. Jianpin, "Eight factors applied in teaching English listening," *School English*, vol. 6, pp. 4-5, 2016.

[3] Z. Pei, "Classroom discourse in college English teaching of China: a pedagogic or natural mode?" *Journal of Multilingual & Multicultural Development*, vol. 36, no. 7, pp. 694–710, 2015.

[4] A. D. Adamson, "Prototype schemas, variation theory, and the structural syllabus," *IRAL - International Review of Applied Linguistics in Language Teaching*, vol. 28, no. 1, pp. 1–26, 1990.

[5] R. A. Berman, "Rule of grammar or rule of thumb?" *IRAL - International Review of Applied Linguistics in Language Teaching*, vol. 17, no. 1, pp. 279–302, 1979.

[6] G. P. Berent, V. J. Samar, and I. Parasnis, "College teachers' perceptions of English language characteristics that identify English language learning disabled deaf students," *American Annals of the Deaf*, vol. 145, no. 4, pp. 342–358, 2000.

[7] L. Sun, Z. H. Lin, and W. University, "The application of CAT techniques:an investigation based on the undergraduates majoring in translation," *Foreign Language Research*, vol. 32, p. 25, 2016.

[8] X. H. Zhou, "Functional analysis of snowman CAT standard edition translation software based on the normal distribution

and similarity model," *Applied Mechanics and Materials*, vol. 427-429, no. 7, pp. 2073–2077, 2013.

[9] M. Fishel, R. Sennrich, M. Popović, and O. Bojar, "TerrorCat: a translation error categorization-based MT quality metric," in *Proceedings of The Workshop on Statistical Machine Translation*, pp. 64–70, Montreal, Quebec, Canada, June 2012.

[10] A. Beeby, M. Fernández, O. Fox et al., "Investigating translation competence: conceptual and methodological issues," *Meta:Translators' Journal*, vol. 50, no. 2, pp. 609–619, 2015.

[11] Y. Sun and M. Tian, "Research and practice of computer-assisted Japanese intensive reading education," *Journal of Physics: Conference Series*, vol. 1648, no. 3, p. 032164, 2020.

[12] C. Li and H. Zhang, "The application of computer aided translation in practice—taking the Chinese-English translation of tourism texts in hetao region as an example," *Journal of Physics: Conference Series*, vol. 1693, no. 1, p. 012005, 2020.

[13] X. Wang, "A study on project-based computer aided translation courses from perspective of language services," *International Core Journal of Engineering*, vol. 6, no. 7, pp. 261–266, 2020.

[14] D. Man, A. Mo, M. H. Chau, J. M. O'Toole, and C. Lee, "Translation technology adoption: evidence from a post-graduate programme for student translators in China," *Perspectives*, vol. 28, no. 2, pp. 253–270, 2020.

[15] L. Tian and C. Zhu, "Making connections through knowledge nodes in translator training," *International Journal of Translation, Interpretation, and Applied Linguistics*, vol. 2, no. 2, pp. 15–29, 2020.

Hindawi
Mobile Information Systems
Volume 2021, Article ID 5512382, 7 pages
https://doi.org/10.1155/2021/5512382

Research Article

Multilabel CNN-Based Hybrid Learning Metric for Pedestrian Reidentification

Yinjun Zhang,[1] **Ryan Alturki**,[2] **Hasan J. Alyamani**,[3] **Mohammed Abdulaziz Ikram**,[4] **Ateeq ur Rehman**,[5] **and Muhammad Haleem**[6]

[1]*School of Mechanical and Electrical Engineering, Guangxi Science & Technology Normal University, Laibing, China*
[2]*Department of Information Science, College of Computer and Information Systems, Umm Al-Qura University, Mecca, Saudi Arabia*
[3]*Department of Information Systems, Faculty of Computing and Information Technology, King Abdulaziz University, Rabigh, Saudi Arabia*
[4]*Computer Science Department, University College in Al-Jamoum, Umm Al-Qura University, Mecca, Saudi Arabia*
[5]*Department of Computer Science, Abdul Wali Khan University Mardan, Mardan 23200, Pakistan*
[6]*Department of Computer Science, Faculty of Engineering and Technology, Kardan University Kabul, Kabul, Afghanistan*

Correspondence should be addressed to Muhammad Haleem; m.haleem@kardan.edu.af

Received 7 February 2021; Revised 8 March 2021; Accepted 24 March 2021; Published 5 April 2021

Academic Editor: Nicola Bicocchi

Copyright © 2021 Yinjun Zhang et al. This is an open access article distributed under the Creative Commons Attribution License, which permits unrestricted use, distribution, and reproduction in any medium, provided the original work is properly cited.

Pedestrian reidentification has recently emerged as a hot topic that attains considerable attention since it can be applied to many potential applications in the surveillance system. However, high-accuracy pedestrian reidentification is a stimulating research problem because of variations in viewpoints, color, light, and other reasons. This work addresses the interferences and improves pedestrian reidentification accuracy by proposing two novel algorithms, pedestrian multilabel learning, and investigating hybrid learning metrics. First, unlike the existing models, we construct the identification framework using two subnetworks, namely, part detection subnetwork and feature extraction subnetwork, to obtain pedestrian attributes and low-level feature scores, respectively. Then, a hybrid learning metric that combines pedestrian attributes and low-level feature scores is proposed. Both low-level features and pedestrian attributes are utilized, thus enhancing the identification rate. Our simulation results on both datasets, i.e., CUHK03 and VIPeR, reveal that the identification rate is improved compared to the existing pedestrian reidentification methods.

1. Introduction

In recent years, pedestrian reidentification emerges as a hot research topic. It has attained considerable attention since it can be applied to many potential applications in human-computer interaction and surveillance tasks. The purpose of pedestrian reidentification algorithms is to search and detect a target from a large set of images. Various cameras capture these images for detecting a target image, where an image or a video sequence can represent the target person. The pedestrian reidentification algorithm is imperative in the development of an automatic video surveillance system. Pedestrian reidentification is an especially difficult topic due to tremendous variations in viewpoints, human poses, light, and other factors. These impacting factors are likely to make two independent images of a single person look quite different. On the contrary, these factors can also make some people's images look pretty similar, creating great difficulties for the identification algorithms. The previous works [1, 2] mainly aim to eliminate the impacts of interference and build a reliable pedestrian reidentification algorithm with solid robustness.

The existing pedestrian reidentification algorithms have two major types, namely, supervised learning and unsupervised learning. For supervised learning-based approaches [3, 4], the work presented in [1] used a deep convolutional neural network (CNN) for learning features continuously, and the resultant matching metrics used in reidentification of individuals

expressively increase the precision of the state-of-the-art model. The authors in [3] presented indiscriminative reinforcement lean strategies and multi-instance multilabel learning methods to solve the pedestrian reidentification within a short-term surveillance system. As for unsupervised learning-based pedestrian reidentification algorithms [5–7], the authors in [5] presented a progressive unsupervised learning (PUL) method for transferring the pretrained model's deep representations to unseen domains. In [6], a transferable approach simultaneously learnt the attribute-semantic and identity-discriminative feature space transferred to new fields for reidentification tasks without new labeled data.

The first significant challenge in designing pedestrian reidentification algorithms is the weak capability to effectively extract and match the features from different views and select mutual patterns. However, one image's features may not necessarily appear the same in the target image due to the pose change caused by view difference [8, 9]. Hence, extracting, embedding, and evaluating features from different image domains are critical in developing a high-performance pedestrian reidentification framework. The other challenge is how to select a good metric that measures the similarity of various features within sampled images, which is the most crucial part of the training process of CNN models. A good metric can increase the learning efficiency of CNN models during training, thus improving the recognition performance.

This work improves pedestrian reidentification by adopting pedestrian multilabel learning and investigating hybrid learning metrics. The contributions of this paper are twofold. First, two subnetworks, namely, part detection subnetwork and feature extraction subnetwork, are used to obtain pedestrian attributes and low-level feature scores. A hybrid learning metric that combines pedestrian attributes and low-level feature scores is proposed to enhance the performance. The experiment results validate the performance of the proposed framework.

The remainder of this paper is in accordance with the following pattern. Section 2 introduces previous works related to pedestrian reidentification. Section 3 describes the proposed multilabel learning algorithms with enhanced learning metrics. Section 4 illustrates the experimental setup and experimental results to validate the performance of the proposed algorithms. Finally, Section 5 concludes the paper.

2. Related Work

This section describes the literature from two different perspectives: pedestrian reidentification using traditional approaches and pedestrian identification using machine learning approaches.

2.1. Pedestrian Reidentification. Pedestrian reidentification can be viewed as the problem of identifying pedestrians from different images captured by different cameras. Figure 1 illustrates some example images of pedestrians captured by using real cameras in the CUHK03 [9] dataset. Pedestrian reidentification typically involves two parts: extracting features from input images and comparing the extracted features' metrics to obtain the rank list. From these two aspects, the previous works on pedestrian reidentification mainly aim at two factors: developing new learning metrics [10, 11] and developing new feature representations [12]. These schemes are used to combat the variations of viewpoint, pose, and color.

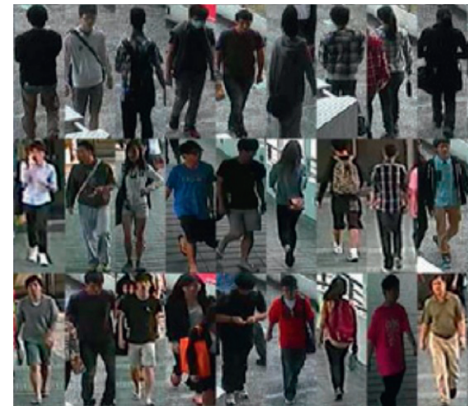

Figure 1: Example images of pedestrians from the CUHK03 [9] dataset.

2.2. Deep Learning-Based Pedestrian Reidentification. With deep learning algorithms' resurgence, deep neural networks [7, 13] have witnessed great success in many fields, especially computer vision tasks. CNNs can extract low-level features while learning more abstract information, including detailed texture and geometry patterns. Based on self-built CNN models, several deep learning methods [1, 2, 9] have been presented to realize pedestrian reidentification tasks and have shown promising performance improvement compared to traditional handcrafted features.

3. The Proposed Pedestrian Multilabel Learning Algorithms

This section introduces proposed algorithms for pedestrian multilabel learning, which includes a part detection subnetwork. Then, the other subnetwork performs feature extraction for the input and evaluates the similarity of two given images. As mentioned above, both subnetworks receive the input paired images and process them in a parallel manner. The following sections describe associated algorithms in detail.

3.1. Overview. The problem of pedestrian reidentification can be described in a similar way to object recognition. The conventional reidentification algorithm takes two input images; each image usually involves the pedestrian's whole body. The identification algorithm outputs the similarity metric between the given images, which shows the probability that the two images depict the same or different people.

The existing frameworks [1, 2, 4, 5] typically utilize bottom-up image cues and end-to-end learning for reidentification. These works improve the performance and accuracy of pedestrian reidentification mainly through two aspects. The first aspect is to design learning architectures

[1, 2], thus enhancing the feature extraction abilities of reidentification models. The second aspect is to develop efficient evaluation metrics [4, 5] and precisely evaluate the distance between correct and trained results, thereby improving the learning capabilities.

One critical problem that limits the performance of conventional pedestrian reidentification is that these works fail to utilize the small semantic parts that contain crucial information of pedestrian attributes, such as hair color and gender. The conventional pedestrian reidentification algorithms mainly emphasize bottom-up image indications while neglecting small semantic parts, thus losing physical pedestrian attributes. Moreover, some of these attributes have local characteristics. Due to the variation of viewpoints and other impacting factors, the failure of taking advantage of this information may become the performance bottleneck. According to the previous works on semantic part detection [14], the pedestrian's multiple attributes can be used to describe and improve the overall accuracy.

Inspired by the multilabel CNN model [15] and part detection approaches [14], we design a pedestrian multilabel learning framework to tackle fine-grained pedestrian attribute recognition. Figure 2 shows the proposed framework of pedestrian reidentification with the aid of multilabel learning. The processes of proposed pedestrian multilabel learning are carried out as follows:

(1) First, the input image passes the part detection subnetwork, responsible for dividing the predefined body parts. A fully connected (FC) layer will calculate the attribute scores associated with divided body parts after the split body parts are flattened.

(2) Then, the same input image passes the feature extraction subnetwork, which extracts the low features hidden in the image. The low-level feature similarity will be calculated by an FC layer similar to the attribute scores in Step 1.

(3) Finally, after the attribute scores and low-level feature similarity scores are obtained, the gallery images will be ranked according to the two metrics.

3.2. Part Division. According to Zhang et al. [14], body movements and other factors may cause the popularly used universal feature illustration approaches to agonize from misalignments. Hence, combating and eliminating the interference that arose from camera viewpoints' variations becomes a challenging task for body part division tasks. The previous work [15] solved this problem by dividing the given image into 15 overlapping areas. Several softmax classifiers were then used to compute various body parts' regression and then obtain the attribute scores. However, there are two defects in this method. Firstly, the positions of the human body part vary in various images. The handcrafted division of areas may not accommodate all the cases, thus resulting in inaccurate body parts. Secondly, the 15 overlapping body parts need to pass multiple CNNs, which requires a considerable amount of computational complexity and makes this scheme inefficient.

We use another body part division scheme to improve the efficiency as well as accuracy. Similar to [14], we adopt a body part detector, named the part detection subnetwork in Figure 2. The part detection subnetwork integrates the state-of-the-art semantic model, R-CNN [16], to detect each body part region. Detecting every part of the human body is difficult since the resolution of images in an existing dataset, such as CUHK03 [9], is low. Hence, we let the part detection subnetwork only find those parts associated with human hair and clothing. Assuming that there are m parts to be detected, the part detection subnetwork has $(m + 1)$ parallel output labels, consisting of m body parts and one gender label, indicating male or female. Based on the loss of R-CNN [16], the part detection subnetwork is trained and optimized using the following multitask loss L_{part}:

$$\mathscr{L}_{\text{part}} = \mathscr{L}_{\text{class}}(s, c) + \lambda[c > 0] \cdot \mathscr{L}_{\text{loc}}\left(b^r, b^{\text{true}}\right), \tag{1}$$

where $s \in [0, 1]$ denotes the confidence score for each regressed bounding box b, which is the output of the part detection subnetwork. $c \in [0, m]$ is the ground-truth class of the body part bounding box, while $\mathscr{L}_{\text{class}}$ represents the loss of the ground-truth class. Besides, $\mathscr{L}_{\text{loc}}$ denotes the loss function for the regressed bounding box for each body part. b^{true} is the ground-truth result, while b^r represents the regressed bounding box of the true class.

The FC layer in Figure 2 acts as the classifier for the feature vector of the body part. As the concatenation fully connected layer in [14], we use the following matrix-vector multiplication and nonlinear activation to compute the combination of various body parts and realize fine-grained classification:

$$y = f\left(\sum_{i=1}^{m+1} \mathbf{W}_i \cdot \mathbf{x}_i\right), \tag{2}$$

where $\mathbf{W}_i$ represents the weight matrix for the i^{th} body part. The feature vector of the i^{th} body part is stored in a vector $\mathbf{x}_i$.

3.3. Learning Metrics. Unlike the conventional frameworks that only compare the extracted low-level features, the extracted attribute scores and low-level feature similarity scores from two subnetworks are aggregated to evaluate the given images' similarity. Pedestrian reidentification algorithms will return a list where the gallery images are ranked by their distances between the probe image and the gallery images. The higher the ground-truth gallery images are ranked, the higher the accuracy is achieved.

The total loss function of the proposed framework is composed of two parts. The first one is the softmax function that computes the loss of all pedestrian attributes. The second part is the cost from the low-level feature similarity. The following equation gives the total loss function:

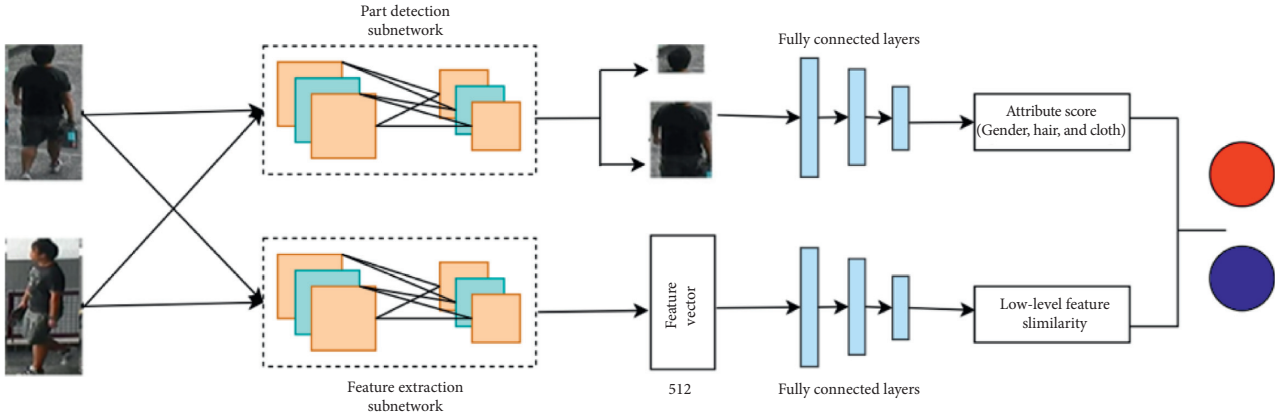

Figure 2: The proposed framework of pedestrian reidentification with the aid of multilabel learning.

$$\mathscr{L}_{ML} = \sum_{i=1}^{I} \lambda_i L_i + \alpha\left(L_p - L_g\right)^T \left(L_p - L_g\right), \tag{3}$$

where L_i denotes the loss of the i^{th} attribute, while I is the total number of features. λ_i denotes the parameter that defines the contribution of the i^{th} attribute. Without an explicit statement, the value of λ_i is $1/I$ which means each attribute contributes equally. L_p and L_g denote the low-level features of given probe images and gallery images, respectively.

The metric L_i in equation (3) is expanded as follows:

$$L_i = -\frac{1}{N} \sum_{n=1}^{N} \sum_{m=1}^{M^i} 1_{\{y_n^i = m\}} \log \frac{e^{\left(w_m^i\right)^T \cdot x_n^i}}{\sum_{m=1}^{M^i} e^{\left(w_m^i\right)^T \cdot x_n^i}}, \tag{4}$$

where N is the number of total training samples, while M^i denotes the number of classes for the i^{th} attribute. Besides, $\{x_n^i, y_n^i\}$ denotes the paired training image sample, and y_n^i denotes the n^{th} sample x_n^i's i^{th} attribute label.

The proposed multilabel learning algorithms for pedestrian reidentification still reserve the end-to-end learning paradigm as previous works [1, 2, 15]. Therefore, the training and inference phases can be done with high parallelism, thus creating no impact on overall system efficiency. The parallel approach will make the model run smoothly and speed up the proposed model's execution time.

4. Experiments

In this section, we conduct detailed experiments to study the performance of the proposed framework. Besides, the obtained results are compared with other existing pedestrian reidentification approaches to demonstrate our proposed models' superior performance.

4.1. Datasets. We utilize the CUHK03 [9] publicly available dataset to evaluate our work and compare the results with other state-of-the-art models. VIPeR [17] and CUHK03 are the two commonly used person reidentification datasets. VIPeR contains a total of 632 pedestrian images, which are captured by using two cameras with different viewpoints. However, the drawback is that the image resolution of VIPeR is relatively low, making it not suitable for body part division. In contrast, CUHK03 is the pedestrian reidentification dataset large enough to overcome deep neural networks' overfitting. It provides the bounding boxes detected correctly and manually label them. CUHK03 consisted of 13,164 images of various pedestrians and was captured with several surveillance cameras, where every identity is detected with two separate camera views. Such settings yielded an average of 4.8 images in each set of view. Furthermore, the dataset comes up with bounding boxes auto-obtained and manually labeled pedestrian bounding boxes. In our work, we present the results on the labeled dataset. To ensure good detection quality, we select CUHK03 as the test dataset in this paper.

4.2. Implementation Settings. The proposed algorithms and framework are implemented using the famous deep learning library PyTorch [18]. Most functional layers are adopted from the library, and those parts associated with the proposed structure are realized on our own. The training and inference of CNN models are performed on multiple NVIDIA TITAN X GPUs to accelerate the speed. The experiments are conducted by optimizing the proposed softmax-based objective function. We first train the CNN models with the minibatch-based stochastic gradient descent. The minibatch size is set to 16 for smooth gradient updating and convergence. We applied $L2$ regularization and dropout (cite dropout) for the earlier layers with a ratio of 0.5 to avoid overfitting and speed up the convergence speed. Initially, we set the learning rate to 0.05 and used a decreasing factor until we obtained the best results. The models are trained for 24,000 iterations, and the learning rates for two subnetworks are identical (0.001). We use the Adam optimizer [19] to adjust the learning rate and accelerate the optimization convergence.

4.3. Evaluation Protocol. We assume the widely adopted single-shot modality to allow a wide-range comparison with state-of-the-art models. For every probe image, we match it in contradiction to the gallery set to obtain the true match's rank. The rank-k recognition rate describes the match at

rank k. At the same time, we record the cumulative values' recognition rate at all ranks due to a specific trail of the cumulative matching characteristic (CMC) result. We evaluated the performance with such settings ten times and reported the average CMC results.

4.4. Model Training. In this section, we discuss the data augmentation, dropout techniques, and training strategies.

4.4.1. Data Augmentation. Even though the selected dataset is large scale, the positive paired data are not as many as opposing pairs. Moreover, the dataset size is relatively small compared to the deep network models. Hence, data imbalance and overfitting may occur. Multiple data augmentation strategies are used to compensate for the performance degradation resulted from insufficient images, overcoming this limitation. Affine transformations are applied to alleviate the overfitting effect. We also augment the dataset by conducting random translations. We sample an equal amount of positive and negative pairs to accomplish data balancing despite creating the negative-positive fixed proportion.

4.4.2. Dropout. In the scenario of person reidentification, because of the considerable misalignment, cross-view variations, occlusions, and pose variations, it is anticipated that specific patches on the identical person (though in various views) may contradict each other. We applied the dropout [20] approach to induce the trained proposed model adequate to misdetection of the similarity. We randomly select some outputs of the first convolutional layer (extracted features with the filter pairs) and set them as zeros at each training iteration and for every training sample as the input. We calculate the gradients in the backpropagation with the randomly muted filter responses to achieve a stable training model.

4.4.3. Training Strategies. It is time-consuming and tedious to train the fast R-CNN model from scratch over large-scale datasets. We use the pretrained fast R-CNN model to avoid complex model tuning and accelerate the training process. The pretrained model significantly reduces the training time and improves the identification accuracy. In the experiment, MobileNetV2 [21] is selected as the feature extraction subnetwork. The MobileNetV2 model uses multiple optimization schemes that achieve a good tradeoff between complexity and performance. The impact of the pretraining effect is also demonstrated experimentally.

4.5. Experiment Results. We compare the result of our model with two person reidentification methods (KISSME [11] and SDALF [22]), two metric learning methods (logistic distance metric learning (LDM) [23] and metric learning to rank (RANK) [24]), and a filter-based approach FPNN [9]. RANK is an optimized approach for ranking-based problems, whereas person reidentification is a ranking problem. LDM is designed for person and face identification scenarios.

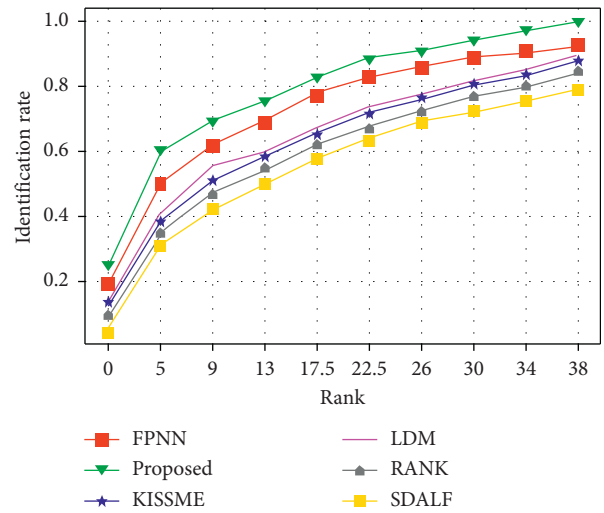

Figure 3: Performance comparison of CMC results with other pedestrian reidentification methods [9, 11] on the CUHK03 dataset.

On the benchmark CUHK03 dataset, we conducted a range of experiments of our proposed and other state-of-the-art models for pedestrian bounding boxes. Figure 3 plots the comparison performance of CMC on various methods on the CUHK03 dataset. It shows that the proposed algorithm significantly outperforms the KISSME [11] model by a large margin with an identification rate improvement of 10% to 18%. As for the other deep neural network-based method, FPNN [9], our approach yields an identification rate improvement by 4% to 8%. The observed performance gain mainly comes from the utilization of pedestrian attribute information.

Since initializing has been instrumental for the performance and convergence of deep learning models [25–27], we propose initializing the proposed model with pretrained weights. Figure 4 presents the performance comparison on the CUHK03 dataset with or without a pretrained subnetwork. From the figure, we can see that the algorithm with a pretrained model achieves a higher identification rate by 2% to 8% for all rank values. The gain comes from the fine-tuning of the R-CNN model which helps the training start at a good point. Moreover, according to our experiments, the training process with a pretrained model converges faster than that without a pretrained model, significantly reducing the time cost of model training.

The experimental results in Figure 5 demonstrate the usefulness of employing dropout to the proposed model. The figure describes the rank-1 identification rates following various sets of training minibatches on the validation set against a range of dropout rates (0% to 20%). Our model's identification rate decreases as the number of training minibatches grows in the absence of dropout. Such behavior indicates the overfitting problem. The convergence speed improves, and the identification rate is high when the dropout is set to 5%, enabling it to be adequate to patch the misdetection of correspondence and result in a good generalization power. However, it does not achieve a reasonable identification rate when the dropout is set to a higher value (20% in this case).

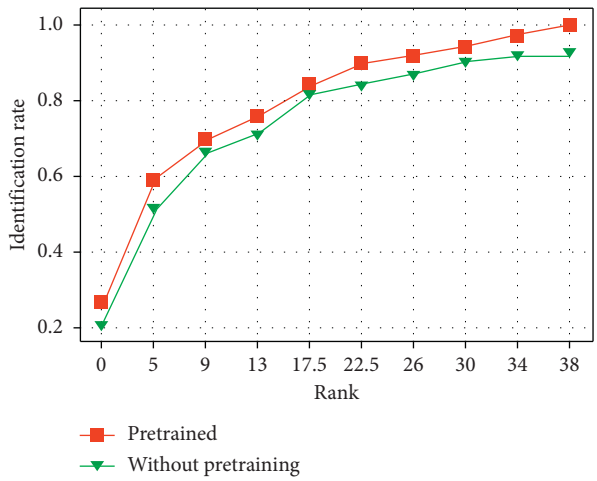

Figure 4: Comparison of CMC results on the CUHK03 dataset with or without the pretrained subnetwork.

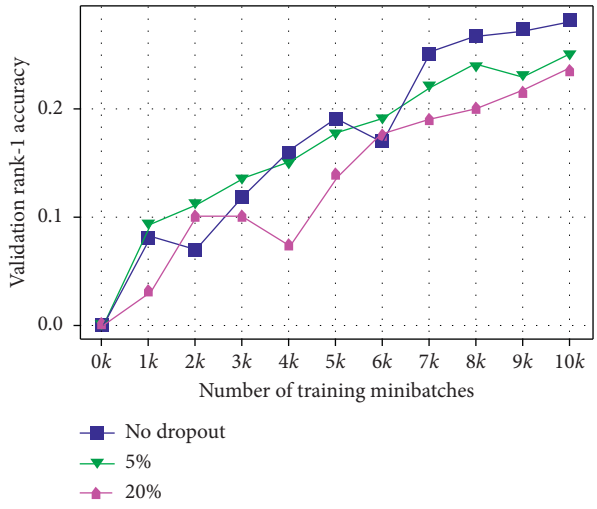

Figure 5: Rank-1 identification of the proposed model on the validation set after a different number of training minibatches.

5. Conclusion

In this paper, we present a novel pedestrian reidentification framework based on multilabel learning CNN models. Besides, we also propose a hybrid algorithm with the aid of pedestrian attributes and low-level features. Both low-level features and pedestrian attributes are utilized to enhance the performance. Experimental results on the popular dataset, CUHK03, show that the identification rate is improved compared to the existing algorithms.

Data Availability

No data were used to support this study.

Conflicts of Interest

The authors declare that they have no conflicts of interest to this work.

Acknowledgments

This work was sponsored by Chongqing Basic Science and Research Project (CSTC2015JCYJBX0133) and NSFC (51375519).

References

[1] E. Ahmed, M. Jones, and T. K. Marks, "An improved deep learning architecture for person re-identification," in *Proceedings of the IEEE Conference on Computer Vision and Pattern Recognition*, pp. 3908–3916, Boston, MA, USA, June 2015.

[2] R. R. Varior, M. Haloi, and G. Wang, "Gated Siamese convolutional neural network architecture for human re-identification," in *European Conference on Computer Vision*, pp. 791–808, Springer, Berlin, Germany, 2016.

[3] Y. Lin, F. Guo, L. Cao, and J. Wang, "Person re-identification based on multi-instance multi-label learning," *Neurocomputing*, vol. 217, pp. 19–26, 2016.

[4] H.-X. Yu, W.-S. Zheng, A. Wu, X. Guo, S. Gong, and J.-H. Lai, "Unsupervised person re-identification by soft multi-label learning," in *Proceedings of the IEEE Conference on Computer Vision and Pattern Recognition*, pp. 2148–2157, Long Beach, CA, USA, 2019.

[5] H. Fan, L. Zheng, C. Yan, and Y. Yang, "Unsupervised person Re-identification," *ACM Transactions on Multimedia Computing, Communications, and Applications*, vol. 14, no. 4, pp. 1–18, 2018.

[6] J. Wang, X. Zhu, S. Gong, and W. Li, "Transferable joint attribute-identity deep learning for unsupervised person re-identification," in *Proceedings of the IEEE Conference on Computer Vision and Pattern Recognition*, pp. 2275–2284, Salt Lake City, UT, USA, June 2018.

[7] K. He, X. Zhang, S. Ren, and J. Sun, "Deep residual learning for image recognition," in *Proceedings of the IEEE Conference on Computer Vision and Pattern Recognition*, pp. 770–778, Las Vegas, NV, USA, June 2016.

[8] A. Vaswani, N. Shazeer, N. Parmar et al., "Attention is all you need," in *Advances in Neural Information Processing Systems*, pp. 5998–6008, MIT Press, Cambridge, MA, USA, 2017.

[9] W. Li, R. Zhao, T. Xiao, and X. Wang, "Deepreid: deep filter pairing neural network for person re-identification," in *Proceedings of the 2014 IEEE Conference on Computer Vision and Pattern Recognition*, pp. 152–159, Columbus, OH, USA, June 2014.

[10] S. Liao, Y. Hu, X. Zhu, and S. Z. Li, "Person re-identification by local maximal occurrence representation and metric learning," in *Proceedings of the IEEE Conference on Computer Vision and Pattern Recognition*, pp. 2197–2206, Boston, MA, USA, June 2015.

[11] M. Koestinger, M. Hirzer, P. Wohlhart, P. M. Roth, and H. Bischof, "Large scale metric learning from equivalence constraints," in *Proceedings of the IEEE Conference on Computer Vision and Pattern Recognition*, pp. 2288–2295, Providence, RI, USA, June 2012.

[12] I. Kviatkovsky, A. Adam, and E. Rivlin, "Color invariants for person re-identification," *IEEE Transactions on Pattern Analysis and Machine Intelligence*, vol. 35, no. 7, pp. 1622–1634, 2012.

[13] N. Carion, F. Massa, G. Synnaeve, N. Usunier, A. Kirillov, and S. Zagoruyko, "End-to-end object detection with transformers," 2020, https://arxiv.org/abs/2005.12872.

[14] H. Zhang, T. Xu, M. Elhoseiny et al., "SPDA-CNN: Unifying semantic part detection and abstraction for fine-grained recognition," in *Proceedings of the 2016 IEEE Conference on Computer Vision and Pattern Recognition*, pp. 1143–1152, Las Vegas, NV, USA, June 2016.

[15] J. Zhu, S. Liao, D. Yi, Z. Lei, and S. Z. Li, "Multi-label CNN based pedestrian attribute learning for soft biometrics," in *Proceedings of the International Conference on Biometrics (ICB)*, pp. 535–540, Phuket, Thailand, May 2015.

[16] S. Ren, K. He, R. Girshick, and J. Sun, "Faster r-CNN: towards real-time object detection with region proposal networks," in *Advances in Neural Information Processing Systems*, pp. 91–99, MIT Press, Cambridge, MA, USA, 2015.

[17] D. Gray and H. Tao, "Viewpoint invariant pedestrian recognition with an ensemble of localized features," in *European Conference on Computer Vision*, pp. 262–275, Springer, Berlin, Germany, 2008.

[18] A. Paszke, S. Gross, S. Chintala et al., "Automatic differentiation in pytorch," in *Proceedings of the Conference on Neural Information Processing Systems*, Long Beach, CA, USA, December 2017.

[19] D. P. Kingma and B. Jimmy, "ADAM: a method for stochastic optimization," 2014, https://arxiv.org/abs/1412.6980.

[20] N. Srivastava, "Dropout: a simple way to prevent neural networks from overfitting," *The Journal of Machine Learning Research*, vol. 15, pp. 1929–1958, 2014.

[21] M. Sandler, A. Howard, M. Zhu, A. Zhmoginov, and L.-C. Chen, "Mobilenetv2: inverted residuals and linear bottlenecks," in *Proceedings of the IEEE Conference on Computer Vision and Pattern Recognition*, pp. 4510–4520, Salt Lake City, UT, USA, June 2018.

[22] M. Farenzena, "Person re-identification by a symmetry-driven accumulation of local features," in *Proceedings of the 2010 IEEE Computer Society Conference on Computer Vision and Pattern Recognition*, June 2010.

[23] M. Guillaumin, J. Verbeek, and C. Schmid, "Is that you? Metric learning approaches for face identification," in *Proceedings of the IEEE 12th International Conference on Computer Vision*.

[24] B. McFee and G. R. G. Lanckriet, "Metric learning to rank," in *Proceedings of the International Conference on Machine Learning*, Haifa, Israel, June 2010.

[25] D. P. Kingma and J. Ba, "ADAM: a method for stochastic optimization," 2014, https://arxiv.org/abs/1412.6980.

[26] D. Erhan, "Why does unsupervised pre-training help deep learning?" in *Proceedings of the Thirteenth International Conference on Artificial Intelligence and Statistics*, Sardinia, Italy, May 2010.

[27] Shah, S. T. Ullah, J. Li, Z. Guo, G. Li, and Q. Zhou, "DDFL: a deep dual function learning-based model for recommender systems," *Database Systems for Advanced Applications*, Springer, Cham, Switzerland, 2020.

Hindawi
Mobile Information Systems
Volume 2023, Article ID 9763973, 1 page
https://doi.org/10.1155/2023/9763973

Retraction

Retracted: Multimedia Teaching of College Musical Education Based on Deep Learning

Mobile Information Systems

Received 8 August 2023; Accepted 8 August 2023; Published 9 August 2023

Copyright © 2023 Mobile Information Systems. This is an open access article distributed under the Creative Commons Attribution License, which permits unrestricted use, distribution, and reproduction in any medium, provided the original work is properly cited.

This article has been retracted by Hindawi following an investigation undertaken by the publisher [1]. This investigation has uncovered evidence of one or more of the following indicators of systematic manipulation of the publication process:

(1) Discrepancies in scope

(2) Discrepancies in the description of the research reported

(3) Discrepancies between the availability of data and the research described

(4) Inappropriate citations

(5) Incoherent, meaningless and/or irrelevant content included in the article

(6) Peer-review manipulation

The presence of these indicators undermines our confidence in the integrity of the article's content and we cannot, therefore, vouch for its reliability. Please note that this notice is intended solely to alert readers that the content of this article is unreliable. We have not investigated whether authors were aware of or involved in the systematic manipulation of the publication process.

Wiley and Hindawi regrets that the usual quality checks did not identify these issues before publication and have since put additional measures in place to safeguard research integrity.

We wish to credit our own Research Integrity and Research Publishing teams and anonymous and named external researchers and research integrity experts for contributing to this investigation.

The corresponding author, as the representative of all authors, has been given the opportunity to register their agreement or disagreement to this retraction. We have kept a record of any response received.

References

[1] W. Li, "Multimedia Teaching of College Musical Education Based on Deep Learning," *Mobile Information Systems*, vol. 2021, Article ID 5545470, 10 pages, 2021.

Hindawi
Mobile Information Systems
Volume 2021, Article ID 5545470, 10 pages
https://doi.org/10.1155/2021/5545470

RETRACTED

Research Article

Multimedia Teaching of College Musical Education Based on Deep Learning

Wei Li

Hunan University of Science and Engineering, Yongzhou 425100, China

Correspondence should be addressed to Wei Li; lw_5535@huse.edu.cn

Received 20 February 2021; Revised 9 March 2021; Accepted 22 March 2021; Published 2 April 2021

Academic Editor: Mian Ahmad Jan

Copyright © 2021 Wei Li. This is an open access article distributed under the Creative Commons Attribution License, which permits unrestricted use, distribution, and reproduction in any medium, provided the original work is properly cited.

In view of the current situation of musical education and the need for reform in China, we adopt two different methods, i.e., literature method and interview method in this research work. From these methods, we read a lot of musical education, multimedia technology, and modern teaching and reform. This research work is divided into two main phases. Firstly, the article mainly discusses the characteristics of college musical education compared with other cultural courses and the feasibility of multimedia technology and the auxiliary function of musical education that is applied in school's musical education. Secondly, brain computing attempts to analyze things by simulating the structure and information processing of biological neural networks. The intelligent learning characteristic of a deep learning algorithm is proposed to monitor the process of musical education teaching and analyze the process quality. Finally, we introduced the design and production of network multimedia courseware which will help in theoretical guidance and reference to the application of multimedia technology in college musical education in China. Moreover, the outcome of the proposed model can play a role in solving and answering questions in the current multimedia application process and Chinese college music workers will apply multimedia technology more effectively and skillfully.

1. Introduction

In recent years, the state has actively promoted the construction of teaching sharing platforms such as network quality courses, microcurriculums, and university video open courses. They provide multidisciplinary and multitype quality education resources for the teaching and independent learning of college teachers and students. As a public foundation course, in college musical education, due to its particularity, teachers use multimedia and network technology in teaching far less than other disciplines. Some data show that computers and multimedia have been used in the teaching of various subjects in colleges and universities, but they have not been truly popularized in college musical education [1, 2]. In March 2012, the Ministry of Education's "Special Plan for Higher Education" notice stressed: "Actively promoted based on "the reform of the network's talent training model, teaching content and teaching methods." As the main teaching task of the college musical education curriculum, the transfer of motor skills requires both a simple language expression and a graceful demonstration of movement. To some extent, the intuitive demonstration of action is greater than the role of language. Multimedia that takes full advantage of computer system imagery, animation, and sound resources can demonstrate accurate virtual 3D motion demonstrations for students. At present, there are still problems in teaching publicity and musical education courses in colleges and universities using multimedia to carry out practical teaching, but there are infinite prospects for expanding the network teaching space. Among the many network platforms, well-known IT brands occupy the favorite independent learning platform for college students. In all kinds of network interaction tools, the search and utilization of semiorganized information are also common [3].

The rapid development of network technology provides a broad space for people to learn, live, and communicate. The development of mobile network technology provides more convenient conditions for people to use the network.

Modern college students have a strong ability to use network technology, especially mobile network technology [4]. Brain computing should not process still images but signals that are spatially and spatially continuous. Although there have been many successful applications of deep learning, if we go further, for example, in video analysis and dynamic visual information processing, we will naturally encounter the same tasks as human brain, requiring some recognition of dynamic spatial and temporal patterns. They can easily browse spatial information at any time through communication tools [5]. How to effectively use these modern technologies to improve the quality of education and expand the teaching space of public musical education curriculum is worthy of serious consideration by the majority of musical education teachers [6]. According to the use of network information by college students, combined with the characteristics of musical education curriculum, this paper discusses the establishment of Q-group-based aerial classroom-assisted teaching. It introduces the experimental study of multimedia teaching and network interaction in musical education. Besides, it explores the network-assisted mode of musical education and realizes the musical education model [7]. The specific contributions of this paper include the following:

(1) The characteristics of college musical education and other cultural courses are discussed

(2) An intelligent learning feature based on a deep learning algorithm is proposed to monitor the process of musical education teaching and analyze the process quality

(3) The application of multimedia technology in college physics teaching is studied

The rest of this paper is organized as follows. Section 2 discusses college students' use of the network situation; the generation of multimedia network teaching is discussed in Section 3. The classification of musical education courseware is discussed in Section 4. The basic structure of multimedia network in teaching platforms in college is discussed in Section 5. Section 6 shows the simulation experimental results, and Section 7 concludes the paper with a summary and future research directions.

2. College Students Use the Network Situation

According to the latest statistics from the China Internet Network Information Center, the total number of Internet users in China has reached 564 million by the end of December 2012 [8, 9]. The number of new Internet users in the country is 50.9 million and the penetration rate of the Internet is 42.1%. It increased by 3.8% in comparison with the end of 2011. Figures 1 and 2 show the scale and penetration rate of Chinese data from 2005 to 2012.

It can be seen from Figure 1 that China had grown from 11 million in 2005 to 564 million in 2012, and the penetration rate of the Internet has increased from 8.5% in 2005 to 42.1% in 2012. Such a clear upward trend and penetration rate indicate that China has entered the ranks of major

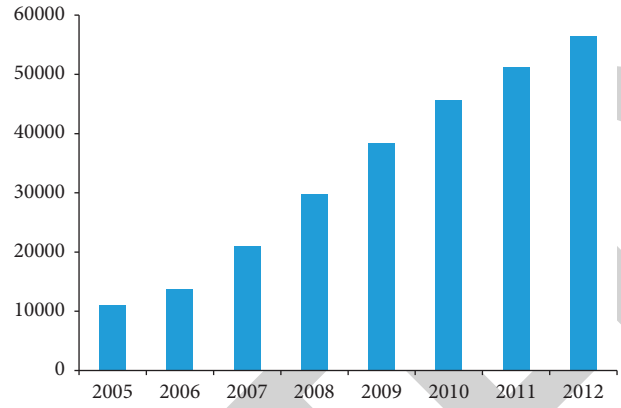

Figure 1: The scale of Chinese citizen.

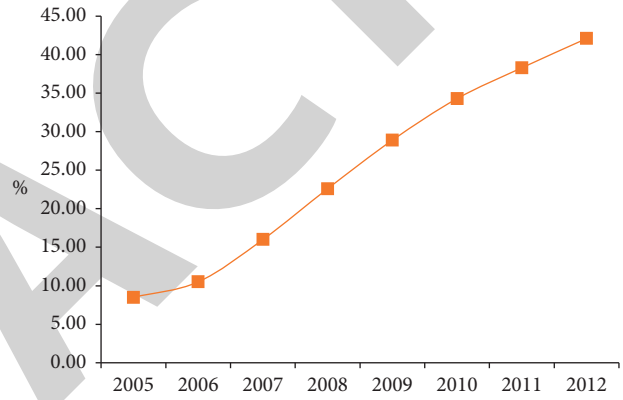

Figure 2: The Internet penetration rate in China.

Internet countries. According to data analysis and statistics released by the China Internet Network Information Center, the scale distribution and Internet penetration rate of various provinces (cities, autonomous regions) in mainland China have increased significantly from 2011 to 2012. It can be seen from Table 1 that China's Internet has been fully covered in various provinces (municipalities and autonomous regions). Although the distribution of various regions is still uneven, some remote and minority areas have relatively low coverage. However, they are relatively low in these areas. The growth rate is increasing. This shows that China has entered a new era of the network [10].

According to a survey conducted by the China Internet Network Information Center (CNNIC) in the survey report on Internet users, the Internet usage rate of college graduates or above reached 96.1% in 2012. Basically saturated, the penetration rate of high school students in the past five years is the most obvious. In 2012, the proportion exceeded 90%, reaching 90.9%. It can be seen that among the users of the current Internet, college students account for the largest proportion.

3. The Generation of Multimedia Network Teaching

There is no unified definition of multimedia network teaching. The so-called multimedia network teaching is to

RETRACTED

Table 1: Size and Internet penetration rate of Internet users in various provinces (municipalities and autonomous regions) in Mainland China, 2011–2012.

Province	Number of citizens (10,000 people)	Popularity rate (%)	Citizen growth rate (%)	Popularity ranking	Citizen growth rate ranking
Beijing	1458	72.2	5.8	1	27
Shanghai	1606	68.4	5.3	2	29
Guangdong	6627	63.1	5.2	3	30
Fujian	2280	61.3	8.5	4	23
Zhejiang	3221	59.0	5.5	5	28
Tianjin	793	58.5	10.3	6	18
Liaoning	2199	50.2	5.1	7	31
Jiangsu	3952	50.0	7.2	8	25
Shanxi	1589	44.2	13.1	9	13
Hainan	384	43.7	13.6	10	12
Xinjiang	962	43.6	9.1	11	21
Qinghai	238	41.9	14.7	11	9
Hebei	3008	41.5	15.9	13	7
Shaanxi	1551	41.5	8.6	14	22
Chongqing	1195	40.9	11.9	15	16
Ningxia	258	40.3	24.5	16	1
Shandong	3866	40.1	6.7	17	26
Hubei	2309	40.1	8.5	18	24
Neimenggu	965	38.9	12.9	19	14
Jilin	1062	38.6	10.0	20	20
Heilongjiang	1329	34.7	10.2	21	19
Guangxi	1586	34.2	17.2	22	4
Hunan	2200	33.3	13.6	23	10
Xizang	101	33.3	12.7	24	15
Sichuan	2562	31.8	14.9	25	8
Anhui	1869	31.3	17.9	26	3
Gansu	795	31.0	13.6	27	11
Henan	2856	30.4	10.6	28	17
Guizhou	991	28.6	17.9	29	2
Yunnan	1321	28.5	15.9	30	6
Jiangxi	1267	28.5	16.5	31	5
National	56400	42.1	9.9	—	—

RETRACTED

fully utilize the most advanced computer network technology and multimedia technology. A new teaching method with organic combination teaching is the implementation of multimedia technology under the support of Internet technology. This makes implementation of a teaching method based on communication and discussion [11, 12].

Multimedia network teaching is a kind of distance learning. According to the development of major media and information technology, multimedia network teaching belongs to the third generation of distance learning. Multimedia network teaching is the product of the development of modern computer network technology and multimedia technology to a certain extent. The famous Chinese scholar made a detailed summary of the three generations of information technology used for teaching and the stage of three generations of distance education. It can be seen from Table 2 that since the 1990s, with the emergence and development of computer network technology and computer multimedia technology, two-way interactive electronic information communication technology has been realized, which makes the teaching process more open and flexible. Therefore, with the emergence and development of new technologies, multimedia network teaching has emerged [13–15].

We also obtained the most published new data by logging on to the Chinese University and found that, by the end of 2012, there are 2,148 universities in China, 31 of which are top universities, 1.44%. 256 colleges and universities with comprehensive music majors accounted for 11.9% of the total number of colleges and universities in China. At present, these colleges have their own independent campus network for the management of school information and the presentation of quality courses for the usual educational system. However, most college websites have not yet built their own multimedia network teaching platforms because there are still many vacancies in the application of multimedia network teaching technology.

4. Classification of Musical Education Courseware

Musical education courseware can be divided into two major categories, namely, the principle teaching mode and the training teaching mode. The principle teaching mode can be divided into principle teaching and technical teaching. The principle teaching is to briefly introduce the

Table 2: Three generations of information technology and three generations of distance education.

Staging	First generation	Second generation	Third generation
Age	From the mid-19th century to the mid-20th century	From the mid-20th century to the end of the 1980s	From the 1990s to the present
Distance education classification	Correspondence education	Distance education in multimedia teaching	Open and flexible distance learning
Information technology	Traditional printing technology. Postal transmission technology. Early audiovisual technology.	One-way transmission-based electronics. Information and communication technology.	Two-way interactive electronic information. Communication technology.
Main media	Printing materials, photography, electricity words, slides, vocals, projections, recording, film, early recording	Mass media (broadcasting, Satellite TV), personal media (audio recording, CD-ROM, microcomputer), early remote electronic communication, computer-aided teaching	Modern remote electronic communication, no line mobile communication, computer multimedia, computer network, knowledge (smart) media, virtual technology

characteristics, origin, evolution, development and rules, venue, and movement methods of the project and help students to establish a complete knowledge concept. Technical teaching is to use the CAI courseware to display the complex technical movements and some of the world's best athletes' scientific and standardized technical actions on the screen by means of "slow motion" and "settlement" on the screen so that students can see clearly and explore the key technical points of the various movements that you have to master, increase the depth of understanding, and enable students to master music knowledge and skills more and better [16, 17].

The training teaching mode should follow the principle of differential treatment, reasonably arrange different practice steps and methods, improve students' understanding of basic knowledge and basic concepts of technology, movements, and methods, and analyze and solve problems. It is seen in Figure 3.

4.1. Basic Requirements for Courseware Design. The design of courseware must fully reflect the characteristics of integrating animation, picture, video, sound, text, and other multimedia into one. It gives full play to the advantages of multimedia teaching. With intuitive expressions, rich media resources, and varied presentation methods, teachers can easily explain and control. Students can easily learn and can fully utilize their initiative, interactivity, and collaboration to better meet the campus. The stable Internet and fast downloading speed are needed for distant education [18].

The overall structure of multimedia courseware is composed of teaching objectives and teaching content. The teaching objectives of the courseware include enhancing the physique of the students, mastering the basic knowledge, skills, cultivating the students' good ideology and morality, and improving the students' ability to observe and imitate, as shown in Figure 4. The teaching content of the courseware includes theoretical and practical lessons, and the content of the courseware teaching content is shown in Figure 4.

5. Basic Structure Multimedia Network in Teaching Platform in College

The multimedia network teaching platform adopts the latest B/S (browser/server) structure, and its structure is shown in Figure 5. The characteristics of the structure are as follows: the environment applied by the client is a standardized and universal web browser and all applications are stored on the webserver, and they can be directly downloaded when needed. It is easier to manage and maintain because the client does not need special software. When upgrading a network application, you only need to update the software in the server; such a structure has good scalability and openness. The B/S structure adopts a standard TCP/IP working protocol, and the school can meet its own development needs and extend the system at any time.

The working principle of the system: teachers and students access the multimedia network teaching platform through the browser. The students use the personal computer equipment to connect with the server through the browser. They carry out related musical education teaching content learning, music resource information query, and the timely time between teachers and students. The administrator of the multimedia network teaching platform and the college musical education teacher can update and maintain the content stored on the server through the browser. It can upload the latest musical education resource information to the server, and at the same time, it can realize online answering with the student. It can make music guidance. The server consists of a web server and a database server. The web server stores various application modules of the system, completes the application function of the client, receives the request of the client user, converts it into a database request, interacts with the database server, and downloads the interaction result to the browser as a web page. The user can observe the result of the request. The database server stores the database and its management software is required by the system. It performs database operations according to the request sent by the web server, and it transmits the result to the webserver.

RETRACTED

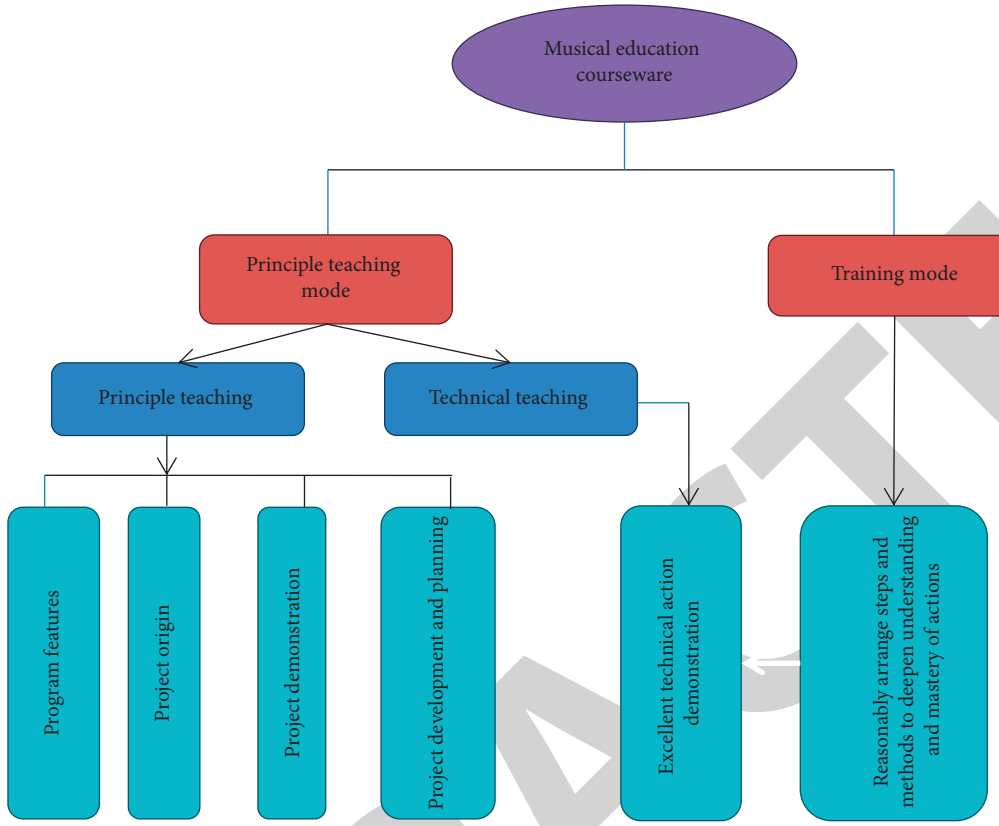

Figure 3: Musical education course structure diagram.

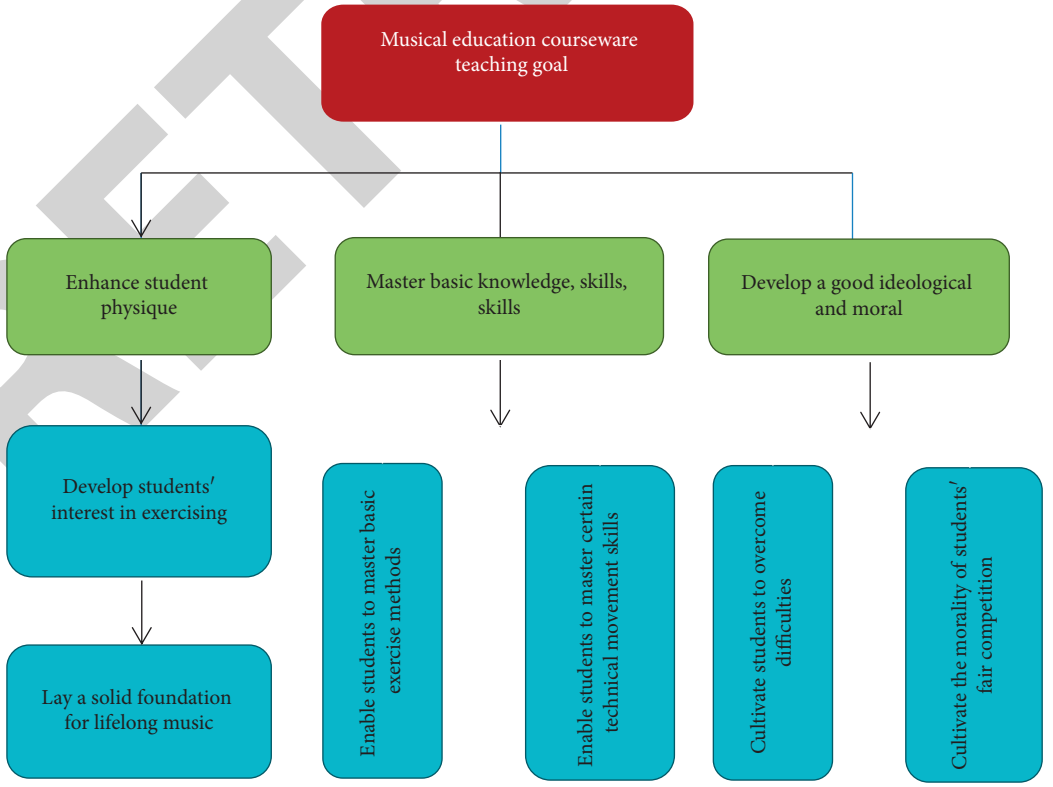

Figure 4: Musical education class multimedia teaching target structure.

RETRACTED

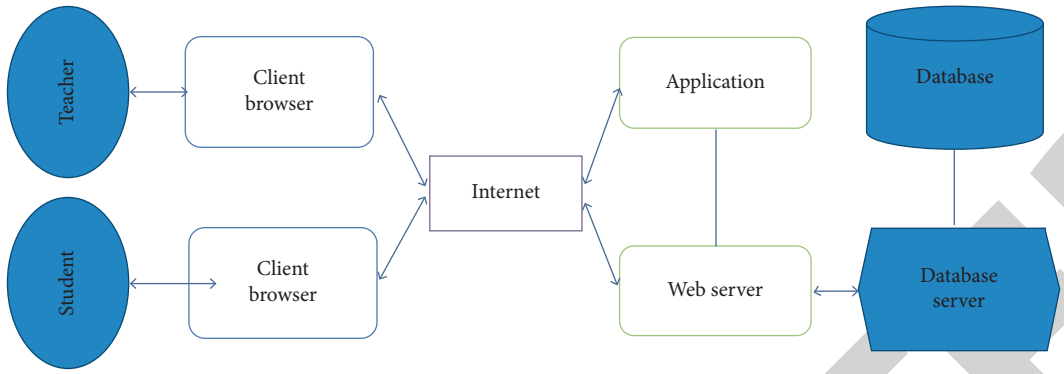

Figure 5: Multimedia network teaching platform structure.

5.1. Supporting Environmental Structure of College Music Multimedia Network Teaching Platform. The promotion of multimedia network teaching platforms in college musical education is inseparable from the construction of the platform environment. According to the Modern Distance Education Teaching Support System in the Technical Specifications for Modern Distance Education Resources Construction, we propose a supporting environment structure diagram for a college music multimedia network teaching platform as shown in Figure 6.

5.2. Musical Education Module. The musical education module is the core module of the college music multimedia network teaching platform. The main function of this module is the display and assistance of the college musical education teaching process. The module includes submodules such as introduction to the course, electronic teaching materials, teaching plans, multimedia network courseware, live teaching, lecture video (including excellent course display), and course resource collection. Through the musical education module, the teacher will edit and upload the information resources of the lectures. Students can use this module to understand the musical education curriculum and conduct independent music learning. With multimedia network courseware, you can also visualize multimedia animations of difficult technical movements that occur during the course of musical education so that students can better understand and master the essentials. Through the implementation of the lectures, the musical education process can be viewed online remotely, and other institutions with relatively poor musical education resources can also conduct musical education courses through this submodule. The lecture video is good for students to review and enhance memory after class. The logical structure and implementation of the live teaching submodule under the musical education module are shown in Figure 7.

5.3. Brain-Like Computing Process. The i-th particle is written as the solution vector $X_i = (x_{i1}, x_{i2}, \ldots, x_{i\,d})$. If the position vector is denoted by $P_i = (p_{i1}, p_{i2}, \ldots, p_{i\,d})$ and the velocity vector is denoted by $V_i = (v_{i1}, v_{i2}, \ldots, v_{i\,d})$, then $x_{i\,d} = \langle p_{i\,d}, v_{i\,d} \rangle$. Calculate the best position bp_i (preferably the position corresponding to the fitness value) experienced by each particle i so far, and call it the optimal position of the individual; calculate the optimal position gP of the entire population up to the current position, and call it the global optimum. Then get the optimal solution through multiple iterations. In each iteration, the particles update their speed and position by tracking and gP, as in the following formula:

$$\begin{aligned} v_{i\,d}^{t+1} &= \omega v_{i\,d}' + c_1 r_1 \left(bp_{i\,d} - x_{i\,d}^t\right) + c_2 r_2 \left(gP_d - x_{i\,d}^t\right), \\ x_{i\,d}^{t+1} &= x_{i\,d}^t + x_{i\,d}^{t+1}. \end{aligned} \tag{1}$$

Among them, t is the number of iterations, ω is the inertia weight, c_1, c_2 are positive acceleration constants, and r_1, r_2 are two random numbers obeying uniformly distributed value between [0, 1].

Sample entropy is a time series complexity measurement method proposed by Richman. The musical meaning represents the rate of new information generated by a nonlinear dynamic system. The larger the sample entropy, the higher the degree of complexity. As an improved algorithm of approximate entropy, its remarkable superiority lies in the fact that it can rely less on the length of time series and better precision, and it is widely used in the processing of physiological signals and various complex signals. For a discrete sequence $x(n)$ of L points, the sample entropy calculation process is as follows: In step 1, a new set of vectors with the embedding dimension m is constructed: $x(i) = [x(i), x(i+1), \ldots, x(i+m-1)]$, where $i = 1, 2, \ldots, L-m+1$ and then the distance between the vectors $X(i)$ and $X(j)$ is defined as follows:

$$d(i,j) = \max_{k=0,1,\ldots,m-1} |x(i+k) - x(j+k)|. \tag{2}$$

In Step 2, given the threshold tr, for each I, count the number of $d(i,j) < \mathrm{tr}$ and the ratio of this number to the total number of distances $L - \mathrm{m} + l$, denoted as $B_i^m(\mathrm{tr})$, and then average:

$$B_i^m(tr) = \left(\sum_{i=1}^{L-m+1} B_i^m(tr) / (L-m+1) \right). \tag{3}$$

In Step 3, increase the dimension to $m+1$, repeat the above steps to obtain $B_i^m(tr)$; in Step 4, obtain the theoretical calculation formula of sample entropy:

RETRACTED

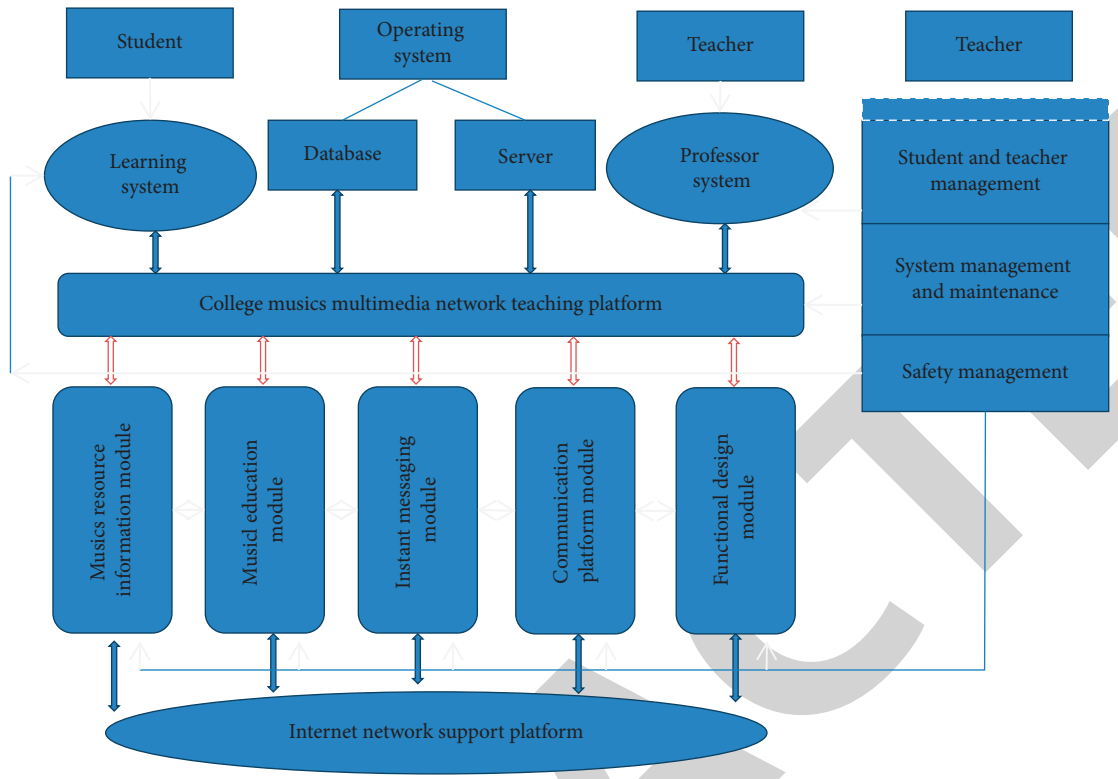

Figure 6: Supporting environment structure diagram of college music multimedia network teaching platform.

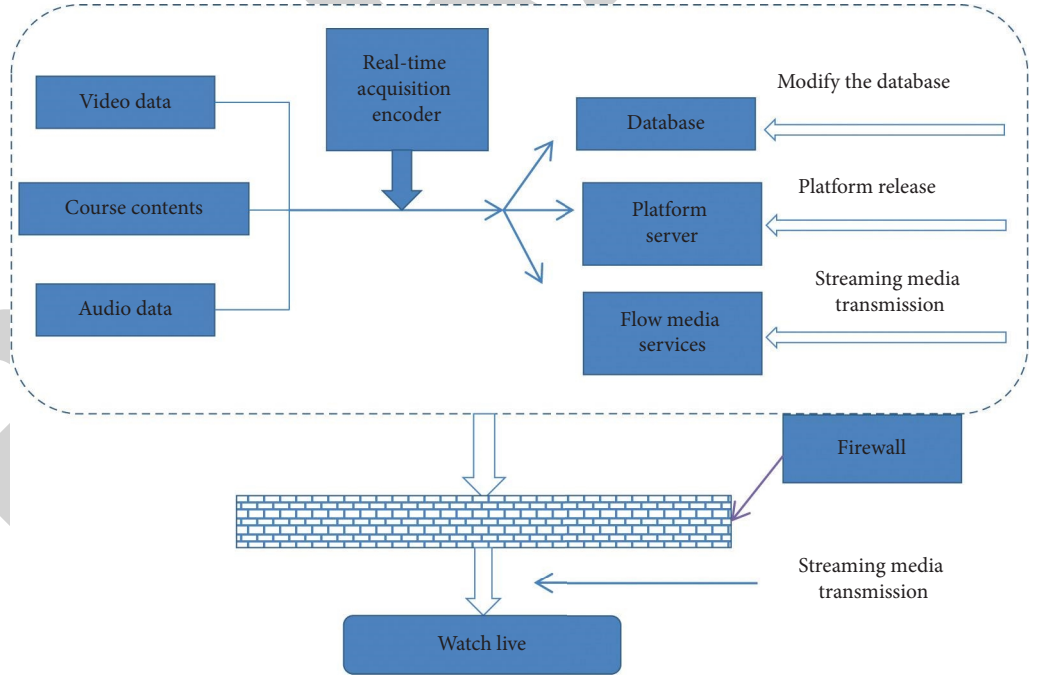

Figure 7: Logical domain implementation of living.

$$\mathrm{Samp}En(m, \mathrm{tr}, L) = \lim_{L \longrightarrow \infty} \left(-\ln \left(\frac{B^{m+1}(\mathrm{tr})}{B^{m}(\mathrm{tr})} \right) \right). \quad (4)$$

In the actual calculation, L takes a finite value, and the sample entropy estimate value obtained when the sequence length is L is

$$\text{Samp}En(m, \text{tr}, L) = \lim_{L \longrightarrow \infty} \left(-\ln \left(\frac{B^{m+1}(\text{tr})}{B^{m}(\text{tr})} \right) \right). \quad (5)$$

6. Analysis and Discussion of Results

We have trained 8,000 samples with 128-size batches, 15 epochs, and $10e-3$ learning frequencies. We have tested multiple hyperparameter values before we have selected certain values. After a few tuning moves, we have reached $10e-3$ for the learning pace. We picked 128 for small batch size, which was the best value that could be used without memory size problems. We used cross-entropy as a loss function for Adam Optimizer. In the 15 epochs, we forced an early break, during which we confirmed the inclination of the model to steadily update training estimates. To ensure that we did not overwrite, we measured the assessment metrics for the training data and correlated them with the validation dataset results.

The frequency distribution table of the gate results is as follows, count (Y) indicates the number of each category (frequency count). Sum (Y) is the total score for everyone. Sum (Y) indicates the cumulative number less than the number. According to the above table, a cumulative histogram can be drawn (the abscissa indicates the score). The ordinate represents less than the number of points. From the frequency histogram and the graph in Table 3 and Figure 8, we can also see that the door score is consistent with the normal distribution.

Similarly, the gate score frequency table is as follows: The number of each group shows count (Y) (frequency count). Sum (Y) for all is the overall score. Sum (Y), as seen in Table 4, means a cumulative number smaller than the number. We draw a cumulative histogram according to Table 4 (the abscissa indicates the score; the ordinate indicates the number less than the score). We can also see that the door score is aligned with the normal divides from the frequency histogram and graph in Tables 4 and Figure 9.

The gate effects frequency table is as follows: count (Y) shall mean the number of each group (frequency count). Sum (Y) is the cumulative ranking for both of us. Sum (Y) means that the cumulative number is smaller than the actual number. By plotting the frequency histogram and the graph in Table 5 and Figure 10, we can see that the test scores of the subject are not usually distributed. There are two peaks, as can be seen from the figure, so the explanation may be that the test questions are complicated. There are so many partial challenges, or students' level of learning is polarized.

The frequency number distribution table of the door score is as follows and the count graph indicates the number of each category (frequency count). Sum (Y) is the total score for everyone. Sum (Y) indicates less than the cumulative number of the number. By plotting the frequency histogram and the graph in Table 6 and Figure 11, we can see that the test scores of the subject are not in a normal distribution. It can be seen from the figure that there are two peaks in the left and right of the average line, which means that the questions are difficult and the problems are easy. Or students at high and low levels

Table 3: The distribution of count (Y) and sum (Y).

	X	Count (Y)	Sum (Y)
1	40	3	3
2	50	4	7
3	60	7	14
4	70	9	23
5	80	6	29
6	90	3	32
7	100	2	34

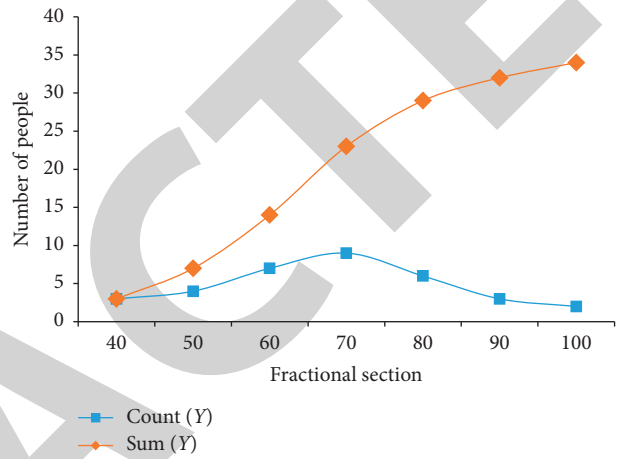

Figure 8: The data of count (Y) and sum (Y).

Table 4: The distribution of count (Y) and sum(Y).

	X	Count (Y)	Sum (Y)
1	50	1	3
2	60	3	7
3	70	8	14
4	80	14	23
5	90	6	29
6	100	2	32

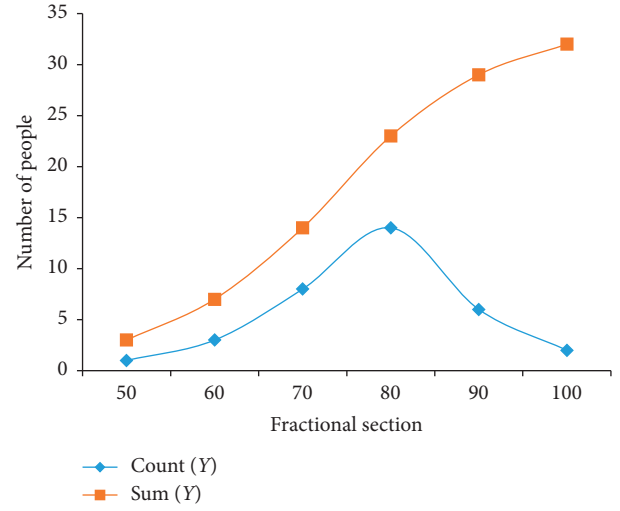

Figure 9: The data of count (Y) and sum (Y).

RETRACTED

Table 5: The distribution of count (Y) and sum(Y).

	X	Count (Y)	Sum (Y)
1	57.5	2	2
2	62.5	0	2
3	67.5	2	4
4	72.5	8	12
5	77.5	6	18
6	82.5	10	28
7	87.5	6	34

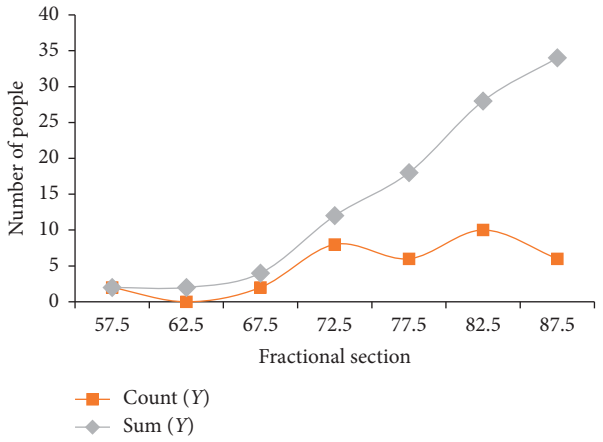

Figure 10: The data of count (Y) and sum (Y).

Table 6: The distribution of count (Y) and sum(Y).

	X	Count (Y)	Sum (Y)
1	52.5	1	1
2	57.5	2	3
3	62.5	0	3
4	67.5	5	8
5	72.5	6	14
6	77.5	6	20
7	82.5	10	30
8	87.5	4	34

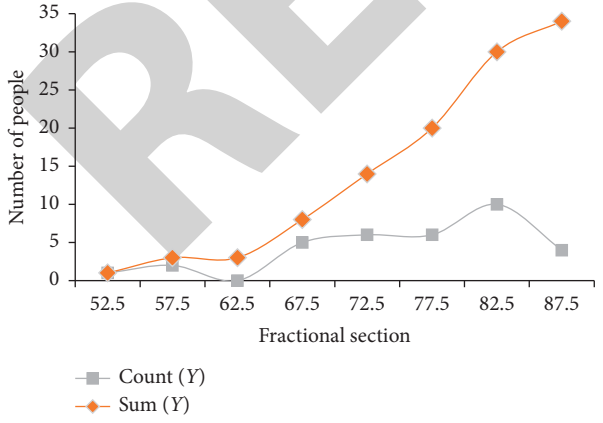

Figure 11: The data of count (Y) and sum (Y).

are distributed in two poles. As can be seen from the figure, the number of students with high scores is higher than the number of students to the left of the average score.

7. Conclusion

Teachers use multimedia for computer-assisted instruction, which provides a new way for education. It changes the relationship between teachers and students, and teachers-centered teaching becomes student-centered teaching. With the continuous development of modern technology, the integration of multimedia, optical discs, and network technologies has changed the way information. It is stored, transmitted, and used. As a new form of education and teaching methods, multimedia will bring great impact and influence to traditional education. The musical education process is the same as the process of students mastering knowledge. There are basic factors such as teachers, students, and teaching content. Musical education activities are very practical bilateral activities of teaching and learning. Both teaching and learning are interdependent and inseparable. Applying deep learning technology to the process of musical education, the impact on teachers, students, and teaching content is of great practical significance.

In the future, we are planning to incorporate, compare, and add tools to study the effects of more in-depth learning frameworks such as the RNN, RCNN, and CRNN.

Data Availability

The datasets used and/or analyzed during the current study are available from the corresponding author upon reasonable request.

Conflicts of Interest

The authors declare that there are no conflicts of interest.

Acknowledgments

This paper was supported by the Educational Planning Project of the 13th Five Year Plan of Hunan Province (XJK20CTW007).

References

[1] P. Antoniou, V. Derri, E. Kioumourtzoglou, and S. Mouroutsos, "Applying multimedia computer-assisted instruction to enhance physical education students' knowledge of basketball rules," *European Journal of Physical Education*, vol. 8, no. 1, pp. 78–90, 2003.

[2] M. Beller and E. Or, "The crossroads between lifelong learning and information technology A challenge facing leading universities," *Journal of Computer-mediated Communication*, vol. 4, no. 2, 2010.

[3] K. Kennedy and L. Archambault, "Offering preservice teachers field experiences in K-12 online learning," *Journal of Teacher Education*, vol. 63, no. 3, pp. 185–200, 2012.

[4] V. Devedzic, "Knowledge modeling—state of the art," *Integrated Computer-Aided Engineering*, vol. 8, no. 3, pp. 257–281, 2001.

[5] N. Winters and Y. Mor, "IDR: a participatory methodology for interdisciplinary design in technology enhanced learning," *Computers & Education*, vol. 50, no. 2, pp. 579–600, 2008.

RETRACTED

Hindawi
Mobile Information Systems
Volume 2021, Article ID 5518424, 8 pages
https://doi.org/10.1155/2021/5518424

Research Article

An Early Risk Warning of Cross-Border E-Commerce Using BP Neural Network

Zhichao Deng,[1] **Meiji Yan**,[1] **and Xu Xiao**[2]

[1]*Guangzhou Panyu Polytechnic, No. 1342 Shiliang Road, Panyu, Guangdong, China*
[2]*Zhejiang Vocational College of Finance, 118 Xueyuan Street, Xiasha Higher Education Park, Hangzhou, Zhejiang Province, China*

Correspondence should be addressed to Zhichao Deng; txeb@hcnu.edu.cn

Received 8 February 2021; Revised 1 March 2021; Accepted 10 March 2021; Published 30 March 2021

Academic Editor: Mian Ahmad Jan

Copyright © 2021 Zhichao Deng et al. This is an open access article distributed under the Creative Commons Attribution License, which permits unrestricted use, distribution, and reproduction in any medium, provided the original work is properly cited.

In this paper, we propose an early warning model of credit risk for cross-border e-commerce. Our proposed model, i.e., KPCA-MPSO-BP, is constructed using kernel principal component analysis (KPCA), improved particle swarm optimization (IPSO), and BP neural network. Initially, we use KPCA to reduce the credit risk index for cross-border e-commerce. Next, the inertia weight and threshold of BP neural network are searched using MPSO. Finally, BP neural network is used for training the data of 13 different enterprises of cross-border e-commerce's credit risk. To analyze the efficiency of our proposed approach, we use the data of five different enterprises for testing and evaluation. The experimental results show that the mean absolute error (MAE) and root mean square error (RMSE) of our model are the lowest in comparison to the existing models and have much better efficiency.

1. Introduction

According to the Wall Street Journal, on September 22, 2014, Alibaba, the giant of cross-border e-commerce [1, 2] was listed as the largest IPO ever with a financing amount of 25 billion USD. Though this achievement was mainly due to the development of cross-border e-commerce applications, the credit risk still exists for these applications. To understand this risk, various studies have been conducted in this context. However, there exists little research when it comes to early warning of credit risk for cross-border e-commerce applications. Based on the risk level, the early warning of credit risk for these applications can be divided into four levels. Among these levels, level 1 represents the lowest risk and level 4 represents the highest risk. During cross-border e-commerce transactions, it is always desirable to select enterprises having better performance for transactions, though the credit risk level of cross-border e-commerce is always dynamic. Selecting an enterprise with better credit among various cross-border e-commerce enterprises for transactions is a major challenge that needs to be studied in detail [3]. Distinguishing the risk level of these enterprises is one of the main reasons that have made this selection quite cumbersome.

In literature, there exist very few studies for early warning of credit risk for cross-border e-commerce. For example, the authors of [4, 5] used the least squares approximate support vector regression model to study early warning for cross-border e-commerce credit risk. In [6–8], the authors employed the Z-score model to analyze the early warning and attained relatively better results. In [9], BP neural network was used to study the early warning of cross-border e-commerce credit risk. From the aforementioned studies, numerous factors were derived that have a direct impact on the credit risk for cross-border e-commerce applications.

In this context, using the financial information disclosed for cross-border e-commerce by listed companies and selecting better and reliable enterprises for conducting research on credit risk seems a viable option. However, there are two main challenges associated with it [10]. First, due to the larger number of financial indicators of listed enterprises, some researchers mainly focused on using the principal component analysis (PCA) for the reduction of

dimensions, but PCA is used for dimension reduction using linear transformation, which is not effective for solving nonlinear problems. There are some nonlinear problems in the credit risk indicators of cross-border e-commerce, which have been proved by previous studies [11]. In this context, neural network seems a much better option but it has few main drawbacks associated with it such as overfitting, poorly generalized performance, and a much slower convergence speed, among others. Neural network can cooperate with PSO algorithm for determining the inertia weight and threshold of a given neural network. However, the PSO algorithm may easily fall into local minimum which ultimately leads to loss of efficiency. Besides, the results of neural network based on PSO are not accurate in most circumstances.

To solve the aforementioned problems, we use KPCA, MPSO, and BP neural network for establishing a framework for early warning of credit risk in cross-border e-commerce applications. The major contributions are as follows:

(1) Initially, the kernel principal component analysis (KPCA) is employed to solve the nonlinear feature vector extraction.

(2) Next, MPSO is used to solve the local pole problem associated with particle swarm optimization (PSO). A small value phenomenon is resolved by dynamically adjusting threshold and inertia weight for a BP neural network. Based on the principle of KPCA, MPSO, and BP neural network, this paper makes an empirical study using the credit risk's early warning of cross-border e-commerce.

The rest of this paper is organized as follows. In Section 2, we discuss our proposed combination model. In Section 3, we discuss the empirical analysis along with experimental results for our proposed model. Finally, the paper is concluded and future research directions are provided in Section 4.

2. Combination Model

In this section, first we discuss the principle of KPCA in Section 2.1. Next, we discuss the principle of MPSO in Section 2.2 followed by the operational principle of BP algorithm in Section 2.3. Finally, we discuss our proposed combination model in Section 2.4.

2.1. Principle of KPCA. KPCA is a multivariate statistical analysis technique that uses a kernel method by applying it to PCA. It maps multiple variables to a high-dimensional feature space via nonlinear mapping, and conducts analysis in a high-dimensional space. Based on ensuring that the relationship between the relevant variables remains unchanged, it strives to minimize the loss of original data information and reduces the credit risk index of cross-border e-commerce. Several main indexes that can reflect the characteristics of the original problem are obtained for this purpose [10–12]. KPCA is a nonlinear feature extraction method, but it has not been applied to the credit risk early warning of cross-border e-commerce. It avoids the complex problem of solving eigenvectors in eigenspace and is realized by solving eigenvectors and eigenvalues of the kernel matrix.

Firstly, for a given cross-border e-commerce credit risk sample, $x_i\,(i = 1, 2, \ldots, n, x_i \in R^n)$ is mapped to the feature space H^D, where H^D is a nonlinear mapping, then the covariance matrix C of the feature space $\phi(\cdot)$ sample is

$$C = \frac{1}{N}\sum_{i=i}^{N}\phi(x_i)^T. \tag{1}$$

In equation (1), the eigenvalue of C is decomposed into

$$\lambda V = CV. \tag{2}$$

In this equation, $\lambda\,(\lambda \geq 0)$ is the eigenvalue of matrix C and V is the eigenvector corresponding to λ. Since, V is a linear combination of $\phi(x_i), \phi(x_2), \ldots \phi(x_n)$, then there exists $\alpha_i\,(i = 1, 2, \ldots, n)$.

$$V = \sum_{i=1}^{n}\alpha_i\phi(x_i). \tag{3}$$

In equation (3), V belongs to the mapping function $\phi(x_t)\,(i = 1, 2, \ldots, n)$ of the characteristic space H^D; the generating space is

$$\lambda\phi^T(x_i) \quad V = \phi^T(x_i)CV, \quad i = 1, 2, \ldots, n. \tag{4}$$

In equation (4), the matrix $K_{i,j}$ defining $n \times n$ has

$$K = \left(k_{ij}\right) = K\left(x_i, x_j\right) = \left(\phi^T(x_i)\phi\left(x_j\right)\right). \tag{5}$$

In equation (5), the eigenvalue problem of $i, j = 1, 2, \ldots, n$, α_i depends on the kernel function K_{ij}, K is a dot product kernel matrix, and equation (5) can be written as

$$K\alpha = n\lambda\alpha. \tag{6}$$

In equation (6), for the kernel principal component extraction of cross-border e-commerce credit risk data, the projection $P(t)$ of test set t in the direction of feature space vector V_l is calculated as follows:

$$\begin{aligned} P(t) = V_l\phi(t) &= \sum_{i=1}^{n}\alpha_{l,i}\left(\phi^T(x_i)\phi(t)\right) \\ &= \sum_{i=1}^{n}\alpha_{i,j}aK(x_i, t), \quad l = 1, 2, \ldots q. \end{aligned} \tag{7}$$

In equation (7), it has been assumed that the training set satisfies equation (1) in the feature space, $\sum_{i=1}^{n}\phi(x_i) = 0$, and it is extremely difficult to satisfy equation (1) in the feature space. To relax the assumption $\sum_{i=1}^{n}\phi(x_i) = 0$, the matrix expression $(I_n)_{ij} = (1/n)$ is introduced, and the kernel matrix is replaced by the following form:

$$\overline{K} = K - I_nK - KI_n + I_nKI_n. \tag{8}$$

In equation (8), the maximum number of principal components extracted by KPCA is n. If the first few feature vectors can reflect all the characteristics of cross-border e-commerce credit risk, the number of principal components extracted can be reduced [13–15].

2.2. Principle of MPSO. Particle swarm optimization (PSO) is an intelligent algorithm inspired from the natural social behavior of fish and birds. In PSO, each "particle" reflects an entity that can be compared to a bird within a search space. The particle is used for solving the optimization problems. Each particle can search, follow, and memorize the current optimal particle within a solution space. The particle has a fitness value, which is determined by an optimization function and a speed that determines its flight direction and distance [16, 17]. Finally, a PSO algorithm finds the optimal solution via iterations. At first, it is initialized as a group of random particles. Particles chase two extremums and update their position in each iteration. One is the global extremum best, which is the optimal solution currently found by the whole group, and the other is the individual extremum best, which is the current optimal solution found by the particles themselves. When the fitness value of this time (current time) is equal to that of the previous time, the PSO will fall into the local minimum. To solve the abovementioned problem, PSO is improved by dynamically adjusting the weight of inertia. When the fitness value of this time is equal to the fitness value of the previous time, the particle swarm will fall into a local minimum. It can be predicted that in all future iterations if the inertia weight is equal, it is impossible to generate such an equal inertia weight. If the number of subsequent iterations is the best fitness value of the inertia weight generated by the current iteration, the inertia weight will inevitably change, and the change is irreversible, which makes PSO fall into the state of local extremum. The improvement method of PSO is introduced below. In the past, some improved algorithms for inertia weight were proposed based on equation (9). The improved inertia weight has serious disadvantages, and the improvement depends on the current iteration times and the maximum iteration times of the algorithm, which will make it fall into a local minimum. Because of these shortcomings, this paper proposes an algorithm to dynamically adjust the inertia weight, i.e., the method of first increasing and then decreasing controlled by the algorithm itself to improve the PSO algorithm [18, 19].

$$\omega = \omega_{\max} - \frac{\omega_{\max} - \omega_{\min}}{iter_{\max}} \times iter. \tag{9}$$

In equation (9), *iter* is the current number of iterations, $iter_{\max}$ is the maximum number of iterations, $\omega_{\min}$ is the minimum value of inertia weight, and $\omega_{\max}$ is the maximum inertia weight. The basic idea is as follows: using a dynamic inertia adjustment strategy, first select the inertia weight of particles with the smaller initial value, so that the initial development ability of particles is stronger. If the fitness value f_{t-1} of the previous iteration is compared with the fitness value f_t of the current iteration, the particle will fall into the local minimum at two fitness values $f = f_{t-1}$. To enhance the global search ability of particles, we can call the linear function: $\omega = \omega + \alpha \times \omega$, where α is a local random number in the interval (0-1), adjust the size of inertia weight, and increase the inertia weight of particles, and particles can jump out of the local extreme point. When the inertia weight increases to 1.4, the exploration ability among particles is the strongest, but the connection between particles is the weakest, i.e., the development ability of particles is the weakest. To enhance the connection between particles, a linear function, $\omega = \omega + \alpha \times \omega$, is used. Here, a local random number in the (0-1) interval is used to linearly reduce the inertia weight to enhance the connection between particles. This method is repeatedly used to make the particles control and adjust the inertia weight dynamically, and the connection of particles is developed in the direction of enhancement so that the exploration ability and development ability of particles can reach the dynamic strategic balance. The adjustment formula of inertia weight is as follows:

$$\omega = \begin{cases} \omega + \alpha \times \omega, & f_t = f_{t-1} \text{ and }, \quad \omega < 1.4, \\ \omega - \alpha \times \omega, & f_t = f_{t-i}, \quad \omega \geq 1.4, \\ \omega, & f \neq f_{t-1}, \end{cases} \tag{10}$$

In this equation, α is a random number between 0 and 1, ω is a linear function, f_t is the fitness value of generation t, and f_{t-1} is the fitness value of generation $t-1$. The dynamic balance between global search and local search of particle swarm optimization is represented by the above equation [20–23].

2.3. BP Algorithm Principle. BP neural network is a predominant artificial neural network (ANN). It comprises an input layer, several hidden layers, and an output layer that has several nodes. Each node reflects a neuron, the lower and the upper nodes are connected through weights. The nodes between layers are fully interconnected, and there exists no connection among the nodes at each layer. A typical case of BP neural network is a three-layer structure network model with a hidden layer, as shown in Figure 1.

In an NN model, the relationship between an output y_t and input $y_{t-1}, y_{t-2}, \ldots, y_{t-p}$ can be expressed using the following equation:

$$y_t = \omega_0 + \sum_{j=1}^{n} \omega_j g\left(\omega_{0_j} + \sum_{i=1}^{m} \omega_{ij} y_{t-i}\right) + \varepsilon_i. \tag{11}$$

In this equation, $\omega_{ij} = (i = 1, 2, \ldots, n)$ and $\omega_j (i = 1, 2, \ldots, n)$ are model parameters, n denotes the number of nodes at the hidden layer, m reflects the number of nodes at the model input layer, and g is a conversion function. The commonly used function is $g(x) = (1/1 + e^{-x})$.

BP neural network model described in equation (11) reflects the linear function mapping relationship between the input and output y_t of the previous observation value of the sequence

$$y_t = f\left(y_{t-1}, y_{t-2}, \ldots, y_{t-p}, \omega\right) + \varepsilon_t. \tag{12}$$

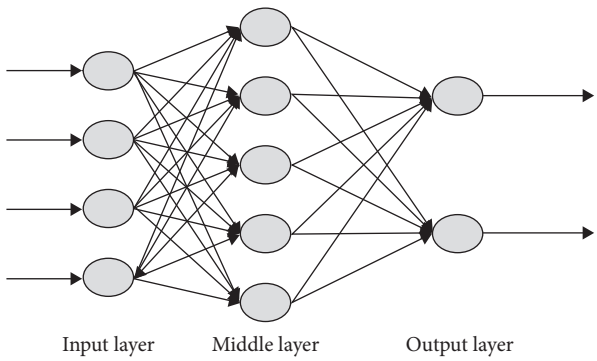

Figure 1: Structure of BP neural network model.

In equation (12), ω is the parameter vector of all models; function $f(\cdot)$ is determined by network structure and weight parameters [24, 25], respectively.

2.4. Combination Model. Our combination model, i.e., KPCA-MPSO-BP, is discussed in detail here. The basic idea of this model is as follows: firstly, the eigenvalues and eigenvectors of the indicators of cross-border e-commerce credit risk are calculated. Then, the kernel principal component eigenvectors with cumulative contribution rate greater than 85% are calculated, and finally, MPSO is used to search the weights and thresholds of BP neural network. The current position and fitness of the particles in the swarm are expressed by the weights, thresholds, and errors of the BP neural network and the results are compared. To analyze whether or not to update the PSO algorithm, BP neural network is used for early warning calculation. The flowchart of our proposed model is shown in Figure 2.

The operation steps of our model are as follows:

(1) Data collection and data preprocessing:

The credit risk indicators of cross-border e-commerce are standardized, and the reverse indicators are converted into positive indicators. The method is 1-index value, that is, $x_{ij} = 1 - x_{ij}$, where x_{ij} is the reverse index and x_{ij} is the positive index after conversion. The formula of normalization is as follows:

$$x''_{ij} = \frac{x_{ij} - x_{\min}}{x_{\max} - x_{\min}}. \tag{13}$$

(2) Calculate the kernel matrix:

After data standardization, the cross-border e-commerce credit risk data is analyzed by KPCA, and the eigenvalues and eigenvectors of covariance are calculated.

(3) Feature values extraction:

KPCA method is used to reduce the dimension of the input eigenvalue. The standard of dimension reduction is to select the kernel principal component eigenvector which contains more than 85% information.

(4) Initialize PSO:

Initialize the initial position and initial velocity of the population, set the minimum fitness value as ε and the maximum number of iterations as m, and transfer the initial position of particles to the initial optimal position of particles.

(5) BP neural network initialization:

The initial position of particles is transferred to BP neural network as the initial threshold and initial value of the BP neural network.

(6) Output and average error:

The output and average error $\varepsilon_1 = (1/1 + e^{-x})$ of the BP neural network are calculated. The comprehensive score of sample data is taken as the expected output value, the average error of the BP neural network is calculated, the fitness value of particle swarm optimization algorithm is determined by the network error εt, and the fitness value of particle swarm optimization algorithm is determined [6].

(7) Training set of BP neural network:

Part of the data of cross-border e-commerce credit risk is taken as the training set of BP neural network, and the training calculation is carried out in the network.

(8) Test set of BP network:

Another part of the data of cross-border e-commerce credit risk is taken as the test set of BP neural network and tested in BP neural network.

(9) Credit warning:

According to the score of the BP neural network, the credit warning of cross-border e-commerce enterprises is carried out. Based on the results of test/inspection, the credit risk of cross-border e-commerce enterprises is given early warning according to the risk level.

(10) Error analysis:

To test the superiority of the KPCA-MPSO-BP model, mean absolute percentage error (MAPE) and root mean square error (RMSE) are calculated. These two metrics are used for error analysis:

$$\text{MAPE} = \frac{1}{n}\sum_{i=1}^{n}\left|\frac{x_i - \widetilde{x}_i}{x_k}\right| \times 100\%, \tag{14}$$

$$\text{RMSE} = \sqrt{\frac{\sum_{i=1}^{n}\left(x_i - \widehat{x}_i\right)^2}{n}}. \tag{15}$$

In equations (14) and (15), smaller the mean absolute error and root mean square error, the better will be the results.

3. Empirical Analysis

According to the characteristics of cross-border e-commerce credit risk enterprises, data sources use the index system of

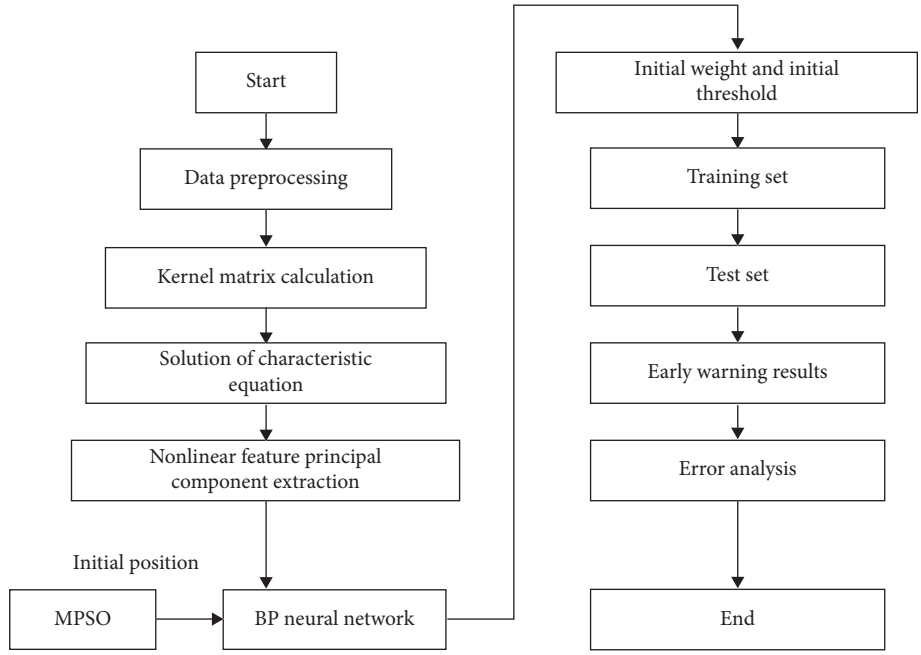

Figure 2: Flowchart of the combination model.

[1, 3] to make an empirical study on cross-border e-commerce credit risk.

3.1. Selection of Research Samples and Indicators. Taking the data of 18 international cross-border e-commerce enterprises as the sample, the selected indicators for our studies are sales profit rate X_1, return on net assets X_2, return on total assets X_3, total assets turnover X_4, cost and expense profit rate X5, inventory turnover X_6, accounts receivable turnover X_7, current assets turnover X_8, interest multiple X_9, digital certificate grade X_{10}, quick ratio X_{11}, current ratio X_{12}, capital accumulation rate X_{13}, platform service provider credit X_{14}, fixed assets renewal rate X_{15}, total assets growth rate X_{16}, contract breaking rate X_{17}, overdue payment rate X_{18}, and trade volume growth rate X_{19}. The 18 enterprises are named enterprise A, enterprise B, and enterprise R, respectively. The index meanings are shown in Table 1.

According to the definition of Table 1, the original data in Table 2 can be obtained by using the data in [3].

3.2. Data Processing. According to the combination processing method in Section 2.4, the standardized transformation of the original data (including the normalization of the reverse index into the positive index) enables the standardized cross-border e-commerce credit risk matrix. We adopt KPCA standard of the dimension reduction for selecting the cumulative contribution rate of the eigenvalue, which accounts for 85%. The initial position of the particle is transferred to BP neural network as the initial threshold and initial value of the BP neural network. First, 13 groups of data are used to form the training set, then the BP neural network is used to train, and then the other 5 groups of data are used to form the test set. Using the prediction test, the credit risk of cross-border e-commerce is divided into four categories: level 1 risk (80100), level 2 risk [60, 80], level 3 risk [30, 60], and level 4 risk [0, 30]. Among them, level 1 and level 2 are in a risk state, while level 3 and level 4 are in a risk-free state. If the score is greater than or equal to 60, it is no alarm, and if the score is less than 60, it is an alarm. The data after standardized processing are shown in Table 3.

3.3. Credit Risk Early Warning Analysis of Cross-Border E-Commerce. According to the early warning of cross-border e-commerce credit risk in Table 3, enterprises are classified, as shown in Table 4.

As can be seen from Table 4, there are 4 enterprises in good condition (level 1 risk). These enterprises include D, E, I, and P, respectively. These enterprises are in good financial condition. Next, there are 6 enterprises in Level 2 risk (normal condition) that include A, G, I, K, N, and Q, respectively. The financial status of these enterprises is good and there is no credit risk. There are 5 enterprises with level 3 risk (slight risk). The financial status of the cross-border e-commerce enterprises in this section is not very good, with slight credit risk. Finally, there are 3 enterprises with grade 4 risk (serious risk), including J, F, and O as the table shows. The financial status of the enterprises in this section is extremely dangerous, with a relatively serious credit crisis.

3.4. Model Combination Fitting Test. For the test of the model, the average absolute error and root mean square error of the model can be compared by BP, PSO-BP, MPSO-BP, and KPCA-MPSO-BP, as shown in Table 5.

Table 1: The meaning of credit risk early warning in cross-border e-commerce.

Serial number	Index name	Indicator meaning
1	Sales profit margin X_1	Sales profit rate = total profit/net sales revenue
2	Return on equity X_2	Return on net assets = net profit/average balance of owner's equity
3	Return on total assets X_3	Return on total assets = profit before interest and tax/average balance of total assets
4	Total assets turnover rate X_4	The turnover rate of total assets = net income of main business/average balance of total assets
5	Cost profit margin X_5	Cost profit rate = total profit/total cost
6	Inventory turnover rate X_6	Inventory turnover rate = inventory turnover times = cost of goods sold/average inventory
7	Accounts receivable turnover rate X_7	The turnover rate of accounts receivable = net income of main business/average balance of accounts receivable
8	Current assets turnover rate X_8	The turnover rate of current assets = net income of main business/average balance of current assets
9	Interest multiple X_9	Multiple of interest earned = profit before interest and tax/interest expense
10	Level of digital certificate X_{10}	Digital certificate is divided into five levels, corresponding to the score, it's 1.0, 0.80, 0.60, 0.40, and 0.20
11	Quick ratio X_{11}	Quick ratio = (current assets inventory)/current liabilities
12	Current ratio X_{12}	Current ratio = current assets/current liabilities
13	Capital accumulation rate X_{13}	Capital accumulation rate = growth of owner's equity in the current year/beginning of the year owner's equity
14	Platform service provider credit X14	According to the degree of recognition, it is divided into five levels, and the corresponding scores 0.80, 0. 60, 0. 40, 0. 20, and 0
15	The renewal rate of fixed assets X_{15}	The update rate of fixed assets = original value of new fixed assets/period end fixed assets
16	The growth rate of total assets X_{16}	The growth rate of total assets = growth amount of total assets in this year/capital at the beginning of the year. Total output × 100%
17	Contract breaking rate X_{17}	Breach rate = total amount of breach contract/total amount of signed contract amount of money
18	Overdue payment rate X_{18}	Overdue loan rate = total number of days beyond the repayment period/total number of days of loan total days
19	The growth rate of trade volume X_{19}	The growth rate of trade volume = trade growth of this year/total trade of this year exchange amount

Table 2: Credit risk data of 18 enterprises.

On	Name	X_1	X_2	X_3	X_4	X_5	...	X_{17}	X_{18}	X_{19}
1	A enterprise	0.362	0.362	0.293	1.263	1.235	...	0.068	0.368	0.259
2	B enterprise	0.282	−0.523	−0.453	1.326	0.686	...	0.089	0.319	0.688
3	C enterprise	−0.342	0.395	0.264	0.984	1.267	...	0.037	0.287	0.577
4	D enterprise	0.293	0.457	0.165	0.885	2.368	...	0.125	0.105	0.496
5	E enterprise	0.146	−0.298	−0.217	1.368	0.889	...	0.053	0.396	−0.285
6	F enterprise	−0.413	0.372	0.648	1.529	0.984	...	0.015	0.687	−0.052
7	G enterprise	0.374	0.254	0.539	0.997	5.235	...	0.076	0.758	0.373
8	H enterprise	0.355	−0.166	−0.391	1.682	0.686	...	0.037	0.499	0.496
9	I enterprise	0.217	0.195	0.342	2.015	4.267	...	0.119	0.852	0.278
10	J enterprise	0.258	0.183	0.503	1.354	5.212	...	0.122	0.463	0.299
11	K enterprise	−0.499	−0.287	−0.185	0.896	0.893	...	0.034	0.644	−0.085
12	L enterprise	0.642	0.391	0.187	1.364	4.374	...	0.075	0.595	0.354
13	M enterprise	0.571	0.388	0.268	1.093	2.675	...	0.057	0.476	0.197
14	N enterprise	0.393	−0.427	−0.329	0.855	0.978	...	0.069	0.317	−0.082
15	O enterprise	−0.132	0.193	0.196	2.995	1.684	...	0.064	0.272	0.241
16	P enterprise	0.095	0.487	0.115	2.687	3.565	...	0.126	0.194	0.386
17	Q enterprise	0.284	−0.448	−0.384	0.974	0.886	...	0.113	0.241	0.654
18	R enterprise	0.487	0.435	0.357	2.686	2.988	...	0.087	0.353	0.545

It can be seen from Table 5 that the RMSE and MAPE of the KPCA-MPSO-BP model are the smallest, which indicates that the KPCA-MPSO-BP model has higher early warning accuracy than the single model, the MPSO-BP model has higher early warning accuracy than the PSO-BP model, and KPCA-MPSO-BP model has the highest early warning accuracy, which indicates that the KPCA-MPSO-BP model has the good fitting degree and the KPCA-MPSO-BP model proposed in this paper is scientific and reasonable.

Table 3: Early warning table of credit risk score of BP neural network training set and test set.

Serial number	Enterprise	Score	Risk level	Is there an alarm	Serial number	Enterprise	Score	Risk level	Is there an alarm
1	A	69	2	No	10	J	22	4	Yes
2	B	46	3	Yes	11	K	72	2	No
3	C	45	3	Yes	12	L	94	1	No
4	D	91	1	No	13	M	39	3	Yes
5	E	87	1	No	14	N	78	2	No
6	F	27	4	Yes	15	O	26	4	Yes
7	G	78	2	No	16	P	89	1	No
8	H	51	3	Yes	17	Q	76	2	No
9	I	64	2	No	18	R	56	3	Yes

Table 4: Cross-border e-commerce credit risk early warning table.

Category	Level 1 risk (no alarm)	Level 2 risk (no alarm)	Level 3 risk (with alarm)	Level 4 risk (with alarm)
Enterprise name	D enterprise E enterprise I enterprise P enterprise	A enterprise G enterprise I enterprise K enterprise N enterprise Q enterprise	B enterprise C enterprise H enterprise M enterprise R enterprise	F enterprise J enterprise O enterprise

Table 5: Comparison of mean absolute error and root mean square error of different models.

Serial number	Prediction model	RMSE	Sort	MAPE (%)	Sort
1	BP	0.2555	4	3.96	4
2	PSO~BP	0.1410	3	2.240	3
3	MPSO-BP	0.0898	2	1.545	2
4	KPCA-MPSO-BP	0.0377	1	1.018	1

4. Conclusion

To improve the ability to prevent the credit risk of cross-border e-commerce enterprises, this paper proposes a combination model of KPCA-MPSO-BP. This model is used to early warn the credit risk of cross-border e-commerce enterprises and analyze the relevant sample data. The results show that the KPCA-MPSO-BP combination model is effective in early warning for any credit risk. Compared with other models, KPCA-MPSO-BP has fewer parameters, faster calculation speed, and better fitting. Though our model has much better results, there is still room for improvement. For example, for enterprises with grade 1 risk (excellent state), there is no credit risk, so it is necessary to strengthen the data collection of credit rating to avoid the occurrence of credit risk. For the enterprises in the level 2 risk (normal state), there is a possibility of credit risk, hence we should strengthen the analysis of the potential factors of credit risk, strengthen the management, and prevent the occurrence of credit risk. For enterprises with level 3 risks (slight risk status), if there is a slight risk and they are in early warning status, we should strengthen the work of enterprise credit risk, improve the credit, and reduce the occurrence of credit risk. The enterprises with level 4 risk (serious risk status) are in the early warning status and have serious credit risk, so they should stop business, strengthen rectification and clean-up, and enter the risk plan procedure to prevent the occurrence of enterprise bankruptcy.

Data Availability

The data used to support the findings of this study are included within the article.

Conflicts of Interest

The authors declare that they have no conflicts of interest.

References

[1] S. Xie, "Prediction of repeat purchase customers in e-commerce platform based on the neural network," *Journal of Changchun Institute of Technology (Natural Science Edition)*, vol. 21, no. 1, pp. 97–100, 2020.

[2] H. Wang, "An e-commerce satisfaction evaluation method based on deep learning," *Electronic Devices*, vol. 43, no. 1, pp. 196–199, 2020.

[3] Z. Xiao, *Research on Trust Evaluation of Social E-Commerce Based on BP Neural Network*, Shenyang University of Technology, Shenyang, China, 2020.

[4] Y. Cao, *Research on Conversational Recommendation System Based on the Neural Network*, Zhejiang University, Hangzhou, China, 2020.

[5] Y. Zhou, *Research on Sentiment Analysis of Commodity Reviews Based on the Convolutional Neural Network*, Nanjing University of Posts and telecommunications, Nanjing, China, 2019.

[6] Y. Wan and Y. Zhang, "Research on abnormal transaction data detection based on the probabilistic neural network," *Communication World*, vol. 26, no. 11, pp. 39-40, 2019.

[7] C. Yi, *Research on Garment Image Retrieval Technology Based on the Convolutional Neural Network*, Zhejiang University of Technology, Hangzhou, China, 2020.

[8] G. C. Yin, *Research on Clothing Style Recognition and Recommendation Based on the Convolutional Neural Network*, Zhejiang University of Technology, Hangzhou, China, 2020.
[9] Y. Mao, *Research on Recommendation Algorithm Based on the Convolutional Neural Network*, West China Normal University, Nanchong, China, 2019.
[10] J. Chen, *Research and Implementation of Commodity Recommendation System Based on the Neural Network*, University of Electronic Science and Technology, Chengdu, China, 2019.
[11] G. Yang and B. Guo, "User behavior prediction of e-commerce platform enhanced by machine learning," *Science and Technology and Innovation*, vol. 3, no. 1, pp. 124-125, 2019.
[12] L. Wang, *E-commerce Image Text Detection and Recognition Based on Deep Learning*, Wuhan Research Institute of Posts and Telecommunications, Wuhan, China, 2019.
[13] Z. Kang, *Research on Cross Border E-Commerce Logistics Risk Evaluation Based on the Genetic Neural Network*, Chang'an University, Xi'an, China, 2018.
[14] W. Yang, *Research and Application of Collaborative Filtering Recommendation Algorithm Based on BP Neural Network*, Wuhan Research Institute of Posts and Telecommunications, Wuhan, China, 2018.
[15] H. Zhang, "Analysis of data mining technology in e-commerce network marketing," *Journal of Chifeng University (Natural Science Edition)*, vol. 33, no. 21, pp. 90-91, 2017.
[16] H. Wang, "Logistics demand forecast of Hangzhou metropolitan area based on BP neural network," *Modern Commerce and Trade Industry*, vol. 29, pp. 46-47, 2017.
[17] W. Shi and X. Wang, "Research on E-commerce credit evaluation model based on clustering and BP neural network," *Fujian Computer*, vol. 33, no. 8, pp. 1–4 + 20, 2017.
[18] C. Yao, H. Shan, H. Hu, and D. Gao, "Risk assessment of cross border e-commerce logistics based on BP neural network," *Economic Research Guide*, vol. 22, pp. 157–159, 2017.
[19] K. Zhou, *Research on Enterprise E-Commerce Credit Risk Early Warning Based on Bagging Method*, Guangxi University, Nanning, China, 2017.
[20] M. Qian, *Repeat Purchase Customer Prediction of E-Commerce Platform Based on Machine Learning*, Lanzhou University, Lanzhou, China, 2017.
[21] K. Zhao, *E-commerce Data Deep Mining Based on the Convolutional Neural Network*, Zhejiang University, Hangzhou, China, 2017.
[22] Y. Huang, *Design and Implementation of E-Commerce Customer Segmentation System Based on Cluster Analysis*, Jiangsu University of Science and Technology, Zhenjiang, China, 2016.
[23] Y. Tang, *Research on Recommendation Algorithm Based on User Behavior in E-Commerce*, Hunan University, Changsha, China, 2016.
[24] X. Lian, *Research on Recommendation Algorithm Based on Sorting Learning and Convolutional Neural Network*, Dalian University of Technology, Dalian, China, 2016.
[25] J. Wu and X. Zhou, "E-commerce credit risk early warning based on KPCA and BP neural network," *Logistics Technology*, vol. 35, no. 4, pp. 97–102, 2016.

Hindawi
Mobile Information Systems
Volume 2021, Article ID 5589154, 8 pages
https://doi.org/10.1155/2021/5589154

Research Article

Sonar Image Target Detection and Recognition Based on Convolution Neural Network

Wu Yanchen

School of Marine Science and Technology, Northwestern Polytechnical University, Xi'an 710072, China

Correspondence should be addressed to Wu Yanchen; 202008064@gxstnu.edu.cn

Received 22 February 2021; Revised 10 March 2021; Accepted 14 March 2021; Published 22 March 2021

Academic Editor: Mian Ahmad Jan

Copyright © 2021 Wu Yanchen. This is an open access article distributed under the Creative Commons Attribution License, which permits unrestricted use, distribution, and reproduction in any medium, provided the original work is properly cited.

Recent advancements in deep learning offer an effective approach for the study in machine vision using optical images. In this paper, a convolution neural network is used to deal with the target task of sonar detection, and the performance of each neural network model in the sonar image detection and recognition task of underwater box and tire is compared. The simulation results show that the neural network method proposed in this paper is better than the traditional machine learning methods and SSD network models. The average accuracy of the proposed method for sonar image target recognition is 93%, and the detection time of a single image is only 0.3 seconds.

1. Introduction

The targets under the sea are not convenient for the human to contact directly, so sonar is needed for detection and recognition. At present, target detection and recognition of sonar images is an important research topic of marine target detection. Traditional sonar detection mainly identifies the features or contours of marine organisms, such as the shape and texture of underwater targets, but the effect of recognizing these features mainly depends on whether the features are clear. However, due to the complexity of the underwater environment and the similarity of some targets, the traditional sonar recognition cannot meet the current detection and recognition of underwater targets. Today, deep learning target detection and identification becomes the mainstream method, and it can be expressed as depth feature extraction target identification and positioning based on deep convolutional neural network. The convolutional neural network (CNN) model has strong characterization and modeling capabilities through supervision or non-supervision training methods. CNN can be denoted by the characteristics of the object layer, and the abstraction and description of the object hierarchism are achieved. Girshick et al. designed a detector (RCNN) based on regional CNN, which is also a milestone in the field of target detection. Since then, the target detection is developed quickly, and many RCNN-based methods are developed in the literature.

In recent years, several computational models have been proposed in the literature for the identification and detection of underwater acoustics using machine learning algorithms. For example, Li et al. [1] and Cheng et al. [2] used the deep learning algorithm for data fusion of sonar multisensor observation data. This article sets out a new approach to SAR image object recognition by designing CNN and improves the unattended detection mechanism, taking advantage of the convolution features. Similarly, Yang et al. [3] and Lei et al. [4] proposed another model based on deep learning for the identification of active sonar signal and semantic segmentation of remote sensing images, respectively. Both the authors produce the promising results, and their strategy was based on how to extract the appropriate number of regional recommendations in order to increase the reliability of target detection. Moreover, Zheng [5] and Liu [6] used the method of passive underwater acoustic using deep learning as classification learning algorithm.

To investigate the convolutional neural network approaches used for remote sensing images' semantic segmentation and to create new technologies and algorithms for greater accuracy, in this paper, we proposed the novel computational model based on convolutional neural

network for the sonar image target detection and recognition. The most important additions and the major contributions of the paper are as follows:

(1) An intelligent and powerful computational model is proposed for the classification of sonar image target detection and recognition

(2) This work proposes an algorithm that can automatically perform target recognition, tracking, or detection works

(3) This work proposes a rigorous model that classifies multitype objects at the same time as the traditional approach using a feature matching technique that can detect one type of object at a time

(4) Finally, the proposed scheme has been extensively tested on comparative experiments and ablation studies

The rest of the paper is organized as follows. In Section 2, literature review is studied in detail, while Section 3 provides the detailed methodology. Section 4 provides detailed results and discussion. Finally, the paper is concluded in Section 5.

2. Design of Convolutional Neural Network Model

In this section, we introduce design of the proposed convolutional neural network model. The architecture of the proposed model is shown in Figure 1 which contains a number of components that are discussed in detail as follows.

2.1. Convolutional Neural Network. A convolution neural network (CNN) is a kind of deep neural network [8–12]. In the 1990s, Lecun first proposed to design and train convolutional neural network lenet5 by using a backpropagation algorithm, which has achieved good results in handwritten digit recognition [13]. In 2006, Professor Hinton of the University of Toronto in Canada proposed the concept of deep learning and solved the gradient dispersion problem of the traditional neural network through the layer pretraining method, which set off an upsurge of deep learning [14]. At present, the convolutional neural network, as the most widely used deep neural network, has made a breakthrough in image processing [15], speech recognition [16], target detection [4, 5], and other fields. Generally speaking, the basic structure of CNN consists of a convolutional layer, pooling layer, fully connected layer, and output layer, as shown in Figure 1.

2.1.1. Convolution Layer. The convolution layer is composed of multiple feature maps. The convolution layer convolutes the input original image with a certain size and step size through the convolution kernel and obtains the feature map of the next layer after activating the function. Convolution kernel is a weight matrix of size n* n. The convolution process is shown in Figure 2.

Each neuron in the convolution layer is connected with the local region of the upper layer by a set of weights, and the pixel weighted sum is obtained. Then, the locally weighted

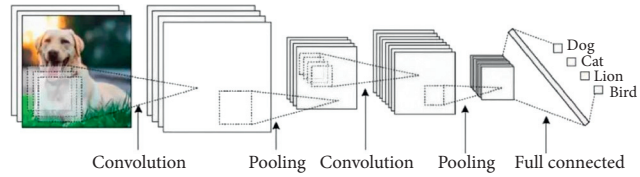

Figure 1: Structure of convolution neural network, adapted from [7].

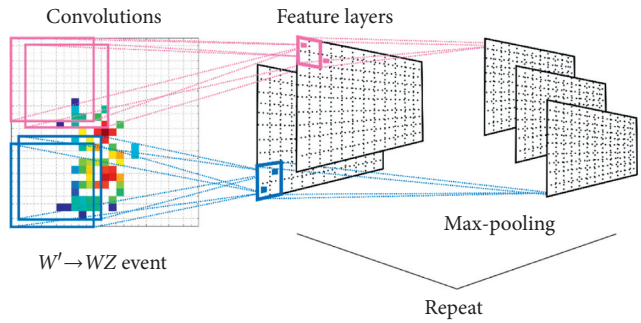

Figure 2: Convolution operation.

sum is transferred to a nonlinear activation function to obtain the value of each neuron in the convolution layer. The calculation formula is as follows:

$$X_j^i = f\left(\sum_{i \in M_j} X_i^{i-1} * W_{ij}^l + b_j^i\right), \tag{1}$$

where X_i^j represents the j-th feature map of the i-th layer, f represents the activation function, X_i^{i-1} represents the i-th feature map of the upper layer, $*$ represents the convolution operation, W_{ij}^i is the convolution kernel, M_j represents the subset of the feature map of the upper layer participating in the operation, and b_i^j represents the offset. The function of the convolution layer is to extract different features of the input image. In CNN, because the convolution process is linear, to increase the nonlinear expression ability of the network, the nonlinear activation function is usually used. The commonly used activation functions are the sigmoid function, tanh function, and ReLU function. Compared with the other two functions, the ReLU function is widely used because of its faster convergence speed and easier implementation. The ReLU, sigmoid, and tanh activation functions can be mathematically expressed using the following equations:

$$\mathrm{ReLU}(x_i) = \max(0, x_i), \tag{2}$$

$$\mathrm{sigmoid}(x_i) = \frac{1}{\left(1 + e_i^{-x}\right)}, \tag{3}$$

$$tanh(x_i) = \frac{2}{\left(1 + e^{-2x_i}\right)} - 1. \tag{4}$$

2.1.2. Pooling Layer. The pooling layer is also composed of multiple feature maps. The pooling operation is similar to

the convolution operation. Each neuron of the pooling layer is also connected with the local area of the previous layer feature map. However, the value of the pooling layer is not the weighted summation of the local area, but the maximum pixel value or average value of the local area is extracted as the value of the pooling layer neuron. The function of the pooling layer is to reduce the size of the feature graph, reduce the computational complexity of the network model, and improve the spatial invariance of the network for the input image object. The common pooling methods are maximum pooling and average pooling. All the networks in this paper adopt maximum pooling. The pooling operation is shown in Figure 3.

2.1.3. Full Connection Layer. The full connection layer is located behind the convolution layer and pooling layer. Each neuron in the full connection layer is connected with all neurons in the previous layer to integrate the feature extracted from the convolution layer or pooling layer. The output value of the last full connection layer is transferred to the output layer to realize the output of classification results. With the rapid development of the convolutional neural network, the target detection method based on the convolutional neural network has been widely used. Using CNN to extract image target features has gradually replaced the traditional target detection method based on manual features and has become the mainstream method of current target detection. In recent years, many excellent target detection models have emerged among which Fast RCNN, YOLOv3, and SSD models are the most widely used.

2.2. Fast RCNN Model. Fast RCNN is a CNN target detection model based on the region proposal proposed by Hu in 2015 [16]. The basic structure of FastRCNN is still CNN, but this model abandons the traditional selective search algorithm [17] in the process of extracting the possible candidate regions, i.e., region recommendation of the target in the image, and then adds a full convolution network (RPN) after the convolution feature map of the last layer of convolution neural network, and the RPN achieved this function. The overall structure of RCNN is shown in Figure 4.

The input of the model is the original image. The feature map is extracted by a deep convolution neural network, i.e., vgg16 [18], and then the coordinate information of candidate regions is extracted by RPN. About 2000 candidate regions are extracted from each image, and then the coordinate information of these candidate regions is mapped back to the position in the original image and compared with the real region. When the overlap ratio between the candidate region and the target region in the original input image is greater than a certain threshold, the default value is 0.7, the target is considered to exist in the region, and then the regression location is carried out according to the positions of the candidate region and the real region, and the probability distribution of the target belonging to a certain category is calculated. Because Fast RCNN realizes the process of candidate region extraction and target detection in a neural network, the operation speed of the model is significantly improved compared with RCNN and Fast RCNN.

2.3. YOLOv3 Model. YOLO (you only look once) is a CNN target detection model based on regression thought [11]. YOLO has gone through the improvement of YOLO [19] and YOL09000 [20], and now it has developed to YOLO3. Different from the Fast RCNN model, the YOLO series model does not need to extract the possible candidate regions of the target in the image but directly performs regression training on the whole image. Firstly, the original image is transformed into a fixed size, and then the feature is extracted by the depth convolution neural network. Finally, the classification result and the target location coordinate information are output.

The basic network used by YOLOv3 is Darknet53 [11]. To avoid the gradient explosion caused by the deepening of network layers, Darknet53 adds RESNET (residual neural network) [21–25] residual structure. When classifying the target objects, YOLOv3 uses several independent logistic regression classifiers. These logistic regression classifiers only judge whether the objects in the target frame belong to the current label or not, which is a simple binary classification. In this way, multilabel classification is realized. Besides, YOLOv3 uses the idea of FPN (feature pyramid networks) [26, 27] for reference and predicts three different scale feature maps, with three target frames predicted for each scale grid. For an image, if it is initially divided into N x N grids and C categories need to be predicted, then the final predicted tensor is $N \times N \times [3 \times (4 + 1) + C]$, which includes the information of four coordinate points and a confidence score. Due to the fusion of the first two-layer feature maps, the model can obtain more low-level and high-level image semantic information, which makes the model prediction more accurate.

2.4. SSD Model. SSD (single shot multibox detector) is another CNN target detection model based on regression idea and is one of the mainstream target detection models at present. The SSD model is mainly divided into two parts: one is a convolutional neural network for feature extraction, which is based on VGG network, replacing the last two full connection layers of VGG with convolution layer and discarding dropout layer and softmax classification layer; the other is multiscale feature detection network closely following VGG network, which is composed of four convolution layers. Each group first uses 1 x 1 convolution kernel to reduce the number of channels and then uses 3* 3 convolution kernel to increase the number of channels. The feature maps of different levels are used for the border regression of different scale targets and the prediction of different category scores. Finally, the final detection result is obtained by NMS [23]. SSD is combined with a multiscale feature map to detect small targets with shallow feature maps with high resolution and large targets with deep feature maps with low resolution so that targets of different scales can be detected.

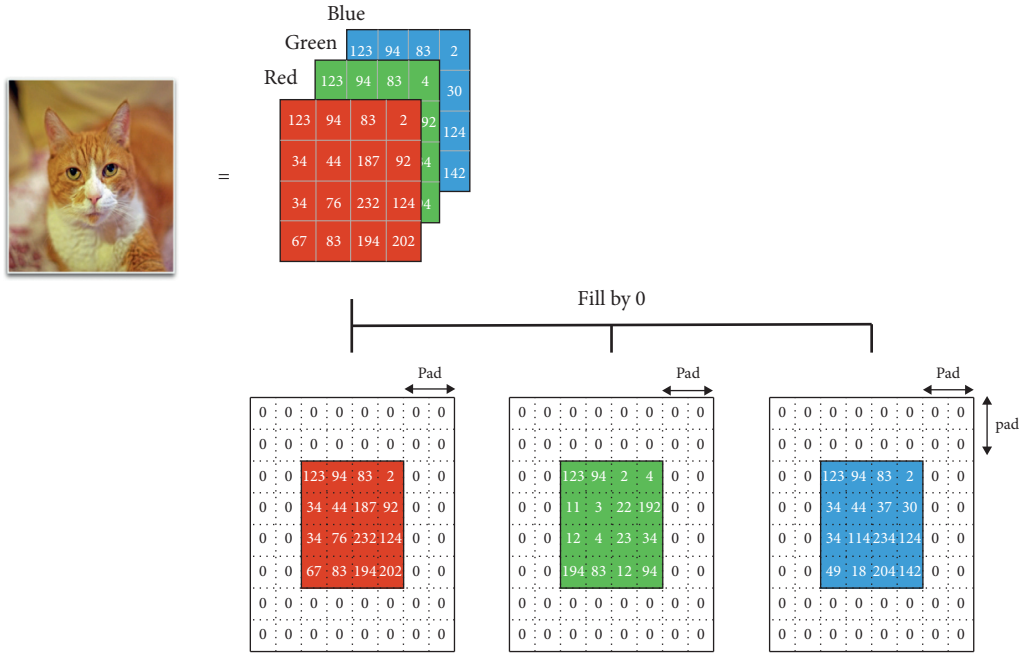

Figure 3: Pooling operation.

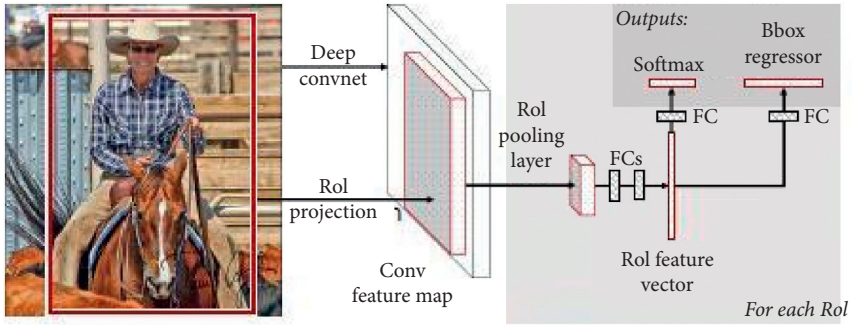

Figure 4: Schematic diagram of the FastRCNN model.

3. Model Performance Evaluation Index

To evaluate the performance of a machine learning algorithm, four parameters are commonly used to check the model reliability and validity [10–12]. These parameters include overall accuracy of the model, specificity as true negative rate, sensitivity as true positive rate, and MCC as Mathew's correlation coefficient. These four metrics calculation formula are as follows:

$$\begin{aligned}
\text{accuracy} &= 1 - \frac{\left(m_{-}^{+} + m_{+}^{-}\right)}{\left(m^{+} + mP^{-}\right)}, \quad 0 \le \text{Acc} \le 1, \\
\text{specificity} &= 1 - \frac{m_{+}^{-}}{m^{-}}, \quad 0 \le \text{Sp} \le 1, \\
\text{sensitivity} &= 1 - \frac{m_{-}^{+}}{m^{+}}, \quad 0 \le \text{Sn} \le 1, \\
\text{Mcc} &= \frac{1 - \left(\left(m_{-}^{+} + m_{+}^{-}\right)/\left(m^{+} + mm^{-}\right)\right)}{\sqrt{1 + \left(\left(m_{+}^{-} - m_{-}^{+}\right)/m^{+}\right)\left(1 + \left(\left(m_{-}^{+} - m_{+}^{-}\right)/m^{-}\right)\right)}}, \quad -1 \le \text{Mcc} \le 1,
\end{aligned} \tag{5}$$

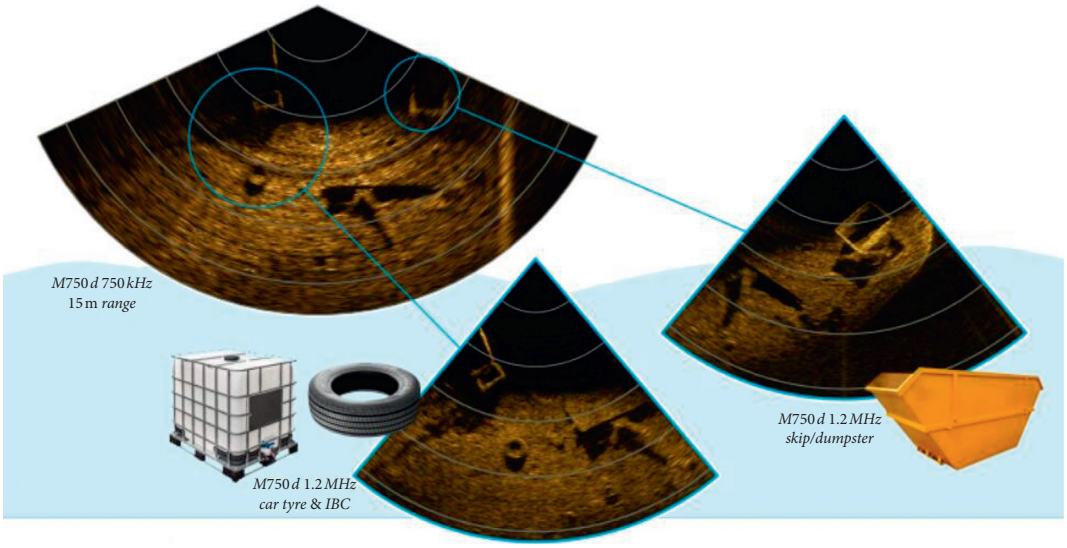

Figure 5: Example of tire and box sonar.

where

(i) m^+ represents true positive
(ii) m^- represents the total true negative
(iii) m_-^+ represents the false positive
(iv) m_+^- represent the false negative

4. Results and Discussion

4.1. Data Preparation. In this paper, sonar image data are obtained through experiments. The sonar used in the experiment is m3 multibeam imaging sonar of Kongsberg Company, UK. The working frequency is 500 KHz, the range resolution is 0.01 M, the nearest distance is 0.2 m, and the farthest distance is 150 m. A total of 2300 sonar images were obtained through several experiments, 80% of which were training sets and 20% were test sets. The final sonar image is shown in Figure 5.

The resolution of the sonar image is 1920 * 1080, the sector area is the scanning range of sonar, the scanning angle is 120, and the origin O of the sector is the scanning center, which is the location of imaging sonar. The longitudinal highlight area on the left and right sides of the image is the pool wall, and the area outside the pool wall is not considered. The white arc is an equidistant line, and the distance from any point on the same equidistant line to O is the same.

4.2. Experimental Setup. In the experiments, we have setup the computing platform with basic hardware and software specifications that include Intel Core i5-10500 processor, NVIDIA Quadro 1060 graphics card, the memory of graphics card is 2G, Tensorflow version is 1.10, CUDA version is 9.0, and operating system is Ubuntu 16.04. To ensure the comparability of the results, the three models use the same super parameters in the training, the learning rate is 0.001, the weight attenuation factor is 0.99, and the momentum parameter is 0.9. The optimization method is random gradient descent, the number of iterations is 10000, and the number of pictures participating in each iteration is 16.

4.3. Analysis of Target Detection. After the training, the test set is used to test, and the results are shown in Table 1 and Figure 6. According to the results shown in Table 1, in the target detection and recognition task of starfish and scallop sonar images, the map of YOLOv3 reaches 92.95%, and the detection accuracy is much higher than that of the faster can and SSD models. In terms of detection speed, it takes 0.255 s for YOLOv3 to detect an image, which is similar to SSD speed but faster than Fast RCNN which is 4 times faster because Fast RCNN needs to extract about 2000 candidate regions from each image and judge these regions separately, which leads to more time consumption. However, YOLOv3 and SSD models use the regression method to output coordinate information directly, so the detection speed is faster. The example of the detection results of the sonar image of starfish scallop by YOLOv3 shows that the model can still detect the target accurately in the case of large background noise.

Furthermore, the quantity of the sample selected by different algorithm is further direction, and the specific results are shown in Figure 7. Overall, each algorithm can basically maintain the relative stability of data distribution, but the model of training is very different, which further indicates that uncertainty + diversity sampling can not only select high information amount of data but also make the sample have minimum redundancy and high representation.

Through the above experiment, it can be seen that the mode of uncertainty + diversity sampling can play a good effect on the dataset even in the distribution and uneven distribution. Further, the uncertainty + diversity sampling in Figure 7 can obtain a better detection effect than all training data by selecting part of the amount of high information and high representative data in the case where the data are small,

Table 1: Detection results of different models on sonar image of starfish scallop.

Test method	Basic network	Picture size	ACC%	Detection speed (s/image)
Faster RCNN	VGG16	1000 × 600	63.03	1.172
YOLOv3	Darknet53	416 × 416	92.95	0.255
SSD	VGG16	300 × 300	31.38	0.224

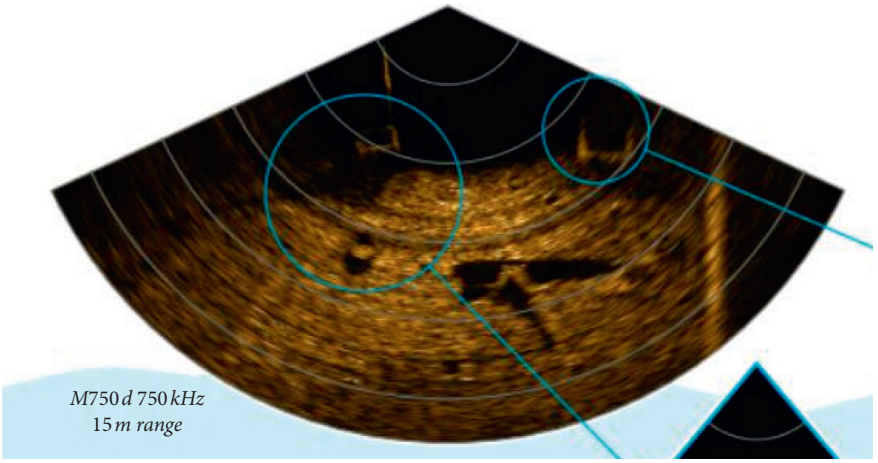

Figure 6: Detection results of the box and tire sonar image by YOLOv3.

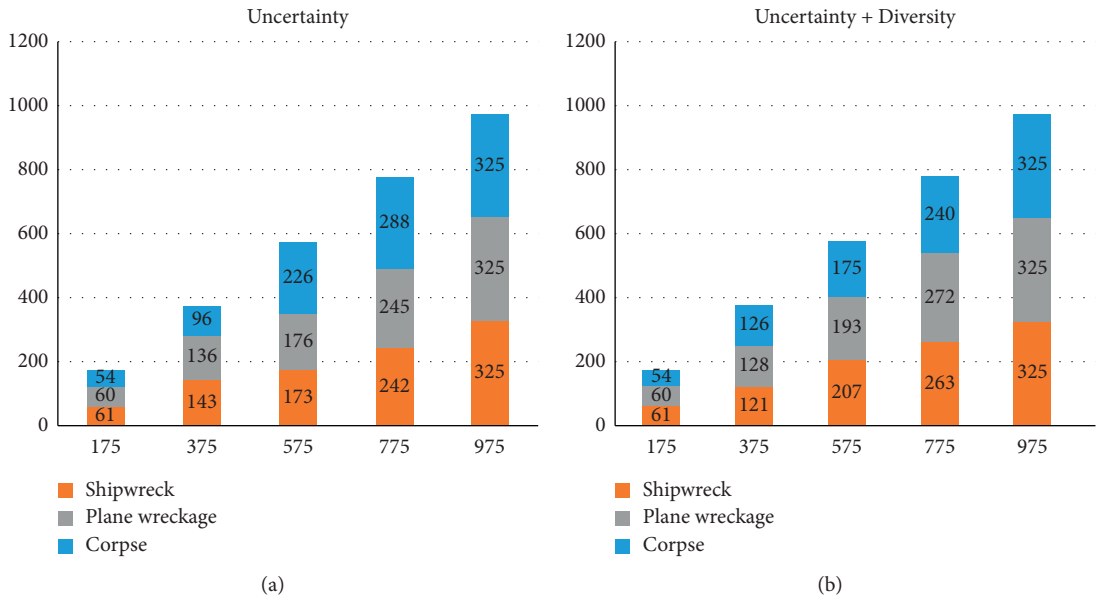

Figure 7: Continued.

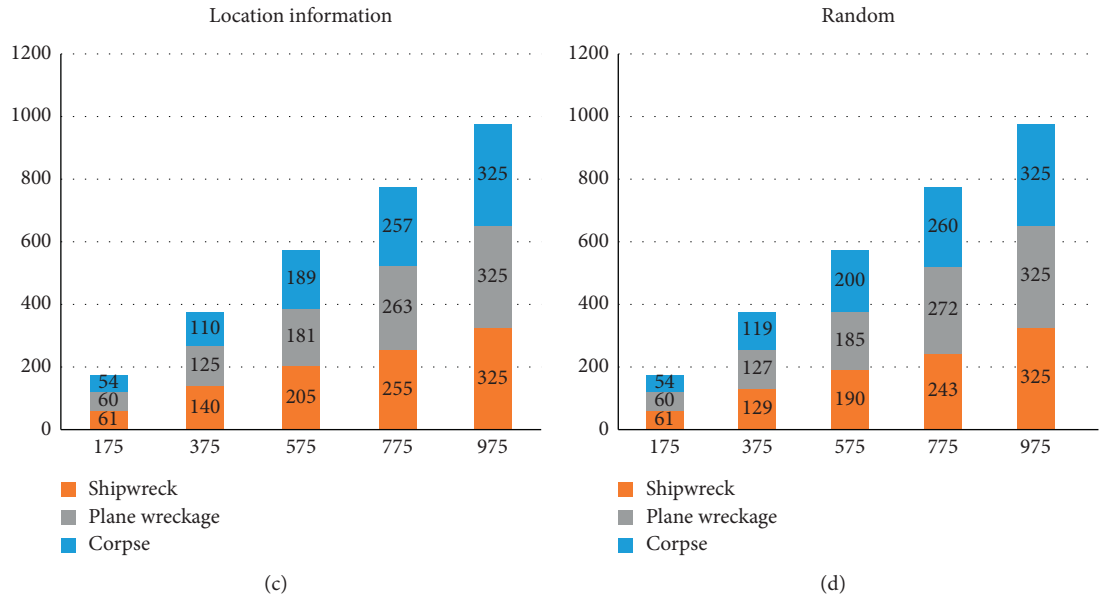

Figure 7: Number of samples selected by different algorithms.

and whether the algorithm has a relief the fit of fit that is a direction worthy of more exploration in the future.

5. Conclusions

This paper presented a convolution neural network model for classification and identification of sonar image. The performance of the proposed model was extensively evaluated, and experimental results showed that the proposed YOLOv3 model is effective to predict the box and tire in the sonar image. We also compare the performance of the proposed model with RCNN and SSD algorithms. The results show that the detection accuracy of YOLOv3 is higher than those of the other two methods in the case of tire sonar image target detection task; and the detection speed is almost the same as that of the SSD model, which is four times faster than that of the Fast RCNN model. In the future, we are planning to incorporate and compare, as well as to add tools, the effects of more in-depth learning frameworks such as the RNN and BNN.

Data Availability

The data used to support the findings of this study are included within the article.

Conflicts of Interest

The author declares that there are no conflicts of interest regarding the publication of this paper.

References

[1] G. Li, Li Xiang, X. Tan, and J. Yan, "Target detection in SAR image based on convolutional neural network," *National Security Geophysics Professional Committee of Chinese Geophysical*, vol. 8, 2020.

[2] L. Cheng, P. Zhou, and J. Han, "High resolution optical remote sensing image target detection based on rotation invariant convolution neural network," *Scientific Observation*, vol. 15, no. 6, pp. 75-76, 2020.

[3] L. M. Yang, X. Hu, and L. Hong, "Aircraft target detection in remote sensing images based on the deformable convolutional neural network," *Foreign Electronic Measurement Technology*, vol. 39, no. 7, pp. 121–126, 2020.

[4] X. Lei, *Research on Hybrid Hole Convolution Neural Network for Image Classification and Target Detection*, Xi'an University of science and technology, Xi'an, China, 2020.

[5] Y. Zheng, *Target Detection and Segmentation of Cervical TCT Image Based on the Convolutional Neural Network*, Xiangtan University, Xiangtan, China, 2020.

[6] S. Liu, *Remote Sensing Image Target Detection Method Based on Deep Convolution Neural Network*, Guangdong University of Technology, Guangzhou, China, 2020.

[7] S. Liu and L. Cheng, "Remote sensing image target detection method based on deep convolution neural network," *Industrial Control Computer*, vol. 33, no. 5, pp. 72–74, 2020.

[8] Q. Cheng, G. Chen, Lu Wang, and C. Guan, "Millimeter-wave image target detection based on the convolutional neural network," *Science Technology and Engineering*, vol. 20, no. 13, pp. 5224–5229, 2020.

[9] J. Yu, Q. Kang, Z. Chen, M. Chu, Z. Hu, and H. Yao, "Sea surface target detection in remote sensing image based on full convolution neural network," *Journal of Missile and Guidance*, vol. 40, no. 5, pp. 15–19, 2020.

[10] Y. Huang, *Application of Convolution Neural Network in Cement Electron Microscope Image Target Detection*, Hubei University of Technology, Wuhan, China, 2020.

[11] Z. Liu and Y. Li, "The target detection method of SAR image based on feature fusion convolutional neural network," *Microprocessor*, vol. 41, no. 2, pp. 31–37, 2020.

[12] S. Yang, *Remote Sensing Image Target Detection Based on Deep Convolution Neural Network*, Hebei Normal University, Shijiazhuang, China, 2020.

[13] X. Chen, *Research on Optical Remote Sensing Image Target Detection Technology Based on Convolution Neural Network*, Harbin Institute of Technology, Harbin, China, 2020.
[14] P. Yin, *Research on Aerial Image Target Detection Algorithm Based on Full Convolution Neural Network*, Harbin Institute of Technology, Harbin, China, 2020.
[15] G. Chen, Q. Cheng, C. Huang, Z. Zhou, and L. Wang, "Millimeter-wave image target detection using deep convolution neural network method," *Telecommunication Technology*, vol. 59, no. 10, pp. 1121–1126, 2019.
[16] Q. Hu, "Remote sensing image target recognition and detection based on deep convolution neural network," *Journal of Ningxia Normal University*, vol. 40, no. 10, pp. 75–79, 2019.
[17] Q. Yao, X. Hu, and L. Hong, "Aircraft target detection in remote sensing images based on multi-scale fusion feature convolution neural network," *Chinese Journal of Surveying and Mapping*, vol. 48, no. 10, pp. 1266–1274, 2019.
[18] H. Jin, *Remote Sensing Image Target Detection Based on SSD Convolutional Neural Network*, Hebei University of Geosciences, Shijiazhuang, China, 2019.
[19] W. Zeng and J. Lu, "Sonar image target detection and recognition based on convolution neural network [a]," in *Proceedings of the 17th symposium on ship underwater noise*, vol. 7, Key Laboratory of Equipment Comprehensive Support Technology of University of National Defense Science and Technology Chinese Society of Shipbuilding Engineering, Beijing, China, January 2019.
[20] H. Li, C. Li, A. Dubai, and J. Ren, "Remote sensing image target detection based on an improved convolutional neural network with an attention mechanism," *Chinese Journal of Image Graphics*, vol. 24, no. 8, pp. 1400–1408, 2019.
[21] X. Wang, Z. Guan, J. Wang, and Y. Wang, "Color image sonar target detection based on convolution neural network," *Computer Applications*, vol. 39, no. S1, pp. 187–191, 2019.
[22] C. Hu, C. Chen, C. He, H. Pei, and J. Zhang, "Ship small target detection in SAR image based on deep convolution neural network," *Chinese Journal of Inertial Technology*, vol. 27, no. 3, pp. 397–405, 2019.
[23] P. Zhang, *Research on Multi-Scale Remote Sensing Image Target Detection Method Based on Convolution Neural Network*, Xi'an University of Electronic Science and Technology, Xi'an, China, 2019.
[24] Q. Wang, *SAR Image Denoising and Target Detection and Recognition Based on the Convolutional Neural Network*, Xi'an University of Electronic Science and Technology, Xi'an, China, 2019.
[25] F. Guo, *Research on Remote Sensing Image Target Detection Algorithm Based on Deep Convolution Neural Network*, Harbin University of science and technology, Harbin, China, 2019.
[26] T. Zhou, *Image Classification and Target Detection Based on the Convolutional Neural Network*, Guangxi Normal University, Guilin, China, 2019.
[27] L. Fang, *Research on High-Resolution Image Target Detection Based on Deep Convolution Neural Network*, Liaoning University of Technology, Jinzhou, China, 2019.

Hindawi
Mobile Information Systems
Volume 2021, Article ID 5579709, 8 pages
https://doi.org/10.1155/2021/5579709

Research Article

Intelligent Integrated Community Model for Ethnic Minority Areas Using Data Analysis and Machine Learning

Xiaoxue Liu

School of Architecture and Art Design, Hebei University of Technology, Tianjin 300130, China

Correspondence should be addressed to Xiaoxue Liu; 2006011@hebut.edu.cn

Received 21 January 2021; Revised 18 February 2021; Accepted 26 February 2021; Published 9 March 2021

Academic Editor: Muhammad Babar

Copyright © 2021 Xiaoxue Liu. This is an open access article distributed under the Creative Commons Attribution License, which permits unrestricted use, distribution, and reproduction in any medium, provided the original work is properly cited.

The intelligent community has become a technological trend with the continuous development of China's Internet economy and the continuous improvement in community cooperative governance. The comprehensive service system in ethnic areas is also one of the reasons for the intelligent community. It plays an important role in community cooperative governance and comprehensive service system construction in ethnic minority areas. This paper briefly analyzes the important opportunities provided by the "wisdom community" for community cooperative governance and comprehensive service system construction in ethnic minority areas. For this purpose, an integrated model for the construction of a "culture sharing cloud system," "public cultural service microplatform," and "interactive end of public cultural service" is proposed. The mode of wisdom community's public culture is utilized in the proposed integrated model. Our proposed model puts forward some countermeasures to accelerate the construction of infrastructure, innovate the digital service system of public culture, and optimize the internal organizational structure of the government. The existing datasets are analyzed to design the proposed model. Machine learning techniques are utilized to design the proposed intelligent community system. The proposed model overcomes the existing communication bottleneck for the public cultural service in ethnic minority areas and accelerates the realization of community coordination governance and the optimization of the comprehensive service system. It also improves the modernization level of minority areas. Finally, the effectiveness of the proposed model is highlighted.

1. Introduction

In recent years, the construction of public culture in minority areas in China has made great achievements under the leadership of the party. Along with the basic aspects of China's economy, new changes have taken place, and the construction and development of public culture in ethnic areas has also entered a new stage. The third Plenary Session of the 18th CPC Central Committee proposed to "promote the innovation of the cultural system and mechanism" to "adhere to the people-centered work orientation, persist in putting social benefits first, and integrate social and economic benefits." To stimulate the vitality of the national culture as the central link, further deepen the reform of the cultural system. "At present, with the continuous improvement of the cultural quality of the masses and the wide application of network technology, the public's demand for public culture has also changed a lot." How to make full use of the technological advantages of the Internet, give full play to the role of the Internet in the optimization and integration of cultural resources allocation, and integrate the innovative achievements of the Internet with public cultural services in depth should be studied. Breaking through the existing communication bottleneck for the public cultural service in the minority areas, accelerating the realization of modernization has brought great opportunities [1]. With the continuous development of the Internet economy in our country and the continuous improvement of the community cooperative governance and comprehensive service system in ethnic areas, "intelligent community" has become a trend of development. It also plays an important role in community cooperative governance and comprehensive service system construction in ethnic minority areas [2].

The community cooperative governance and comprehensive service system is dominated by government organizations and investment, supplemented by the participation

of social forces, and is mainly used to serve and improve the quality of farmers. A comprehensive system for providing public cultural services products and services to farmers. It mainly includes the rural public cultural facilities system, the public cultural network system, the public welfare cultural service system, the public culture management system, and so forth [3–5]. The construction of community cooperative governance and comprehensive service system is an important content of the construction of new socialist countryside and an important embodiment of the implementation of the scientific concept of development and the construction of a harmonious socialist society. At present, the construction of community cooperative governance and comprehensive service system in ethnic minority areas is not perfect, the rural cultural infrastructure is relatively weak, the funds are insufficient, and the grass-roots cultural talents are lacking [6]. To perfect the community cooperative governance and comprehensive service system in ethnic minority areas, we should make great efforts to innovate the construction mode of community cooperative governance and comprehensive service system, perfect the talent training system, and construct the investment mechanism combining government and social participation [7], strengthening cultural infrastructure construction and other aspects of work. The socialization of urban community public service in minority areas is an effective way to realize the harmonious promotion of urbanization and urban public service. Through the construction of the intelligent community, we can give full play to the optimization and integration of the Internet in the allocation of cultural resources and deeply integrate the innovative achievements of the Internet and the intelligent community with the public cultural services.

There is a need of an intelligent centralized system to promote the process of socialization of public services on the basis of correctly understanding the nature of public goods and public services. In the process, it is necessary to improve the effective degree of community residents' public service demand expression, improve the community residents' public service demand expression mechanism, strengthen community cultural construction by establishing a strong community spirit, and reorganize community resources to pursue public interests. The centralized system can be based on the available data that define the responsibility of the government. Under the background of "intelligent community," this article constructs the community cooperative governance and integrated service system in ethnic areas. The paper further describes the system based on the available data by utilizing them with machine learning algorithms. It analyzes briefly the important opportunities provided by the "intelligent community" for the construction of community cooperative governance and comprehensive service system in ethnic areas. It also puts forward the construction of "culture sharing cloud system," "public cultural service microplatform," and "interactive end of public cultural service" by using the mode of "wisdom community public culture." This paper puts forward some countermeasures to accelerate the construction of infrastructure, innovate the digital service system of public culture, and optimize the internal organizational structure of the government [8–10].

The proposed model puts forward some countermeasures to accelerate the construction of infrastructure, innovate the digital service system of public culture, and optimize the internal organizational structure of the government. The existing datasets are analyzed to design the proposed model. Machine learning techniques are utilized to design our proposed intelligent community system. The proposed model overcomes the existing communication bottleneck.

2. Community Cogovernance and Comprehensive Service System

At current, the government pays more consideration to the effort of community social facility in minority zones. Due to the encouragement of geographical aspects, the deployment rate of community cultural services and resources in minority areas is low. Therefore, there is a need of an intelligent system for the community for ethnic areas.

2.1. Intelligent Community Construction. The "intelligent community" can greatly promote the innovation of the public cultural service mechanism in ethnic minority areas and use the Internet to carry out digital cultural services, from physical services to virtual services and, at the same time, in the process of constructing the service system, improve the service system through big data and improve the pertinence and effectiveness of public cultural services in ethnic areas. Simultaneously, the full use of the thinking of an "intelligent community" can greatly promote the mode of public cultural service in ethnic areas of our country and improve the efficiency of public cultural service in ethnic areas [11]. Governments at all levels may, through the combination of the Internet and cultural departments and based on the national public cultural digital support platform, establish a grass-root public digital cultural service management platform in ethnic minority areas and formulate corresponding platform construction, management, and application standards. To realize the integrated intelligent management of the basic level public cultural service network facilities and the project of benefiting the people [12], the architecture of the smart community can be divided into four levels: the perception level, the network level, application level, and the terminal level. The sensing layer uses sensing devices to collect data and monitor devices. The network layer is used to transmit information in the smart community. The application layer provides various services for residents, and the terminal layer allows users to use various services of the intelligent community through various intelligent terminals. The architecture of the smart community is shown in Figure 1.

2.1.1. Perception Layer. The sensory layer is used for the meter set of data. Perceptual devices use sensing devices such as gateways, sensors, and modules to fully inspect and collect real-time information about the infrastructure. The sensing layer equipment of the infrastructure management system is

a variety of instruments and gateways. The meters are responsible for collecting residents' water, electricity, and gas usage information and transmitting the information to the gateway. The gateway transmits the data to the network layer. Administrators can fully understand the usage of water, electricity, and gas in real time through water, electricity, gas, and other information and realize a fully aware function.

2.1.2. Network Layer. Perceived devices, application servers, and smart terminals are connected at the network layer, and various subsystems are brought together at the network layer to form a unified smart community service platform. The network and fourth-generation mobile communication technologies will play a catalytic role in the development of smart communities. Besides, they include sensor networks and wireless networks. The infrastructure management system will use acquisition servers and networks as the network layer for data transfer.

2.1.3. Application Layer. The function of the application layer is to process the sensed data and provide people with various application services, including infrastructure management, smart home, community security, billing services, e-commerce, telemedicine, and remote monitoring. Among them, infrastructure management includes elevator management, street lamp management, instrument management, drainage management, monitoring, and management. The infrastructure management system processes the data collected by the instrument to provide users with instrument management services and payment services, which makes it easier for administrators to manage instruments and other equipment and, at the same time, makes it easier for people to pay.

2.1.4. Application Layer. Community residents use terminal devices to use smart community services. Terminal equipment includes mobile phones, home smart terminals, smart remotes, and tablet computers. In the infrastructure management system, people can use mobile phones and carry out payment and inquiries.

2.2. National Public Culture Service System Promotion in the Wisdom Community. The wisdom community promotion is the key to the success of the national public cultural service system. The detailed description of the required promotion components is discussed in the upcoming sections.

2.2.1. Culture Sharing Cloud. Integrate superior resources and establish a "culture sharing cloud" system in ethnic areas. Cloud computing, big data, and mobile Internet are today's three hot topics of information technology. In combination with the latest practice of public digital culture and the development trend of information technology, we can build a "culture sharing cloud" system in minority areas with all-round coverage, multiterminal access, cross-platform, and multichannel distribution. When the mobile terminal installs the corresponding software and browses the corresponding website, it can understand a series of cultural activities information anytime and anywhere, enjoy the one-stop public cultural service, and effectively solve the information asymmetry of the public cultural activities. Facilities resource utilization rate is not high [13].

2.2.2. Microplatform. Activate the market potential and establish the microplatform of public cultural service in minority areas. The Internet has a full impact on the world today, and all industrial areas will be redefined, including cultural industries. Zhoushan City in Zhejiang Province, with the help of the Taobao model, launched the "Amoy Culture Network" to let cultural teams of all kinds produce cultural products to act as "sellers" and organizations or groups of consumers' cultural products to act as "buyers." In addition to placing orders, buying, and selling, you can also evaluate services to build a freely chosen platform between buyers and sellers. Ethnic regions have very rich traditional cultural resources, can rely on "Zhoushan mode," through the integration of resources to build a new demand-oriented cultural supply and demand docking network platform, draw lessons from the Taobao operation model, relying on the Internet, and set up an efficient and convenient service platform for government, market, and masses.

2.2.3. Information Asymmetry. To set up the interactive end of public cultural service in ethnic areas, "information asymmetry" has always been a difficult problem for community coordination governance and comprehensive service system construction in ethnic minority areas: on the one hand, people always say that they do not know what cultural activities are being held; on the other hand, cultural venues often complain about lack of popularity. Similarly, some local governments invest a lot of manpower and material resources in cultural service projects, and the public may not like them. This requires the government to attach great importance to the interactive construction of public cultural services. It is necessary to use the Internet as an important platform for the investigation, collection, and analysis of the cultural needs of the masses, to establish a microplatform for interaction with the masses in ethnic areas, and to publish some cultural resources information through government portals, official WeChat, Weibo, and other interactive terminals. Let the masses truly express their cultural needs and meet the needs of the masses.

3. Path Choice of Proposed System in Minority Areas

There are several options to choose the best one. We have proposed a mechanism to choose the right path.

3.1. Strategic Significance of Proposed System Construction in Ethnic Areas. The 17th Session of the Third Plenary Session of the Communist Party of China (CPC) adopted the Decision of the Central Committee of the Communist Party of China on several important issues concerning the development of rural reform and further called for the acceleration of the development of rural public undertakings and the improvement in the overall progress of the rural society [14]. Firstly, it is an important content of building a new socialist countryside. The production and development, living allowance, township wind civilization, village cleanness, and management democracy are the general requirements of the construction of socialist new countryside. The core of the new socialist countryside construction is to strengthen the construction of rural culture [15]. The community management structure is shown in Figure 2.

Secondly, it is an unavoidable requisite to completely execute the scientific growth and shape a harmonious socialist harmonious society [16, 17]. It is necessary to accelerate the construction of community cooperative governance and comprehensive service system, realize good, maintain good, develop the basic cultural rights and interests of the masses of peasants, reflect the scientific development of the cultural undertakings, promote the comprehensive integration and effective utilization of various cultural resource elements, such as government resources, social resources, service resources, and management resources, and promote the comprehensive, coordinated and sustainable development of culture and society.

Thirdly, it is an essential obligation to attain the shared agreement of the peoples and the shared success and growth. It is also a necessary strategy of the Central Government to provision the fast-tracked growth of ethnic minorities and ethnic areas [18]. The ethnic minorities require an urgent action in the context of COVID 19 [19]. The National unity is the fundamental guarantee for maintaining national unity and realizing the common development of all peoples. The only development in the minority areas can be stabilized. The culture is the spiritual power of strengthening unity and urging people to move forward. The cultural level is also lower than that of the central and eastern regions and ethnic areas. It is possible to develop a public cultural service system, foster the comprehensive quality of the masses of the masses, and train new citizens who can meet the requirements of the socialist market economy, and it is an effective way to promote the common prosperity of the peoples [20, 21]. It is a strong link between the people of our country and the people of our country to work together for common prosperity and development. It is an important role to build a public cultural service system, develop rich and colorful and unique ethnic cultures, and play an important role in strengthening the unity and cooperation of all peoples and realizing the common prosperity of the peoples.

3.2. Improvement of Proposed System in Ethnic Areas. The improvement of the Community Cooperative Governance and Integrated Service can be done in the following ways.

3.2.1. Establish and Improve the Elementary System of Rural Public Culture in Ethnic Areas. The establishment and improvement of the elementary system of rural public culture in ethnic areas are required to improve the system for the ethnic areas. The construction of cultural infrastructure in the minority areas has been greatly improved in recent years, but the cultural infrastructure is still relatively backward compared with the eastern region. Therefore, Party and Government must attach great importance to the improvement of public cultural infrastructure.

3.2.2. Improving Talent Training System. The talent training system and its strengthening are also required in the construction of rural cultural teams in ethnic areas. First, we should strengthen the management of the existing talents, use the existing talents, improve the treatment, and devote themselves to the development of the cultural undertakings in the minority areas. Secondly, we should strengthen the cultivation of the new people, build the endogenous mechanism of the rural public cultural services, and cultivate the new rural cultural subjects. Most of the ethnic areas are located in remote areas with inconvenient traffic, poor information, underdeveloped economy, strong measures are required to meet the needs of the people's spiritual and cultural needs in these areas, and the training of the cultural information resources is in sharing engineering talents, the introduction of professional technical personnel, and the organization of a high-level resource construction, software development, and website maintenance technical backbone team; thirdly, in the face of the deterioration of the cultural environment of minority nationality, the cultivation of cultural construction management talents, such as radio and television and library and information, is mandatory.

3.2.3. Innovative Community Cooperative Governance and Integrated Service System Construction Model. In the construction of community cogovernance and comprehensive service system, the mode of innovation must be innovated. Firstly, it is necessary to fundamentally change the development mode with the external one-way input as the main and to focus on the integration of the advanced culture of socialism with the folk culture of the excellent national folk culture in our country.

3.2.4. Input Mechanism of the Combination of Government and Social Participation. The shortage of funds is the most direct reason for the lag of rural cultural development in the minority areas. The abundant capital investment is the basic guarantee for the construction of public culture in rural areas. On the one hand, the government should increase the input of rural public culture funds and, on the other hand, should establish scientific and institutionalized investment mechanisms to form an investment safeguard mechanism of a virtuous circle. To encourage the multi-input of community cooperative governance and comprehensive service system, we should encourage the multi-input of community cooperative governance and comprehensive service system,

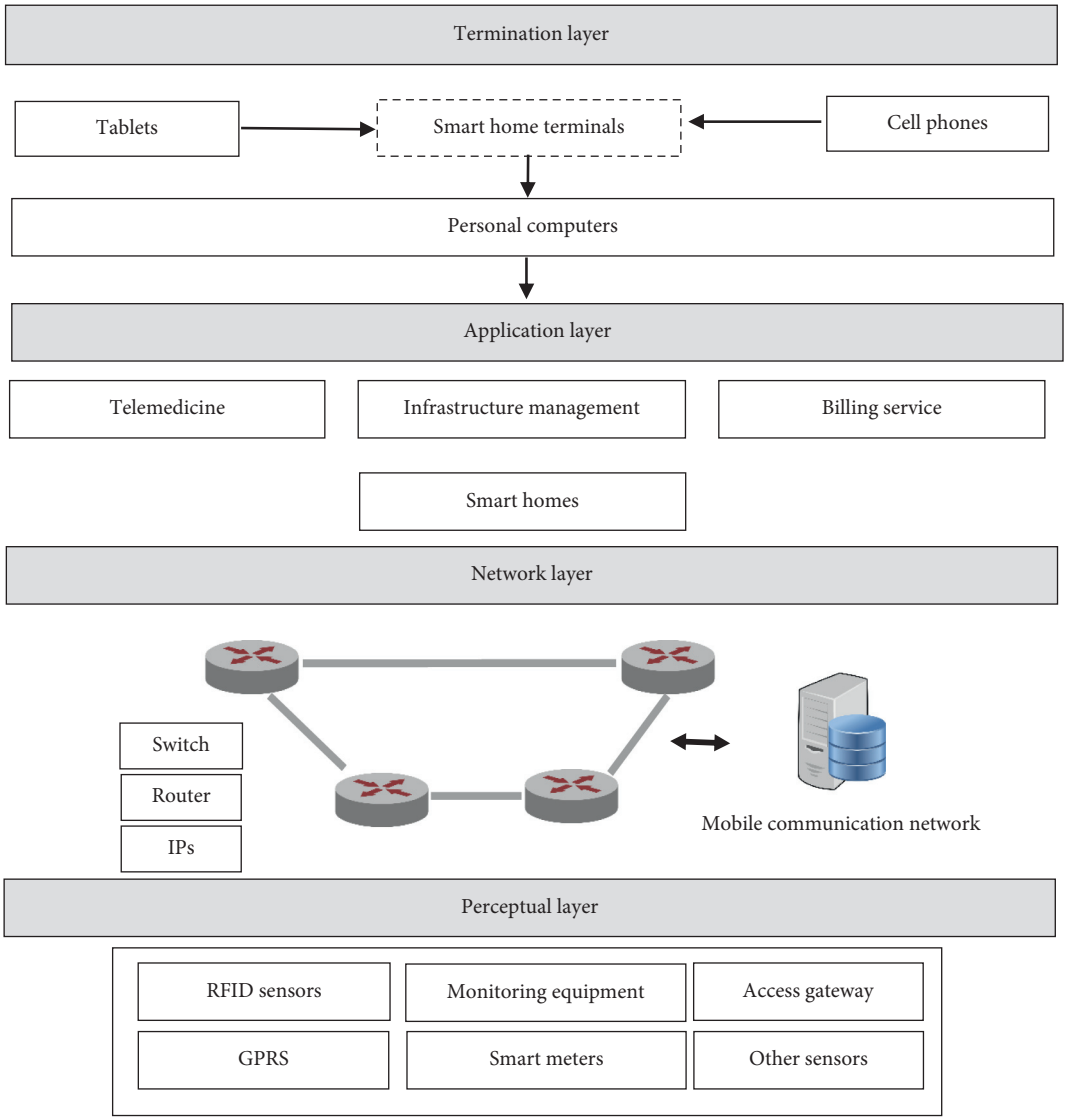

Figure 1: Smart and intelligent community architecture.

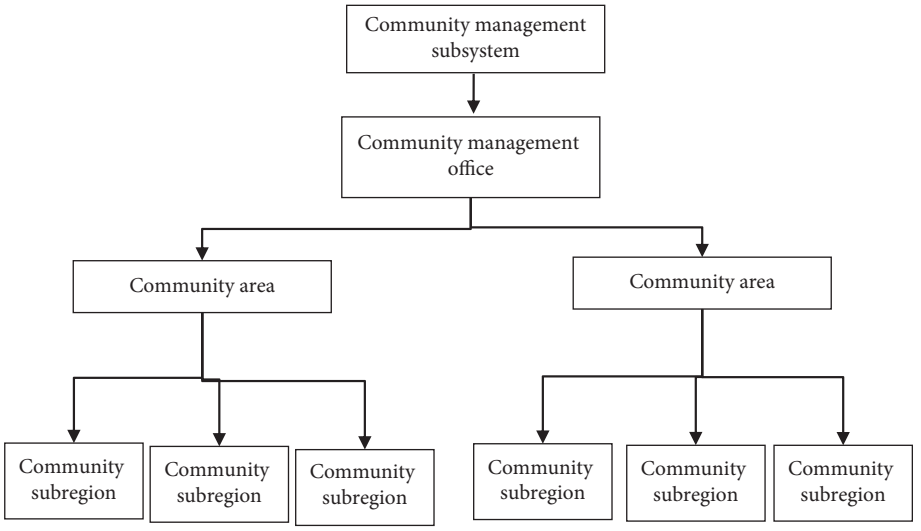

Figure 2: Structural diagram of smart community management.

Table 1: Comparison of existing and proposed systems.

Existing system	Proposed system
Does not support decision-making	Support decision-making
Not adaptable	Adaptable
Static	Dynamic
Manual services	Digital services
Not optimized	Optimized
Does not provide training	Include training system
Only tradition elementary services	Improved elementary services
Does not support telemedicine	Support telemedicine
Does not support smart services	Support smart services

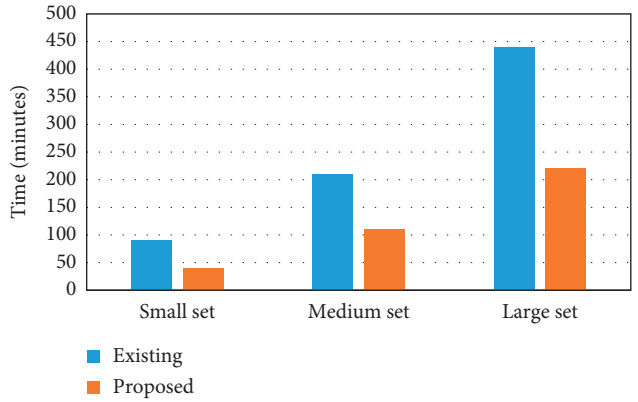

Figure 3: Comparison of execution time.

cultivate the pluralism of the main body, encourage the community to participate in the construction of rural public culture, and implement and perfect the preferential policies for the donation and sponsorship of rural cultural undertakings.

4. Countermeasures and Suggestions

The countermeasures and suggestions of "Wisdom Community" are also required for the Construction of Community Coordination and Integrated Service systems in minority areas. This mechanism highlights the effectiveness.

4.1. Multiple Investors and Internet Infrastructure. In this section, we need to create multiple investors and speed up the construction of Internet infrastructure. The construction of a public cultural service system in minority areas needs to gradually adjust the investment means of the government to the end, actively play the role of folk capital, broaden the channels of investment in public cultural services, and establish. The multi-investment mechanism is constructed based on government investment and supplemented by social multichannel investment. Ethnic regions have unique cultural and geographical advantages, and local governments can also seek cooperation with the eastern developed provinces to attract folk capital and other ways, to construct the diversification of investment subjects, to mobilize social forces to participate widely, and to contribute to the infrastructure construction in minority areas.

4.2. Cultural Development Modernization and Digital Service System Innovation. We need to speed up the modernization of cultural development and innovate the digital service system of public culture. By the end of December 2017, China's Internet users had reached 1029 million, including 820 million mobile phone users, according to CNNIC, the China Internet Information Center. Mobile Internet has become the most important way for people to obtain cultural information. The construction of public culture in minority areas can use modern science and technology to integrate public cultural services, promote the public digital cultural service network, and create a digital service platform covering urban and rural areas, with the Internet as the main service means. Local governments can share cultural resources as a whole, strengthen digital processing and integration of public cultural information and products in minority areas, and develop and produce traditional cultural information and satellite data for the needs of ethnic minorities. Resources especially focus on the intangible cultural heritage and minority languages and other traditional cultural resources "digital" protection.

4.3. Internal Structure Optimization and Cultural Resources Utilization. Finally, we need to optimize the internal structure of the government and coordinate and integrate the utilization of cultural resources. The construction of a modern public cultural service system involves the production and distribution of cultural products. The whole system design including management and resource

guarantee system must integrate the power of government and society and break through the system limitation of trade barrier and public resource system. The establishment of a coordination mechanism for the construction of a public cultural service system is a strong organizational guarantee for the construction of an "intelligent community public culture" in ethnic areas. The governments of ethnic minority areas should take the opportunity of deepening the reform of the cultural system to set up a cultural sector-led, economic, propaganda, financial, radio, and television industry. The coordinating body of sports and other departments is responsible for the work of "public cultural service in intelligent community" and responsible for organizing, planning, coordinating, carrying out, examining, coordinating regional cultural resources, and speeding up the formation of the scientific and effective macrocultural management system. Through a sound and perfect organizational system, the construction of "public culture in intelligent communities" should be promoted into a new stage of development so that the broad masses of the people in minority areas can share the fruits of reform and development and enrich the cultural life. The comparison of the proposed system based on the Intelligent Community Model with the existing system is depicted in Table 1. The comparison of process execution time with the existing system is also provided in Figure 3 regarding different classes of the processes (e.g., small set, medium set, and large set). The small process set is up to 10 processes, the medium process set includes 10–20 processes, while the large set is having around 20–30 processes.

5. Conclusions

This article proposes an intelligent system model to realize the socialization of public services in minority areas. The cooperative governance and integrated service system in minority areas is an important process. The proposed model is the integration on the construction of "culture sharing cloud system," "public cultural service microplatform," and "interactive end of public cultural service." The existing datasets are analyzed to design the proposed model. Machine learning techniques are utilized to design the proposed intelligent community system. Under the background of "intelligent community," it optimizes the construction of community cooperative governance and comprehensive service system in ethnic minority areas, mobilizes social forces to participate extensively, and contributes to the construction of infrastructure in minority areas. The innovative achievements of the Internet and the intelligent communities are deeply integrated with the public cultural services, to serve the public in minority areas. The effectiveness of the proposed model is also highlighted. Besides, it also improves the modernization level of minority areas. The proposed model overcomes the existing communication bottleneck for the public cultural service in minority areas.

Data Availability

We have already included the analysis data in our manuscript.

Conflicts of Interest

The author declares that there are no conflicts of interest.

References

[1] L. Mao, "Practice and thinking of promoting community cooperative governance and comprehensive service system construction," *Jiangnan Forum*, vol. 11, no. 2, pp. 23–25, 2008.

[2] J. Chen, "On the construction of community synergetic governance and integrated service system in ethnic areas," *Guizhou Ethnic Studies*, vol. 2, pp. 16–19, 2008.

[3] Z. Xiao, L. Zhu, F. Dongyu, and D. Zhang, "Performance optimization of distributed database aggregation computing," *Journal of Computer Applications*, vol. 37, no. 5, pp. 1251–1256, 2017.

[4] J. Han, E. Haihong, G. Le et al., "Survey on NoSQL database," in *Proceedings of the 20116th International Conference on Pervasive Computing and Applications*, pp. 363–366, IEEE, Piscataway, NJ, USA, May 2011.

[5] J. Han, M. Song, and J. Song, "A novel solution of distributed memory NoSQL database for cloud computing," in *Proceedings of the 2011 IEEE/ACIS 10th International Conference on Computer and Information Science*, pp. 351–355, IEEE, Piscataway, NJ, USA, May 2011.

[6] H. Kaur and J. Singh, "Improvement in load balancing technique for MongoDB clusters," *International Journal of Applied Information Systems*, vol. 8, no. 4, pp. 31–35, 2015.

[7] J. Ean and S. Ghemawat, "MapReduce:simplified data processing on large clusters," *Communications of the ACM*, vol. 51, no. 1, pp. 107–113, 2008.

[8] E. Dede, M. Govindaraju, D. Gunter et al., "Performance evaluation of a MongoDB and Hadoop platform for scientific data analysis," in *Proceedings of the 4th ACM Workshop on Scientific Cloud Computing*, pp. 13–20, ACM, New York, NY, USA, June 2013.

[9] Y. Liu, Y. Wang, and Y. Jin, "Research on the improvement of MongoDB auto-sharding in cloud environment," in *Proceedings of the 20127th International Conference on Computer Science & Education*, pp. 851–854, IEEE, Piscataway, NJ, USA, July 2012.

[10] P. Kookarinrat and Y. Temtanapat, "Analysis of range-based key properties for sharded cluster of MongoDB," in *Proceedings of the 2015 2nd International Conference on Information Science and Security*, pp. 1–4, IEEE, Piscataway, NJ, USA, December 2015.

[11] V. Dyo, S. A. Ellwood, D. W. Macdonald et al., "Wildsensing," *ACM Transactions on Sensor Networks*, vol. 8, no. 4, pp. 1–33, 2012.

[12] D. Miorandi, S. Sicari, F. De Pellegrini, and I. Chlamtac, "Internet of things: vision, applications and research challenges," *Ad Hoc Networks*, vol. 10, no. 7, pp. 1497–1516, 2012.

[13] S. K. Chong, M. M. Gaber, S. Krishnaswamy, and S. W. Loke, "Energy conservation in wireless sensor networks: a rule-based approach," *Knowledge and Information Systems*, vol. 28, no. 3, pp. 579–614, 2011.

[14] L. M. Oliveira and J. J. Rodrigues, "Wireless sensor networks: a survey on environmental monitoring," *Journal of Communications*, vol. 6, no. 2, pp. 143–151, 2011.

[15] G. Hackmann, F. Sun, N. Castaneda, C. Lu, and S. Dyke, "A holistic approach to decentralized structural damage localization using wireless sensor networks," *Computer Communications*, vol. 36, no. 1, pp. 29–41, 2012.

[16] S. Li, "Research on the construction of legal mechanism of socialist harmonious society based on computer simulation," in *Journal of Physics: Conference Series,* vol. 1544, no. 1, IOP Publishing, Article ID 012200, 2020.
[17] C. P. Pow, "Building a harmonious society through greening: ecological civilization and aesthetic governmentality in China," *Annals of the American Association of Geographers*, vol. 108, no. 3, pp. 864–883, 2018.
[18] H. Weber, "The educational divide over feelings about ethnic minorities: does more education really lead to less prejudice?" *Journal of Ethnic and Migration Studies*, vol. 2020, pp. 1–20, 2020.
[19] K. Khunti, L. Platt, R. Ash, and K. Abbasi, "Covid-19 and ethnic minorities: an urgent agenda for overdue action," *BMJ*, vol. m2503, 2020.
[20] A. Y. Lo, "Carbon trading in a socialist market economy: can China make a difference?" *Ecological Economics*, vol. 87, pp. 72–74, 2013.
[21] G. Sigley, "Chinese governmentalities: government, governance and the socialist market economy," *Economy and Society*, vol. 35, no. 4, pp. 487–508, 2006.

Hindawi
Mobile Information Systems
Volume 2021, Article ID 5595833, 8 pages
https://doi.org/10.1155/2021/5595833

Research Article

Prediction of Volleyball Competition Using Machine Learning and Edge Intelligence

Qiang Liu and Qiannan Liu

The Graduate School, Woosuk University, Wanju, Republic of Korea

Correspondence should be addressed to Qiannan Liu; emma@hgu.edu.cn

Received 17 January 2021; Revised 7 February 2021; Accepted 27 February 2021; Published 8 March 2021

Academic Editor: Muhammad Babar

Copyright © 2021 Qiang Liu and Qiannan Liu. This is an open access article distributed under the Creative Commons Attribution License, which permits unrestricted use, distribution, and reproduction in any medium, provided the original work is properly cited.

Data analysis and machine learning are the backbones of the current era. Human society has entered machine learning and data science that increases the data capacity. It has been widely acknowledged that not only does the number of information increase exponentially, but also the way of human information management and processing is completed to be changed from manual to computer, mainly depending on the transformation of information technology including a computer, network, and communication. This paper is aimed at a solution to the lag of the methods and means of volleyball technique prediction in China. Through field visits, it is found that the way of analysis and research of techniques and tactics in Chinese volleyball practice is relatively backward, which to a certain extent affected the rapid development of Chinese volleyball. Therefore, it is a necessary and urgent task to realize the reform of the methods and means of volleyball technical and tactical analysis in China. The data analysis and prediction are based on the machine learning and data mining algorithm applied to volleyball in this paper is an inevitable trend. The proposed model is applied to the data produced at the edges of the systems and thoroughly analyzed. The Apriori algorithm of the machine learning algorithm is utilized to process the data and provide a prediction about the strategies of a volleyball match. The Apriori algorithm of machine learning is also optimized to perform better data analysis. The effectiveness of the proposed model is also highlighted.

1. Introduction

The development of the modern Olympic Games for more than 100 years has proved that the improvement of the performance of competitive sports has gone through the following four stages in turn. Machine learning is widely used to predict sports [1]: the period of natural growth, the period of a large amount of movement, the period of high-intensity growth, and the period of scientific growth [2]. A detailed review is also provided in this context [3]. At present, competitive sports are in the fourth stage when its remarkable feature is that science and technology have been involved in the whole process of competitive sports from material selection, training, and competition to recovery. In other words, science and technology are the wings of competitive sports [4]. Now the human society has entered the IT Era when the marked sign is that not only does the number of information increase exponentially but the way of information management and processing relies mainly on information technology including a computer, network, and communication. In other words, the level of information collection, management, processing, and analysis is the determinant of the correctness of human decision-making and behavior selection [5].

It is reported that Liu Xiang, a Chinese track and field athlete who won the gold medal in the 110-meter hurdles at Athens Olympic Games, has more than 70 scientific research institutes and sports companies at home and abroad. They did scientific research for him in the design of running shoes, nutrition supply, recovery and rest, tactical analysis, and other aspects. Only during the preliminaries and finals, there were more than 10 scientific research personnel of the National Sports Administration Institute, Shanghai Sports Scientific Research Institute, and CCTV analyzing and comparing the hurdles and tactics of the athletes Liu Xiang

and Alan Johnson in both Beijing and Athens by modern computer information means, such as video acquisition, comparison on the same screen, the transmission of streaming media network, and so on. Also, this staff provided feedback of the information to Liu Xiang in time, which made him know himself as well as the enemy and make the best use of the advantages and bypass the disadvantages. Liu Xiang played his competitive level normally and even supernormally in the game and contributed to the historical breakthrough of Chinese track and field [6].

Data mining technology and tactics statistics of sports are excavated through two technologies, data mining and correlation analysis and visualization [7]. The use of the volleyball technique and tactics analysis model (BTT) is applicable not only to precompetition preparation and postgame summary, but also to the analysis of technical and tactical data in the game [8, 9]. In the field of data mining, this study attempts to use association analysis and visualization technology to make a preliminary excavation of the information behind the volleyball technical and tactical data. As far as the breadth of mining means and the depth of the mining content are concerned, it is far from enough, so these deficiencies will be the direction and task of the follow-up study. The Apriori technique is used for the recurrent element set mining [10]. It is also based on the learning of the association rule over relational Database Management systems (DBMS). It operates by recognizing the recurrent distinct objects in the DBMS and outspreading them to bigger and bigger object sets until necessarily repeated in the DBMS.

2. Literature Review

Machine learning methods and tactics statistics of volleyball can be mined through two types of machinery, which are data mining and correlation analysis and visualization [11]. The usage of the volleyball practice and strategies investigation model is appropriate for precompetition preparation and postgame summary [12]. It can also be utilized to analyze the technical and tactical data during the game. In the field of data mining, this study attempts to use association analysis and visualization technology to make a preliminary excavation of the information behind the volleyball technical and tactical data [13]. As far as the breadth of mining means and the depth of the mining content are concerned, it is far from enough, so these deficiencies will be the direction and task of the follow-up study. The Apriori technique is used for the recurrent element set mining [14]. It is also based on the learning of the association rule over relational Database Management systems (DBMS). It operates by recognizing the recurrent distinct objects in the DBMS and outspreading them to bigger and bigger object sets until necessarily repeated in the DBMS.

For many years, scholars at home and abroad have carried out the substantive study of volleyball techniques and tactics at the same time along several different paths. The scholars use the logical method of history to find the time and background of the appearance of various volleyball techniques, such as variable direction dribble appearing in 1908, volleyball hook shot appearing in 1940, and so on [15]. The scholars have put forward a new point of view through the analysis of kinematics and dynamics of volleyball technique by using biomechanics; with the help of high-speed photographic instruments, the athletes' technical movements are photographed, with three-dimensional kinematics and dynamics analysis of the film or simplified processing of motion technology to build a model for mechanical analysis. Also, using kinematics, classical mechanics, anatomy, and even aerodynamics knowledge and principles, scholars have made some useful discussions on the posture, aiming point, and rotation of the ball. For example, the direction of the arm and the finger should be close to the middle axis of the human body.

Association rule mining is largely apprehensive with unseen, motivating, and valued relationships among relational databases (RDMS), transaction databases, and massive data items [16]. These huge and massive data items are in the form of information storage, which is one of the important research contents in data mining. Among them, the Apriori algorithm is the most classical association rule extraction algorithm. The hollow ball cast aiming point should be selected in the net rather than the traditional textbook advocated distal proximal, and the ball in the air should spin, which is conducive to high arc [17]. Scholars also put forward a study of volleyball technology from the perspective of psychology. For example, the use of positive self-hints in a free throw can help the completion of a technical movement. In volleyball training, the imagination training method, the image training method, the simulated competition scene training method, and the self-confidence training method are used [18]. There are several proposals that are focusing on sports prediction [19–21].

Edge computing is carried out to improve the processing of the systems. Edge computing is a viewpoint of computer networking that is based on the idea of carrying processing as close to the data. It improves the processing. The Apriori method of machine learning can be applied to edge computing to perform faster processing. The traditional data analysis can also be improved by utilizing the machine learning mechanism. The Apriori method is one of the widely used methods to perform data analysis. The processing activity can also be improved if the data computation is done using the edge computing concept. The traditional Apriori has several challenges including the bottleneck challenge. Therefore, there is a need for optimization of this algorithm to solve the bottleneck problem of the Apriori algorithm and improve the efficiency of the algorithm.

3. Proposed Methodology

This section describes the proposed methodology for the prediction of volleyball matches using edge-enabled data analysis. The proposed model is based on a machine learning algorithm. The classical Apriori algorithm of machine learning is utilized in this research. The classical Apriori algorithms are extended and optimized to overcome the challenges faced by the traditional approach. The Apriori technique is used for the recurrent element set mining. It is

also based on the learning of the association rule over relational database management systems (DBMS). It operates by recognizing the recurrent distinct objects in the DBMS and outspreading them to bigger and bigger object sets until necessarily repeated in the DBMS. The detailed description of the proposed extended Apriori algorithms is shown below.

3.1. Extended Apriori Algorithm. Association rule mining is mainly concerned with hidden, interesting, and valuable laws between relational databases, transaction databases, and massive data items in information storage, which is one of the important research contents in data mining. Among them, the Apriori algorithm is the most classical association rule extraction algorithm, and other related algorithms are improved or extended based on the algorithm. To further study the algorithm of association rule mining, we first introduce the classic Apriori algorithm. The Apriori algorithm uses an iterative method of layer-by-layer exploration, and the k-term set is used to find the $(k+1)$-itemset. First, the frequent 1-term set Li is obtained, and the frequent 2-term set $L2$ is searched with Li, and $L2$ is used to search for $L3$, and so on, until the frequent $(k+1)$-itemset cannot be found. Among them, the largest frequent itemsets are k-frequent itemsets, and each Lk needs to scan a database once. The nature of Apriori: the nonempty subset of any frequent itemset is also a frequent itemset. The nature of Apriori is used to search for frequent itemsets with two steps: connection and pruning. In the connection part, the $\mathrm{Lk}-i$ is connected with the $\mathrm{Lk}-i$ to generate a possible candidate itemset; in the pruning part, the candidate itemsets with infrequent subsets are deleted by using the Apriori property.

From the description of the above algorithms, it is not difficult to find that although the Apriori algorithm reduces the number of candidate items, in the execution of the "connection-pruning" iteration it is still inevitable to test a large number of candidate sets frequently and to scan the database repeatedly. When the database is large enough to repeatedly scan the external needs, the efficiency is low. Processing I/O operations for large-scale data has become a bottleneck for improving efficiency. Therefore, to improve the efficiency of the Apriori algorithm, the defects of the Apriori algorithm will be improved in the next chapter. A matrix candidate itemset and frequent itemsets are proposed. To reduce the time overhead of the corresponding operation, the matrix is compressed according to the related properties.

The set item F_q': the result attribute in the matching relational database is the case of R_k and the attribute value is d; if the item $R_k(d \longrightarrow \sim d)$ is expressed as F_q^m, then r^m: $F_1^m \wedge F_2^m \wedge \ldots \wedge F_{L'}^m \Rightarrow F_q^m$. F_i' belongs to the state before the change, and F_i'' belongs to the state that has changed. In this case, the support degree sup (R), lifting quantity lift-measure (R), and confidence conf (R) of rule R are as follows:

$$\begin{aligned} \sup(r) &= \sup(r'), \\ \text{lift_measure}(r) &= \text{lift}(r') - \text{lift}(r''), \\ \text{con}(r) &= \frac{\text{lift}(r') - \text{lift}(r'')}{\text{lift}(r')} = \frac{\text{lift_measure}(r)}{\text{lift}(r')}. \end{aligned} \tag{1}$$

The degree of support in the rule represents the scope of influence, which shows the usefulness of the rules. Lifting capacity showed the degree of change, enhancing the degree of higher representatives will be the value of the F_i property from a_i to a_j; the R_k property value is d in reducing the more. Confidence is the certainty that shows the change. Then for the nature of lift_measure, for association rules, the lifting degree belongs to a class of relative low complexity measures. The formula for calculating the lifting degree between A and B is

$$\text{lift}\ (A, B) = \frac{P(A \cup B)}{P(A)P(B)}. \tag{2}$$

By the expression of lift in the association rules, the correlation metric formula based on the lifting quantity can be expressed as

$$\text{corr}_{(A1 \longrightarrow A2)\cdot(B \longrightarrow \sim B)} = \text{lift}\ (A1, B) - \text{lift}\ (A2, B). \tag{3}$$

It is important to note that, in the form, $A1$ represents the set of initial sets, and $A2$ represents the set of itemsets for $A1$ mutex, and B represents the set of the result. Here we contact to reduce the occurrence of B. The proposed extended algorithm is also optimized to effectively utilize and achieve better results. The algorithm efficiency is improved in the context of bottleneck challenges.

3.2. Algorithm Optimization. The proposed algorithm is optimized to solve the bottleneck problem of the Apriori algorithm and improve the efficiency of the algorithm. This research improves the efficiency in the context of the few concepts. First, the source database is scanned, based on the source transaction database, and the transaction matrix D is constructed according to the definition. The transaction is the line and the itemset is the column when the transaction matrix is constructed. In order to facilitate the compression of a matrix, a column of sum_c is added to the matrix to record the number of items contained by each firm. And a row of sum_r is added to the matrix to record the count of each item's support. According to the definition, the minimum support transaction number min_supsh is calculated and the matrix is compared. If the value of an element is less than min_supsh, the column corresponding to the element is deleted, from which we get frequent 1-term sets. The sum_c column is recalculated; if the value of an element is 0, the line

of the element is deleted. Thus, the matrix $D1$ is produced. When compressing the matrix $D1$, K-frequent itemset ($k \geq 2$) is produced. According to the property 1, the column corresponding to the item Ij of the frequent $(k-1)$-itemset less than k is deleted. The sum_c column is recalculated again, and then according to the property 2, if the value of an element is less than k, the element corresponding to the element is deleted. Recalculate the sum_r line; if the value of an element is less than min_supsh, the column corresponding to the element is deleted. The matrix is compressed repeatedly until it can not be compacted again. The matrix Dk after the compression is obtained.

Set up an auxiliary two-dimensional array, which is used to record the frequency and the corresponding combination of subscript mix, so you can more easily find frequent itemsets k-($k \geq 2$). According to definition 3, we collected the column vector of the matrix Dk corresponding K dimensional combination and for each combination of vector and bitwise operations on a K column and for "number 1" and to obtain the K dimension of the support number. If the support number of K dimension is not less than min_supsh, then the itemset in the combination pair is a frequent k-itemset. The results are stored in a two-dimensional array, the front is the subscript of the corresponding set of items, and the last column is the itemset to support the number of transactions. According to the nature, if the number of frequent k-itemsets is less than $k+1$, the search frequent itemsets are terminated. Otherwise, repeat the above call until the generated frequent itemsets are empty. This process improves the efficiency of the proposed extended Apriori algorithms.

4. Result and Discussion

This section describes the results of the simulation. The results are generated using the proposed extended and optimized machine learning algorithm. The dataset is achieved using the edge computing concepts. As mentioned above, although volleyball is a collective event, the one or two players, especially the core players or role players, are not the decisive players, but not all players, because the volleyball match is the winning or losing of the score on both sides of the game, and the precondition of hitting the ball is the right to have the ball. In the game, there are five players on one side, and there is only one volleyball, so the chance of each player is unbalanced in terms of the right of the ball. Volleyball is controlled and disposed by core players in most of the time and crucial moments, and the tactics of the team are also designed and run around core players and role players. So the core and role players of a team, as well as the restrictions on the core and role players of the team, are the key to winning the game. So as long as the analysis of the team's core players and the main players is almost equal to the analysis of a team, the strategic line map of the core players and the main players is shown in Figure 1.

For the high level volleyball players, their technical and tactical patterns are in a dynamic pattern, and the characteristics of attack and defense are relatively fixed. For example, the choice of the way of attacking the ball and the

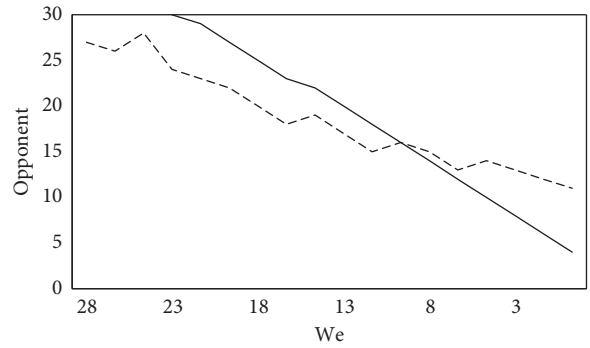

Figure 1: Core player and main player strategic line.

area, the defensive position, and the choice of the tactics have certain rules, which provides the possibility for the analysis of tactics and tactics. As shown in Figure 2, the gray part of the picture shows that Liu Wei's free throw score in the first 19 rounds of the CBA League 2005 to 2006 season accounts for the percentage of his total score.

The stability of step point affects the pace of running and the full degree of take-off. In this paper, the difference between the 6 take-off steps is analyzed by Liu Wei (whose running number is 23 steps) as an example. The step position statistics is shown in Table 1. The data unit in the table is meter. It can be seen from Table 1 that the repeatability of the 6 training steps of the athletes is poor, and the accuracy of the pedal is low.

Oksa is the core of Shanghai attacks and defense blocking net score. Therefore, the use of good oksa has become the key to the success of the development of East Shanghai. Here is oksa as the research object, using the time efficient association rules of the competitive ability of technical and tactical data mining. The sources of data are as follows: the video data in the CBA League oksa in 2005~2006 season before the 19 rounds of the competition are gotten by setting game time to query and extract multimedia database of volleyball technique and tactics. We counted the total score of three points, scoring three points, hitting number, three hits and two points, hitting number two and two free throws, hit rate, free throws, free throw percentage, backcourt number, front to back ball number, number, number of backcourt steals, cover number, error number, number of fouls assists, number, number, number of effective defensive tactics in the technical and tactical indicators in 6 minutes, 7 minutes, 8 minutes, 9 minutes, 10 minutes, 11 minutes, and 12 minutes.

We only study the total score and the score two points and two free throws along with the hit rate of free throw percentage. In addition, the offensive backcourt number, stealing the ball back cover number, number of fouls, failure assists, and effective defensive tactics are also taken into consideration. The number of technical and tactical indicators is focused on too. According to the player's tactical competitive ability efficiency formula, division between the corresponding values was weighted and this season has been the game and getting a coefficient. The set of values is as follows: the player's continuous playing time (minutes per minute, its TID value is

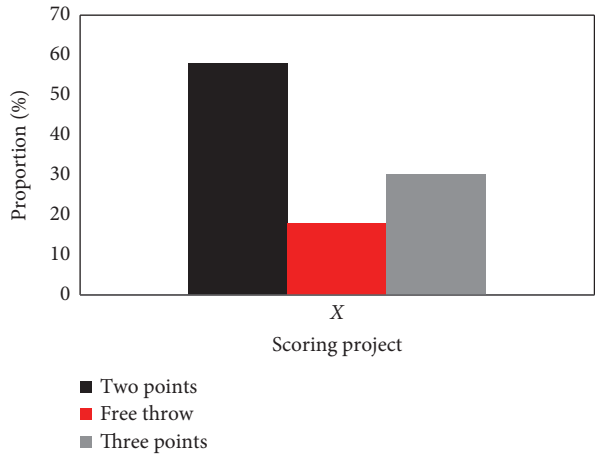

Figure 2: Liu Wei's shooting.

Table 1: Statistics of the full range steps.

Steps	First time	Second time	Third time	Fourth time	Fifth time	Sixth time
1	4.44	4.86	4.92	6.43	6.61	6.44
2	6.97	7.21	7.24	7.79	7.99	7.88
3	8.17	8.34	8.38	8.9	9.12	8.98
4	9.76	9.88	9.68	10.34	10.49	10.46
5	11.27	11.36	11.31	11.74	11.91	11, 87
6	13.13	13.14	13.02	13.49	13.79	13/77
7	14, 97	14.92	14.77	14.2	14.49	14.46
8	17.04	16.84	16.71	17.07	17–49	17.62
9	19.04	18.73	18.64	18.94	19.46	19.64
10	21.24	20.88	20.74	21.06	21.73	21.94
11	23.21	22.87	22.78	23.08	23.68	23.93
12	24.39	24.04	24.00	24.26	24.9	26.06
13	27.43	27.12	27.1	2121	27.89	28.04
14	29.6	29.33	29, 36	29.43	30.22	30.23
15	31.67	31.37	31.42	31.64	32.3	32.29
Foul line	48.32	48.32	48.32	48.32	48.32	48.32
Foul distance	−0.15	−0.15	−0.23	−0.17	0.15	0.24

PToxa1, PToxa2, PToxa3, PToxa4, PToxa5, PToxa6, and PU) is [7–12]. The value of technical and tactical competitive efficiency (its TID PRoxa) is [0-infinity] (its TID is PRoxa1, PR, oxa2, and PEoxa3). To analyze the quality of attack and defense, the analysis mode of volleyball technique and tactics in this study can be analyzed by the following two perspectives: comparative visualization of technical and tactical statistics on both sides of the game and the quality curve of time attack and defense for both sides of the game. The CBA2005-2006 season Shanghai East and Zhejiang Wanma games (January 4, 2006, Yiwu) are an example to discuss the game tactics analysis of the main content and method.

The technical statistics of the game between Shanghai Oriental and Zhejiang Wanma is shown in Figure 3. As shown in Figure 3, although the Shanghai team finally failed in 87 : 94, they were on the low side in the number of free throws (18 : 33), backcourt times (40 : 49), blocked times (2 : 6), and fouls (30 : 19). But in the times of error (8 : 14), the number of fast attacks (4 : 0), and other indicators, Shanghai was in the upper east. So the good aspects, such as the quick attack, should continue to be carried forward, such as too many fouls (11 times more than the other). It should be carefully analyzed whether the defensive consciousness of a player is in place or not.

In the attack, as shown in Figure 4, Zhejiang cyclones in the first quarter have 10 times the use of the 1 tactical team (Let Wu Naiqun and Samaki stand on both sides of the waist and put the ball into the inside line and they finish the attack or assists. Give play to the height advantage of internal line foreign aid, Samaki, and the technology of the experience of the forward Wu Naiqun, the former net strong attack, the latter follow-up). And they get a lot of success. There was the beginning of the start of the 12 : 5 lead and the end of this section of Shanghai behind at 16 : 25. Shanghai East called a pause, changing the strategy of attack and defense in the east of Shanghai. Foreign aid Oksana avoided opponents edge, to attack distance shots, the defensive front. Samaki had the ball by Wang Ligang then wrapped but also caused the Zhejiang cyclones perimeter defense to weaken accordingly. So the effect is not obvious. Shanghai East, respectively, was

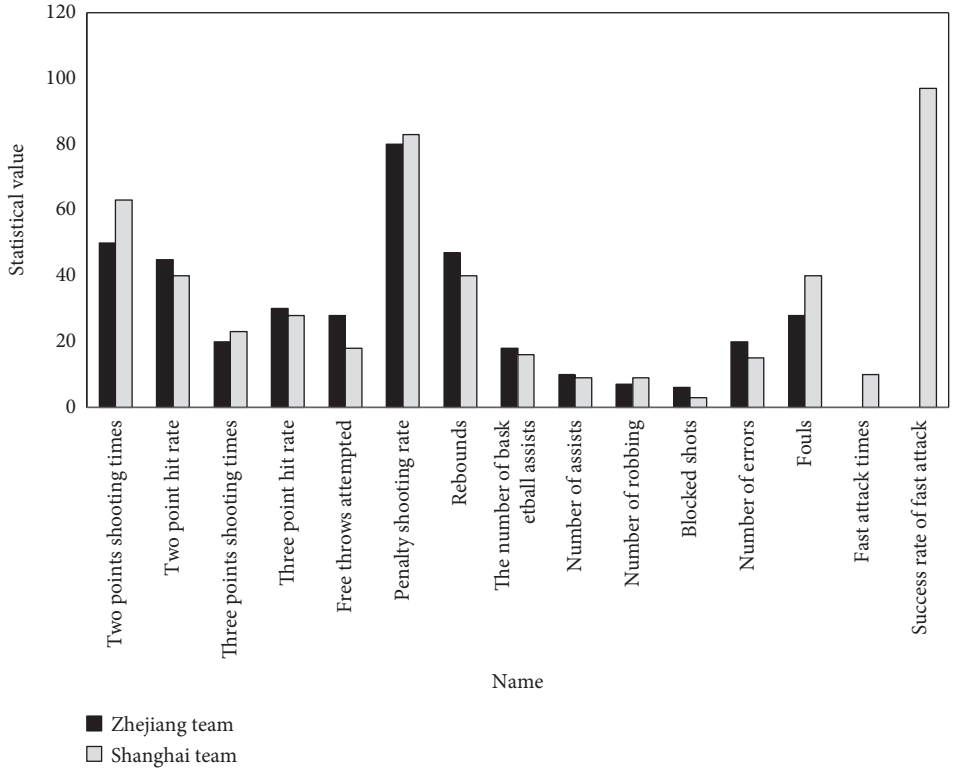

Figure 3: Technical statistics of Shanghai Oriental and Zhejiang Wanma game.

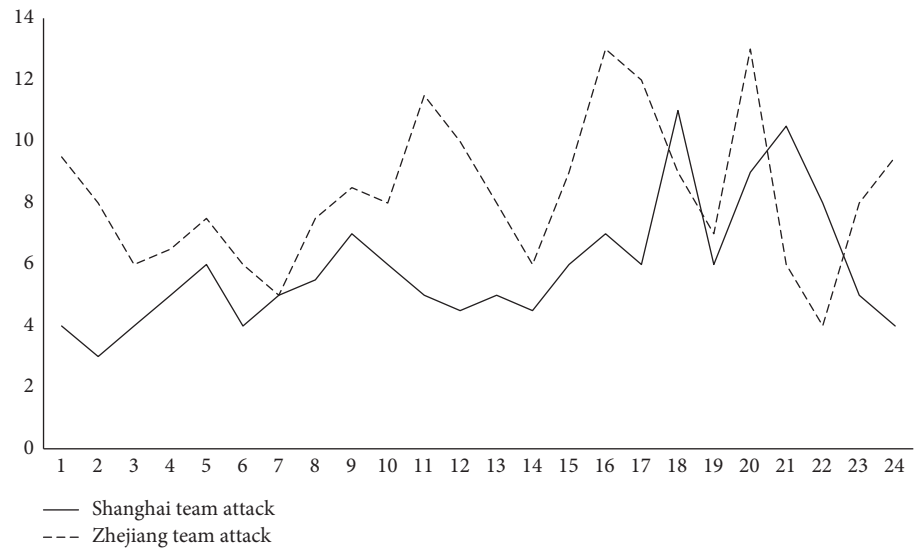

Figure 4: Contrast of attack quality in competition.

attacked by Samaki's cap in second and fifth minutes and two turnovers in seventh and tenth minutes. Therefore, there are several inflection points on the curve.

The quality of the attack comparison is provided in Figure 5. As shown in Figure 5, the lead at the start of the third quarter of Zhejiang Wanma bianzhao let Samaki rest, by a small foreign aid ball by Zhang Weigang M. Rudge, in charge. Liu Wei has made 3 mistakes because of his quick strategy for Rudge and the effect of it. Center Zhang Weigang although a larger force, but the pace is

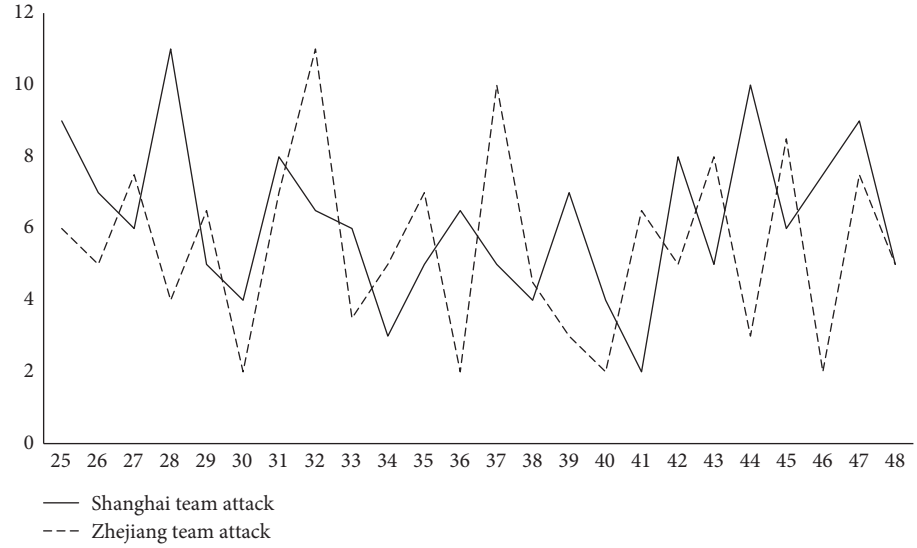

Figure 5: Quality attack comparison.

slow, so the poor offensive and defensive Zhejiang cyclones were a disadvantage. In the third section of the Shanghai east to 21 : 11 in the lead, quality of defense graph is Shanghai east line trend compared to the Zhejiang cyclones.

5. Conclusion

This article planned to put forward the idea of applying modern data management and data mining to volleyball technology and tactics multimedia data analysis. This article further highlights the idea of designing and developing the multimedia database of volleyball technology and tactics and puts forward the multimedia data analysis method of volleyball technique and tactics based on modern information technology. The proposed model is applied to the data produced at the edges of the systems and thoroughly analyzed. The machine learning algorithm is utilized to process the data and provide a prediction about the strategies of a volleyball match. The classical Apriori algorithm of machine learning is utilized in this research. The classical Apriori algorithm is extended and optimized to overcome the challenges faced by the traditional approach. This paper is mainly aimed at a solution to the lag of the methods and means of volleyball technique and tactics analysis in China. This way can provide intelligence support for coaches and players to enhance their core competitiveness. The proposed optimized Apriori algorithm is implemented and the effectiveness is also highlighted.

Data Availability

The data used to support the findings of this study are included in the article.

Conflicts of Interest

The authors declare that they have no conflicts of interest.

References

[1] H. Li, "Analysis on the construction of sports match prediction model using neural network," *Soft Computing*, vol. 24, pp. 8343–8353, 2020.

[2] F. Wunderlich and D. Memmert, "Forecasting the outcomes of sports events: a review," *European Journal of Sport Science*, vol. 12, pp. 1–14, 2020.

[3] B. P. Kelley, C. Klochko, S. Halabi, and D. Siegal, "Datafish multiphase data mining technique to match multiple mutually inclusive independent variables in large PACS databases," *Journal of Digital Imaging*, vol. 29, no. 3, pp. 331–336, 2015.

[4] P. Wicker and B. Christoph, "Analysis of problems using data mining techniques-findings from sports clubs in Germany," *European Journal for Sport and Society*, vol. 7, no. 2, pp. 131–140, 2010.

[5] C. Soto Valero, "Predicting win-loss outcomes in MLB regular season games—a comparative study using data mining methods," *International Journal of Computer Science in Sport*, vol. 15, no. 2, 2016.

[6] X. Yu, F. Jiang, J. Du, and D. Gong, "A cross-domain collaborative filtering algorithm with expanding user and item features via the latent factor space of auxiliary domains," *Pattern Recognition*, vol. 94, pp. 96–109, 2019.

[7] D. Yang, "Application of data mining technology in the subject tactical teaching of badminton," *International Journal of Emerging Technologies in Learning*, vol. 13, no. 7, 2018.

[8] G. Raiola, G. Altavilla, C. De Luca, and P. Alfredo Di Tore, "Analysis on some aspects of the service in volleyball," *Sport Science*, vol. 9, no. 1, pp. 74–77, 2016.

[9] M. Silva, R. Marcelino, D. Lacerda, and P. Vicente João, "Match analysis in volleyball: a systematic review," *Montenegrin Journal of Sports Science and Medicine*, vol. 5, no. 1, pp. 35–46, 2016.

[10] L. Tianbiao and H. Andreas, "Apriori-based diagnostical analysis of passings in the football game," in *Proceeding of the IEEE International Conference on Big Data Analysis (ICBDA)*, pp. 1–4, IEEE, Hangzhou, China, March 2016.

[11] S. Wenninger, D. Link, and M. Lames, "Performance of machine learning models in application to beach volleyball

data," *International Journal of Computer Science in Sport*, vol. 19, no. 1, pp. 24–36, 2020.

[12] J. V. Haaren, H. B. Shitrit, J. Davis, and F. Pascal, "Analyzing volleyball match data from the 2014 world championships using machine learning techniques," in *Proceedings of the 22nd ACM SIGKDD International Conference on Knowledge Discovery and Data Mining*, pp. 627–634, San Francisco, CA, USA, August 2016.

[13] F. A. Salim, D. B. W. Postma, R. Van Delden et al., "Volleyball action modelling for behavior analysis and interactive multi-modal feedback," in *Proceeding of the 15th International Summer Workshop on Multimodal Interfaces*, Ankara, Turkey, July 2019.

[14] S. Wenninger, D. Link, and M. Lames, "Data mining in elite beach volleyball-detecting tactical patterns using market basket analysis," *International Journal of Computer Science in Sport*, vol. 18, no. 2, pp. 1–19, 2019.

[15] X. Yu, J. Yang, and Z. Xie, "Training SVMs on a bound vectors set based on fisher projection," *Frontiers of Computer Science*, vol. 8, no. 5, pp. 793–806, 2014.

[16] Q.-Y. Li, "Appliance of apriori algorithm on technical-tactics analysis of volleyball," in *Proceeding of the International Conference on Virtual Reality and Intelligent Systems (ICVRIS)*, pp. 164–167, IEEE, Changsha, China, August 2018.

[17] S. Lee, K. Jin, J. Kim, and G. Heo, "Development of a data-mining methodology for spent nuclear fuel forensics," *Journal of Radioanalytical and Nuclear Chemistry*, vol. 312, no. 3, pp. 495–505, 2017.

[18] X. Yu, Y. Chu, F. Jiang, Y. Guo, and D. Gong, "SVMs classification based two-side cross domain collaborative filtering by inferring intrinsic user and item features," *Knowledge-Based Systems*, vol. 141, pp. 80–91, 2018.

[19] Z. Haiyun and X. Yizhe, "Sports performance prediction model based on integrated learning algorithm and cloud computing hadoop platform," *Microprocessors and Microsystems*, vol. 79, Article ID 103322, 2020.

[20] Y. Li, L. Wang, and F. Li, "A data-driven prediction approach for sports team performance and its application to national basketball association," *Omega*, vol. 98, Article ID 102123, 2019.

[21] A. Dubbs, "Statistics-free sports prediction," *Model Assisted Statistics and Applications*, vol. 13, no. 2, pp. 173–181, 2018.

Hindawi
Mobile Information Systems
Volume 2021, Article ID 6617286, 11 pages
https://doi.org/10.1155/2021/6617286

Research Article

A 3D Machine Vision-Enabled Intelligent Robot Architecture

Yanjun Zhang,[1,2] Jianxin zhao,[1,2] and Heyong Han [1,2]

[1]*College of Mechanical Engineering, Taiyuan University of Science and Technology, Taiyuan 030024, China*
[2]*Research Center for Basic Hydraulic Components and Intelligent Manufacturing Engineering of Major Equipment, Taiyuan 030024, China*

Correspondence should be addressed to Heyong Han; hhy@tyust.edu.cn

Received 15 December 2020; Revised 7 February 2021; Accepted 23 February 2021; Published 4 March 2021

Academic Editor: Mian Ahmad Jan

Copyright © 2021 Yanjun Zhang et al. This is an open access article distributed under the Creative Commons Attribution License, which permits unrestricted use, distribution, and reproduction in any medium, provided the original work is properly cited.

In this paper, the principle of camera imaging is studied, and the transformation model of camera calibration is analyzed. Based on Zhang Zhengyou's camera calibration method, an automatic calibration method for monocular and binocular cameras is developed on a multichannel vision platform. The automatic calibration of camera parameters using human-machine interface of the host computer is realized. Based on the principle of binocular vision, a feasible three-dimensional positioning method for binocular target points is proposed and evaluated to provide binocular three-dimensional positioning of target in simple environment. Based on the designed multichannel vision platform, image acquisition, preprocessing, image display, monocular and binocular automatic calibration, and binocular three-dimensional positioning experiments are conducted. Moreover, the positioning error is analyzed, and the effectiveness of the binocular vision module is verified to justify the robustness of our approach.

1. Introduction

Internet of Robotic Things (IoRT) allows intelligent physical devices to monitor various events, gather data from multiple sources, and fuse them to extract useful features [1]. IoRT uses local and distributed intelligence for determining the best course of action. Based on this intelligence, various actions are taken and objects of the real-world are manipulated. IoRT allows the Internet of Things (IoT) and robotic devices to intersect by providing advanced robotic features. The concept of IoRT has made the realization of advanced and novel applications and has felt its presence in industries, businesses, and various other sectors. IoRT works based on the concept of computer vision. Though computer vision research has made considerable progress, there are also many controversies. According to the school of three-dimensional reconstruction led by Marr, vision is a procedure for information processing to obtain the description of external world, i.e., to recover three-dimensional scenes from image features such as edge points, contours, lines, curves, textures, grey levels, and colors. The features are obtained from either single or multiple two-dimensional images, and then used to recognize, locate, and analyze the three-dimensional scenes [2, 3]. In fact, the inverse process of image restoration often leads to unsolvability or instability of Horn's optical flow field constraint equation due to some ill-posed problems in the scene. Many works have been carried out around this problem, but so far, no real successful practical system has been developed.

More than 70% of the external information received by human beings is obtained through vision. As an imitation product, the realization and generalization of the vision system of home service robot is particularly important [4, 5]. First of all, the visual sensor has the advantages of low cost, abundant information, and high reliability. Secondly, the environment of intelligent service robots is usually an unstructured indoor environment. Vision can provide rich environmental information for robots, so as to achieve navigation, recognition, control, and other tasks. As a general-purpose robot vision platform, the system should have abundant and universal communication interfaces, so as to facilitate the exchange of information with various robot control hosts [6–8]. The system should have powerful processing functions, because the amount of visual information data is extremely large, and the requirement of video processing for processors is very high. Besides, the system

should also have good software and hardware expansion capabilities to facilitate the expansion of the system functions.

At the end of 1980s and the beginning of 1990s, a behavioural and application-oriented purposivism school emerged. It puts forward the concepts of active vision and qualitative vision. It says that vision is purposeful and pursues the purpose more actively. Some objects in the scene need quantitative analysis, while others need only qualitative description [9–11]. They accomplish their tasks together according to a certain purpose. This viewpoint has been criticized by the "reconstruction" school, which holds that "purposivism" uses specific tasks as restrictions to avoid problems and deal with facts. Secondly, the active sensing technology for acquiring scene data has many problems, such as single function and large noise impact, which lead to its limitations on the use of occasions and objects. On the other hand, from the initial remote-control manipulator to the intelligent robot with certain intelligence, the robot has gone through half a century, forming a unique information, energy, and material transformation feature system of the robot.

Machine vision has attained significant attention in recent times. In fact, machine vision is used as a unit of robot to feel the external information, its theory and methods, which cannot be separated from the large-scale system requirements of robots to discuss [12–15]. In this paper, we address all these issues and concerns. The major contributions of this paper are as follows:

(1) We start the discussion with the architecture of general-purpose intelligent robots and aim at different viewpoints in machine vision research in this context. After analyzing the generality and particularity, this paper puts forward a general research scheme of hierarchical modular structure of machine vision, and a vision integrated sensor supporting this system.

(2) Using experimental results, we justify the validity and feasibility of designing a 3D machine vision-enabled intelligent robot architecture.

The rest of the paper is organized as follows. In Section 2, we present the platform required for designing a robot vision system. In Section 3, we discuss the realization of binocular camera 3D vision location. In Section 4, the experimental process and result analysis are discussed. Finally, the paper is concluded and future research directions are provided in Section 5.

2. Platform Design of the Robot Vision System

Images can be classified into two categories according to their description properties: intrinsic and nonintrinsic. The former refers to the images that represent the objective characteristics of the scene and the scene that have nothing to do with the nature of the observer and the collector, for example, the most commonly used depth images, where each pixel value represents the distance between the pixel and the camera. The physical quantity of the latter is related not only to the scene, but also to the nature of the observer and the collector as well as the surrounding environment [16–18]. A typical representation is the grey image. Each pixel reflects the light radiation received and reflected by the observer. To accomplish the vision task mentioned above is to solve the problem of restoring intrinsic features from nonintrinsic images. The imaging process of noneigenvalue image is a degenerate transformation process, in which a lot of physical information about scene is mixed up in noneigenvalue image, but these pieces of information are not completely lost. There are always a lot of redundant information in the image, and various processing techniques (such as distance transformation) can be used to eliminate the degradation and "restoration of" intrinsic characteristics. In order to restore the scene, it is necessary to directly collect intrinsic images or nonintrinsic images containing stereo information. In this way, certain image acquisition equipment (imaging device) and a certain image acquisition mode (imaging mode) are needed. In the following subsections, we first discuss designing an image acquisition device followed by system architecture.

2.1. Design of Image Acquisition Device. The imaging devices are stimulated by external radiation (visible light radiation, etc.), which is converted into electrical signals, and then this signal response is converted into digital signals that can be processed with a computer. There are two functions of the image acquisition device. One is to accept the excitation, and the other is the conversion of analog signal. There are many kinds of image acquisition devices, usually consisting of video source and video acquisition. Of course, digital technology has made it possible to integrate these two functions into a packaged device such as digital camera on hardware [19]. Considering the maturity, advantages, and environmental adaptability of technology, the structure composed of camera and acquisition card is still adopted in mobile robot vision system at present (the first half of Figure 1). The hardware of the image capture card will bring greater flexibility and performance improvement. Generally, video cards integrate user conversion, signal amplification, filtering, and other processing of signals. With the progress of technology and the development of manufacturing industry, some cards also integrate functions that are usually completed by software, such as directly compressing into a certain data format (such as MPEG4) or even matrix operation, which will greatly speed up data processing.

At present, the charging source device is mainly used in video devices. It is a kind of solid-state camera device which works by charge storage, transmission, and readout. It has the advantages of low reading noise, large dynamic range, and high response sensitivity. With the continuous progress of technology, its resolution is gradually improved, and color restoration is becoming more realistic. It is a high cost-effective imaging device at present. The working principle of CCD is that the object reflects light and propagates to the lens. The lens focuses on the CCD chip. According to the intensity of the light, the CCD accumulates corresponding charges and discharges periodically to produce electrical

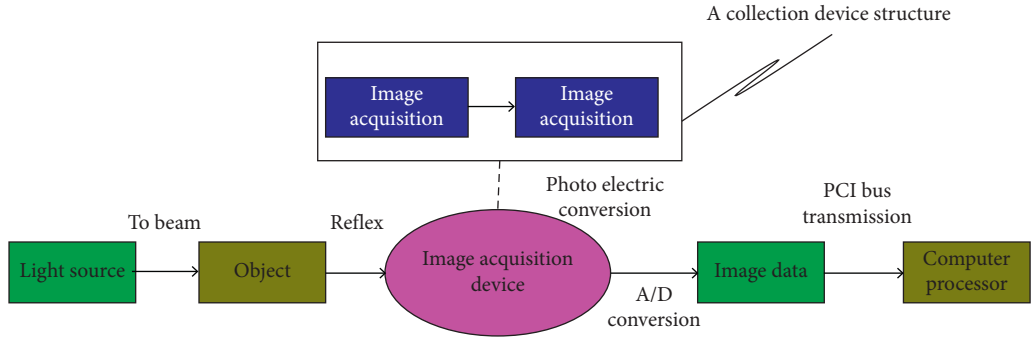

Figure 1: Image acquisition process.

signals representing a picture [20]. After filtering and amplification, a standard compound video signal is generated through the output terminal of the camera. CCD is the main sensing component of the camera. It has the characteristics of high sensitivity, small distortion, long life, antivibration, antimagnetic field, small volume, and no residual shadow. CCD can change light into charge, store and transfer charge, and take out the stored charge to change voltage. Therefore, it is an ideal camera element. It is a new device instead of traditional camera tube sensor. Because of the richness and importance of color information, we use color CCD as image collector. The image acquisition process is shown in Figure 1.

The acquisition card is the process of importing video data or mixed data of video and audio output from other data sources into the computer, transforming them into digital signals by processing, and storing these pieces of information. This analog-to-digital conversion is carried out by the acquisition chip or related software on the video acquisition card, so that the acquisition card can be divided into real-time acquisition card and nonreal-time acquisition card. According to the data sources, it can be divided into three categories: digital acquisition, analog acquisition, and digital-analog acquisition. Considering that more than one video source is needed to construct stereo vision, a multichannel acquisition card will be more feasible. As mentioned above, data compression will be extremely important in this context. Therefore, the acquisition card has the following functions: hardware compression, 1 card multiplex, and real-time analog acquisition.

2.2. System Structure. In our proposed approach, imaging is determined mainly by the position and movement of the three sources, the video source, and the scenery. The simplest part is monocular imaging, which uses a video source to take a picture from the scene in a fixed position. Stereo vision is a method of perceiving distance by binocular cues. Two video sources are used to get images of the same scene in one location. Parallax generated between two images is used to help find the distance between video sources and objects so as to realize the perception of three-dimensional information. In principle, it is based on triangulation. Therefore, the specific means of implementation are not limited to the use of two cameras as the source of video. For example, it is also possible to use one camera to take images of the same scene at multiple locations, and to use more than two cameras to image the same scene from different locations.

Let us analyze and compare the commonly used stereoscopic imaging methods. First of all, the general principle of binocular vision is expounded. Figure 2 is a hint of the simplest case.

In this figure, C_L and C_R are the lens centers of the left and right cameras, the distance between them is b (called baseline), and the focal length between the cameras is f. Here, P is the point on the surface of the object. The projection points on the two cameras are rulers, where the distance between P and the central line of the lens of the two cameras is d, the vertical line from C_L and C_R to the horizon is A_L and A_R, the vertical line from P to the horizon is B, and the intersection point between the extension line and the central line of the lens is C. In this way, it is easy to get the distance between the object point and the camera from two pairs of triangles: ΔPP_RB and ΔPC_RC, $\Delta P_LA_LC_L$ and ΔP_LBP.

$$d = f\frac{a + l_a}{b} = \frac{bf}{l_a - l_b}. \tag{1}$$

Obviously, d is related to b and $l_a - l_b$, one of which is called parallax formed by P in the two viewing planes. For a visual system, b and f are known, so the key to achieve ranging is to obtain parallax, that is, to achieve the correspondence of a point in space between the projection points on the left and right images, which is the process of image registration.

The principle of binocular imaging is very simple, but image registration is still a difficult problem. Stereo matching is the most difficult and important step in stereo vision. When a three-dimensional scene is projected into a two-dimensional image, the image of the same scene will be very different in different viewpoints, and many changes and unpredictable factors in the scene, such as illumination conditions, noise, geometric shape of the scene, and the characteristics of the camera, are integrated into a single image color/gray value. Conversely, it is a morbid problem to determine the three-dimensional information from the single image color/gray value, which has not been solved well up to now. Binocular registration has a large search space for corresponding points, which is often complex. Therefore, a trinocular registration method is proposed, that is, taking three images of an object at the same time, so as to increase

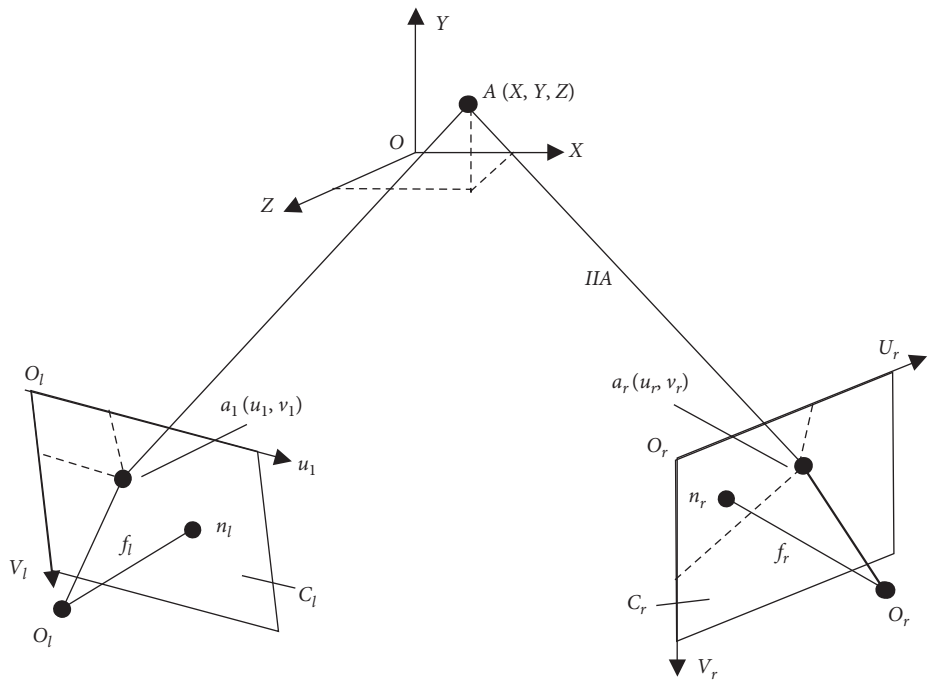

Figure 2: Geometric principle of binocular vision parallax ranging.

the constraints of registration and simplify the registration problem.

Next, we discuss the light displacement imaging and structural light imaging. The basic principle of the former is that the brightness of the same scene is different under different illumination conditions, so the surface orientation of the object can be obtained by light moving image, which is different from several other techniques, so that the absolute depth information cannot be obtained, but the surface shape description of the object can be obtained. Since our mobile robot is moving in an unknown environment, it will be difficult to control the mobile light source, so we do not consider this technique. The latter is to explain the surface shape of the scenery by the projection mode collected. This method can fix the light source and the acquisition and rotate the scenery. It can also fix the scenery and move the light source and the acquisition around the scenery together. With the progress of science and technology, especially the emergence of various new sensors, more means of acquiring distance appear. If one eye in binocular vision is replaced by a laser source, the light source produces a series of point or line lasers to illuminate the object surface, and the illumination part is recorded by the light sensitive camera, the depth information can be obtained directly. However, other information on the surface of the object will be ignored. The schematic diagram of robot vision information acquisition system is shown in Figure 3.

Trinocular and multiocular imaging, which involves the calibration of multiple cameras, is mostly used in three-dimensional reconstruction in virtual reality human-computer interaction and other fields. For mobile robots, the uncertainty of their environment will bring many unpredictable factors. At the same time, the processing of some environmental information also needs some real-time requirements (such as obstacle avoidance). Therefore, too complex imaging methods will have many limitations in practical applications. Therefore, the general mobile robot system adopts binocular imaging in visual information. However, for unknown environments, the task facing robots is not only to ensure that they can safely avoid obstacles and move smoothly, but also to obtain as much environmental information as possible in order to realize the process of recognizing the unknown. The real objective environment is three-dimensional, and the reconstruction of three-dimensional environment has naturally become an important aspect of cognition. Therefore, we also attach enough importance to this function in our system. Obviously, the existing imaging methods alone cannot meet the needs of vision system for mobile robots in unknown environments. The combination of multiple imaging methods will be a worthy consideration. Considering the above-mentioned imaging methods and system requirements, we decided to construct a visual platform by combining binocular imaging and monocular imaging, in order to make full use of the advantages of various imaging methods. Redundant design methods will lead to the avoidance of using a single method as far as possible, while information fusion and flexible combination of imaging methods will bring higher reliability, flexibility, and fault tolerance.

3. Realization of Binocular Camera 3D Vision Location

In this section, we discuss the 3D vision location of binocular camera. First, we discuss the realization of binocular camera

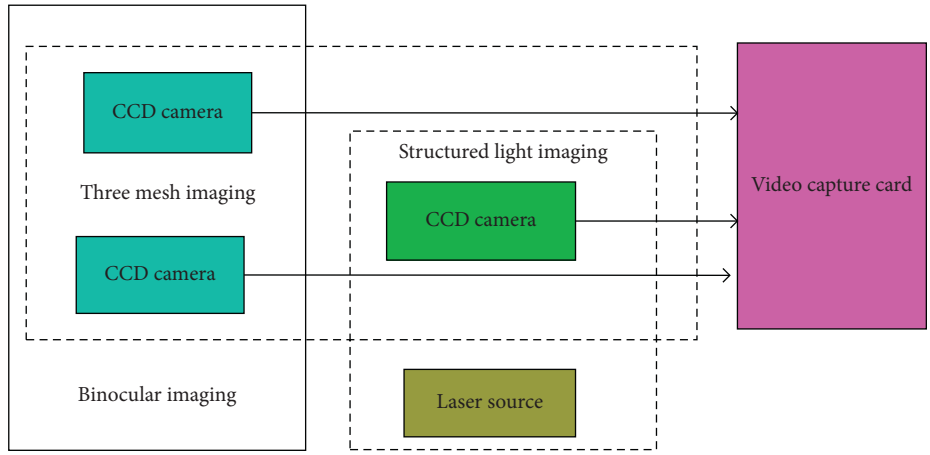

Figure 3: Schematic diagram of robot vision information acquisition system.

calibration in Section 3.1 followed by binocular 3D positioning of target points in Section 3.2.

3.1. Realization of Binocular Camera Calibration. Binocular vision refers to the simultaneous imaging of the overlapping parts of the field by two cameras. The matching algorithm is used to obtain the image position of the same spatial point in two cameras. Based on the matching algorithm, the three-dimensional location of the scene is realized according to the internal parameters of the two cameras and the spatial position and attitude relationship between the two cameras. The task of dual target determination is to determine the internal parameters of two cameras and the relationship between the relative position and attitude of two cameras. The internal parameters of the two cameras can be achieved by performing single target calibration algorithm for them, and the spatial relative position and attitude relationship between them can be obtained by transforming the external parameters of the two cameras for the same position calibration target.

When the target is set at a certain position, the transformation matrix from the world coordinate system to the left-eye camera (i.e., the external reference matrix of the left-eye camera) is $[R_1]$, and the transformation matrix from the world coordinate system to the right-eye camera (i.e., the external reference matrix of the right-eye camera) is $[R_2]$. Then, the relationship between (x, y, z) points in the world coordinate system and (x_1, y_1, z_1) coordinates in the right camera coordinate system and (x_2, y_2, z_2) coordinates in the left camera coordinate system satisfies the following formulas:

$$\begin{bmatrix} x_2 \\ y_2 \\ z_2 \end{bmatrix} = [R_2] \begin{bmatrix} X \\ Y \\ Z \end{bmatrix}, \tag{2}$$

$$\begin{bmatrix} x_1 \\ y_1 \\ z_1 \end{bmatrix} = [R_1] \begin{bmatrix} X \\ Y \\ Z \end{bmatrix}, \tag{3}$$

Both sides can get the same $[R_2]^{-1}$:

$$\begin{bmatrix} X \\ Y \\ Z \end{bmatrix} = [R_2]^{-1} \begin{bmatrix} x_2 \\ y_2 \\ z_2 \end{bmatrix}. \tag{4}$$

The coordinate transformation relation of the same point in the left and right cameras can be obtained as follows:

$$\begin{bmatrix} x_1 \\ y_1 \\ z_1 \end{bmatrix} = [R_1][R_2] \begin{bmatrix} x_2 \\ y_2 \\ z_2 \end{bmatrix}. \tag{5}$$

That is, the position and attitude transformation matrix of left and right cameras is $[R_1][R_2]^{-1}$.

The process of binocular automatic calibration software is shown in Figure 4.

3.2. Realization of Binocular 3D Positioning of Target Points. According to the analysis of camera imaging transformation and the principle of three-dimensional positioning of target points, the focus and target points of two cameras can be transformed into the same coordinate system through a series of coordinate transformation. In this paper, we choose to convert them all into the camera coordinate system of the left-eye camera, and then use these four points to establish two equations of imaging light. By solving the equations composed of these two equations, we can get the coordinates of the target point in this coordinate system. However, due to the following reasons, this method is almost infeasible in practical applications:

(1) Firstly, there is a certain gap between the practical camera and the simplified camera model, and the camera that meets the ideal camera model actually does not exist

(2) Secondly, in the process of camera calibration, because of the simplification of camera model, the discretization of digital imaging, and the calculation errors introduced in the process of numerical

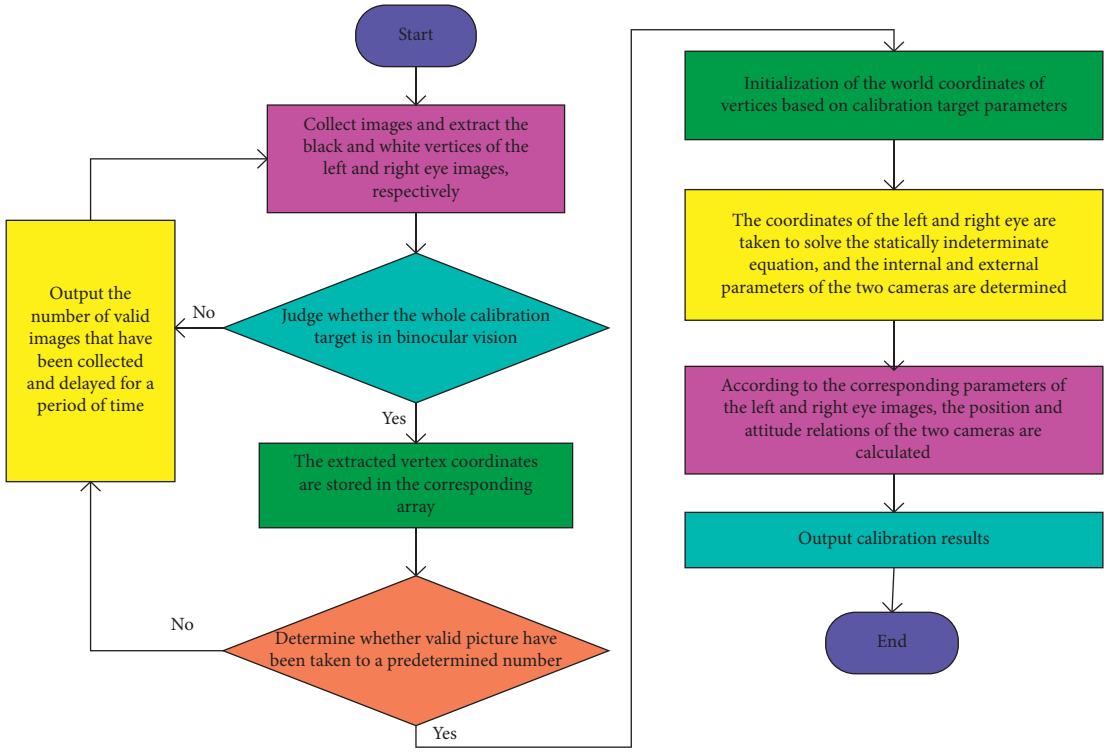

Figure 4: Software flow chart of binocular automatic calibration algorithm.

solution, it is almost impossible for the two transformed imaging rays to be intersecting lines

(3) Finally, even if two imaging rays intersect, it is a relatively difficult problem to solve directly the equations whose parameters change at any time by digital method

Based on the above reasons, in order to achieve the three-dimensional positioning of the target point, this paper adopts the method of restoring two imaging rays, using the method of solving the points in the common perpendicular line segment of the spatial heterogeneous straight line to approximately replace the position of the target point, and gives the length of the common perpendicular line segment as the credible error range of the calculation. In the process of solving the problem, the general equation of the imaging light of the left camera is set as follows: the imaging light of the left camera cannot pass through the origin of the camera coordinate in the XY plane of the camera coordinate system at the same time, and the imaging light of the left camera must pass through the origin of the camera coordinate.

$$\frac{x}{a_0} = \frac{y}{b_0} = \frac{z}{1}. \tag{6}$$

Similarly, the general equation for imaging light on the right camera is set as

$$\frac{x - x_1}{a_1} = \frac{y - y_1}{b_1} = \frac{z - z_1}{1}. \tag{7}$$

The parameters of $a_0, b_0, a_1, b_1, x_1, y_1, z_1$ in the general formula are determined by the coordinates of image points and focus points converted to the coordinates of the left-eye camera.

According to the theory of analytic geometry, the algorithm for solving the length of common vertical line and its midpoint coordinates of the two straight lines can be realized by writing C language code. The software flow of binocular 3D positioning algorithm for target point is shown in Figure 5.

In this paper, the principle of camera imaging is studied, and the transformation model of camera calibration is analyzed. Based on Zhang Zhengyou's camera calibration method, an automatic calibration method for monocular and binocular cameras is developed on a multichannel vision platform, which realizes the automatic calibration of camera parameters under the call of human-machine interface of the host computer. Based on the principle of binocular vision, a feasible three-dimensional positioning method for binocular target points is proposed, and the algorithm implementation program is compiled to provide a basis for the experiment of binocular three-dimensional positioning of target in simple environment.

4. Experimental Process and Result Analysis

In this section, first we discuss image acquisition and preprocessing followed by calibration of monocular and binocular cameras.

4.1. Image Acquisition and Preprocessing. The multichannel vision platform designed in this paper supports four-channel video input at most. The experiment of image acquisition

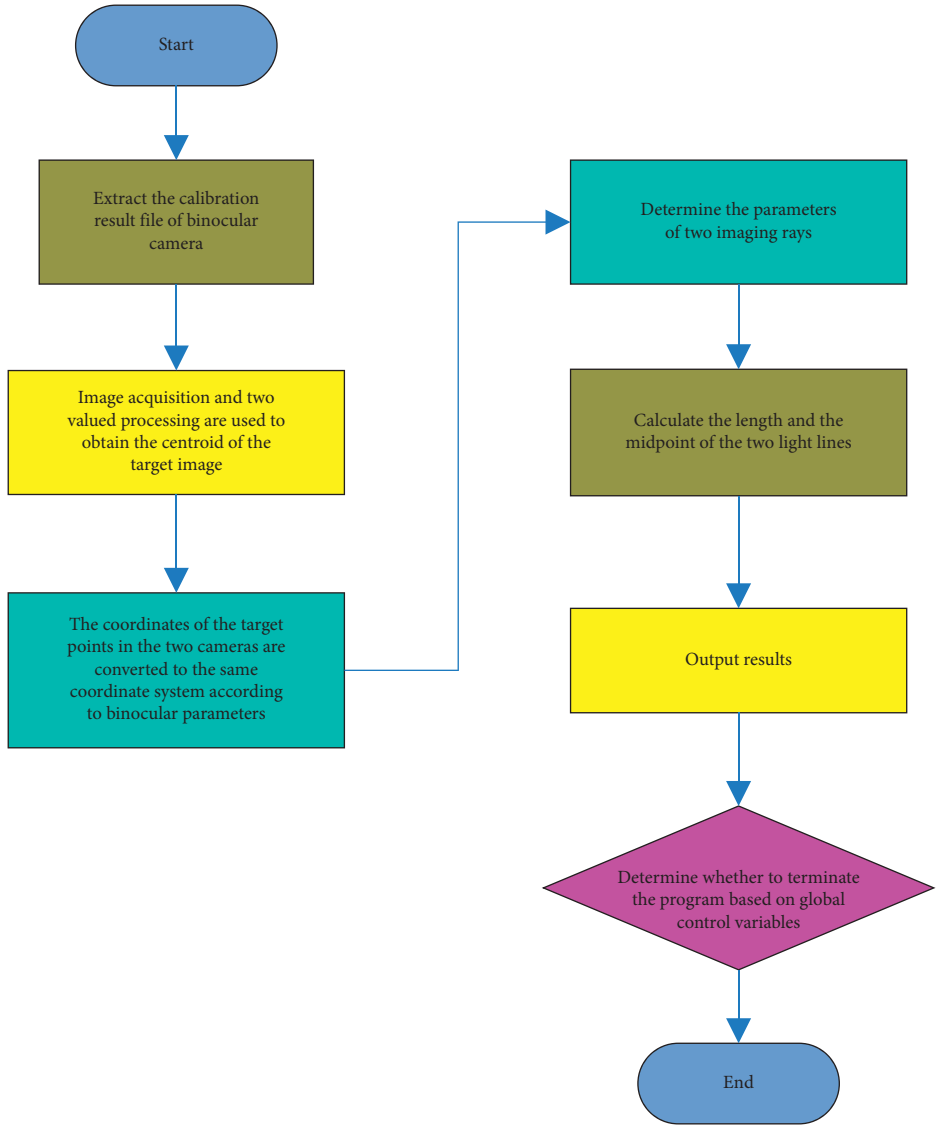

Figure 5: Software flow chart of binocular 3D location algorithm for target points.

and preprocessing is to verify the effectiveness of the system's input-output interface control and the ability of the system's dual-core architecture to coordinate work. The software structure used in the experiment of single-channel image acquisition and preprocessing as shown in Figure 6 includes three parts: PC user interface program, embedded system management program on ARM, and preprocessing algorithm program on DSP.

The execution process of the program is that when a preprocessing algorithm instruction is pressed on the PC user interface, the PC sends the corresponding control command string to the embedded system through the serial port. After receiving the command string, the embedded system management program running on the ARM processor starts the video capture threads by modifying the global control variables in turn. Control the CCD camera to capture the image and store the image in the corresponding memory space, start the algorithm call thread, call the corresponding preprocessing algorithm of the DSP processor to execute the program, realize the corresponding preprocessing of the collected image, and control the video back end to display the processed image to the TV. After that, the communication control thread monitors the instruction of the network port and serial port, decides whether to transmit the processed image to the host computer according to the instruction state of the network port, changes the preprocessing algorithm, or terminates the processing program according to the instruction of the serial port.

4.2. Automatic Calibration of Monocular and Binocular Cameras. As shown in Figure 7, the calibration algorithm of monocular and binocular camera automatic calibration test runs on PC, and the embedded system runs in the image acquisition mode. It receives the instructions of the host computer to provide single- or multichannel image information for the host computer and displays the video information collected by the camera to the TV.

In the PC user interface, press the single target or binocular calibration button to start the calibration program. Then,

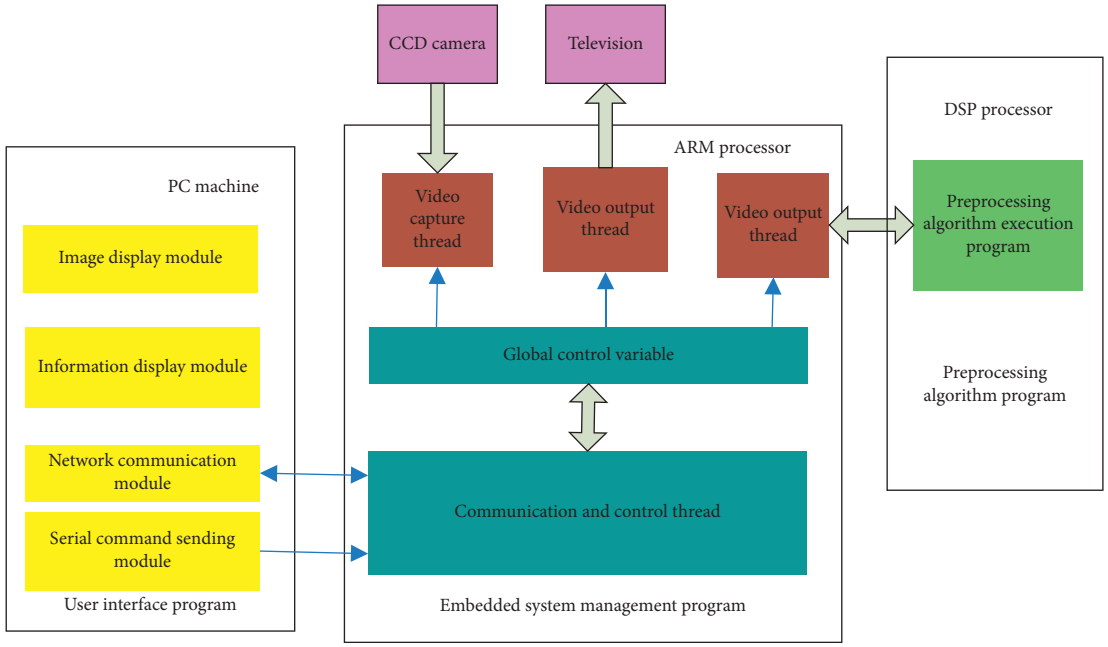

Figure 6: Single-channel image acquisition and preprocessing experimental system structure diagram.

according to the prompt information displayed on the PC user interface, the position and attitude of the calibration target can be changed so that the system can acquire 10 valid calibration images to complete the calibration under the condition of ensuring the whole calibration target in the field of vision. The calibration results are displayed on the man-machine interface. At the same time, the system stores the calibration results in document form and saves 10 calibration images in JPEG format. In order to evaluate the results of automatic calibration algorithm, 10 calibration images used in automatic calibration are calibrated with the calibration toolbox of MATLAB. The comparison of calibration results is shown in Table 1.

Compared with the calibration results of the MATLAB toolbox, the error of focal length calibration is about 5%, and the deviation of image center is basically zero. The results of automatic binocular calibration are shown in Table 2 and Figure 8.

Experiments show that the automatic calibration method is feasible. The validity of the calibration value needs further verification by three-dimensional positioning experiment.

4.3. Binocular 3D Positioning Experiment. As shown in Figure 9, the binocular three-dimensional positioning experimental system is similar to the image preprocessing experimental system, which consists of three parts. The three-dimensional positioning algorithm runs on the DSP, and the processing results are displayed on the PC user interface through network communication.

Binocular localization algorithm is sensitive to errors in Z-direction (along the optical axis). The comparison between the location output and the measured data is shown in Table 3 and Figure 10.

The reliability of the proposed binocular three-dimensional positioning method is verified by positioning experiments, and the validity of the results of binocular automatic calibration is indirectly proved. The errors between positioning results and actual measurements in the range of 2 m are less than 10 cm. The larger errors mainly occur in the range of Z coordinates less than 50 cm and greater than 150 cm. The main sources of errors are two aspects. On the one hand, there is a gap between the mathematical model established by the positioning method and the actual camera imaging model. The positioning model algorithm itself is sensitive to the Z-direction error, which results in a larger error when the Z coordinate is greater than 150 cm. On the other hand, because the errors caused by image distortion during camera imaging are not taken into account in the ranging model, the tangential distortion of image has a greater impact on the results when Z coordinates are smaller, which results in larger errors when Z coordinates are less than 50 cm.

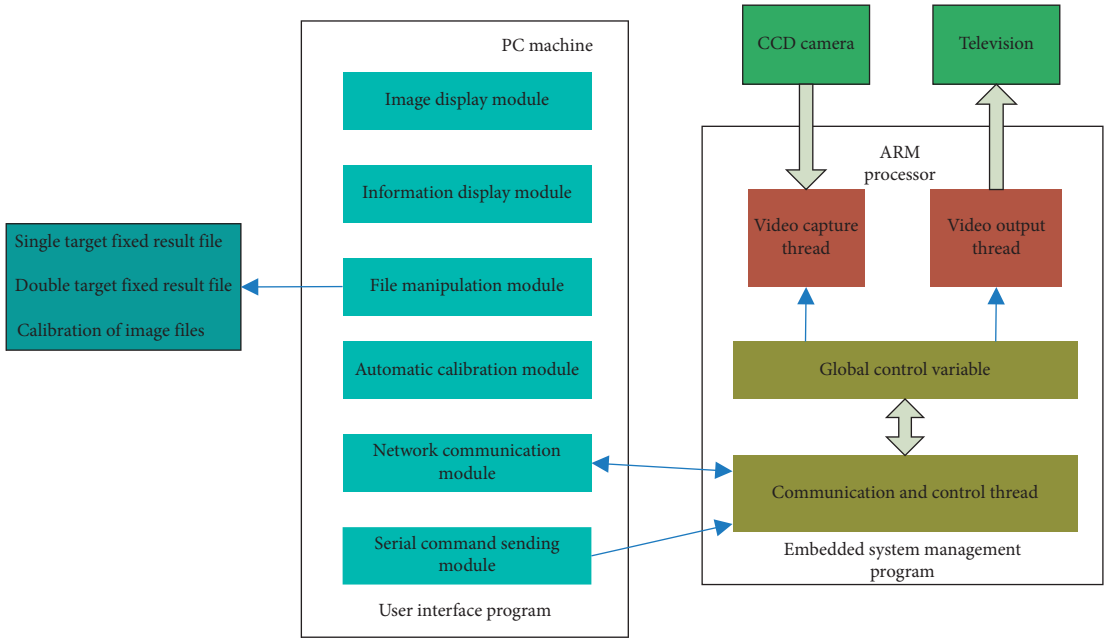

Figure 7: Structure chart of automatic calibration system for single and binocular vision.

Table 1: Comparison between automatic calibration results of monocular and calibration results of MATLAB toolbox.

Calibration parameters	f_x	f_y	C_x	C_y
Automatic calibration results	798.48	878.67	360.6	240.6
MATLAB calibration results	813.85	886.79	360.6	240.1

Table 2: Automatic calibration results of binocular.

Calibration parameters	f_x	f_y	C_x	C_y
Left-eye camera	394.22	435.16	180.6	153.1
Right-eye camera	394.22	427.62	180.6	153.1

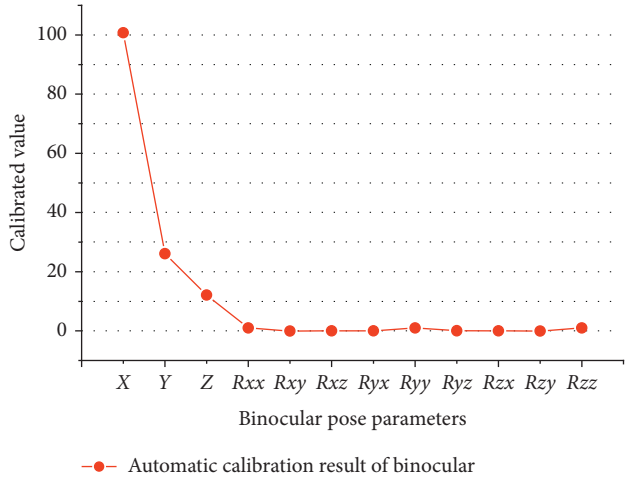

Figure 8: Automatic calibration results of binocular.

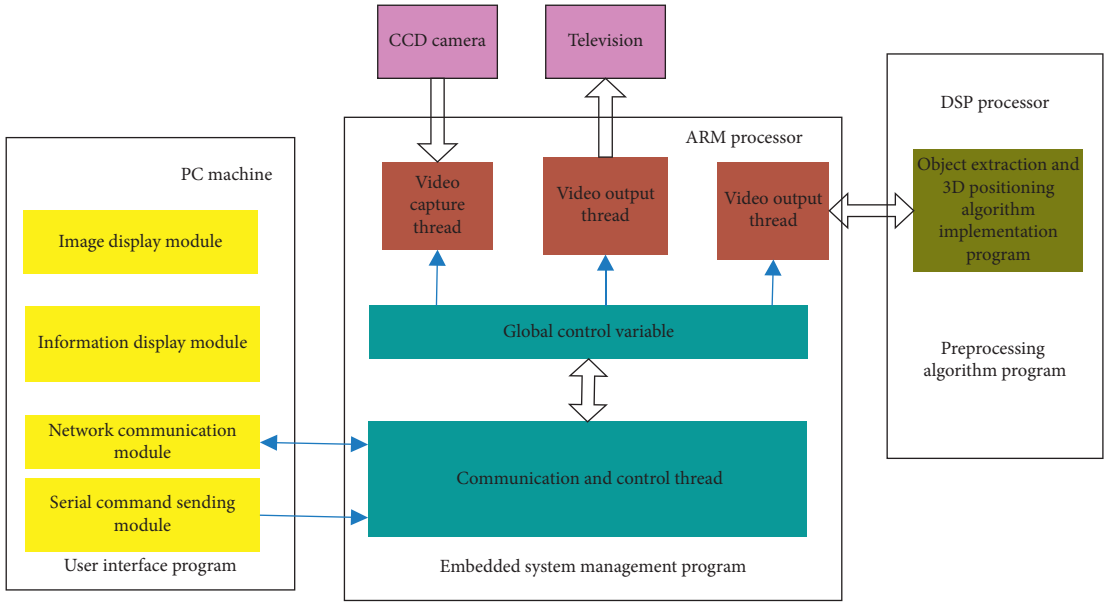

Figure 9: System structure diagram of binocular 3D positioning experiment.

Table 3: Comparison table of Z-axis coordinate experiment results of binocular 3D positioning (unit: cm).

Experimental value	25	50	75	100	125	150	175	200
Location experiment results	24.63	54.8	71.36	99.97	127.42	164.7	180.73	208.75
Location error estimation	4.14	2.36	1.46	1.28	1.17	4.27	7.76	12.57
Measured error	3.63	3.79	0.36	0.25	1.42	3.7	4.73	7.73

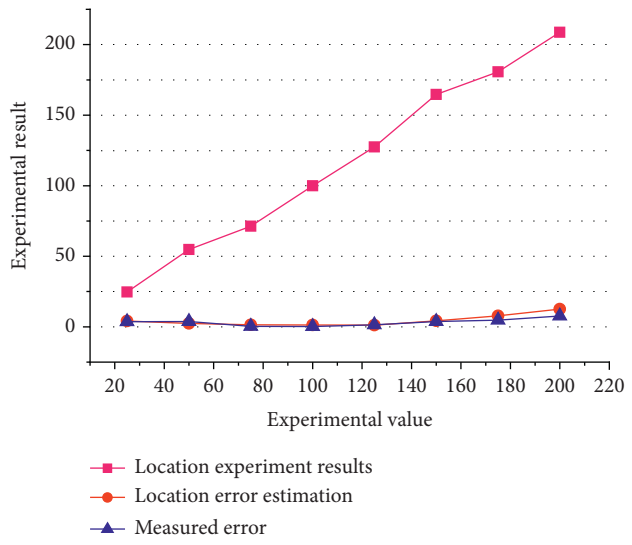

Figure 10: Comparison table of Z-axis coordinate experiment results of binocular 3D positioning.

5. Conclusion

Using the human intelligence system, and combining the theory and methods of artificial intelligence and computer vision, this paper proposes an intelligent reconfigurable mobile robot vision system and studies the appropriate structure on the hardware and software levels. On the basis of the existing work, the function expansion method is adopted to gradually improve each module so that it can achieve the desired effect with the support of a large system structure. The imaging principle of the camera is studied, and the transformation model of the camera calibration is analyzed. Based on the Zhang Zhengyou camera calibration method, the automatic calibration method of the single-binocular camera is developed on the multichannel vision platform, and the camera automatic parameters under the human-machine interface are realized. A feasible three-dimensional positioning method for binocular target points is proposed based on the principle of binocular vision, and the algorithmic implementation is provided for the binocular three-dimensional positioning experiment of the target in a simple environment. Finally, image acquisition, preprocessing, image display, single and double eye automatic calibration, and binocular three-dimensional positioning experiment were examined and evaluated via the experimental results. The positioning error was analyzed to verify the effectiveness of the binocular vision module.

Data Availability

All data can be obtained upon request to the corresponding author.

Conflicts of Interest

The authors declare that they have no conflicts of interest.

Acknowledgments

This work was supported by the College of Mechanical Engineering, Taiyuan University of Science and Technology, Shanxi.

References

[1] P. P. Ray, "Internet of robotic things: concept, technologies, and challenges," *IEEE Access*, vol. 4, pp. 9489–9500, 2016.

[2] B. Tovar, F. Cohen, L. Bobadilla et al., "Combinatorial filters: sensor beams, obstacles, and possible paths," *Acm Transactions on Sensor Networks*, vol. 10, no. 3, pp. 317–332, 2013.

[3] P. Leica, J. M. Toibero, F. Roberti, and R. Carelli, "Switched control to robot-human bilateral interaction for guiding people," *Journal of Intelligent & Robotic Systems*, vol. 77, no. 1, pp. 73–93, 2015.

[4] M. Birem and F. berry, "DreamCam: a modular FPGA-based smart camera architecture," *Journal of Systems Architecture*, vol. 60, no. 6, pp. 519–527, 2014.

[5] C. Astua, R. Barber, J. Crespo, and A. Jardon, "Object detection techniques applied on mobile robot semantic navigation," *Sensors*, vol. 14, no. 4, p. 6734, 2014.

[6] W. Song, G. Wang, J. Xiao, G. Wang, and Y. Hong, "Research on multi-robot open architecture of an intelligent CNC system based on parameter-driven technology," *Robotics and Computer-Integrated Manufacturing*, vol. 28, no. 3, pp. 326–333, 2012.

[7] Y. Zhou and W. K. Huang, "The study on robot control using underwater sensor network," *Advanced Materials Research*, vol. 490-495, pp. 813–817, 2012.

[8] Y. Zhi-Gang and A. Yi, "Research of intelligent glue-coating robot based on visual servo," *Shanxi Electronic Technology*, vol. 24, pp. 2165–2171, 2012.

[9] M. D. Truong, N. N. Yu Feng, and L. Ricky, "Intelligent autonomous navigation system for the wheeled mobile robot," *Advanced Materials Research*, vol. 383-390, 2012.

[10] H. Sun, Z. Shi, J. Wu et al., "Research on multi-functional intelligent boiler slag-cleaning robot at the coal-fired power stations," *Lecture Notes in Electrical Engineering*, vol. 143, no. 11, pp. 601–608, 2012.

[11] T. Krajnik, N. Matias, J. Faigl et al., "A practical multirobot localization system," *Journal of Intelligent & Robotic Systems*, vol. 76, no. 3-4, pp. 539–562, 2014.

[12] H. Zhao, L. Xiong, Y. Liu et al., "Dynamic environment sensing using an intelligent vehicle," *Contemporary Issues in Early Childhood*, vol. 6, no. 2, pp. 63–74, 2012.

[13] X. W. . Wang, "Three-dimensional vision applications in GTAW process modeling and control," *International Journal of Advanced Manufacturing Technology*, vol. 80, no. 9-12, pp. 1601–1611, 2015.

[14] H. Mousazadeh, "A technical review on navigation systems of agricultural autonomous off-road vehicles," *Journal of Terramechanics*, vol. 50, no. 3, pp. 211–232, 2013.

[15] A. Araújo, D. Portugal, M. S. Couceiro, and R. P. Rocha, "Integrating arduino-based educational mobile robots in ROS," *Journal of Intelligent & Robotic Systems*, vol. 77, no. 2, pp. 281–298, 2015.

[16] M. Carol, F. M. Iván, C. Pascual, and S.-L. Jose Luis, "A hierarchical tracking strategy for vision-based applications on-board UAVs," *Journal of Intelligent & Robotic Systems*, vol. 72, no. 3-4, pp. 517–539, 2013.

[17] F. Flacco, T. Kroeger, A. D. Luca et al., "A depth space approach for evaluating distance to objects," *Journal of Intelligent & Robotic Systems*, vol. 80, no. 1, pp. 7–22, 2015.

[18] C. Rasmussen, K. Yuvraj, R. Vallett et al., "Towards functional labeling of utility vehicle point clouds for humanoid driving," . *Intelligent Service Robotics*, vol. 7, no. 3, pp. 133–143, 2013.

[19] S. Mohammed, C. Ramos, R. S. Chang et al., "Advanced sensor technology and applications in industrial control system," *International Journal of Distributed Sensor Networks*, vol. 2013, no. 3, 2 pages, 2013.

[20] M. Uhart, O. Patrouix, and Y. Aoustin, "Improving manufacturing of aeronautical parts with an enhanced industrial Robotised Fibre Placement Cell using an external force-vision scheme," *International Journal on Interactive Design & Manufacturing*, vol. 10, no. 1, pp. 1–21, 2015.

Hindawi
Mobile Information Systems
Volume 2021, Article ID 5523553, 11 pages
https://doi.org/10.1155/2021/5523553

Research Article

RSSI-Controlled Long-Range Communication in Secured IoT-Enabled Unmanned Aerial Vehicles

Inam Ullah Khan,[1] **Ryan Alturki**,[2] **Hasan J. Alyamani**,[3] **Mohammed Abdulaziz Ikram**,[4] **Muhammad Adnan Aziz**,[1] **Vinh Truong Hoang**,[5] **and Tanweer Ahmad Cheema**[1]

[1]*Department of Electronic Engineering, School of Engineering and Applied Sciences, Isra University, Islamabad, Pakistan*
[2]*Department of Information Science, College of Computer and Information Systems, Umm Al-Qura University, Makkah, Saudi Arabia*
[3]*Department of Information Systems, Faculty of Computing and Information Technology, King Abdulaziz University, Rabigh, Saudi Arabia*
[4]*Computer Science Department, University College in Al-Jamoum, Umm Al-Qura University, Makkah, Saudi Arabia*
[5]*Faculty of Computer Science, Ho Chi Minh City Open University, Ho Chi Minh city, Vietnam*

Correspondence should be addressed to Vinh Truong Hoang; vinh.th@ou.edu.vn

Received 6 January 2021; Revised 13 February 2021; Accepted 21 February 2021; Published 1 March 2021

Academic Editor: Mian Ahmad Jan

Copyright © 2021 Inam Ullah Khan et al. This is an open access article distributed under the Creative Commons Attribution License, which permits unrestricted use, distribution, and reproduction in any medium, provided the original work is properly cited.

Unmanned aerial vehicle (UAV) has recently gained significant attention due to their efficient structures, cost-effectiveness, easy availability, and tendency to form an ad hoc wireless mobile network. IoT-enabled UAV is a new research domain that uses location tracking with the advancement of aerial technology. In this context, the importance of 3D aerial networks is attracting a lot of attention recently. It has various applications related to information processing, communication, and location-based services. Location identification of wireless nodes is a challenging job and of extreme importance. In this study, we introduced a novel technique for finding indoor and open-air three-dimensional (3D) areas of nodes by measuring the signal strength. The mathematical formulation is based on a path loss model and decision tree machine learning classifier. We constructed 2D and 3D models to gather more accurate information on the nodes. Simulation findings demonstrate that the proposed machine learning-based model excels in nodes location estimation, the actual and estimated distance of different nodes, and calculation of received signal strength in aerial ad hoc networks. In addition, the decision tree constructs an offline phase control in the flying vehicle's location to enhance the time complexity along with experimental accuracy.

1. Introduction

Due to recent advancements in communication and networking, the flying ad hoc network (FANET) is considered as a more feasible alternative to the wireless sensor network (WSN). To meet growing high-speed networking and communication requirements, unmanned aerial vehicles are the optimal choice for communication. They are used for different cellular network applications such as border surveillance, search operations, crime scene security, home-based security, emergency assistance, and rescue operations. Unmanned aerial vehicles use air-to-air communication (a2a communication) like UAV communicating with other UAVs and air-to-ground communication (a2g communication) like UAV communicating with the ground base station. Air-to-air communication between different UAVs generally requires less energy as compared to air-to-ground communication. UAVs face different challenges such as limited power, short-communication ranges, rapid topological changes, low bandwidth, and handover.

Generally, for radio-range transmission communications, WLAN or WiFi networking is considered, but for long range communication requirements, 802.15.4 is used. WLAN induces heavy overheads due to which it is usually discouraged. Single UAV cannot create FANET; therefore, multiple UAV's are required, and not every UAV needs to be

connected to the base station. UAV does usually have a speed between 30 and 360 km/h due to which communication problems in multiple unmanned aerial vehicles arise. In flying ad hoc networks, there must be a sparse density with a large distance between unmanned aerial vehicles; however, it also depends upon the nature of flying ad hoc networks. The communication between UAV's can be affected due to their high speed, changing topology, changing location, connection failure, and updated processing needed every time. Localization means selecting the location of each UAV even at high speed. There is a need for efficient and accurate localization within short intervals of time according to the high speed.

The weighted centroid algorithm depends upon the beacon frames sent from nodes. These nodes are either expressed in 2D or 3D space. It is measured through the received signal strength identifier (RSSI) for indoor and outdoor environments. This study presents a novel strategy for aerial ad hoc networks using the three-dimensional measurement of received signal strength power which shows optimal outcome in terms of location and the distance of nodes. Calculation of signal strength is performed using a log-normal model. Signal strength plays an important role from aerial vehicles to the land station where cyber-security attacks can be deployed by intruders to overcome and hijack the network which causes disruption. Optimal flying signals transmission mitigates aerial data congestion which reduces many problems in smart cities. Intelligent signaling systems directly mixup in the field of smart cities which improve decision making, the interaction of information, and also smart flying things that increase the behavior of human interaction, energy, and context awareness. The main contributions of this study are as follows.

IoT-based unmanned aerial vehicles are used to improve signal strength in smart cities

Secure communication channels in flying ad hoc networks utilize a two-ray model and centroid algorithm for node localization

Machine learning framework decision tree is applied on the network topology to improve signal strength

Rest of the study is structured with Section 1 which consists of introduction, while Section 2 is composed of brief literature having past data about the problem. Similarly, detailed classification is incorporated in Section 3; also, Section 4 represents the proposed model. Section 5 demonstrates results of the algorithm. The theoretical analysis and future direction is discussed in Section 6, which is explained in conclusion section.

2. Related Survey

In [1], Bilal et al. discussed that the hexahedral method is being replaced by centroid localization algorithms. They compared the performance of the proposed approach with maximum likelihood estimation (MLE); this is further compared with the two-dimensional weighted centroid localization algorithm.

Syed et al. [2] designed a new routing protocol which can select cluster head (CH) for path planning and intelligent routing. The protocol design is based on selecting the group leader in the nodes. The group leader must have some specific attributes or characteristics. The group leader selects nodes and senses the environmental changes; whereas, the OPEN protocol performs better results as compared with the traditional routing techniques which improve energy lifetime.

In [3], Liu et al. compared optimal ant-based distance protocols. The analysis of different protocols is performed by using primary metrics. These routing protocols are evaluated in simulation-based environments, rather than real-time scenario. In this study, almost all of the protocols are based on transition probability, which is pheromone and heuristic-based, and the operation level is energy level control and distance transmission control.

Network topology such as flat and hierarchical describes routing challenges in ant-based protocols. This study also highlights the latest developments in this research field. Pu et al. [4] projected a novel idea in this study. The motivation of the study is a result of rapid development in technology such as sensors and communications in multisized UAVs leading to flying ad hoc networks. Because of the easy deployment of nodes and configurations, FANET is used in many applications such as search operations, rescue operations, and civil family functions. Due to high topological changes in communication links failure, there is an intentional jamming in unmanned aerial vehicles. This work can be further extended by making a connectivity-based mobility model for unmanned aerial vehicles.

Qiang et al. [5] explained the problem of the single connected flying ad hoc network, which can be segmented because of the special attributes of unmanned aerial vehicles. They also described different movements using k hope physical structure; this algorithm is studied in a three-dimensional FANET in numerical computation using a simulation environment. The proposed algorithm is compared with the local and also with the roof of a brief time, offset distance, cascade movement of motes, and also maintaining the original link at the same time.

Guillen-Perez and Cano et al. [6] came up with a new area in the network communication that is flying networks in which we find some different attributes from other areas. This study presents brief literature on mobility models of flying ad hoc networks positioning, propagating proposed for FANETs such as path planning. They used a pure randomized structural approach. In this study, they performed two experiments to advance state of the art by measuring the drones' onboard WiFi radiation patterns. To achieve, this experiment is performed in a controlled environment. Different wireless technologies such as WiFi, LTE, and WiMAX are used. Through these technologies quantifying the influence of radiation pattern onboard communication, the communication is mainly carried out in two-dimensional boundary, but in the future, we can use three-dimensional boundary for this practical experimentation.

Anis and Basit [7] described technical and experimental data on Internet of drones. This technology opens a new

horizon on smart tracking of drones through web and android-based applications using the robot operating system. This study explains object tracking through drones using Internet. Drone tracker uses drone map planner. A cloud-based system manages drones over Internet. Practical experimentation is performed, which shows drone tracking systems with a low speedy destination.

In [8], Zhang et al. [8] presented radio frequency identification for unmanned aerial vehicles that provides 6 degrees of freedom. They attached modern ultrahigh frequency tags that are interrogated. For this purpose, the Bayesian algorithm is used. The proposed experimentation was tested on rich structure for inside environments. SVD-based algorithm and Bayesian filter is used, and this method is efficient for different aerial vehicles. An unscented Kalman filtering mechanism is applied on directional antenna-based aerial networking to estimate the position of unmanned aerial vehicles [9].

According to the past research, we have found that most of the research work was conducted on wireless sensor networks based on the two-dimensional centroid localization algorithm; whereas, we have seen many limitations in the work such as calculating range-based methods; the availability of the data on sensors/hubs is part of range free calculation, and later, the received signal strength power was introduced. Formulation of signal strength on receiving flying nodes makes use of wireless infrastructure which enhances the capabilities of line-of-sight in air-2-ground signals multiplication to maximize the sensor networks. Achieving the optimal signal strength directly increases received signal power; whereby, wireless radio energy of the channel can uphold the power level in flying ad hoc networks. The industrial Internet of things is concerned where communication workstation security and reliable data transmission are the most important factors to safeguard the information centers. Pervasive edge computing is proposed to secure IIoT [10]. However, for lightweight mutual authentication, the client-server model utilizes encryption to secure sessions among the nodes [11, 12]. Threat intelligence can be minimized in dynamic malware analysis using a decision tree to examine behavior and overcome security risks [13]. In the decentralized web of networks, cognitive radio gives optimal results that employ the hidden Markov model to dedicate direct short range communication channels for transmission [14, 15]. Maintain the quality of service in multihop communication to detect Sybil attack; whereas for this purpose, QoS-aware secure communication technique can be easily deployed using Internet of things-based networks, which can be performed on large scale data [16].

3. Detail Classification

3.1. Aerial Networks. Topology construction plays an important role in aerial networks. In UAV networks, every node is a nonstatic node and moves in three axes. We do a study on how far is the node from the base station and how far is the drone away from the cluster head; for tackling these problems, making topology is important. Kim [17] discussed that due to rapid fluctuations in topological parameters of futuristic networks, UAV networks are promising technology due to the versatile behavior. This study describes the optimization of topological management to maximize the performance by optimizing the location and movements of unmanned aerial vehicles. It is achieved by adapting the topological changes while carrying out UAV's missions. Therefore, for this purpose, two algorithms were proposed, one for topology construction based on swarm optimization and the second one is adjusting topological changes in flying ad hoc networks, which is based on aerial flying networks. Shi et al. [18] introduced a new area that is a drone-assisted vehicular network (DAVN), which provides connectivity between vehicles and futuristic networks of unmanned aerial vehicles. In [18], they further discussed a brief architecture of software define the drone-assisted vehicular network (DAVN) by cooperating with vehicle infrastructure that can improve connectivity between drones and vehicles. The architecture is constructed on a mobile ad hoc network that includes static nodes and a remote server/node for communication; then, this process was updated into flying ad hoc networks that comprise a base station and drones. A pictorial representation of DAVN is presented in Figure 1.

3.2. Localization. Localization means to measure the distance between the nodes; there are two types of localization: one is indoor localization and the second one is open-air/outdoor localization. Yves and Peng [19] in their study described that low cost received signal strength can be found by simple experimentation of two devices that will be connected to a database to store the data. The algorithm works on the location of an unknown mote by using the received signal strength indicator (RSSI) with angle-based localization estimation (RALE). RSSI value gets increased when it comes near to hidden workstations which keep away from angle unreliable RSSI. The results obtained after the practical experiment show that RALE only requires RSSI and the angles. It does not require a complex computationally expensive algorithm. Furthermore, they suggested that this research can be tested on the position and height of the node. Wireless sensor networks mostly work in the bounded area of communication that forms clusters; the tracking of a static node or cluster is very easy, and these issues can be tackled by dynamic programming. As communication advances in many areas, hybridization of many heterogeneous sensor networks offers low power in high communication networks. Akter et al. [20] described the tracking and localization algorithm in wireless sensor networks. Due to the drawbacks in the static clustered routing, this research incrementally updates, creates maintenance through online learning, and shows us energy-efficient tracking and localization in wireless sensor networks. Some nodes decrease computational complexity calculation and give us proper information of the coordinate systems. Our research study will make use of signal strength power that shows how much is received which will be opposite to the distance between unmanned aerial vehicles.

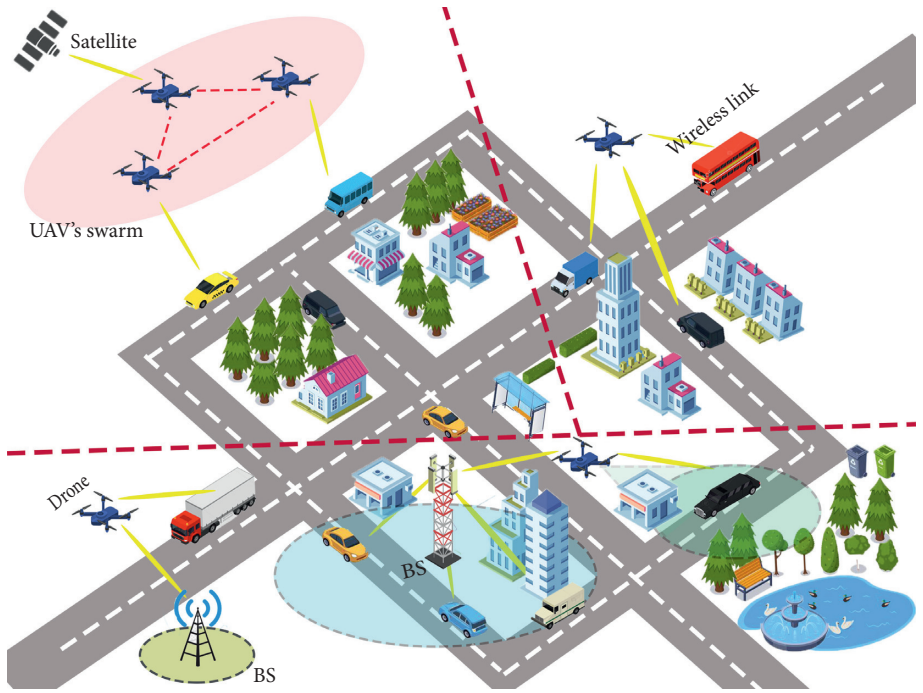

Figure 1: Drone-assisted vehicular networks.

3.3. Localization Strategies and Algorithm. As discussed in Section 3.2, localization is the estimation of the distance from one node to another node, such as environmental monitoring checking animals' habitat, fire surveillance, water quality checking from where the water is coming, search operations, and intrusion detection systems. Wireless sensor localization is the process to estimate the location of the sensors having unknown locations, time, distance, angle of arrival, and how the motes are connected. As far as the global positioning system (GPS) is a concern, this is very expensive to implement in every mote; so that is why we go for the technique of localization. Sensor with a known location of position information is called anchors. Range free localization includes pattern matching and hop-count-based localization. There is another branch called target/source localization, which includes single and multiple target localizations.

Yu et al. [21] in their study introduced two algorithms that give us better results to localize a node. First, error terms of the estimated distance between anchor motes. Second, the QDV-Hop algorithm minimizes error to obtain optimal localization. Almost both proposed algorithms achieve similar accuracy by solving unconstrained optimization issues. Later, localization can be improved by reducing computational complexity while improving accuracy.

The range free estimation can be expressed using centroid algorithms, DV-Hop, and APTI algorithms. In Figure 2, we briefly presented localization taxonomy that comprises of (i) target/source localization, (ii) distribution, (iii) mobility, (iv) ranging, (v) coordinates, and (vi) location. Figure 3 elaborates the classification of node localization strategies for wireless technology like 802.1, which mainly covers centralized and distributed localization. Distribution localization techniques further extend to six modules such as bacon based, relaxation based, coordinate system, hybrid, error propagation, and interferometer ranging. Bacon-based techniques have three more modes, which are diffusion, gradient, and bounding box. The 2D view of sensor workstations in flying vehicles gives the flat view where the three-dimensional implication displays a real-time field of vision in the network topology. Deep insight idea of the 3D location where flying nodes is having practical applications is utilizing sensor nodes. Besides, working on 3D-based environments on Internet of drones to improve node localization is a difficult task. Our simulation environment is based on a 3D centroid algorithm which will estimate not only node distance computation but also signal power between two unmanned aerial vehicles to measure the distance between aerial vehicles. Figure 2 represents the taxonomy ladder of localization, where Figure 3 shows wireless sensor communication networks' distribution in terms of centralized or either distributed localization.

3.4. Proposed Model. Signal strength power measurement commonly known as the received signal strength identifier (RSSI) is a technique for calculating the distance between two UAVs or wireless nodes. Signal strength varies as the distance between nodes changes. However, if you compare it to the real environment, the received signal strength indicator is highly influenced by environmental noise. Gao et al. [22] used a two-ray model for their proposed scheme for node localization. They tested the proposed technique in the rice field. With advancements in wireless communication technologies, there must be some efficient mathematical models that can be used to improve the accuracy in motes

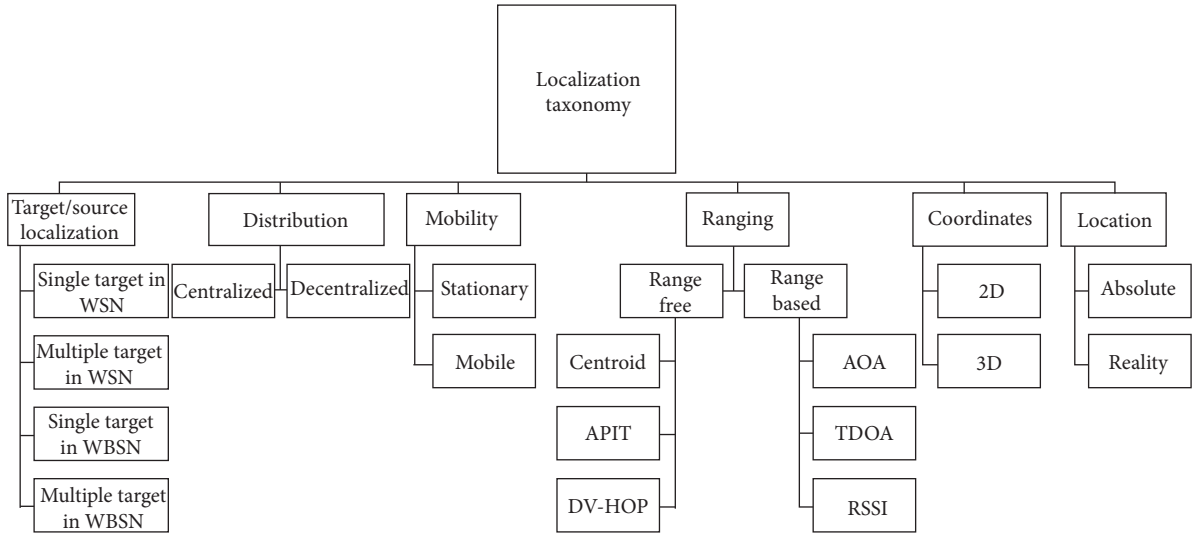

Figure 2: Localization taxonomy.

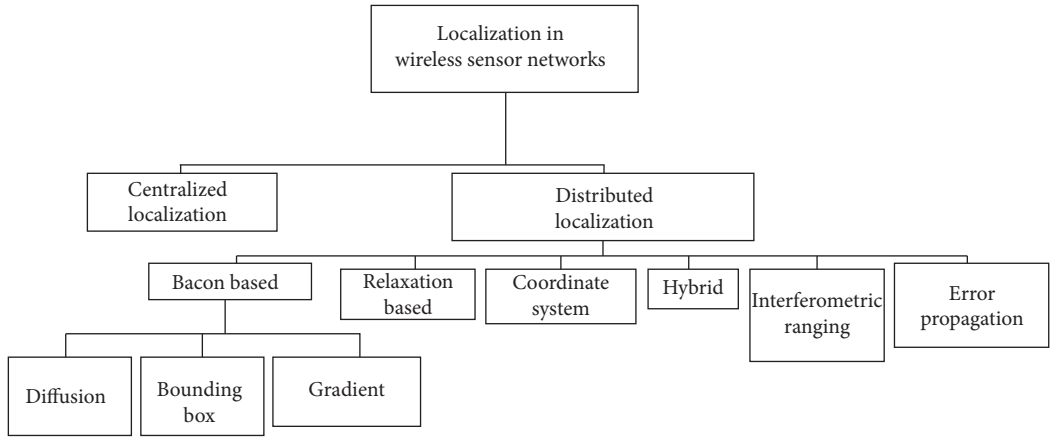

Figure 3: Classification of localization in wireless sensor networks.

localization algorithms. Received signal strength measurement is based on distance; we applied this technique in the centroid algorithm for node localization in aerial technology. Figure 4 elaborates the ideal relationship of received signal strength and distance between nodes.

$$\begin{aligned} \text{RSSI} &= -k \log d + a, \\ d &= 10\left[\frac{(a - \text{rssi})}{k}\right]. \end{aligned} \tag{1}$$

Syed et al. [1] discussed that remote signal plays a vital role in wireless communication; so remote received signals and motes relationship is given in the following equation:

$$P_r = P_t\left(\frac{1}{d}\right). \tag{2}$$

We must take ten times logarithm on both sides and convert it into dBm, as given in the following equation.

$$P_R\,(\text{dBm}) = A - 10n \log d. \tag{3}$$

Syed et al. [1] further discussed that the above equations are for urban environments, and the equation for received signal strength on the receiver side is given by the following equation.

$$P_r\,(\text{dB}) P_t G_t G_r * \left(\frac{{h_t}^2 {h_r}^2}{d^4}\right). \tag{4}$$

The shadowing model using signal strength power can be briefly explained using the following equation.

$$P(d) = P(d_0) - 10\eta \log 10\left(\frac{d}{d_0}\right) + X\sigma. \tag{5}$$

η is the signal attenuation used for some specific environments even when some obstacles come on the path of signal. $X\ \sigma$ is the Gaussian random variable, for smaller values and larger distances calculation of error for small values of measured signal strength.

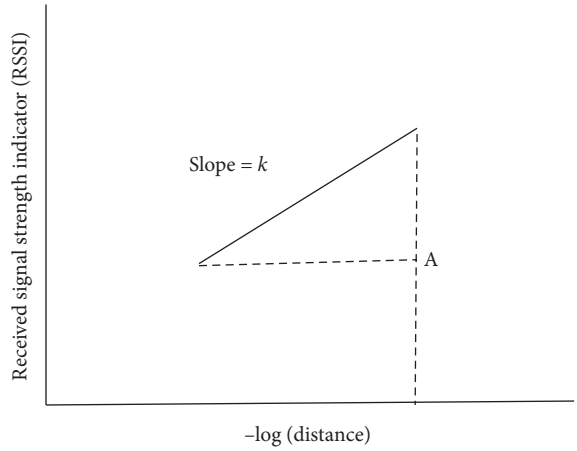

Figure 4: Relationship between RSSI and distance.

$$d = 10 - \frac{(P(d) - P(d_0) - X_\sigma)}{10\eta},$$
$$d = 10 - \frac{(P(d) - P(d_0) + X\sigma 1)}{10} \quad \text{if } P(d) \geq P1, \tag{6}$$
$$d = 10 - \frac{(P(d) - P(d_0) + X\sigma 2)}{10\eta 2} \quad \text{if } P(d) < P1.$$

In wireless communication using static access points, indoor localization is having importance, through which accuracy can be improved. Wang et al. [23] proposed that access point for indoor localization in 2D space is divided by special access points. They suggested that regions are divided by different locations, and the distance of the rank is provided to each region on access point. Location sequenced is obtained by using channel status information (CSI) between the access points. This algorithm is compared with the traditional method, i.e., received signal strength indicator (RSSI), and the simulations results show us accuracy of about 24.31%.

3.5. Wireless Technology. Short range communication is mostly used in aerial technology by using ZigBee. ZigBee is a low cost, easy to configure IEEE 802.15.4-based specification, which is generally used to create personal wireless area networks. It is used in different applications such as agriculture, smart homes, and military. Yu et al. described 3D localization in [24]. It uses a well-known loop invariant technique for division, with reference to point anchor bounded in an outer side using parameter points known as parametric loop division (PLD), for the measurement of noise. In Figure 5, we presented a novel technique called the three-dimensional centroid algorithm and RSSI framework in FANETs.

$$P_L(\text{dB}) = 10 \log Q,$$
$$P_L(\text{dB}) = -10 \log\left\{\frac{R}{S}\right\}. \tag{7}$$

Let G_t and G_r unite. L does not affect

$$X^2 + Y^2 = M_i^2, \quad i = 1, 2, 3, \ldots,$$
$$X^2 + Y^2 - M_i^2 = 0, \quad \text{If} \neq 0, \text{then} = \text{ei},$$
$$X_i^2 + X^2 - 2X_iX_0 + Y_i^2 + Y^2 - 2Y_iY_0 - M_i^2 = 0, \tag{8}$$
$$M_i^2 - X_i^2 - Y_i^2 = \left(X^2 + Y^2\right) - 2X_iX_0 - 2Y_iY_0.$$

Using the prior n-1 formulas minus n-1$^{\text{th}}$ formula,

$$X_i^2 + Y_i^2 - X^2 - Y^2 - M_i^2 + M^2 = 2X_0(X_i - X_n) + 2Y_0(Y_i - Y_0),$$
$$AX = B. \tag{9}$$

Basically, A is a tall matrix, whose inverse does not exist; so, premultiply with A^T:

$$A^TAX = A^TB. \tag{10}$$

A^TA = square matrix.

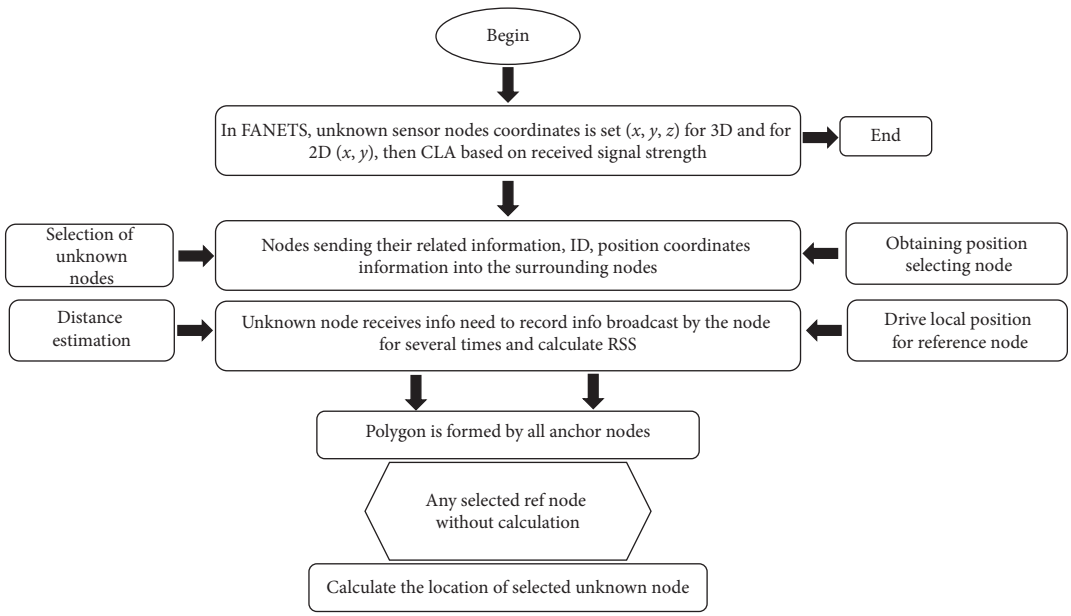

Figure 5: Three-dimensional centroid algorithm and RSSI framework in FANETS.

$$X = \left(A^T A\right)^{-1} A^T B. \tag{11}$$

4. Mathematical Formulation for Three-Dimensional (3D) Calculation

$$\begin{aligned} X_i^2 + X_0^2 - 2X_i X_0 + Y_i^2 + Y_0^2 - 2Y_i Y_0 + Z_i^2 + Z_0^2 - 2Z_i Z_0 &= M_i^2, \\ \left(X_0^2 + Y_0^2 + Z_0^2\right) - 2X_i X_0 - 2Y_i Y_0 - 2Z_i Z_0 &= M_i^2 - X_i^2 - Y_i^2 - Z_i^2. \end{aligned} \tag{12}$$

Using the prior (n-1) formula minus the n^{th} formula,

$$\begin{aligned} &\left(X_0^2 + Y_0^2 + Z_0^2\right) - 2X_0\left(X_i - X_n\right) - 2Y_0\left(Y_i - Y_n\right) - 2Z_0\left(Z_i - Z_n\right), \\ &\quad X_i^2 + Y_i^2 + Z_i^2 - X_n^2 - Y_n^2 - Z_n^2 - M_i^2 - M_n^2, \\ &A^T AX = A^T B, \\ &X = \left(A^T A\right)^{-1} A^T B. \end{aligned} \tag{13}$$

5. Simulation Results

We used Matlab for the simulation of the proposed model. We deployed 9 nodes randomly in the topology. All the nodes used in the topology are mobile and move in all three access at the same time. We constructed two scenarios one for 2D space and another for 3D. Pictorial representation of 2D and 3D topologies are presented in Figures 6 and 7, respectively. Few important simulation parameters are presented as follows.

(1) Number of nodes: 9.

(2) Calculation method for RSSI: log-normal method.

(3) Path loss for reference distance: 55 db.

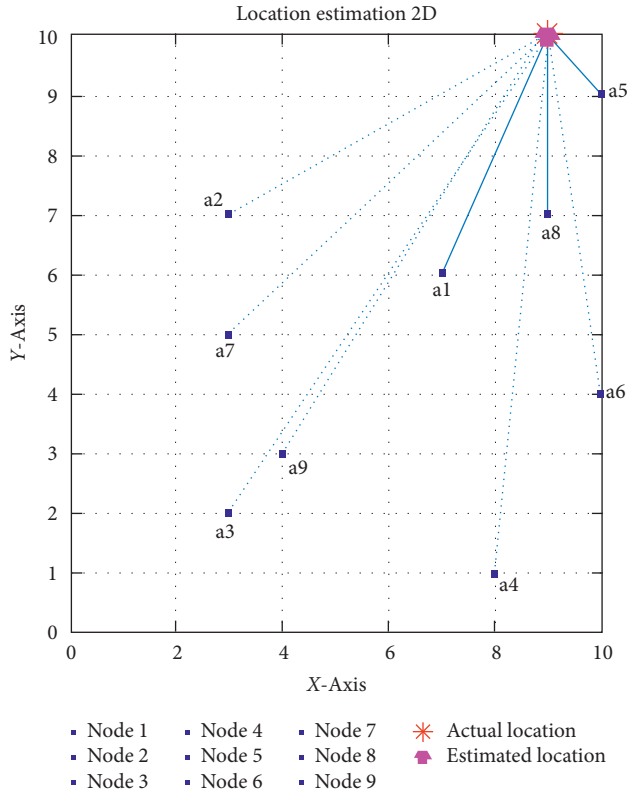

Figure 6: 9 UAVs deployed randomly in 2D.

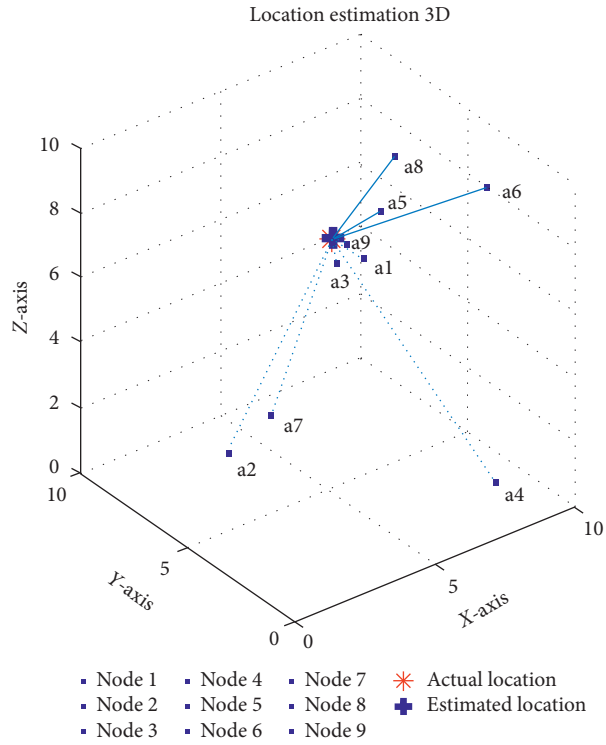

Figure 7: UAVs deployed randomly in 3D.

Estimation of 3D location with the decision tree algorithm for flying Ad hoc networks
Number of nodes: 9
Actual distance from node 1: 2.828427e + 00
Actual distance from node 2: 7.280110e + 00
Actual distance from node 3: 2.236068e + 00
Actual distance from node 4: 7.071068e + 00
Actual distance from node 5: 7.071068e + 00
Actual distance from node 6: 4.690416e + 00
Actual distance from node 7: 5.099020e + 00
Actual distance from node 8: 8.774964e + 00
Actual distance from node 9: 6.557439e + 00
Calculation of received signal strength by the log-normal model
Path loss for reference distance: 55 dB
Path loss exponent: 1
Reference distance: 1 m
Noise variance: 7
Received signal strength from node 1: 5.748455e + 01
Received signal strength from node 2: 5.337862e + 01
Received signal strength from node 3: 5.850515e + 01
Received signal strength from node 4: 5.350515e + 01
Received signal strength from node 5: 5.350515e + 01
Received signal strength from node 6: 5.528789e + 01
Received signal strength from node 7: 5.492513e + 01
Received signal strength from node 8: 5.256755e + 01
Received signal strength from node 9: 5.383266e + 01
Estimated distance from node 1: 5.643454e – 01
Estimated distance from node 2: 1.452573e + 00
Estimated distance from node 3: 4.461542e – 01
Estimated distance from node 4: 1.410864e + 00
Estimated distance from node 5: 1.410864e + 00
Estimated distance from node 6: 9.358610e – 01
Estimated distance from node 7: 1.017388e + 00
Estimated distance from node 8: 1.750836e + 00
Estimated distance from node 9: 1.308381e + 00
Node with good signal strength: node 3
Node with good signal strength: node 1
Node with good signal strength: node 6
Node with good signal strength: node 7
Actual location: (5, 3, 1)
Estimated location with the decision tree algorithm: (5.009588e + 00, 3.019663e + 00, 1.041434e + 00)

Figure 8: Decision tree for FANETS (3D).

(4) Path loss exponent: 1.

(5) Reference distance: 1 m.

(6) Noise variance: 7.

(7) Machine learning classifier: decision tree.

(8) Cost function: mean square error.

Figures 8 and 9 are MATLAB generated results which show some parameters such as estimated distance, nodes with signal strength, and actual distance among the aerial vehicles. Figure 8 is utilized for 2D and Figure 9 for 3D using Internet of flying vehicles.

Table 1 shows the comparison between the proposed solution and wireless sensor node localization which represents optimal results by using a decision tree to improve receive signal strength in the dynamic network. Therefore, signal power is improved more while utilizing machine learning technique as compared with the static node localization.

Estimation of 2D location with the decision tree algorithm
Number of nodes: 9
Actual distance from node 1: 2
Actual distance from node 2: 4.123106e + 00
Actual distance from node 3: 2.236068e + 00
Actual distance from node 4: 5
Actual distance from node 5: 5.830952e + 00
Actual distance from node 6: 4.242641e + 00
Actual distance from node 7: 5.099020e + 00
Actual distance from node 8: 7.211103e + 00
Actual distance from node 9: 4.242641e + 00
Calculation of received signal strength by the log-normal model
Path loss for reference distance: 55 dB
Path loss exponent: 1
Reference distance: 1 m
Noise variance: 7
Received signal strength from node 1: 5.898970e + 01
Received signal strength from node 2: 5.584776e + 01
Received signal strength from node 3: 5.850515e + 01
Received signal strength from node 4: 5.501030e + 01
Received signal strength from node 5: 5.434261e + 01
Received signal strength from node 6: 5.572364e + 01
Received signal strength from node 7: 5.492513e + 01
Received signal strength from node 8: 5.341998e + 01
Received signal strength from node 9: 5.572364e + 01
Estimated distance from node 1: 3.990525e – 01
Estimated distance from node 2: 8.226677e – 01
Estimated distance from node 3: 4.461542e – 01
Estimated distance from node 4: 9.976312e – 01
Estimated distance from node 5: 1.163428e + 00
Estimated distance from node 6: 8.465181e – 01
Estimated distance from node 7: 1.017388e + 00
Estimated distance from node 8: 1.438804e + 00
Estimated distance from node 9: 8.465181e – 01
Node with good signal strength: node 1
Node with good signal strength: node 3
Node with good signal strength: node 2
Actual location: (5, 3)
Estimated location with the decision tree algorithm: (5.005643e + 00, 2.995822e + 00)

Mean square error for 3D position: 7.317732e – 04 m
Mean square error for 2D position: 1.643185e – 05 m

Figure 9: Decision tree for FANETS (2D).

Table 1: Comparison of the proposed work with WSN-based node localization.

Ref/Proposed work	Number of nodes	WSN-based node localization	Flying things node localization	Node with good RSS using decision tree and dynamic mobility	Node with good RSS using WSN nodes	2D or 3D
[1]	9	YES	NO	NO	5.704609	Both
Proposed work	9	NO	YES	5.850515	NO	Both

6. Conclusions

Aerial networks refer to flying ad hoc networks or unmanned aerial vehicles. The rapidly changing dynamic structure of drones using different mobility models and topologies makes a challenge in implementing an algorithm that can measure signal strength power accurately. This study implementation presented a theoretical analysis and provided a brief discussion on using the three-dimensional centroid localization technique, step by step sequences using only 9 UAV's which have improved received signals on some UAVs. In the future, we can make use of different locations

on using distinct topological arrangements in aerial vehicles. Simulation results show that our decision tree-based model has shown good potential to address this problem.

Data Availability

This research is based on simulations, which are performed in a simulator. Therefore, there is no dataset used in this research.

Conflicts of Interest

The authors declare that they have no conflicts of interest.

References

[1] B. S. Syed, Z. Chen, F. Yin et al., "3D weighted centroid algorithm & RSSI ranging model strategy for node localization in WSN based on smart devices," *Sustainable cities and Society*, vol. 39, pp. 298–308, 2018.

[2] B. H. S. Syed, Z. Chen, and Y. Fuliang, "OPEN: optimized path planning algorithm with energy efficiency and extending network–lifetime in WSN," *Journal of Computing and Information Technology*, vol. 25, no. 1, pp. 1–14, 2017.

[3] X. Liu, "Routing protocols based on ant colony optimization in wireless sensor networks: a survey," *Institute of Electrical and Electronics Engineers Access*, vol. 5, pp. 26303–26317, 2017.

[4] C. Pu, "Jamming-resilient multipath routing protocol for flying ad hoc networks," *Institute of Electrical and Electronics Engineers Access*, vol. 6, pp. 2169–3536, 2018.

[5] Q. Guo, J. Yan, and W. Xu, "Localized fault tolerant algorithm based on node movement freedom degree in flying ad hoc networks," *Symmetry*, vol. 11, no. 1, p. 106, 2019.

[6] A. Guillen-Perez and M.-D. Cano, "Flying AD HOC networks: a new domain for network communications," *Sensors*, vol. 18, no. 10, p. 3571, 2018.

[7] K. Anis and Q. Basit, "Dronetrack: cloud-based real-time object tracking using unmanned aerial vehicles over the internet," *Institute of Electrical and Electronics Engineers Access*, vol. 6, pp. 13810–13824, 2018.

[8] J. Zhang, X. Wang, Z. Yu et al., "Robust RFID based 6-DoF localization for unmanned aerial vehicles," *Institute of Electrical and Electronics Engineers Access*, vol. 7, pp. 77348–77361, 2019.

[9] J. Yan, H. Zhao, X. Luo, C. Chen, and X. Guan, "RSSI-based heading control for robust long-range aerial communication in UAV networks," *Institute of Electrical and Electronics Engineers Internet of Things Journal*, vol. 6, no. 2, pp. 1675–1689, 2019.

[10] F. Khan, M. A. Jan, A. U. Rehman, S. Mastorakis, M. Alazab, and P. Watters, "A secured and intelligent communication scheme for IIoT-enabled pervasive edge computing," *Institute of Electrical and Electronics Engineers Transactions on Industrial Informatics*, vol. 2020, 2020.

[11] M. A. Jan, F. Khan, R. Khan et al., "A lightweight mutual authentication and privacy-preservation scheme for intelligent wearable devices in industrial-CPS," *Institute of Electrical and Electronics Engineers Transactions on Industrial Informatics*, vol. 2020, 2020.

[12] J. Li, J. Cai, F. Khan et al., "A secured framework for sdn-based edge computing in IOT-enabled healthcare system," *Institute of Electrical and Electronics Engineers Access*, vol. 8, pp. 135479–135490, 2020.

[13] N. Usman, S. Usman, F. Khan et al., "Intelligent dynamic malware detection using machine learning in IP reputation for forensics data analytics," *Future Generation Computer Systems*, vol. 118, p. 124, 2021.

[14] W. Yao, A. Yahya, F. Khan et al., "A secured and efficient communication scheme for decentralized cognitive radio-based internet of vehicles," *Institute of Electrical and Electronics Engineers Access*, vol. 7, pp. 160889–160900, 2019.

[15] F. Khan, A. Rehman, and M. Ahmad Jan, "A secured and reliable communication scheme in cognitive hybrid ARQ-aided smart city," *Computers & Electrical Engineering*, vol. 81, 2020.

[16] F. Khan, A. U. Rehman, A. Yahya et al., "A quality of service-aware secured communication scheme for internet of things-based networks," *Sensors*, vol. 19, no. 19, p. 4321, 2019.

[17] D. -Y. Kim and J. -W. Lee, "Integrated topology management in flying ad hoc networks: topology construction and adjustment," *Institute of Electrical and Electronics Engineers Access*, vol. 4, pp. 2169–3536, 2016.

[18] W. Shi, H. Zhou, J. Li, W. Xu, N. Zhang, and X. S. Shen, "Drone assisted vehicular networks: architecture, challenges and opportunities," *Institute of Electrical and Electronics Engineers Network*, vol. 32, no. 3, pp. 130–137, 2018.

[19] A. J. Yves and H. Peng, "RSSI-based indoor localization using RSSI-with-angle-based localization estimation algorithm," *International Journal of Sensor Networks and Data Communications*, vol. 4, no. 1, 2015.

[20] A. Mahmuda, R. Obaidur, I. Nazrul, M. M. Hassan, A. Alsanad, and A. K. Sangaiah, "Energy-efficient tracking and localization of objects in wireless sensor networks," *IEEE Access*, vol. 6, pp. 17165–17177, 2018.

[21] X. Yu, Y. Chu, F. Jiang, Y. Guo, and D. Gong, "SVMs classification based two-side cross domain collaborative filtering by inferring intrinsic user and item features," *Knowledge-Based Systems*, vol. 141, pp. 80–91, 2018.

[22] Z. Gao, W. Li, Y. Zhu et al., "Wireless channel propagation characteristics and modeling research in rice field sensor networks," *Sensors*, vol. 18, no. 9, p. 3116, 2018.

[23] Z. Wang, Y. Chen, and H. Wang, "Sequence-based indoor localization with channel status information," *Sensors*, vol. 18, no. 6, p. 1818, 2018.

[24] X. Yu, J. Yang, and Z. Xie, "Training SVMs on a bound vectors set based on fisher projection," *Frontiers of Computer Science*, vol. 8, no. 5, pp. 793–806, 2014.

Hindawi
Mobile Information Systems
Volume 2021, Article ID 6674479, 13 pages
https://doi.org/10.1155/2021/6674479

Research Article

Analyzing and Evaluating Smart Cities for IoT Based on Use Cases Using the Analytic Network Process

Chao Huang[1] **and Shah Nazir**[2]

[1]*Tianjin University of Technology, Tianjin 300384, China*
[2]*Department of Computer Science, University of Swabi, Swabi, Pakistan*

Correspondence should be addressed to Chao Huang; chaohuang_tjut@sina.com and Shah Nazir; snshahnzr@gmail.com

Received 28 December 2020; Revised 11 January 2021; Accepted 18 January 2021; Published 23 February 2021

Academic Editor: Mian Ahmad Jan

Copyright © 2021 Chao Huang and Shah Nazir. This is an open access article distributed under the Creative Commons Attribution License, which permits unrestricted use, distribution, and reproduction in any medium, provided the original work is properly cited.

With the passage of time, the world population is growing. Proper utilization of resources and other devices is tremendously playing an important role to easily examine, manage, and control the resources of the Internet of Things (IoT) in the smart city. Research in the field of IoT has revolutionized the services mostly in smart cities. In the smart city, the applications of IoT are utilized without human involvement. Diverse IoT devices are connected with each other and communicate for different tasks. With the existence of a huge number of IoT devices in the forthcoming years, the chances of privacy breach and information leakage are increasing. Billions of devices connected on IoT producing huge volume of data bound to cloud for processing, management, and storage. Sending of whole data to the cloud might create risk of security and privacy. Various needs of the smart city should be considered for both urgent and effective solutions to support requirements of the growing population. On the other side of rising technology, the IoT evolution has massively produced diverse research directions for the smart city. Keeping in view the use cases of the smart city, the proposed study presents the analytic network process (ANP) for evaluating smart cities. The approach of ANP works well in the situation of complexity, and vagueness exists among the available alternatives. The experimental results of the planned approach show that the approach is effective for evaluating the smart cities for IoT based on the use cases.

1. Introduction

With the passage of time, the population of the world is rising. According to the United Nations report, the population of the world will increase by 2.5 billion in 2050. About 55% of the world populations exists in cities, and it is estimated that, in the coming 30 years, this percentage will reach 68% [1]. Such incredible rise in population will give birth to diverse challenges and issues on cities. These issues can include sustainability management and urban areas development of smart cities. Research in the field of IoT has revolutionized the services mostly in smart cities. In the smart city, the applications of IoT are utilized without human involvement. Diverse IoT devices are connected with each other and communicate for different tasks. With the existence of a huge number of IoT devices in the forthcoming years, the chances of privacy breach and information leakage are increasing. Billions of devices connected on IoT producing huge volume of data bound to cloud for processing, management, and storage. Sending of whole data to the cloud might create risk of security and privacy. The paradigm of cloud computing subjugated through fog computing and acted as a channel between cloud and IoT.

Various approaches are being practiced by practitioners and researchers for diverse issues of smart cities. Sadhukhan [2] proposed an approach as appropriate framework for the services of smart city relying on IoT for addressing the issues of internet connectivity in smart city and to deal with heterogeneous technologies. Sabrina [3] proposed a model of structural relationship-based access control that can be used as an agent for the access of rights to resources for users

in the scenario of IoT at large scale. The model used public blockchain and smart contracts to manage access control for users that are external and with a local off-blockchain storage to manage access control for internal users of the organization. Lee et al. [4] suggested the function of service platform and whole architecture with details of the uses of platform with the help of analyzing road surface as a case study. The study analyzed the data services which can be associated with the applications of smart city and recommended generic directions of the services of urban data for services of advanced city. Li et al. [5] presented a semi-automated process of role mapping for the setting of dynamic accesses of smart city enabling access control. Mora-Sánchez et al. [6] proposed scalability complaint infrastructure as a validation approach consisting of the properties of interoperability, modularity, and resilience. The approach is relying on the top practices accomplished during a living lab at the Smart Cities Innovation Center in Universidad de Guadalajara implementation. Gebru et al. [7] addressed the prospect of quantifying flow and detection of people in the street of city to implementation of commercial sensors linked with the network of 5G capturing analyses of WiFi communicated through smartphones of people. The issues and motivation of these scenarios were outlined. After this, the study illustrated the proposed approach and presented the results obtained from live measurement in a testbed employed in Turin city within the project of 5G-EVE. The contributions of the planned study are given as follows:

(i) To present the ANP approach for assessing smart cities

(ii) To plot the smart cities according to the criteria defined for the available alternatives to achieve a specific goal of smart city

(iii) Results of the proposed approach show that the approach is effective for evaluating the smart cities for IoT based on the use cases

The paper is organized as follows: Section 2 shows the literature on the diverse issues of the smart cities. Section 3 briefly shows the methodology with the background of the smart cities use cases and the approach of the ANP for assessing the smart cities. The paper is concluded in Section 4.

2. Related Work

Various approaches are in practice by researchers and practitioners for smart city. Rout et al. [8] presented a model of IoT network based on technique of fuzzy logic data fusion for IoT. The process of data fusion estimates the congestion of location specific through human input and sensory data from the crowd. An open-source routing engine computes the congestion-aware shortest route through retorting to live updates of traffic in network of road. Besides, a node of sensor has been intended to gather the speed and emissions of moving vehicles on the road. An Android application was developed for gathering information of blockage on the road. Gheisari et al. [9] presented the concept of software defined networking paradigm to equip the IoT based smart city. The approach mounts privacy preserving for accomplishing packets of data flowing of split IoT device data. Several simulations were done by Mininet-WiFi for showing efficiency of the approach. Alamgir Hossain et al. [10] have used the concept of edge computing for empowering state awareness in IoT based smart city and for minimizing the latency of the edge devices producing data to be moved to cloud. From the user endpoint, huge data is produced, so processing of this data can expressively increase performance. The results of the experiments showed that processing IoT raw data at the devices of edge delivers situational awareness and is efficient for latency smart city decision makers. Araujo et al. [11] studied the performance assessment of FIWARE, which is a platform of cloud based IoT. The results were gathered from widespread performance assessment and developed testbed and produced MQTT and CoAp data for emulating IoT deployments at large scale.

Meng et al. [12] presented blockchain empowered single character frequency-based ESM building a confirmable database of malicious payloads through blockchain. In the assessment, the performance of the method was investigated under flooding character padding attacks in the real IoT and simulated surroundings. Sharma et al. [13] used multicriteria decision-making methods and acknowledged 15 implementations' IoT barriers from the existing literature hindering the implementation of IoT in smart cities in India. The acknowledged IoT barriers were investigated by approach of total interpretative structure model. The Fuzzy Matrices' Impacts Croises Multiplication Classement model, the decision-making trial, and evaluation laboratory approach were used. Serrano [14] presented blockchain random neural network for the applications of cybersecurity in a complete physical and digital cybersecurity user and channel methods of authentication. The approach empowers the gaps, the confidential identity can be mined, and attackers can be identified. Abbas et al. [15] achieved two objectives in the study: the first is the enhancement of Narrowband Internet of Things spectral efficiency, while the second one is to lessen the burden of signaling during transmission request for SMs. Koumetio Tekouabou et al. [16] proposed a system that integrated the predictive model based on ensemble approaches and IoT for optimizing the expectation of space availability in the smart parking. The Birmingham parking dataset was endorsed for reaching a Mean Absolute Error of 0.06% by applying Bagging regression. Pimpinella et al. [17] proposed smart urban routing services designed for cyclists and pedestrians disposed of movements in the city. The system allows retrieving the top route between a location of the source and destination based on the defined objective function of the user.

Srinivasa Desikan et al. [18] offered techniques of topology control for managing and constructing network of IoT for large-scale smart city. The problem of topology control was approached in two phases, the construction and maintenance. Based on fog gateways, cost-efficient IoT network was built in the construction phase, while resource utilization was done in the maintenance phase. Marques et al.

[19] proposed a multilevel infrastructure management architecture for IoT based smart city. The issue of waste management was considered for evaluating the performance of the system. The experimental results of the study show that the idea of the architecture is capable of managing up to 3902 garbage bins instantaneously. Atitallah et al. [20] presented a comprehensive review of the existing literature associated with DL and IoT for developing smart cities. The study begins with defining the IoT and then lists the properties of IoT produced big data. Furthermore, the study presented various infrastructures of computing used for big data analytics of IoT consisting of fog, cloud, and edge computing. Additionally, they surveyed the common DL models and presented the current innovations employing both the DL and IoT for developing services and smart applications for smart cities. The issues and challenges that existed during the developments of smart cities are highlighted. Bibri [21] aimed to review the associated literature with the objective of finding and discussing the state-of-the-art applications of sensor based big data empowered through the IoT surrounding sustainability and platforms of associated data processing and models of computing for smart sustainable cities. The issues and challenges affecting analytics of big data and IoT were identified.

Zahmatkesh and Al-Turjman [22] considered the probable applications of fog computing and technologies toward sustainable smart cities in the environment of IoT. The study discussed different approaches of artificial intelligence, various techniques of caching, unmanned aerial vehicle, and machine learning in data caching for fog based IoT. The study also highlighted the issues and challenges faced by the system. Singh et al. [23] provided a detailed review of the literature of the problems and issues impacting the blockchain deployment in smart cities. The study presented review of the main factors to the blockchain convergence and technologies of IoT for supporting a sustainable smart society. The study also discussed the solutions of security improvements and summarized the different main points that can be used to develop different transportation system based on AI-enabled blockchain. Majumdar et al. [24] predicted the congestion propagation across network of road based on long-short memory. The model predicts the propagation of congestion according to speed of vehicle from sensors of traffic at two sites. Rani et al. [25] presented a review on the cloud ecosystem and IoT role in smart cities with evaluation parameters and forthcoming directions of research in smart cities. Ouerhani et al. [26] offered an approach of dynamic control and management for streetlight based on architecture of IoT. Considerable influence is carried out for the interoperability level through the idea of device connection relying on communication of model driven agents for speeding up the cooperation of actuators and sensors to platform of IoT. The experimental results from tests of the real world with employed dynamic streetlights in urban spaces are shown.

Merlino et al. [27] presented an approach for the design and implementation of software defined cities approach which is a cloud infrastructure initiated from the idea of software-defined paradigms. The architecture in focus is on aspect of infrastructure and function virtualization with details of software stacks used. Santos et al. [28] presented PortoLivingLab, an infrastructure of multisource sensing that influences technology of IoT for achieving four occurrences of city-scale sensing. These occurrences include environment, weather, people flows, and public transport. A vehicular network is deployed, containing 600 vehicles and 19 environmental static sensors. Platform of crowdsensing that is effortlessly reconfigurable is conceded to various crowdsensing campaigns with above 600 participants. The architecture and elements of PortoLivingLab mentioning the technologies of IoT and issues faced are described. Various use cases are presented as evidence of idea. Omarov and Altayeva et al. [29] offered an approach of multiagent based implementation of smart microgrid that can be a base in building smart city converged platform. Mora et al. [30] proposed a blockchain as a potential for conciliating privacy versus security. The approach discussed the initial employment of a control access system incorporating blockchain. The study discussed the advantages and issues in detail.

3. Methodology

The following sections describe the methodology section of the paper.

3.1. Identification of Use Cases for Smart Cities. The world population is growing with the passage of time. Resources utilization and other devices are tremendously playing a significant role to certainly analyze, manage, and control the resources of the IoT in the smart city. In smart city, the applications of IoT are utilized without human involvement. Diverse IoT devices are connected with each other and communicate for different tasks. Figure 1 shows the depiction of smart city ecosystem, which demonstrates how data are accumulated from smart sensors of edge then transforming to the cloud and fog for processing, management, and storage and then interpreting for serving various applications of IoT [20].

Diverse sectors through the city have in recent times expanded the capability of smart technologies and actions [20, 31, 32]. These sectors of smart cities are given as follows:

(i) Smart homes: these are the residence containing devices connected to the internet. These devices can include lights, fridges, and televisions, communicating with each other and sharing the data to its users.

(ii) Smart healthcare: the smart healthcare consists of the devices that can monitor and measure the activities of user health. These devices are mostly wearable and nonwearable, which can measure user temperature, user blood pressure, heartbeat rate, blood sugar, and many other diseases.

(iii) Smart environment: intelligent sensors are installed for the development of city infrastructure. These sensors control and monitor the conditions of the surroundings for providing healthier environment.

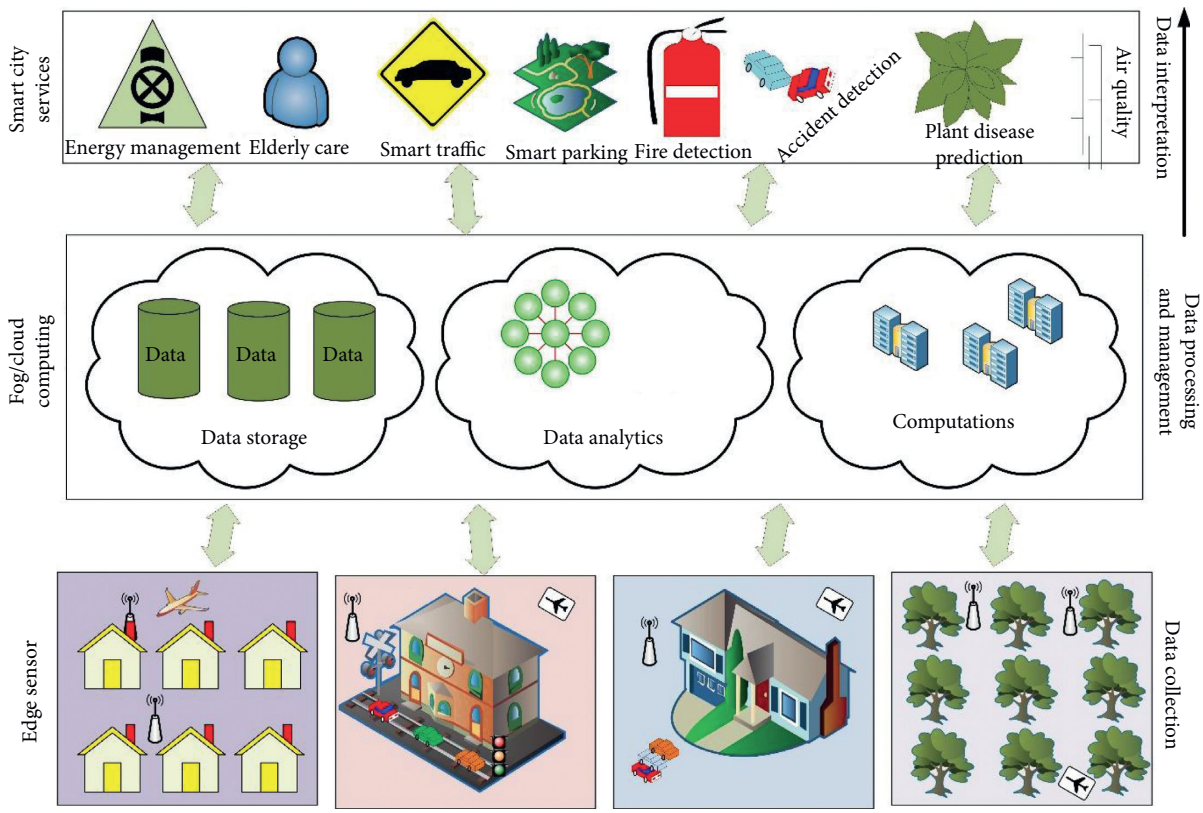

Figure 1: Smart city ecosystem.

(iv) Smart transportation: optimized services and innovative devices are used for enhancement of smart cities transportation. The services are smart parking, traffic flow, and so on.

(v) Smart surveillance: diverse devices of surveillance such as camera are installed for prevention of incidents. Smart security can be achieved by collecting real-time data and then analyzing it for different purposes.

(vi) Smart agriculture: the deployment of IoT devices in agriculture is for automation and providing good services against outdated approaches. These services support the agriculture and guarantee healthier crop production and improve harvesting, smart crop counting, and so on.

The proposed study has considered the six use cases from hypothetical smart cities which were earlier identified [31, 32]. These use cases are smart home, smart transportation, smart healthcare, smart environment, smart agriculture, and smart surveillance. These use cases of smart cities are described in Figure 2.

3.2. Analyzing the Smart Cities Based on Use Cases. Various libraries were searched for identification of relevant materials associated with the proposed study. The search results indicate that the extent of research is increasing in the field of smart cities. Various types of analysis were done. These types of analysis include the years of publication with papers published, the type of articles, the place, and titles of publications. Figure 3 shows the papers with the years of publication in ScienceDirect.

Figure 4 shows the paper types in the same library.

Figure 5 presents the discipline of publications. In the figure, it is revealed that a high number of papers were published in the field of computer science.

Figure 6 shows locations of conference held with the articles number in the IEEE.

Figure 7 graphically shows the topics of publications.

Figure 8 depicts the types of papers.

Figure 9 depicts the publications with the disciplines in the Springer library.

Figure 10 shows the publication types in the same library.

3.3. Evaluating Smart Cities for IoT Based on Use Cases. Researches in the area of IoT have transformed the services commonly in smart cities. In smart city, the applications of IoT are exploited deprived of human participation. Various devices of IoT are linked with each other, communicating for different activities and tasks. With the existence of a huge number of IoT devices in the forthcoming years, the chances of privacy breach and information leakage are increasing. Billions of devices connected on IoT producing huge volume of data bound to cloud for processing, management, and storage. Sending of whole data to the cloud might create risk of security and privacy. The proposed study considers

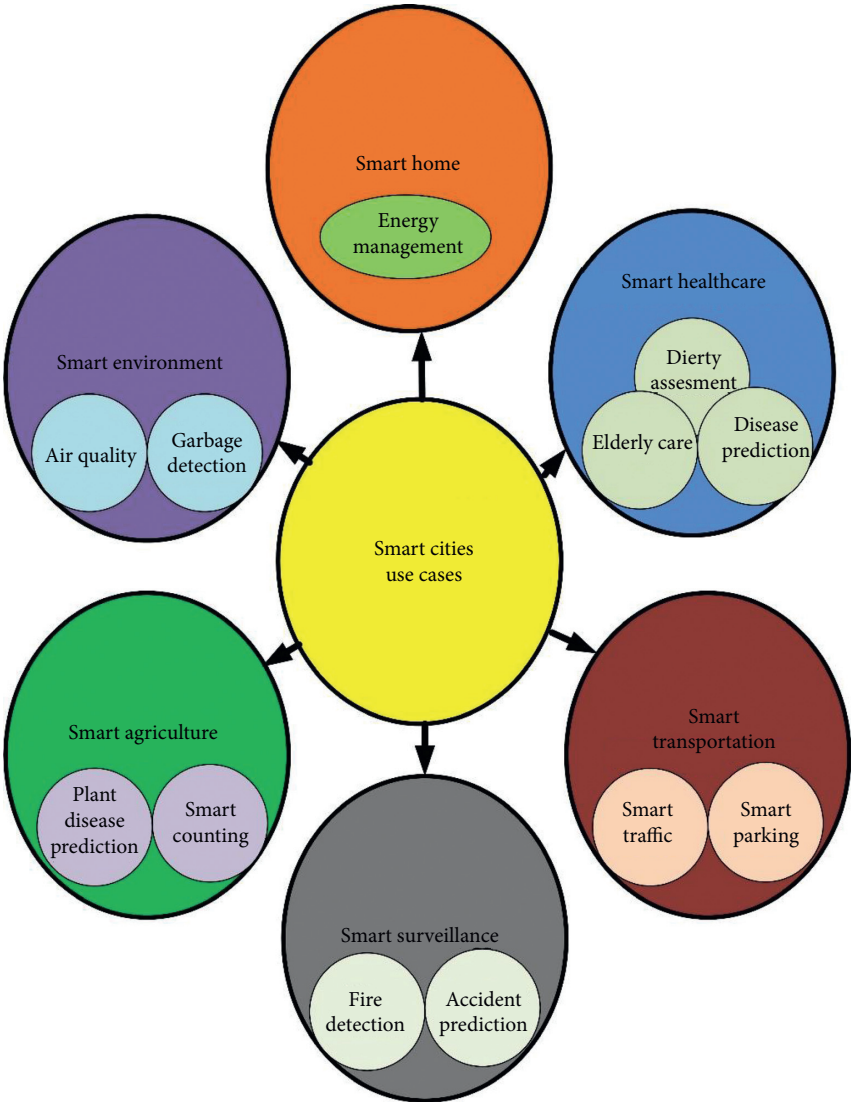

Figure 2: Smart cities' use cases.

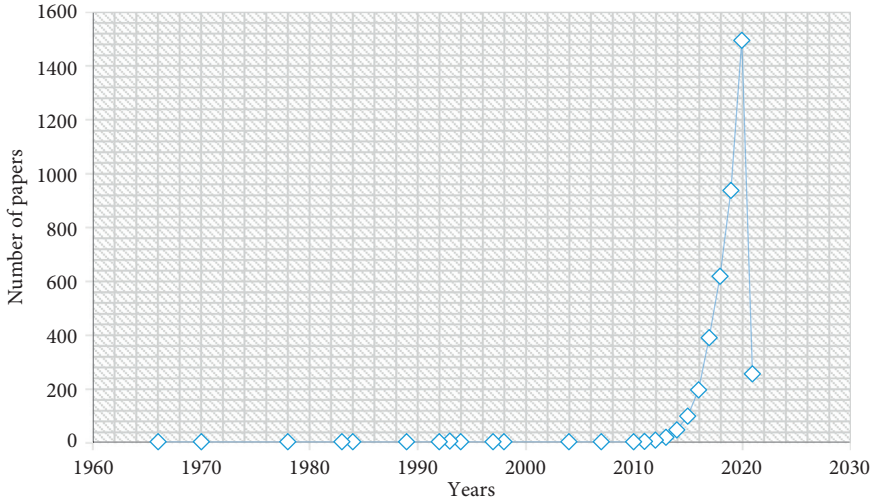

Figure 3: Years with publications.

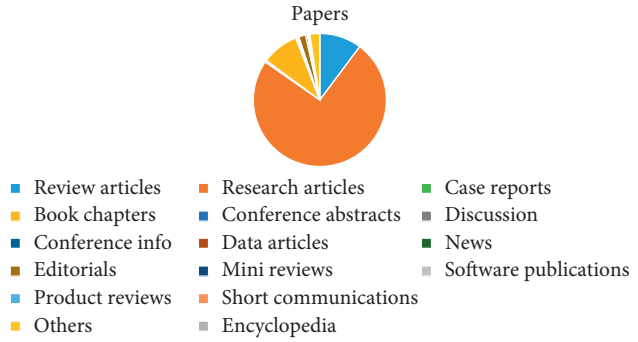

Figure 4: Publication types.

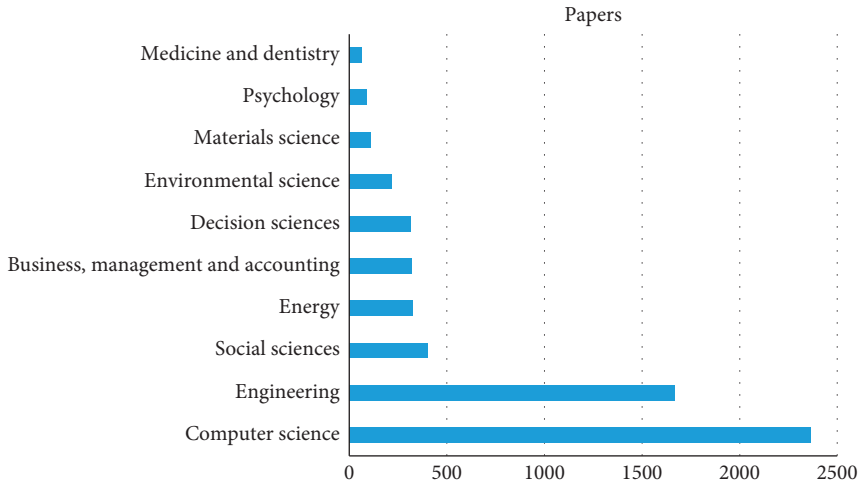

Figure 5: Disciplines of publications.

Figure 6: Locations of conferences held.

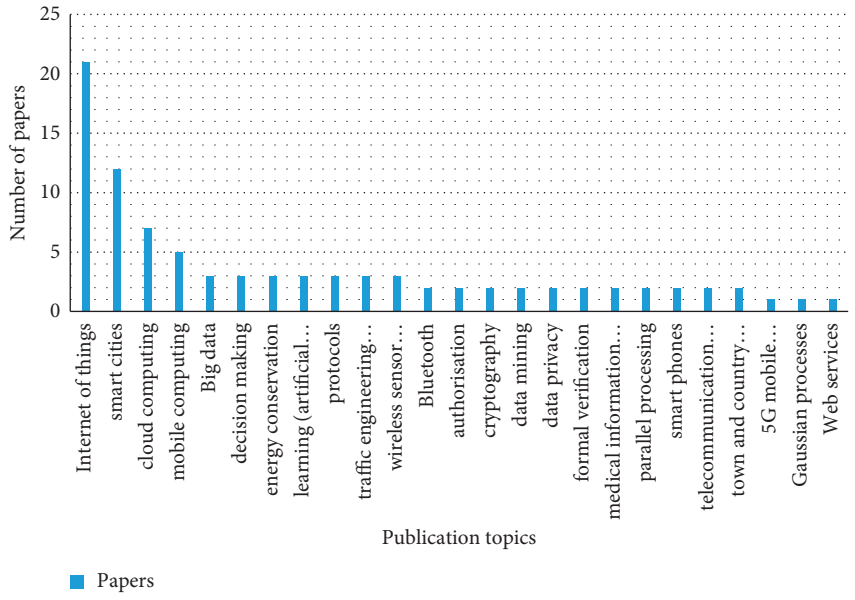

Figure 7: Publication topics.

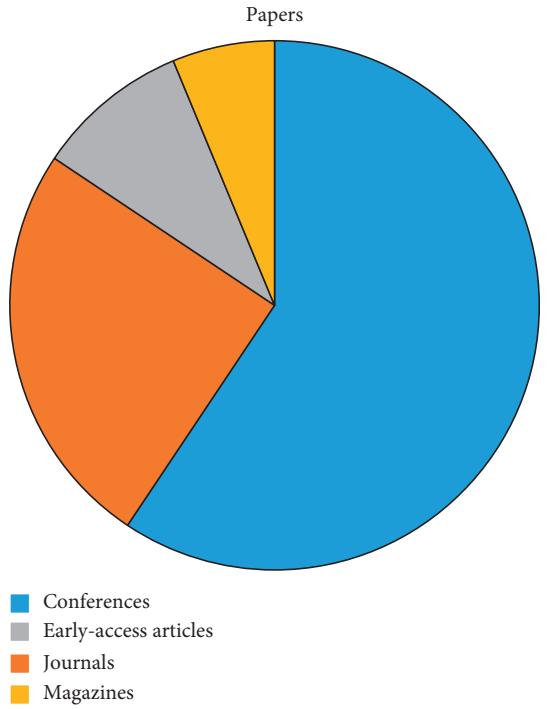

Figure 8: Publication types.

different use cases of the smart cities on the basis of which smart cities are assessed. These use cases are smart home, smart transportation, smart healthcare, smart environment, smart agriculture, and smart surveillance. The approach of ANP has been used for the purpose of evaluation of the smart cities. The ANP has various applications [33–38]. Three parts of the approach were considered as the significant parts consisting of goal, criteria, and alternatives. The details of the ANP approach can be found in [39]. The following algorithm was followed for the process of evaluation of the proposed study (Algorithm 1).

The process of the above algorithm was followed to evaluate the smart cities. The random consistency table was given by Satty [39] (Table 1).

The process of calculating the pairwise comparison was done for each of the alternatives and criteria to achieve the goal of smart city. The whole process of calculation was done but here only a few tables are given for understanding of the

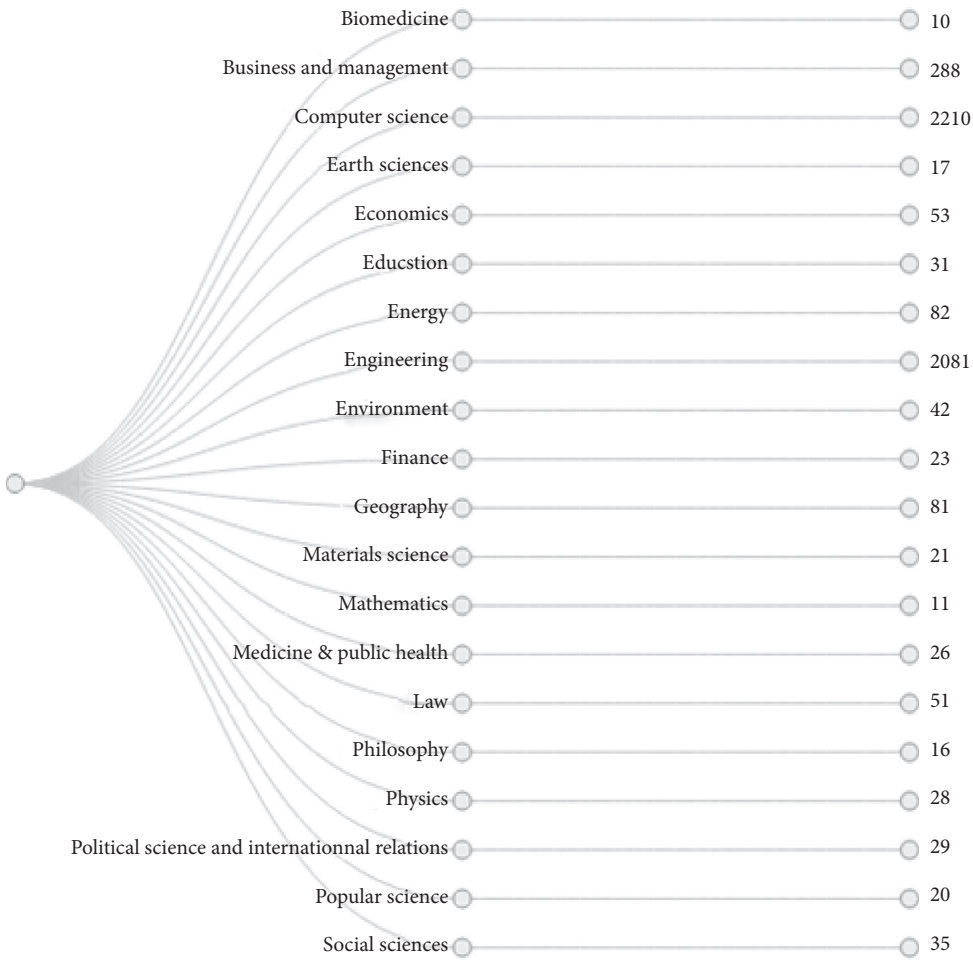

Figure 9: Papers with disciplines.

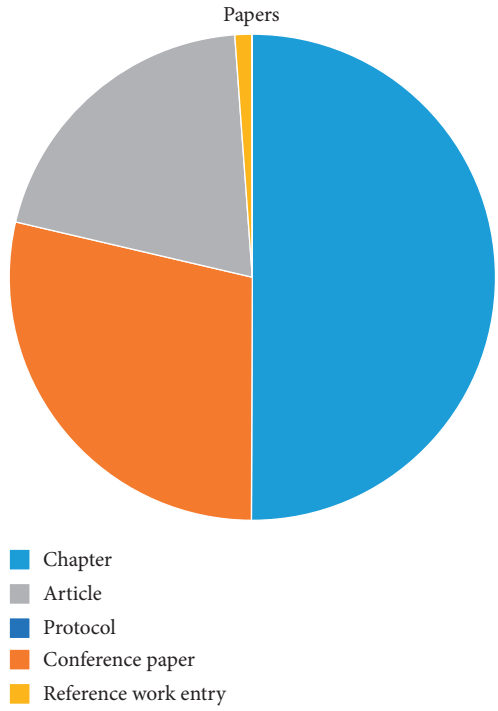

Figure 10: Publication types.

readers. Table 2 shows the pairwise comparison of smart city 1 for available use cases.

The process in Table 2 is normalized, and the normalization process is shown in Table 3.

Table 4 shows the available smart cities which are evaluated for the use cases.

Table 4 is normalized, and the normalized table is shown in Table 5.

After all of the processes of pairwise comparison, the normalized matrices are combined into a single matrix, which formed a weighted supermatrix. The weighted supermatrix is shown in Table 6.

The weighted supermatrix was converted into limit matrix for decision-making. This table was obtained by taking the square of the weighted matrix till all the values of rows become the same. Table 7 shows the limit matrix.

On the basis of the limit matrix given in Table 7, the decision of smart cities can be made. This decision was graphically plotted for showing visibility of the decision of evaluation of smart cities based on use cases. The smart city SC1 obtained high rank of 0.453 followed by SC2 and then others. So, among the available smart cities, SC1 was considered the topmost priority. Figure 11 shows the ranking of the smart cities against the available based on the use cases.

(a) Plot the criteria into subparts
(b) Qualitative scale of measure between 1 and 9
(c) Pairwise comparison is done
(d) Relative importance is found
(e) Finding the principal eigenvalue and the related eigenvector of the matrix
(f) Measuring the consistency of the matrix
(g) Priority vector "w" is calculated as follows: $A_w = \lambda_{\max} w$
(h) $\lambda_{\max}$ is the major eigenvalue of matrix "A" and "w" is its eigenvector.
(i) Calculating the consistency index (CI) and consistency random (CR) of the pairwise comparison matrix computed by the following equation: $C_i = (\lambda_{\max} - n)/(n-1)$, CR = CI/RI
(j) The value of CR should be less than 0.1
(k) Construction of the supermatrix
(l) Conversion of the weighted supermatrix into the limit matrix
(m) Decision based on the limit matrix

Algorithm 1: Process of the proposed approach.

Table 1: Random consistency index.

	1	2	3	4	5	6	7	8	9	10	11	12	13	14	15
RI	0	0	0.58	0.9	1.12	1.24	1.32	1.41	1.45	1.49	1.51	1.48	1.56	1.57	1.59

Table 2: Pairwise comparison of smart city 1 for available use cases.

	Smart home	Smart healthcare	Smart transportation	Smart surveillance	Smart environment	Smart agriculture
Smart home	1	3	2	5	4	4
Smart healthcare	1/3	1	2	3	2	3
Smart transportation	1/2	1/2	1	3	3	2
Smart surveillance	1/5	1/3	1/3	1	2	2
Smart environment	1/4	1/2	1/3	1/2	1	3
Smart agriculture	1/4	1/3	1/2	1/2	1/3	1

Table 3: Normalization of Table 2.

	Smart home	Smart healthcare	Smart transportation	Smart surveillance	Smart environment	Smart agriculture	E.V.
Smart home	0.39	0.53	0.32	0.38	0.32	0.267	0.371
Smart healthcare	0.13	0.18	0.32	0.23	0.16	0.200	0.204
Smart transportation	0.20	0.09	0.16	0.23	0.24	0.133	0.176
Smart surveillance	0.08	0.06	0.05	0.08	0.16	0.133	0.094
Smart environment	0.10	0.09	0.05	0.04	0.08	0.200	0.093
Smart agriculture	0.10	0.06	0.08	0.04	0.03	0.067	0.062

CR = 0.78.

Table 4: Available smart cities for use cases.

	SC1	SC2	SC3	SC4
SC1	1	2	4	2
SC2	1/2	1	2	3
SC3	1/4	1/2	1	2
SC4	1/2	1/3	1/2	1

Table 5: Normalization of Table 4.

	SC1	SC2	SC3	SC4	E.V.
SC1	0.44	0.52	0.53	0.25	0.437
SC2	0.22	0.26	0.27	0.38	0.281
SC3	0.11	0.13	0.13	0.25	0.156
SC4	0.22	0.09	0.07	0.13	0.125

CR = 0.087.

Table 6: Weighted supermatrix.

Node label		Use cases						Smart cities			
		Smart home	Smart healthcare	Smart transportation	Smart surveillance	Smart environment	Smart agriculture	SC1	SC2	SC3	SC4
Use cases	Smart home	0.000	0.000	0.000	0.000	0.000	0.000	0.371	0.320	0.357	0.397
	Smart healthcare	0.000	0.000	0.000	0.000	0.000	0.000	0.204	0.227	0.191	0.193
	Smart transportation	0.000	0.000	0.000	0.000	0.000	0.000	0.176	0.162	0.170	0.145
	Smart surveillance	0.000	0.000	0.000	0.000	0.000	0.000	0.094	0.131	0.125	0.114
	Smart environment	0.000	0.000	0.000	0.000	0.000	0.000	0.093	0.100	0.093	0.098
	Smart agriculture	0.000	0.000	0.000	0.000	0.000	0.000	0.067	0.063	0.067	0.056
Smart cities	SC1	0.437	0.501	0.404	0.406	0.489	0.441	0.000	0.000	0.000	0.000
	SC2	0.281	0.247	0.320	0.316	0.245	0.309	0.000	0.000	0.000	0.000
	SC3	0.156	0.158	0.170	0.154	0.148	0.163	0.000	0.000	0.000	0.000
	SC4	0.125	0.094	0.105	0.124	0.118	0.087	0.000	0.000	0.000	0.000

Table 7: Limit matrix.

		Use cases						Smart cities			
	Node label	Smart healthcare	Smart healthcare	Smart transportation	Smart surveillance	Smart environment	Smart agriculture	SC1	SC2	SC3	SC4
Use cases	Smart home	0.361	0.361	0.361	0.361	0.361	0.361	0.000	0.000	0.000	0.000
	Smart healthcare	0.209	0.209	0.209	0.209	0.209	0.209	0.000	0.000	0.000	0.000
	Smart transportation	0.169	0.169	0.169	0.169	0.169	0.169	0.000	0.000	0.000	0.000
	Smart surveillance	0.113	0.113	0.113	0.113	0.113	0.113	0.000	0.000	0.000	0.000
	Smart environment	0.096	0.097	0.096	0.097	0.097	0.097	0.000	0.000	0.000	0.000
	Smart agriculture	0.065	0.065	0.065	0.065	0.065	0.065	0.000	0.000	0.000	0.000
Smart cities	SC1	0.000	0.000	0.000	0.000	0.000	0.000	0.453	0.452	0.452	0.452
	SC2	0.000	0.000	0.000	0.000	0.000	0.000	0.287	0.287	0.287	0.287
	SC3	0.000	0.000	0.000	0.000	0.000	0.000	0.161	0.160	0.160	0.160
	SC4	0.000	0.000	0.000	0.000	0.000	0.000	0.114	0.114	0.114	0.114

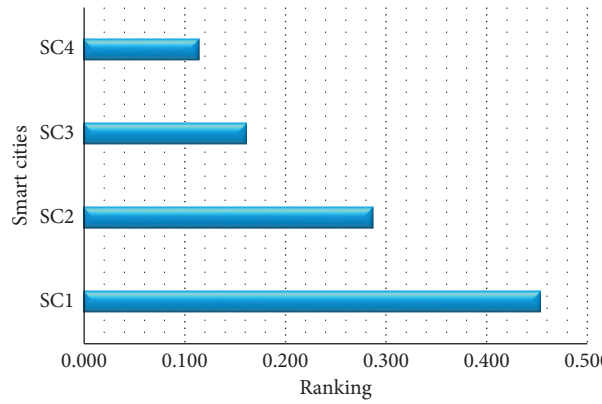

Figure 11: Ranking of smart cities based on the use cases.

4. Conclusion

Research in the field of IoT has transfigured the services of life, mostly in smart cities. In the smart city, the applications of IoT are utilized without human involvement. Various devices of IoT are connected with each other and communicate for different tasks. Billions of devices connected on IoT producing huge volume of data bound to cloud for processing, management, and storage. Sending of whole data to the cloud might create risk of security and privacy. Various needs of the smart city should be considered for both the urgent and effective solutions to support requirements of the growing population. On the other side of rising technology, the IoT developments have enormously shaped diverse research directions for the smart city. Keeping in view the use cases of the smart city, the proposed study presents the approach of the ANP for evaluating smart cities. The method was mainly based on the criteria defined for the smart cities with the aim of selecting the smart city. The selection of the smart city can further play an important role for living in the future. The experimental results of the proposed study show that the approach is effective for evaluating the smart cities for IoT based on the use cases.

Data Availability

The data can be provided upon request.

Conflicts of Interest

The authors declare no conflicts of interest.

Acknowledgments

This work was sponsored in part by Tianjin Philosophy and Social Science Project 2018 (TJYJ18-019).

References

[1] U. Nation, "68% of the world population projected to live in urban areas by 2050," 2018, https://www.un.org/development/desa/en/news/population/2018-revision-of-world-urbanization-prospects.html.

[2] P. Sadhukhan, "An IoT based framework for smart city services," in *Proceedings of the 2018 International Conference on Communication, Computing and Internet of Things (IC3IoT)*, vol. 15-17, pp. 376–379, Chennai, India, Febuary 2018.

[3] F. Sabrina, "Blockchain and structural relationship based access control for IoT: a smart city use case," in *Proceedings of the 2019 IEEE 44th Conference on Local Computer Networks (LCN)*, pp. 137–140, Osnabrück, Germany, October 2019.

[4] R. Lee, R.-Y. Jang, M. Park, G.-Y. Jeon, J.-K. Kim, and S.-H. Lee, "Making IoT data ready for smart city applications," in *Proceedings of the 2020 IEEE International Conference on Big Data and Smart Computing (BigComp)*, vol. 19–22, pp. 605–608, Busan, South Korea, Febuary 2018.

[5] F. Li, H. Wang, L. Diao, I. Yen, and F. Bastani, "Toward semi-automated role mapping for IoT systems in smart cities," in *Proceedings of the 2019 IEEE International Smart Cities Conference (ISC2)*, pp. 14–17, Casablanca, Morocco, October 2019.

[6] O. B. Mora-Sánchez, E. López-Neri, E. J. Cedillo-Elias, E. Aceves-Martínez, and V. M. Larios, "Validation of IoT infrastructure for the construction of smart cities solutions on living lab platform," *IEEE Transactions on Engineering Management*, vol. 9910 pages, 2020.

[7] K. Gebru, C. Casetti, C. F. Chiasserini, and P. Giaccone, "IoT-based mobility tracking for smart city applications," in *Proceedings of the 2020 European Conference on Networks and Communications (EuCNC)*, pp. 326–330, Dubrovnik, Croatia, Croatia, June 2020.

[8] R. R. Rout, S. Vemireddy, S. K. Raul, and D. V. L. N. Somayajulu, "Fuzzy logic-based emergency vehicle routing: an IoT system development for smart city applications," *Computers & Electrical Engineering*, vol. 88, Article ID 106839, 2020.

[9] M. Gheisari, G. Wang, W. Z. Khan, and C. Fernández-Campusano, "A context-aware privacy-preserving method for IoT-based smart city using software defined networking," *Computers & Security*, vol. 87, Article ID 101470, 2019.

[10] S. Alamgir Hossain, M. Anisur Rahman, and M. A. Hossain, "Edge computing framework for enabling situation awareness in IoT based smart city," *Journal of Parallel and Distributed Computing*, vol. 122, pp. 226–237, 2018.

[11] V. Araujo, K. Mitra, S. Saguna, and C. Åhlund, "Performance evaluation of FIWARE: a cloud-based IoT platform for smart cities," *Journal of Parallel and Distributed Computing*, vol. 132, pp. 250–261, 2019.

[12] W. Meng, W. Li, S. Tug, and J. Tan, "Towards blockchain-enabled single character frequency-based exclusive signature matching in IoT-assisted smart cities," *Journal of Parallel and Distributed Computing*, vol. 144, pp. 268–277, 2020.

[13] M. Sharma, S. Joshi, D. Kannan, K. Govindan, R. Singh, and H. C. Purohit, "Internet of Things (IoT) adoption barriers of smart cities' waste management: an Indian context," *Journal of Cleaner Production*, vol. 270, Article ID 122047, 2020.

[14] W. Serrano, "The blockchain random neural network for cybersecure IoT and 5G infrastructure in smart cities," *Journal of Network and Computer Applications*, vol. 175, Article ID 102909, 2021.

[15] A. M. Abbas, K. Y. Youssef, I. I. Mahmoud, and A. Zekry, "NB-IoT optimization for smart meters networks of smart cities: case study," *Alexandria Engineering Journal*, vol. 59, no. 6, 2020.

[16] S. C. Koumetio Tekouabou, E. A. Abdellaoui Alaoui, W. Cherif, and H. Silkan, "Improving parking availability prediction in smart cities with IoT and ensemble-based model," *Journal of King Saud University-Computer and Information Sciences*, 2020.

[17] A. Pimpinella, A. E. C. Redondi, and M. Cesana, "Walk this way! an IoT-based urban routing system for smart cities," *Computer Networks*, vol. 162, Article ID 106857, 2019.

[18] K. E. Srinivasa Desikan, V. J. Kotagi, and C. Siva Ram Murthy, "Topology control in fog computing enabled IoT networks for smart cities," *Computer Networks*, vol. 176, Article ID 107270, 2020.

[19] P. Marques, D. Manfroi, E. Deitos et al., "An IoT-based smart cities infrastructure architecture applied to a waste management scenario," *Ad Hoc Networks*, vol. 87, pp. 200–208, 2019.

[20] S. B. Atitallah, M. Driss, W. Boulila, and H. B. Ghézala, "Leveraging deep learning and IoT big data analytics to support the smart cities development: review and future directions," *Computer Science Review*, vol. 38, Article ID 100303, 2020.

[21] S. E. Bibri, "The IoT for smart sustainable cities of the future: an analytical framework for sensor-based big data applications for environmental sustainability," *Sustainable Cities and Society*, vol. 38, pp. 230–253, 2018.

[22] H. Zahmatkesh and F. Al-Turjman, "Fog computing for sustainable smart cities in the IoT era: caching techniques and enabling technologies - an overview," *Sustainable Cities and Society*, vol. 59, Article ID 102139, 2020.

[23] S. Singh, P. K. Sharma, B. Yoon, M. Shojafar, G. H. Cho, and I.-H. Ra, "Convergence of blockchain and artificial intelligence in IoT network for the sustainable smart city," *Sustainable Cities and Society*, vol. 63, Article ID 102364, 2020.

[24] S. Majumdar, M. M. Subhani, B. Roullier, A. Anjum, and R. Zhu, "Congestion prediction for smart sustainable cities using IoT and machine learning approaches," *Sustainable Cities and Society*, vol. 64, Article ID 102500, 2021.

[25] R. Rani, V. Kashyap, and M. Khurana, "Role of IoT-cloud ecosystem in smart cities : review and challenges," *Materials Today: Proceedings*, 2020.

[26] N. Ouerhani, N. Pazos, M. Aeberli, and M. Muller, "IoT-based dynamic street light control for smart cities use cases," in *Proceedings of the 2016 International Symposium on Networks, Computers and Communications (ISNCC)*, pp. 1–5, Yasmine Hammamet, Tunisia, May 2016.

[27] G. Merlino, D. Bruneo, F. Longo, A. Puliafito, and S. Distefano, "Software defined cities: a novel paradigm for smart cities through IoT clouds," in *Proceedings of the 2015 IEEE 12th Intl Conf on Ubiquitous Intelligence and Computing and 2015 IEEE 12th Intl Conf on Autonomic and Trusted Computing and 2015 IEEE 15th Intl Conf on Scalable Computing and Communications and Its Associated Workshops (UIC-ATC-ScalCom)*, vol. 10-14, pp. 909–916, Beijing, China, Auguest 2015.

[28] P. M. Santos, C. Queiros, S. Sargento et al., "PortoLivingLab: an IoT-based sensing platform for smart cities," *IEEE Internet of Things Journal*, vol. 5, no. 2, pp. 523–532, 2018.

[29] B. Omarov and A. Altayeva, "Towards intelligent IoT smart city platform based on OneM2M guideline: smart grid case study," in *Proceedings of the 2018 IEEE International Conference on Big Data and Smart Computing (BigComp)*, pp. 701–704, Kyoto, Japan, January 2018.

[30] O. B. Mora, R. Rivera, V. M. Larios, J. R. Beltrán-Ramírez, R. Maciel, and A. Ochoa, "A use case in cybersecurity based in blockchain to deal with the security and privacy of citizens and smart cities cyberinfrastructures," in *Proceedings of the*

2018 IEEE International Smart Cities Conference (ISC2), pp. 1–4, Kansas City, MO, USA, September 2018.

[31] M. M. Rathore, A. Paul, A. Ahmad, and S. Rho, "Urban planning and building smart cities based on the internet of things using big data analytics," *Computer Networks*, vol. 101, no. 63–80, 2016.

[32] R. Khatoun and S. Zeadally, "Smart cities," *Communications of the ACM*, vol. 59, no. 8, pp. 46–57, 2016.

[33] S. Nazir, S. Shahzad, I. Zada, and H. Khan, "Evaluation of software birthmarks using fuzzy analytic hierarchy process," in *Proceedings of the Fourth International Multi-Topic Conference*, pp. 171–175, 2015.

[34] S. Nazir, S. Shahzad, M. Nazir, and H. U. Rehman, "Evaluating security of software components using analytic network process," in *Proceedings of the 11th International Conference on Frontiers of Information Technology (FIT)*, pp. 183–188, IEEE, Islamabad, Pakistan, December 2013.

[35] S. Nazir, S. Shahzad, Z. Hussain, M. Iqbal, and A. Keerio, "Evaluating student grades using analytic network process," *Sindh University Research Journal (Science Series)*, vol. 47, no. 1, pp. 1–5, 2015.

[36] S. Nazir, S. Anwar, S. A. Khan et al., "Software component selection based on quality criteria using the analytic network process," *Abstract and Applied Analysis*, vol. 2014, Article ID 535970, 12 pages, 2014.

[37] J. Li, "Attributes based decision making for selection of requirements elicitation techniques using the analytic network process," *Mathematical Problems in Engineering*, vol. 2020, Article ID 2156023, 13 pages, 2020.

[38] X. Huang and S. Nazir, "Evaluating security of internet of medical things using the analytic network process methods," *Security and Communication Networks*, vol. 2020, Article ID 8829595, 14 pages, 2020.

[39] T. L. Saaty, "Relative measurement and its generalization in decision making why pairwise comparisons are central in mathematics for the measurement of intangible factors the analytic hierarchy/network process," *Revista de la Real Academia de Ciencias Exactas, Fisicas y Naturales. Serie A. Matematicas*, vol. 102, no. 2, pp. 251–318, 2008.

Hindawi
Mobile Information Systems
Volume 2021, Article ID 5578490, 13 pages
https://doi.org/10.1155/2021/5578490

Research Article

A Dual-Mode Medium Access Control Mechanism for UAV-Enabled Intelligent Transportation System

Muhammad Asghar Khan,[1] **Tanweer Ahmad Cheema**,[1] **Insaf Ullah**,[2] **Fazal Noor**,[3] **Sajjad Ur Rehman**,[4] **Ateeq Ur Rehman**,[5] **and Muhammad Adnan Aziz**[1]

[1]*Department of Electronic Engineering, ISRA University, Islamabad 44000, Pakistan*
[2]*Hamdard Institute of Engineering & Technology, Islamabad 44000, Pakistan*
[3]*Department of Computer Science and Information Systems, Islamic University of Madinah, Madinah 400411, Saudi Arabia*
[4]*Department of Electrical Engineering, Namal Institute, Mianwali, Pakistan*
[5]*Department of Computer Science, AWKUM Shankar Campus, Mardan, Pakistan*

Correspondence should be addressed to Muhammad Asghar Khan; khayyam2302@gmail.com

Received 14 January 2021; Revised 1 February 2021; Accepted 6 February 2021; Published 15 February 2021

Academic Editor: Muhammad Bilal

Copyright © 2021 Muhammad Asghar Khan et al. This is an open access article distributed under the Creative Commons Attribution License, which permits unrestricted use, distribution, and reproduction in any medium, provided the original work is properly cited.

With the exponential growth in technologies for the vehicular Internet of things applications and high demands for autonomous road vehicles, future transportation systems are projected to be revolutionized on a global scale. This new landscape requires a stable, flexible, and business-friendly base of connectivity, networking, and computing technology, in which Unmanned Aerial Vehicles (UAVs) can play an important role. A UAV-enabled Intelligent Transportation System (ITS) can provide a cost-effective communication solution to improve the safety and efficiency of the transportation system, particularly if the data traffic is nonhomogeneous and nonstationary. Typically, wireless is the communication medium between vehicles and UAVs in an ITS setting, which is based on the IEEE802.11p MAC protocol adopted by car manufactures. However, the IEEE 802.11p MAC protocol is modified solely for omnidirectional antennas, which restricts network coverage, delay, and throughput. In comparison, the directional antenna has greater network coverage, spatial reuse, and bandwidth. In addition, a multiaccess edge computing (MEC) facility at the backhaul link will provide ultralow latency and high bandwidth services to meet the increasingly growing demand for latency-sensitive vehicle applications such as vehicular video data analytics, autonomous driving, and intelligent navigation. Therefore, this article aims to propose a novel dual-mode MAC protocol that can work in two antenna modes, i.e., directional and omnidirectional. For modeling and simulation purposes, we use the Optimized Network Engineering Tool (OPNET) and aim to seek an evaluation with respect to throughput, media access delay, and retransmission attempts. The results obtained demonstrate the effectiveness of the proposed scheme.

1. Introduction

Technical advances are underway exponentially in the automotive market, with the focus of progress turning towards ubiquitous connectivity and fully autonomous vehicles. When independent, autonomous vehicles become connected with each other and with Vehicle-to-Everything (V2X) communications, the potential of such a transformation will be completely disclosed. Based on shared planned movements from nearby vehicles, V2X will create a collective understanding of the surrounding environment and help make more informed decisions for the vehicles. To achieve this, connected and automated vehicles require continuous access to sensory data from which vehicles can carry out advanced trajectory planning and more complicated high-speed maneuvers [1]. The vehicle can use onboard sensor information for short-term trajectory decisions, but for long-term decisions, the car requires data and information from other nearby vehicles. The sharing of sensor data is, therefore, an essential factor requiring a stable connection between vehicles that are subjected to the strict quality of service (QoS) guidelines [2, 3]. This new

paradigm of fully autonomous connected vehicles will pave the way for an Intelligent Transport System (ITS), an important part of which will be UAVs. Integrating UAVs into ITS provides enormous opportunities for new applications and services to be developed [4] as they provide on-the-fly communication facilities in a cost-effective way. In addition, due to their high mobility, autonomous operation, three-dimensional (3D) movement, and communication/processing capabilities, UAVs can play a key role in the Intelligent Transportation System (ITS). As the number of vehicles grows, the existing communication framework does not satisfy the data transmission demands, especially when there are hot spots (e.g., road intersections) during rush hours. A UAV-enabled ITS has several advantages over the traditional transportation system. Firstly, since the UAV can fly closer to vehicles compared to stationary base stations, the path loss will be much lower. Secondly, the UAV is versatile in changing the transmission control depending on the mobility of the vehicle. Thirdly, the performance of UAV-to-Vehicle connections is typically better than that of terrestrial links due to the line-of-sight (LoS) communication.

Automation of the entire transportation infrastructure cannot be done by merely automating road vehicles [5]. It is also important to automate other components of the road and end-to-end transport infrastructures, such as the field support unit, the traffic police, road surveys, and rescue teams. Figure 1 illustrates the sample network architecture of UAVs-enabled ITS. A road support team, for example, maybe supplemented or supported by a set of UAVs that may fly around an incident site and provide basic support, or at least bring back an incident survey report. In addition, UAVs that can fly over vehicles on a highway to track and record potential traffic violations may also be substituted or assisted by a traffic police officer. On the one hand, UAV-enabled ITS can provide an effective means not to implement traffic rules and help on-the-ground traffic officers only but also to provide efficient traffic information (i.e., intelligent traffic management) to road users. On the other hand, it suffers from limited onboard energy, restricted computing capability, insufficient bandwidth, and other issues that preclude UAVs from being the prevalent part of the ITS network.

IEEE 802.11p is the typical wireless MAC standard, which is an enhancement to 802.11 (the basis of devices sold as Wi-Fi) adopted by car manufacturers to support applications for Intelligent Transportation Systems (ITS) [6]. By default, the IEEE 802.11p standard has been optimized for low-delay and small-bandwidth wireless communication applications. In addition, the IEEE 802.11p is designed with omnidirectional antenna settings in mind. It assumes that all packets, i.e., RTS/CTS/DATA/ACK, are sent and received as omnidirectional signals. However, with an omnidirectional antenna, network coverage, delay, and throughput, etc., will remain limited. In comparison, directional antennas deliver several advantages over omnidirectional antennas, such as greater coverage, spatial reuse, and high bandwidth, due to the concentration of total RF energy in one direction. Nonetheless, these advantages pose some unique challenges for the MAC layer. The primary challenge with the directional antenna is the error in location estimation for high-speed UAVs and road vehicles [7, 8]. For this reason, the combination of multiple navigation systems is the central requirement for the practical solution of error reduction in the position estimation. Therefore, the UAVs must be fitted with a GPS-based Inertial Measurement Unit (IMU) device so that other UAVs can be placed accurately at any time. IMU can be rated by GPS signal and therefore, can provide position and angle at a faster rate [9].

1.1. Authors' Motivation and Contributions. Designing an appropriate MAC protocol for UAV-enabled ITS is very necessary for achieving high throughput, low latency, and fewer retransmission attempts, etc., for efficient communication. The primary objective of this MAC protocol is to overcome data packet transmission collisions, provide reduced channel access delay, and allow numerous UAVs to share a common medium efficiently with improved data transfer rate and network coverage. Therefore, in this article, we present the MAC protocol based on the IEEE 802.11p standard, which consists of two antenna modes: directional and omnidirectional. Under the 3D terrain model, network density, coverage area, routing protocols, and speed of both UAVs and ground vehicles are considered to check the performance of the proposed protocol. Some of the highlights of our research contribution in this article can be summarized as follows:

(i) We propose a dual-mode Medium Access Control (MAC) protocol. The protocol is based on the IEEE 802.11p standard, which consists of two antenna modes: directional and omnidirectional.

(ii) We assume a 3D terrain model, where each of the UAVs flies at different altitudes in order to achieve realistic results.

(iii) The proposed scheme is modeled and implemented using Optimized Network Engineering Tool (OPNET) and deployed on Intelligent Transportation System (ITS) as a case study.

(iv) We compare the proposed protocol in terms of throughput, media access delay, data dropped, and retransmission attempts to its existing counterpart, i.e., omnidirectional antenna-based MAC protocol.

(v) The findings from the comparison results demonstrated the superiority of the proposed scheme over conventional omnidirectional based MAC protocol.

1.2. Organization of the Paper. The rest of the article is structured as follows. In section 2, we address the related work. An overview of the IEEE 802.11p specification is provided in section 3. In section 4, the proposed MAC dual-mode protocol is presented. Section 5 describes the simulation environment using the OPNET tool. Section 6 includes the results and analysis followed by concluding remarks in section 7.

2. Literature Review

In the literature, very few research studies are found in the field of directional antennas focusing on the UAVs network. In 2004, Ulukan and Gürbüz [10] presented a MAC angular

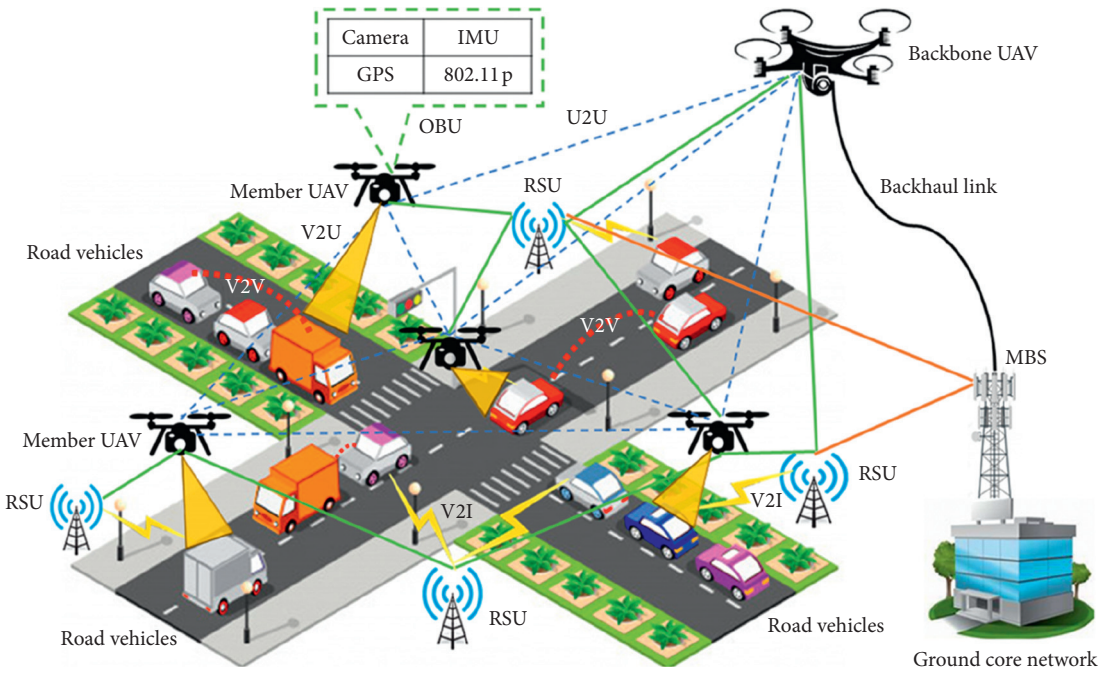

Figure 1: Sample architecture of UAV-enabled ITS.

protocol (AN-MAC) to improve the network's performance with directional beams. The proposed protocol allows stations to classify busy sectors with a location-based scheduler to prevent collisions and congestion on the network. The authors intend to check the performance analysis of AN-MAC on different topologies with an increased number of antennas per node. In [11], the authors introduced an Adaptive Medium Access Control (AMAC) protocol in which two directional antennas and two omnidirectional antennas were mounted on each UAV. It is observed that the performance of UAVs network with directional antennas in terms of bandwidth, range, and delay is comparatively better than omnidirectional antennas. However, this scheme can be further improved for transmitting and receiving packets using multiple directional antennas mounted on UAVs. Huba and Shenoy [12] presented an aerial network in which UAVs are mounted with directional antennas. The proposed approach combines scheduling and clustering with a single algorithm in the MAC layer, providing a robust and scalable solution. Temel and Bekmezci [13] researched various flight scenarios and used directional antennas to demonstrate the effect of the distance between the operating UAVs and the main beam angles. The authors have not, however, focused on improving network efficiency in terms of both data rate and latency.

Biomo et al. [14] researched the efficiency of current routing protocols using FANET directional antennas. The proposed mechanism for this scheme will result in improved performance of the network in terms of packet delivery ratio (PDR) and latency. The authors further examined the fact that the directional antenna offers a wider coverage with the same number of nodes. However, the authors used only one flow in 2D sight. In 2019, Khan et al. [15] directional antenna-based medium access control (MAC) protocol using multiple directional antennas for FANETs. The proposed scheme was modeled and implemented in the OPNET Modeler. It has been shown that major improvements can be made in terms of end-to-end delay and retransmission attempts using directionally based MAC. However, in the proposed scheme all the six antennas were active without any on/off mechanism. Finally, in 2020, the authors introduced a dual channel MAC protocol based on a directional antenna for the underwater acoustic sensor networks [16]. However, the switching time between the omnidirectional directional and directional antenna modes has been ignored, and in real-world scenarios, it cannot be ignored. To this end, in our work, the promising results have inspired us for the extended version of the same scheme, as [14, 15] adopted a similar approach for the UAVs network.

For ITS, analysis of the research works is provided using IEE 802.11p [17] for MAC and PHY layers [18–23]. Arena et al. [6] presented an overview of IEEE 802.11p, with a special emphasis on its adoption in an ITS environment. They studied both MAC and PHY layers explicitly in a dedicated short-range communication (DSRC) environment.

3. Overview of IEEE 802.11p

The IEEE 802.11p protocol has a series of specifications that are useful to allow connectivity in the vehicle environment, i.e., in the environment where sudden changes take place. The operating frequency of the 802.11p band, which is set in the DSRC, is 5.850–5.925 GHz. IEEE 802.11p uses a physical (PHY) layer based on OFDM (Orthogonal Frequency Division Multiplexing). In modulation and coding strategies with data rates from 3 to 27 Mbps, the IEEE 802.11p standard is identical to IEEE 802.11a. The basic medium access

method known as CSMA/CAA is often used for IEEE 802.11p (Carrier Sense Multiple Access with Collision Avoidance). In CSMA/CA, a node has to sense the channel before it sends a message. The node will not transmit in events if the channel is being used by another node. If the channel is detected to be idle, the nodes will only initiate their transmission and postpone the transmission until the completion of the ongoing transmission if the channel is detected to be busy. When the received power intensity of the signal is higher than the Clear Channel Assessment (CCA) threshold, the radio channel is interpreted as busy. The CCA threshold is expected to be greater than the receiver's sensitivity level, i.e., the threshold of sensing power. After the channel is observed busy, the node waits for a backoff period to eliminate collisions during contention with other nodes that have already postponed their transmission. The time of the channel is separated into synchronization intervals of a fixed period of 100 ms. It consists of intervals of equal duration, which varies between the CCH (Control Channel) and the SCH (Signaling Channel). For safety-related messaging and device control data exchange, all nodes must tune in to the CCH frequency during the CCH interval. A guard time of 4 ms is set at the beginning of each interval so that the delay in radio switching and timing inaccuracies in the systems can be taken into account.

Seven 10 MHz channels are arranged in the DSRC spectrum, in which 5 MHz is the guard band, as seen in Figure 2. Channel 178 is intended for safety-related communications only and is known as the control channel (CCH). It has the most important beacons and alarms. Both networks are used at the edge of the spectrum for future uses and specific employment, such as automated collision prevention and the use of public protection. For residual applications and routine correspondence, the remaining channels are service channels (SCH). It is also possible to merge pairs of these neighboring channels into a 20 MHz channel.

As seen in Figure 3, each layer practices various protocols in the DSRC architecture. IEEE standards1609.2, 1609.3, and 1609.4 are incorporated in the upper layers for special services, such as security services (1609.2), network services (1609.3), and channel switching (1609.4). The IEEE 802.11p is deployed for the PHY and MAC layers. The WAVE Short Message Protocol (WSMP) also operates on the network layer, but it is also acceptable to use other protocols such as IPv6.

4. Proposed Dual-Mode MAC Protocol

By default, the directional antenna in the OPNET simulator is not available on any node. Therefore, we need to design our own directional antenna, which enables users to define the representation of antenna patterns using an antenna pattern editor. The antenna pattern can be connected with a radio transmitter and/or receiver using a node editor antenna module to give the gain defined by the pattern. We implemented the standard 802.11p DCF MAC for designing the proposed protocol. Typically, the IEEE 802.11p protocol uses 10 MHz bandwidth. It operates in the frequency band of 5.9 GHz ranging from 5.850 to 5.925 GHz and adopts OFDM. It is offering fast data speeds between 3 Mbps and 27 Mbps. This protocol uses CMSA/CA, an important technique in the WLAN MAC layer with Distributed Coordination Function (DCF) as ITS performance decreases with a variety of factors such as high speed, 3D movement, regular distance changes between UAVs and road vehicles, and link quality fluctuations. Thus, the distance between connected UAVs and vehicles in the proposed scheme will not reach the transmission limit of the directional antenna. A medium access table is set up with the help of RTS/CTS messages to know the destination location information and adjacent UAVs. More information on the proposed MAC protocol can be found below.

4.1. Station Model. UAV station model is designed so that each UAV is fitted with four directional and antennas covering an area of 360. The proposed model also has mounted external GPS, IMU, and altimeter pod (radar, lidar, and others) to track and update the neighboring UAV's position, altitude, and distance. The standard 802.11p uses RTS/CTS packets to book medium-to-exchange packages.

4.2. Terrain Model. We assume a 3D terrain model, where each UAV would fly at different heights to achieve more realistic results. To achieve the desired results, each UAV is fitted with an altimeter pod (consisting of radar, lidar, and others) that retains its height relative to the terrain to which it flies. Therefore, it is evident that the geographical characteristics of the regions will affect UAV communication.

4.3. Antenna Model. The proposed scheme uses a switched-beam directional antenna with $N = 4$ separate antenna beams. All four beams can cover an area of 360° in total, as shown in Figure 4. The beamwidth of each antenna is 90°. Thus, to design the proposed mechanism as shown in Figure 5, four separate RF modules with a single MAC chip are required. We used the Friis transmission equation in the proposed system to get parameters for the antenna.

$$P_r = \frac{P_t G_t G_r \lambda^2}{(4\pi R)^2}, \tag{1}$$

$$P_r = P_t G_t G r \left(\frac{\lambda}{4\pi R}\right)^2. \tag{2}$$

In equation (2), P represents power and G denotes gain; respectively, subscript t and r stand for transmitted and received. In addition, λ is the wavelength and R is determining the range of transmission.

For omnidirectional antennas, setting the parameters in the OPNET simulator as follows will provide the transmission of 1000 meters: Pr = -95dBm, Pt = −196 dBm, Frequency = 5.885 GHz and Gr = Gt = 0 dB:

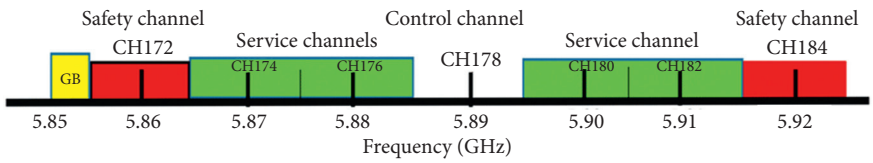

Figure 2: DSRC spectrum.

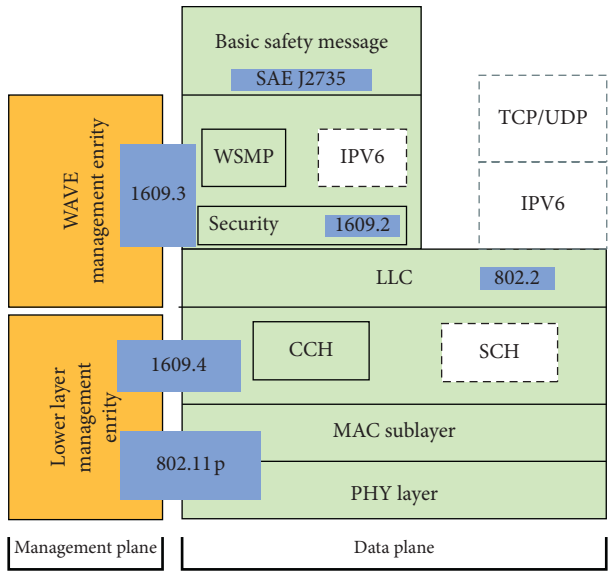

Figure 3: DSRC architecture.

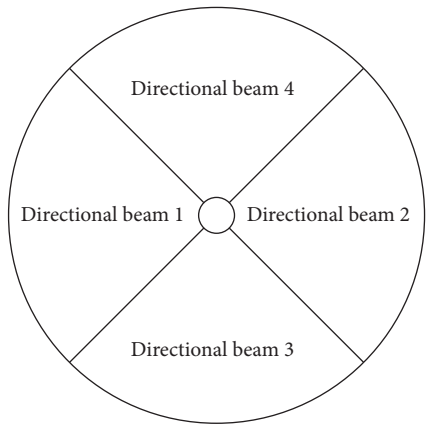

Figure 4: Beams configuration for directional and omnidirectional modes.

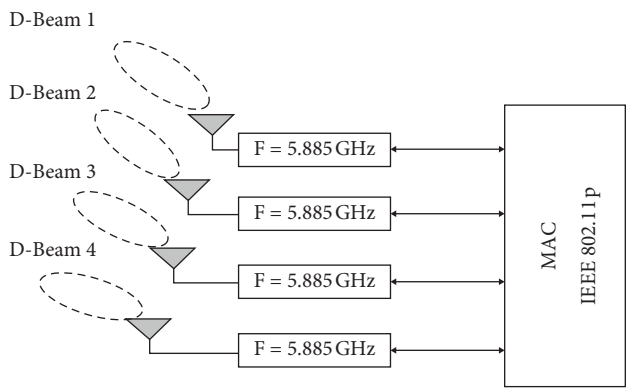

Figure 5: Single MAC chip integrated with directional and omnidirectional beams.

$$\frac{60}{360}\pi r^2 = \pi R^2,$$
$$r = R\sqrt{4} \Longrightarrow 1000\sqrt{4} \approx 2000m. \tag{3}$$

In the case of a 4-beam directional antenna, with the same transmission range, i.e., 2000 m, we will have Pt ≈ −200 dBm.

4.4. Interference Model. In a directional antenna, some power is still radiating in the side lobes, although most of the power is directed towards the central beam. This power is considered an interference among the remaining UAVs. The interference zone between directional antennas is illustrated in Figure 6. The maximum transmission range of the main lobe beam R_m, side lobe beam R_s, and guard zone R_g is defined as follows [13]:

$$R_m = \sqrt[\alpha]{P_t/P_r},$$
$$R_s = \sqrt[\alpha]{R_m + G_s}, \tag{4}$$
$$R_g = \sqrt[\alpha]{R_s G_s}.$$

P_t, P_r, and G_s are the transmitted power, received power, and side lobe gain, respectively, as mentioned in equation (4).

UAVs in the Indirect Interference Zone (IIZ) will concentrate their antennas beyond beam N. The total volume of IIZ expressed in m^3, is the sum of the conic zone linked to the receiver antenna and the sphere connected to the sidelobe gain of the receiver. The probability distribution function (PDF) is used for the deployment of K number of UAVs with their initial locations over a terrain. The volume of the spherical zone V_c and the side lobe sphere V_s is determined from equations (5) and (6). Moreover, in equations (7) and (8), the total volume of IIZ, VIIZ, and the volume of DIZ, VDIZ, are determined.

$$V_C = \frac{\theta}{2\pi}\left(\frac{4}{3}\pi R_m^3\right), \tag{5}$$

$$V_S = \left(\frac{4}{3}\pi R_s^3\right), \tag{6}$$

$$V_{IIZ} = V_C + V_Z\,\frac{\theta}{2\pi}\left(\frac{4}{3}\pi {}^3_{Rs}\right), \tag{7}$$

$$V_{DIZ} = V - V_{DIXZ}. \tag{8}$$

The total interference (I_t) and SIR experienced by all the UAVs can be measured from equations (9) and (10) as follows:

$$I_t = \frac{P_t G_s G_s}{I_t d^{\alpha}}, \tag{9}$$

$$SIR = \frac{P_t G_m G_m}{I_t d^{\alpha}}. \tag{10}$$

The maximum number of UAVs without affecting the ongoing communication in the field can be expressed as in the following equation:

$$UAV_{act} = \frac{SIR}{SIR_{th}}. \tag{11}$$

4.5. Mobility Model. In the UAV-enabled ITS, due to the agile motion of the UAVs, it is necessary to select the appropriate model of mobility to achieve maximum accuracy in the simulation results. There are many circumstances in which a group of UAVs is tasked with acting against a common point to patrol a particular area. Therefore, in the proposed scheme, we used Reference Point Group Mobility (RPGM) [24] for the simulation of a UAVs group. In the RPGM model, in order to achieve collective work, UAVs are grouped around a centralized node, called a group head (backbone UAV). The movement pattern of the reference point describes the movement of the whole group, including position, altitude, velocity, and direction. The group head follows a random viewpoint (RWP) mobility model, and the rest of the UAVs revolves around the center with their movement patterns (see Figures 7(a) and 7(b)) [25]. There are several types of mobility models, such as columns (CLMN) [25], nomadic community (NC) [25], and purse (PRS).

4.6. Protocol Operation. The proposed MAC protocol consists of two antenna modes, namely directional and omnidirectional. In the directional mode of operation, only one antenna beam will be active at a time. The beam can only be deactivated by settings its gain up to −200 dB that results in 0 linear gain. We have set an active sector gain of 7.8 dB. The entire process is well presented in [14, 26]. By comparison, in the case of omnidirectional mode, all four sectors are active with a gain of 0 dB resulting in linear gain 1. UAVs will remain in this mode if there is no RTS-CTS-Data-ACK exchange. In the proposed scheme, initially, each UAV with pending data sends an RTS frame using N beams in all directions. By default, these RTS messages are sent using a traditional CSMA/CA algorithm. All the connected UAVs that are idle or in a backoff state hear the channel omnidirectionally. When the intended UAV receives the RTS packet, it disables all other beams with the maximum power except the one receiving the signal. The UAV in question then sends a CTS packet through the maximum signal strength beam. Similarly, the transmitting UAV also selects the beam with maximum power that receives the CTS. Using the beam, it will then send data in the same direction. Also, ACK packets are sent in a directional pattern. The flowchart of the proposed dual-mode MAC protocol is illustrated in Figure 8.

5. Simulation Environment

Modeling and simulation of the proposed scheme are achieved using OPNET Modeler 14.5 [27]. OPNET consists of an antenna pattern editor where an antenna directionality is modeled and an antenna gain is set. We made changes to the IEEE 802.11a standard due to the unavailability of IEEE 802.11p in the OPNET modeler as shown in Figure 9. We

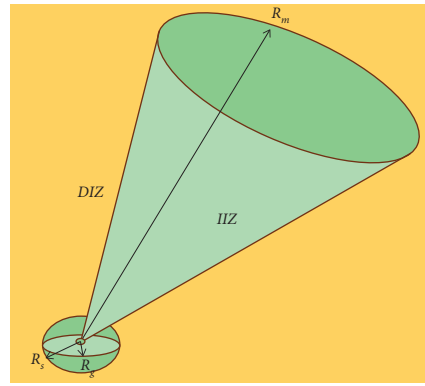

Figure 6: The maximum transmission ranges of DIZ and IIZ zones.

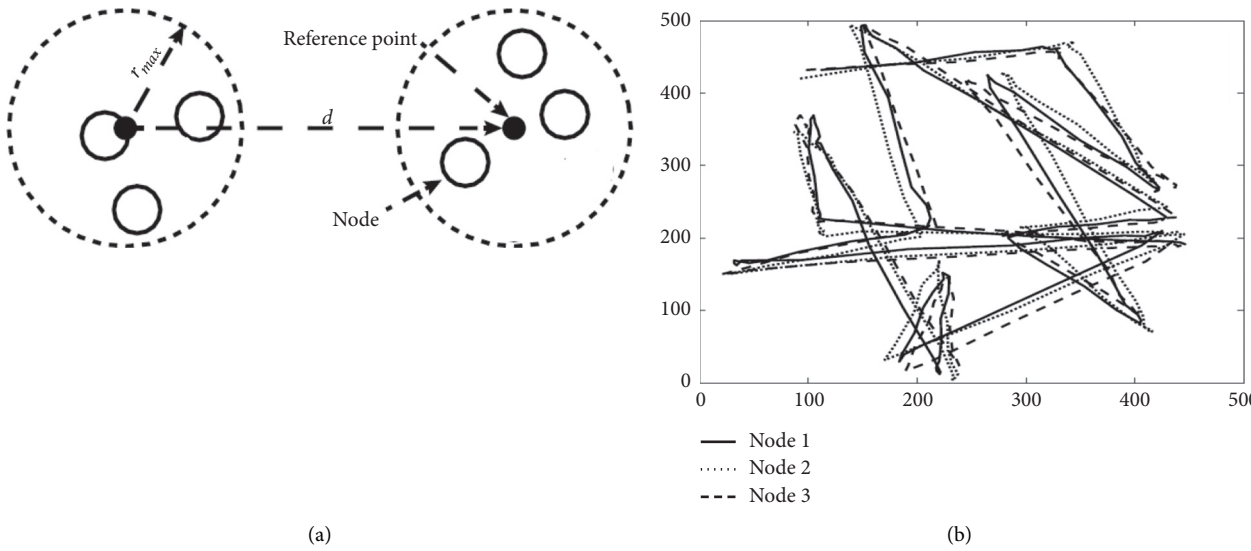

Figure 7: Mobility models: (a) Nomadic community (NC) with three UAVs. (b) Mobility pattern of one group (i.e., three UAVs) using RPGM.

also made modifications in the MANET node model according to which the proposed MAC protocol for both directional and omnidirectional antennas can be implemented. As shown from Figures 10 and 11, the UAV and vehicle node model consist of three main parts: the lower part (physical layer), the middle part (data link layer), and the upper part (upper layer). The transmitter, receiver, and antenna module are part of the physical layer. Wireless connectivity between the associated nodes is the duty of these modules. The middle part, i.e., the data link layer, consists of the MAC module using the IEEE 802.11p standard. By default, it is primarily designed to work with omnidirectional antennas. This module is designed to run collectively to support the proposed scheme. The TRAF SRC, UDP, MANET RTE MGR, DHCP, IP ENCAP, ARP, IP, and CPU modules are included in the upper layers, i.e., the top part.

The directional antenna node model provides all of the compulsory interfaces that are set in each antenna for working with four separate beams. In the proposed model, each UAV has a 60° beam width that enables them to cover an area of 360° with the help of four directional antennas. For all beams, the UAV will sense the signal intensity and mark the beam with maximum signal strength for data communication. The UAV can also block all other beams except the one with maximum signal strength. We choose all the suitable parameters. For more detailed information, further parameters are summarized in Table 1.

When the UAVs start flying, along with height sensors, IMU, GPS units, and other embedded equipment such as flight controllers, the network formation starts. We presume that UAVs are well aware of the zone ID, position, altitude, and velocity of their neighbors when network creation begins. The performance of the proposed MAC protocol is evaluated on the basis of throughput, media access delay, data dropped, and retransmission attempts.

6. Results and Discussion

Figures 12–14 show the performance of the proposed dual-mode MAC protocol with the default omnidirectional based IEEE 802.11p protocol in terms of throughput, media

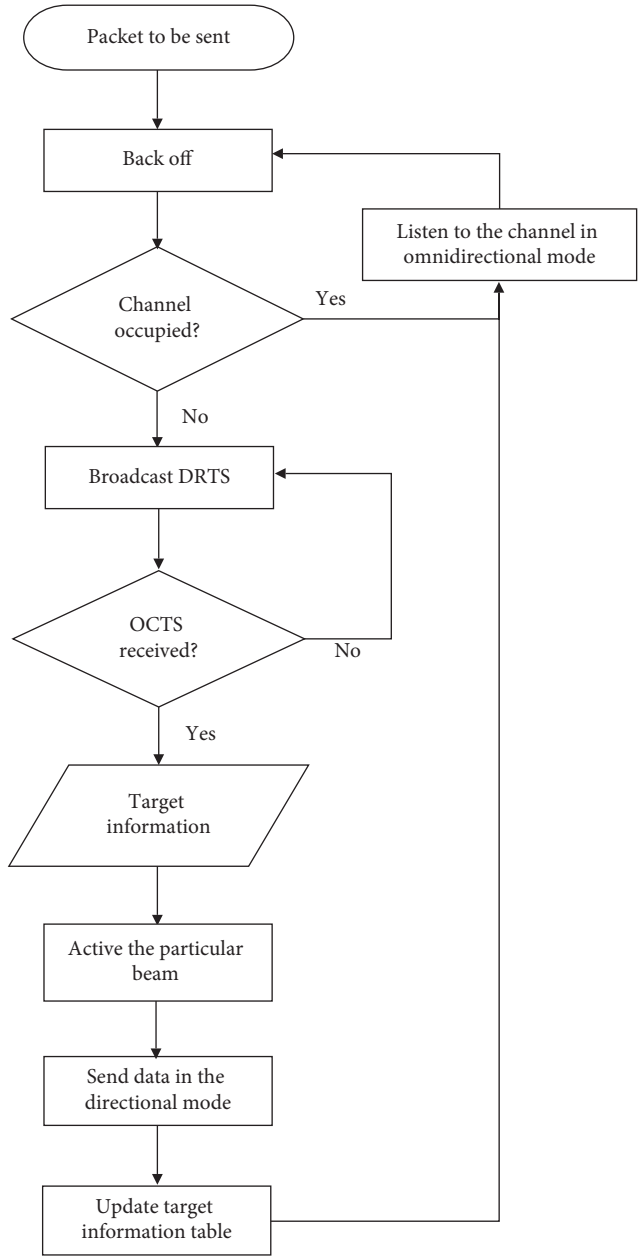

Figure 8: Flowchart of the proposed dual-mode MAC protocol (UAV side).

access delay, and retransmission attempts, respectively. In the graphs, the x-axis specifies simulation time and the y-axis stipulates the throughput in bits, media access delay in seconds, data dropped in bits, and retransmission attempts in packets, respectively. The proposed scheme is tested under the area of 2000 m × 2000 m composed of 60 nodes. The simulation using the OPNET simulator is performed for two different scenarios, i.e., proposed dual-mode MAC protocol with and default IEEE 802.11p, respectively, under the RPGM mobility model. We chose the RPGM model because, under the RPGM model, the movement of UAVs is controlled by a reference point, which is the group head in a particular zone. That way, the network stays fully connected all the time. The results of the simulation authenticate that the proposed dual-mode MAC protocol meets the desired QoS requirements. That is, the use of directional antenna in terms of throughput, media access delay, data dropped, and retransmission attempts provides better performance than that of the default MAC protocol using omnidirectional antennas. Using an omnidirectional antenna, the distance between the nodes increases and network performance deteriorates. For this purpose, each UAV in the same Basic Service Set (BSS) assumes that other UAVs will terminate communication before transmitting frames if the MAC protocol is based on the use of an omnidirectional antenna. Each UAV that is available in the same BSS must, therefore, wait until the other UAV completes its transmission by the same protocol. In comparison, the proposed dual-mode MAC protocol, which uses directional antennas, allows each

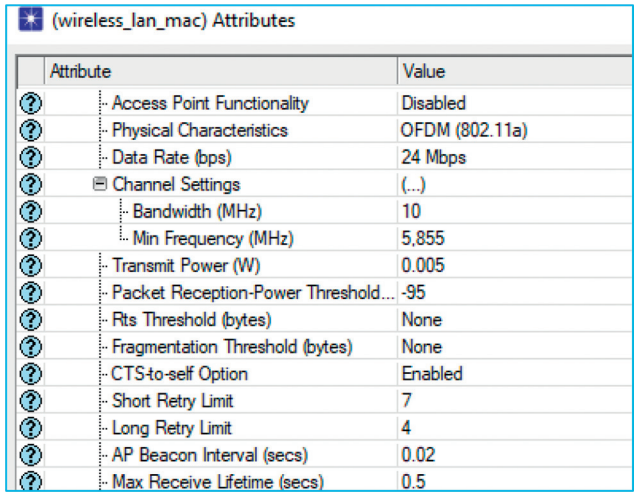

Figure 9: Setting parameters for IEEE 802.11p applied to the nodes in OPNET.

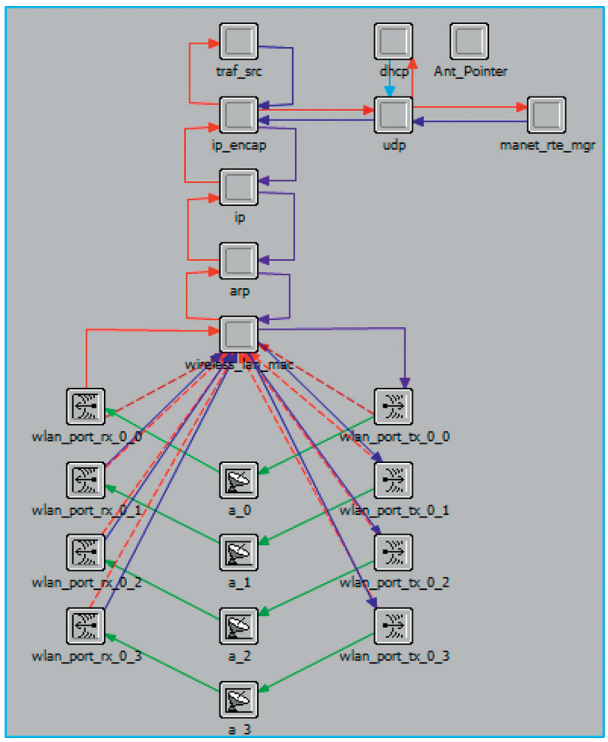

Figure 10: Designing of node model for UAV in OPNET.

UAV to concurrently use the same channel for transmitting data with other UAVs over the same BSS. Moreover, the proposed scheme would require retransmission of each UAV against any transmission that fails. They will continue to transmit until the receiving UAV sent an ACK frame or up to the maximum retransmission limit. Therefore, the

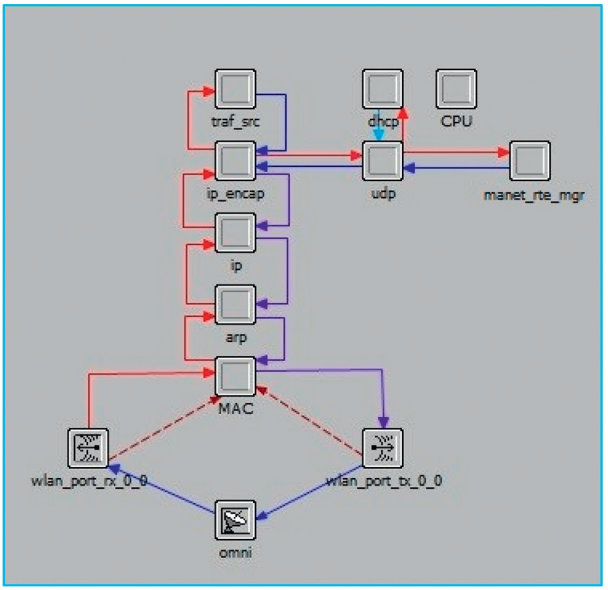

Figure 11: Node model for vehicle in OPNET.

Table 1: Simulation parameters.

Parameter	Value
Dimensions	2000 m × 2000 m
Number of UAVs	30
Number of vehicles	30
Mobility model	Random point group mobility (RPGM)
Frequency	5.885 GHz
Application	Simple source
Packet interval	Exponential (1) sec
Packet size	1024 byte
Simulation time	1800 sec
Road vehicles	Mobile
UAVs type	Mobile
UAVs altitude	25 m
Speed of UAVs	50 m/s
Speed of vehicles	30 m/s
CTS-to-self option	Enabled

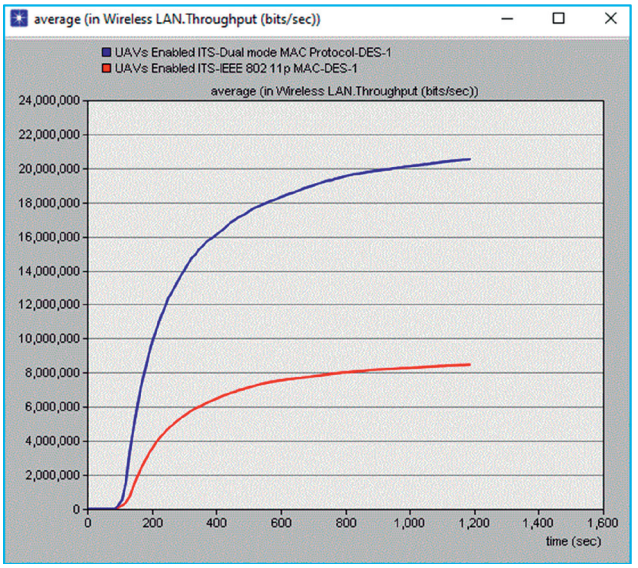

Figure 12: Throughput (in bits/sec).

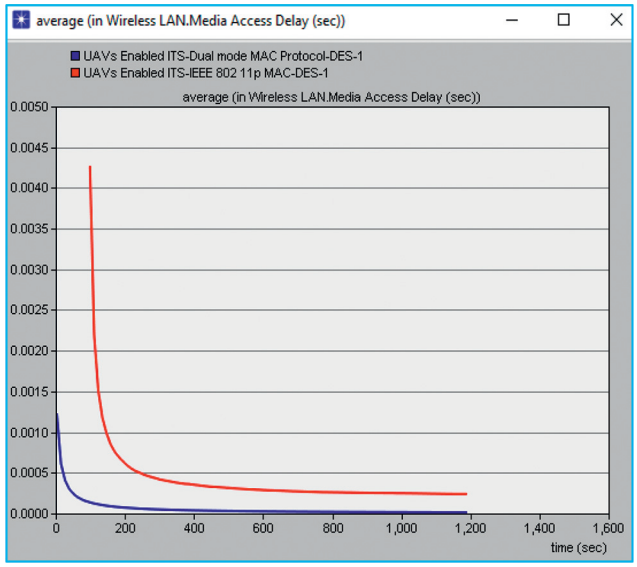

Figure 13: Media access delay (in sec).

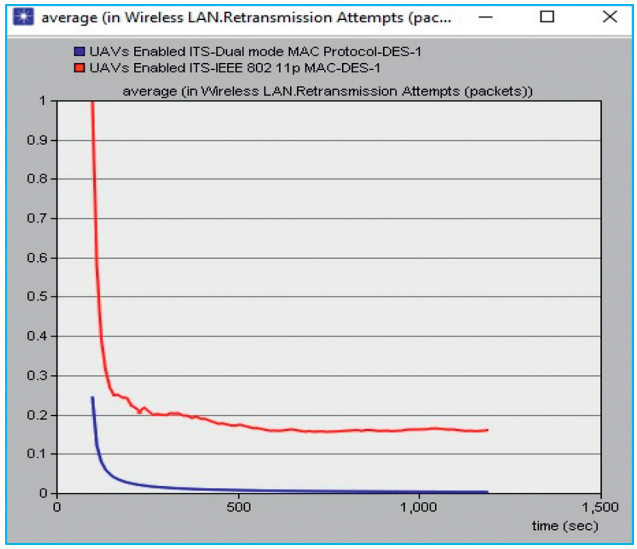

Figure 14: Retransmission attempts (in packets).

results show that the proposed dual-mode MAC has a better performance than that of default IEEE 802.11p in all three evaluation metrics.

7. Conclusions

In this article, a dual-mode Medium Access Control (MAC) protocol is proposed, which is based on the IEEE 802.11p standard. It consists of two antenna modes: directional and omnidirectional. The proposed MAC mechanism integrates the antenna's directivity with CSMA and SDMA, allowing each UAV to share bandwidth simultaneously with other UAVs and road vehicles in the same BSS becomes fair. Moreover, the proposed scheme overcomes the unique challenges associated with a MAC protocol based on directional antennas. The proposed scheme is modeled and implemented using Optimized Network Engineering Tool (OPNET) and deployed on Intelligent Transportation System (ITS) as a case study. The simulation results in terms of the throughput, media access delay, data dropped, and

retransmission attempts confirm that the proposed scheme is better than the default IEEE 802.11p omnidirectional antenna-based MAC protocol.

Data Availability

All the data generated or analyzed during this study are included in this article.

Conflicts of Interest

The authors declare no conflicts of interest with respect to the research, authorship, and/or publication of this article.

References

[1] I. Mavromatis, A. Tassi, R. J. Piechocki, and A. Nix, "Efficient v2v communication scheme for 5 g mmwave hyper-connected cars," in *Proceedings of the IEEE International Conference on Communications*, Kansas City, MO, USA, May 2018.

[2] I. Chatzigeorgiou and A. Tassi, "Decoding delay performance of random linear network coding for broadcast," *IEEE Transactions on Vehicular Technology*, vol. 66, no. 8, pp. 7050–7060, 2017.

[3] I. Tassi, I. Ahmad, E. Ahmed, A. Gani, M. Imran, and N. Guizani, "Overcoming the key challenges to establishing vehicular communication: is sdn the answer?" *IEEE Communications Magazine*, vol. 55, no. 7, pp. 128–134, 2017.

[4] H. Menouar, I. Guvenc, K. Akkaya, A. S. Uluagac, A. Kadri, and A. Tuncer, "UAV-enabled intelligent transportation systems for the smart city: applications and challenges," *IEEE Communications Magazine*, vol. 55, no. 3, pp. 22–28, 2017.

[5] M. Zhu, X.-Y. Liu, and X. Wang, "Deep reinforcement learning for unmanned aerial vehicle-assisted vehicular networks," 2019, https://arxiv.org/abs/1906.05015.

[6] F. Arena, G. Pau, and A. Severino, "A review on IEEE 802.11p for intelligent transportation systems," *Journal of Sensor and Actuator Networks*, vol. 9, no. 2, p. 22, 2020.

[7] G. Choudhary, V. Sharma, and I. You, "Sustainable and secure trajectories for the military Internet of drones (IoD) through an efficient medium access control (MAC) protocol," *Computers & Electrical Engineering*, vol. 74, pp. 59–73, 2019.

[8] S. Vashisht, S. Jain, and G. S. Aujla, "MAC protocols for unmanned aerial vehicle ecosystems: review and challenges," *Computer Communications*, vol. 160, pp. 443–463, 2020.

[9] D. Jung and P. Tsiotras, "Inertial attitude and position reference system development for a small UAV," in *Proceedings of the 26th AIAA Aeroacoustics Conference*, pp. 1–15, Rohnert Park, CA, USA, May 2007.

[10] E. Ulukan and O. Gurbuz, "Using switched beam smart antennas in wireless ad hoc networks with angular MAC protocol," in *Proceedings of the IEEE 12th Signal Processing and Communications Applications Conference*, pp. 1–8, Bodrum, Turkey, April 2004.

[11] A. I. Alshbatat and L. Dong, "Adaptive MAC protocol for UAV communication networks using directional antennas," in *Proceedings of the 2010 International Conference on Networking, Sensing and Control (ICNSC)*, pp. 598–603, Chicago, IL, USA, November 2010.

[12] W. Huba and N. Shenoy, "Airborne surveillance networks with directional antennas," in *Proceedings 2011 Third International Conference on Communication Systems and Networks (COMSNETS 2011)*, pp. 1–7, St. Louis, MO, USA, January 2012.

[13] S. Temel and I. Bekmezci, "Scalability analysis of flying ad hoc networks (FANETs): a directional antenna approach," in *Proceedings of the 2014 IEEE International Black Sea Conference on Communications and Networking (BlackSeaCom)*, pp. 185–187, Odessa, Ukraine, May 2014.

[14] J.-D. M. M. Biomo, T. Kunz, and M. St-Hilaire, "Directional antennas in FANETs: a performance analysis of routing protocols," in *Proceedings of the 2017 International Conference on Selected Topics in Mobile and Wireless Networking (MoWNeT)*, pp. 1–8, Avignon, France, November 2017.

[15] M. A. Khan, I. M. Qureshi, I. U. Khan, A. Nasim, U. Javed et al., "On the performance of flying ad-hoc networks (FANETs) with directional antennas," in *Proceedings of the 2018 5th International Multi-Topic ICT Conference (IMTIC)*, pp. 1–8, Jamshoro, Pakistan, April 2018.

[16] J. Yang, G. Qiao, Q. Hu, J. Zhang, and G. Du, "A dual channel medium access control (MAC) protocol for underwater acoustic sensor networks based on directional antenna," *Symmetry*, vol. 12, no. 6, pp. 1–18, 2020.

[17] IEEE, *IEEE Standard for Information Technology–Local and Metropolitan Area Networks–specific Requirements–Part Wireless LAN Medium Access Control (MAC) and Physical Layer (PHY) Specifications Amendment 6: Wireless Access in Vehicular Environments; IEEE Std 802.11p-2010 (Amendment to IEEE Std 802.11-2007 as Amended by IEEE Std 802.11k-2008, IEEE Std 802.11r-2008, IEEE Std 802.11y-2008, IEEE Std 802.11n-2009, and IEEE Std 802.11w-2009)*, IEEE, Piscataway, NJ, USA, 2010.

[18] G. Cecchini, A. Bazzi, B. Masini, and A. Zanella, "Performance comparison between IEEE 802.11p and LTE-V2V in-coverage and out-of-coverage for cooperative awareness," in *Proceedings of the 2017 IEEE Vehicular Networking Conference (VNC)*, pp. 109–114, Torino, Italy, November 2017.

[19] Y. Harkat, A. Amrouche, E.-S. Lamini, and M. T. Kechadi, "Modeling and performance analysis of the IEEE 802.11p EDCA mechanism for VANET under saturation traffic conditions and error-prone channel," *AEU-International Journal of Electronics and Communications*, vol. 101, pp. 33–43, 2019.

[20] S. Cao and V. C. S. Lee, "An accurate and complete performance modeling of the IEEE 802.11p MAC sublayer for VANET," *Computer Communications*, vol. 149, pp. 107–120, 2020.

[21] R. Ramanathan, "An Empirical study on MAC layer in IEEE 802.11p/WAVE based Vehicular Ad hoc Networks," *Procedia Computer Science*, vol. 143, pp. 720–727, 2018.

[22] S. Chen, W. Nai, D. Dong, W. Zheng, and W. Jing, "Key indices analysis of IEEE 802.11p based vehicle to infrastructure system in highway environment," *Procedia-Social and Behavioral Sciences*, vol. 96, pp. 188–195, 2013.

[23] A. Bazzi, B. M. Masini, A. Zanella, and I. Thibault, "On the performance of IEEE 802.11p and LTE-V2V for the cooperative awareness of connected vehicles," *IEEE Transactions on Vehicular Technology*, vol. 66, no. 11, pp. 10419–10432, 2017.

[24] H. Hong, M. Gerla, G. Pei, and C.-C. Chiang, "A group mobility model for ad hoc wireless network," in *Proceedings of the 2nd ACM international workshop on Modeling, analysis and simulation of wireless and mobile systems-MSWiM*, pp. 53–60, Seattle, WA, USA, October 1999.

[25] A. Guillen-Perez and M. D. Cano, "Flying ad hoc networks: a new domain for network communications," *Sensors*, vol. 18, no. 10, pp. 1–23, 2018.
[26] G. Boggia, P. Camarda, C. Cormio, and L. A. Grieco, "A BIBD based MAC protocol for wireless ad hoc networks with directional antennas," in *Proceedings of the 2008 6th International Symposium on Communication Systems, Networks and Digital Signal Processing*, pp. 25–29, Poznan, Poland, February 2008.
[27] OPNET simulator. https://www.riverbed.com/sg/products/steelcentral/opnet.html 2020.

Hindawi
Mobile Information Systems
Volume 2021, Article ID 6699420, 8 pages
https://doi.org/10.1155/2021/6699420

Research Article

Innovative Marketing Framework for Enterprises Using Edge-Enabled Data Analysis

Guangming Wang[1] **and Yifeng Wang**[2]

[1]*School of Politics and Public Administration, Zhengzhou University, Zhengzhou 450001, China*
[2]*School of Economics & Management, Xidian University, Xi'an 710126, China*

Correspondence should be addressed to Guangming Wang; zzdxwgm@zzu.edu.cn

Received 16 December 2020; Revised 2 January 2021; Accepted 22 January 2021; Published 8 February 2021

Academic Editor: Muhammad Babar

Copyright © 2021 Guangming Wang and Yifeng Wang. This is an open access article distributed under the Creative Commons Attribution License, which permits unrestricted use, distribution, and reproduction in any medium, provided the original work is properly cited.

An effective marketing strategy has become a challenging task with the development of the social economy for the reform and innovation of many domestic and foreign enterprises. The idea of edge computing is also gaining prominence and is broadly recognized. Edge-enabled solutions provide computing, analysis, storage, and control nearer to the edge of the network. The existing literature highlights the concepts of social media marketing and evaluates the advantages of social media for communication between individuals and companies. However, there is a lack of an effective marketing strategy for enterprises. This article proposes an innovative marketing framework for enterprises using data analysis and wireless networks. The proposed framework is composed of two different modules. Initially, a corporate innovation and marketing framework module is established through edge computing to carry out a wireless transmission of relevant data and information at the edges of the network. Later, the enterprise marketing resource optimization module is constructed based on the particle swarm algorithm. The proposed framework performs efficient calculation and storage using a resource optimization module. The feasibility and effectiveness of the proposed framework are verified using the analysis of the actual case test results. This proposed framework can effectively improve the innovation efficiency level of existing enterprises and the optimization of marketing management resources.

1. Introduction

Entering the new era of social development, an effective marketing strategy has become a challenging task. The enterprises face development challenges to adapt to high-quality development and an ever-changing market economy. Enterprises should transform from manufacturing to brand development goals, actively promote industrial upgrading and transformation, and develop toward the goal of high quality, excellent structure, stable growth, and innovation [1–3]. This requires strengthening product quality and brand building projects. To comply with national policy requirements and adapt to the pressure of market competition, various enterprises have responded and deeply analyzed the current internal status of enterprises and the external business environment [4]. By organizing and participating in various development forums under the high-quality perspective, enterprises seek high-quality development strategies with product services, brand building, marketing strategies, organizational structures, and other factor-driven methods [5].

With the rise of wireless networks, the idea of edge computing is also gaining prominence and is broadly recognized. Edge-enabled solutions provide computing, analysis, storage, and control nearer to the edge of the network to resolve the issues of scalability and latency. Edge computing offloading technology uses computing-intensive and delay-sensitive computing that is difficult to handle by mobile devices. The migration of tasks to the servers surrounding the mobile device not only improves the processing capacity of the mobile device but also ensures the energy rate of the device. Since the implementation of the reform and opening

policy, the social and economic construction has adhered to the principles of internal reform and opening to the outside world. It also adheres to the comprehensive deepening of reforms and adheres to the combination of importing and going out. While promoting the rapid development of the enterprise industry, it also forces the enterprises to adjust their development strategies in an all-round way to deal with the impact of globalization and to build a high-quality enterprise development layout with efficient brand marketing strategies [6, 7]. Marketing theory started relatively early abroad, and the theory is more advanced. In 1955, Levy and Gardner first proposed brand theory [8]. In 1956, American marketing master Philip Kotler created the famous STP analysis model [9]. The 4P marketing concept was put forward by E. Jerome McCarthy in 1960. This theoretical significance made the focus of brand marketing gradually shift from the product itself to the needs and desires of consumers [10]. H. Weihrich created the SWOT (strength, weakness, opportunity, and threats) model construction method to find the best marketing strategy through a comprehensive analysis of the company. Robert F. Lauterborn put forward the 4C marketing concept, an in-depth analysis of the brand's influence on winning consumers [11].

With the advent of the Internet era, new media has changed the way of brand development, network marketing has become a new form of sales, and related theoretical research has also been developed rapidly. Stuart Dillov conducted high-level research on brand building and brand communication and published "How to Create a Brand" to provide a reference for business management [5]. Duane. E. K proposed that the brand marketing strategy consists of five steps, namely, market research, brand reputation establishment, brand development planning, brand culture promotion, and product advantages [5]. Tybout. A. M's research concluded that a brand is an identification of products and services, and a brand can be associated with specific products and the unique value of the brand itself [12].

There are certain limitations in the use and practical application of data in the context of a wireless network. The existing literature highlights the concepts of social media marketing and evaluates the advantages of social media for communication between individuals and companies. However, there is a lack of an effective marketing strategy for enterprises. This paper develops a type of enterprise innovative marketing architecture based on data analysis and wireless networks [13, 14]. The existing enterprise innovation and marketing technology is analyzed and compared with the current wireless network and data analysis techniques in the actual enterprise innovation and marketing problems. We have discussed and designed the architecture scheme of wireless network equipment and data analysis technology and related communication methods. We establish a corporate innovation and marketing framework through wireless networks and carry out a wireless transmission of relevant data and information. Based on the particle swarm algorithm, the enterprise marketing resource optimization model is constructed. The proposed model effectively improves the efficiency level of existing enterprise innovation and marketing management resource optimization. It adapts the enterprise to high-quality development and changing market economy.

2. Background and Literature Review

This section provides the background concerning the use of edge computing technologies in enterprise communication and marketing management.

2.1. Mobile Edge Computing. Mobile edge computing (MEC) provides the possibility to overcome the challenges of the traditional computing model for mobile devices with insufficient computing power and energy storage. Edge computing offloading technology uses computing-intensive and delay-sensitive computing that is difficult to handle by mobile devices. The migration of tasks to the servers surrounding the mobile device not only improves the processing capacity of the mobile device but also ensures the energy rate of the device. The server can be a single network element, or it can integrate its functions into a large node [15, 16].

This kind of architecture scheme is conducive for the server to obtain relevant information in the coverage area through the base station, but there are billing and security issues. Trust evaluation is an effective and lightweight method to deal with malicious node attacks inside nodes. Aiming at the problem of internal malicious attacks on nodes, we propose a multidimensional trust evaluation method to comprehensively evaluate the trust value of nodes. In the node trust evaluation mechanism, the most important link is to collect and use node index information for evaluation. The collected trust index data can be used in the trust formula to calculate the trust value. Commonly used trust indicators in wireless sensor networks include node energy remaining, the number of received data packets, interactive information between nodes, and so on. This paper comprehensively utilizes different indicators of nodes, divides the evaluation of node trust value into direct trust and indirect trust, and determines the method of node trust evaluation according to the environmental location of the node in the network [17].

2.2. Wireless Network. Wireless mobile communication technology has developed rapidly from the second generation (2G) and third-generation (3G) technology to the current fifth-generation technology. Cellular mobile communication technology has undergone many innovations, and the corresponding number of mobile users and smart terminals explosive growth has also taken place [18]. With the continuous advancement of science and technology, mobile users have higher and higher requirements for communication services. More vertical fields such as autonomous driving demand for low latency and the demand for high mobility on high-speed trains put forward higher requirements on wireless networks. The enterprise marketing and innovation architecture design diagram is shown in Figure 1.

More and more new technologies are proposed to meet the needs of users, such as MIMO (multiple-input multiple-

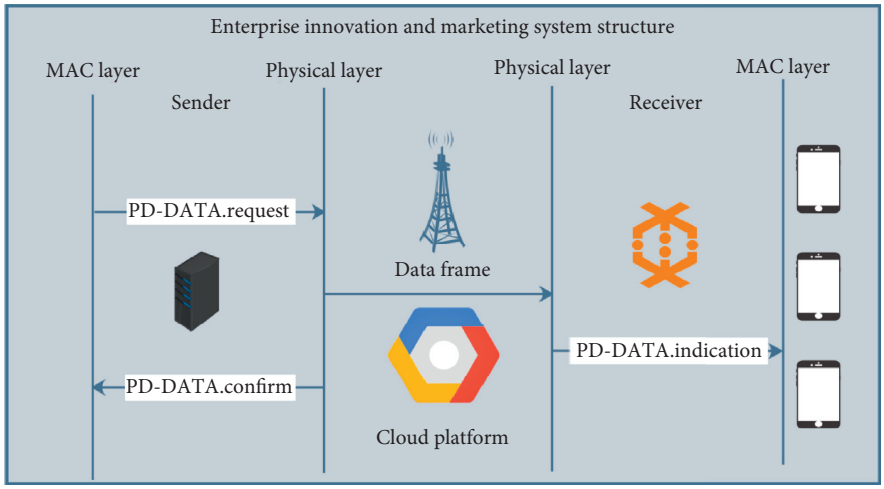

Figure 1: Enterprise marketing architecture.

output), network slicing, ultra-dense cells, mobile edge computing (mobile edge computing, MEC), and other new technologies are in communication technological innovations to meet the needs of future networks for greater throughput and lower latency [19]. Sensor nodes have data fusion capabilities in wireless sensor networks. Due to a large number of sensor nodes, many nodes will collect data of the same type. Therefore, it is usually required that some of the nodes have data fusion capabilities, which can fuse data collected from multiple sensor nodes and then send them to the information processing center. Data fusion can reduce redundant data, which can reduce energy consumption during transmission and extend network life [20].

2.3. Enterprise Innovation and Marketing Management. Marketing strategy management is the core link of the consulting and training industry in the company's operation and management. Marketing is the direction indicator that guides the development of enterprises and determines the success or failure of enterprise operations [21]. How to improve the market competitiveness of an enterprise and achieve healthy and sustainable development requires the management of the enterprise to brainstorm and combine the status quo to find a marketing strategy suitable for the development of the enterprise. A company faces changes in the industry during the development process, and changes in customer training needs are discussed. The company's existing marketing strategy can no longer adapt to the current business environment [22]. Through research and analysis of various problems and challenges that have emerged, combined with the company's current development stage and its advantages, it proposes market positioning and strategic combination plans to help companies solve the current development dilemmas.

Porter's five forces include the competitive ability of current competitors, the ability of potential competitors to enter, the substitute ability of substitutes, the bargaining power of suppliers, and the bargaining power of buyers [23, 24]. The article is used to analyze the industry market environment facing. Due to the scientificalization of corporate marketing strategies and the emergence of many manufacturers, brand marketing has gradually been regarded as one of the best ways to promote the high-quality development of enterprises. There are also more research and analysis on this. Researchers believe that brand marketing strategies include product innovation, price positioning, channel management, and promotion policies, ensuring that the implementation of marketing strategies needs to be refined to brand image promotion and maintenance, and they have given inspiration and suggestions for crisis management.

3. Proposed Innovative Marketing Framework for Enterprises

The proposed framework is composed of two different modules. Initially, a corporate innovation and marketing framework module is established through edge computing to carry out a wireless transmission of relevant data and information at the edges of the network. Later, the enterprise marketing resource optimization module is constructed based on the particle swarm algorithm.

3.1. Enterprise Innovation and Marketing Architecture. The proposed innovation and marketing architecture is based on a wireless network and edge computing. The network is composed of several edges. Currently, companies are pursuing high-quality and long-term development, and brand marketing strategies must fully adapt to changes in the market environment. For modern enterprises, being in line with globalization and keeping up with big data can establish credibility with high-quality brand images and win consumers' praise with high-quality brand services [25, 26]. Such market requirements are equally strict for enterprises. At the same time, the development of the enterprise industry fluctuates greatly, and there are many influencing factors. The international and domestic markets of enterprises are still bad. A schematic diagram of enterprise innovation and marketing management data analysis process is shown in Figure 2.

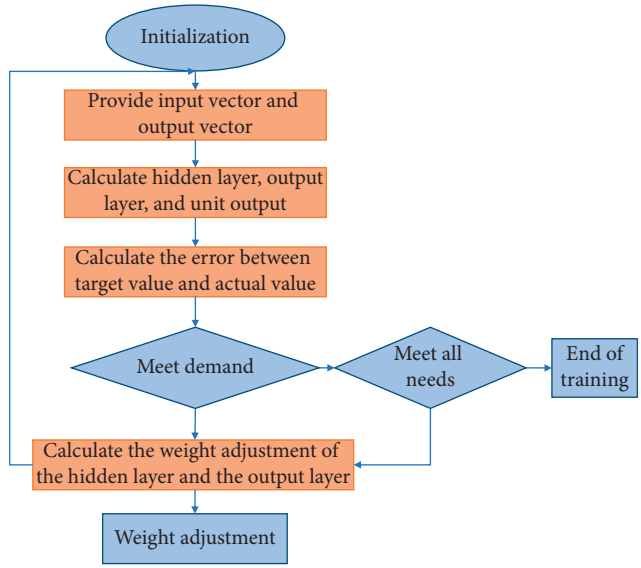

Figure 2: Data analysis process of the proposed framework.

The goal of shaping the high-quality development of an enterprise is to improve the quality of products, especially when the enterprise is seeking high-quality development. High-quality development must emancipate the mind, keep up with the forefront of science and technology, improve the company's target market positioning, and focus on creating quality products and star projects. Enterprises enter the high-end market through high-quality development. Product quality represents brand competitiveness. Without quality assurance, there will be no brand image and no brand competitiveness [27]. The market is cruel. Many small- and medium-sized enterprises are facing bankruptcy. It is high-quality products that customers choose in the market. The creation of high-quality projects is also the basis for the survival of the corporate brand.

3.2. Enterprise Innovation and Marketing Optimization. The proposed optimization module is based on data analysis. Researchers believe that brand marketing strategies include product innovation, price positioning, channel management, and promotion policies, ensuring that the implementation of marketing strategies needs to be refined to brand image promotion and maintenance, and they have given inspiration and suggestions for crisis management. To this end, we will research enterprise innovation and marketing optimization based on data analysis [28]. This kind of architecture scheme is conducive for the server to obtain relevant information in the coverage area through the base station, but there are billing and security issues. Trust evaluation is an effective and lightweight method to deal with malicious node attacks inside nodes. Aiming at the problem of internal malicious attacks on nodes, we propose a multidimensional trust evaluation method to comprehensively evaluate the trust value of nodes.

The particle swarm algorithm comes from the swarm intelligence embodied in the foraging process of fish or birds. In the process of foraging for food, a school of fish or birds uses a one-way flow of information and relies on the judgment of the group to correct the route to find the target [29, 30].

$$\begin{aligned} X \Theta X' &= \{x \mid x \in X \cup X' - X \cap X'\}, \\ \tilde{P}_2 &= s \cdot P_2 \cdot R + L. \end{aligned} \tag{1}$$

Among them, the individual in the group is not intelligent, and the correction of the target direction only depends on the best direction of itself and the group, and the entire group depends on the information flow of all the monomers to have the intelligent characteristic of being able to judge the position correctly [31, 32].

$$\begin{aligned} Pr[A(X) \in \hat{D}] &\leqq e^{[X, X']} Pr\left[A(X') \in \hat{D}\right], \\ E(P_{k1}, P_{k2}) &= \left\| P_{k1} - (s \cdot P_{k1} \cdot R + L) \right\|. \end{aligned} \tag{2}$$

In order to improve the search ability of the algorithm, a particle swarm algorithm with weight coefficients is adopted [33, 34].

$$\begin{aligned} v_{ij}^{e+1} &= W + V_{IJ}^{e} + C_1 * R_1 * \left(pBest_{ij} - P_{ij}^{e}\right) \\ &\quad + C_2 * R_2 * \left(gBest_{ij} - P_{ij}^{e}\right), \\ \Delta P &= P_1(I) - P_1(J). \end{aligned} \tag{3}$$

According to the above analysis, when the initial particle number of the particle swarm algorithm reaches 20, the accuracy and efficiency of the algorithm reach the best state, and the registration correction problem when the information in the image is lacking can be solved [35, 36].

$$W = W_{\max} - \left(W_{/\max} - W_{\min}\right) \frac{g}{G}. \tag{4}$$

It is concluded that 20 can be used as the upper limit of the parameter adjustment of the initial particle number of the algorithm, and the algorithm dynamically adjusts the initial particle number under this upper limit [37, 38]. When

the number of particles is less than 10, the average maximum mutual information drop rate obtained by the algorithm is accelerated, and the maximum mutual information value drops by an order of magnitude and does not meet the actual registration accuracy required. 10 is used as the lower limit of the initial particle number parameter adjustment [39, 40].

$$s = \frac{tr\left(P_{K1}^{T} \cdot P_{k2} \cdot R\right)}{tr\left(P_{K2}^{T} \cdot P_{k2}\right)}. \quad (5)$$

When the number of particles reaches 15, the average maximum mutual information basically meets the requirements of the actual problem on the efficiency of the algorithm, and 15 can be used as a reference value for the dynamic adjustment of the initial particle number [41, 42].

4. A Case Study: Analyses of Proposed Optimization

4.1. Data Source and Test Environment. In this section, we set up an example scenario, using a cloud server as the cloud service layer and 4 laptops as edge servers to collect the original video of the camera. The server is configured with Intel Xeon CPU and equipped with 8GB memory [43]. The goal of shaping the high-quality development of an enterprise is to improve the quality of products, especially when the enterprise is seeking high-quality development [44]. High-quality development must emancipate the mind, keep up with the forefront of science and technology, improve the company's target market positioning, and focus on creating quality products and star projects. Enterprises enter the high-end market through high-quality development [45, 46]. The comparison of enterprise innovation and marketing management structure rate under different ρ values (SNR = 10 dB) is shown in Figure 3.

The edge server is configured with Intel Core i7-6200U and has NVIDIA GeForce 940MX graphics card. At the same time, the communication bandwidth rate transmitted to the cloud service layer is limited to 1 MB/s. In order to evaluate the performance of the proposed algorithm, a series of simulation experiments are carried out.

4.2. Comparison of Enterprise Innovation and Marketing Network Speed. In the simulation, consider a mobile social network consisting of 5 base stations and 15 D2D transmitters [27]. Assuming that there are a total of 10 types of content distributed in the network, the cache status of each content follows the Markov model, the content popularity follows the distribution, and the morphological parameter is 1.5. In the simulation, the probability of staying in the same state in the buffer state transition probability matrix is set to 0.6, and the transition probability from one state to another state is set to 0.4. For the transmitter, the state transition probability that the buffer state remains unchanged is 0.3. The transition probability from one state to another is 0.74 [47, 48]. The calculation state of the MEC server follows the Markov model. It is assumed that the computing power status of the MEG server is divided into five types: very low, low, medium, high, and very high. The comparison of enterprise innovation and marketing management structure rate under different ρ values (SNR = 10 dB) is shown in Figure 4 [49].

Figure 4 shows the convergence of the proposed DRL-MSN resource joint allocation scheme. It can be seen from the figure that in the initial stage of the learning process, the total utility value of the DRL-MSN scheme is very low. As the number of nodes increases, the total utility continues to increase until it converges to a relatively stable value, about 5900. In addition, the convergence performance of deep reinforcement learning algorithms under different learning rates is compared. When the learning rate is 0.001, the convergence speed is faster than when the learning rate is 0.0001. However, this does not mean that a higher learning rate is always better because a higher learning rate may lead to a local optimal rather than a global optimal. For example, when the learning rate is 0.01, the algorithm converges to about 4900, which is much lower than the convergence value obtained by other learning rates. Therefore, it is important to choose the right learning rate for a particular problem. In the following simulation, a learning rate of 0.001 was selected.

4.3. The Impact of Data Analysis and Optimization on Experimental Results. In the above, the data source and the prediction model built are introduced in detail. For a neural network prediction model or other machine learning algorithm model, it is necessary to judge the pros and cons of the prediction algorithm based on the quantitative measurement of its prediction performance. At the same time, for a built model, there are many changes in the parameters of the model. The model needs to be tuned to make the prediction results accurate. The changes of corporate marketing indicators under different methods are shown in Figure 5.

In the following, first the evaluation index used in this article and the meaning of the evaluation index are introduced, and the parameters of the model built in this article are selected. After that, the prediction results of the model built in this article are shown, and the prediction results of other machine learning algorithms to prove its superiority are compared. The effect diagram of enterprise innovation and marketing management optimization-Gaussian noise is shown in Figure 6.

Figure 7 shows the effect diagram of enterprise innovation and marketing management optimization under data optimization. The impact of the average size of each content on the total reduced backhaul link traffic. It can be seen from the figure that as the average size of each content increases, the reduced backhaul link traffic will increase. The effect of enterprise innovation and marketing management optimization-salt and pepper noise is shown in Figure 7.

The gain of cache utility decreases, and the system tends not to cache, which leads to a decrease in cache revenue. Therefore, the traffic on the backhaul link is reduced even more. In addition, without indirect observation of the trust value of mobile users, the accuracy of the social trust value evaluation of the DRL-MSN-wind scheme is low, which

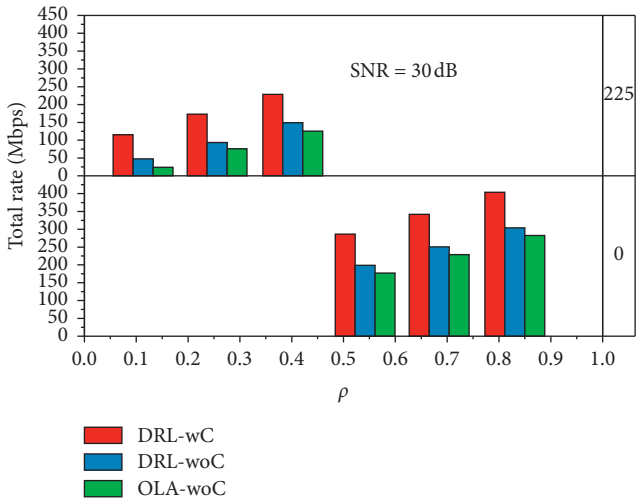

Figure 3: Comparative analysis: rates under different ρ values (SNR = 30 dB).

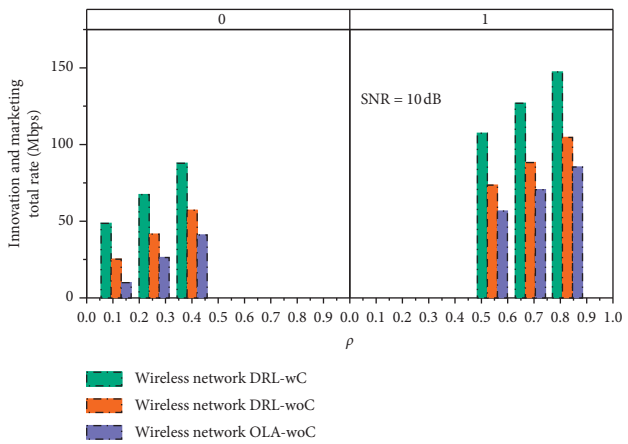

Figure 4: Comparative analysis: rates under different ρ values (SNR = 10 dB).

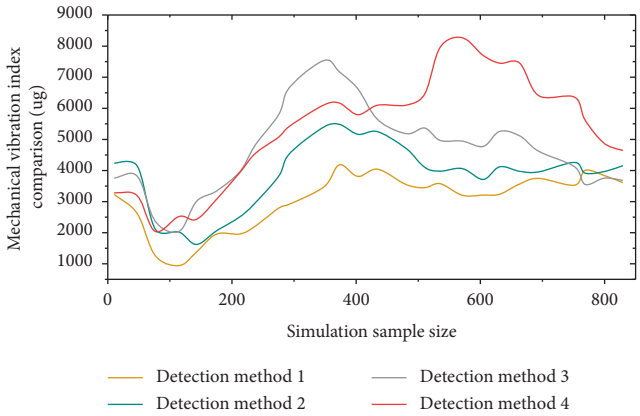

Figure 5: Changes in corporate marketing indicators under different methods.

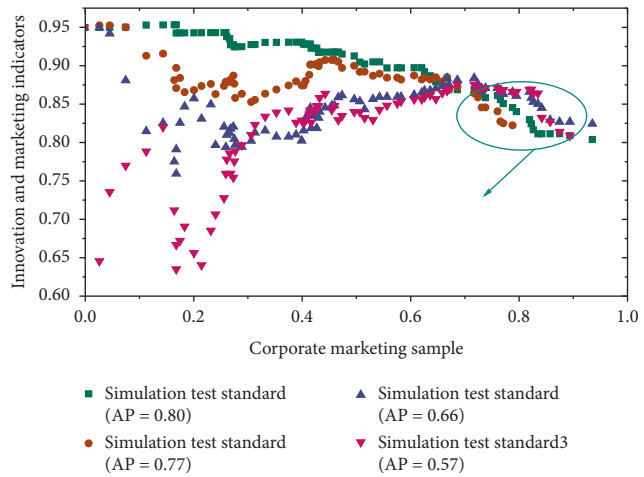

Figure 6: The effect of the proposed optimization-Gaussian noise.

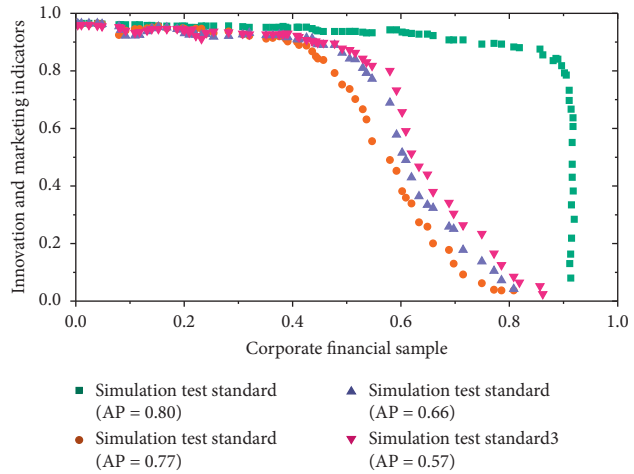

Figure 7: The effect of the proposed optimization-salt and pepper noise.

leads to MEC and cache. The utility gain is reduced, and the traffic of the backhaul link is increased.

5. Conclusion

This article puts forward a novel enterprise innovation and marketing model to overcome the challenges faced by the enterprises. This article proposes a new resource optimization scheme that combines data mining and wireless network. We establish enterprise innovation and marketing structure through a wireless sensor network with the advent of edge computing and carried out the wireless transmission of relevant data and information at the edge of the network. The proposed model comprised of an edge-enabled corporate innovation and marketing framework module for wireless transmission of data and the enterprise marketing resource optimization module using the particle swarm algorithm. The proposed framework performs efficient calculation and storage using a resource optimization module. The feasibility and effectiveness of the proposed

framework are verified using the analysis of the actual case test results. This proposed framework can effectively improve the innovation efficiency level of existing enterprises and the optimization of marketing management resources.

Data Availability

The data used to support the findings of this study are obtained from the corresponding author upon request.

Conflicts of Interest

The authors declare that they have no conflicts of interest regarding the publication of this paper.

References

[1] Z. Zhou, N. Bambos, and P. Glynn, "Deterministic and stochastic wireless network games: equilibrium, dynamics, and price of anarchy," *Operations Research*, vol. 66, no. 6, 2018.

[2] D. Zhang, Q. Liu, L. Chen, and W. Xu, "Survey on coexistence of heterogeneous wireless networks in 2.4GHz and TV white spaces," *International Journal of Distributed Sensor Networks*, vol. 13, no. 4, Article ID 155014771770396, 2018.

[3] Y.-G. Yang, S.-N. Cao, Y.-H. Zhou, and W.-M. Shi, "Quantum wireless network communication based on cluster states," *Modern Physics Letters A*, vol. 35, no. 21, Article ID 2050178, 2020.

[4] J. Wind and V. Mahajan, "Marketing hype: a new perspective for new product research and introduction," *Journal of Product Innovation Management*, vol. 4, no. 1, pp. 43–49, 1987.

[5] K. S. Swan, M. Luchs, and M. Creusen, "Perspective: a review of marketing research on product design with directions for future research," *Journal of Product Innovation Management*, vol. 33, no. 3, pp. 320–341, 2016.

[6] M. Pióro, A. Tomaszewski, and A. Capone, "Maximization of multicast periodic traffic throughput in multi-hop wireless networks with broadcast transmissions," *Ad Hoc Networks*, vol. 77, pp. 119–142, 2018.

[7] J. Pedersen, A. G. I. Amat, I. Andriyanova, and F. Brannstrom, "Optimizing MDS coded caching in wireless networks with device-to-device communication," *IEEE Transactions on Wireless Communications*, vol. 18, no. 1, pp. 286–295, 2019.

[8] M. C. Oliveira, G. A. M. Pereira, E. A. Ferreira et al., "Additive design: the concept and data analysis," *Weed Research*, vol. 58, 2018.

[9] H. Moon, D. R. Miller, and S. H. Kim, "Product design innovation and customer value: cross-cultural research in the United States and Korea," *Journal of Product Innovation Management*, vol. 30, no. 1, pp. 31–43, 2013.

[10] M. Meler, "Marketing approach to the tourism product conceptualization in a globalization condition," *Applied Optics*, vol. 39, no. 39, pp. 770–775, 2004.

[11] S. K. Markham, "Research on the management of innovation: the Minnesota studies (book)," *Journal of Product Innovation Management*, vol. 19, no. 3, pp. 253-254, 2002.

[12] S. Wan, Y. Xia, L. Qi, Y. H. Yang, and M. Atiquzzaman, "Automated colorization of a grayscale image with seed points propagation," *IEEE Transactions on Multimedia*, vol. 22, no. 7, pp. 1756–1768, 2020.

[13] S. Wan, X. Xu, T. Wang, and Z. Gu, "An intelligent video analysis method for abnormal event detection in intelligent transportation systems," *IEEE Transactions on Intelligent Transportation Systems*, p. 2, 2020, In press.

[14] S. Wan, R. Gu, T. Umer, and K. Salah, "Toward offloading Internet of vehicles applications in 5G networks," *IEEE Transactions on Intelligent Transportation Systems*, p. 2, 2020, In press.

[15] Z. Gao, H. Xue, and S. Wan, "Multiple discrimination and pairwise CNN for view-based 3D object retrieval," *Neural Networks*, vol. 125, pp. 290–302, 2020.

[16] S. Wan and S. Goudos, "Faster R-CNN for multi-class fruit detection using a robotic vision system," *Computer Networks*, vol. 168, Article ID 107036, 2020.

[17] A. D. Jong, W. Verbeke, and E. Nijssen, "Editorial of special issue on: sales and innovation," *Journal of Product Innovation Management*, vol. 34, no. 1, pp. 234–245, 2014.

[18] N. T. Javan, M. Sabaei, and M. Dehghan, "To-send-or-not-to-send: an optimal stopping approach to network coding in multi-hop wireless networks," *International Journal of Communication Systems*, vol. 31, no. 2, 2018.

[19] F. Hempelmann and A. Engelen, "Integration of finance with marketing and R&D in new product development: the role of project stage," *Journal of Product Innovation Management*, vol. 32, no. 4, pp. 636–654, 2015.

[20] Y. He, Z. Zhang, F. R. Yu et al., "Deep-reinforcement-learning-based optimization for cache-enabled opportunistic interference alignment wireless networks," *IEEE Transactions on Vehicular Technology*, vol. 66, no. 11, pp. 10433–10445, 2017.

[21] E. Hansen, E. Nybakk, and R. Panwar, "Firm performance, business environment, and outlook for social and environmental responsibility during the economic downturn: findings and implications from the forest sector," *Canadian Journal of Forest Research*, vol. 43, no. 12, pp. 1137–1144, 2013.

[22] A. Griffin, "PDMA research on new product development practices: updating trends and benchmarking best practices," *Journal of Product Innovation Management*, vol. 14, no. 6, pp. 429–458, 1997.

[23] K. Brockhoff and A. K. Chakrabarti, "R&D/marketing linkage and innovation strategy: some West German experience," *IEEE Transactions on Engineering Management*, vol. 35, no. 3, pp. 167–174, 1988.

[24] J. B. D. Assuncao, "From the special issue editor: bridging marketing and operations in new product development," *Journal of Product Innovation Management*, vol. 25, no. 5, pp. 414–417, 2008.

[25] J. West and M. Bogers, "Leveraging external sources of innovation: a review of research on open innovation," *Journal of Product Innovation Management*, vol. 31, no. 4, pp. 814–831, 2014.

[26] A. Anand and G. D. Veciana, "Resource allocation and HARQ optimization for URLLC traffic in 5G wireless networks," *IEEE Journal on Selected Areas in Communications*, vol. 36, no. 11, pp. 2411–2421, 2018.

[27] M. Alzenad, M. Z. Shakir, H. Yanikomeroglu, and M. S. Alouini, "FSO-based vertical backhaul/fronthaul framework for 5G+ wireless networks," *IEEE Communications Magazine*, vol. 56, no. 1, pp. 218–224, 2018.

[28] M. Ahsaini, A. Kassogue, M. F. Tazi et al., "Emphysematous cystitis and emphysematous pyelitis: a clinically misleading association.####Procalcitonin: diagnostic value in systemic infections in chronic kidney disease or renal transplant

patients.####Medical therapy alone can be sufficient for bilater," *Applied Optics*, vol. 46, no. 22, pp. 4896–4906, 2007.

[29] F. Zhou, Y. Wu, R. Q. Hu, and Q. Yi, "Computation rate maximization in UAV-enabled wireless powered mobile-edge computing systems," *IEEE Journal on Selected Areas in Communications*, vol. 36, no. 9, pp. 1927–1941, 2018.

[30] Q. Yuan, H. Zhou, J. Li, Z. Liu, F. Yang, and X. S. Shen, "Toward efficient content delivery for automated driving services: an edge computing solution," *IEEE Network*, vol. 32, no. 1, pp. 80–86, 2018.

[31] B. Yang, X. Cao, J. Bassey, X. Li, and L. Qian, "Computation offloading in multi-access edge computing: a multi-task learning approach," *IEEE Transactions on Mobile Computing*, no. 1, p. 99, 2020, In press.

[32] T. Tran and D. Pompili, "Adaptive bitrate video caching and processing in mobile-edge computing networks," *IEEE Transactions on Mobile Computing*, vol. 18, no. 9, pp. 1965–1978, 2019.

[33] D. Norbert, C. Octavian, E. Marius, and T. Eliza, "C?T?Lin, Negrea, Edge computing for space applications: field programmable gate array-based implementation of multiscale probability distribution functions," *Review of Scientific Instruments*, vol. 12, no. 4, pp. 412–423, 2018.

[34] H. Marylesa, M. C. Hock, B. T. Meehan, and L. E. Dresselhaus-Cooper, "A locally adapting technique for edge detection using image segmentation," *SIAM Journal on Scientific Computing*, vol. 40, no. 4, pp. B1161–B1179, 2018.

[35] J. H. Huh, "Refer container monitoring system using PLC-based communication technology for maritime edge computing," *Journal of Supercomputing*, vol. 76, no. 7, pp. 5221–5243, 2020.

[36] Y. Huang, X. Song, F. Ye, Y. Yang, and X. Li, "Fair and efficient caching algorithms and strategies for peer data sharing in pervasive edge computing environments," *IEEE Transactions on Mobile Computing*, vol. 19, no. 4, pp. 852–864, 2020.

[37] Y. Huang, B. Sheng, F. Yang et al., "Immune system for the Internet of things using edge technologies," *IEEE Internet of Things Journal*, vol. 6, no. 3, pp. 4774–4781, 2019.

[38] T.-Y. Hsieh, S.-E. Chan, C.-R. Chen, P.-C. Li, and C.-H. Ho, "A no-reference error-tolerability test technique for videos via edge and extreme-value checking and its hardware implementation," *Microelectronics Reliability*, vol. 99, pp. 1–11, 2019.

[39] X. Hong, L. Liang, X. Jie, and A. Nallanathan, "Joint task assignment and resource allocation for D2D-enabled mobile-edge computing," *IEEE Transactions on Communications*, vol. 67, no. 6, pp. 4193–4207, 2019.

[40] L. He, K. Ota, and M. Dong, "Learning IoT in edge: deep learning for the internet of things with edge computing," *IEEE Network*, vol. 32, no. 1, pp. 96–101, 2018.

[41] M. Gairing and R. Savani, "Computing stable outcomes in symmetric additively separable hedonic games," *Mathematics of Operations Research*, vol. 44, 2019.

[42] A. Ebrahimzadeh and M. Maier, "Distributed cooperative computation offloading in multi-access edge computing fiber-wireless networks," *Optics Communications*, vol. 452, pp. 130–139, 2019.

[43] G. Duan, F. Xiao, and L. Wang, "Asynchronous periodic edge-event triggered control for double-integrator networks with communication time delays," *IEEE Transactions on Cybernetics*, vol. 48, no. 99, pp. 675–688, 2018.

[44] F. Andreas, D. J. Dürrenmatt, and H. Stefanie, "Using data mining to assess environmental impacts of household consumption behaviors," *Environmental Science & Technology*, vol. 52, no. 15, pp. 8467–8478, 2018.

[45] X. Xu, Q. Wu, L. Qi, W. Dou, S.-B. Tsai, and M. Z. A. Bhuiyan, "Trust-aware service offloading for video surveillance in edge computing enabled Internet of vehicles," *IEEE Transactions on Intelligent Transportation Systems*, 2020, In press.

[46] X. Xu, B. Shen, X. Yin et al., "Edge server quantification and placement for offloading social media services in industrial cognitive IoV," *IEEE Transactions on Industrial Informatics*, vol. 17, no. 4, p. 2910, 2021.

[47] L. S. Álvaro, G. P. Jesús, P. L. Alberto, M. R. Ricardo, J. F. Ortega, and L. Alejandro, "Hormonal and neuromuscular responses during a singles match in male professional tennis players," *PLos One*, vol. 13, no. 4, Article ID e0195242, 2018.

[48] I. Afolabi, A. Ksentini, M. Bagaa, T. Taleb, M. Corici, and A. Nakao, "Towards 5G network slicing over multiple-domains," *IEICE Transactions on Communications*, vol. E100, no. 11, pp. 1992–2006, 2017.

[49] A. Poordavoodi, M. Reza Moazami Goudarzi, A. Haj Masoud Rahmani, A. M. Rahmani, and M. Izadikhah, "Toward a more accurate web service selection using modified interval DEA models with undesirable outputs," *Computer Modeling in Engineering & Sciences*, vol. 123, no. 2, pp. 525–570, 2020.

Hindawi
Mobile Information Systems
Volume 2021, Article ID 6628739, 11 pages
https://doi.org/10.1155/2021/6628739

Review Article

Big Data Insights and Comprehensions in Industrial Healthcare: An Overview

Weiwei He[1], **Shah Nazir**[2] **and Zahid Hussain**[3]

[1]*Sichuan Academy of Medical Sciences & Sichuan Provincial People's Hospital, Chengdu, China*
[2]*Department of Computer Science, University of Swabi, Swabi, Pakistan*
[3]*Department of Information Technology, Quaid-e-Awam University Nawabshah, Nawabshah, Pakistan*

Correspondence should be addressed to Weiwei He; weiweihehot@sina.com and Shah Nazir; snshahnzr@gmail.com

Received 22 December 2020; Revised 17 January 2021; Accepted 20 January 2021; Published 31 January 2021

Academic Editor: Mian Ahmad Jan

Copyright © 2021 Weiwei He et al. This is an open access article distributed under the Creative Commons Attribution License, which permits unrestricted use, distribution, and reproduction in any medium, provided the original work is properly cited.

Big data are the data which need to be shaped for their volume, size, and shape in order to extract meaningful information for an explicit purpose. Data are ever playing a significant role in organization and industry for their daily activities to functional smoothly. The volume of healthcare data is increasing with the rising of technology and passage of time. This rise in volume of data can be a challenging task toward analysing the big data for industry and Internet of things (IoT). Numerous approaches, techniques, and tools exist in the literature for supporting, to handle, and manage processing of data. A review of the literature is needed in order to collect existing evidence from the literature to show which method or tool works for which particular situation. Therefore, the current study presents a review of the existing techniques of big data insights and scientific programming in the industry of healthcare. The report presents the summary of the literature. The study collects evidences from the existing literature and organizes it through the process of literature review with some derivations. This review will benefit practitioners to identify the right techniques for their specific purpose of research.

1. Introduction

With the rising technology and digital innovation, the healthcare technology is refined at a high rate. Healthcare data are continuously growing, and their volume is drastically increasing. Such data can make it harder to identify useful form of data producing meaningful information. Big data analytics are a useful delivery of data, producing valuable and useful insights for huge volume of data. Several advantages are there with the use of big data such as identification of patient disease in the early stage, delivering enhanced services of healthcare, reducing cost, and producing quality care. Various sources of big data are available in healthcare. These sources include electronic healthcare data, biometric data, registration, medical imaging, biomarker data, patient-reported data, clinical data, and administration data. Such data can be visualized in order to extract meaningful and valuable information. Analytic tools of big data play a significant role in analysing and integrating huge volume of unstructured, semistructured, and structured data providing diverse hospital, clinical, and many other decision services. Diverse applications of big data in healthcare are presented as follows [1–4].

Panda et al. [5] concentrated on mobile-based development of application through which the patient can send query of symptoms to the doctors. The application of mobile will be fitted out with instruction of first aid based on the severity and nature of the symptoms. Huge bulk of data was gathered from doctors and users, and the data were used for training the machine for automating the task to some level. Beneficial insights for improving efficiency and quality of care were gathered from the collected data. The patient is able to reach out for the solution of health with easiness and cheap. The approach is used as an analytic tool for gathering data for the delivery purpose and extracting useful information. Mian et al. [6] described the real-time exploration of data for datasets of healthcare through in-memory databases. Two databases of in-memory were considered for

comparing and studying the ability and responsiveness for handling complexity of classic data of health for exploring tasks. The study outlined the issues which need addressing for future developments of big data. Gonzalez-Alonso et al. [7] presented an approach for addressing the technologies of big data analytics incorporated into the care provider. Katsis [8] described the applications of big data in efficient use of public health discoveries. The study showed that the analytic approaches classically applied in public health are not up to the data task currently existing. The results elaborated the big data case study which was carried out in San Diego, California. The study analyzed thousands of variables associated to health for gaining useful insights on the determination of various health outcomes. The contribution of the proposed study is given as follows:

(i) To deliver a review report of the existing approaches for big data insights in the industry of healthcare.

(ii) To provide an in-depth review of the available sources from different point of views by publishing the papers in different areas of big data in healthcare.

(iii) To provide a gateway on the basis of which researchers can devise new approaches, techniques, and tools to facilitate healthcare.

The organization of the paper is as follows. Section 2 provides the literature study to the big data insights in the industry of healthcare. Section 3 shows the library-based study process of the searching materials and their analysis. The paper concludes in Section 4.

2. Literature Review

Numerous approaches are in practice to deal with diverse perspectives of big data. The data can be viewed to extract meaningful insights for delivering quality services. Cha et al. [9] proposed the technical architecture of the data analytic platform for health offering a methodological solution for analysis of big health data which are produced from various sources. Data standardization was used as the main feature of the architecture, and SNOMED-CT was considered as a standard for standardizing data of health from various sources. With the help of the case study involved, huge volumes of data based on the laboratory are incorporated and analyzed through this platform. Li et al. [10] introduced the big data analytics proof-of-concept framework for development of the risk-tuning patient expenditure model. The approach is based on the strategy of "divide and conquer" for exploiting the big-yet-rich data for enhancing the accuracy of the model. The MapReduce tool was used for implementation of the machine learning algorithms for the dataset. The framework determined the predictive analytics' effectiveness through the random forest algorithm and distributed-computing platform efficiency. Straton et al. [11] presented an approach for evaluation of predictions and post engagement on Facebook. The study focused on insights into associated indicators leading to the engagement with posts of healthcare on Facebook. The approaches of unsupervised and supervised are used. The study elaborated the strategy of healthcare for engaging users and building the prevention mechanism by contents posted on Facebook about informative healthcare. Sterling [12] reviewed the associated concepts from the literature of organizational communications and elaborated technology acquisition theories. The study described the possible benefits and the issues in the area. The study has further emphasized on the issues of resources like cost of human, patient privacy, and thoughtful of technology interventions.

Pandey and Subbiah [13] proposed architecture of big data storage containing the storage cluster and application cluster for facilitating read, write, or update data optimization as well as speedup. The application cluster facilitates effective storage and retrieval function from the user, while the services of storage are provided by the storage cluster. Ambigavathi and Sridharan [14] analyzed the properties of big data, analytics tools of big data, and various phases through healthcare economy from the collection of data for the stage of data delivery. The study reported the challenges of research with possible findings. Zhang et al. [15] examined the three knowledge modes achieving beneficial use of big data analytics with electronic health records. The authors surveyed 580 nurses of a hospital in China in 2019. For examining the association of electronic health records and knowledge, structured equation modelling was used. The study contributed to the available literature of big data and digital health through exploring the analytical tools to electronic health records from various modes of knowledge to extract useful big data analytics. Mande et al.'s [16] goal was establishing of a collaborating processing environment with patient data through technologies of open source software. The structures of distributed data were produced from hospital explicit metadata for extracting side effects in the patient through the query of whole clinical trial data to develop, repurpose, and reposition drugs. Harerimana et al. [17] identified the data sources, technologies, techniques, main issues, and future directions of healthcare big data analytics. The study elaborated a do-it-yourself review delivering a simplified, easily understandable, and holistic view of different technologies' applications for developing incorporated analytic applications of health. Nazir et al. [18] presented a comprehensive and detailed report on the big data visualization in cardiology. The study is based on the last 10 years from 2009 to 2018. 53 studies were filtered based on the inclusion and exclusion criteria, quality assessment, and some derivations derived. They elaborated that the study is associated to cardiology and will help researchers and practitioners in the area for devising new solutions based on the existing evidences. Several other studies are of the same authors related to big data are available [19–22].

Singh et al. [23] explained the usefulness of real-time data for analysis and prediction of severe emergency cases. They explained that without approaches of Hadoop cluster and analytics of big data, the data become useless. Xu and Kumar [24] presented a framework based on machine learning for analytics of big data and tested for improvement of performance and quality of auxiliary power-unit services of health monitoring. They developed and employed useful

technologies and practical analytics of big data for application of industries in aviation and aerospace. Ojha and Mathur [25] gave an overview of how the patient record can be saved as digital data in the form of electronic health record and how useful information can be produced from the saved records through approaches of analytics and tool supporting in saving money and time of both the doctors and patients. The study was done in the hospital of Maharaja Yeshwantrao, Indore, Madhya Pradesh, India. From this hospital, huge amount of heterogeneous data is generated from various sources such as laboratory tests, patient health records, electronic medical requirements, social media, health insurance data, genome research, drug research, clinical outcome, and transaction from Mahatma Gandhi Memorial Medical Mollege, working under Maharaja Yeshwantrao. Analytics of big data can be used for making useful information for retrieval. Sabharwal et al. [26] focused on the applications and analytics of big data and issues in the IoH care. Rao et al. [27] presented different possible solutions of security for harnessing the probable of big data affecting healthcare in vastly regulated surroundings. Ajayi et al. [28] proposed a particle swarm optimization approach for selection of feature and tuning parameters of the gradient boosting machine approach on 1,349,239 data points of an incident dataset. The ability of prediction of the proposed approach was compared to the traditional tree-based approach discovered about accurate prediction of the model on test data. Khennou et al. [29] explored efficiently the appropriate adaptation of analytical tools for electronic health records for upgrading the usage through practitioners of health. A case study of the implementation process of electronic health record relies on open electronic health record and identifies analytics of health adoption in every phase of the approach.

Gaitanou et al. [30] performed a systematic literature review of the applications of big data in healthcare systems for improving clinician behaviour, experiences of the patient, and quality of care facilitated to the patient. The PubMed database was searched for the search process and identifying associated research papers. 12 research papers were selected based on the inclusion and exclusion criteria from the 108 research papers searched in the library. The derivations of the study show that 9 papers were showing the positive effects of big data, while some papers resulted negative. The key advantages of the applications of big data include enhanced usability, positive behaviour change, and effective decision support, while issues were traced for acceptance of technology. The key issue happened in the systems' process heterogeneous datasets, outcomes reported by patients, and in motion data, as different to electronic health records. The study highlighted round about areas of research where exploration is needed for understanding the applications of big data in healthcare and improving its success. Talukder [31] pointed out that a huge amount of patient data is available in hospitals. Apart from this, large medical knowledge of body exist in the digital form in various repositories. The focus of the study has addressed the issues ariseing from such data with the analytic solutions combining the knowledge bodies and data by technology of big data integrated with mathematical models, artificial intelligence, and translation medicine "*Evidence Based Precision Medicine—the perfect decision outcome with perfect knowledge backing*." Several benefits exist for various stakeholders such as cost of payer are reduced considerably. The medical decision accuracy in improved and enhanced productivity of hospital, reduced burden of disease, decreased medical errors, and reduced wastage and fraud.

3. Big Data Insights and Comprehensions in Industrial Healthcare Based on Famous Libraries

Insights of big data is the essential process of mining and analysing big data for producing operational and business information at exceptional scale and specificity. Han et al. [32] presented a nonsystematic review for identifying associated gray and scientific literature related to the current state and restrictions of assessment of health involvement and infrastructure of health data in the US. The study comprised the literature on nations with unified data systems. The aim of the study was producing in-depth analysis of the available endeavors for use and standardized data collection through encounters of patient with doctors for the purpose of public health. Ravikumaran et al. [33] elaborated the fields of big data analytics developing in healthcare, giving details of the advantages, and presented architectural framework and approach. The sources of data were identified and the tools and platforms for technologies, approaches, and analytics were recommended, and the issues and derivations were discussed. The study elaborated that analytics of big data in healthcare is an encouraging area for facilitating in-depth insights from huge volume of datasets. Aceto et al. [34] systematically surveyed the adoption of technologies of Industry 4.0 applied for the domain of health. The study provided details of the key paradigms and technologies' applications to Healthcare 4.0, discussed the key application scenarios, and examined benefits, new cross-disciplinary issues, and lessons learned. Istepanian and Al-Anzi [35] provided the associated issues of big data from the perceptions of mobile health. The study also presented the associated issues of rapprochement of analytics of big m-health data. Galetsi et al. [36] surveyed a systematic review associated to big data analytics in healthcare. The study focused on different resources utilization for creating capabilities/values for organization; based on the publications selected, the study discussed the big data types' classifications associated to healthcare, the analysis approaches, stakeholders value, the tools and platforms to handle data of big health, and forthcoming aspects in the area. Pragmatic examples were given for showing the advancements of healthcare.

Wang et al. [37] developed the transformation model for analytics of big data accordingly to the practice-based view revealing the casual association among analytics of big data abilities, benefits' dimensions, IT-enabled practices of transformation, and business values. The system was validated in the environment of healthcare. Wami et al. [38] evaluated the possible utility of Mosaic groups for the purpose of research in health through identifying

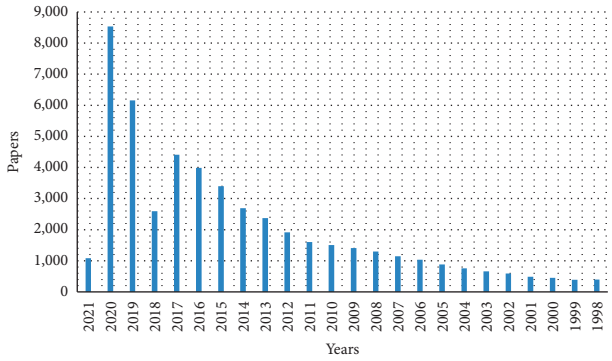

Figure 1: Year wise distribution of articles.

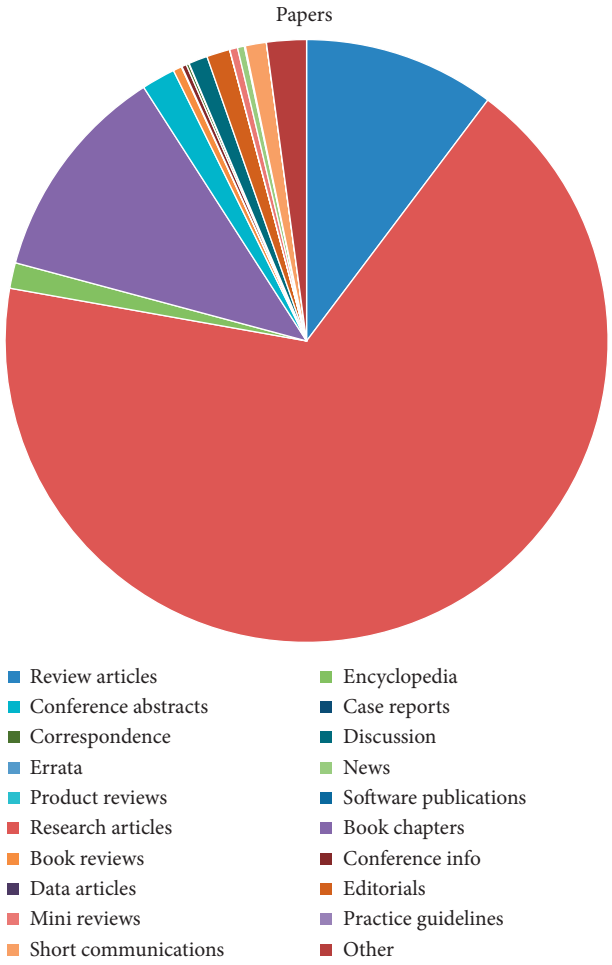

Figure 2: Article types with the ratio of papers based on its types.

the associations with indices of multiple, driven to the population of British. Various popular libraries were searched for identifying associated studies. Figure 1 depicts year-wise distribution of papers in the library of Sciencedirect. Figure 2 depicts article types with the ratio of papers based on its types. Figure 3 shows the publications' titles with the total of papers in the library. Figure 4 presents the subject areas with the total of papers. The library of IEEE was searched for finding the related materials. Figure 5 shows the publications' topics in the library. Figure 6 presents the total papers in the conferences held. Figure 7 depicts the title of publications with the total number of papers. Figure 8 shows the publication types in the given library.

The library of Springer and PubMed were searched for related research studies. Bates et al. [39] elaborated the

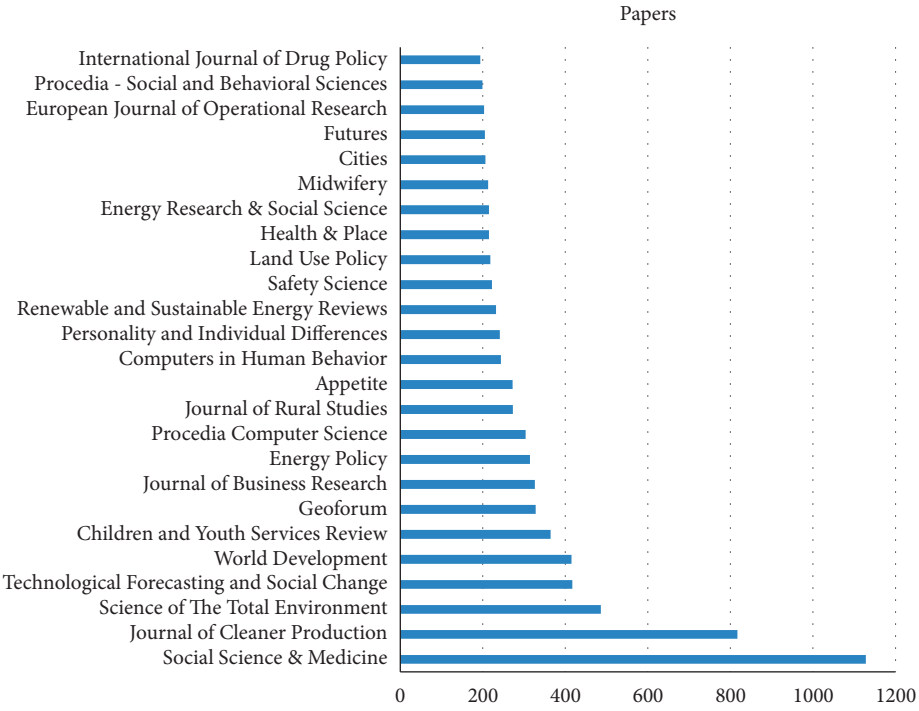

Figure 3: Publications titles with the total of papers.

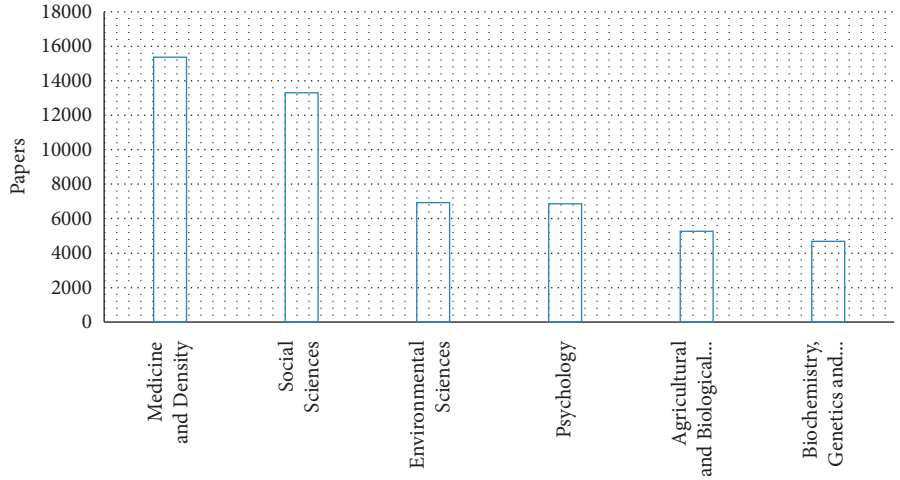

Figure 4: Subject areas with total of papers.

insights' types such as emerging from clinical analytics, types of analytics for obtaining insights, algorithms, monitoring devices, evaluation scores, registries, and analytics infrastructure needed for organization for performing the essential analysis and implementing changes for enhancing care at low costs. Nanayakkara et al. [40] surveyed the biomedical big data in healthcare advancements, issues, and limitations with the focus on oral health and elaborated the possible forthcoming applications of big data for oral health for improving the efficiency and quality of personalized healthcare. Madanian et al. [41] identified and examined the issues associated to the existing status of India's healthcare system with the emphasis on mHealth and technologies of big data analytics. For addressing these issues, the study proposed a framework for incorporating the produced mHealth big data and employed the results in healthcare of India. The study was conducted with the use of electronic sources between December 2018 and February 2019 with the publications' language as English. Brennan and Bakken [42] presented a study consisting of investigation of emergent initiative of federal big data and explored exemplars from informatics of nursing research for benchmark where nursing are previously poised for

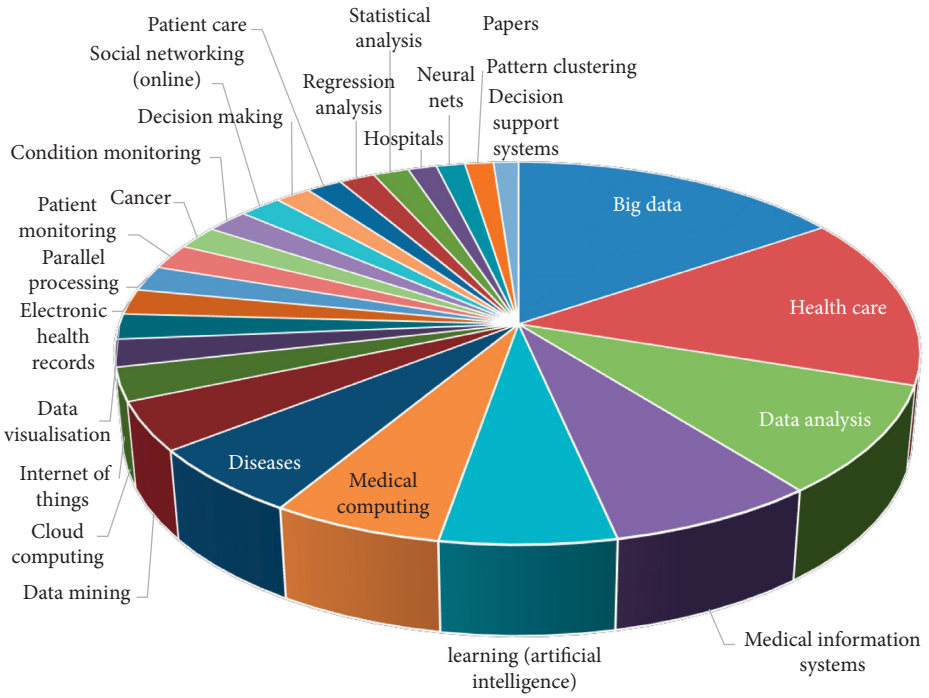

Figure 5: Publications topics.

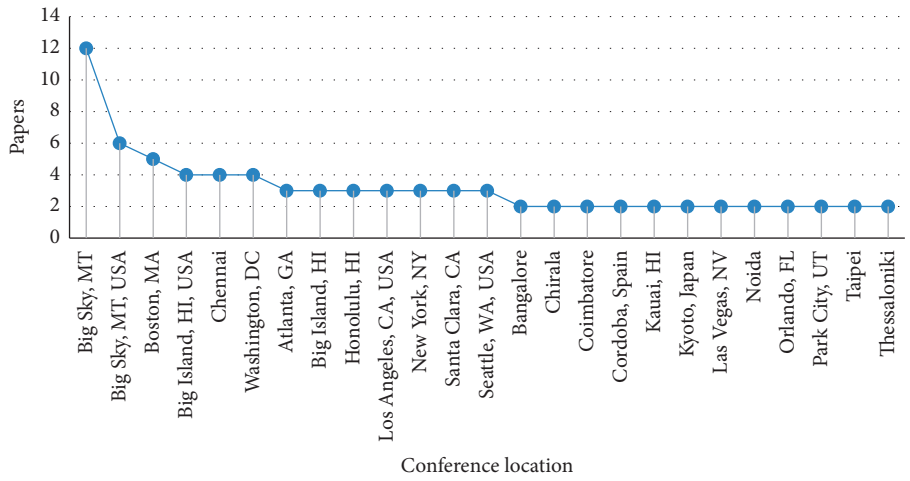

Figure 6: Total papers in the conferences.

participating in the revolution of big data. Reflections and observations were provided on experiences in the initiatives of emerging big data. Luo et al. [43] reviewed and elaborated the applications of big data in four key subdisciplines of biomedical including the clinical informatics, bioinformatics, imaging informatics, and public health informatics. The study reviewed the advances and breakthroughs of the applications of big data in the domains of healthcare and surveyed the issues, opportunities, and gaps for improving and advancements of healthcare big data applications. Sukumar et al. [44] presented a study with the aim of highlighting the quality of data issues in context of healthcare big data analytics. The insights described in the study were results of analytics research performed in various organizations on different datasets of health. The datasets included Medicaid claims and Medicare, provider datasets from electronic health records and private and public sources from health centers available through partnership with claims of healthcare under privacy-protected policies of health. Slime et al. [45] presented a study focussing on application enhancements of the technology in the field of health. The

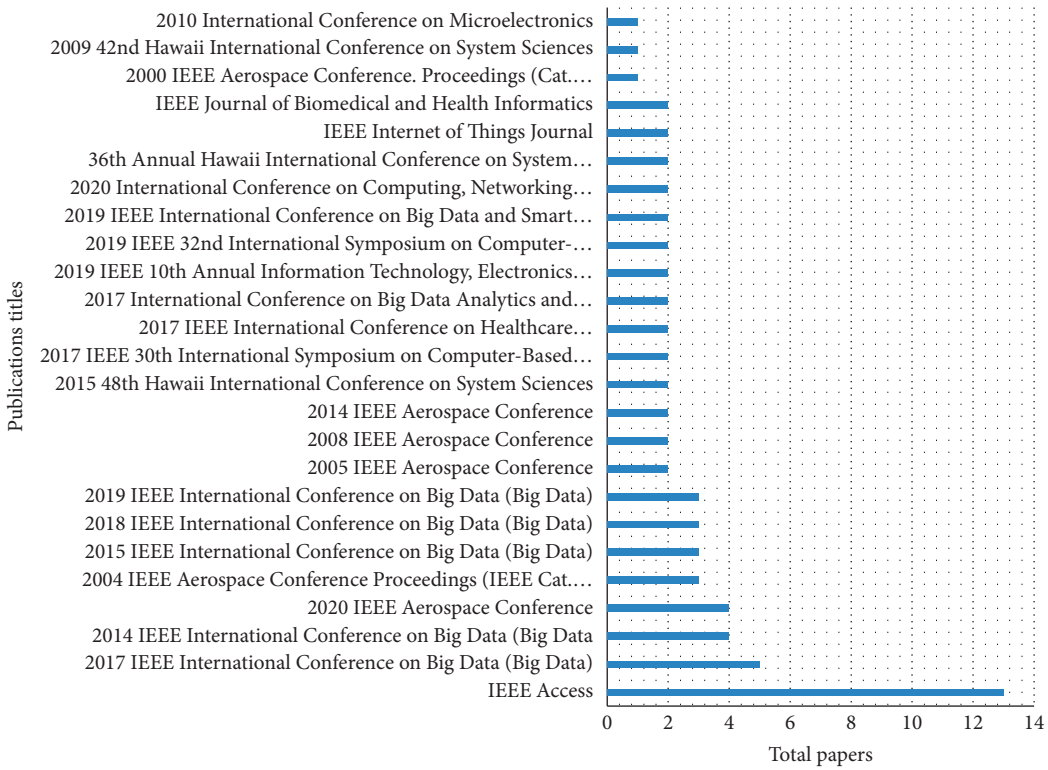

Figure 7: Title of publications with total papers.

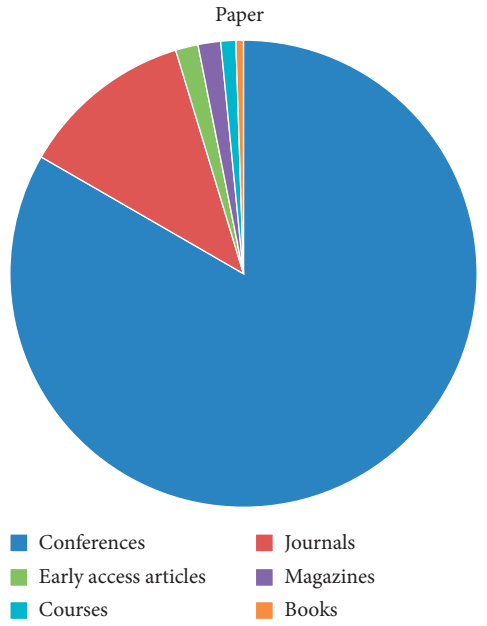

Figure 8: Types of papers.

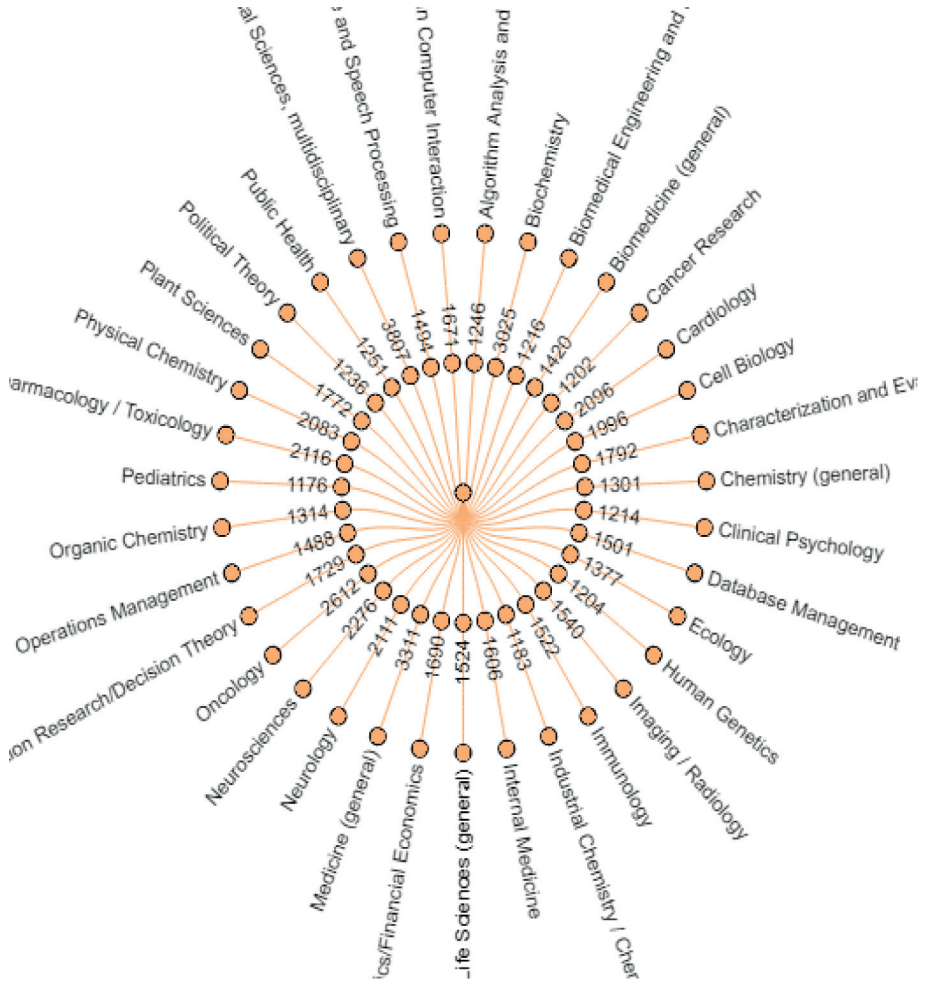

Figure 9: Publication topics and total of papers.

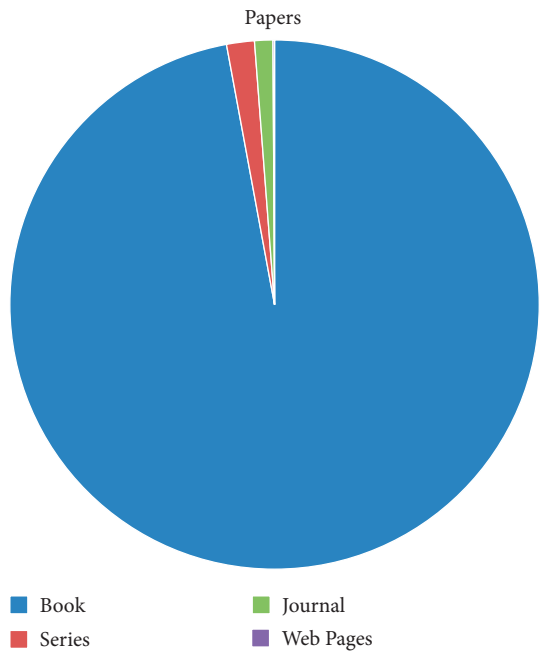

Figure 10: Publications types with ratio of papers.

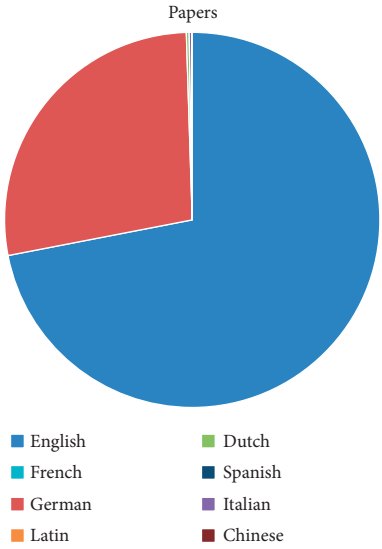

Figure 11: Languages in which the papers are published.

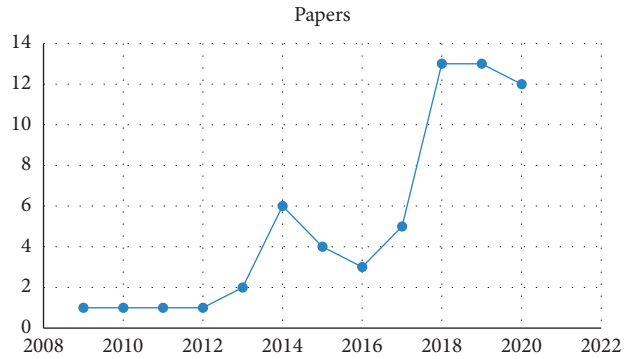

Figure 12: Publications in the given years.

aspects of big data are discussed, giving some implementation and elaborating various architecture of big data in healthcare. Figure 9 depicts the topics of publications with total of publications. Figure 10 depicts the publications' types with the ratio of papers. Figure 11 represents the languages in which the papers are published. Figure 12 shows the publications in the given years.

4. Conclusion

With the growing technology and digital revolution, the technology of healthcare is getting advanced at a high rate. Healthcare data are always rising and drastically increasing the volume of healthcare data. Such data can make it tougher to recognize useful form of data generating meaningful information. The data are always playing a significant role in organization and industry for their daily activities to function smoothly. This rise in big data volume can be a challenging task concerning analysing the data for normal industry and IoT. Numerous tools, approaches, and techniques are existing in literature for supporting, to handle, and manage the process of big data. A review of the literature is needed in order to gather current evidences from the literature to show which method or tool works for which particular situation. The proposed study presents a review of the existing techniques of big data insights and scientific programming in the industry of healthcare. The report presents the summary of the literature. The study collects evidences from the existing literature and organizes it through the process of literature review with some derivations. This review will benefit practitioners to identify the right techniques for their specific purpose of research.

Data Availability

The data are not available.

Conflicts of Interest

The authors declare that they have no conflicts of interest regarding the publication of this paper.

References

[1] K. Waldhör, "Rezension big data and E-health," *HMD Praxis der Wirtschaftsinformatik*, vol. 56, no. 5, pp. 1085-1086, 2019.

[2] C. Katzenmeier, "Big data, E-health, M-health, KI und Robotik in der Medizin," *Medizinrecht*, vol. 37, no. 4, pp. 259–271, 2019.

[3] J. Roski, G. W. Bo-Linn, and T. A. Andrews, "Creating value in health care through big data: opportunities and policy implications," *Health affairs*, vol. 33, no. 7, pp. 1115–1122, 2014.

[4] S. Zillner and S. Neururer, "Big data in the health sector," in *New Horizons for a Data-Driven Economy*, pp. 179–194, Springer, Cham, Switzerland, 2016.

[5] M. Panda, S. M. Ali, and S. K. Panda, "Big data in health care: a mobile based solution," in *Proceedings of the 2017 International Conference on Big Data Analytics and Computational Intelligence (ICBDAC)*, pp. 149–152, Chirala, India, March 2017.

[6] M. Mian, A. Teredesai, D. Hazel, S. Pokuri, and K. Uppala, "Work in progress - in-memory analysis for healthcare big data," in *Proceedings of the 2014 IEEE International Congress on Big Data*, pp. 778-779, Anchorage, AK, USA, July 2014.

[7] P. Gonzalez-Alonso, R. Vilar, and F. Lupiañez-Villanueva, "Meeting technology and methodology into health big data analytics scenarios," in *Proceedings of the 2017 IEEE 30th International Symposium on Computer-Based Medical Systems (CBMS)*, pp. 284-285, Thessaloniki, Greece, June 2017.

[8] Y. Katsis, "Big data techniques for public health: a case study," in *Proceedings of the 2017 IEEE/ACM International Conference on Connected Health: Applications, Systems and Engineering Technologies (CHASE)*, pp. 222–231, Philadelphia, PA, USA, July 2017.

[9] S. Cha, A. Abusharekh, and S. S. Abidi, "Towards a "big" health data analytics platform," in *Proceedings of the 2015 IEEE First International Conference on Big Data Computing Service and Applications*, pp. 233–241, Redwood City, CA, USA, April 2015.

[10] L. Li, S. Bagheri, H. Goote, A. Hasan, and G. Hazard, "Risk adjustment of patient expenditures: a big data analytics approach," in *Proceedings of the 2013 IEEE International Conference on Big Data*, pp. 12–14, Santa Clara, CA, USA, October 2013.

[11] N. Straton, R. R. Mukkamala, and R. Vatrapu, "Big social data analytics for public health: comparative methods study and performance indicators of health care content on Facebook," in *Proceedings of the 2017 IEEE International Conference on Big Data (Big Data)*, pp. 2772–2777, Boston, MA, USA, December 2017.

[12] M. Sterling, "Situated big data and big data analytics for healthcare," in *Proceedings of the 2017 IEEE Global Humanitarian Technology Conference (GHTC)*, p. 1, San Jose, CA, USA, October 2017.

[13] M. K. Pandey and K. Subbiah, "A novel storage architecture for facilitating efficient analytics of health informatics big data in cloud," in *Proceedings of the 2016 IEEE International Conference on Computer and Information Technology (CIT)*, pp. 578–585, Nadi, Fiji, December 2016.

[14] M. Ambigavathi and D. Sridharan, "Big data analytics in healthcare," in *Proceedings of the 2018 Tenth International Conference on Advanced Computing (ICoAC)*, pp. 269–276, Chennai, India, December 2018.

[15] C. Zhang, R. Ma, S. Sun, Y. Li, Y. Wang, and Z. Yan, "Optimizing the electronic health records through big data analytics: a knowledge-based view," *IEEE Access*, vol. 7, pp. 136223–136231, 2019.

[16] R. Mande, G. JayaLakshmi, and K. C. Yelavarti, "Leveraging distributed data over big data analytics platform for healthcare services," in *Proceedings of the 2018 2nd International Conference on Trends in Electronics and Informatics (ICOEI)*, pp. 1115–1119, Tirunelveli, India, May 2018.

[17] G. Harerimana, B. Jang, J. W. Kim, and H. K. Park, "Health big data analytics: a technology survey," *IEEE Access*, vol. 6, pp. 65661–65678, 2018.

[18] S. Nazir, M. Nawaz Khan, S. Anwar et al., "Big data visualization in cardiology-A systematic review and future directions," *IEEE Access*, vol. 7, pp. 115945–115958, 2019.

[19] S. Nazir, M. Nawaz, A. Adnan, S. Shahzad, and S. Asadi, "Big data features, applications, and analytics in cardiology-A systematic literature review," *IEEE Access*, vol. 7, no. 1, pp. 143742–143771, 2019.

[20] S. Nazir, S. Khan, H. U. K. S. Ali, I. García-Magariño, R. B. Atan, and M. Nawaz, "A comprehensive analysis of healthcare big data management, analytics and scientific programming," *IEEE Access*, vol. 8, 2020.

[21] S. Nazir, S. Ali, M. Yang, and Q. Xu, "Deep learning algorithms and multi-criteria decision making used in big data- a systematic literature review," *Security and Communication Networks*, vol. 2020, Article ID 2836064, 18 pages, 2020.

[22] S. Khan, S. Nazir, I. García-Magariño, and A. Hussain, "Deep learning based urban big data fusion in smart cities: towards traffic monitoring and flow-preserving fusion," *Computers & Electrical Engineering*, vol. 89, Article ID 106906, 2020.

[23] M. Singh, V. Bhatia, and R. Bhatia, "Big data analytics: solution to healthcare," in *Proceedings of the 2017 International Conference on Intelligent Communication and Computational Techniques (ICCT)*, pp. 239–241, Jaipur, India, December 2017.

[24] B. Xu and S. A. Kumar, "Big data analytics framework for system health monitoring," in *Proceedings of the 2015 IEEE International Congress on Big Data*, pp. 401–408, New York, NY, USA, July 2015.

[25] M. Ojha and K. Mathur, "Proposed application of big data analytics in healthcare at Maharaja Yeshwantrao Hospital," in *Proceedings of the 2016 3rd MEC International Conference on Big Data and Smart City (ICBDSC)*, pp. 1–7, Muscat, Oman, March 2016.

[26] S. Sabharwal, S. Gupta, and K. Thirunavukkarasu, "Insight of big data analytics in healthcare industry," in *Proceedings of the 2016 International Conference on Computing, Communication and Automation (ICCCA)*, pp. 95–100, Noida, India, April 2016.

[27] S. Rao, S. N. Suma, and M. Sunitha, "Security solutions for big data analytics in healthcare," in *Proceedings of the 2015 Second International Conference on Advances in Computing and Communication Engineering*, pp. 510–514, Dehradun, India, May 2015.

[28] A. Ajayi, L. Oyedele, O. Akinade et al., "Optimised big data analytics for health and safety hazards prediction in power infrastructure operations," *Safety Science*, vol. 125, Article ID 104656, 2020.

[29] F. Khennou, Y. I. Khamlichi, and N. E. H. Chaoui, "Improving the use of big data analytics within electronic health records: a case study based OpenEHR," *Procedia Computer Science*, vol. 127, pp. 60–68, 2018.

[30] P. Gaitanou, E. Garoufallou, and P. Balatsoukas, "The effectiveness of big data in health care: a systematic review," in *Research Conference on Metadata and Semantics Research*, pp. 141–153, Springer, Berlin, Germany, 2014.

[31] A. K. Talukder, "Big data analytics advances in health intelligence, public health, and evidence-based precision medicine," in *Proceedings of the International Conference on Big Data Analytics*, pp. 243–253, Springer, Hyderabad, India, December 2017.

[32] A. Han, A. Isaacson, and P. Muennig, "The promise of big data for precision population health management in the US," *Public Health*, vol. 185, pp. 110–116, 2020.

[33] P. Ravikumaran, K. Vimala Devi, K. Kartheeban, and N. Narayanan Prasanth, "Health data analytics: framework & review on tool & technology," *Materials Today: Proceedings*, 2020.

[34] G. Aceto, V. Persico, and A. Pescapé, "Industry 4.0 and health: internet of things, big data, and cloud computing for healthcare 4.0," *Journal of Industrial Information Integration*, vol. 18, Article ID 100129, 2020.

[35] R. S. H. Istepanian and T. Al-Anzi, "m-Health 2.0: new perspectives on mobile health, machine learning and big data analytics," *Methods*, vol. 151, pp. 34–40, 2018.

[36] P. Galetsi, K. Katsaliaki, and S. Kumar, "Big data analytics in health sector: theoretical framework, techniques and prospects," *International Journal of Information Management*, vol. 50, pp. 206–216, 2020.

[37] Y. Wang, L. Kung, W. Y. C. Wang, and C. G. Cegielski, "An integrated big data analytics-enabled transformation model: application to health care," *Information & Management*, vol. 55, no. 1, pp. 64–79, 2018.

[38] W. M. Wami, R. Dundas, O. R. Molaodi, M. Tranter, A. H. Leyland, and S. V. Katikireddi, "Assessing the potential utility of commercial "big data" for health research: enhancing small-area deprivation measures with Experian™ Mosaic groups," *Health & Place*, vol. 57, pp. 238–246, 2019.

[39] D. W. Bates, S. Saria, L. Ohno-Machado, A. Shah, and G. Escobar, "Big data in health care: using analytics to identify and manage high-risk and high-cost patients," *Health affairs*, vol. 33, no. 7, pp. 1123–1131, 2014.

[40] S. Nanayakkara, X. Zhou, and H. Spallek, "Impact of big data on oral health outcomes," *Oral Diseases*, vol. 25, no. 5, pp. 1245–1252, 2019.

[41] S. Madanian, D. T. Parry, D. Airehrour, and M. Cherrington, "mHealth and big-data integration: promises for healthcare

system in India," *BMJ Health & Care Informatics*, vol. 26, no. 1, 2019.

[42] P. F. Brennan and S. Bakken, "Nursing needs big data and big data needs nursing," *Journal of Nursing Scholarship*, vol. 47, no. 5, pp. 477–484, 2015.

[43] J. Luo, M. Wu, D. Gopukumar, and Y. Zhao, "Big data application in biomedical research and health care: a literature review," *Biomedical Informatics Insights*, vol. 8, 2016.

[44] S. R. Sukumar, R. Natarajan, and R. K. Ferrell, "Quality of big data in health care," *International Journal of Health Care Quality Assurance*, vol. 28, no. 6, pp. 621–634, 2015.

[45] K. Slime, A. Maizate, and L. Hassouni, "Processing and analyzing health data in a big data context: aspects and implementations," in *Proceedings of the International Conference on Advanced Intelligent Systems for Sustainable Development*, pp. 299–307, Springer, Marrakech, Morocco, July 2019.